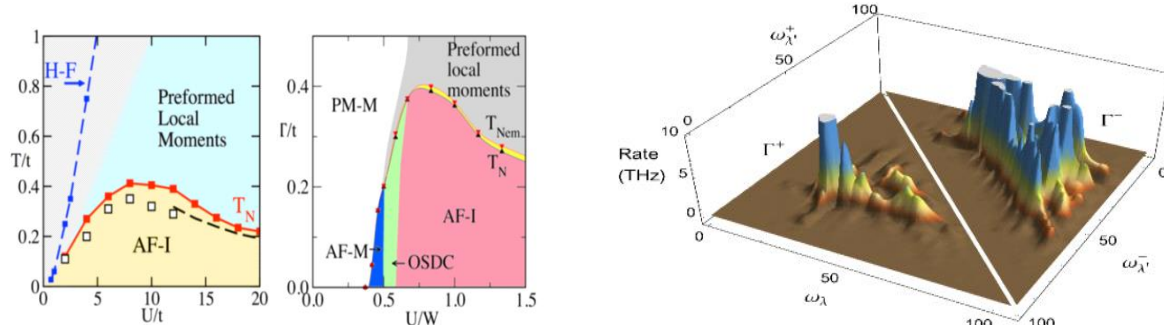
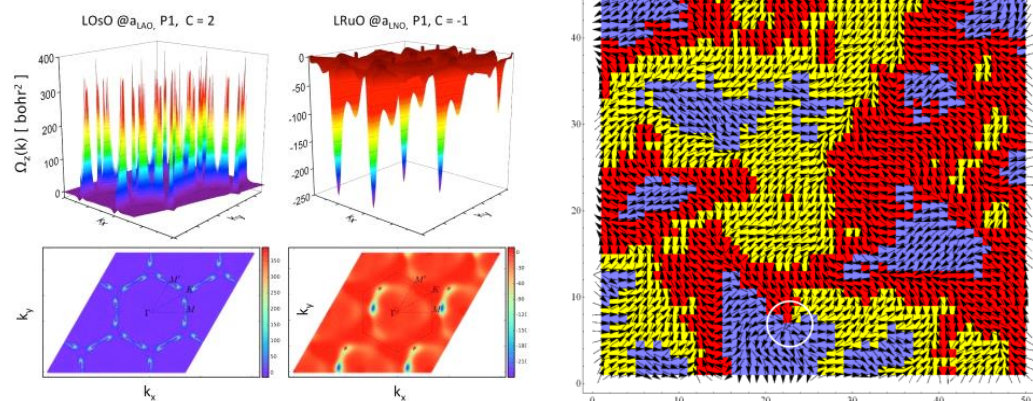
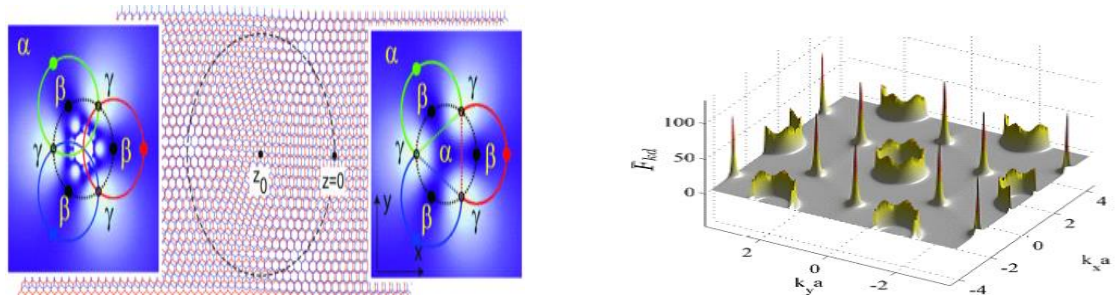


Theoretical Condensed Matter Physics

Principal Investigators' Meeting

August 15–17, 2016

Gaithersburg, Maryland



Office of Basic Energy Sciences
Division of Materials Sciences and Engineering



Office of
Science

On the Cover

- Top left: Strain-optimized stacking texture in bilayer graphene. Wire frame rendering (center) and potential energy densities of local stacking configurations. X Gong & E J Mele, Phys Rev B **89**, 121415(R) (2014)
- Top right: Time-averaged Berry curvature for a phase of a Floquet Chern Insulator corresponding to Chern number of 3. H Dehghani & A Mitra, Phys Rev B **92**, 165111 (2015)
- Middle left: Berry curvature (top, perspective view; bottom, top view) of buckled bilayer of LaOsO₃; with Chern number of 2; right side, and buckled bilayer of LaRuO₃ with Chern number of -1. W E Pickett, unpublished.
- Middle right: Imry-Ma domains in the ferromagnetic state of the 2d XY model at zero-applied field, with a vortex in the lower part inside the white circle. D A Garanin & M Chudnovsky, European Physics Journal B (Condensed Matter and Complex Systems) **88**, 81 (2015)
- Bottom left: Phase diagram for the half-filled one orbital Hubbard model (left) compared to the two-orbital Hubbard Model (right). A Mukherjee, N D Patel, A Moreo & E Dagotto. Phys Rev B **93**, 085144 (2016)
- Bottom right: Anharmonic scattering rates for three-phonon processes in the Heusler semiconductor Ba₂AuBi at 300 K. The lower left segment shows the absorption rates, whereas the upper right panel indicates the rates for emission processes. J He, M Amsler, Y Xia, S Shahab Naghavi, V I Hegde, S Hao, S Goedecker, V Ozolinš, & C Wolverton. Phys Rev Lett **117**, 046602 (2016)

This document was produced under contract number DE-AC05-06OR23100 between the U.S. Department of Energy and Oak Ridge Associated Universities.

The research grants and contracts described in this document are supported by the U.S. DOE Office of Science, Office of Basic Energy Sciences, Materials Sciences and Engineering Division.

Foreword

This volume provides descriptions of supported projects in the Theoretical Condensed Matter Physics (TCMP) Program, Materials Sciences and Engineering Division (MSED) in the Office of Basic Energy Sciences (BES) of the U.S. Department of Energy (DOE). It is intended to provide material for the third TCMP Principal Investigator meeting, held August 15–17, 2016 in Gaithersburg, Maryland.

BES supports fundamental research to understand, predict, and ultimately control matter and energy at the electronic, atomic, and molecular levels and fundamental research which provides the foundations for new energy technologies relevant to DOE's missions in energy, environment and national security. Condensed matter theory plays a key role in both the discovery of new organizing principles and the clarification of the origin of newly discovered phenomena.

The TCMP program emphasizes quantum materials, materials discovery, non-equilibrium transport, ultrafast response, and fundamental research in materials related to energy technologies. Ongoing research includes strongly correlated electron systems, quantum phase transitions, topological states, computational and data driven materials design, magnetism, superconductivity, optical response, semiconductors, thermoelectric materials, and neutron and photon scattering. Computational techniques include quantum Monte Carlo, improvements to density functional theory, extensions of dynamical mean field theory, density matrix renormalization group, self-consistent GW calculations and field theoretical approaches.

The TCMP program has recently expanded its portfolio through the interagency Materials Genome Initiative and support for new large projects in Computational Materials Sciences, designed to provide widely used, experimentally validated software and data to the materials community. An ongoing emphasis is toward exascale computing and joint programs with the Chemical Sciences, Geosciences and Biosciences Division of BES and the Office of Advanced Scientific Computing in DOE

The purpose of the BES biannual PI meetings is to bring together researchers funded by BES to foster an awareness of the research of others in the program, to facilitate the exchange of new results and research highlights, to promote new ideas and collaborations among participants and BES scientific user facilities, and to identify and pursue new scientific opportunities and new frontiers. For BES the PI meetings provide an opportunity to see the entire portfolio at one time and to assess the state of the program and chart new scientific directions.

We thank all the meeting participants for their active contributions in sharing their ideas and research accomplishments. We wish to thank Teresa Crockett in MSED and Linda Severs at the Oak Ridge Institute for Science and Education (ORISE) for their outstanding work in all aspects of the meeting organization.

Dr. James W. Davenport & Dr. Matthias J. Graf
Program Managers, Theoretical Condensed Matter Physics
Materials Sciences and Engineering Division, Basic Energy Sciences
Office of Science, U.S. Department of Energy

Table of Contents

Agenda xi

Poster Listing xvii

Abstracts

Static and Dynamic Thermal Effects in Solids

Philip B. Allen 1

Theory of Fluctuating and Critical Quantum Matter

Leon Balents 5

Electronic Structure, Spectroscopy and Correlation Effects in Novel Materials

Arun Bansil and Robert S. Markiewicz 9

Revealing Quantum Impurity Critical States via the Environment

Harold U. Baranger 13

Quantum Phenomena in Few-Layer Group IV Monochalcogenides: Interplay
among Structural, Thermal, Optical, Spin, and Valley Properties in 2D

Salvador Barraza-Lopez 17

Properties of Multiferroic Nanostructures from First Principles

Laurent Bellaiche 23

Theoretical Investigations of Nano and Bio Structures

J. Bernholc 27

Geometry, Entanglement and Disorder in Topological Phases

Ravindra N. Bhatt, F. Duncan M. Haldane, Edward H. Rezayi, and Kun Yang 32

Near-Field Electrodynamics of Carbon Nanostructures

Igor Bondarev 38

Interacting Topological Quantum Matter

Claudio Chamon 42

Quantum Embedding and First Principles Electronic Structure for Correlated
Materials

Garnet Kin-Lic Chan 46

Computational Theory Applied to Nanostructures <i>James R. Chelikowsky</i>	50
Computational Approach to Complex Interfaces and Junctions <i>Hai-Ping Cheng and James N. Fry</i>	54
Quantum Dynamics in Complex Magnets: Excitations, Transport, and Disorder <i>Alexander Chernyshev</i>	59
Dynamics of the Magnetic Flux in Superconductors <i>Eugene M. Chudnovsky</i>	63
Spin Driven Phenomena in Highly Correlated Materials <i>Piers Coleman</i>	68
First Principles Predictions of Phase Stability in Complex Oxides <i>Valentino R. Cooper</i>	72
Theoretical Study of Complex Collective Phenomena <i>Elbio Dagotto, Randy Fishman, Adriana Moreo, and Satoshi Okamoto</i>	77
Moments Study of Anharmonicity of Vibrational Modes in Solids <i>Murray S. Daw</i>	81
Time-Dependent Phenomena in Correlated Materials <i>Adrian Feiguin</i>	86
Competing Orders in Correlated Materials: Impact of Disorder and Non-equilibrium Perturbations <i>Rafael M. Fernandes</i>	90
Thermal and Thermoelectric Phenomena in Novel Materials and Systems of Disordered and Interacting Electrons <i>Alexander Finkel'stein</i>	95
Theoretical Description of Pump-Probe Experiments in Ordered Materials <i>J. K. Freericks</i>	99
Odd-Parity Superconductors: Nematic, Chiral and Topological <i>Liang Fu</i>	103
Theory of Fluctuations in Strongly-Correlated Materials <i>Victor M. Galitski</i>	106
Midwest Integrated Center for Computational Materials <i>Giulia Galli</i>	110

Semiconductor Nanostructures by Scientific Design <i>Giulia Galli</i>	113
Non-equilibrium Effects in Conventional and Topological Superconducting Nanostructures <i>Leonid Glazman and Alex Kamenev</i>	117
Simulation of Correlated Lattice and Impurity Systems out of Equilibrium <i>Emanuel Gull</i>	121
High-Performance First-Principles Molecular Dynamics for Predictive Theory and Modeling <i>Francois Gygi, Giulia Galli, and Eric Schwegler</i>	125
Quantum Quench Dynamics – Crossover Phenomena in Non-Equilibrium Correlated Quantum Systems <i>Stephan Haas, Hubert Saleur, and Stefan Kettemann</i>	129
Symmetry in Correlated Quantum Matter <i>Michael Hermele</i>	133
Quantitative Studies of the Fractional Quantum Hall Effect <i>Jainendra K. Jain</i>	137
Targeted Band Structure Design and Thermoelectrics Materials Discovery Using High-Throughput Computation <i>Anubhav Jain</i>	141
Mapping and Manipulating Materials Transformation Pathways and Properties <i>Duane D. Johnson</i>	145
Network for Ab Initio Many-Body Methods: Development, Education and Training <i>Paul Kent, Anouar Benali, David M. Ceperley, Miguel A. Morales, and Luke Shulenburger</i>	150
Emergence of High Tc Superconductivity out of Charge and Spin Ordered Phases <i>Eun-Ah Kim</i>	154
Correlation Effects and Magnetism in Actinides: Elements and Compounds <i>Gabriel Kotliar</i>	158
Non-collinear Magnetism and Dynamic Effects in Dzyaloshinskii-Moriya Magnets <i>Alexey Kovalev</i>	162

Toward High-Accuracy Point Defect Calculations in Materials using the Quasiparticle-Self-Consistent GW Method <i>Walter R. L. Lambrecht</i>	166
Structure and Dynamics of Material Surfaces, Interphase Interfaces and Finite Aggregates <i>Uzi Landman</i>	171
Strongly Correlated Electronic Systems: Local Moments and Conduction Electrons <i>Patrick A. Lee</i>	175
Design of Functional Materials based on New Principles of Disorder <i>Andrea J. Liu</i>	180
Theory of Materials Program at the Lawrence Berkeley National Laboratory <i>Steven G. Louie, Marvin L. Cohen, Dung-Hai Lee, Jeffrey B. Neaton, and Lin-Wang Wang</i>	184
Charge Carrier Holes Correlations and Non-Abelian Physics in Nanostructures, Quantum Hall Effect and Hybrid Superconductor/Semiconductor Structures <i>Yuli Lyanda-Geller</i>	188
Correlation between Electron Transport and Antiferromagnetic Ordering <i>Allan H. MacDonald and Qian Niu</i>	192
Structure and Electronic Properties of Dirac Materials <i>Eugene Mele</i>	196
Surface and Interface Physics of Correlated Electron Systems <i>A. J. Millis</i>	200
Optical, Transport Phenomena, and Interaction Effects in Novel Low-Dimensional Electron Systems <i>Eugene Mishchenko</i>	204
Variable Spins in Electronic Structure Quantum Monte Carlo and the Fixed-Phase Approximation <i>Lubos Mitas</i>	208
Nonequilibrium Phenomena in Topological Insulators <i>Aditi Mitra</i>	212
Non-equilibrium Physics at the Nanoscale <i>Dirk K. Morr</i>	216

Materials Theory	
<i>J. R. Morris, V. R. Cooper, M. H. Du, L. R. Lindsay, and D. S. Parker</i>	220
 Designing allostery-inspired response in mechanical networks	
<i>Sidney Nagel</i>	226
 Condensed Matter Theory	
<i>Mike Norman, Olle Heinonen, Alex Koshelev, Peter Littlewood, Ivar Martin, and Kostya Matveev</i>	230
 Symmetry Effects on the Interplay between Strong Correlation and Spin-Orbit Coupling	
<i>Warren E. Pickett</i>	234
 Emergent Properties of Highly Correlated Electron Materials	
<i>Srinivas Raghu</i>	238
 Theoretical and Computational Studies of Functional Nanomaterials	
<i>Talat S. Rahman</i>	243
 Physical Analysis of the Bulk Photovoltaic Effect for Solar Harvesting Materials	
<i>Andrew M. Rappe</i>	247
 Extending the Reach of Computational-Theoretical Methods to Materials at the Energy Frontier	
<i>Fernando A. Reboredo, G. Malcolm Stocks, Markus Eisenbach, and Jaron T. Krogel</i>	251
 Next Generation Photon and Electron Spectroscopy Theory	
<i>John J. Rehr</i>	257
 Percolative Metal-Insulator Transition in the Perovskite Oxides	
<i>Sashi Satpathy</i>	261
 Quantum Monte Carlo Studies of Multiband Hubbard Models	
<i>Richard Scalettar</i>	265
 Strongly Correlated Electrons	
<i>Pedro Schlottmann</i>	268
 Theoretical Studies in Very Strongly Correlated Matter	
<i>Sriram Shastry</i>	272
 Novel Fractional Quantum Hall Effect and New Topological Phase in Interacting Systems	
<i>Donna N. Sheng</i>	276

Many-Body Theory of Energy Transport and Conversion at the Nanoscale <i>Charles A. Stafford</i>	282
Non-equilibrium Relaxation and Aging Scaling of Driven Topological Defects in Condensed Matter <i>Uwe C. Täuber and Michel Pleimling</i>	287
Unconventional Metals in Strongly Correlated Systems <i>Senthil Todadri</i>	291
Orbital-Free Quantum Simulation Methods for Applications to Warm Dense Matter <i>Samuel B. Trickey, J. W. Dufty, F. E. Harris, and K. Runge</i>	295
Quantum Simulations of Orbitally Controlled Physics and Nanoscale Inhomogeneity in Correlated Oxides <i>Nandini Trivedi</i>	299
Non-equilibrium Thermodynamics in Magnetic Nanostructures <i>Yaroslav Tserkovnyak</i>	303
Strongly Correlated Systems: Further Away from the Beaten Path <i>Alexei M. Tsvelik, R. M. Konik, Wei Ku, and Weiguo Yin</i>	307
Collective Charge and Spin Dynamics in Low-Dimensional Itinerant Electron Systems with Spin-Orbit Coupling <i>Carsten A. Ullrich</i>	316
Materials Genome Innovation for Computational Software (MAGICS) <i>Priya Vashishta</i>	320
Time-Dependent Density Functional Theories of Charge, Energy and Spin Transport and Dynamics in Nanoscale Systems <i>Giovanni Vignale and Massimiliano Di Ventra</i>	325
Quantum Mesoscopic Materials <i>Valerii Vinokur and Andreas Glatz</i>	330
Accelerated Molecular Dynamics Methods <i>Arthur F. Voter and Danny Perez</i>	334
Gutzwiller Density Functional Theory for First-Principles Calculation of Strongly Correlated Electron Systems <i>Cai-Zhuang Wang, Kai-Ming Ho, Yongxin Yao, Vladimir Antropov, and Viatcheslav Dobrovitski</i>	338
Disorder and Interaction in Correlated Electron Materials <i>Ziqiang Wang</i>	342

Tensor Networks and Density Functional Theory for Electronic Structure <i>Steven R. White and Kieron Burke</i>	347
Thermodynamic Stability and Elasticity of High Entropy Alloys <i>Michael Widom</i>	352
Thermodynamics and Kinetics of Phase Transformations in Energy Materials <i>Christopher Wolverton and Vidvuds Ozolins</i>	356
Probing Fluctuation Induced Interactions in Nanostructured Materials <i>Lilia M. Woods</i>	361
First Principles Investigations for Magnetic Properties of Innovative Materials <i>Ruqian Wu</i>	365
Quantum Mechanical Simulations of Complex Nanostructures for Photovoltaic Applications <i>Zhigang Wu</i>	369
Interfacial Magnetic Skyrmions and Proximity Effects <i>Jiadong Zang</i>	373
Laser-Induced Ultrafast Magnetization in Ferromagnets <i>Guoping Zhang</i>	377
Theory of Defects in Electronic Materials <i>Shengbai Zhang</i>	381
Electronic Structure and Fundamental Physics of Semiconductor Nanostructures <i>Alex Zunger</i>	386
Unconventional Spin and Orbital Ordering in Semiconductor Nanostructures <i>Igor Zutic</i>	390
Author Index	397
Participant List	401

X

AGENDA

**2016 Theoretical Condensed Matter Physics
Principal Investigators' Meeting
Materials Sciences and Engineering Division, Office of Basic Energy Science
U. S. Department of Energy**

Program Chairs: Jim Davenport & Matthias Graf, TCMP Program Managers

SUNDAY, AUGUST 14, 2016

*****Arrival, Dinner on Your Own*****

MONDAY, AUGUST 15, 2016

7:00 – 8:30 am	***Breakfast***
8:30 – 9:00 am	Matthias Graf, Program Manager, Theoretical Condensed Matter Physics <i>TCMP Program Overview</i>
Session I	Title: Quantum Materials Chair: Andrey Chubukov, University of Minnesota
9:00 – 9:30 am	Elbio Dagotto, Oak Ridge National Laboratory <i>Complex magnetic phase diagrams of models for iron pnictides and chalcogenides</i>
9:30 – 10:00 am	Liang Fu, Massachusetts Institute of Technology <i>Odd-parity superconductors: nematic, chiral and topological</i>
10:00 – 10:30 am	***Break***
10:30 – 11:00 am	Pedro Schlottmann, Florida State University <i>Commensurate and incommensurate spin-density waves, non-Fermi liquid behavior and the superconducting dome in heavy electron systems</i>
11:00 – 11:30 am	Nandini Trivedi, Ohio State University <i>Orbital frustration and orbital entanglement in 5d transition metal oxides</i>
11:30 – 12:15 pm	Linda Horton, Director, Materials Sciences and Engineering Division <i>BES Program Updates</i>
12:15 – 1:00 pm	***Working Lunch*** <i>Overview of Poster Session I: Presenters with Highlights</i>

Session II	Title: Multi-Ferroics, Magnetism and More Chair: Samuel Trickey, University of Florida
1:00 – 1:30 pm	Laurent Bellaiche, University of Arkansas <i>Electric-field control of magnetism in rare-earth substituted BiFeO₃</i>
1:30 – 2:00 pm	Qian Niu, University of Texas <i>Transport, magnetic, and optical properties in noncollinear antiferromagnets</i>
2:00 – 2:30 pm	Andrew Rappe, University of Pennsylvania <i>Physical analysis of the bulk photovoltaic effect for solar harvesting materials</i>
2:30 – 3:00 pm	Richard Scalettar, University of California Davis <i>Magnetism and superconductivity on depleted lattices</i>
3:00 – 3:30 pm	***Break***
Session III	Title: The 2-Dimensional World Chair: James Morris, Oak Ridge National Laboratory
3:30 – 4:00 pm	Steven Louie, Lawrence Berkeley National Laboratory <i>Atomically thin quasi two-dimensional materials: electrons, excitons and plasmons</i>
4:00 – 4:30 pm	Eugene Mele, University of Pennsylvania <i>Bending rules in graphene kirigami</i>
4:30 – 5:00 pm	Lilia Woods, University of South Florida <i>Probing fluctuation induced interactions in nanostructured materials</i>
5:00 – 5:30 pm	Valentino Cooper, Oak Ridge National Laboratory <i>Computational materials design of high response piezoelectrics</i>
6:00 – 7:30 pm	***Working Dinner*** <i>Scientific Highlights of the Day: Discussion and Input from Attendees</i>
7:30 – 9:30 pm	***Poster Session I***

TUESDAY, AUGUST 16, 2016

7:00 – 8:00 am

Breakfast

Session IV

Title: Correlated States – First Principles Approaches

Chair: Emanuel Gull, University of Michigan

8:00 – 8:30 am

Garnet Chan, California Institute of Technology

Ab-initio models of the cuprates

8:30 – 9:00 am

Lubos Mitas, North Carolina State University

Variable spins in electronic structure quantum Monte Carlo and the fixed-phase approximation

9:00 – 9:30 am

Sriram Shastry, University of California Santa Cruz

Analytical calculation of the temperature dependent resistivity for an extremely correlated model

9:30 – 10:00 am

Steven White, University of California Irvine

Tensor networks and electronic structure

10:00 – 10:30 am

Break

Session V

Title: MGI etc.

Chair: Olle Heinonen, Argonne National Laboratory

10:30 – 10:50 am

Jim Davenport, DOE

Computational materials science, materials genome, exascale and all that

10:50 – 11:10 am

Giulia Galli, Argonne National Laboratory & University of Chicago

Midwest Integrated Center for Computational Materials

11:10 – 11:30 am

Gabriel Kotliar, Brookhaven National Laboratory & Rutgers University

Center for Computational Design of Functional Strongly Correlated Materials and Theoretical Spectroscopy

11:30 – 11:50 am

Priya Vashishta, University of Southern California

Materials genome innovation for computational software

12:00 – 1:15 pm

Working Lunch

Overview of Poster Session II: Presenters with Highlights

Session VI

Title: Materials in Our World

Chair: Michael Norman, Argonne National Laboratory

1:15 – 1:45 pm

James Chelikowsky, University of Texas

Simulating subatomic images of the covalent bond

1:45 – 2:15 pm

Francois Gygi, University of California Davis

High-performance first-principles molecular dynamics

2:15 – 2:45 pm

Duane Johnson, Ames Laboratory

Mapping and manipulating materials transformation pathways and properties

2:45 – 3:15 pm

Michael Widom, Carnegie Mellon University

Thermodynamic stability of high entropy alloys

3:15 – 3:45 pm

Break

Session VII

Title: What About Transport?

Chair: Leonid Glazman, Yale University

3:45 – 4:15 pm

Alexander Finkel'stein, Texas A&M University

Thermal transport and the Wiedemann-Frantz law in a system of disordered interacting electrons

4:15 – 4:45 pm

Alexey Kovalev, University of Nebraska

Magnon-mediated torque, spin and energy currents in chiral magnets

4:45 – 5:15 pm

Charles Stafford, University of Arizona

Local thermoelectric probes of nonequilibrium quantum systems

5:15 – 5:45 pm

Giovanni Vignale, University of Missouri

Towards a density functional theory of thermoelectric phenomena: recent progress and challenges

6:15 – 7:30 pm

Working Dinner

Scientific Highlights of the Day: Discussion and Input from Attendees

7:30 – 9:30 pm

Poster Session II

WEDNESDAY, AUGUST 17, 2016

7:00 – 8:00 am

Breakfast

Session VIII

Title: Out of Equilibrium

Chair: Andrew Millis, Columbia University

8:00 – 8:30 am

Yuli Lyanda-Geller, Purdue University

Topological matter in charge carrier hole systems

8:30 – 9:00 am

Aditi Mitra, New York University

Entanglement properties of Floquet Chern insulators

9:00 – 9:30 am

Kun Yang, Florida State University

Geometry, entanglement and disorder in fractional quantum Hall liquids

9:30 – 10:00 am

Andrea Liu, University of Pennsylvania

Scaling theory of the non-equilibrium jamming transition

10:00 – 10:30 am

*** Break***

Session IX

Title: The World is Not Static

Chair: Piers Coleman, Rutgers University

10:30 – 11:00 am

Dirk Morr, University of Illinois at Chicago

Non-equilibrium transport in topological and correlated materials

11:00 – 11:30 am

Ivar Martin, Argonne National Laboratory

Quasicrystals in space and time

11:30 – 12:00 pm

Adrian Feiguin, Northeastern University

Thermal and pump-driven dynamical behavior of a spin-full Luttinger liquid

12:00 – 12:30 pm

Talat Rahman, University of Central Florida

Time-dependent density-functional theory with dynamical mean-field theory: towards ab initio tools for strongly correlated and/or out-of-equilibrium systems

12:30 – 1:00 pm

Wrap-up, debriefing, evaluation

Meeting Feedback, Suggestions for Future Meetings

TCMP PI Meeting

Poster session I, Monday 7:30 – 9:30 PM

1. **Philip B. Allen**, Stony Brook University
Static and Dynamic Thermal Effects in Solids
2. **Leon Balents**, University of California, Santa Barbara
Theory of Fluctuating and Critical Quantum Matter
3. **Jerry Bernholc**, North Carolina State University
Theoretical Investigations of Nano and Bio Structures
4. **Harold Baranger**, Duke University
Revealing Quantum Impurity Critical States via the Environment
5. **Igor Bondarev**, North Carolina Central University
Near-Field Electrodynamics of Carbon Nanostructures: 1D Transport in Hybrid Metal-Semiconductor Nanotube Systems
6. **Claudio Chamon**, Boston University
Interacting Topological Quantum Matter
7. **Eugene Chudnovsky**, City University of New York
Disorder in Classical and Quantum Systems with Continuous-Symmetry Order Parameter: Flux Lattices, Josephson Junction Arrays, Spin Systems, Charge Density Waves
8. **Murray Daw**, Clemson University
Effects of Anharmonicity on Flexural Modes of Graphene
9. **Rafael Fernandes**, University of Minnesota
Competing Orders in Correlated Materials: Impact of Disorder and Non-equilibrium Perturbations
10. **Victor Galitski and Mehdi Kargarian**, University of Maryland
Amperean Pairing at the Surface of Topological Insulators
11. **Emanuel Gull**, University of Michigan
Simulation of Correlated Lattice and Impurity Systems out of Equilibrium
12. **Stephan Haas**, University of Southern California
Quantum Quench Dynamics – Crossover Phenomena in Non-equilibrium Correlated Quantum Systems

13. **Michael Hermele**, University of Colorado Boulder
Symmetry in Correlated Quantum Matter: Topological Phases Protected by Point Group Symmetry
14. **Anubhav Jain**, Lawrence Berkeley National Laboratory
Targeted Band Structure Design and Thermoelectrics Materials Discovery using High-Throughput Computation
15. **Leonid Glazman**, Yale University
Non-equilibrium Effects in Conventional and Topological Superconducting Nanostructures
16. **Paul Kent**, Oak Ridge National Laboratory
Network for Ab Initio Many-Body Methods: Development, Education and Training
17. **Walter Lambrecht**, Case Western Reserve University
Toward High-Accuracy Point Defect Calculations in Materials using the Quasiparticle-Self-Consistent GW Method
18. **Uzi Landman**, Georgia Institute of Technology
Structure, Transport and Topological Effects in Atomically Precise Graphene Nanostructures: Fabry-Pérot Oscillations in Segmented Nanoribbons and Charge Fractionization in Rings
19. **Patrick Lee**, Massachusetts Institute of Technology
Interaction of Light with Weyl Semimetals
20. **Steven G. Louie**, Lawrence Berkeley National Laboratory
Theory of Materials Program at LBNL
21. **Hector Ochoa**, UCLA
Topological Spin-Transfer Drag Driven by Skyrmion Diffusion
22. **Andrey Chubukov**, University of Minnesota
Novel Physics in Fe-Based Superconductors

TCMP PI Meeting

Poster Session II, Tuesday 7:30 – 9:30

1. **John J. Rehr**, University of Washington
Next Generation Photon and Electron Spectroscopy Theory: Cumulant Approach for Inelastic Losses and Satellites in X-ray Spectra
2. **Sashi Satpathy**, University of Missouri
Percolative Metal-Insulator Transition in LaMnO₃: A Variational Gutzwiller Study
3. **Uwe C. Täuber and Michel Pleimling**, Virginia Tech
Non-equilibrium Relaxation and Aging Scaling of Driven Topological Defects in Condensed Matter
4. **Senthil Todadri**, Massachusetts Institute of Technology
Dimensional Decoupling at Continuous Quantum Critical Mott Transitions
5. **Samuel B. Trickey**, University of Florida
Thermal DFT Functionals and Software for Extreme Condition Material Simulations
6. **Yaroslav Tserkovnyak**, UCLA
A Realization of the Haldane-Kane-Mele Model in Spin Systems
7. **Alexei Tsvelik**, Brookhaven National Laboratory
Composite Order Parameters, Their Universality Classes and Relation to Topological Order
8. **Carsten A. Ullrich**, University of Missouri
Spin-Wave Dynamics in a Paramagnetic 2DEG with Spin-Orbit Coupling
9. **Arthur F. Voter and Danny Perez**, Los Alamos National Laboratory
Accelerated Molecular Dynamics Methods
10. **Jiadong Zang**, University of New Hampshire
Magnetic Skyrmions in Confined Geometries
11. **C. Z. Wang**, Ames Laboratory
Gutzwiller Density Functional Theory for First-Principles Calculation of Strongly Correlated Electron Systems
12. **Ruqian Wu**, University of California, Irvine
Oxygen Adsorption as the Origin of 1/f Flux Noise in SQUIDS
13. **Guoping Zhang**, Indiana State University
Laser-Induced Ultrafast Demagnetization and All-Optical Switching

14. **Shengbai Zhang**, Rensselaer Polytechnic Institute
Criticality of Interfacial Plasmon and Ultrafast Charge Transfer between Transition Metal Dichalcogenides
15. **Salvador Barraza-Lopez**, University of Arkansas
Layered Group-IV Monochalcogenides: A Playground for Phase Transitions and Tunable Material Properties in 2D
16. **Valerii Vinokour**, Argonne National Laboratory
Quantum Mesoscopic Materials: Non-Hermitian Approach to Far-from-Equilibrium Phase Transitions
17. **Andy Rappe**, University of Pennsylvania
Photovoltaic Effects in Halide Perovskites
18. **Arun Bansil**, Northeastern University
Electronic Structure, Spectroscopy and Correlation Effects in Novel Matter
19. **Andy Millis**, Columbia University
*Surface and Interface Phenomena in Correlated Electron Materials
(plus: analytical continuation from machine learning)*
20. **Warren Pickett**, University of California, Davis
Symmetry Effects on the Interplay between Strong Correlation and Spin-Orbit Coupling
21. **Alexander Balatsky**, Los Alamos National Laboratory
Driven Dirac Materials: Transient Collective States
22. **Srinivas Raghu**, Stanford University
Composite Fermions and the 2D Field-Tuned Superconductor-Insulator Transition
23. **Vidvuds Ozolins**, University of California, Los Angeles
Ultralow Thermal Conductivity in Full Heusler Semiconductors
24. **Peter Hirschfeld**, University of Florida
Incipient Band Pairing in Fe-based Superconductors
25. **Fernando Reboredo**, Oak Ridge National Laboratory
Unraveling the Role of Site-Specific Oxygen Vacancies in a Transition-Metal-Oxide Superlattice with Diffusion Monte Carlo

Static and Dynamic Thermal Effects in Solids

Philip B. Allen, Stony Brook University

Key words: Temperature Shift, Thermal Broadening, Polaron, Piezo-electric, Pyroelectric

Project Scope

The current project (with student Jean Paul Nery) is about the temperature shift of electronic band structures. The specific example we study is the conduction band minimum and valence band maximum of zincblende structure GaN. This project is motivated by the recent realization by Ponce *et al.*¹ that in polar materials, Fröhlich electron-phonon interactions are not correctly treated by the adiabatic approximation which works well for other phonon modes. The correct treatment requires keeping non-adiabatic corrections and using an integration mesh for numerical sums, which is prohibitively fine if DFT methods are used. We work around this by introducing an analytic correction, as shown in Fig. 1.

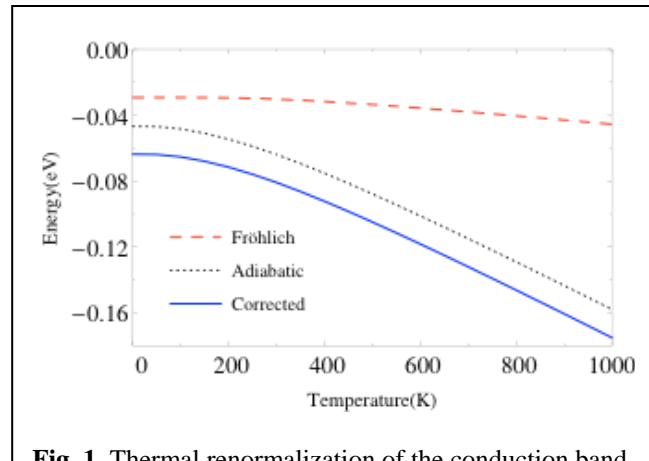


Fig. 1. Thermal renormalization of the conduction band minimum of GaN computed using the code² *Abinit* (dotted line, adiabatic approximation). The blue line shows the corrected answer after adding our analytic approximation for missing part of the Fröhlich polar phonon contribution. The red line shows the complete Fröhlich polar phonon contribution.

We have also realized that there is another phonon mode where adiabatic approximation fails, namely acoustic phonons in piezo-electric materials^{3,4}. Part of our work is about to be published in Phys. Rev. B. We are extending this work in several directions.

A recent paper, by Antonius *et al.*⁵ shows that dynamical effects (keeping the full Green's function form of perturbation theory, with a complex frequency $\omega + i\eta$) makes a significant change in theoretical predictions of thermal shifts. We are now studying the dynamical theory for single electrons in the conduction band or holes in the valence band. These interact with acoustic phonons, both piezo and non-piezo, and polar optical phonons. One main object of study is the spectral function, defined by

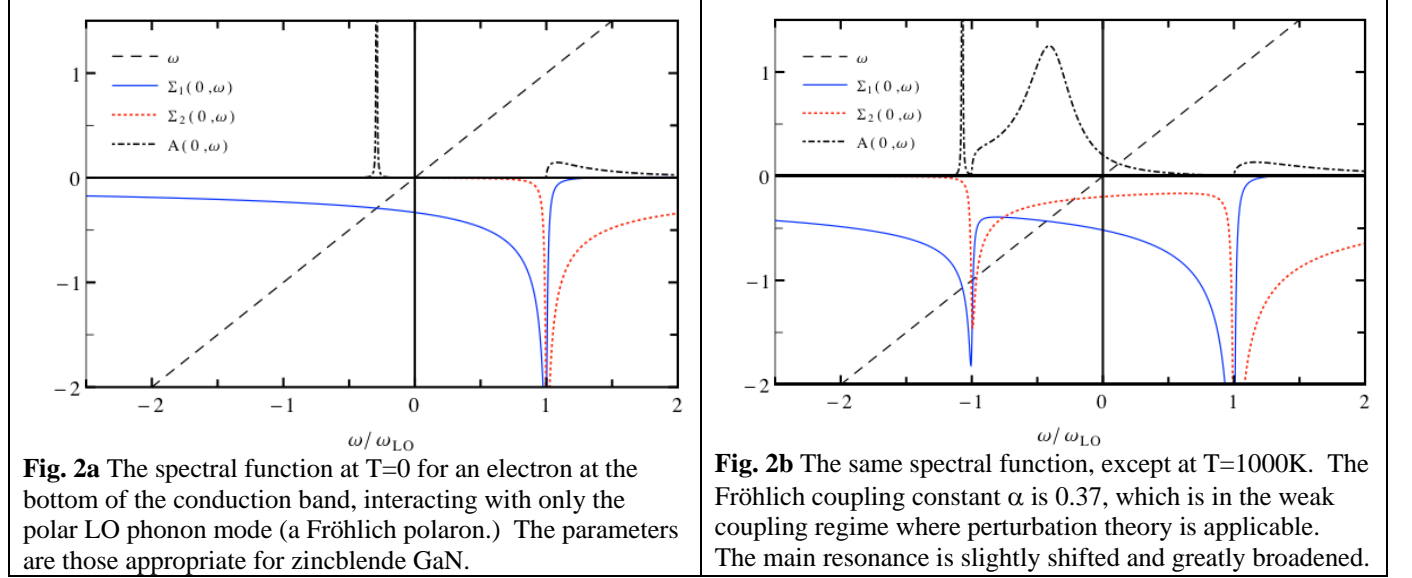
$$G(kn, \omega) = \left[\omega + i\eta - \varepsilon_{kn}^r - \Sigma(kn, \omega + i\eta) \right]^{-1}$$

$$A(kn, \omega) = \frac{-1}{\pi} \text{Im} G(kn, \omega)$$

In the usual treatment of electron renormalization in semiconductors, the self-energy Σ is treated

as a constant shift $\Sigma(kn, \omega) \approx \Delta(kn)$, with lifetime broadening ignored. The spectral function is then $A(kn, \omega) \approx \delta(\omega - \varepsilon(kn) - \Delta(kn))$. For a Fröhlich polaron, the shift is $\Delta = -\alpha\hbar\omega_{LO}$.

Two examples are shown below, where only the Fröhlich polar phonon interaction is included. At zero temperature, the standard Fröhlich resonance is seen at $-\alpha\hbar\omega_{LO}$, with additional spectral weight starting at $\omega = +\hbar\omega_{LO}$, where the electron probed at frequency ω has enough energy to emit a phonon. At high temperatures, significant lifetime broadening is seen.



We are still learning how to think about these results. One thing we have found is that the Fröhlich term is not the only part of the self-energy where significant ω -dependence and lifetime broadening occurs. By 1000K, ordinary acoustic phonon emission and absorption gives an equally important contribution. Also, of course, there is a large real part of $\Delta(kn)$ coming from virtual intraband and interband transitions, which we know how to include. One of the puzzles is that the LO phonon emission bump shown in Fig. 2 starts at $\omega=\omega_{LO}$, rather than at energy ω_{LO} higher than the quasiparticle peak at $-\alpha\omega_{LO}$. This suggests that the self energy needs to be computed self-consistently using the renormalized Green's function $G(kn, \omega)$. However, the literature on polarons discourages doing this based on insights from non-perturbative work. Another aspect we are working on is experimental implications of the dynamical treatment of the coupled one-electron/phonon system, such as infrared probes of existing polarons or soft uv excitation of electron-hole polaronic pairs. Such things are quite well understood for electrons in metals (see, for example, publication 3), but the physics here is a bit different and doesn't seem to have been completely worked out.

Recent Progress

Pyroelectricity is measured by the pyroelectric coefficient $p_s = dPs/dT$, a direct measure of the thermal shift of the intrinsic polarization of polar materials. Old theories of Born⁶ and Szigeti⁷ acknowledged two types of contribution, one from anharmonicity, and the other lying within harmonic theory. Theoretical formulas were given for the first of these by both Born and Szigeti. No formula has even been derived for the second, which Szigeti discounted, but which I believe is real and derives from electron-phonon interactions. No one has previously published an actual computation of the first (anharmonic) contribution. We have now done this (publication 5), using density functional calculations of the shifts of harmonic phonon frequencies when the “internal” (meaning not a macroscopic strain) distortion linked to polarization is changed. We find reasonable agreement with experiment for GaN and ZnO.

Future Plans

Two new projects are closely related to the ones described above. The electron-phonon interaction causes thermal shifts of electron charge density and of electrical polarization in polar materials. Batterman and others⁸ have measured the temperature shift of the (222) x-ray reflection of silicon. If all electron charge clouds around silicon atoms were spherical, this reflection would be forbidden in harmonic approximation. Therefore this x-ray reflection provides a particularly sensitive measure of the charge density of the valence electrons. The intensity depends on temperature because anharmonic vibrations increase, but more important, because the electron-phonon interaction renormalizes the (non-spherical) charge. Chelikowski and Cohen⁹ have already studied this contribution, but their method is now known to be very incomplete. They used temperature-dependent Debye-Waller factors to modify the pseudopotential strengths $V(G)$. This does indeed provide part of the answer, but there is another part which is probably larger, from the first-order electron-phonon interaction, used in second-order perturbation theory. This has never before been studied for electron charge density, and should make a serious change in the Chelikowsky-Cohen answer.

In a similar way, the electron-phonon renormalization should alter the polarization field of a polar semiconductor like GaN. As mentioned under “recent progress,” my former student Jian Liu already computed the effect of anharmonicity on the polarization. He gets the right sign and magnitude of the effect. I believe the electron-phonon effect will be at least as big. It was left out of the formulas of Szigeti and Born^{6,7}, probably because Born didn’t know how to put it in, and Szigeti decided it likely wasn’t there. Modern understanding does not support Szigeti. I am fairly sure the effect will be as important as the anharmonic effect that Liu already computed in GaN and ZnO, but we will not know until the theory has been formulated and computed.

Another project, less related to the ones above, is underway. The aim is to learn how to correctly solve the non-local Boltzmann transport equation for phonons carrying heat across an

interface. Specifically, the aim is to discover whether the temperature gradient close to the boundary remains constant (as always assumed in prior work) or evolves when the distance to the interface is similar to, or less than, the phonon mean free path.

References

1. S. Poncé, Y. Gillet, J. L. Janssen, A. Marini, M. Verstraete, and X. Gonze, Temperature dependence of the electronic structure of semiconductors and insulators, *J. Chem. Phys.* **143**, 102813 (2015).
2. X. Gonze et al., *ABINIT: First-principles approach to material and nanosystem properties*, *Comput. Phys. Commun.* **180**, 2582 (2009).
3. A. R. Hutson, *Piezoelectric scattering and phonon drag in ZnO and CdS*, *J. Appl. Phys.* **32**, 2287 (1961).
4. P. B. Allen, *Low temperature semiconductor band gap thermal shifts*, (arXiv:1605.01980).
5. G. Antonius et al., *Dynamical and anharmonic effects on the electron-phonon coupling and the zero-point renormalization of the electronic structure*, *Phys. Rev. B* **92**, 085137 (2015).
6. M. Born, *On the Quantum Theory of Pyroelectricity*, *Rev. Mod. Phys.* **17**, 245-251 (1945).
7. B. Szigeti, *Temperature Dependence of Pyroelectricity*, *Phys. Rev. Lett.* **35**, 1532-34 (1975).
8. J. B. Roberto, B. W. Batterman, and D. T. Keating, *Diffraction studies of the (222) reflection in Ge and Si: Anharmonicity and the bonding electrons*, *Phys. Rev. B* **9**, 2590-99 (1974).
9. J. R. Chelikowsky and M. L. Cohen, *Electronic Charge Densities and the Temperature Dependence of the Forbidden (222) Reflection in Silicon and Germanium*, *Phys. Rev. Lett.* **33**, 1339-1342 (1974).

Publications

1. P. B. Allen, *Size Effects in Thermal Conduction by Phonons*, *Phys. Rev. B* **90**, 054301:1-8 (2014); erratum *Phys. Rev. B* **92**, 019904 (2015)
2. P. B. Allen, *Anharmonic Phonon Quasiparticle Theory of Zero-point and Thermal Shifts in Insulators: Heat Capacity, Bulk Modulus, and Thermal Expansion*, *Phys. Rev. B* **92**, 064106:1-10 (2015).
3. P. B. Allen, *Electron self-energy and generalized Drude formula for infrared conductivity of metals*, *Phys. Rev. B* **92**, 054305:1-4 (2015).
4. B. Pamuk, P. B. Allen, and M.-V. Fernández-Serra, *Electronic and nuclear quantum effects on the ice XI/ice Ih phase transition*, *Phys. Rev. B* **92**, 134105:1-8 (2015).
5. J. Liu, M.-V. Fernández-Serra, and P. B. Allen, *First-principles study of pyroelectricity in GaN and ZnO*, *Phys. Rev. B* **93**, 081205(R) (2016).
6. J. Liu, M.-V. Fernández-Serra, and P. B. Allen, *Special Quasi-ordered Structures: role of short-range order in the semiconductor alloy (GaN)_{1-x}(ZnO)_x*, *Phys. Rev. B* **93**, 054207:1-8 (2016).
7. J. P. Nery and P. B. Allen, *Influence of Fröhlich polaron coupling on renormalized electron bands in polar semiconductors. Results for zincblende GaN*, *Phys. Rev. B* (accepted, 2016). (arXiv:1603.04269)

Theory of Fluctuating and Critical Quantum Matter

Leon Balents, University of California, Santa Barbara

Keywords: quantum criticality, frustration, strong correlations, spin liquid, mott transition

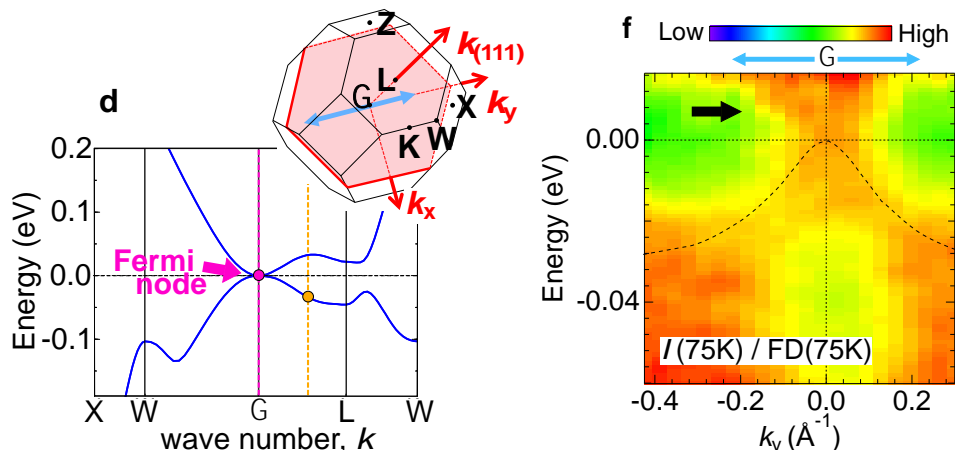
Project Scope

The proposal centers on the theory of phenomena in electronic materials involving strong quantum fluctuations, which arise due to frustration, exotic interactions (especially those originating from spin-orbit coupling), and proximity to quantum critical points. The projects are divided roughly into two areas: phases of frustrated quantum magnets, and quantum critical points in itinerant systems with frustrated or exotic interactions. All components are connected both to specific experiments and materials, and to general issues at the forefront of the theory of correlated quantum matter.

Recent Progress

Pyrochlore iridates: We collaborated with experimental groups at the ISSP in Japan on studies of the electronic properties of these materials. We compared first principles electronic structure calculations, which predict a quadratic Fermi node at the Fermi level for $\text{Pr}_2\text{Ir}_2\text{O}_7$, to angle resolved photoemission measurements of the same material, and found remarkable agreement. This result firmly places $\text{Pr}_2\text{Ir}_2\text{O}_7$ on the verge of a number of electronic instabilities, which may explain its complex low temperature properties.

In a second work, we studied the effect of applied magnetic fields on the insulating state in $\text{Nd}_2\text{Ir}_2\text{O}_7$. We found a first order zero temperature insulator to metal transition at a field



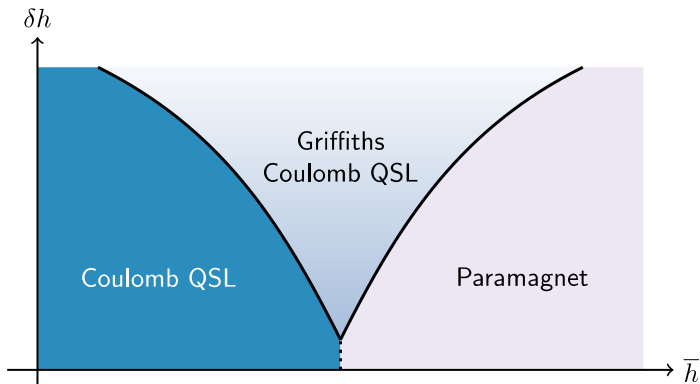
Theoretical (left) and experimental (right) electronic structure of $\text{Pr}_2\text{Ir}_2\text{O}_7$, showing the existence of a quadratic Fermi node.

of 12T, which we argued corresponds to the loss of Ising magnetic order. This transition occurs only for a field along the crystalline (100) axis, which is explained by the effects of Ising-like Nd rare earth spins, making the full description of this material and Kondo lattice model.

In a third study, we extended the photoemission measurements to Nd₂Ir₂O₇, and observed the evolution of the electronic structure below the onset of magnetic ordering. Pronounced correlation effects were observed, and explained in the context of an interacting Fermi liquid (not Fermi gas) description, and suggested a Slater to Mott crossover interpretation.

In a fourth, theoretical work, we complemented our earlier theory of an Ising antiferromagnetic quantum critical point with quadratic band touching, relevant to the all-in-all-out ordering seen in Nd₂Ir₂O₇, to the analogous theory for ferromagnetic ordering. While this is not observed experimentally, it might be induced by appropriate magnetic doping of materials with this band structure. We found that in the ferromagnetic case there is an intrinsic instability to *incommensuration*, induced by coupling to the itinerant fermions. Consequently, an intermediate spin density wave state appears when the ferromagnetic order weakens.

Disorder-enhanced quantum spin ice: We considered the effects of non-magnetic disorder in non-Kramers spin ice systems.¹ We argued that in this situation the dominant effect of disorder is to introduce local crystal fields which act as quantum transverse fields. Thus they induce faster spin dynamics rather than a tendency to freezing, which is completely opposite to naive expectations. This is actually a generic effect of disorder in non-Kramers magnets. In spin ice, it goes further, and we argue that disorder can induce a quantum spin liquid phase even in an otherwise classical spin ice material, i.e. even when it provides the only source of dynamics. This context opens up an intriguing set of problems involving the combination of strong disorder physics and spin liquid physics of strong entanglement.



Phase diagram showing disorder-induced entangled phases in quantum spin ice.

Optical and dielectric response at a spin-orbital quantum critical point: Using a theoretical model developed several years ago in our group, we calculated the optical and dielectric response near a quantum critical point

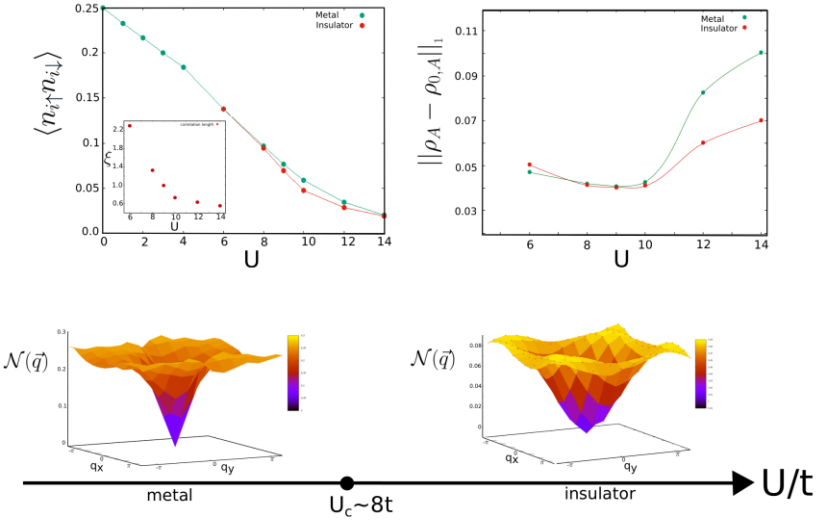
believed to apply to FeSc₂S₄. Our theory gives the dispersion and splitting of optical excitations versus field and temperature, as well as a two-particle continuum contribution to the dielectric susceptibility. The results explain several recent experimental observations.

Density matrix embedding theory of highly entangled states: We are currently working to develop a new computational method which aims to connect exact calculations for small clusters to the long-distance structure of entanglement of wavefunctions in the thermodynamic limit. The basic problem of connecting wavefunctions for small systems to a larger environment is a central one in quantum many body systems. One very successful approach to this is cluster DMFT, which treats the environment as a bath with structure in energy but not in position, and approaches the problem from high temperature. However, there is no ground state wavefunction associated with DMFT, and as such it cannot describe any physics of long-range entanglement. Phases with for example topological order are therefore outside the DMFT approach. Recently, Garnet Chan's group proposed DMET,² which has a cluster+bath decomposition but works directly with wavefunctions. We have been working to extend this approach to treat wavefunctions with long-range entanglement. Eventually this may provide a quantitative accurate computational approach to topologically ordered or quantum spin liquid systems, which has the virtue of treating short-distance physics exactly. Currently we are developing and testing our approach on a two dimensional triangular lattice Hubbard model, and preliminary results are promising.

Review articles: We wrote a couple of review articles. One long review on quantum spin liquids,³ solicited by Reports on Progress of Physics, is still under review, and the other, on strongly correlated materials with strong spin orbit coupling, is published (paper 9 under Publications).

Future Plans

We will continue to develop DMET and related cluster approaches to strongly correlated conductors and insulators, and in particular extend our version of DMET to spin Hamiltonians. We will use this and other methods to study the magnetic excitations of Yb₂Ti₂O₇, which have recently been studied in more experimental detail by Coldea. A more quantitative comparison with experiment of the evolution of these excitations with field and temperature should be a



Preliminary results from DMET on the triangular lattice Hubbard model using variational Monte Carlo evaluation of a highly entangled trial wavefunction. Top: double occupancy and trace-norm error in the density matrix versus U . Bottom: density structure factor showing metal and insulating states. Calculations are for a 2 site cluster.

strong test of theory. We plan also to apply the basic idea of disorder-induced dynamics in non-Kramers systems to other materials beyond the spin ice class.

References

1. L. Savary and L. Balents, *Disorder-Induced Entanglement in Spin Ice Pyrochlores*, arXiv:1604.04630 (2016).
2. Knizia, G. and Chan, G.K.L., *Density matrix embedding: A simple alternative to dynamical mean-field theory*, Physical review letters **109**, 186404 (2012).
3. L. Savary and L. Balents, *Quantum spin liquids*. arXiv:1601.03742 (2016).

Publications

1. M. Nakayama, T. Kondo, Z. Tian, J. J. Ishikawa, M. Halim, C. Bareille, W. Malaeb, K. Kuroda, T. Tomita, S. Ideta, K. Tanaka, M. Matsunami, S. Kimura, N. Inami, K. Ono, H. Kumigashira, L. Balents, S. Nakatsuji, and S. Shin. *Slater to mott crossover in the metal to insulator transition of Nd₂Ir₂O₇*, Phys. Rev. Lett., **117**, 056403 (2016).
2. Z. Tian, Y. Kohama, T. Tomita, H. Ishizuka, T. H. Hsieh, J. J. Ishikawa, K. Kindo, L. Balents, and S. Nakatsuji., *Field-induced quantum metal-insulator transition in the pyrochlore iridate Nd₂Ir₂O₇*. Nat Phys, **12**, 134–138 (2016).
3. T. Kondo, M. Nakayama, R. Chen, J. J. Ishikawa, E. G. Moon, T. Yamamoto, Y. Ota, W. Malaeb, H. Kanai, Y. Nakashima, Y. Ishida, R. Yoshida, H. Yamamoto, M. Matsunami, S. Kimura, N. Inami, K. Ono, H. Kumigashira, S. Nakatsuji, L. Balents, and S. Shin. *Quadratic Fermi node in a 3d strongly correlated semimetal*, Nature communications, **6**, 10042 (2015).
4. D. Ish and L. Balents. *Theory of excitations and dielectric response at a spin-orbital quantum critical point*, Phys. Rev. B, **92**, 094413 (2015).
5. J. M. Murray, O. Vafek, and L. Balents. *Incommensurate spin density wave at a ferromagnetic quantum critical point in a three-dimensional parabolic semimetal*, Phys. Rev. B **92**, 035137 (2015).
6. J. Iaconis and L. Balents, “Many-body effects in topological kondo insulators”, Phys. Rev. B **91**, 245127 (2015).
7. L. Mittelstädt, M. Schmidt, Z. Wang, F. Mayr, V. Tsurkan, P. Lunkenheimer, D. Ish, L. Balents, J. Deisenhofer, and A. Loidl, *Spin-orbiton and quantum criticality in FeSc₂S₄*, Phys. Rev. B **91**, 125112 (2015).
8. L. Savary, E.-G. Moon, and L. Balents. *New type of quantum criticality in the pyrochlore iridates*, Phys. Rev. X **4**, 041027 (2014).
9. W. Witczak-Krempa, G. Chen, Y.-B. Kim, and L. Balents, *Correlated quantum phenomena in the strong spin-orbit regime*, Annual Review of Condensed Matter Physics **5**, 57–82 (2014).

Electronic Structure, Spectroscopy and Correlation Effects in Novel Materials

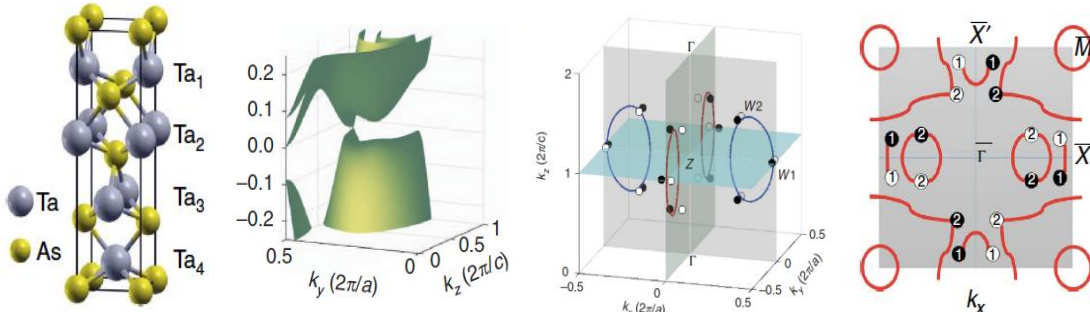
Principal Investigator: Arun Bansil; Co-PI: Robert S. Markiewicz
Physics Department, Northeastern University, Boston MA 02115
ar.bansil@northeastern.edu

Project Scope

This project concerns theoretical studies of electronic structure, spectroscopic response, and correlation effects in a wide variety of novel materials of current interest. Our overarching goal is to undertake realistic modeling of various highly resolved spectroscopies of materials for providing discriminating tests of competing theoretical scenarios, and as a rational basis for future experimentation. We emphasize that spectroscopies do not provide a direct map of electronic states, but act as a complex 'filter' or 'mapping' of the underlying spectrum. This link between electronic states and measured spectra—the 'matrix element effect'—is in general extremely complex, but a good understanding of this link is crucially important for fully exploiting various spectroscopies. Accordingly, we are working toward formulating and implementing increasingly sophisticated methodologies for making direct connection with angle-resolved photoemission (ARPES), resonant inelastic x-ray scattering (RIXS), scanning tunneling microscopy/spectroscopy (STM/STS), magnetic and non-magnetic Compton scattering, positron annihilation, neutron scattering and optical spectroscopies. Specific systems considered are topological insulators and other exotic topological phases of quantum matter, cuprates, pnictides, manganites, nano-particles, and 2D ultrathin films beyond graphene. Although the LDA provides an important baseline, 'beyond LDA' schemes are invoked for modeling the underlying electronic spectrum in correlated materials in order to incorporate the physics of superconducting orders, pseudogaps, impurities and nanoscale heterogeneities, and how matrix element effects can enhance/suppress related signatures in spectroscopies. The present project thus aims to help fill a critical gap in the available tools for understanding, analyzing and interpreting spectroscopies in wide use today, and to obtain through direct comparisons between theory and experiment new insights into electron correlation effects, Fermi surfaces, magnetism and related issues.

Recent Progress

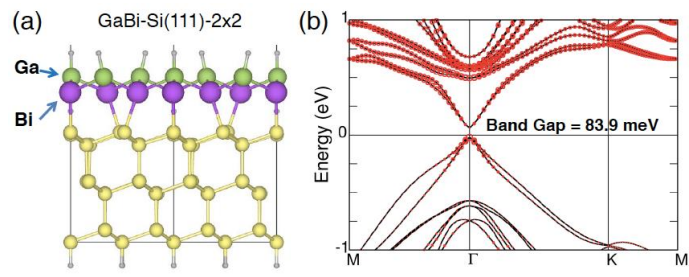
Successful Prediction of the First Weyl Semi-metal TaAs Class Material, Modeling ARPES Spectral Intensities and Spin Textures of Topological States



We predicted successfully last year that the TaAs class, highlighted in the figure on the preceding page, can host Weyl fermions in a single-phase non-magnetic material. The crystal structure is fairly simple body-centered tetragonal (left panel). One of the Weyl nodes where the conduction and valence bands touch is shown in the middle left panel. The total of 24 Weyl nodes in TaAs result from the evaporation of line nodes lying in the high symmetry planes in the absence of spin-orbit coupling into pairs of nodes, see middle right panel. Finally, the rightmost panel emphasizes the unique surface state structure, which includes FS arcs connecting Weyl nodes of opposite polarities for the Ta-terminated (001) surface. The results for TaP, NbAs and NbP are similar. Our key theoretically predicted bulk and surface features of the TaAs class have been verified experimentally. The TaAs class is still the only experimentally realized Weyl material. [Nat. Commun. 6, 7373 (2015); Science 349, 613 (2015); Nat. Phys. 11, 748 (2015); Science Advances 1, e1501092 (2015)]

2D Thin Films Beyond Graphene, Predicting Robust 2D Topological Phases, Quantum Transport.

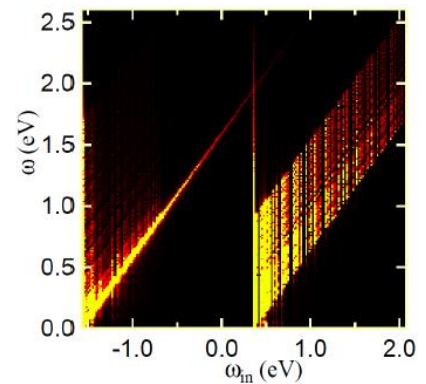
The available 2D TIs or quantum spin Hall (QSH) insulators are still limited to the HgTe/CdTe and InAs/GaSb/AlSb quantum wells with very small band gaps. In this connection, we have examined a wide variety of ultrathin films of elements of groups III, IV and V and their alloys, including effects of substrates, strains and passivations. The figure highlights the results for a



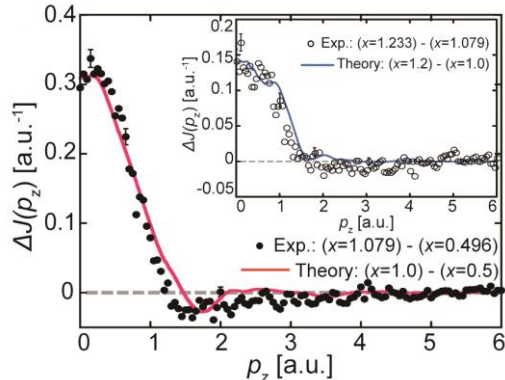
GaBi bilayer on Si(111) with the top and bottom layers passivated with H atoms. The relaxed structure is shown in the left panel. The band structure (right panel) is inverted around Γ with a robust band gap of 83.9 meV, which is large enough for room temperature applications. The film supports a surface state Dirac cone well-isolated from the bulk bands. [Nano Lett. 14, 2505 (2014); Nano Lett. 15, 6568 (2015); Nat. Sci. Reports 5, 15463 (2015); PRB 93, 035429 (2016); Nat. Sci. Reports 6, 18993 (2016)]

Relation of Strong Core Hole to the X-Ray Edge Singularity in RIXS.

Using a lattice model, we show how the classic approach of Nozieres and di Domenicis for treating the edge-singularity in x-ray absorption/emission can be generalized to the more complex case of the RIXS process, including effects of the intermediate states in the presence of the core hole. We numerically solve our lattice model essentially exactly to obtain a novel form of edge-singularity at the RIXS threshold energy. The figure on the right shows the weights for all zero- and one-pair states for a 35×35 lattice where ω is the energy transferred and ω_{in} is the initial photon energy with respect to the resonant energy. Our RIXS spectrum thus naturally includes both the well- and poorly-screened spectral components and their dispersions, and allows its separation into pair- and multiple-pair excitations. Our lattice model provides a robust basis for gaining insight into the K-, L- and M-edge RIXS spectra of materials. [PRL 112, 237401 (2014)]



In-Situ/Operando Advanced Characterization of Li-Battery Materials via High-Resolution X-Ray Compton Scattering. The figure shows the measured and computed changes in the valence Compton profiles, $\Delta J(p_z)$, in $\text{Li}_x\text{Mn}_2\text{O}_4$ for two different Li contents, x , with respect to the baseline of the Mn-O matrix. Computations are based on our all electron, fully self-consistent KKR-CPA methodology to model the random occupation of the host matrix by Li. The good agreement between theory and experiment allows us to adduce that the orbital involved in Li insertion/extraction is mainly the O- $2p$, and that 0.16 ± 0.05 3d electrons/Mn experience spatial delocalization. Since high-energy x-rays can easily penetrate matter, Compton scattering provides a unique window for probing closed electrochemical cells in sharp contrast to other spectroscopic techniques involving charged particles. Our approach paves the way for an advanced characterization and design/engineering of battery materials. [PRL 114, 087401 (2015); J. App. Phys. 119, 025103 (2016)]



Planned activities

Highlights of ongoing/planned activities are: (1) Modeling/analysis of spin-textures of topological states in 2D and 3D topological materials and the associated ARPES and STS/STM spectra. (2) New topological materials prediction to expand the menu of available materials, especially materials hosting Weyl, Dirac and Majorana fermions. (3) Thin film materials beyond graphene, especially those with large spin-orbit coupling, their topological phases, and their quantum transport characteristics in the presence of external electric and magnetic fields. (4) Modeling/analysis of the doping and temperature dependencies of the electronic spectra of novel superconductors using our comprehensive, beyond LDA intermediate coupling scheme and its multi-orbital extensions. (5) Generalizations of our work on realistic modeling of STS/STM spectra of homogeneous phases to treat STS/STM spectra of defects and impurities, including relativistic generalizations for handling spin-orbit coupled materials. (6) Modeling electronic structures of ordered/disordered phases of various Li-battery materials, and the associated inelastic x-ray scattering spectra to develop the potential of these techniques as unique, in situ/operando advanced characterization tools with the capability to probe closed electrochemical cells. (7) Modeling of K-, L- and M-edge RIXS spectra of cuprates and extensions of our methodology for treating dissipation effects and time-domain problems.

Selected Publications (2015-)

1. S-Y. Xu, I. Belopolski, N. Alidoust, M. Neupane, C. Zhang, R. Sankar, G. Chang, Z. Yuan, Chi-Cheng Lee, Shin-Ming Huang, H. Zheng, G. Bian, Jie Ma, D. S. Sanchez, BaoKai Wang, Arun Bansil, Fangcheng Chou, Pavel P. Shibayev, Hsin Lin, Shuang Jia, and M. Zahid Hasan: "Discovery of a Weyl fermion semimetal and topological Fermi arcs," *Science* 349, 613 (2015).

2. I. Zeljkovic, Y. Okada, M. Serbyn, R. Sankar, D. Walkup, W. Zhou, J. Liu, G. Chang, Y. J. Wang, M. Z. Hasan, F. Chou, H. Lin, A. Bansil, L. Fu and V. Madhavan: "Dirac mass generation from crystal symmetry breaking in topological crystalline insulators," *Nature Materials* **14**, 318 (2015).
3. J. He, T. Hogan, T. R. Mion, H. Hafiz, Y. He, J. D. Denlinger, S.-K. Mo, C. Dhital, X. Chen, Q. Lin, Y. Zhang, M. Hashimoto, H. Pan, D. H. Lu, M. Arita, K. Shimada, R. S. Markiewicz, Z. Wang, K. Kempa, M. J. Naughton, A. Bansil, S. D. Wilson, R-H. He: "Spectroscopic evidence for negative electronic compressibility in a quasi-3D spin-orbit correlated metal," *Nature Materials* **14**, 577 (2015).
4. S-Y. Xu, I. Belopolski, D. S. Sanchez, C. Zhang, G. Chang, C. Guo, G. Bian, Z. Yuan, H. Lu, T-R. Chang, P. Shibayev, M. Prokopovych, N. Alidoust, H. Zheng, C-C. Lee, S.-M. Huang, R. Sankar, F. Chou, C-H. Hsu, H.-T. Jeng, A. Bansil, T. Neupert, V. N. Strocov, H. Lin, S. Jia and M. Z. Hasan: "Experimental discovery of Weyl semimetal state TaP," *Science Advances* **1**, e1501092 (2015).
5. K. Suzuki, B. Barbiellini, Y. Orikasa, N. Go, H. Sakurai, S. Kaprzyk, M. Itou, K. Yamamoto, Y. Uchimoto, Y-J. Wang, H. Hafiz, A. Bansil, Y. Sakurai: "Extracting Redox Orbitals in Li Battery Materials with High-Resolution X-Ray Compton Spectroscopy," *PRL* **114**, 087401 (2015).
6. J.T. Okada, P.H.-L. Sit, Y. Watanabe, B. Barbiellini, T. Ishikawa, Y.J. Wang, M. Itou, Y. Sakurai, A. Bansil, R. Ishikawa, M. Hamaishi, P.-F. Paradis, K. Kimura, T. Ishikawa, S. Nanao: "Visualizing mixed bonding properties of liquid boron with Compton scattering," *PRL* **114**, 177401 (2015).
7. S.-M. Huang, S-Y. Xu, I. Belopolski, C.-C. Lee, G. Chang, B. Wang, N. Alidoust, G. Bian, M. Neupane, C. Zhang, S. Jia, A. Bansil, H. Lin and M. Z. Hasan: "A Weyl fermion semimetal with surface Fermi arcs in the transition metal monopnictide TaAs class," *Nature Communications* **6**, 7373 (2015).
8. S.-Y. Xu, N. Alidoust, I. Belopolski, Z. Yuan, G. Bian, T.-R. Chang, H. Zheng, V. Strokov, D. S. Sanchez, G. Chang, C. Zhang, D. Mou, Y. Wu, L. Huang, C.-C. Lee, S.-M. Huang, B. Wang, A. Bansil, H.-T. Jeng, T. Neupert, A. Kaminski, H. Lin, S. Jia, and M. Z. Hasan: "Discovery of a Weyl Fermion state with Fermi arcs in niobium arsenide," *Nature Physics* **11**, 748 (2015).
9. Christian P. Crisostomo, Liang-Zi Yao, Zhi-Quan Huang, Chia-Hsiu Hsu, Feng-Chuan Chuang, Hsin Lin, Marvin A. Alba and Arun Bansil: "Robust Large Gap Two-Dimensional Topological Insulators in Hydrogenated III-V Buckled Honeycombs," *Nano Letters* **15**, 6568 (2015).
10. Q. Jia, N. Ramaswamy, H. Hafiz, U. Tylus, K. Strickland, G. Wu, B. Barbiellini, A. Bansil, E. F. Holby, P. Zelenay and S. Mukerjee: "Experimental Observation of Redox-Induced Fe-N Switching Behavior as a Determinant Role for Oxygen Reduction Activity," *ACS Nano* **9**, 12496 (2015).
11. S.-M. Huang, S-Y. Xu, I. Belopolski, C.-C. Lee, G. Chang, T.-R. Chang, B. Wang, N. Alidoust, G. Bian, M. Neupane, D. Sanchez, H. Zheng, H.-T. Jeng, A. Bansil, T. Neupert, H. Lin, and M. Z. Hasan: "New type of Weyl semimetal with quadratic double Weyl fermions," *PNAS* **113**, 1180 (2016).
12. T.-R. Chang, S-Y. Xu, G. Chang, C.-C. Lee, S-M. Huang, B. Wang, G. Bian, H. Zheng, D. S. Sanchez, I. Belopolski, N. Alidoust, M. Neupane, A. Bansil, H-T. Jeng, H. Lin and M. Z. Hasan: "Prediction of an arc-tunable Weyl Fermion state in $M_{0.8}W_{1-x}Te_2$," *Nature Communications* **7**, 10639 (2016).
13. G. Bian, T-R. Chang, R. Sankar, S-Y. Xu, H. Zheng, T. Neupert, C-K. Chiu, S-M. Huang, G. Chang, I. Belopolski, D. S. Sanchez, M. Neupane, N. Alidoust, C. Liu, B. Wang, C-C. Lee, H-T. Jeng, C. Zhang, Z. Yuan, S. Jia, A. Bansil, F. Chou, H. Lin, and M. Z. Hasan: "Topological nodal-line fermions in spin-orbit metal $PbTaSe_2$," *Nature Communications* **7**, 10556 (2016).
14. W. Shi, S. W. H. Eijt, C. S. S. Sandeep, L. D. A. Siebbeles, A. J. Houtepen, S. Kinge, E. Bruck, B. Barbiellini, A. Bansil: "Ligand-surface interactions and oxidation of colloidal PbSe quantum dots by thin-film positron annihilation methods," *Applied Physics Letters* **108**, 081602 (2016).
15. A. Bansil, Hsin Lin and Tanmoy Das: "Colloquium: Topological Band Theory," *Reviews of Modern Physics* **88**, 021004 (2016).

Revealing Quantum Impurity Critical States via the Environment

PI: Harold U. Baranger, Dept. of Physics, Duke University; baranger@phy.duke.edu

Keywords: quantum phase transition, quantum noise, quantum transport, non-equilibrium steady state, nanoscale

Project Scope

Quantum fluctuations and coherence are key distinguishing ingredients in quantum matter. Two phenomena to which they give rise are *quantum phase transitions* and *quantum noise*, the ubiquitous quantum fluctuations in the environment of any system. It is natural to suppose that decoherence produced by the quantum noise will suppress quantum effects, and in particular inhibit or destroy a quantum critical state. In this project, my primary goal is to show how connecting an electronic quantum impurity system to an environment can produce or enhance quantum critical states, and then to study the equilibrium and non-equilibrium properties of these remarkable systems. In some cases, the environment can be viewed as emulating interactions in the electronic system; in others, it acts to suppress effects that then allow the critical state to be observed. The models studied are directly relevant to nanoscale systems that can be studied experimentally via quantum transport. Steady-state non-equilibrium properties are a key focus of the project as the nonlinear I-V curve is readily measured.

Recent Progress

Rescuing a Quantum Phase Transition with Quantum Noise

We have discovered and analyzed a striking counter-example to the notion that noise necessarily harms quantum many-body effects: in the system we study, the addition of (equilibrium) quantum noise stabilizes a non-Fermi-liquid quantum critical state. The team consists of the PI, graduate student Gu Zhang, and collaborator Eduardo Novais (Brazil).

We consider the phase diagram of two quantum dots connected to two leads in the presence of environmental noise (Fig. 1). The noiseless model has a quantum phase transition that is transformed into a crossover by charge transport across the double dot. We show that quantum fluctuations of the source and drain voltage counteract this charge transport. The competition between these two processes results in a more coherent system, as in “quantum frustration of decoherence” for a qubit but here for a many-body system. The result is that the quantum phase transition is rescued from the undesired crossover for *any* strength of the noise.

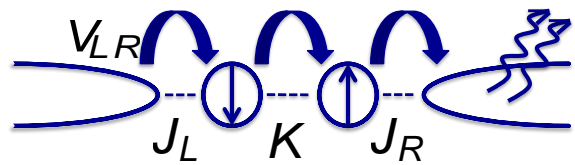


Fig. 1. Schematic of the system: two quantum dots coupled to left and right leads. $J_{L,R}$ and K are the Kondo and exchange coupling strengths, respectively. V_{LR} is the strength of the direct charge transport between the leads. Dissipative modes in the leads are represented by wiggly arrows.

In our double quantum dot setup (Fig.1), the leads are resistive, thereby coupling the electrons to an ohmic EM environment. Experimentally, the ingredients for a study are available: double dots have been made in several materials, and environmental effects on a single quantum dot have been studied in detail [1]. In the absence of noise, the system is modeled by a two-impurity Kondo (2IK) model that arises from a single-level Anderson model. In 2IK, there is a quantum phase transition (QPT), at a critical value of the exchange K_c , between a local singlet phase (LSFP, spins in the dots are locked) and a Kondo phase (KFP, singlet between each dot and its lead). When charge transfer between the two leads is introduced, the system flows to a crossover, rendering the 2IK QPT invisible.

The EM environment (the noise) is treated as a bosonic field coupled to the lead charge and phase operators. Tunneling from one lead to another excites the environment via a charge-shift operator that depends on the lead resistance, $r=Re^2/h$. Only terms involving inter-lead charge transfer excite the environment; terms in which net charge flow is absent are unaffected.

The key to obtaining our results is a detailed analysis via bosonization at the quantum critical point, closely following known results in the noiseless case [2]. We arrive at the following scenario: (i) For $r=0$, the noiseless case, there is a line of Fermi-liquid fixed points between the LSFP and KFP. (ii) For $0 < r < 1/2$, the line of Fermi-liquid fixed points is unstable; a new intermediate fixed point emerges, denoted IFP₂. (iii) For $r > 1/2$, IFP₂ becomes unstable, while the flow is into the fixed point that evolves from the 2IK QPT, IFP₁. The scaling dimension of operators around the fixed points yields the power-law dependence of the conductance shown in Fig 2.

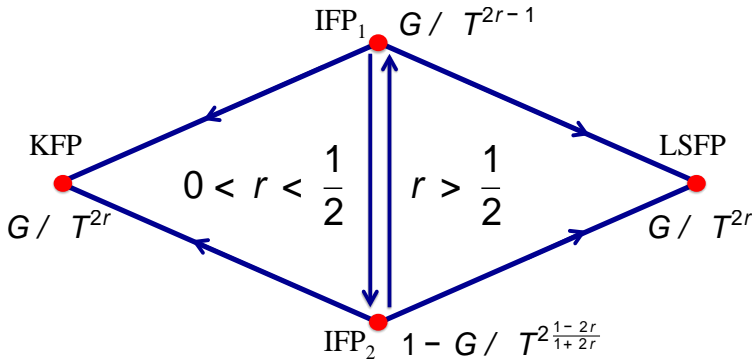


Fig. 2. **Stability diagram** for different noise strengths r , and the temperature dependence of the conductance at each fixed point. The KFP and LSFP are stable for any non-zero r , while the nature of the IFP changes as a function of r . For $r < 1/2$, the intermediate state is controlled by IFP₂—the fixed point that evolves from one of the $r=0$ Fermi-liquid fixed points. In contrast, for $r > 1/2$, IFP₁—which evolves from the two-impurity-Kondo IFP—is relevant. For $r=1/2$ a line of fixed points connects IFP₁ to IFP₂.

Nonlinear I-V Curve at a Quantum Impurity Quantum Critical Point

Non-equilibrium phenomena in quantum many-body systems reveal novel aspects of the interacting states involved, motivating study of non-equilibrium effects near quantum phase transitions. A key non-equilibrium phenomenon that is naturally measured in experiments is the steady-state charge transport through the system—the nonlinear I-V curve.

We have carried out an analytical calculation of the full nonlinear I-V curve at a QCP. (Team: PI, G. Zhang (grad student), collaborator C.-H. Chung (Taiwan) and his student.) The system is a

quantum dot coupled to resistive leads—a spinless resonant level coupled to an ohmic EM environment in which a QCP similar to the two-channel Kondo QCP occurs. Recent experiments [1] studied this criticality via transport measurements: the conductance approaches unity when tuned to the QCP (on resonance and symmetric barriers) and approaches zero in all other cases.

To obtain the current at arbitrary temperature and bias, we write the problem as a 1d field theory and scale from electrons in the left/right leads to right-going and left-going channels between which there is weak two-body backscattering.

This is done via bosonization at weak-coupling, a duality transformation to the strong-coupling QCP, and repermionization into new effective modes. These new modes couple to an environment: a backscattering event excites the environment via a shift operator.

The deviation of the current from an ideal conductor can be treated in perturbation theory in the weak backscattering. Indeed, this is exactly the situation treated by dynamical Coulomb blockade theory—perturbative in the tunneling but to all orders in the coupling to the (effective) environment. Drawing on those results, we obtain an explicit expression for the full nonlinear I-V curve. Fig. 3 shows the comparison with the experimental result in a scaling plot. The agreement is remarkable.

Future Plans

Non-Equilibrium Effects at Quantum Critical Points

Opening a quantum impurity system to an environment produces new quantum critical states that involve complex entanglement among the interacting electronic and bosonic degrees of freedom. Such “open quantum-many-body systems” occur naturally in making nanoscale devices, as well as in a variety of novel materials physics contexts. In nanophysics, such quantum critical states can be studied experimentally with exquisite control via quantum transport measurements in both equilibrium and (steady-state) non-equilibrium.

We are extending our study of open-system quantum critical points to more complex states produced by nanosystems with more structure, i.e. more quantum dots, reservoirs, or internal degrees of freedom such as spin or valley. Currently, we have obtained the weak-coupling RG

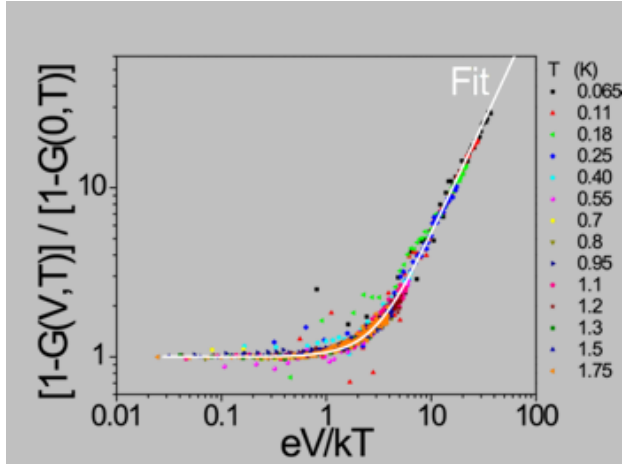


Fig. 3. **I-V curve, theory & experiment:** Normalized I-V curve on log-log scale, $[1-G(V,T)]/[1-G(0,T)]$ with $G(V,T)=dI/dV$ the non-equilibrium differential conductance. The resistance of the dissipative leads is $r=0.5$. The white curve is our calculation with no free parameters. The unpublished data is from C.-T. Ke, et al. [G. Finkelstein group].

equations for a number of these situations, and are generalizing them to non-equilibrium situations through the frequency dependent RG techniques.

Quantum Hall & Superconductivity in Graphene

I plan to pursue a new way to produce interesting quantum states that can be probed with quantum transport in both equilibrium and highly non-equilibrium situations. The system involves combining quantum Hall effect (QHE) edge states with superconductivity. Because QHE occurs at relatively low magnetic field in graphene ($\sim 1\text{ T}$), it can be combined with superconductors. Several experimental groups worldwide are actively pursuing this system; there has recently been, for instance, an experiment observing supercurrent [3].

This is an excellent system on which to build future studies of interesting quantum states and non-equilibrium effects. Because the 2DEG in graphene has structure—valley and sublattice degrees of freedom—the interaction with the superconductor has non-trivial effects. Non-equilibrium situations in which electrons are injected via the edge channels, as in the “electron quantum optics” experiments in regular 2DEG, would be particularly interesting. The interplay between the superconductor and graphene would allow manipulation of the internal graphene degrees of freedom, and the presence of the superconductor would itself produce entirely new edge-channel effects. Using fractional QHE edge states, novel quasi-particles, such as parafermions, may provide a useful low-energy description. The response of these in non-equilibrium situations could be probed in this system.

References

1. H. T. Mebrahtu, I. V. Borzenets, H. Zheng, Y. V. Bomze, A. I. Smirnov, S. Florens, H. U. Baranger, G. Finkelstein, *Observation of Majorana quantum critical behaviour in a resonant level coupled to a dissipative environment*, Nat. Phys. **9**, 732-737 (2013).
2. J. Gan, *Solution of the two-impurity Kondo model: Critical point, Fermi-liquid phase, and crossover*, Phys. Rev. B **51**, 8287-8309 (1995); J. Malecki, E. Sela, I. Affleck, *Prospect for observing the quantum critical point in double quantum dot systems*, Phys. Rev. B **82**, 205327 (2010).
3. F. Amet, C. T. Ke, I. V. Borzenets, J. Wang, K. Watanabe, T. Taniguchi, R. S. Deacon, M. Yamamoto, Y. Bomze, S. Tarucha, G. Finkelstein, *Supercurrent in the quantum Hall regime*, Science **352**, 966-969 (2016).

Publications (August 2014 – July 2016)

1. S. Bera, A. Nazir, A. W. Chin, H. U. Baranger, and S. Florens, *Generalized Multipolaron Expansion for the Spin-Boson Model: Environmental Entanglement and the Biased Two-State System*, Phys. Rev. B **90**, 075110 (2014).
2. S. Bera, H. U. Baranger, and S. Florens, *Dynamics of a Qubit in a High-Impedance Transmission Line from a Bath Perspective*, Phys. Rev. A **93**, 033847 (2016).
3. Gu Zhang, E. Novais, and H. U. Baranger, *Rescuing a Quantum Phase Transition with Quantum Noise*, submitted to Phys. Rev. Lett. (2016); arXiv:1604.07440.

Quantum phenomena in few-layer group IV monochalcogenides: interplay among structural, thermal, optical, spin, and valley properties in 2D

Principal Investigator: Salvador Barraza-Lopez.

Department of Physics. University of Arkansas, Fayetteville

sbarraza@uark.edu

Keywords: Two-dimensional atomic materials, two-dimensional phase transitions, material properties

Program Scope

The driving concept is the fact that two-dimensional materials with a degenerate structural ground state such as monochalcogenide monolayers are phase-tunable materials that are prone to disorder at finite temperature, as recently described by the PI. The PI will link structural properties of these materials before and after their thermal transition, including the effects of time-independent external fields, to their electronic, spin, valley, and optical behavior. For this purpose, his team can carry out comprehensive computational and theoretical studies to determine the relations among structure, number of layers, time-independent external fields (such as light or other electromagnetic perturbations, strain and/or heat), on the electronic, valley, and spin properties of these materials. This knowledge will dictate the design of new device paradigms based on few-layer monochalcogenides that account for their two-dimensional order/disorder properties. The PI collaborates with Churchill's experimental team at Arkansas in topics related to this program.

Specific projects are: (i) the determination of the 2D order/disorder transition temperature in bulk layered monochalcogenides; (ii) determining the effective electronic/spin/valley properties of disordered monochalcogenide monolayers; (iii) assessing the interplay among a giant piezoelectric response and the Pnma-Cmcm transition in layered monochalcogenides; (iv) investigating the excitonic spectrum of monochalcogenide monolayers; (v) determining the material properties of stacks of monochalcogenides with other 2D materials; (vi) assessing the chemical degradation of few-layer monochalcogenides; (vii) generalizing the discovery of two-dimensional disorder to other puckered two-dimensional materials beyond graphene; and (viii) investigating new paradigm for thermoelectrics by design on layered materials with degenerate ground states.

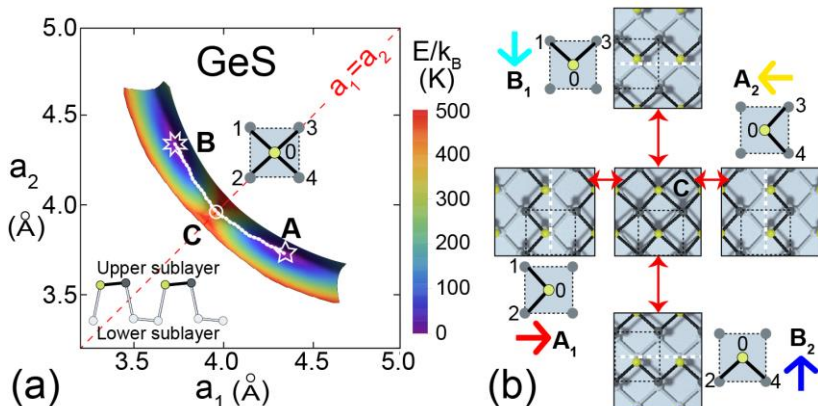


Figure 1. (a) Elastic energy landscape $E(a_1, a_2)$ as a function of lattice parameters for a GeS monolayer at zero temperature. A dashed white curve joins points A and B that label two degenerate minima ($E_A = E_B = 0$). The saddle point C corresponds with a Cmcm atomistic structure in which atom 0 forms bonds to four in-plane neighbors, and the elastic energy barrier is defined by Ec. (b) Atomistic decorations (i.e., the specific pair of atoms bonding atom 0) increase the structural degeneracies. The degenerate ground states A₁, A₂, B₁ and B₂ are assigned in-plane arrows that label them uniquely.

monochalcogenide monolayers; (iii) assessing the interplay among a giant piezoelectric response and the Pnma-Cmcm transition in layered monochalcogenides; (iv) investigating the excitonic spectrum of monochalcogenide monolayers; (v) determining the material properties of stacks of monochalcogenides with other 2D materials; (vi) assessing the chemical degradation of few-layer monochalcogenides; (vii) generalizing the discovery of two-dimensional disorder to other puckered two-dimensional materials beyond graphene; and (viii) investigating new paradigm for thermoelectrics by design on layered materials with degenerate ground states.

Prior Research

Four-fold degenerate structural ground-state and structural phase transitions. The PI outlined an atomistic mechanism leading to this transition that applies to monolayers of materials with a layered *Pnma* structure, including SnSe (42) that transition onto a *square* phase. 2D materials with orthorhombic unit cells have an initial structural degeneracy in their ground state upon exchange of in-plane lattice vectors. Such exchange is illustrated for a GeS monolayer by the elastic distortion that initiates at point A ($a_1 > a_2$) and ends at point B ($a_2 > a_1$) along the white line on the elastic energy landscape in Figure 1(a) (43). Points A and B are the initial and final degenerate minima in this elastic process.

The saddle (thus unstable) point with ($a_1 = a_2$), labeled by the letter C on the energy landscape, determines the (elastic) energy cost E_C required to exchange the in-plane lattice vectors. E_C has a value of 460 K for GeS (Figure 1(a)).

Now, as seen in Figure 2, E_C decays exponentially as a function of the mean atomic number:

$$\bar{Z} = \frac{1}{4} \sum_{i=1}^4 Z_i$$

with Z_i the atomic number of atom i on a monolayer unit cell that contains four atoms. E_C is equal to 300 K for GeSe monolayers, and about 100 K for SnSe monolayers. In general, layered orthorhombic monochalcogenides with average atomic numbers larger than 30 (red vertical line in Figure 1) have values of E_C that are smaller than room temperature. In going from SnS to SnTe, the two minima seen at $a_1 > a_2$ and $a_2 > a_1$ collapse onto a single minima at point C where $a_1 = a_2$, and E_C goes all the way down to 0K accordingly. This is so because ultra-thin monochalcogenides with a rock-salt structure (SnTe, PbS, PbSe, PbTe) have a non-degenerate ground state with $a_1 = a_2$ and hence a zero barrier. Black phosphorus has the largest values of a_1/a_2 and E_C and it is listed for comparison purposes. Figure 2 has consequences for the stability of black arsenic (atomic number 33) at room temperature as well.

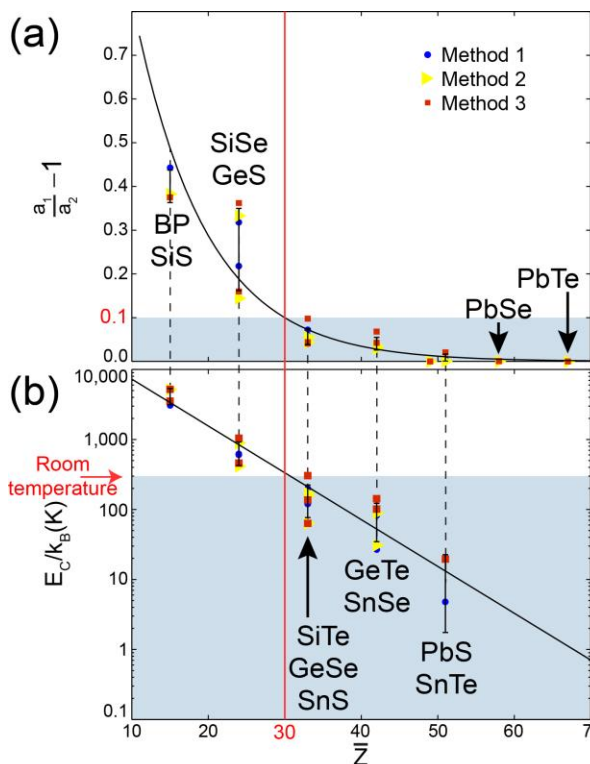


Figure 2. (a) Ratio among lattice parameters and (b) magnitude of E_C as a function of the average atomic number for BP and many monochalcogenides.

An additional source of structural degeneracy originates from the atomic arrangement of the four basis atoms, also known as the decoration of the unit cell. The ridges so characteristic of these orthorhombic layered structures can have two dispositions related by a reflection with respect to the axes shown by white dashed lines on the atomistic models in Figure 1(b). Considering axis exchanges and reflections, there are four degenerate structural ground states that are labeled A_1 , A_2 , B_1 and B_2 and assigned in-plane arrows (\rightarrow corresponding to A_1 , \leftarrow to A_2 , \downarrow to B_1 , and \uparrow to B_2) that mimic the local decoration of the ridges in Figure 1(b).

It is a well-known fact that degeneracies of the ground state lead to the disorder at finite temperature, but this realization may be a first within the field of two-dimensional atomic crystals (44), and the degeneracies of the structural ground state (Figure 1) and the elastic energy barrier E_c required to switch among these states (Figure 2) is all that is needed to describe the disordered phase. This basic theory applies to monolayers of these compounds, and it will be laid out in two gradual steps next.

The first step, provided by snapshots of room-temperature Car-Parrinello molecular dynamics in Figure 3, validates the hypothesis that monolayer structures with an average atomic number larger than 30 are disordered at room temperature, and shows that the atomistic process triggering disorder is the switching mechanism indicated in Figure 1(b). Indeed, monolayers having $E_c > 300$ K undergo “arrow flips” where unit cells originally with a A_1 (\rightarrow) pattern acquire an A_2 , B_1 , or a B_2 decoration (\leftarrow , \downarrow , or \uparrow) at the onset of disorder.

A GeS monolayer has a mean atomic number of 24 and $E_c=460$ K (Figures 1 and 2). In Figure 3 GeS is verified to be ordered at room temperature, because most unit cells have an A_1 decoration; there is only a single flip onto a B_1 structure (\rightarrow to \downarrow) due to thermal fluctuations that is highlighted by a blue oval at the upper left corner of the figure. SnS and SnSe monoayers, on the other hand, have values of E_c close to 100K and become disordered at room temperature by recommitting

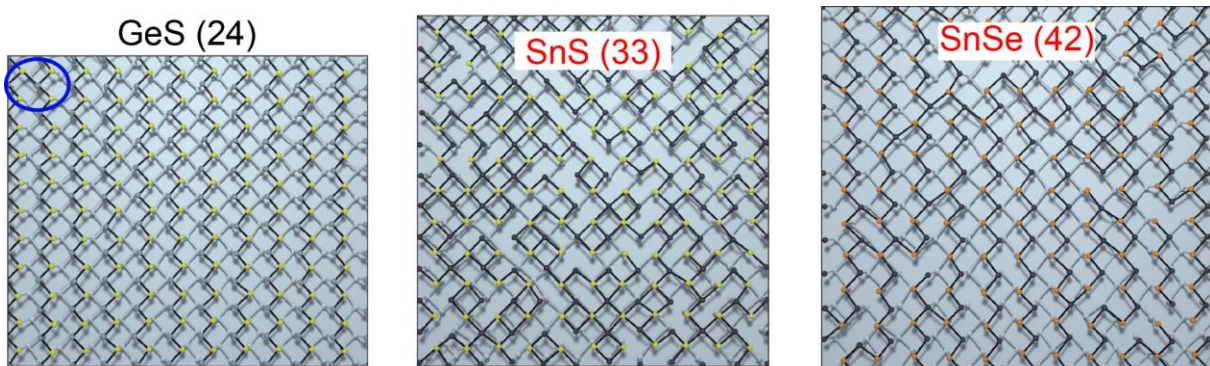


Figure 3. Car-Parrinello atomistic structure of GeS, SnS, and SnSe monolayers at room temperature and at 1 ns (equivalent to 1,000 molecular dynamics steps). The structures marked in red are disordered, in the sense given by Fig 4b. The average atomic number is shown in parenthesis.

atoms in the form indicated on Figure 2b. The second step alluded to in previous page proceeds as follows: the labeling of the four degenerate structural states with in-plane arrows in Figure 1 was established to map the observed energetics to a planar (clock) Potts model with $q=4$ and coupling strength E_c . This perfect mapping is demonstrated by the evolution of the total energy in Car-Parrinello molecular dynamics calculations with respect to temperature, because sharp changes on the total energy are unmistakable indicators of phase transitions.

The configurational energy from Car-Parrinello runs for GeS and GeSe is represented by dots, squares, and triangles on Figure 4(a) at various temperatures and supercell sizes, and it displays an abrupt increase at around E_c/k_B , as confirmed by a finite-difference “derivative” having a sharp peak at a temperature close to E_c at the lower subplot on Figure 4(a).

The *ab initio* energetics are indeed fully reproduced by the planar Potts model having E_c as its only fitting parameter. The dynamical behavior is characterized by an in-plane “spin” pointing along a specific in-plane direction (\rightarrow , \leftarrow , \downarrow , or \uparrow) per unit cell, with “next-unit-cell” coupling:

$$\hat{H} = -E_C \sum_{\langle i,j \rangle} \cos(\theta_i - \theta_j)$$

In previous equation, θ_i takes any of the four ($q=4$) values 0 (\rightarrow), $\pi/2$ (\uparrow), π (\leftarrow), or $3\pi/2$ (\downarrow). This model favors the “ferromagnetic” coupling among neighboring unit cells and assigns the largest energy penalty to neighboring unit cells displaying an “antiferromagnetic” coupling. This feature of the model is consistent with the number of individual atomic bonds being altered in these “flip” events. When used as an input of a Monte Carlo solver, the dynamics from previous equation yields the configurational energy per unit cell shown by the red lines in Figure 4(a), that reproduces the energetics of Car-Parrinello molecular dynamics up to $T \sim 1.5 E_C$ entirely. There is a transition from this disordered phase onto a gas at about $T \sim 1.8 E_C$ that is highlighted by the vertical black arrow in Figure 4(a) and is not relevant for solid-state device applications. For this reason, the Potts model does not describe that second transition.

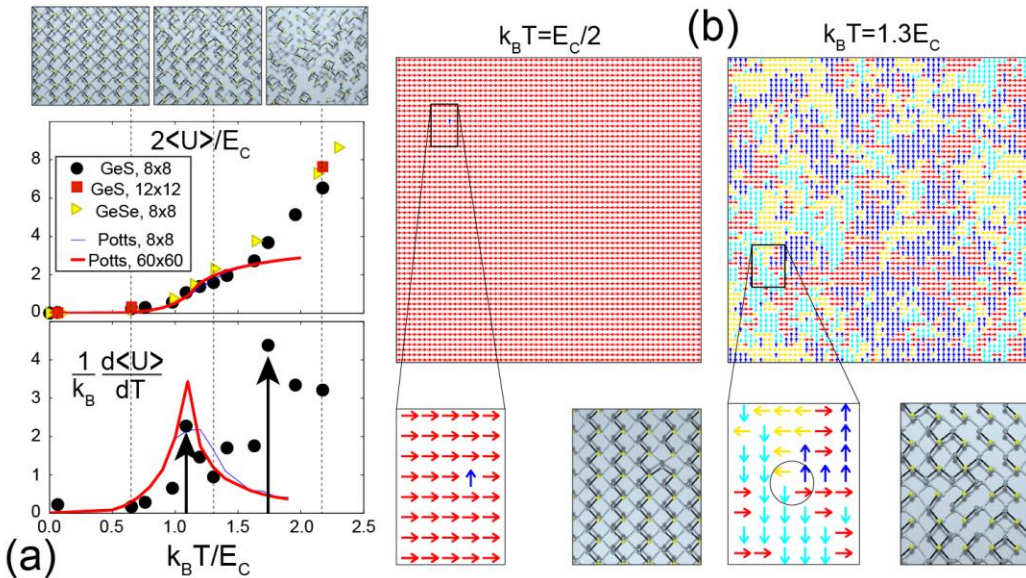


Figure 4. (a) Monochalcogenide monolayers become disordered at a critical temperature $T_c = 1.1 E_C / k_B$ (k_B is Boltzmann constant). This prediction can be experimentally demonstrated by sharp peaks on the specific heat. The second peak, at about $1.75 E_C / k_B$ is at the onset of a transition onto a gas phase. (b) The Potts model maps the microscopic phenomena into an effective system in which the transition to 2D disorder can be formally studied.

As shown on Figure 4(b), the Potts model can be employed to map the disordered 2D structure right after the order/disorder transition at larger spatial scales, in order to determine domain size and vortex creation. The phase transition onto a disordered phase is thus firmly established for monolayers now.

This result provides a new atomistic insight into the onset of such displacive transition, namely that **the anharmonicity of the Sn environment (4) in these layered materials arises from a degenerate structural ground state (53)**. Monochalcogenides with a rocksalt structure lack degeneracies on their ground state and the picture here developed does not apply to them.

Future Plans

Transition temperature in bulk layered monochalcogenides: Monochalcogenide monolayers undergo a two-dimensional order/disorder transition, and the question is whether coupling among

layers can help raise or otherwise tune the transition temperature with respect to its value in isolated monolayers.

To answer this question, Car-Parrinello molecular dynamics (MD) calculations with fixed number of particles, pressure, and temperature (NPT) will be carried out at increasing temperatures and at atmospheric pressure on 8x8x2 supercells that contain about 600 atoms and have dimensions close to (25 Å)³ for GeSe. Additional calculations will be carried out for bulk SnSe, given the great interest commanded by this layered monochalcogenide for thermoelectrics, and in order to establish the generality of the theoretical trend to arbitrary group-IV monochalcogenides in the bulk. These calculations will be carried out with the SIESTA density functional theory code using standard basis sets and a set of highly-accurate pseudopotentials deployed by the PI.

Effective electronic/spin/valley properties of disordered monochalcogenide monolayers: The prediction of valleytronics with spin-polarized valleys on this material platform relies on monolayers with a *Pnma* structure that lack inversion symmetry. The ensuing discussion indicates that, out of GeS, GeSe, SnS, and SnSe, only GeS has an ordered *Pnma* structure at temperatures up to 460 K. This prompts the following two questions:

What is the electronic structure of these monolayers as a function of temperature, especially while crossing the 2D order/disorder transition? This question can be addressed experimentally with ARPES measurements, and the PI will provide band structures by means of the well-known zone-folding method.

What is the interplay of uniaxial strain, piezoelectricity and electronic/valley/spin behavior at the onset of disorder on monochalcogenide monolayers? Can this interplay lead to novel device functionalities? Strain is a very important handle to tune the properties of two-dimensional crystals. The relation among uniaxial strain, disorder, and the electronic and valley properties of monochalcogenide monolayers will be elucidated with the specific goal of designing device paradigms that are based on the indirect optical transitions in the crystalline phase, and on the direct transitions and additional number of momentum pockets in the disordered 2D phase. In Sn-based monolayers, spin-orbit coupling could also be relevant as it leads to a spin splitting at the bottom of the conduction band. Using the zone-folding method, the PI will determine whether disorder at finite temperature can degrade this spin-polarization at individual valleys.

Once the effect of structural disorder in the absence of external fields is understood, we will explore the effect of transverse electrostatic fields (field effect) on the materials properties.

Excitonic spectrum of monochalcogenide monolayers: Electron-hole pairs in two-dimensional materials are one class of excitons that arise due to the strong Coulomb interaction that originates due to the reduced dimensionality. Such excitons are generated optically. Black phosphorus is a monoatomic layered material with a *Pnma* structure similar to that of layered monochalcogenides. Black phosphorus monolayers sustain a very anisotropic excitonic response that can be experimentally observed through photoluminescence. The anisotropy of this response can be used to quickly determine the two axes of symmetry.

Two-dimensional disorder in other puckered two-dimensional materials: This proposal is about the consequences of two-dimensional disorder on the properties of few-layer monochalcogenides, and it is appropriate to end this document with a project that shows the generality of the concepts introduced thus far to arbitrary 2D materials with structural degeneracies in their ground state.

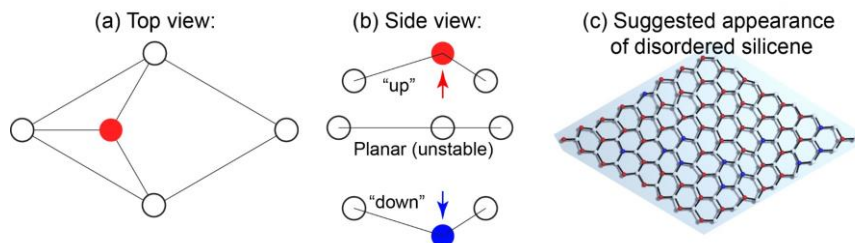


Figure 5. All 2D materials with a degenerate ground state will be prone to disorder at finite temperature; this will be the case for silicene, germanene, and low-buckled stanene. (a) Top and (b) side views of the unit cell; the side view highlights the two-fold structural degeneracy and the planar structure which is necessary to determine E_c . (c) Artistic view of disordered silicene.

given by the energy difference among the low-buckled and the planar phenomena can be modeled by an Ising-type interaction with interaction strength E_c . As far as the PI knows, nobody else has realized this propensity towards disorder on 2D materials with structural degeneracies, nor their potential use in thermoelectric materials.

Publications

A list of selected publications follows below.

Two-dimensional disorder in black phosphorus and monochalcogenide monolayers. M. Mehboudi, A.M. Dorio, W. Zhu, A. van der Zande, H.O.H. Churchill, A.A. Pacheco-Sanjuan, E.O. Harriss, P. Kumar, and S. Barraza-Lopez. *Nano Lett.* **16**, 1704 (2016).

Strain-tunable topological quantum phase transition in buckled honeycomb lattices. J.-A. Yan, M. A. Dela Cruz, S. Barraza-Lopez, and L. Yang. *Appl. Phys. Lett.* **106**, 183107 (2015).

Systematic pseudopotentials from reference eigenvalue sets for DFT calculations. P. Rivero, V. M. Garcia-Suarez, D. Pereniguez, K. Utt, Y. Yang, L. Bellaiche, K. Park, J. Ferrer, and S. Barraza-Lopez. *Comp. Mat. Sci.* **98**, 372 (2015).

Stability and properties of high-buckled two-dimensional tin and lead. P. Rivero, V. M. Garcia-Suarez, J.-A. Yan, J. Ferrer, and S. Barraza-Lopez. *Phys. Rev. B* **90**, 241408(R) (2014).

Structural phase transition and material properties of few-layer monochalcogenides. M. Mehboudi, B. M. Fregoso, Y. Yang, W. Zhu, A. van der Zande, J. Ferrer, L. Bellaiche, P. Kumar, and S. Barraza-Lopez. arXiv:1603.03748 (submitted on 1/18/2016).

For example, two-dimensional materials such as silicene, germanene, and stanene have a two-fold degenerate ground state that arises by whether an atom on the B-sublattice protrudes “up” (\uparrow) or “down” (\downarrow) with respect to the three nearest neighbors belonging to the A-sublattice, and the energy barrier E_c is

``Properties of multiferroic nanostructures from first principles''

Laurent Bellaiche

Keywords: Multiferroics; magnetism, electric field

Project Scope

Multiferroics are materials that can simultaneously possess ferroelectricity (that is, a spontaneous electrical polarization that can be switched by applying an electric field) and magnetic ordering. Such class of compounds exhibits a magnetoelectric coupling that is of high technological relevance, since it implies that electrical properties are affected by a magnetic field or, conversely, that magnetic properties can be varied by an electric field.

The broad objectives of this proposal are to gain a deep understanding of multiferroics, in general, and to reveal original, exciting phenomena in low-dimensional multiferroics, in particular.

To achieve these objectives, several research projects on multiferroic nanostructures have been conducted (and are currently conducted) by developing and/or using state-of-the-art techniques from first principles. Collaborations with internationally-recognized groups, having vital experimental programs in multiferroics are further strengthened, which allow us to ground our simulations and to fully, deeply understand the complex materials under investigation.

Recent Progress

We discovered several novel phenomena (see list of publications). In particular, we will report here some works about $(\text{Bi},\text{R})\text{FeO}_3$ materials [1,2], with R being a rare-earth ion and for which an original first-principle-based effective Hamiltonian was developed. Such development led to the discoveries of (1) novel complex states (that we identified as nanotwins) in some compositional range of disordered $(\text{Bi},\text{R})\text{FeO}_3$ solid solutions; and (2) a five-state path resulting in the switching of polarization and magnetization under an electric field in (hybrid improper ferroelectric) $\text{BiFeO}_3/\text{NdFeO}_3$ superlattices.

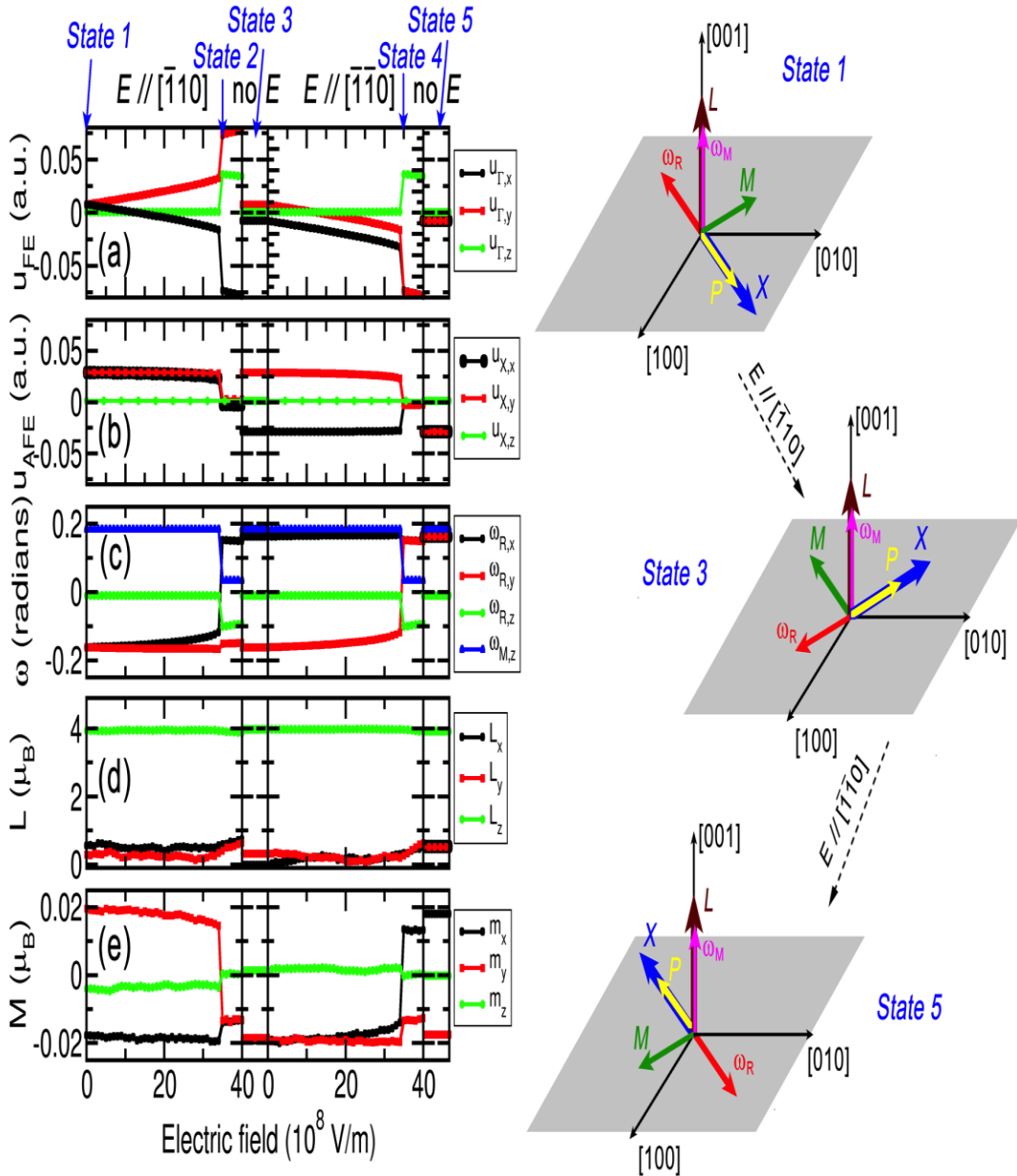


Figure captions: The five-state switching mechanism for $(\text{BiFeO}_3)_1/(\text{NdFeO}_3)_1$ superlattice. a,b) The local modes (upper panel: u_{Γ} ; lower panel: u_x characterizing ferroelectricity and antiferroelectricity, respectively); c) oxygen octahedra tilting vectors (ω_R and ω_M characterizing anti-phase and in-phase tiltings, respectively); d) the AFM vector; and e) the weak FM vector under a sequence of applied electric fields, i.e., 1) an increasing field along the $[110]$ direction (perpendicular to the initial polarization); 2) field removed; 3) an increasing field along the $[110]$ direction (antiparallel to the initial polarization); 4) field removed. The insets show schematics of the five-state switching mechanism.

Future Plans

We will continue to investigate properties of multiferroics and related materials. Examples of ongoing and future studies are as follows:

- Understanding the appearance of an improper electrical polarization in nominally-paraelectric ABO_3 perovskites that exhibit magnetic orderings at both the A and B sublattices.
- Design of novel multiferroics from defect-engineering.
- Joint theoretical and experimental collaboration on ultrafast switching of electrical polarization in multiferroic thin films.
- Joint theoretical and experimental collaboration on the combined effect of uniaxial stress and electric field on properties of multiferroic thin films.
- Simulation of the frequency-dependent complex dielectric and magnetic susceptibilities in multiferroic nanostructures, in the search for the so-called electromagnons.
- Discovery of multiferroic solid solutions having large energy storage density.
- Investigating rare-earth garnets.

References

1. ``Finite-temperature Properties of Rare-Earth-Substituted BiFeO_3 Multiferroic Solid Solutions," Bin Xu, Dawei Wang, Jorge Iniguez and L. Bellaiche, Advanced Functional Materials 25, 552 (2015).
2. ``Hybrid Improper Ferroelectricity in multiferroic superlattices: Finite-temperature Properties and Electric-field-driven Switching of Polarization and Magnetization," Bin Xu, Dawei Wang, Hong Jian Zhao, Jorge Iniguez, Xiang Ming Chen and Laurent Bellaiche, Advanced Functional Materials 25, 3626 (2015).

Publications (10 most relevant)

1. "Creating multiferroics with large tunable electrical polarization from paraelectric rare-earth orthoferrites," Hong Jian Zhao, Yurong Yang, Wei Ren, Ai-Jie Mao, Xiang Ming Chen, and Laurent Bellaiche, *J. Phys.: Cond. Mat.* 26, 472201 (2014).
2. "Structural, magnetic, and electronic properties of GdTiO_3 Mott insulator thin films grown by pulsed laser deposition," M. N. Grisolia, F. Y. Bruno, D. Sando, H. J. Zhao, E. Jacquet, X. M. Chen, L. Bellaiche, A. Barthelemy and M. Bibes, *Applied Physics Letters* 105, 172402 (2014).
3. "Finite-temperature Properties of Rare-Earth-Substituted BiFeO_3 Multiferroic Solid Solutions," Bin Xu, Dawei Wang, Jorge Iniguez and L. Bellaiche, *Advanced Functional Materials* 25, 552 (2015).
4. "Prediction of a Stable Post-Post-Perovskite Structure from First Principles," Changsong Xu, Bin Xu, Yurong Yang, Huafeng Dong, A. R. Oganov, Shanying Wang, Wenhui Duan, Binglin Gu, and L. Bellaiche, *Phys. Rev. B* 91, 020101(R) (2015).
5. "Predicting a Ferrimagnetic phase of $\text{Zn}_2\text{FeOsO}_6$ with Strong Magnetoelectric Coupling," P. S. Wang, W. Ren, L. Bellaiche, and H. J. Xiang, *Phys. Rev. Lett.* 114, 147204 (2015).
6. "Electronic properties of electrical vortices in ferroelectric nanocomposites from large-scale ab-initio computations," Z. Gui, L.-W. Wang and L. Bellaiche, *Nano Letters* 15, 3224 (2015).
7. "Hybrid Improper Ferroelectricity in multiferroic superlattices: Finite-temperature Properties and Electric-field-driven Switching of Polarization and Magnetization," Bin Xu, Dawei Wang, Hong Jian Zhao, Jorge Iniguez, Xiang Ming Chen and Laurent Bellaiche, *Advanced Functional Materials* 25, 3626 (2015).
8. "Relativistic interaction Hamiltonian coupling the angular momentum of light and the electron spin," R. Mondal, M. Berritta, C. Paillard, S. Singh, B. Dkhil, P. M. Oppeneer and L. Bellaiche, *Phys. Rev. B* 92, 100402(R) (2015).
9. "Magnetoelectric effects via pentagonal interactions," Hong Jian Zhao, M. N. Grisolia, Yurong Yang, Jorge Iniguez, M. Bibes, Xiang Ming Chen, and L. Bellaiche, *Physical Review B* 92, 235133 (2015).
10. "A multiferroic on the brink: Uncovering the nuances of strain-induced transitions in BiFeO_3 ," D. Sando, Bin Xu, L. Bellaiche, and V. Nagarajan, *Applied Physics Reviews* 3, 011106 (2016) (Invited Review).

Theoretical Investigations of Nano and Bio Structures

J. Bernholc (PI)

**Department of Physics, North Carolina State University
Raleigh, NC 27695-7518, bernholc@ncsu.edu**

Keywords: nanoscale electronics, molecular sensors, non-equilibrium quantum transport

Project Scope

This proposal addresses fundamental issues in nanoscale science and technology, namely the design of nanostructured materials and devices with desired, novel characteristics. The research projects will focus on nanoscale materials and devices for the beyond Moore's law era, and electrical detection of DNA sequences. These projects build on the work accomplished during the prior proposal periods, which included investigations of (i) detection mechanisms of carbon-nanotube-based molecular sensors; (ii) monitoring of DNA replication with a nanocircuit, and (iii) major performance and capability improvements in the real space multigrid methodology. Our newly developed capabilities enable multi-petaflop electronic structure calculations, the ability to include over ten thousand atoms in multi-terminal non-equilibrium Green's function simulations of realistic device structures, and a new diagonalization method that speeds up this key bottleneck by almost an order of magnitude.

Recent Progress

Nanoscale electronics beyond Moore's law era

The current silicon-based semiconductor technology is facing a limit at about 5 nm feature size. Current leakage, already a problem in current devices, prevents strict Moore's scaling and results in much increased energy use. Indeed, information technology is estimated to already consume 5-10% of world's electricity. Future energy and computational trends call for nanoscale electronics based on nearly atomic-scale features, operating at much lower voltages. Graphene nanoribbons (GNR) are very promising building blocks for future nanoscale devices, due to their very high mobilities, simple 2D wire-like structure and the potential for high quality growth. However, we have previously shown that nearly perfect edges are essential for maintaining the electronic properties of nanoribbons. Furthermore, nanoribbon properties change with their widths and edge directions. Since accurate control over GNR's structure is difficult to achieve with top-down fabrication, bottom-up synthesis from well-defined molecular precursors is preferable, because it results in GNRs with exactly defined structures.¹ However, currently synthesized bottom-up GNRs are far too short for electrical measurements, let alone for applications. We pursue an in-depth study of the mechanisms of growth of GNRs in collaboration with the experimental group of An-Ping Li at ORNL. We have identified a low-barrier growth pathway

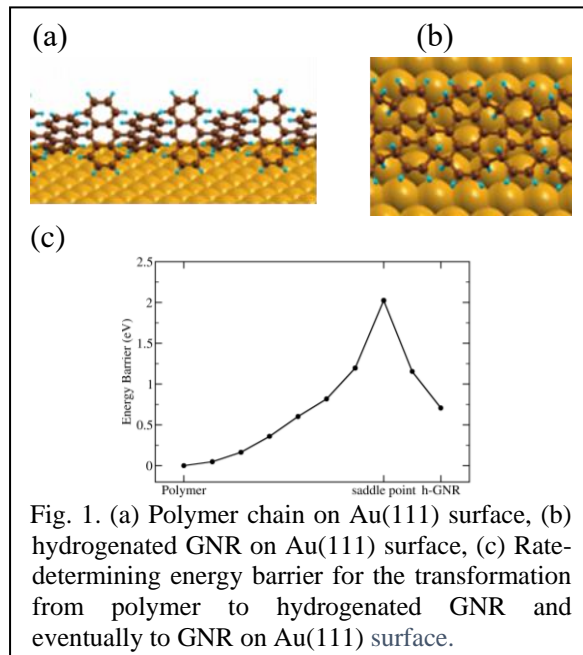


Fig. 1. (a) Polymer chain on Au(111) surface, (b) hydrogenated GNR on Au(111) surface, (c) Rate-determining energy barrier for the transformation from polymer to hydrogenated GNR and eventually to GNR on Au(111) surface.

and showed that the metal substrate is critical in enabling conversion of twisted polymer chains to GNRs at moderate temperatures, in agreement with experimental data. The pathway consists of an electrocyclization step, which transforms the twisted polymer blocks into a planar structure that temporarily forces the C atoms at block boundaries into an sp^3 coordination, followed by dehydrogenation on both sides of the growing ribbon. Once the growth mechanism is established, we can computationally screen different substrates and growth conditions to identify best scenarios for growing long GNRs.

We have also explored potential GNR-based device structures, using our high-accuracy quantum transport code, which self-consistently applies the full non-equilibrium Green's function formalism to calculate electron distribution and ballistic transport with full DFT accuracy. For short channel devices we find that $\text{mod}(n,3)=0$ GNRs with graphene contacts are the most suitable. A calculation of I-V characteristics for a paradigmatic transistor structure is shown in Fig. 2. It involved $\sim 4,500$ atoms in a three-terminal NEGF calculation.

Molecular sensing and DNA sequencing Carbon nanotubes are highly promising for molecular detection and biological sensing, owing to their high chemical and mechanical stabilities, high surface areas and unique electronic properties. We have carried out extensive ab initio studies of the mechanisms of detection of small molecules: ammonia, nitrogen dioxide, glucose and ethylene, and simulations of nano circuits involving a nanotube functionalized with a fragment of polymerase I enzyme. The nano circuit monitors replication of a single-stranded DNA and can potentially be used to sequence DNA by detecting electrical signatures of the adding bases. For ammonia and nitrogen dioxide, for which the detection mechanism is still controversial, we find that only adsorption near the nanotube-metal contact results in a sizable change in current.

As a model of a glucose sensor, we consider the experimentally studied configuration² in which a CNT is non-covalently functionalized with pyrene-1-boronic acid. The calculated transmission of this device before and after glucose attachment in Fig. 3 shows a clear difference between the two cases, confirming that glucose can be detected by this method. An example of a covalently functionalized CNT small molecule detector is the ethylene sensor employing a Cu(I) complex.³ Calculated transmission spectra are shown in Fig. 3. The resulting current change is 85% at 100 mV bias.

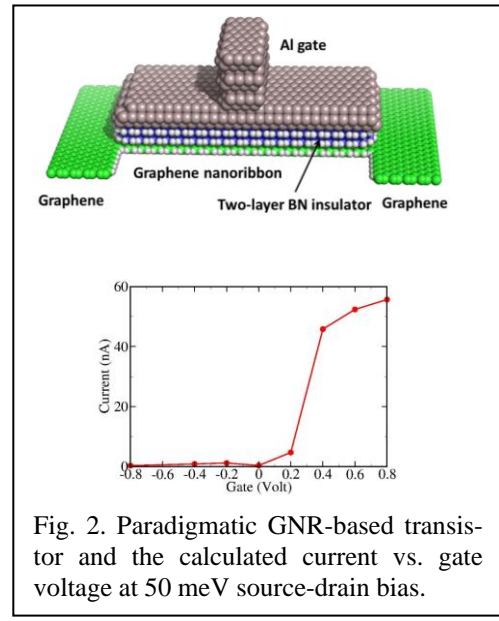


Fig. 2. Paradigmatic GNR-based transistor and the calculated current vs. gate voltage at 50 meV source-drain bias.

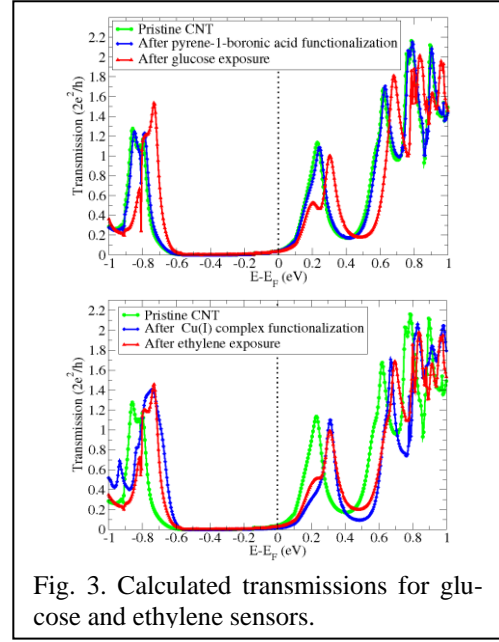


Fig. 3. Calculated transmissions for glucose and ethylene sensors.

Turning to a nanocircuit for monitoring DNA replication, we consider a CNT-Klenow Fragment (KF) nanocircuit, which could potentially be used for fully electrical sequencing of DNA, replacing the cumbersome and expensive fluorescent labeling and electrophoresis procedures.. KF is a member of DNA polymerase I family that performs DNA replication, starting from a single-stranded DNA as a template to assemble the complementary strand. It was recently demonstrated⁴ that the addition of nucleotides during replication can be detected by monitoring the current passing through the CNT. We have initiated collaboration with the experimentalists and performed molecular mechanics simulations of the KF enzyme involving over 100,000 atoms to obtain snapshots of the open and closed states of the enzyme. Equilibrated structures of both open and closed states are then used as inputs to NEGF calculations for ~5,000 atoms. Here, only atoms closer than 2 nm to CNT surface are retained. The positions of the charged residues relative to the CNT surface are shown in Fig. 4. We calculate a substantial current change between the open and closed states of the enzyme, in agreement with experiment. However, the currents at zero bias are similar when different nucleotides are attached, both in experiments and in calculations, which prevents sequencing. Stimulated by experiment,⁵ we have investigated several atomic substitutions in the nucleotides, which replace specific O atoms with either S or Cl. We show that when these substitutions are combined with gate potential scanning (Fig. 4), it should possible to distinguish between G and T, and separate T and G signals from the others. However, additional changes are needed to identify A and C. Our work has attracted the attention of Illumina Inc., the dominant supplier of DNA sequencing equipment in the world, which sponsored an investigation of similar processes using KF on silicon.

Real-space MultiGrid (RMG) electronic structure code We develop and publicly distribute RMG open-source DFT-based code. Designed for highly parallel systems from inception, RMG scales to 200k CPU cores and 20k GPUs, reaching multipetaflops performance (>6.5 PF on ORNL's Cray XK7). It uses real space grids to represent wave functions, charge densities and ionic potentials. Multigrid pre-conditioning accelerates convergence by employing a sequence of grids of varying resolutions, while the finest, highest-resolution grid serves as the physical basis. An extensive default set of pseudopotentials, both norm-conserving and ultrasoft, is built-in.

As an example, in Fig. 5 we compare the performance of RMG v. 2.0 with PWSCF, which is a highly regarded and widely used open-source plane wave code. For 1000 water molecules run on 64-256 Cray XE6 nodes, RMG is substantially

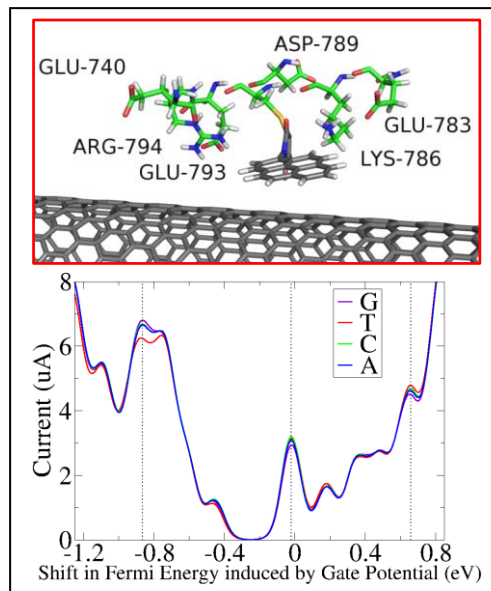


Fig. 4. Part of the Klenow Fragment attached to CNT and calculated current difference for open and closed states of KF with nucleotide substitutions.

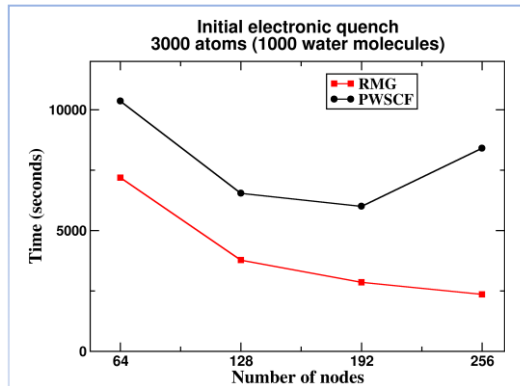


Fig. 5. Scaling comparison between RMG v. 2.0 and PWSCF (Quantum Espresso) for 1000 water molecules run on Cray XE6.

faster and scales dramatically better than PWSCF. We attribute most of the performance difference to different scaling of FFT- and real-space-based algorithms.

When simulating large systems ($>1,000$ atoms), a substantial part of RMG's running time is spent on sub-space diagonalization, which has $O(N^3)$ scaling. To improve its performance, we have developed a new diagonalization method, a partitioned folded spectrum scheme (PFSM), which takes into account the iterative nature of the electronic structure eigenvalue problem and performs well on massively parallel systems. It distributes submatrices among nodes, takes full advantage of GPUs and significantly outperforms the standard SCALAPACK and MAGMA eigensolvers. We should stress that because PFSM performs full diagonalization, metallic systems are treated as easily as those with a gap, and level crossing is not a problem.

RMG version 1.0 was released in November 2014 and v. 2.0 in June 2016. In v. 2.0 the code base was largely rewritten in templated C++ with C++11 threads, which led to a major reduction in the size of the code while improving performance, readability, maintainability, robustness and portability. Since its release, RMG has attracted nearly 1,600 downloads. We observe major spikes in downloads after our conference presentations. We also gave well-attended RMG tutorials at the last two Electronic Structure Workshops. The source code, documentation and binaries for Linux, Windows, Mac OS X, and Cray systems can be downloaded from www.rmgdft.org. We also maintain a wiki, forums, and welcome feature requests. A future release will include non-equilibrium Green's function module for self-consistent calculations of ballistic transport.

Future Plans

We plan to continue research on 2D materials and nano device architectures, first focusing on avenues to grow sufficiently long nanoribbons to allow for device structures with well-determined properties and performance. Other 2D materials will also be explored in addition to graphene. We also plan to incorporate RMG into neutron spectroscopy analysis software at the Spallation Neutron Source, to enable high throughput collection and vibrational analysis of neutron scattering data, with focus on novel, multicomponent materials for hydrogen storage.

RMG is very well suited to many-core and multi-GPU architectures, because of scalability and locality of the real-space multigrid formulation. We plan to adapt to future architectures, including institutional and group-level clusters, as well as pre-exascale and exascale systems. An NEGF module, capable of handling over 10k atoms will also be released.

References

- J. Cai, P. Ruffieux, R. Jaafar, M. Bieri, T. Braun, S. Blankenburg, M. Muoth, A. P. Seitsonen, M. Saleh, X. Feng5, K. Müllen, and R. Fasel, *Atomically precise bottom-up fabrication of graphene nanoribbons*, *Nature* **466**, 470 (2010).
- M. B. Lerner, N. Kybert, R. Mendoza, R. Villechenon, M. A. B. Lopez, and A. C. Johnson, *Scalable, non-invasive glucose sensor based on boronic acid functionalized carbon nanotube transistors* *Appl. Phys. Lett.* **102**, 183113 (2013).
- B. Esser, J. M. Schnorr, and T. M. Swager, *Selective Detection of Ethylene Gas Using Carbon Nanotube-based Devices: Utility in Determination of Fruit Ripeness*, *Angew. Chem. Int. Ed.* **51**, 5752 (2012).
- T. J. Olsen, Y. Choi, P. C. Sims, O. T. Gul, B. L. Corso, C. Dong, W. A. Brown, P. G. Collins, and G. A. Weiss, *Electronic Measurements of Single-Molecule Processing by DNA Polymerase I (Klenow Fragment)*, *J. Am. Chem. Soc.* **135**, 7855 (2013).
- K. M. Pugliese, O. T. Gul, Y. Choi, T. J. Olsen, P. C. Sims, P. G. Collins, and G. A. Weiss, *Processive Incorporation of Deoxynucleoside Triphosphate Analogs by Single-Molecule DNA Polymerase I (Klenow Fragment) Nanocircuits*, *J. Am. Chem. Soc.* **137**, 9587 (2015).

Publications

1. Y. Li, M. Hodak, and J. Bernholc, *Enzymatic Mechanism of Copper-Containing Nitrite Reductase*, ACS Biochemistry, **54**, 1233 (2015),
2. B. Tan, M. Hodak, W. Lu, and J. Bernholc, *Charge Transport in DNA Nanowires*, Phys. Rev. B **92**, 075429 (2015).
3. E. L. Briggs, C. T. Kelley, and J. Bernholc, *Parallel implementation of electronic structure eigensolver using a partitioned folded spectrum method*, <http://arxiv.org/pdf/1502.07806.pdf>.
4. Y. Li, M. Hodak, W. Lu, and J. Bernholc, *Mechanisms of NH₃ and NO₂ detection in carbon-nanotube-based sensors: An ab initio investigation*, Carbon **101**, 177 (2016).
5. Y. Li, M. Hodak, W. Lu, and J. Bernholc, *Selective sensing of ethylene and glucose using carbon-nanotube-based sensors: An ab initio investigation*, submitted (2016).

Geometry, Entanglement and Disorder in Topological Phases

Principal Investigator: Professor Ravindra N. Bhatt, Department of Electrical Engineering, Princeton University, Princeton, NJ 08544 (ravin@princeton.edu).

Co-Principal Investigators: Professor F. Duncan M. Haldane, Department of Physics, Princeton University, Princeton, NJ 08544 (haldane@princeton.edu); Professor Edward H. Rezayi, Department of Physics, California State University, Los Angeles, CA 90032 (erezayi@calstatela.edu); Professor Kun Yang, Department of Physics and NHFML, Florida State University, Tallahassee, FL 32310 (kunyang@magnet.fsu.edu)

Project Scope

Carried out in a synergistic manner, our project aims to provide a detailed understanding of topological phases and phase transitions in two-dimensional electron systems in the fractional quantum Hall (FQH) regime, as well as in related systems. This includes the quantum geometry characterizing the phases, their quantum entanglement properties, and the effect of disorder, invariably present in experiment. We use a variety of numerical techniques in conjunction with fundamental theory to achieve our goals.

Research Accomplishments (7/14 – 7/16)

(I) Geometry of Fractional Quantum Hall States

The geometric “Hall viscosity” property of incompressible FQH fluids was investigated, establishing a relationship between the edge-dipole moment and the momentum polarization of the entanglement spectrum [1], and showing how to determine the “gravitational” or thermal quantum Hall anomaly from the orbital entanglement spectrum. We also studied the geometry of Landau orbits in two-dimensional systems without rotational symmetry [23], using dispersions with quartic terms. A natural metric related to the Hall viscosity tensor and a topological “Landau orbit spin” was identified, exposing the generic properties of Landau orbits hidden in standard Galilean invariant models.

A detailed numerical investigation of the dynamical degree of freedom corresponding to quantum geometry of phases of matter with intrinsic topological order was applied [15] to the $v = 1/3$ Laughlin state using exact diagonalization and DMRG methods. Perturbing the system by a smooth, spatially dependent metric deformation, we find that the response of the quantum Hall fluid is given by the Gaussian curvature of the metric. We apply this probe to experimentally relevant settings, e.g., systems with band mass anisotropy and systems in the presence of an electric field gradient.

We showed [18] that the long-wavelength quadrupolar graviton mode in a FQH liquid predicted earlier by Haldane could be excited using acoustic waves in the crystal (which behave like a gravitational wave). This provides a way to probe this mode experimentally.

(II) Composite Fermi Liquid and Fractional Quantum Hall Phases

Two new DMRG based codes [4,6] were developed and tested, one in collaboration with other groups. A collaborative project using infinite cylinder DMRG provides compelling numerical evidence [17] for the existence of a Fermi sea of composite fermions for realistic interactions at $v = 1/2$. The state is found to be particle-hole symmetric, unlike the Halperin-Lee-Read state, consistent with the proposal that composite fermions are massless Dirac particles, like the surface state of a 3D topological insulator. A numerical test shows the suppression of $2k_F$ backscattering characteristic of Dirac particles.

DMRG was used to study 12/5 and 13/5 FQH states [22], using experimentally realistic parameters (spin, Landau level mixing, finite thickness). It explains the experimental observation that 12/5 is an incompressible liquid, while 13/5 is a reentrant integer QH state. Both states were found to be in close proximity to a liquid-solid transition; Landau-level mixing pushes 13/5 towards the solid phase, hence the absence of the plateau in experiments. The 12/5 state was identified to be the Read-Rezayi parafermion state.

The competition between electron-solid and quantum-liquid phases in higher Landau levels of graphene was studied [19]. Differing Coulomb potential in graphene compared to GaAs affects the competition between solid and liquid phases. The liquid phase is found to dominate in the $n=1$ Landau level, whereas the Wigner crystal and electron-bubble phases become more prominent in the $n=2$ and $n=3$ graphene Landau levels.

A new formalism [14] was developed to construct quantum Hall many-body parent Hamiltonians in geometries beyond disk and sphere, which straightforwardly generalizes to the multicomponent SU(n) cases with a combination of spin or pseudospin (layer, sub-band, or valley) degrees of freedom. The approach allows determination of previously unknown parent Hamiltonians of e.g. non-Abelian multicomponent states. Results were verified by numerically computing entanglement properties.

Bilayer QH Systems: Using a two-component pseudopotential applicable to bilayers cold atom systems with dipolar interactions, we performed an exact diagonalization study [3] and showed that one can obtain both strong and weak d-wave paired quantum Hall states, with the Haldane-Rezayi state as the critical point separating them. Three projects on bilayer QH systems were completed with collaborators. Two comprehensive studies [12,13] explored bilayer systems with total filling $v = 2/3$, especially competing Abelian and non-Abelian topological orders, and studied the effect of various two-body interlayer couplings. For dominant interlayer hollow-core interaction, a non-Abelian bilayer Fibonacci state was found. The third [16] was a quantitative study of the phase diagram of the bilayer bosonic FQH system on the torus geometry for total filling factor $v = 1$ ($\frac{1}{2} + \frac{1}{2}$) in the lowest Landau level. Short-range inter- and intra-layer interactions plus interlayer tunneling leads to a fully polarized system and a Moore-Read phase. Two other phases are found: Halperin (220) and coupled Moore-Read states.

(III) Fractional Chern Insulators

Fractional Chern Insulators (FCI) occur in interacting flat band systems with topological phases for rational fractional band fillings. We showed [10] that long-range dipolar interactions can lead to non-Abelian states like $v = \frac{1}{2}$ Moore-Read and $v = \frac{3}{5}$ Read-Rezayi states in Fermionic models, and multiparticle interactions are not required.

We extended our study of quasiholes in fractionally quantized systems by characterizing the *geometry* (Section I) of quasiholes in FCI with $1/3$ filling on different lattices [7]. By comparing with the corresponding FQH problem, we showed that similar structures were obtained for quasiholes on different lattices, involving just a length rescaling.

A model [5] of the [111] surface of the pyrochlore lattice with spin-orbit coupling was generically found to exhibit surface states with Fermi arcs, while in the bulk the model, depending on the parameters, exhibits Weyl semimetal as well as fractional Chern insulating phases, including a $C = 2$ generalization of the Moore-Read state. More recently, we have devised local lattice models [20] whose ground states are ideal FCI, i.e. Abelian and non-Abelian topologically ordered states characterized by exact ground state degeneracies at any finite size, and infinite entanglement gaps. These could potentially help design experimental platforms with novel ground states.

(IV) Quantum Entanglement, Disorder and Localization

Quantum Entanglement has been found to be particularly helpful in classifications of the topological phases of matter. Collaborating with Shao (Binghamton) and Kim (Cornell), we obtained the entanglement entropy of the $v = \frac{1}{2}$ state [11] using a new, determinantal form of the composite-fermion Fermi-liquid wavefunction in periodic (toroidal) boundary conditions, making it convenient for Monte-Carlo evaluation. By partitioning the torus with a “trivial cut”, the second Renyi entropy can be evaluated by Monte-Carlo sampling of the swap operator. The entanglement entropy calculated numerically is found to have a logarithmic correction to the “area law” ($L^* \log L$) just like a free fermion state.

As a precursor to studying effects of disorder in topological systems, we studied the Anderson model in dimensions $d = 1$ to 3 , using Large Disorder Renormalization Group [2] as well as quantum entanglement [8] methods numerically. The former showed promise in culling the Hilbert space of many-body models; the latter demonstrated that the area law for entanglement entropy is obeyed in both metallic and insulating phases.

We also studied numerically the effect of coupling a many-body localized system to a bath [9], demonstrating the evolution of eigenvalues statistics from Poisson (many-body localized) to GOE (Gaussian Orthogonal Ensemble, for extended or thermalized). While the data are consistent with the expectation that many-body localization (MBL) occurs only at zero coupling in the thermodynamic limit, strong signatures of incomplete localization survive in spectral functions of local operators at finite coupling that are

experimentally measurable. This offers hope for designing experiments to detect MBL. In a subsequent numerical study [21] of the level statistics of the entanglement spectrum of MBL and thermalizing phases of 1D and 2D Hamiltonian, and periodically driven Floquet systems, a semi-Poisson distribution was found (indicating a degree of level repulsion), in contrast to the Poisson distribution of energy splittings with no level repulsion.

Most recently, we studied the transition from the $v = 1/3$ FQH state to insulator with the addition of disorder using quantum entanglement as a diagnostic in the torus geometry [24]. This method does not require averaging over boundary conditions, unlike earlier methods that used Chern numbers, and is therefore much faster. The *derivative* of the entanglement entropy with respect to disorder was found to have a sharp peak at a characteristic disorder strength. The peak height grows significantly with size of the system, and appears to diverge in the thermodynamic limit; further, it exhibits finite size scaling, from which the critical exponent is extracted. Our work provides motivation for experimental studies of the FQH – insulator transition in samples with tuned disorder.

Future Plans

Numerical calculations to test the predictions of the graviton mode for FQH states will be done by Rezayi and Yang. Bhatt and coworkers plan to extend their study using quantum entanglement to other FQH-Insulator transitions; a comprehensive study of the plateau transitions using tight-binding and other projected models is also underway. Haldane plans to work on the two-particle reduced density matrix for Landau level problems, and with Rezayi, on a new efficient formalism for Monte Carlo studies.

List of Publications (partial, chronological)

1. *Guiding-center Hall viscosity and intrinsic dipole moment along edges of incompressible fractional quantum Hall fluids*, YeJe Park and F. D. M. Haldane, Physical Review B **90**, 045123 (2014).
2. *Large Disorder Renormalization Group Study of the Anderson Model of Localization*, Sonika Johri and R. N. Bhatt, Physical Review B **90**, 060205(R) (2014).
3. *Existence of strong-pairing quantum Hall phase in bilayer cold-atom systems with dipolar interactions*, Yuihui Zhang, E. H. Rezayi and Kun Yang, Physical Review B **90**, 165102 (2014).
4. *Matrix-Product-State Algorithm for Finite Fractional Quantum Hall Systems*, Zhao Liu and R. N. Bhatt, Journal of Physics: Conference Series 640, 012044 (2015) (XXVI IUPAP Conference on Computational Physics – CCP2014).
5. *Topology and Interactions in a Frustrated Slab: Tuning from Weyl Semimetals to $C > 1$ Fractional Chern Insulators*, E. J. Bergholtz, Zhao Liu, M. Trescher, R. Moessner and M. Udagawa, Physical Review Letters **114**, 016806 (2015).

6. *Infinite Density Matrix Renormalization Group for Multicomponent Quantum Hall Systems*, Michael P. Zaletel, Roger S. K. Mong, Frank Pollmann, and Edward H. Rezayi, Physical Review B **91**, 045115 (2015).
7. *Characterization of quasiholes in Fractional Chern Insulators*, Zhao Liu, R. N. Bhatt and Nicolas Regnault, Physical Review B **91**, 045126 (2015).
8. *Entanglement Area Law in Disordered Free Fermion Anderson Model in One, Two and Three Dimensions*, Mohammad Pouranvari, Yuhui Zhang and Kun Yang, Advances in Condensed Matter Physics, 397630 (2015).
9. *Many-Body Localization in Imperfectly Isolated Quantum Systems*, Sonika Johri, Rahul Nandkishore and R. N. Bhatt, Physical Review Letters **114**, 117401 (2015)
10. *Fermionic non-Abelian fractional Chern insulators from dipolar interactions*, Dong Wang, Zhao Liu, Wu-Ming Liu, Jun-Peng Cao and Heng Fan, Phys. Rev. B **91**, 125138 (2015)
11. *Entanglement entropy of the $\nu = \frac{1}{2}$ composite fermion non-Fermi liquid state*, Junping Shao, Eun-Ah Kim, F. D. M. Haldane and Edward H. Rezayi, Physical Review Letters **114**, 206402 (2015).
12. *Competing Abelian and Non-Abelian Topological orders in $\nu = 1/3 + 1/3$ quantum Hall bilayers*, Scott Geraedts, Michael P. Zaletel, Zlatko Papic and Roger S. K. Mong, Physical Review B **91**, 205139 (2015)
13. *Non-Abelian phases in two-component $\nu = 2/3$ fractional quantum Hall states: Emergence of Fibonacci Anyons*, Zhao Liu, Abolhassan Vaezi, Kyungmin Lee and Eun-Ah Kim, Physical Review B **92**, 081102(R) (2015)
14. *Geometric Construction of Quantum Hall Clustering Hamiltonians*, Ching Hua Lee, Zlatko Papić, and Ronny Thomale, Phys. Rev. X **5**, 041003 (2015).
15. *Probing the geometry of the Laughlin state*, Sonika Johri, Z. Papic, P Schmitteckert, R N Bhatt and F D M Haldane, New Journal of Physics **18**, 025011 (2016).
16. *Phase diagram of $\nu = 1/2 + 1/2$ bilayer bosons with inter-layer couplings*, Zhao Liu, Abolhassan Vaezi, Cécile Repellin, and Nicolas Regnault, Phys. Rev. B **93**, 085115 (2016).
17. *The half-filled Landau level: The case for Dirac composite fermions*, Scott D. Geraedts, Michael P. Zaletel, Roger S. K. Mong, Max A. Metlitski, Ashvin Vishwanath and Olexei I. Motrunich, Science **352**, 197 (2016).

18. *Acoustic Wave Absorption as a Probe of Dynamical Geometrical Response of Fractional Quantum Hall Liquids*, Kun Yang, Phys. Rev. B **93**, 161302(R) (2016).
19. *Electron-solid and electron-liquid phases in graphene*, M. E. Knoester, Z. Papić and C. Morais Smith, Physical Review B **93**, 155141 (2016).
20. *Model Fractional Chern Insulators*, Jörg Behrmann, Zhao Liu, Emil J. Bergholtz, Physical Review Letters **116**, 216802 (2016).
21. *Many body localization and thermalization: insights from the entanglement spectrum*, Scott D. Geraedts, Rahul Nandkishore and Nicolas Regnault, Phys. Rev. B **93**, 174202 (2016). [Editor's Suggestion].
22. *Fibonacci anyons and charge density order in the 12/5 and 13/5 plateaus*, Roger S. K. Mong, Michael P. Zaletel, Frank Pollmann and Zlatko Papić, arXiv:1505.02843 (submitted to Physical Review).
23. *Geometry of Landau orbits in the absence of rotational symmetry*, F. D. M. Haldane and Yu Shen, arXiv1512.04502, (submitted to Physical Review).
24. *Quantum Entanglement as a Diagnostic of Phase Transitions in Disordered Quantum Hall Liquids*, Zhao Liu and R. N. Bhatt arXiv 1607.04762 (submitted to Physical Review Letters).

Near-Field Electrodynamics of Carbon Nanostructures

Principle investigator: Igor Bondarev, Professor, PhD, DSc (Habilitation)
Department of Math & Physics, North Carolina Central University, Durham, NC 27707
ibondarev@nccu.edu

Project Scope

The objective of this research is to advance the frontiers of fundamental knowledge on near-field electrodynamic processes in complex carbon nanostructures. The project seeks to explore how one can use near-fields of low-energy collective plasmon excitations of individual constituent carbon nanotubes (CNs) to tailor the optoelectronic properties of double (multi-) wall CNs and hybrid quantum systems of metal-atomic-wire encapsulating CNs. Quantum near-field theory is being developed for exciton-plasmon Bose-Einstein condensation and superfluidity in pristine double (multi-) wall CN systems. Transport properties of hybrid metal-encapsulating semiconducting CNs are being explored. Clear understanding of the properties of collective excitations, and how individual constituents of complex systems communicate with one another in the near field and what it does to the entire complex system, is a natural prerequisite for advances ranging from new applications, such as coherent light emission, enhanced electromagnetic absorption, scattering and conversion of ambient electromagnetic radiation, to the development of new concepts for future generation carbon based plasmonic nanomaterials engineering. The project focuses on new directions for fundamental nanoplasmonics and near-field optics research, currently mostly dealing with metallic nanoparticles, to include a new area of nanotube optoplasmonics.

Recent Progress

Below are some highlights of progress made in the past two years. A more comprehensive publication list is appended below the highlights.

1D transport in hybrid metal-semiconductor nanotube systems – An electron transport model is developed for the one-atom-thick, finite-length metallic wire (AW) encapsulated into a semiconducting CN with the bandgap broader than the AW conduction band (Fig.1, left panel and top right), in order to understand the interplay between the AW intrinsic 1D conductance and the near fields of nanotube's collective interband plasmon excitations. The model uses the matrix Green's function formalism to derive an analytical expression for the electron transmission coefficient $T(E)$ through such a hybrid metal-semiconductor system. The conductance $g = T(E \sim E_F)$ of the system can be affected significantly by the AW-CN plasmon coupling when $2V(E_p - E_F) = N\mu^2$ (μ is the AW-CN coupling constant, E_p is the CN plasmon energy, N , E_F and V are the number of atoms, the Fermi energy and the hopping parameter of the AW, respectively), to result in the Fano resonances in the electron transmission, whereby the AW-CN near-field interaction blocks some of the pristine AW transmission band channels to open up new coherent channels in the CN bandgap outside the AW transmission band. This makes the entire hybrid system transparent in the energy domain where neither AW nor CN is individually transparent. (Fig.1, right panel) These generic features of the Fano resonances may also manifest themselves in those metal-nanotube combinations where the AW transmission band is broader than the CN bandgap. They may affect both the electron transport in the CN conduction band and the hole transport in the CN valence band, to block some of the transmission channels inside and/or to provide extra plasmon-mediated coherent transmission channels outside of the bands of states. This effect can be used to control, optimize and manipulate by the charge transfer in hybrid metal-semiconductor CN based devices for nanoscale energy conversion, separation, and storage. Work done in collaboration with M.Gelin, Chemistry Dept., TU-Munich, Germany. [Figure 1; [M.F.Gelin and I.V.Bondarev, Physical Review B 93, 115402 \(2016\)](#)]

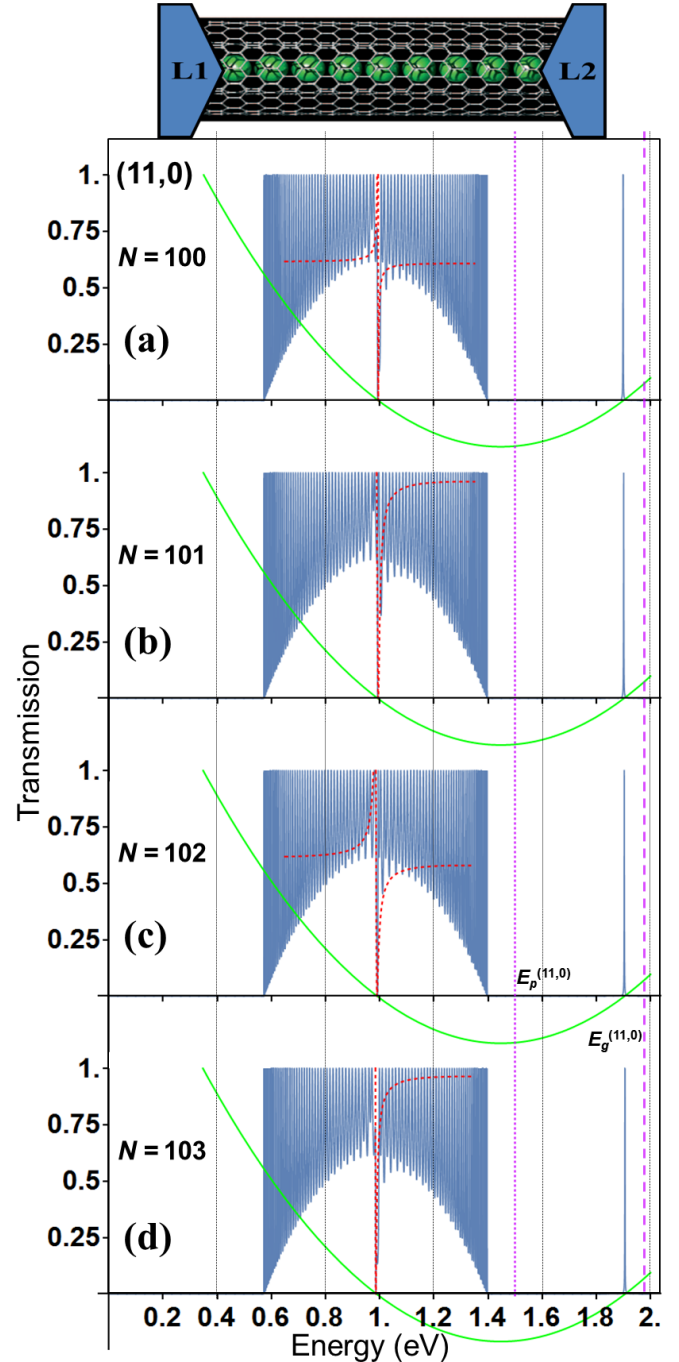
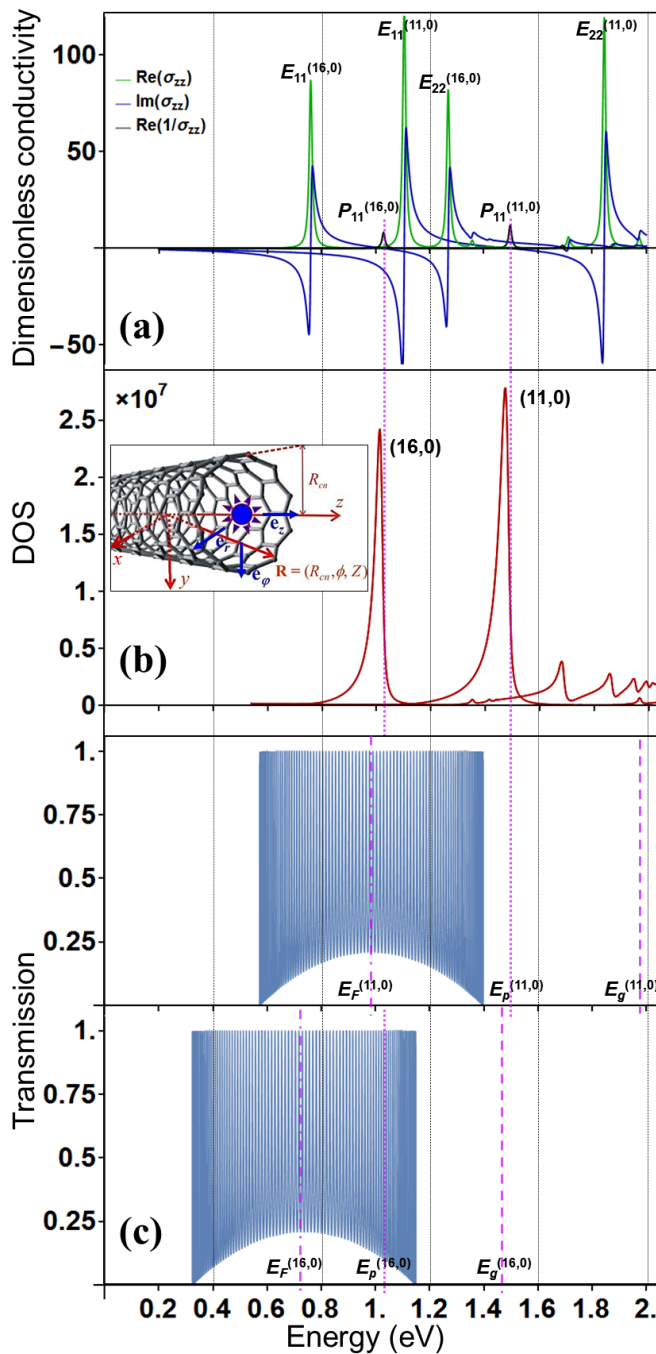


Fig. 1: *Top right:* Schematic of the hybrid system studied. *Left panel:* (a) Calculated axial surface conductivities σ_{zz} (normalized by $e^2/2\pi\hbar$) for the semiconducting $(11,0)$ and $(16,0)$ CNs. Peaks of $\text{Re}(\sigma_{zz})$ and $\text{Re}(1/\sigma_{zz})$ represent excitons (E_{11} , E_{22}) and interband plasmons (P_{11}), respectively. (b) Photonic density-of-states (DOS) for non-radiative spontaneous decay with CN plasmon excitation for a two-level dipole emitter on the symmetry axis (inset) of the $(11,0)$ and $(16,0)$ CN. Dotted vertical lines show the correspondence between the DOS peaks and interband plasmon resonances of the conductivities for the respective CNs. (c) Electron transmission band for the free AW of 100 sodium atoms with energy counted from the bottom of the fundamental bandgap E_g of the $(11,0)$ and $(16,0)$ CNs (top and bottom, respectively); also shown are the AW Fermi energies E_F and CN first interband plasmon energies E_p . *Right panel, (a)-(d):* An example of the calculated transmission coefficient versus energy for the coupled hybrid system (sketched on top) of the AW with $N=100$, 101, 102, and 103 sodium atoms inside the $(11,0)$ CN. Green lines are the parabolas whose zeros give the positions of two Fano resonances that appear due to the AW-CN plasmon coupling to block the AW transmission band center and to open up a new coherent transmission channel in the CN forbidden gap outside the AW band. Red dashed lines are zone-center approximations of the transmission formula obtained.

M.F.Gelin and I.V.Bondarev, Phys. Rev. B 93, 115402 (2016)

Plasmon enhanced Raman scattering near CNs – Quantum theory of the resonance Raman scattering is developed for a two-level system (TLS) coupled to a low-energy ($\sim 1\text{--}2$ eV) interband plasmon resonance of a carbon nanotube. The theory applies to atomic type species that are physisorbed on the CN walls, whereby there is no local electronic orbitals hybridization between the CN and the atomic transition levels involved. The theory covers both weak and strong TLS-plasmon coupling, and predicts a dramatic enhancement of the Raman scattering intensity in the strong coupling regime. Previously, most of the applications of CNs to enhance Raman scattering have been to decorate them with metallic nanoparticles – to use plasmons of metal as spectroscopic enhancers with CNs only serving as their supporters. Here, individual CNs are shown to provide a strong resonance Raman enhancement effect due to their intrinsic interband plasmon modes. The theory developed will help establish new design concepts for future CN based nanophotonics platforms for single atom detection, precision spontaneous emission control, and optical manipulation, which will benefit from the extraordinary stability and precise tunability of the physical properties of CNs by means of their diameter and chirality variation. [Figure 2; I.V.Bondarev, Optics Express 23, 3971 (2015)]

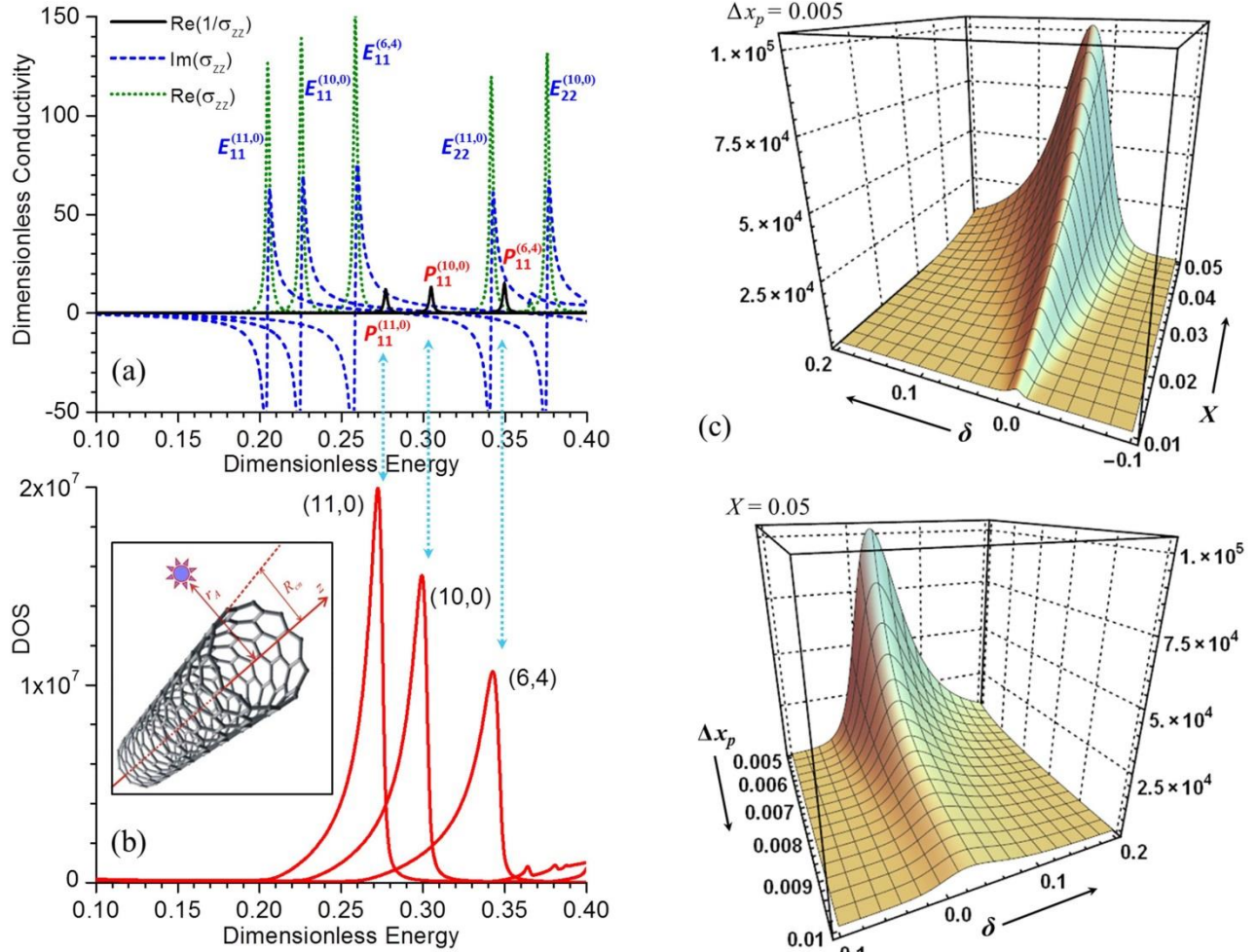


Fig. 2: *Left panel:* (a) Axial surface conductivities σ_{zz} normalized by $e^2/2\pi\hbar$ for the (6,4), (10,0), and (11,0) CNs of increasing diameter (cf. Fig.1, left). Peaks of $\text{Re}(\sigma_{zz})$ represent excitons (E_{11}, E_{22}); peaks of $\text{Re}(1/\sigma_{zz})$ indicate interband plasmons (P_{11}). (b) Photonic DOS for the TLS placed 2.84 Å away from the surface of the nanotubes (see inset) whose axial surface conductivities are presented in (a). Dotted double-end vertical arrows show the correspondence between the DOS peaks and interband plasmon resonances of the conductivities for the respective CNs. (c), *upper & lower panels:* Raman scattering enhancement factor for the $P_{11}(6,4)$ resonance in (a) with typical X , Δx_p , and δ to stand, respectively, for the TLS Rabi splitting energy, plasmon resonance width and TLS detuning from the plasmon resonance. The enhancement factor increases dramatically for $X/\Delta x_p \gg 1$ (strong coupling regime). Energies are in units of the double C-C overlap integral (5.4 eV). Conductivities are calculated using the $(k\cdot p)$ -scheme [T.Ando, J. Phys. Soc. Jpn. 74, 777 (2005)]. DOS functions are obtained per theory by Bondarev & Lambin [PRB 72, 035451 (2005)]. **I.V.Bondarev, Optics Express 23, 3971 (2015)**

Future Plans

Exciton-plasmons in double (multi-) wall carbon nanotubes – The main focus will be on the derivation of the exciton-plasmon dispersion relation and the analysis of the possibility for the exciton Bose-Einstein condensation (BEC) in double wall CNs with matching exciton/plasmon resonances. Double (multi-) wall CN systems in which an exciton resonance of one tubule overlaps with a plasmon resonance of another tubule is expected to provide the strong exciton-plasmon coupling condition that is necessary for the exciton BEC to occur. The quantum electrodynamics approach developed previously by the PI is being used to advance this problem. Once the quasi-particle dispersion relation is obtained, the pairs of nanotubes will be identified that are capable of providing the most efficient exciton-plasmon coupling and, presumably, the exciton BEC. The BEC theory will then be developed to obtain typical BEC temperatures and temperature-dependent exciton emission line profiles, to show how the phenomenon is expected to manifest itself experimentally. Further development will be to study the connection between the exciton BEC and superfluidity in the appropriately chosen double wall CNs, focusing on temperature dependences and (weak) temperature gradients. Apart from the fundamental aspect, this will give insight into photoluminescence peculiarities of multi-wall CNs and their aggregates that are of relevance to energy related applications.

Nonlinear optical response of advanced quasi-1D/2D nanomaterials – These include quasi-1D periodic chains of organic polymer molecules and quasi-2D semiconductor nanostructures such as coupled quantum wells, van der Waals bound graphitic and transition metal dichalcogenide bilayer heterostructures. In the latter, indirect excitons, biexcitons, and trions formed by indirect excitons are likely to control the formation of correlated Wigner-crystal-like electron-hole structures. Binding energy calculations for the biexciton and trion electron-hole complexes formed by indirect excitons will be the main thrust of this effort. The focus will be on testing the capability and correctness of the configuration space method developed recently by the PI for the binding energy calculations of excitonic complexes in reduced dimensionality semiconductor systems. The configuration space method can help develop understanding of how stable Wigner crystallization could be in these quasi-2D nanostructures. Wigner-like electron-hole crystal structures are of great interest for future spintronics applications.

Publications

(2014-16)

I.V.Bondarev, Configuration space method for calculating binding energies of exciton complexes in quasi-1D/2D semiconductors, *Modern Physics Letters B* **2016**, *at press*

M.F.Gelin and I.V.Bondarev, One-dimensional transport in hybrid metal–semiconductor nanotube systems, *Physical Review B* **93**, 115422 (2016)

I.V.Bondarev, Plasmon enhanced Raman scattering effect for an atom near a carbon nanotube, *Optics Express* **23**, 3971 (2015)

I.V.Bondarev and A.V.Gulyuk, Electromagnetic SERS effect in carbon nanotube systems, *Superlattices and Microstructures* **87**, 103 (2015)

I.V.Bondarev, Relative stability of neutral and charged exciton complexes in quasi-one-dimensional semiconductors, *Physical Review B* **90**, 245430 (2014)

I.V.Bondarev and A.V.Meliksetyan, Possibility for exciton Bose-Einstein condensation in carbon nanotubes, *Physical Review B* **89**, 045414 (2014)

M.F.Gelin, I.V.Bondarev, and A.V.Meliksetyan, Optically promoted bipartite entanglement in hybrid metallic carbon nanotube systems, *The Journal of Chemical Physics* **140**, 064301 (2014)

I.V.Bondarev, M.F.Gelin, and A.V.Meliksetyan, Tunable plasmon nano optics with carbon nanotubes, In: *Dekker Encyclopedia of Nanoscience and Nanotechnology*, 3rd ed., CRC Press: New York, 2014, pp. 4989-5001

Interacting topological quantum matter

Principal Investigator: Claudio Chamon
Department of Physics, Boston University
chamon@bu.edu

Project scope:

The study of topological phases of matter is a very active area of research in contemporary condensed matter physics. One of the many facets of the field is the study of fractionalized phases and their classification. It is possible to construct 2D interacting topological phases by coupling 1D quantum wires, and to use this strategy to classify their possible Abelian phases. This scheme, in addition to advancing the theoretical goal of better understanding topological phases through classification efforts, has the potential to provide a blueprint for building topologically based devices.

The objective of this project is to progress with this type of dimensional augmentation approach. The work aims at the construction of Abelian and non-Abelian topological phases in both 2D and 3D using assemblies of quantum wires or quantum spin chains as building blocks. The theoretical analysis deploys the technique of non-Abelian bosonization. The analytical work is complemented by numerical studies of quantum spin chains and ladders that serve as the building blocks.

Recent progress:

Non-Abelian topological spin liquids from arrays of quantum wires or spin chains

We constructed 2D non-Abelian topologically ordered states by strongly coupling arrays of 1D quantum wires via interactions. In our scheme, all charge degrees of freedom are gapped, so the construction can use either quantum wires or quantum spin chains as building blocks, with the same end result. The construction gaps the degrees of freedom in the bulk, while leaving decoupled states at the edges that are described by conformal field theories (CFTs) in (1+1)-dimensional space and time. We considered both the cases where time-reversal symmetry (TRS) is present or absent. When TRS is absent, the edge states are chiral and stable. We prescribed, in particular, how to arrive at all the edge states described by the unitary CFT minimal models with central charges $c < 1$. These non-Abelian spin liquid states have vanishing quantum Hall conductivities, but non-zero thermal ones. When TRS is present, we described scenarios where the bulk state can be a non-Abelian, non-chiral, and gapped quantum spin liquid, or a gapless one. In the former case, we found that the edge states are also gapped.

The non-Abelian bosonization technique utilized in this work is a powerful tool for understanding the possible 2D topological phases that can be reached by strongly coupling 1D systems. As a simple illustration of its power, we showed how to easily recover the ten-fold way classification of two-dimensional non-interacting topological insulators using the Majorana representation that naturally arises within non-Abelian bosonization. Within this scheme, we showed that the classification reduces to counting

the number of null singular values of a mass matrix, with gapless edge modes present when left and right null eigenvectors exist.

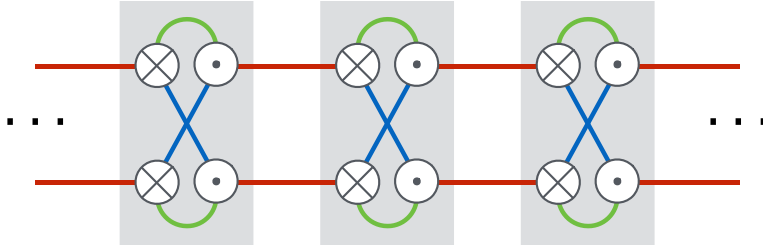


Figure 1: Schematic representation of the Hamiltonian for a state with non-Abelian topological order arising from interactions between electronic quantum wires. Each \otimes and \odot represents the right-moving and left-moving (spinful) electrons of a quantum wire coming out of the plane of the page. Each gray area represents an interaction that gaps out charge fluctuations on the bundle of wires that it encloses. Each line represents a SU(2) symmetric Heisenberg interaction between the spin densities of left-movers and right-movers that it connects. Lines of the same color represent interaction terms of the same strengths.

Wire constructions of Abelian topological phases in three or more dimensions

Coupled-wire constructions have proven to be useful tools to characterize Abelian and non-Abelian topological states of matter in 2D (see above, for example). In many cases, their success has been complemented by the vast arsenal of other theoretical tools available to study such systems. In 3D, however, much less is known about topological phases. Since the theoretical arsenal in this case is smaller, it stands to reason that wire constructions, which are based on 1D physics, could play a useful role in developing a greater microscopic understanding of 3D topological phases.

We provided a comprehensive strategy, based on the geometric arrangement of commuting projectors in the toric code, to generate and characterize coupled-wire realizations of strongly-interacting 3D topological phases. We showed how this method can be used to construct pointlike and linelike excitations, and to determine the topological degeneracy. We also pointed out how, with minor modifications, the machinery already developed in 2D can be naturally applied to study the surface states of these systems, a fact that has implications for the study of surface topological order. Finally, we show that the strategy developed for the construction of 3D topological phases generalizes readily to arbitrary dimensions, vastly expanding the existing landscape of coupled-wire theories. We discussed Z_m topological order in three and four dimensions as a concrete example of this approach, but the approach itself is not limited to this type of topological order.

Planned activities:

The planned effort for the next year will focus on two directions. The first is to extend to 3D the scheme that we utilized to build 2D *non-Abelian* topological phases from coupled 1D quantum wires or spin chains. We have made substantial progress already, and we have identified a way to devise the proper interactions between the wires that gap all degrees of freedom when periodic boundary conditions are imposed. The nature of surface states, or whether we have gapped or gapless degrees of freedom at the boundary, is a topic we will address. After determining the nature of the surface modes, the subsequent step is to construct the operators that lead the fractionalized excitations in the bulk, and investigate the ground state degeneracy for periodic boundary conditions. If successful, this approach will establish a concrete approach for designing 3D non-Abelian topological phases from 1D building blocks.

Our second research direction is to build a 2D non-Abelian topological phase starting directly from a microscopic model, a system of coupled quantum spin $\frac{1}{2}$ ladders. Our constructions thus far have taken as starting point the field theoretical description of wires. The couplings that gap the bulk states were written in terms of the non-Abelian currents that describe the wire degrees of freedom; these couplings should correspond to some microscopic couplings written directly in terms of local degrees of freedom in the wires. For example, in the case of quantum spin chains, the current-current interactions within the non-Abelian bosonization scheme are the result of microscopic spin interactions. We are currently focusing on engineering a specific 1D spin model that lead, once the chains are coupled, to a non-Abelian 2D topological state with gapless Majorana modes at the boundary. We have identified the model for the 1D building blocks, and we are currently using DMRG studies to show that this 1D building block model is gapless, and that these chains are gapped once coupled to neighboring chains. The DMRG studies are being carried in collaboration with Adrian Feiguin.

Publications: DOE support, explicitly referred to as ‘‘DOE Grant DEFG02-06ER46316’’, is acknowledged in every publication listed below for the period 11/15/15 to 07/22/16.

1. “Non-Abelian topological spin liquids from arrays of quantum wires or spin chains”
Po-Hao Huang, Jyong-Hao Chen, Pedro R. S. Gomes, Titus Neupert,
Claudio Chamon, and Christopher Mudry
Phys. Rev. B 93, 205123 (2016)
Featured as Editor’s suggestion

2. “Wire constructions of Abelian topological phases in three or more dimensions”
Thomas Iadecola, Titus Neupert, Claudio Chamon, and Christopher Mudry
Phys. Rev. B 93, 195136 (2016)

3. “Two-Component Structure in the Entanglement Spectrum of Highly Excited States”
Zhi-Cheng Yang, Claudio Chamon, Alioscia Hamma, and Eduardo R. Mucciolo
Phys. Rev. Lett. 115, 267206 (2015)
4. “Driven-dissipative Ising model: Mean-field solution”
Garry Goldstein, Camille Aron, and Claudio Chamon
Phys. Rev. B 92, 174418 (2015)
5. “Electrons at the monkey saddle: a multicritical Lifshitz point”
Alex Shtyk, Garry Goldstein, and Claudio Chamon
arXiv:1606.04950
6. “D-wave superconductivity in boson+fermion dimer models”
Garry Goldstein, Claudio Chamon, and Claudio Castelnovo
arXiv:1606.04129
7. “Dissipationless conductance in a topological coaxial cable”
Thomas Schuster, Thomas Iadecola, Claudio Chamon, Roman Jackiw, and So-Young Pi
arXiv:1606.01905

Quantum embedding and first principles electronic structure for correlated materials

Garnet Kin-Lic Chan

Division of Chemistry and Chemical Engineering,
California Institute of Technology,
Pasadena, CA 91125

Project Scope

The main goals of my research are (i) to develop new methods that can quantitatively describe strong correlation effects in materials, and (ii) to use these methods to make definitive numerical statements about correlation driven phenomena for problems ranging from lattice models to real materials. In the last two years, the DOE program has supported work in my group in two areas. The first is the development and application of density matrix embedding theory (DMET), a technique which allows calculations on finite systems to mimic those performed in the thermodynamic limit. We have applied DMET to carry out high accuracy studies of various cuprate models of increasing complexity, and have obtained several definitive results, discussed further below. We have also developed fundamental extensions of the method, e.g. to superconductivity, electron-phonon coupling, and time-dependent problems. The second area of our efforts has been to explore the systematic diagrammatic approach contained in coupled cluster approximations, to compute first principles materials spectra beyond the level of the GW/BSE paradigm. Our spectral CC methods have been applied to the uniform electron gas, where they accurately treat satellite features, and most recently, we have extended the work to a fully first principles implementation, which can be used to simulate real materials spectra. All of our work is made available through open-source software, and our first-principles methods are implemented as part of a new simulation package, PySCF, that targets in particular correlated electron simulations in molecules and materials.

Recent Progress

Ground-state phase diagram of the 2D Hubbard model. Although the 2D Hubbard model is one of the most widely studied models in condensed matter physics, consensus on the ground-state phases, such as regarding the absence or presence of superconductivity in the physically relevant parameter regime, has been elusive. Using density matrix embedding theory with clusters of up to 16 sites we have computed an accurate ground-state phase diagram of the 2D Hubbard model [1]. (We have since carried out additional benchmark calculations with up to 100 cluster sites) [2]. As one measure of accuracy of the calculations, we find that our extrapolated energies at half-filling are in error by less than 0.001t. Using careful extrapolations of the order parameters to the thermodynamic limit, we determine the phase diagram as shown in Fig. 1. The converged phase diagram shows a clear region of robust d-wave superconductivity at intermediate doping and coupling (e.g. U=4-6), coexistence between AFM and SC order, as well as many inhomogeneous phases in the underdoped regime.

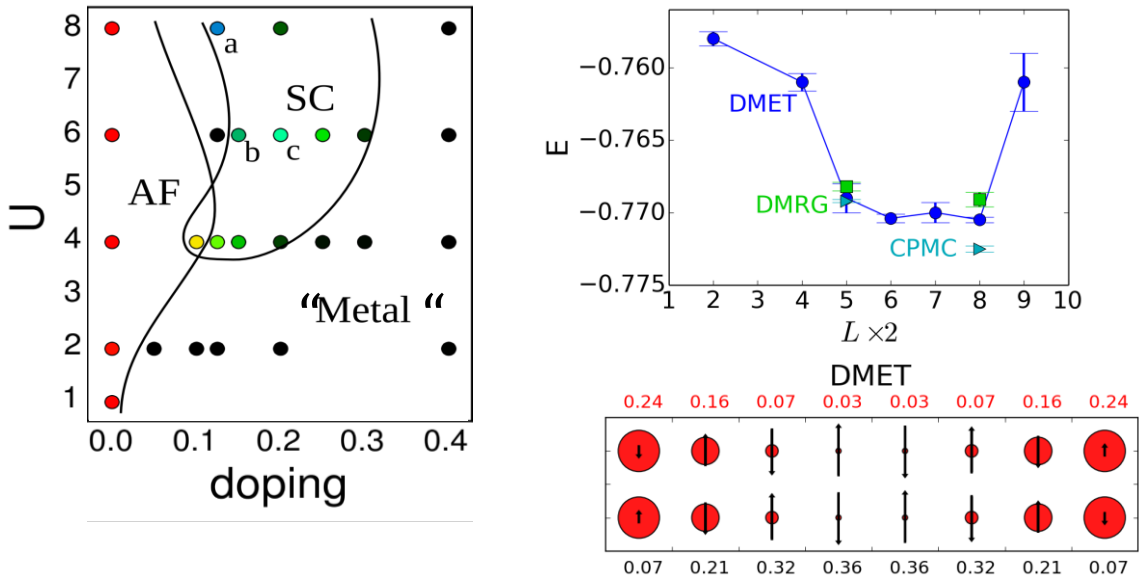


Figure 1 Left: Ground-state phase diagram of the 2D Hubbard model from DMET. From Ref. [1] Right top: stripe-wavelength and energy at $U=8$, $1/8$ doping using different methods. Right bottom: Stripe order from DMET.

Resolving the order in the underdoped 2D Hubbard model ground-state. Our work on the Hubbard model phase diagram, as well as earlier work in the community, had previously observed several competing orders in the underdoped region of the 2D Hubbard model. We thus tried to answer the question: are these orders artifacts of the different computational methods used? If not, can we determine the true order in the underdoped region? Using DMET calculations in conjunction with DMRG, AFQMC, and iPEPS simulations by our collaborators, we could definitively establish that the predominant order in the $1/8$ doping regime is a vertically striped state (see Fig. 1). The stripe wavelength is nearly degenerate between wavelengths 5-8 (on the scale of $0.001t$) with a small preference for a stripe of wavelength 8 and with vanishing superconducting order. This is one of the first conclusive numerical resolutions of order in the underdoped region of the 2D Hubbard model.

Beyond the 2D Hubbard model. We are currently extending our DMET calculations to go beyond the single band Hubbard model. For example, we are computing the ground-state phase diagram of the 3-band model using a variety of parameters sets that are in the literature. Already early calculations indicate interesting behavior, including evidence for bond order in the unit cell, as detected in RIXS studies. In collaboration with Lucas Wagner, we will also explore the 3-band model phase diagram with material specific 3-band parameters sets determined from QMC, in order to correlate cuprate materials directly with their superconducting properties.

Developments in density matrix embedding theory. We have carried out many extensions of the DMET methodology in the last two years, including (i) extensions to

superconducting ground-states (e.g. as applied above) [1], (ii) a dynamical cluster formulation [2], (iii) extensions to coupled fermion-boson Hamiltonians (to study the effects of phonons in the presence of interactions) [3], (iv) spectral functions [4], (v) extensions to non-equilibrium, time-dependent systems. The latter provides the exciting possibility of studying pump-probe experiments in correlated systems, with the DMET being used to mitigate the finite size effects that plague existing time-dependent simulations.

Model Hamiltonian derivation. We have also worked on model reduction via canonical transformations. Here, a common difficulty is the divergence of canonical transformations near perturbation theory singularities. We have found a particularly simple regularization of perturbation theory that allows for qualitatively accurate model Hamiltonians in molecules to be derived by a simple second order canonical transformation. [5]

Spectral functions of the uniform electron gas. A second main thrust of our work has been to advance the first principles simulation of spectra in moderately correlated materials. For materials with modest correlations, the standard first principles method is GW (for single-particle spectra) or GW/BSE (for optical spectra). While this approach has been remarkably successful over several decades, especially for understanding semiconductor physics, the time has come to consider improvements particularly to treat more correlated spectral features (such as satellites) and more correlated materials. The coupled cluster hierarchy of quantum chemistry provides a systematic resummation of diagrams beyond GW theory, which, even at the lowest order (CCSD), contains all ring and ladder diagrams and a subset of the self-energy terms that couple the two. We have recently demonstrated the accuracy of CCSD and CCSDT spectra as compared to GW, GW+C, in the finite uniform electron gas. (Fig. 2.) We find that CC significantly improves the satellite structure and removes the dependence on starting point that is a well-known problem with GW methods. [6]

Beyond GW and BSE: correlated first principles materials spectra from coupled cluster. Building on our work on the uniform electron gas, we have generalized our spectral function coupled cluster implementation from the uniform electron to full ab-initio materials. We can now calculate, for the first time, correlated band structures in materials (with and without pseudopotentials) with the full coupled cluster theory. (Fig. 2). Employing successive levels of the CC hierarchy will allow for the determination of spectra with decreasing error bars, allowing for precise convergence to the exact limit. This work is currently being extended to optical spectra as well.

PySCF: a first principles molecular and materials simulation package. All the methods we develop are made available through free- and open-source software. Developing and maintaining this software is a major activity in the group. The density matrix embedding code is available via several DMET implementations [6]. First principles methods are available through PySCF. PySCF is a new open-source ab-initio

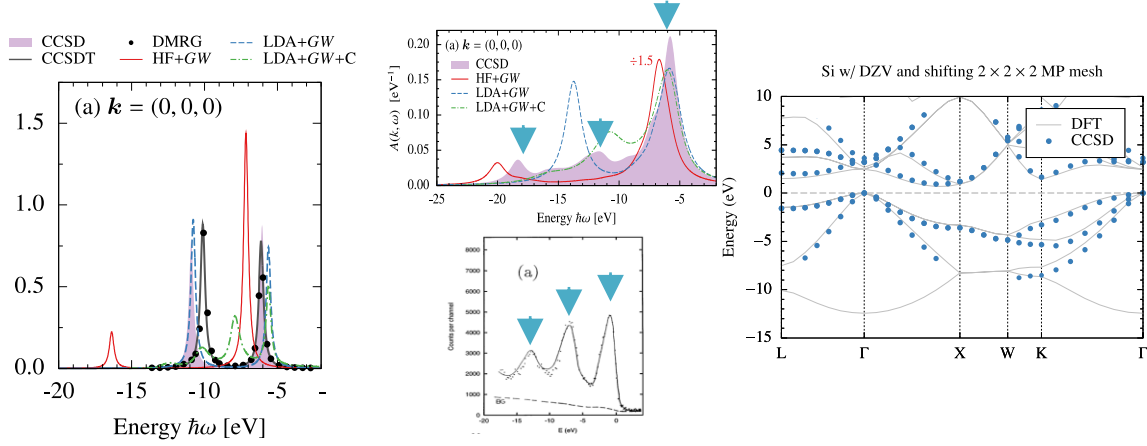


Figure 2 Left: Spectral function for a small finite UEG. CC shows perfect agreement with the “exact” DMRG results. Middle: Spectral function for a large UEG. The CC spectral function has a 3-peak structure unlike the GW spectral function; this 3-peak structure is reproduced in the experimental PES of Na. From Ref. [4]. Right: Full ab-initio coupled cluster calculation of the correlated band-structure of silicon.

code developed by the group which supports both state-of-the-art molecular computation as well as calculations in materials. It is designed to have leading performance while maintaining extreme simplicity for developers. PySCF is available for download from <https://github.com/sunqm/pyscf>.

References

1. Ground-state phase diagram of the square lattice Hubbard model from density matrix embedding theory, B.-X. Zheng, G. K.-L. Chan, Phys. Rev. B 93, 035126 (2016)
2. Cluster size convergence of density matrix embedding theory with an auxiliary field quantum Monte Carlo solver: original and dynamical cluster formulations, B.-X. Zheng, J. S. Kretchmer, H. Shi, S. Zhang, and G. K.-L. Chan, submitted
3. Density matrix embedding theory for interacting electron-phonon systems, B. Sandhoefer, G. K. Chan, arxiv:1602.04195
4. Spectral functions of strongly correlated extended systems via an exact quantum embedding, G. H. Booth, G. K.-L. Chan, Phys. Rev. B 91, 155107 (2016)
5. Correct quantum chemistry in a minimal basis from effective Hamiltonians, T. J. Watson Jr, G. K.-L. Chan, J. Chem. Theory Comput. 12, 512 (2015)
6. Spectral Functions of the Uniform Electron Gas via Coupled-Cluster Theory and Comparison to the GW and Related Approximations, J. McClain, J. Lischner, T. Watson, D. A. Matthews, E. Ronca, S. G. Louie, T. C. Berkelbach, G. K.-L. Chan, Phys. Rev. B, 93, 235139 (2016)
7. A practical guide to density matrix embedding theory in quantum chemistry, S. Wouters, C. A. Jiménez-Hoyos, Q. Sun, G. K.-L. Chan, J. Chem. Theory Comput. 12, 2706 (2016)

Computational theory applied to nanostructures

Principal investigator: Professor James R. Chelikowsky

Center for Computational Materials, Institute of Computational Engineering and Sciences,
Departments of Physics and Chemical Engineering, University of Texas, Austin, TX 78712
jrc@utexas.edu

Project Scope

This program targets the electronic and structural properties of nanostructured materials. Computational methods for predicting and understanding the properties of materials at the nanoscale are being developed and applied to electronic materials. Within the nanoscale, phenomena occur that are characteristic of neither the atomic limit, nor the macroscopic limit. Properties that are intensive at the macroscopic scale become size dependent at the nanoscale. These phenomena can have direct consequence for understanding and characterizing materials used in electronic, optical, and micro-mechanical applications related to energy sciences and technologies. To capitalize properly on predicting and understanding such phenomena in this nano regime, a deeper understanding of the quantum properties of materials will be required.

Recent Progress

Simulating atomic force microscopy images.

Characterization of surfaces and interacting molecular species is important for investigating the physical properties of materials. Recent progress in the field of two-dimensional materials such as graphene extends the applicable areas of characterization methods from surfaces to materials themselves. Non-contact atomic force microscopy (nc-AFM), an imaging technique that measures the frequency shift of an oscillating cantilever is one of the most widely used surface characterization methods. A typical AFM set up is shown in Fig. 1. A major benefit of AFM compared to other surface characterization methods such as scanning tunneling microscopy is its flexibility and ease of application: AFM can be used to image virtually any flat solid surface without sample preparation whereas in STM a conducting sample is required.

However interpreting AFM is difficult. Two noteworthy issues complicate the simulation of nc-AFM images. First, the morphology of the tip is in general unknown. As such, models of the tip are required based on *ad hoc* assumptions. Second, nc-AFM simulations require numerous force calculations between the tip and the specimen of interest over a fine three dimensional grid. This procedure can require thousands if not tens of thousands of geometries to be considered.

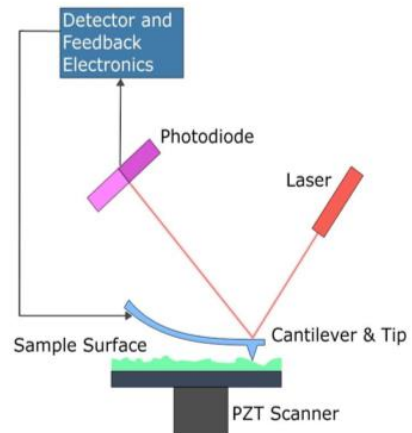


Fig. 1. Typical AFM setup, after Geissibl, Rev. Mod. Phys. 2003.

Simplified approaches to this problem were developed based on (a) avoiding an explicit description of the tip or (b) fixing the electrostatic field of the specimen. In the first case, the image can be determined by treating the tip as a classical object and attributing the shift of frequency in the probe to an induced dipole. In the second case, the tip is allowed to respond to the fixed field of the specimen. This approach allows one to include the functionalization of the tip by adsorbed species. In both cases *quantum* forces are computed. These approaches can result in a dramatic reduction of the computational load, often by more than several orders of magnitude.

Recently, carbon monoxide functionalized tips have been successfully used to obtain high resolution of chemical bonds in organic molecules and 2D materials such as graphene. However, the role of the CO molecule in enhancing the AFM resolution is not well understood. Using a classical tip model with no functionalizing agent and with a CO tip allows one to establish how the CO molecular orbitals account for the differing resolution. In Fig. 2, this difference is illustrated for a dibenzo(cd,n)naphtho(3,2,1,8-pqra)perylene.

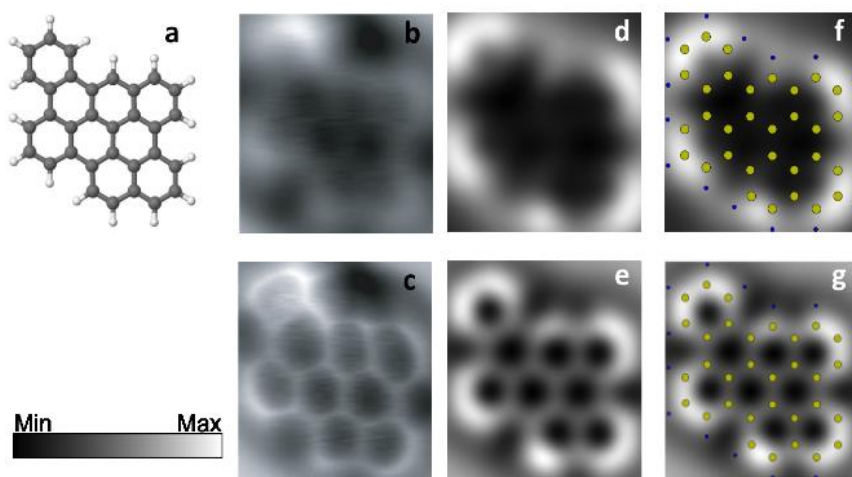


Fig. 2. Non-contact AFM images for a DBNP molecule. (a) Ball and stick model. Experimental nc-AFM images (Mohn et al. Appl. Phys. Lett. (2013)) with the Xe-tip termination (b) and the CO-tip termination (c). Simulated nc-AFM images without an explicit tip model (d) and with a CO-tip model (e). Atom positions are indicated with yellow (carbon) and blue (hydrogen) circles in (f) and (g).

(DBNP) molecule. There are two cases shown: one with a Xe terminated tip and one with a CO tip:

Experimentally, the CO tip results in a subatomic resolution of the covalent bonds in contrast to the Xe results. The simulations exhibit the same trend. The classical tip model fails to resolve the bonds, but the CO functionalized tip does. This difference can be attributed to the special nature of the CO molecular orbitals. Other work on AFM images included examining image inversion and explaining anomalies in imaging hydrogen bonds.

The role of quantum confinement on charged and neutral defects in nanostructures. It is well known that the activation energy of dopants in semiconducting nanomaterials is

higher than in bulk materials owing to dielectric mismatch and quantum confinement. This quenches the number of free charge carriers in nanomaterials. Though a higher doping concentration can compensate for this effect, there is no clear criterion on what the doping concentration should be. Using P-doped Si[110] nanowires as the prototypical system, this project established a doping limit by first-principles electronic structure calculations. By examining how a defect within a crystalline material responds to small changes in its charge state, the electronic properties of an ionized defect can be modeled by an effective work function and capacitance. As the nanowire gets thinner, the interaction range of the P dopants shortens and the doping concentration can increase concurrently. Hence, heavier doping can remain nondegenerate for thin nanowires. Also, this capacitance approach leads to a correction formula to the total energy of a charged periodic system and allows a comparison between the electronic band structure of the ionized defect to its corresponding neutral one. The correction formula can be related to the potential alignment method and Makov-Payne correction widely adopted in charged periodic systems. The new approach suggests both an alternative interpretation and improvements to the popular Makov-Payne and potential alignment scheme.

Computational methods for predicting the Raman spectra of nanostructures, including the role of defects. The vibrational modes and Raman spectra of P-doped Si nanocrystals were examined using the Placzek approximation. The Si nanocrystal vibrations are largely unaffected by the introduction of P dopants; however, the Raman spectra of doped nanocrystals are enhanced relative to those of pristine nanocrystals, and demonstrate a strong dependence on dopant position. An analysis showed that vibrational modes involving atoms in the vicinity of the dopant give the largest contributions to the Raman spectra. In addition, the vibrational and Raman spectra for Li doped Si nanocrystals were calculated. The insertion of Li atoms into Si nanocrystals disrupts the Si crystal structure forming a region of Li-Si alloy. The Raman spectrum for this alloy exhibits a Li induced peak at $440\text{-}480\text{ cm}^{-1}$. An accompanying reduction in the size of the dominant bulk-like Si peak at 520 cm^{-1} was found. Both of these results are consistent with experiment.

The vibrational properties and Raman spectra of Si-Ge core-shell nanostructures were examined. Not surprisingly, the dominant features of the Raman spectrum for the Si-Ge core-shell structure consisted of a superposition of the Raman spectra of the Ge and Si nanocrystals with optical peaks around 300 and 500 cm^{-1} , respectively. A Si-Ge "interface" peak at 400 cm^{-1} was observed for the first time. The Ge shell causes the Si core to expand from the equilibrium structure. This strain induces a significant redshift in the Si contribution to the vibrational and Raman spectra, while the Ge shell is largely unstrained and does not exhibit this shift. The ratio of peak heights is strongly related to the relative size of the core and shell regions. This project demonstrates that Raman has the potential of being developed as a tool for probing structural properties of nanostructures.

Future Plans

Work will focus on the following three themes: (1) Constructing a practical approach for probe microscopy of nanoscale systems in order that structural information from atomic

force microscopy can be quantified and correctly interpreted. A target will be to retain the quantum nature of the probe and sample, while obviating the need for extensive computation. (2) Developing computational methods for predicting the Raman spectra of nanostructures, including complex nanostructures with defects. (3) Predicting the response of complex molecular species, photovoltaic materials and two dimensional materials such as graphene and MoS₂ to external electric fields.

Selected Publications

1. M. Kim and J.R. Chelikowsky, "Simulated non-contact atomic force microscopy for GaAs surfaces based on real-space pseudopotentials," *Appl. Surf. Sci.* **303**, 163 (2014).
2. T.-L. Chan, A. Lee and J.R. Chelikowsky, "An effective capacitance model for computing the electronic properties of charged defects in crystals," *Comp. Phys. Comm.* **185**, 1564 (2014).
3. A.J. Lee, T.-L. Chan and J.R. Chelikowsky, "Dopant binding energies in P-doped Ge[110] nanowires using real-space pseudopotentials," *Phys. Rev. B* **89**, 075419 (2014).
4. K.H. Khoo and J.R. Chelikowsky, "First-Principles Study of Vibrational Modes and Raman Spectra in P-Doped Si Nanocrystals," *Phys. Rev. B* **89**, 195309 (2014).
5. N. Marom, T. Korzdorfer, X. Ren, A. Tkatchenko and J. R. Chelikowsky, "Size Effects in the Interface Level Alignment of Dye-Sensitized TiO₂," *J. Phys. Chem. Lett.* **5**, 23985 (2014).
6. N.S. Bobbitt, M. Kim, N. Marom, N. Sai and J.R. Chelikowsky, "Real space pseudopotential calculations for size trends in Ga- and Al-doped zinc oxide nanocrystals with wurtzite and zincblende structures," *J. Chem. Phys.* **141**, 094309 (2014).
7. T.-L. Chan, A.J. Lee, W.K. Mok and J.R. Chelikowsky, "The interaction range of P-dopants in Si [110] nanowires: Determining the non-degenerate limit," *Nano Lett.* **14**, 6306 (2014).
8. M. Kim, N. Marom, N. Scott Bobbitt, and J.R. Chelikowsky, "A first-principles study of the electronic and structural properties of Sb and F doped SnO₂ nanocrystals," *J. Chem. Phys.* **142**, 044704 (2015).
9. T.-L. Chan, J. Souto-Casares J. R. Chelikowsky, K.-M. Ho, C.-Z. Wang and S. Zhang, "The effect of interface on quantum confinement and electronic structure across the Pb/Si(111) junction," *Solid State Comm.* **217**, 43 (2015).
10. M. Kim and J.R. Chelikowsky, "CO tip functionalization in subatomic resolution atomic force microscopy," *Appl. Phys. Lett.* **107**, 163109 (2015).
11. T.-L. Chan, A. Lee and J.R. Chelikowsky, "Ionization of a P-doped Si(111) nanofilm using 2D periodic boundary conditions," *Phys. Rev. B* **95**, 235445 (2015).
12. N.S. Bobbitt and J.R. Chelikowsky, "First-principles study of vibrational properties and Raman spectra in Li-doped Si nanocrystals," *Chem. Phys. Lett.* **646**, 136 (2016).
13. Y. Sakai, A.J. Lee and J.R. Chelikowsky, "First-principles non-contact atomic force microscopy image simulations with frozen density embedding theory," *Nano Lett.* **16**, 3242 (2016).
14. N.S. Bobbitt and J.R. Chelikowsky, "Real-space pseudopotential study of vibrational properties and Raman spectra in Si-Ge core-shell nanocrystals," *J. Chem. Phys.* **144**, 124110 (2016).
15. J. Lee, M. Kim, J.R. Chelikowsky and G. Kim, "Computational simulation of noncontact AFM and STM images for graphene/hexagonal boron nitride heterostructures with intercalated defects," *Phys. Rev. B* (in press).

Computational approach to complex interfaces and junctions

PI: Professor Hai-Ping Cheng^{1,2}; SP: Professor James N. Fry¹

Department of Physics¹ and the Quantum Theory Project², University of Florida
Gainesville, FL 32611

Keywords: electron and spin transport, tunneling field-effect, interfaces, layered 2D materials

Program Scope

This DOE/BES funded project aims to understand fundamental physical processes at interfaces and across nano-molecular-junctions. We investigate electron and spin transport, interfacial electronic and magnetic structure, and the interplay between structure and properties. In the current funding period, we are working on 1) tunneling field-effect on electronic structure and spin transport through 2D junctions, 2) theoretical development and algorithm/code implementation of the many-body GW method, and 3) phonon-assisted electron relaxation processes

Recent Progress

1) Tunneling Field-Effect and Electron-Spin Transport

We have implemented the effective screening method (ESM) in the density functional theory framework for simulating gate voltage. This development provides a powerful approach to simulating tunneling field-effect transistors via first-principles methods [1,2].

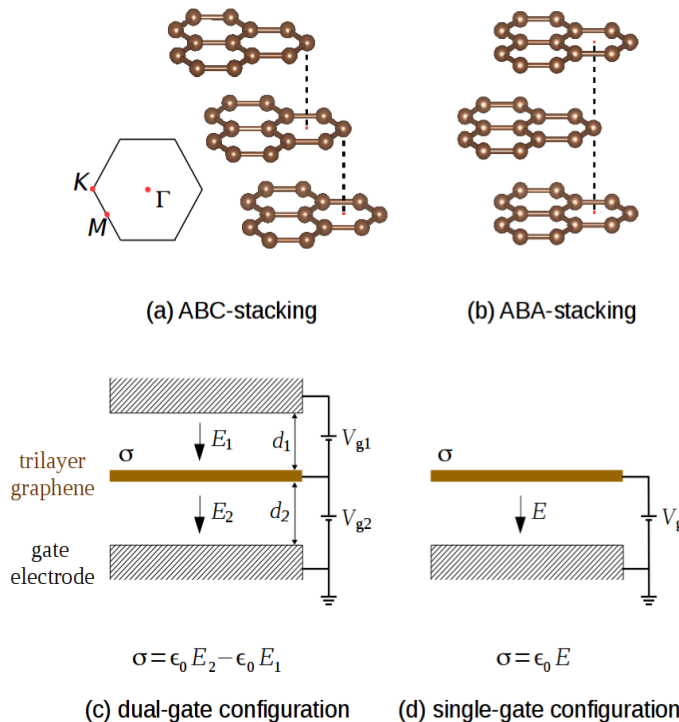


Fig.1 Schematics of the (a) ABC and (b) ABA stacking orders of trilayer graphene, and the (c) dual- and (d) single-gate configurations used in simulations. The first Brillouin zone of trilayer graphene is shown in the insert in (a). In (c,d) the net charge density on the trilayer graphene is denoted by σ , and the electric field between graphene and gate electrodes is denoted by E . Vacuum (permittivity ϵ_0) is used as the medium between graphene and gate electrodes in our simulations.

We have investigated both single-gate and double-gate graphene-based layered junctions. One example is the effect of an electric field on the electronic structure of trilayer graphene with ABC- and ABA-stacking orders (Fig.1). We thoroughly analyzed

the band gaps/overlaps induced by electric fields in ABC/ABA-stacked trilayer graphene. Our simulations are based on the dual-gate configuration, which enables us to examine separately the effects of electric field and of charge doping. (The single-gate configuration as shown in Fig. 1 (d) is a special case of the dual-gate configuration, setting V_{g1} and E_1 to zero). Changes in the band gap of ABC-stacked graphene trilayer are symmetric for hole and electron doping, but the symmetry is broken in ABA-stacked trilayer graphene. From the dual-gate configuration simulation, we show that the single-gate field-effect on the band structure arises from both the electric field and the charge-doping. Our findings are of great importance in guiding future experimental and computational searches aiming to control band structure. Another example is the tunneling transistors that consist of a graphene|h-BN|graphene multilayer structure. The distribution of free carriers and the band structure of both top and bottom graphene layers are calculated self-consistently. The dielectric properties of *h*-BN thin films sandwiched between graphene layers are computed layer-by-layer following the theory of microscopic permittivity. We find that the permittivities of BN layers are very close to those of crystalline *h*-BN. The effect of the interface with graphene on the dielectric properties of *h*-BN is weak, according to an analysis of the interface charge redistribution. The ESM is also applied to study the electronic and magnetic structures of quasi-one-dimensional interfaces along the zigzag direction in two dimensional GaN/SiC heterostructures [3]. We find that a bulk electric field will develop only when both interfaces hold no gap states and the net charge at interfaces are of opposite sign. Geometries studied exhibit an intriguing quasi-one-dimensional conductor character, of which some show finite nonzero magnetic moment. We relate the magnetization at the interfaces the Stoner instability.

After developing an algorithm that combines the idea of scattering theory that underlies the layer Korringa-Kohn-Rostoker (KKR) electronic structure code and pseudopotentials in conjunction with a planewave expansion, we finished code implementation for electronic transport and complex band calculations. The basic equation for each slice is written as, $\mathbf{Y}_{out} = \mathcal{S}\mathbf{Y}_{in} + \mathbf{F}_o$, where \mathcal{S} is the scattering matrix when the local potential is present alone, and \mathbf{F}_o is the special solution including the non-local potential. We applied our new method to study graphene side-contact electron and spin transport [3]. Our code interfaces with the Quantum Espresso package and also utilizes subroutines from the layer KKR code. This development is a significant step beyond our effort that generalizes the current implementation of planewave-based transport theory in PWCOND. The calculated transmission coefficients can be used as inputs in the Boltzmann equation [5-7] to compute resistance of metal and tunneling junctions.

2) All-electron self-consistent GW in the Matsubara-time domain

The GW approximation, originally proposed by Hedin, provides a route to improve electronic descriptions and band gap results using many-body perturbation theory. Although studies employing the GW approximation have enjoyed early success in improving band gap predictions, many implementations rely on the pseudopotential approximation in which pseudo wavefunctions and valence-core interactions are still treated at the level of DFT. We eliminate this disadvantage by implementing the GW method in an all-electron, linearized augmented plane wave (LAPW) code. In addition to

including valence-core interactions within this framework, we also solve for the self-energy in the Matsubara-time domain, which avoids the computationally costly convolution of the Green's function and screened Coulomb interaction in frequency space. Using this methodology, we have calculated the electronic structure for a range of semiconductors and insulators within the single-shot G_0W_0 , GW_0 , and fully self-consistent GW approximations. We have applied the full GW method to study a wide range of systems [8]. Our results show that the full GW improves the band gap greatly (Fig.2). We have also demonstrated the computational efficiency and rapid convergence of the self-energy with respect to Matsubara-time points and emphasize the importance of including valence-core interactions in such calculations.

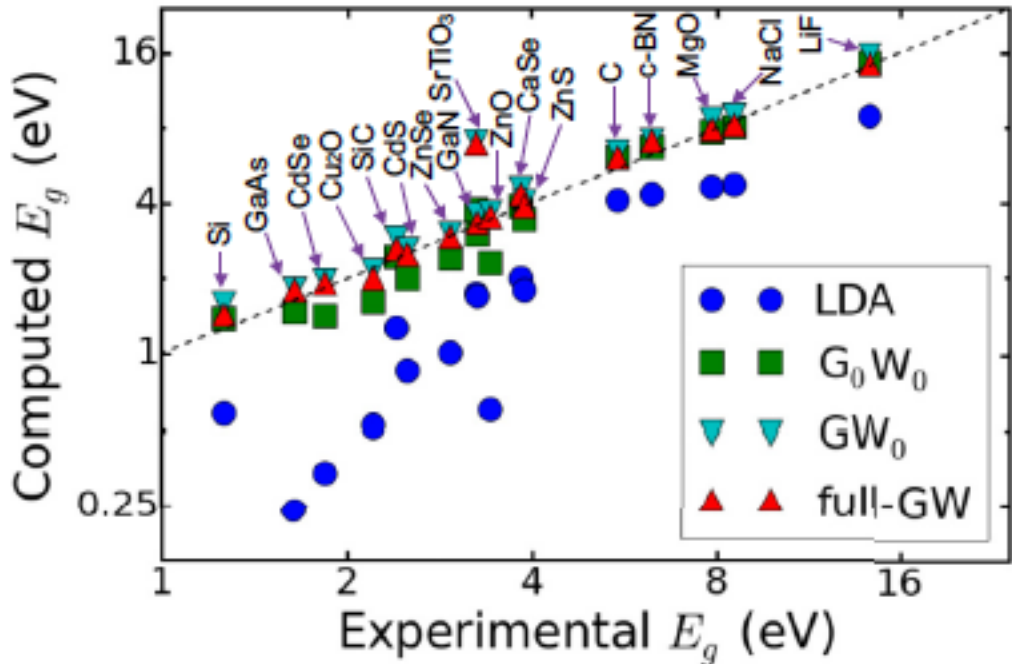


Fig.2 Computed electronic band gap at DFT-LDA as well as GW levels versus the experimental counterpart for all the compounds studied in this work except for Ge. A logarithmic scale is adopted for both axes.

3) Electron relaxation and phonon bottleneck in graphene quantum dots

We have developed method and codes to study slow phonon-induced relaxation in quantum dots [9]. The phonon bottleneck is crucial for next-generation photovoltaics; however the phenomenon has been difficult to realize experimentally, due to defects and ligands introducing strongly coupled states that expedite relaxation. Graphene quantum dots are an intriguing system to avoid these problems due to chemical synthesis methods that minimize defects. Large transition energies between excitonic and higher-energy states in low-screening materials such as graphene offer a possibility to create a bottleneck, but first-principles theoretical methods are too expensive to explore this possibility in large systems. We develop a state of-the-art reduced density matrix method with linear response theory to study carrier dynamics taking into account excitonic states and use this to study such a bottleneck in graphene quantum dots. By treating excitonic

states below the electronic band gap, we identify a distinct timescale attributed to relaxation to these bound states. Carbon chain ligands and edge geometry dramatically extend or reduce this timescale and suggest experimental routes to control the bottleneck.

Future Plans are 1) Wrap up investigations and a paper on spin-orbit coupling in 2D crystals (e.g. WS₂ and MoS₂) as a function of gate voltage in graphene-2D-graphene junctions, interface processes as well as electron transport as function of gate voltage; 2) Wrap up investigations and a paper on graphene-azobenzene-graphene systems, field effects and transport; 3) Wrap up a paper on DFT+DMFT calculations of Mott insulators (NiO, MnO, FeO etc), and 4) Develop/Implement a combined ESM and non-equilibrium Green function method.

References

1. First-principles simulations of a graphene-based field-effect transistor Wang, Yun-Peng; Cheng, Hai-Ping, PHYSICAL REVIEW B Volume: 91 Issue: 24 Article Number: 245307 Published: JUN 12 2015
2. First-principles studies of electric field effects on the electronic structure of trilayer graphene, Yun-Peng Wang, Xiang-Guo Li, James N. Fry, and Hai-Ping Cheng (Submitted 2016)
3. Two-dimensional lateral GaN/SiC heterostructures: first-principles studies of electronic and magnetic properties, Guo-Xiang Chen, Xiang-Guo Li, Yun-Peng Wang, James N. Fry, and Hai-Ping Cheng (submitted 2016).
4. Electron transport in graphene/graphene side-contact junction by plane-wave multiple-scattering method, Li, Xiang-Guo; Chu, Iek-Heng; Zhang, X. -G. Cheng, H.-P., PHYSICAL REVIEW B Volume: 91 Issue: 19 Article Number: 195442 Published: MAY 28 2015
5. Electronic resistances of multilayered two-dimensional crystal junctions, Yun-Peng Wang, James Fry, Xiaoguang Zhang and Hai-Ping Cheng (submitted 2015)
6. Resistance of Ag-silicene-Ag junctions: A combined nonequilibrium Green's function and Boltzmann transport study, Wang, Yun-Peng; Fry, J. N.; Cheng, Hai-Ping PHYSICAL REVIEW B Volume: 88 Issue: 12 Article Number: 125428 Published: SEP 23 2013
7. Plane-wave transport method for low-symmetry lattices and its application By: Srivastava, Manoj K.; Wang, Yan; Zhang, X. -G.; Cheng, Hai-Ping, PHYSICAL REVIEW B Volume: 86 Issue: 7 Article Number: 075134 Published: AUG 20 2012
8. All-electron self-consistent GW in the Matsubara-time domain: Implementation and benchmarks of semiconductors and insulators By: Chu, Iek-Heng; Trinastic, Jonathan P.; Wang, Yun-Peng; Eguiluz, AG; Kozhevnikov, A; Schultheiss, TC; CHENG, Hai-Ping. PHYSICAL REVIEW B Volume: 93 Issue: 12 Article Number: 125210 Published: MAR 28 2016
9. Manipulating the Phonon Bottleneck in Graphene Quantum Dots: Phonon-Induced Carrier Relaxation within the Linear Response Theory, By: Trinastic, Jonathan P.; Chu, Iek-Heng; Cheng, Hai-Ping, JOURNAL OF PHYSICAL CHEMISTRY C Volume: 119 Issue: 39 Pages: 22357-22369 Published: OCT 1 2015

Publications

1. First-principles simulations of a graphene-based field-effect transistor Wang, Yun-Peng; Cheng, Hai-Ping, PHYSICAL REVIEW B Volume: 91 Issue: 24 Article Number: 245307 Published: JUN 12 2015
2. Electron transport in graphene/graphene side-contact junction by plane-wave multiple-scattering method, Li, Xiang-Guo; Chu, Iek-Heng; Zhang, X. -G. Cheng, H.-P., PHYSICAL REVIEW B Volume: 91 Issue: 19 Article Number: 195442 Published: MAY 28 2015
3. All-electron self-consistent GW in the Matsubara-time domain: Implementation and benchmarks of semiconductors and insulators By: Chu, Iek-Heng; Trinastic, Jonathan P.; Wang, Yun-Peng; Eguiluz, AG; Kozhevnikov, A; Schultheiss, TC; CHENG, Hai-Ping. PHYSICAL REVIEW B Volume: 93 Issue: 12 Article Number: 125210 Published: MAR 28 2016
4. Manipulating the Phonon Bottleneck in Graphene Quantum Dots: Phonon-Induced Carrier Relaxation within the Linear Response Theory, By: Trinastic, Jonathan P.; Chu, Iek-Heng; Cheng, Hai-Ping, JOURNAL OF PHYSICAL CHEMISTRY C Volume: 119 Issue: 39 Pages: 22357-22369 Published: OCT 1 2015
5. Physisorption and Chemisorption on Silver Clusters By: Schmidt, Martin; Masson, Albert; Cheng, Hai-Ping; et al. CHEMPHYS-CHEM Volume: 16 Issue: 4 Pages: 855-865 Published: MAR 16 2015
6. Electronic resistances of multilayered two-dimensional crystal junctions, Yun-Peng Wang, James Fry, Xiaoguang Zhang and Hai-Ping Cheng (submitted 2015)
7. First-principles studies of electric field effects on the electronic structure of trilayer graphene, Yun-Peng Wang, Xiang-Guo Li, James N. Fry, and Hai-Ping Cheng (Submitted 2016)
8. Two-dimensional lateral GaN/SiC heterostructures: first-principles studies of electronic and magnetic properties, Guo-Xiang Chen, Xiang-Guo Li, Yun-Peng Wang, James N. Fry, and Hai-Ping Cheng (submitted 2016).

Quantum Dynamics in Complex Magnets: Excitations, Transport, and Disorder

Principal Investigator: Alexander Chernyshev

Institution: Department of Physics and Astronomy, University of California, Irvine
sasha@uci.edu

Project Scope

The central objective of this program is the study of quantum effects in complex magnets with a particular focus on their dynamical and transport properties, and those induced or influenced by disorder. Examples of the focus topics include the dynamical properties of quantum ferromagnets on the geometrically-frustrated lattices, which have recently attracted attention due to their unusual transport properties, the order-by-disorder phenomena and enigmatic ordered phases in anisotropic antiferromagnets, the experimentally puzzling spectral anomalies in the transverse-field Ising and ladder materials, the disorder-induced scattering in noncollinear magnets, and the effect of the phonon scattering in the thermal transport properties of one-dimensional spin systems. These research topics are closely connected and progress in one of them will influence the development of the others. The pursued effort can be expected to explain observed anomalies and yield predictions of new phenomena that will result in a deeper understanding of quantum materials, providing crucial theoretical insights into experiments.

Recent progress

Disorder-induced spin-pseudogap in 1D chains

We have addressed the problem of strong disorder in the spectral properties of 1D spin-1/2 chains [1], a cornerstone example of quantum criticality with scale-free antiferromagnetic correlations. The theoretical component of this work is by the PI in collaboration with a broad experimental team that has involved material-science and neutron-scattering groups from ETH, IFW Dresden, Brookhaven, ORNL, ISIS, and ILL. Both the NMR and the neutron-scattering experiments on one of the best known spin-chain materials SrCuO₂ showed a depletion of the low-energy magnetic states in samples disordered by low-level doping, referred to as the “spin-pseudogap”. This is opposite to the expectations from the strong-disorder Renormalization Group (RG) theory, which predicts *divergent* low-energy density of states and spin structure factor.

The main message of our work is that the spin dynamics of $S=1/2$ antiferromagnetic chains can be fully explained by the effective fragmentation of the spin chains by the screened defects, regardless of the nature of the latter [in-chain or out-of-chain]. We have also argued that such a pseudogap is a *generic* spectral feature of $S=1/2$ antiferromagnetic chains with a low concentration of weak links or defects, a situation which is far from the strong-disorder RG fixed point. Finally, we have demonstrated that defects do not wipe out the universal scaling properties of the correlation functions. The latter are only “masked” by a universal envelope function described by our theory, and can be recovered. A model based on the idea of the effective fragmentation of the spin chains, has *no adjustable parameters*, yet it quantitatively accounts for the experimental data in the entire experimental temperature range and allows to represent the momentum-integrated dynamic structure factor in a universal scaling form, see Fig. 1.

The extreme depletion of spectral weight at low energies [pseudogap] is shown to be due to the exponentially low probability of having very long uninterrupted chain segments in the diluted system. Perhaps the most convincing argument in favor of our interpretation, is that the same envelope function that follows from fragmentation theory can simultaneously reproduce the measurements at all available temperatures. Our approach is argued to be generic and can be applied to describing the spin dynamics in chains with other types of defects, such as vacancies or broken bonds.

Quantum ground-state selection in kagome-lattice antiferromagnets.

The PI in collaboration with Mike Zhitomirsky have significantly advanced theoretical understanding of quantum effects in kagome-lattice antiferromagnets and provided deep insight into the quantum order-by-disorder mechanism, which is important for the broad class of the frustrated spin systems [2,3].

In the search for an unusual ground states and exotic spin dynamics, frustrated spin systems have been the focus of an intense theoretical and experimental investigations in recent years. In frustrated magnetic systems, such as kagome-lattice antiferromagnets, the energies of various spin configurations are massively degenerate. The competition between them often leads to a highly unusual low-temperature spin structures and dynamics. In our work, we have challenged general expectation that quantum fluctuations simply follow thermal ones in selecting the ground state and have presented a rare example

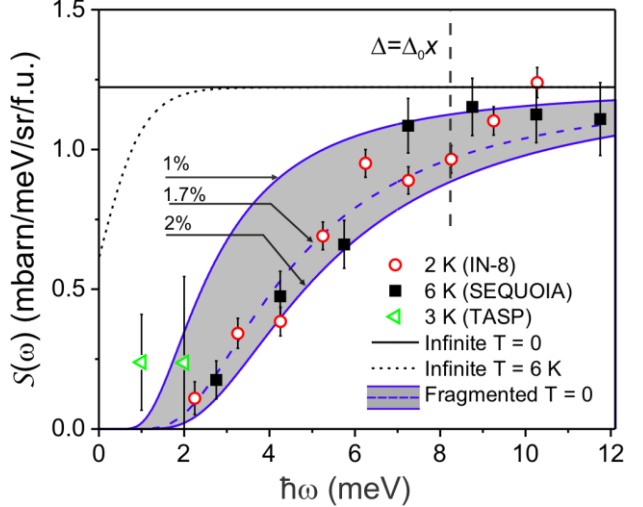


Fig. 1: E-dependence of the momentum-integrated dynamical structure factor with theoretical expectation for defect-free and for doped spin chains.

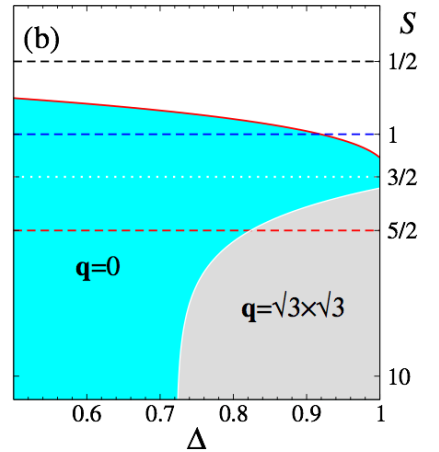


Fig. 2: S- Δ phase diagram of the anisotropic kagome-lattice model.

of the situation when quantum order-by-disorder defies this trend and yields the ground state that is different from the one favored by thermal fluctuations. We have also demonstrated that the order selection is generated by *topologically nontrivial* tunneling processes, making loops around elementary hexagons of the underlying lattice [2]. These non-trivial paths naturally generate a new energy scale in the system, suggesting a common origin of the unusual scale hierarchy in various ground-state and dynamical properties that are observed in many frustrated models. Based on these findings, we have proposed a tentative phase diagram of the XXZ model on the kagome lattice, see Fig. 2, and suggested further studies. More recently, we have provided further extension of our order-by-disorder study onto related kagome-lattice models [3].

Thermal conductivity of 1D spin-chains.

The PI in collaboration with Alex Rozhkov have recently provided a consistent microscopic theory for thermal transport and scattering in 1D spin chains [4], which stands out from previous attempts at such a theory by having a weak spin-phonon coupling and conforming to the analogy of the phonon scattering to that on impurities. We have successfully fit the available experimental data and discussed possible extensions of our theory. Our approach should be applicable to the thermal conductivity in spin-ladder materials and can be extended to the transport phenomena in a variety of Luttinger liquids and ultracold atomic gases. Numerical verification of our results is also called for.

We have proposed that the heat conductivity by spin excitations can be *quantitatively* described within the bosonization framework with the large-momentum scattering by optical phonons or impurities. For weak impurities, scattering grows stronger at lower temperature, a feature intimately related to a critical character of the $S=1/2$ Heisenberg chains. Taking into account multi-spin-boson processes, it follows naturally from our microscopic calculations that scattering by phonons bears a close similarity to that by weak impurities, except that the phonons are thermally populated and thus control heat transport at high T . This is also in accord with a physical picture of phonons playing the role of impurities for the fast spin excitations. Within this picture, the corresponding mean-free path fits excellently the available experimental data, see Fig. 3.

As a crucial distinction of our study, we have emphasized an important physical constraint on the strength of spin-phonon coupling, which is weak in materials of interest. A simple piece of phenomenological evidence for this criterion is the absence of the spin-Peierls transition in real compounds down to very low temperatures. Our theory easily satisfies the proposed constraint, setting itself apart from previous approaches.

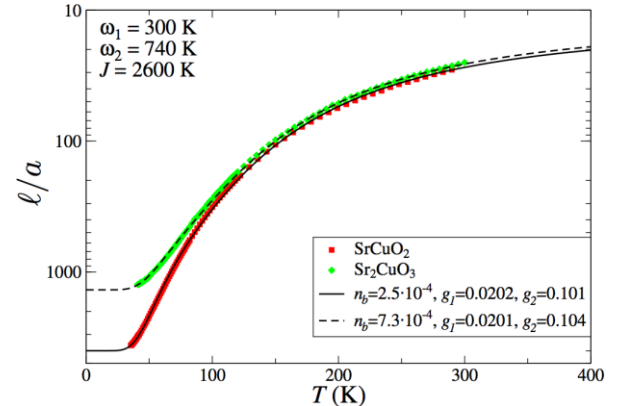


Fig. 3: Mean-free path of spin excitations in Sr_2CuO_3 and SrCuO_2 . Lines are theory fits.

Damped topological magnons in the kagome-lattice ferromagnets

The PI together with Pavel Maksimov (graduate student) have very recently demonstrated [5] that the idea of non-interacting topologically nontrivial bands, familiar from fermionic systems, cannot be trivially transplanted to bosonic systems such as ferromagnets on the geometrically frustrated lattices. The key difference is in the particle-non-conserving terms that are generated by the same interactions that are necessary for the sought-after Berry curvature of the bands. These terms, combined with a ubiquitous degeneracy of the two-magnon continuum, produce a substantial broadening of magnon bands precisely in the ranges of \mathbf{k} and ω that are essential for the topological properties to occur, thus potentially undermining the entire free-band consideration. How the topologically-nontrivial properties of the bands can be defined in the presence of a substantial broadening remains an open question.

Specifically, the anharmonic coupling, facilitated by the Dzyaloshinsky-Moria interaction, and a highly-degenerate two-magnon continuum yield a strong, non-perturbative damping of the high-energy magnon modes in the kagome-lattice ferromagnet. We have provides a detailed account of the effect and proposed further experiments.

Future plans

For the next years, we plan to continue our studies of the dynamical properties and order in complex magnets and of their transport properties. Specifically, next year:

- we will advance the theory of the dynamical response of the XXZ triangular-lattice antiferromagnets in a field, relevant to $\text{Ba}_3\text{CoSb}_2\text{O}_9$
- we plan to provide a theoretical description of the unusual spectral properties of noncollinear antiferromagnets due to a direct magnon-phonon coupling
- we will provide a theoretical support to an experimental discovery of a long-sought field-induced magnon decays in the layered 2D antiferromagnet
- we plan to continue our studies of the dynamical properties of frustrated spin systems, including real kagome-lattice and pyrochlore materials

Publications

- [1] G. Simutis, S. Gvasaliya, M. Mansson, **A. L. Chernyshev**, A. Mohan, S. Singh, C. Hess, A. T. Savici, A. I. Kolesnikov, A. Piovano, T. Perring, I. Zaliznyak, B. Buchner, and A. Zheludev, "Spin pseudogap in Ni-doped SrCuO_2 ", **Phys. Rev. Lett.** **111**, 067204 (2013).
- [2] A. L. Chernyshev and M. E. Zhitomirsky, "Quantum Selection of Order in an XXZ Antiferromagnet on a Kagome Lattice", **Phys. Rev. Lett.** **113**, 237202 (2014).
- [3] A. L. Chernyshev and M. E. Zhitomirsky, "Order and excitations in large-S kagome-lattice antiferromagnets", **Phys. Rev. B** **92**, 144415 (2015). (Editors' Suggestion).
- [4] A. L. Chernyshev and A. V. Rozhkov, "Heat Transport in Spin Chains with Weak Spin-Phonon Coupling", **Phys. Rev. Lett.** **116**, 017204 (2016).
- [5] A. L. Chernyshev, and P. A. Maksimov, "Damped Topological Magnons in the Kagome-Lattice Ferromagnets", **arxiv:1606.09249** (2016).

DYNAMICS OF THE MAGNETIC FLUX IN SUPERCONDUCTORS
DOE/BES Grant No. DE-FG02-93ER45487

Principal Investigator: Dr. Eugene M. Chudnovsky, Distinguished Professor
Department of Physics and Astronomy
Herbert H. Lehman College & CUNY Graduate School
The City University of New York
250 Bedford Park Boulevard West, Bronx, NY 10468-1589
Email: Eugene.Chudnovsky@Lehman.CUNY.edu

Keywords: random fields, magnets, flux lattices

Project Scope

The ongoing work on the DOE/BES grant and research planned for the nearest future include analytical and large scale numerical studies of the effect of randomness on classical and quantum systems with continuous-symmetry order parameter, as well as studies of S/F/S/ Josephson junctions. This abstract focuses on the first topic in application to flux lattices, Josephson junction arrays, spin systems, and charge density waves. Previously we have demonstrated (PRL 2014) that the behavior of the n -component order parameter in d dimensions is governed by the presence and structure of topological defects. These findings have been confirmed numerically on lattices containing up to one billion sites. They have been extended to the investigation of glassy properties and memory effects in systems with quenched randomness, to models with dilute random fields in applications to systems with impurities, and to random-anisotropy systems. Mapping of quantum models of Josephson-junction arrays onto classical XY spin models have allowed us to perform comprehensive studies of persistent currents and effects of disorder in 1d Josephson junction rings and 2d Josephson junction arrays.

Recent Progress

To study the metastability effects in the random field model in three dimensions we have performed the most extensive to date numerical simulations on lattices containing up to one billion sites [1]. Glassy properties and memory effects have been elucidated. Thermal stability of the ordered state has been studied by Monte Carlo method. Evidence has been found of the qualitative difference of the ground state of the XY model and the ground state for the three-component order parameter.

Our study [2] of the effect of dilute random field on a continuous-symmetry order parameter relates to pinned vortex lattices, pinned charge-density waves, and ferromagnets with magnetic impurities, see Figs. 1a and 1b. We have argued and then proved numerically on lattices containing a few million sites that the critical current in superconductors should scale as square of the concentration c_r of strong pinning centers. In a similar manner the area of the hysteresis loop in a ferromagnet containing magnetic impurities scales as square of the concentration of impurities. The correlation length of the charge density wave scales inversely with the

concentration of pinning centers. Our predictions can be directly tested in experiments on superconductors, ferromagnets, and charge density waves with impurities.

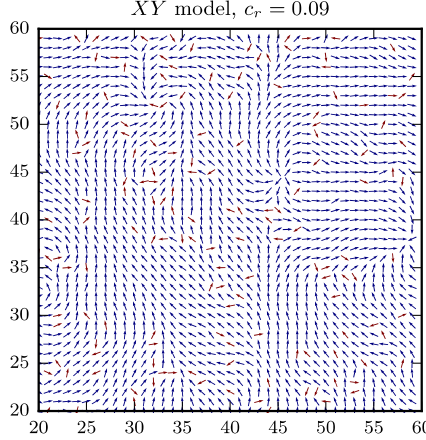


Fig. 1a: XY model with diluted random field

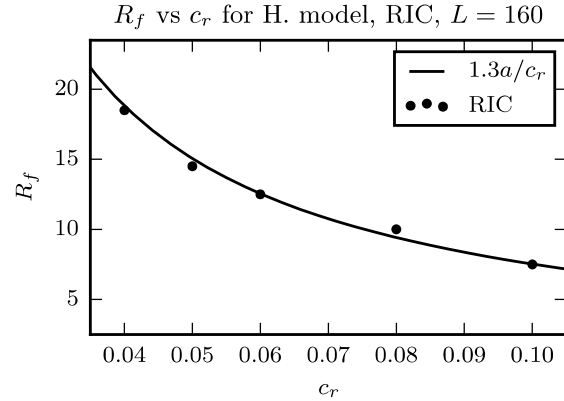


Fig. 1b: Correlation length vs impurity concentration

We also investigated numerically and analytically the coercivity of amorphous and sintered magnets [3], see Figs. 2a and 2b. Coercivity of a 3d amorphous ferromagnet has been found to scale as the fourth power of the local magnetic anisotropy D_R and the sixth power of the amorphous structure factor (the sixth power of the grain size for a nanosintered magnet). Numerical results agree with analysis based upon Flory-Imry-Ma argument. Our findings suggest a path towards manufacturing of extremely soft magnetic materials.

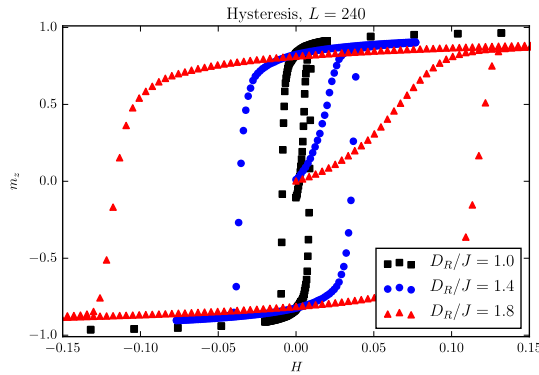


Fig. 2a: Unscaled hysteresis curve

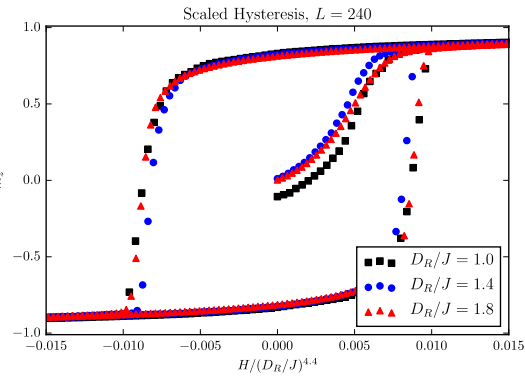


Fig. 2b: Scaled hysteresis curve

We have studied the persistent current in a ring consisting of $N \gg 1$ Josephson junctions threaded by the magnetic flux [4]. When the dynamics of the ring is dominated by the capacitances of the superconducting islands the system is equivalent to the XY spin system in 1+1 dimensions at the effective temperature $T^* = (2JU)^{1/2}$, with J being the Josephson energy of the junction and U being the charging energy of the superconducting island. The numerical problem is challenging due to the absence of thermodynamic limit and slow dynamics of the Kosterlitz-Thouless transition. It has been investigated on lattices containing up to one million sites.

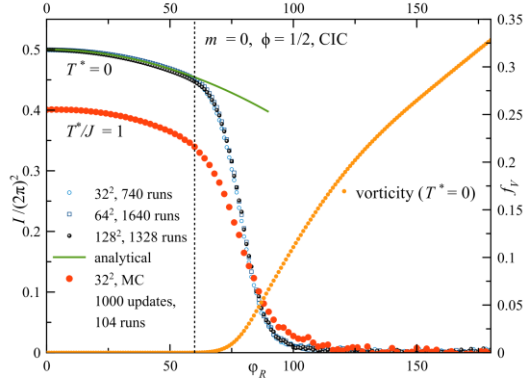


Fig. 3a: Persistent current vs random phase

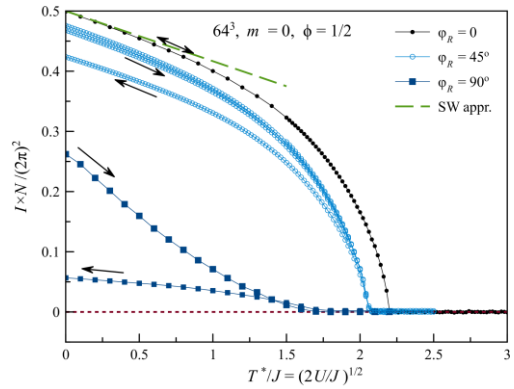


Fig. 3b: Persistent current vs quantum temperature

Switching to two dimensions, we proposed a new system for the study of the persistent current: A Josephson junction array wrapped around a cylinder [5]. The $T = 0$ quantum statistical mechanics of the array is now equivalent to the statistical mechanics of a classical XY spin system in 2+1 dimensions. For weak disorder and $T^* \ll J$ the dependence of the persistent current on the strength of the phase disorder φ_R and on T^* computed numerically agrees quantitatively with the analytical result derived within the spin-wave approximation, see Figs. 3a and 3b. The high- T^* and/or strong-disorder behavior are dominated by instantons corresponding to the vortex loops in 2+1 dimensions. The current becomes destroyed completely at the quantum phase transition into the Cooper-pair insulating phase.

Future Plans

Spin models with quenched disorder describe behavior that, among other systems, is relevant to the pinning of flux lattices, properties of amorphous and sintered magnets, disordered Josephson junction arrays, and spin density waves with impurities. Despite significant effort, many fundamental questions in this area of condensed matter physics remain unanswered. To answer them we plan further large-scale simulations on record-size lattices that are required by large correlation lengths pertinent to systems with weak disorder. Such simulations, that were not possible in the past, have become available in recent years due to increased computational powers.

Our recent numerical studies of the Kosterlitz-Thouless (KT) transition revealed some interesting features in the unbinding of vortex-antivortex pairs, see Figs. 4a and 4b. Contrary to the popular narrative we have not observed any dramatic behavior in the average distance between vortices or for the total vorticity at the KT transition, although the computed persistent current in the Josephson junction array does become zero at the KT temperature. Rather surprisingly, however, the average size of the vortex pair and the vorticity remain small at the KT transition and then increase gradually on raising temperature. Somewhat stronger temperature dependence has been observed in the average distance to the first, second, and third nearest antivortex. These are preliminary results that will be investigated on lattices containing $10^4 \times 10^4$ sites. The dynamics of the process will be studied as well within the stochastic Landau-Lifshitz-Langevin equation. Although it requires substantial computing resources we have prior experience with such

computations. Pinning of vortices by quenched disorder is expected to have a profound effect on the transition.

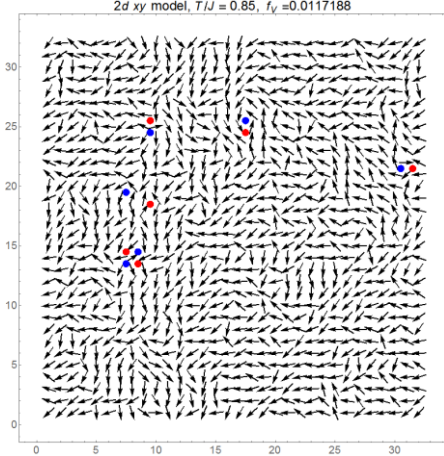


Fig. 4a: Vortex pairs in the XY model

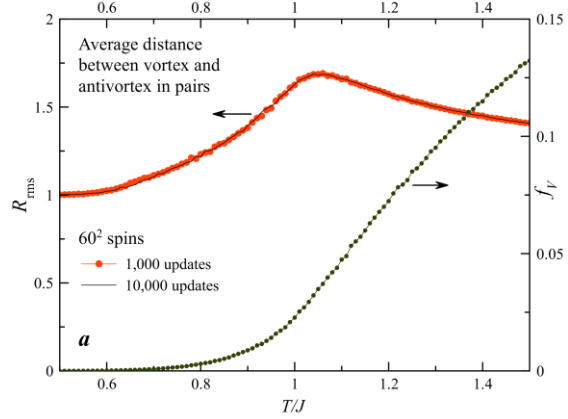


Fig. 4b: Size of vortex pair and vorticity vs temperature

Similar studies will be conducted for the Heisenberg model in two dimensions that possesses skyrmions and for the Heisenberg model in three dimensions that possesses hedgehogs. Previously we have computed the lifetime of a microscopic skyrmion against collapse due to the discreteness of the crystal lattice. Analytical theory agreed well with numerical results. The disorder has a tendency to stabilize skyrmions by providing an additional length that together with the lattice spacing breaks the scale invariance. We plan to study the conditions of pinning and stabilization of skyrmions analytically and numerically. Thermal properties of skyrmion and hedgehog glasses generated by quenched randomness will be investigated.

References

1. D. A. Garanin and E. M. Chudnovsky, Ordered vs Disordered States of the Random-Field Model in Three Dimensions, European Physics Journal B **88**, 81-(19) (2015).
2. T. C. Proctor and E. M. Chudnovsky, Effect of Dilute Random Field on Continuous-Symmetry Order Parameter, Physical Review B **91**, 140201-(4)(R) (2015).
3. T. C. Proctor, E. M. Chudnovsky, and D. A. Garanin, Scaling of Coercivity in a 3d Random Anisotropy Model, Journal of Magnetism and Magnetic Materials **384**, 181-185 (2015).
4. D. A. Garanin and E. M. Chudnovsky, Quantum Decay of the Persistent Current in a Josephson Junction Ring, Physical Review B **93**, 094506-(9) (2016).
5. D. A. Garanin and E. M. Chudnovsky, Persistent Current in a 2D Josephson Junction Array Wrapped Around a Cylinder, arXiv:1605.08451 [cond-mat.supr-con] 26 May 2016.

Publications (August 2014 – July 2016, DOE/BES support acknowledged)

1. R. Zarzuela, E. M. Chudnovsky, and J. Tejada, Josephson Junction with a Magnetic Vortex, *Journal of Superconductivity and Novel Magnetism* **28**, 1959-1965 (2015).
2. D. A. Garanin and E. M. Chudnovsky, Ordered vs Disordered States of the Random-Field Model in Three Dimensions, *European Physics Journal B* **88**, 81-(19) (2015).
3. T. C. Proctor and E. M. Chudnovsky, Effect of Dilute Random Field on Continuous-Symmetry Order Parameter, *Physical Review B* **91**, 140201-(4)(R) (2015).
4. T. C. Proctor, E. M. Chudnovsky, and D. A. Garanin, Scaling of Coercivity in a 3d Random Anisotropy Model, *Journal of Magnetism and Magnetic Materials* **384**, 181-185 (2015).
5. D. A. Garanin and E. M. Chudnovsky, Quantum Decay of the Persistent Current in a Josephson Junction Ring, *Physical Review B* **93**, 094506-(9) (2016).
6. J. Tejada, R. Zarzuela, A. Garcia, I. Imaz, J. Espin, D. Maspoch, and E. M. Chudnovsky, Enhanced Spin Tunneling in a Molecular Magnet Mixed With a Superconductor, *Journal of Superconductivity and Novel Magnetism* **29**, 5096-5099 (2016)
7. E. M. Chudnovsky, Quantum Tunneling of the Magnetic Moment in the S/F/S Josephson ϕ_0 -Junction, *Physical Review B* **93**, 144422-(5) (2016).
8. D. A. Garanin and E. M. Chudnovsky, Persistent Current in a 2D Josephson Junction Array Wrapped Around a Cylinder, arXiv:1605.08451 [cond-mat.supr-con] 26 May 2016.

Spin Driven Phenomena in Highly Correlated Materials

Principal Investigator: Professor Piers Coleman,
Department of Physics and Astronomy, Rutgers University, Piscataway NJ 08854.
coleman@physics.rutgers.edu

Project Scope

My current DOE sponsored research covers three research areas.

- 1) Topological Kondo Insulators (TKI's) particularly SmB₆.
- 2) Iron Based Superconductivity.
- 3) Emergent Kosterlitz Thouless phases in frustrated 2D Heisenberg Antiferromagnets.

Topological Kondo Insulators: In 2009 the PI and collaborators predicted that the Kondo insulators such as SmB₆ are candidate strongly interacting topological insulators, or Topological Kondo Insulators (TKI). Growing support for the topological character of this material has since come from the confirmation of robust conducting surfaces and from ARPES spectroscopy. Many other probes, such as de Haas van Alphen, optics and tunneling are starting to reveal unexpected aspects of SmB₆ which make this a very active field of current research.

During the past funding cycle, the PI and collaborators studied how magnetic interactions in a topological Kondo insulator give rise to properties that delineate it from weakly interacting topological band insulators.

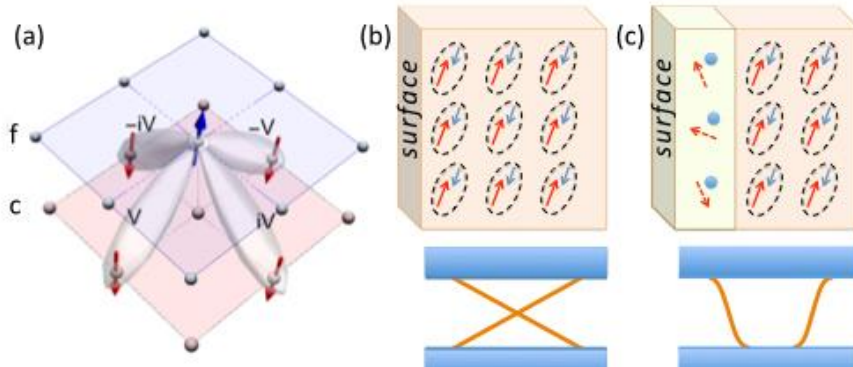


Figure 1 Kondo breakdown at the surface of a topological Kondo insulator (§3). (a) Opposite parities of the f and d orbitals generate a non-local p-wave hybridization. Surface states (b) before and (c) after Kondo breakdown. The Dirac node drops into the valence band, giving rise to light, fast surface states.

In [3] we set out to understand why the surface states seen in ARPES measurements are much lighter than expected for heavy electrons. The key idea we developed is that a break-down of the Kondo effect occurs on the surface ("Kondo breakdown"), which acts to dope and lighten the surface states. Unlike one dimension, topological behavior survives surface Kondo breakdown in three dimensions, with interesting consequences (see Fig. 1). The removal of f-electrons from the surface Kondo singlets has the effect of "doping" the surface states, enlarging the Fermi surface

area of the topological Dirac surface states while also raising the Fermi velocity by a factor of about ten (see Fig 1(b) and 1(c)); both results agree with ARPES experiments. Additionally, the Dirac node is submerged into the valence band, so that the resulting surface states are more robust. From these results, we showed that the minimal model for the surface of a topological Kondo insulator is a chiral Kondo lattice, with local moments interacting with a Dirac sea of chiral, topological surface conduction states.

[5] discusses the paradox posed by recent quantum oscillation experiments in SmB_6 , which interpret the observed de Haas van Alphen oscillations in terms of a 3D bulk Fermi surface, even though SmB_6 is bulk insulator up to very high magnetic fields ($H_c > 100\text{T}$). Moreover a deviation from Lifshitz-Kosevich formula at low temperatures suggests an unconventional character for the quasiparticles, possibly quantum criticality. In this first work we argued that topological surface states are sufficient to explain the data.

Iron Based Superconductors: One of the key questions in iron based superconductors concerns the mechanism by which the pairing avoids the strong Coulomb interaction on the iron sites. In the quasi-particle band structure of the iron-based superconductors the hopping between t_{2g} orbitals at different sites mixes the orbital character in a momentum-dependent fashion, playing the role of an orbital Rashba field. This observation motivated us to propose [6] the idea of orbital triplet pairing, the orbital analogue of the fully gapped condensate in He-3B.

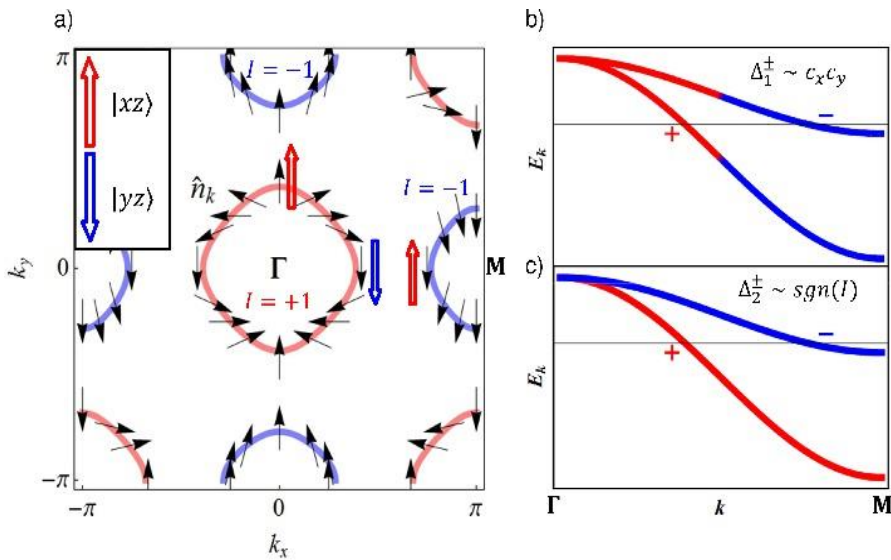


Figure 2 (a) Orientations of the orbital Rashba field n_k (black arrows) and orbital moment I (hollow arrow) in a two-orbital model of Fe-based superconductors after [8], where “up” and “down” represent xz and yz orbital content. The orbital Rashba field n_k rotates twice passing around the Γ and Γ' point, leading to a non-trivial topology.

(b) Conventional s^\pm pairing, in which the sign of the gap is determined by the $\cos k_x \cos k_y$ form factor.

(c) orbital triplet s^\pm pairing in which the sign of the gap is determined by the orbital helicity $I = I^\square \cdot n_k$.

[8] developed a theory for an orbitally entangled s^\pm state (Fig. 2 c), containing a condensate of d-wave pairs, concealed by their entanglement with the iron-orbitals. We showed how it is possible to entangle d-wave ($L = 2$) pairs with the internal angular momenta I of the iron-orbitals to form a low spin ($J = L + I = 0$) s^\pm singlet superconductor. This state is symmetry-equivalent to the conventional s^\pm state on the Fermi surface, but differs topologically in the entanglement of its

orbitals away from the Fermi surface. Our model permits us to understand the transition to a nodal gap state, when the electron pockets are eliminated in KFe_2As_2 as a reconfiguration of the orbital and internal atomic angular momenta into a high spin ($J = L + I = 4$) configuration; the related transition into a fully gapped state under pressure can also be interpreted as a high-to-low spin phase transition of the Cooper pairs. We proposed that polarized laser ARPES measurements can be used to detect a change in orbital entanglement that would accompany formation of this condensate.

BKT order in a frustrated Heisenberg Model: This research examines the role of frustration effect in producing new forms of magnetic order: an example is the fluctuation-induced Z_2 order in the J_1-J_2 Heisenberg model, thought to be responsible for the nematic phase observed in the iron-pnictides. In [9-11], we sought new generalizations of this mechanism.

Conventional 2D Heisenberg magnets do not develop algebraic order at finite temperatures, because the interaction of the Goldstone modes drives the spin-wave stiffness to zero. However, in his pioneering work on this topic, Alexander Polyakov speculated that algebraic long-range order might occur were the system to develop a “vacuum degeneracy”. [9-11] analyzed a frustrated classical 2D Heisenberg model in which order-from disorder provides a mechanism to realize Polyakov’s hypothesis through development of an emergent XY order parameter. A new aspect of this work was the use of Friedan’s Gravitational “Ricci flow” approach to solve the rather complex scaling equations and to show that the emergent $U(1)$ degree of freedom decouples at long distances. In our theory (see Fig. 3) the emergent $U(1)$ order parameter is subject to a Z_6 order-by-disorder potential at short distances. At intermediate temperatures this potential is irrelevant and scales to zero, leading to emergent power-law correlations. Remarkably, the stiffness of the emergent $U(1)$ order parameter remains finite despite the short-range correlations of the underlying Heisenberg spins. In this XY manifold the binding of logarithmically interacting defect vortices leads to multi-step ordering via two consecutive transitions in the Berezinskii-Kosterlitz-Thouless (BKT) universality class. In [11] we carried out an extensive set of Monte-Carlo simulations which directly detected the development of an emergent XY order parameter and definitively confirmed the associated Berezinskii-Kosterlitz Thouless phase transitions.

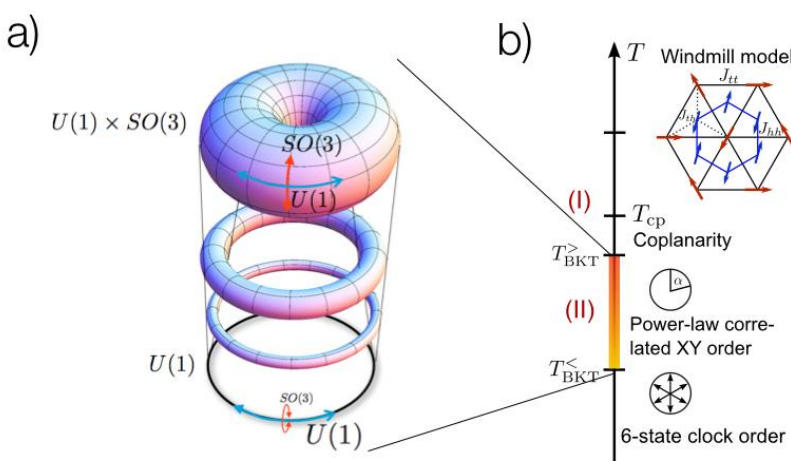


Figure 3. “Ricci Flow”. (a) The manifold of states in the two layer windmill model is $SU(2) \times U(1)$. At long distances, this undergoes a dimensional reduction to a $U(1)$ order parameter representing the relative phase between the upper and lower layer order parameters (b) Temperature Phase diagram for the windmill Heisenberg model, showing power-law phase.

Ongoing and Future work.

Topological Kondo Insulators: More recent data dHva suggests that the observed quantum oscillations may be truly bulk in character. We are currently exploring more radical ideas, based on the idea that in strongly correlated TKI's, there may be gapless Fermi surfaces of Majorana Fermions. We are also exploring the idea of non-symorphic Kondo insulators, and believe that Ce₃Bi₄Pt₃ and CeNiSn may lie in this class [12].

Iron Based Superconductivity: The original work on orbital triplet pairing was restricted to a simple 2 orbital model. We are currently expanding this work to a more realistic 3 orbital model and also examining the effects of spin orbit coupling.

Frustrated Magnetism: Developments in molecular beam epitaxy (MBE) make it possible to synthesize new kinds of magnetic structures, in which the geometric frustration of conventional magnetic order can give rise to new kinds of emergent order. Working in collaboration with materials experts, we will analyze the physics of frustrated, bilayer Heisenberg magnets, seeking to understand the new kinds of emergent magnetic order than result from magnetic frustration.

Publications

- 1) *Cubic Topological Kondo Insulators*, V. Alexandrov, M. Dzero, P. Coleman, Phys. Rev. Lett. **111**, 226403, (2013).
- 2) *End States in a 1-D Topological Kondo Insulator* V. Alexandrov, P. Coleman, Phys. Rev. B **90**, 115147 (2014).
- 3) *Kondo Breakdown in Topological Kondo Insulators*, V. Alexandrov, P. Coleman, O. Erten, Phys. Rev. Lett. **114**, 177202 (2015).
- 4) *Topological Kondo Insulators*, M. Dzero, J. Xia, V. Galitski & P. Coleman, Annual Review of Condensed Matter Physics, Volume **7**, 249-280 (2016).
- 5) *Possible observation of Kondo breakdown in the Quantum oscillations of SmB₆*, O. Erten, P. Ghaemi and P. Coleman, Phys. Rev. Lett. **116**, 046403 (2016).
- 6) *TAO pairing: a fully gapped pairing scenario for the Iron-Based Superconductors*, T. Tzen Ong, Piers Coleman, Phys. Rev. Lett. **111**, 217003 (2013).
- 7) *³He-R: A Topological s[±] Superfluid with Triplet Pairing*, T. Tzen Ong and P. Coleman, Phys. Rev. B **90**, 174506 (2014).
- 8) *Entangled Orbital Triplet Pairs in Iron-Based Superconductors*, T. Tzen Ong, P. Coleman, J. Schmalian, Proceedings of the National Academy of Sciences, 113, 5486-5491 (2016).
- 9) *Emergent Critical Phase and Ricci Flow in a 2D Frustrated Heisenberg Model*, P. Orth, P. Chandra, P. Coleman, J. Schmalian, Phys. Rev. Lett. **109**, 237205 (2012).
- 10) *Emergent Criticality and Friedan Scaling in a 2D Frustrated Heisenberg Antiferromagnet*, P. Orth, P. Chandra, P. Coleman, J. Schmalian, Phys. Rev. B **89**, 094417- 47 (2014).
- 11) *Emergent Powerlaw Phase in the 2D Heisenberg Windmill Antiferromagnet: a Computational Experiment*, B. Jeevanesan, P. Chandra, P. Coleman and P. Orth, Phys. Rev. Lett. **115**, 177201 (2015).
- 12) *Mobius Kondo Insulators*, Po-Yao Chang, O. Erten and P. Coleman, Nature Physics (submitted) 2016.

First Principles Predictions of Phase Stability in Complex Oxides

Valentino R. Cooper, Oak Ridge National Laboratory

Keywords: Oxides, Piezoelectrics, Interfaces, Ferromagnetism, Antiperovskites

Project Scope

The goal of this project is to use first principles methods to predict materials with enhanced properties that can be synthesized and remain active under device relevant conditions. This project aims to develop and implement robust, high-throughput computational approaches for exploring phase stability. The ultimate goal is to facilitate the prediction-to-synthesis process through a synergistic effort involving (i) electronic structure calculations for properties predictions, (ii) phenomenological/empirical models and Monte Carlo simulations for examining phase stability and (iii) experimental validation. The abundance of possible cation chemical identities and arrangements makes complex oxides (such as perovskites) an ideal playground for first principles studies. This variability gives rise to an array of physical, chemical, electrical and magnetic properties as well as possible competing structures. This effort emphasizes the study of complex oxides; primarily ferroelectric/piezoelectric oxides, multiferroics and oxide interfaces and surfaces.

Recent Progress

Towards high-response, Pb-free piezoelectrics - Experimental Validation: [V. R. Cooper *et al.* *J. Adv. Dielect.* 6, 1650011 (2016)] A key challenge to predicting material synthesizability is the assessment of stability relative to competing phases/end member compounds in the case of a solid solution. Previously, using density functional theory calculations combined with a simple entropy of mixing model, we predicted that a solid solution of 50% $\text{Bi}(\text{Zn}_{1/2}\text{Ti}_{1/2})\text{O}_3$ (BZT)-50% $\text{La}(\text{Zn}_{1/2}\text{Ti}_{1/2})\text{O}_3$ (LZT) could be stabilized, despite experimental evidence of immiscibility in solid solutions containing large relative fractions of either end member compounds (see Figure 1a). Recently, through collaboration with ORNL synthesis efforts, we were able to demonstrate that this solid solution could indeed be formed. Figure 1 depicts the X-ray crystal diffraction, XRD, spectra for an initial synthesis attempt of 50/50 BZT-LZT. The diffraction pattern shows peaks consistent with a cubic or pseudo-cubic perovskite structure, but not consistent with other non-bismuth containing perovskite phases. Although some impurities, most likely excess Bi oxides, are present, these initial synthesis

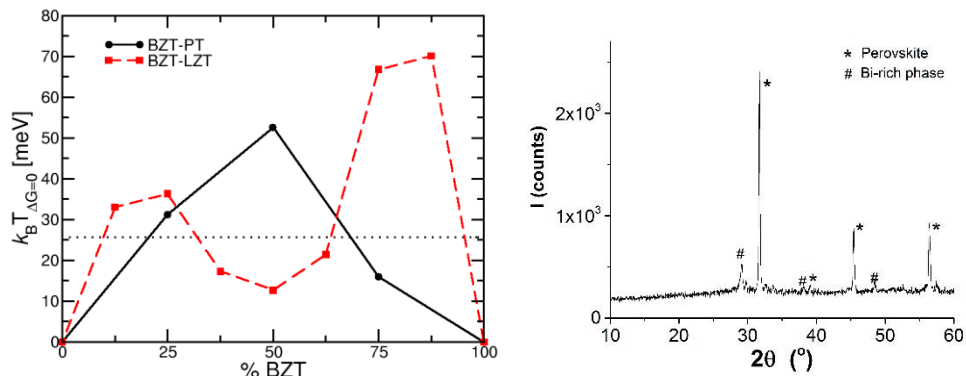


Figure 1 (left) Temperature (in units of $k_B T$ [meV]) at which $\Delta G=0$ (Gibbs free energy including the simple entropy of mixing model) for the BZT-PT and BZT-LZT solid solutions. The dotted line indicates $k_B T$ at room temperature, below which it is assumed that a solid solution will form. (right) XRD spectra for the 50% BZT/50% LZT solid solution.

efforts signal promise for growing solid solutions of this phase. Furthermore, our predictions for the regions of stability in the BZT–PbTiO₃ (PT) phase diagram are in excellent agreement with regards to the phases of BZT-PT that have been grown to date. This approach has most recently been applied to the prediction of the presence of a morphotropic phase boundary in a Pb-free piezoelectric: BZT-LZT-SrTiO₃ (BZT-LZT-ST), an analog to our previous effort on the BZT-LZT-PT compound [Voas *et al.* *to be submitted*].

Towards high-response, Pb-free piezoelectrics – Temperature-dependent phase transitions: [Yuk *et al.* *to be submitted*] Some of the most common tactics to efficiently study ferroelectric phase transitions include: 1) performing Monte Carlo (MC) simulations on first-principles derived effective Hamiltonians, or 2) using atomistic potentials, such as the shell-model or bond-valence approaches, to predict phase transition temperatures via molecular dynamics simulations (MD). Uncertainties in DFT exchange-correlation functionals, however could have fundamental consequences for these predictions.

In preparation for finite temperature studies, we have studied how the choice of exchange-correlation functionals (LDA, PBE, PBEsol and vdW-DF-C09) affects the prediction of the structural and ferroelectric properties of prototypical ferroelectric perovskites: PbTiO₃ (PTO), BaTiO₃ (BTO), and KNbO₃ (KNO). As expected, we find that LDA underestimates both lattice parameters and spontaneous polarizations, while PBE overestimates them. Overall, vdW-DF with C09 exchange (vdW-DF-C09) and PBEsol give the best agreement with the experimental values. Figure 2 depicts the DFT spontaneous polarizations relative to experiment ($P_{\text{DFT}}/P_{\text{Expt}}$) as a function of the DFT bulk modulus relative to experiment ($B_{\text{DFT}}/B_{\text{Expt}}$). These values are particularly important when predicting the electromechanical coupling (piezoelectric response in these materials). Here, again we see the importance of choice of exchange correlation functional for getting a balanced description of these quantities. The overall strong performance of a functional which contains dispersion interactions (vdW-DF-C09) has significant consequences for surface studies that may explore the use of such ferroelectrics as dynamically activated materials for processes such as surface catalysis. Furthermore, it demonstrates the potential for using vdW-DF-C09 as a general-purpose functional for studying a wide range of materials and physical/chemical properties. Current efforts now seek to employ these different functionals with MC methods in order to examine how discrepancies in the predictions of macroscopic properties affect predicted phase transition temperatures. In the process, we seek to build a feasible MC code that interfaces directly with current DFT codes to evaluate the energy of a configuration. This will enable the prediction of finite-temperature responses/behavior of complex, multiphase/multicomponent materials which are often inhibited by the ability to parameterize effective Hamiltonians or empirical potentials.

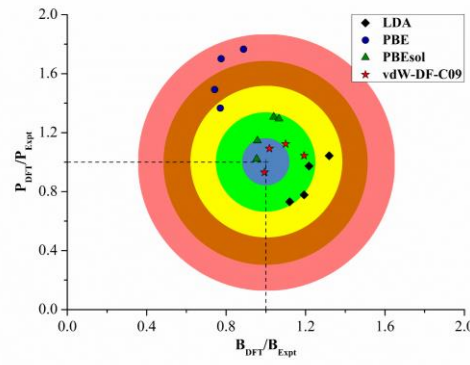


Figure 2 Comparison of bulk modulus (BDFT) and spontaneous polarizations (PDFT) of PTO, BTO, and KNO in the different crystal phases relative to the experimental values.

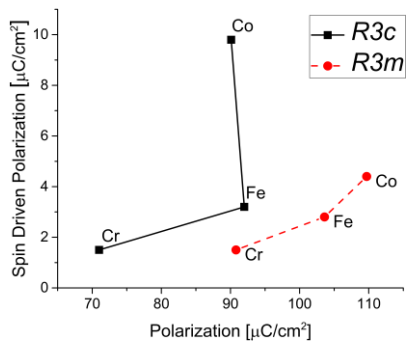


Figure 3 Polarization versus spin driven polarization for BiCrO_3 (Cr), BFO (Fe) and BiCoO_3 (Co) in both the $R3c$ (green squares) and $R3m$ (red circles) phases. The $R3m$ phase exhibits an almost linear dependence of SDP on the polarization, whereas the $R3c$ phase has a strong deviation from linearity for BiCoO_3 ; arising from enhanced couplings to anti-ferrodistortive modes.

such as BiCrO_3 and BiCoO_3 . We found that in their respective ground states BiCrO_3 ($C2/c$) and BiCoO_3 ($P4mm$) only exhibit modest SDPs of -0.08 and $-2 \mu\text{C}/\text{cm}^2$, respectively. However, in the BFO $R3c$ space group, both materials see an enhancement in the SDP to -1 and $-10 \mu\text{C}/\text{cm}^2$ for BiCrO_3 and BiCoO_3 , respectively. The SPD in BiCoO_3 is the largest predicted SDP to date. Interestingly, we find that transformation to the $R3m$ structure only shows a modest decrease in the SDP in BFO and BiCrO_3 . However, BiCoO_3 exhibits a large decrease in the SDP to $-4 \mu\text{C}/\text{cm}^2$. This large change in SDP in BiCoO_3 suggests that the order parameter for the SDP in the $R3c$ phase is not simply the polar ferroelectric modes as can be induced for the $R3m$ phase (see Figure 3). Instead, we find large couplings to the antiferrodistortive rotational modes as often seen in hybrid improper ferroelectrics. As such, we can conclude that the SDP in the BiCoO_3 $R3c$ phase are in part driven by these improper order parameters. Studies of the strain-dependence of the BiCoO_3 $R3c$ phase versus the ground state $P4mm$ phase indicates that it should be possible to stabilize the $R3c$ phase through epitaxial growth at roughly 3% tensile strain. These results demonstrate that the use of couplings of magnetic degrees of freedom with antiferrodistortive modes (i.e. octahedral rotations) and strain may be a unique route towards the enhancement of SDP in multiferroic perovskite oxides.

Defects in hybrid, antiperovskites: [KC *et al.* *in preparation*] Inorganic lithium-ion-conducting solid electrolytes are attractive for their higher energy densities, and reduced safety issues relative to conventional organic based liquid electrolytes. However, challenges exist in achieving high ionic conductivity and maintaining electrochemical stability. Of particular concern are the presence and identity of defects in these materials as they have consequences for both material stability and Li-ion mobility.

In this project, we are exploring the stability of vacancies and anti-site defects in a model antiperovskite Li_3OBr in order to gain an understanding of the relevant defect populations in this material. To this end we are working on developing a thermodynamic model to give *ab initio*

predictions of the reference temperature-dependent chemical potentials in order to obtain accurate predictions of the formation energies of each of these species. This will allow us to predict relative temperature-dependent defect populations without any experimental input as standard for these types of studies. We anticipate that this approach will help provide us with more direct comparisons with experimental data on solid electrolytes. Further work will use this information as a starting point for identifying the experimental signatures in these materials as we previously did by modeling Raman frequencies for the Li_2MnO_3 system [*Ruther et al. J. Phys. Chem. C* **119**, 18022 (2015)]. Additional work will explore ion mobility within these materials in an attempt to understand how this material could be used in the context of a Li-ion battery.

Future Plans

In the upcoming year, we plan to continue our efforts towards understanding the prediction-to-synthesis cycle. Focus will remain on (i) the discovery of high performance piezoelectrics, (ii) exploring the physics at oxide interfaces and (iii) tailoring the properties of oxide composite materials. The focus of the upcoming year will be on the development and application of methods for examining phase stability. We have already implemented a Wang-Landau (WL) Monte Carlo + Quantum Espresso (QE) code to examine phase transitions in bulk ferroelectrics. In this regard, parallel WL algorithms in coordination with the GPU accelerated version of QE will be exploited through our recently awarded INCITE proposal in order to examine the feasibility of this effort. Simultaneously, we are working on the incorporation of machine learning techniques in order to reduce the number of DFT calls in an effort to accelerate the process. (Currently a project by a summer ASTRO intern at ORNL). After initial studies using this approach to study the effects of exchange-correlation functionals on single component bulk oxides, we will extend these studies to other Pb-free ferroelectrics and multicomponent multiferroics in order to study temperature-dependent phase transitions. Two candidate systems will include $(\text{K},\text{Na})\text{NbO}_3$ system that we previously studied using the special quasirandom structure (SQS) approach and the promising high piezoresponse $\text{Bi}(\text{Zn},\text{Ti})\text{O}_3\text{-La}(\text{Zn},\text{Ti})\text{O}_3\text{-SrTiO}_3$ compound. A large part of the upcoming effort will also be centered on the development of the framework for the exploration of the compositional space using density functional theory. We will continue our collaboration with J. Krogel in the development of the NEXUS high throughput simulation package which is currently interfaced with VASP and Quantum Espresso. We will further investigate how this workflow could be used to assist in the acceleration of the WL-QE approach discussed earlier.

Publications

- H. Dixit, W. Zhou, J.-C. Idrobo, J. Nanda and V. R. Cooper, *Facet dependent disorder in pristine high voltage Lithium-Manganese-rich cathodes* *ACS Nano* **8**, 12710 (2014)
- J. H. You, J. H. Lee, S. Okamoto, V. R. Cooper and H. N. Lee *Strain engineering of the electronic properties in δ -doped oxide superlattices* *J. Phys. D: Appl. Phys.* **48**, 085303 (2015)
- H. Dixit, C. Beekman, W. Siemons, M. Chi, H. M. Christen and V. R. Cooper *Understanding strain-induced phase transformations in BiFeO_3 thin films* *Adv. Sci.* **2**, 1500041 (2015)
- R. E. Ruther, A. M. Pezeshki, H. Dixit, R. L. Sacci, V. R. Cooper, J. Nanda and G. M. Veith *Correlating local structure with electrochemical activity in Li_2MnO_3 : A combined*

experimental and theoretical Raman spectroscopic investigation J. Phys. Chem. C **119**, 18022 (2015)

- H. Dixit, J. H. Lee, J. Krogel, S. Okamoto and V. R. Cooper *Stabilization of weak ferromagnetism by strong magnetic response to epitaxial strain in multiferroic BiFeO₃* Sci. Rep. **5**, 12969 (2015)
- A. Glavic, H. Dixit, V. R. Cooper and A. A. Aczel *Exchange coupling between ferro- and antiferromagnets in NdMnO₃/SrMnO₃ superlattices* Phys. Rev. B (R) **93**, 140413(R) (2016)
- V. R. Cooper, B. K. Voas, C. A. Bridges, J. R. Morris and S. P. Beckman *First principles materials design of novel functional oxides* J. Adv. Dielect. **6**, 1650011 (2016)

Theoretical study of complex collective phenomena

Principal investigator: Prof. Elbio Dagotto [1,2] edagotto@utk.edu

Co-PIs: Dr. Randy Fishman [2] fishmanrs@ornl.gov; Prof. Adriana Moreo [1] amoreo@utk.edu; Dr. Satoshi Okamoto [2] okapon@ornl.gov

[1] Department of Physics, University of Tennessee, Knoxville, TN

[2] Materials Science and Technology Division, Oak Ridge National Lab, Oak Ridge, TN

Project Scope

The overarching goal of this project is to achieve a quantitative understanding of the rich phase diagrams exhibited by materials with complex collective electronic behavior, and to predict functionalities with potential technological value. Materials such as high critical temperature superconductors, frustrated spin systems, and oxide heterostructures display correlated behavior where the motion of one particle is severely affected by the rest and the ensemble behaves as a unique quantum collective state. Often these states emerge from the subtle interplay among many simultaneously active degrees of freedom. Because they have similar energies, these states often compete, and small external fields can drastically alter the material's properties by inducing transitions from one collective state to another.

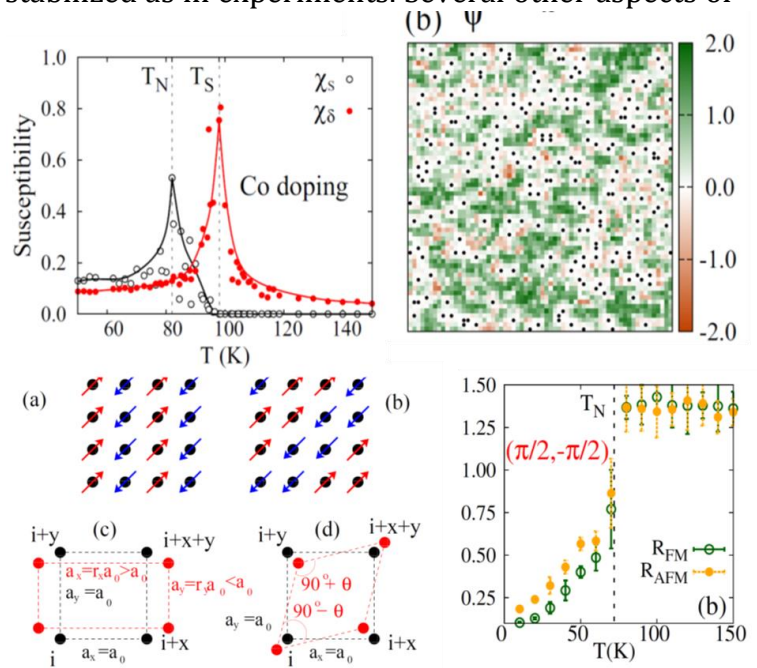
The theoretical study of correlated electronic systems is fundamentally different from the study of simpler materials, such as semiconductors. Typically, model Hamiltonians are used to address the patterns of spin, orbital, and charge that emerge in the ground state due to frustration and phase competition. Because the accurate study of Hamiltonians is challenging, we use several many-body tools including Monte Carlo and optimization computational methods, analytical calculations via perturbative expansions in several parameters, and both static and dynamical mean field approximations.

Recent Progress

Spin fermion model for iron-based superconductors. Several experiments for the new family of superconductors based on iron indicate the coexistence of itinerant and mobile electronic degrees of freedom. Our group and others are using spin fermion models for this description, relying on itinerant fermions for the dominant orbitals at the Fermi level and localized spins for the rest. This approach mathematically resembles the double exchange model for manganites, from where computational techniques can be borrowed. As a continuation of previous efforts, recently two main results were obtained: (1) Incorporating quenched disorder [1.1], we found a robust window of nematicity between the nematic and Néel critical temperatures as shown in Fig. 1 upper left. The intermediate region contains patches that favor $(\pi,0)$ magnetic order locally but the disorder renders the ensemble incoherent over a broad temperature range (Fig. 1 upper right);

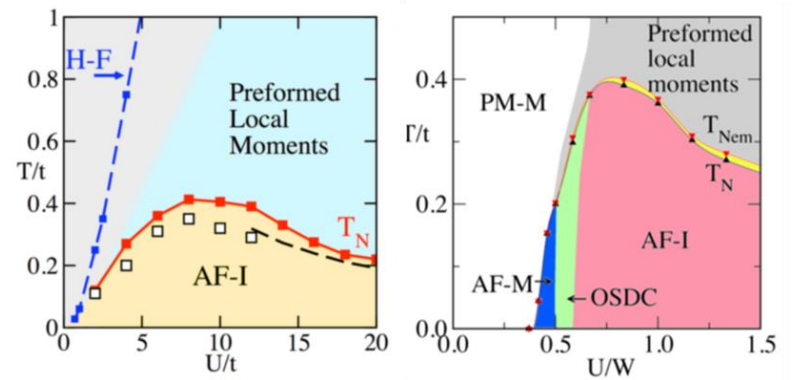
(2) Monoclinic distortions as in FeTe (Fig. 1 lower left) were included in recent efforts using the spin fermion model [1.2]. Incorporating the associated spin-lattice coupling, we found that the E-phase (Fig. 1 lower left) is stabilized as in experiments. Several other aspects of the phenomenology of FeTe are reproduced by this procedure including the puzzling reversed resistivity between the FM and AFM directions (Fig. 1 lower right)

Figure 1. *Upper left:* lattice (red) and magnetic (black) susceptibilities, reproduced from [1.1]. Results are at 5% doping and provide a robust difference of 20K between the critical temperatures. *Upper right:* example of a configuration in the nematic range. Green (orange) are $(\pi,0)$ ($(0,\pi)$) clusters. The $(\pi,0)$ order is not long ranged at this temperature. *Lower left:* C- and E-type magnetism, with associated orthorhombic and monoclinic distortions. *Lower right:* resistance vs temperature in the E-phase showing the “reversed” effect as in 122 compounds [1.2].



Study of multiorbital Hubbard models using Monte Carlo mean field techniques. Most materials of interest require a multiorbital theoretical formalism. Recently, we have developed a many-body tool that combines the mean-field approximation with the Monte Carlo computational technique, dubbed MC-MF. The method was successfully tested in the one orbital case (Fig. 2 left). We recently applied the technique for two orbitals unveiling a new transport regime [2], metallic in one direction and insulating in the other (Fig. 2 right).

Figure 2. *Left:* MC-MF phase diagram for the half-filled one orbital Hubbard model. Red (white) points are MC-MF (quantum MC) [2]. *Right:* results for two orbitals recently published. The novel phase OSDC (orbital selective directional conductor) is metallic along one direction and insulating along the other [2].



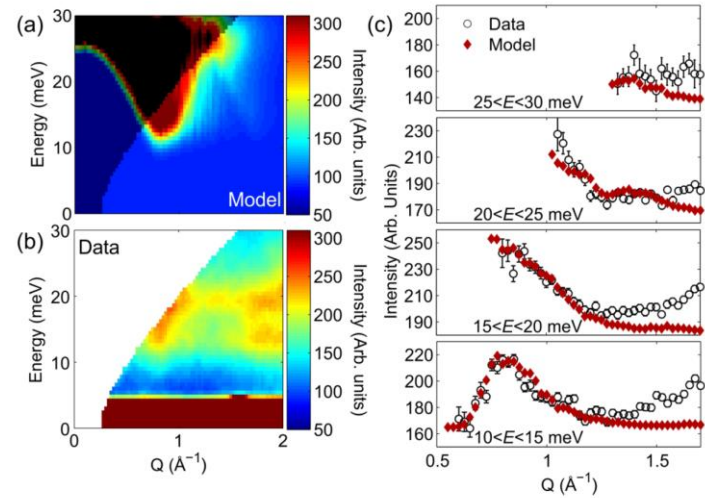
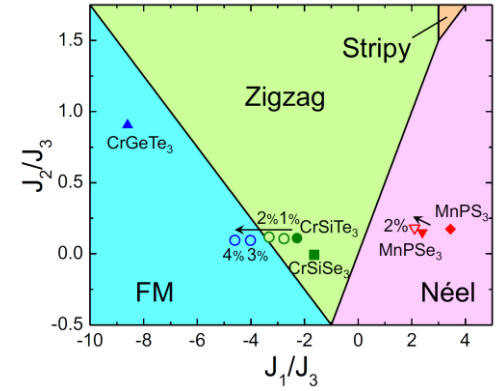
Magnetic properties of ABX_3 monolayers. A special area of focus of our group is the study of interfaces and thin films of complex materials. In particular, the magnetic ground state of semiconducting transition metal trichalcogenide monolayers ABX_3 was analyzed, such as CrSiTe_3 and CrGeTe_3 . Their properties were studied by density functional theory and

Heisenberg models. A variety of ground states were identified, from ferro to antiferromagnetism. Strain was proposed to be the knob to tune the magnetic properties.

Figure 3. Ground-state magnetic phase diagram for our spin model vs J_1/J_3 and J_2/J_3 (standard notation) from [3]. Since our calculation finds J_3 to be always AF, only $J_3 > 0$ is considered. Spins are treated classically. All compounds studied are at the parameters shown. Open symbols are positions under tensile strains; arrows indicate the change from the unstrained cases.

Modelling of neutron scattering data. One of our main goals is to collaborate with neutron scattering experimentalists working at the users facilities of ORNL. As a representative of this work, consider the recent neutron scattering experiments which reveal a large spin gap in the magnetic excitation spectrum of weakly-monoclinic double perovskite $\text{Sr}_2\text{ScOsO}_6$, with a $5d^3$ Os ion. This system was successfully modeled via linear spin-wave theory, including nearest neighbor interactions in a Heisenberg Hamiltonian with exchange anisotropy. The presence of this spin-orbit-induced anisotropy is essential for the explanation of the properties of the Os-based compound [4].

Figure 4: (a) Simulated spectra, modeled using linear spin wave theory. (b) The equivalent experimental data collected at $T = 6$ K. The intensity at high Q in the data is due to phonon scattering, which is not included in the model. The shaded region in the calculations indicates the region of (Q,E) space which is inaccessible in the experiment. (c) Constant-energy cuts through the calculation and data. A global scale factor has been used for the calculation, and a flat background applied for each cut. Reproduced from [4].



Future Plans

Spin fermion and MC-MF approaches. The three orbital Hubbard model will be studied with MC-MF in search of the orbital selective Mott phase, where one orbital has exactly one electron, and its finite temperature properties. The spin fermion model for FeTe will be studied in the presence of disorder and also exploring new types of nematic order involving spin order along diagonals. The interaction orbital-lattice will also be added.

Multiferroic and frustrated spin systems: Work on doped $\text{Mn}_{1-x}\text{Co}_x\text{WO}_4$ will be carried out using the spin wave expansion. Experiments have revealed a rich phase diagram with three different non-collinear multiferroic phases. Long-range exchange interactions are expected to be of relevance. Also work on BiFeO_3 will be performed addressing directional dichroism, from where the magnetoelectric couplings can be extracted.

New states at oxide interfaces. We will develop the continuous-time quantum Monte Carlo impurity solver for DMFT, combined with DFT in collaboration with ORNL experts, to address the effects of strain and reduced dimensionality on the properties of nickelates and manganites. We will also study correlation effects in (111) bilayers made of 4d oxides. Preliminary results suggest that a topological insulator can be stabilized in LaPdO₃.

Publications (partial list)

- [1.1] S. Liang, C. B. Bishop, A. Moreo, and E. Dagotto, “Isotropic in-plane quenched disorder and dilution induce a robust nematic state in electron-doped pnictides”, Phys. Rev. B **92**, 104512 (2015). For details see S. Liang, A. Mukherjee, N. D. Patel, C. B. Bishop, E. Dagotto, and A. Moreo, “Diverging nematic susceptibility, physical meaning of T* scale, and pseudogap in the spin fermion model for the pnictides,” Phys. Rev. B **90**, 184507 (2014), and references therein.
- [1.2] C. B. Bishop, A. Moreo, and E. Dagotto, “Bicollinear Antiferromagnetic Order, Monoclinic Distortion, and Reversed Resistivity Anisotropy in FeTe as a Result of Spin-Lattice Coupling”, arXiv:1606.00904 (2016).
- [2] A. Mukherjee, N. D. Patel, A. Moreo, and E. Dagotto, “Orbital selective directional conductor in the two-orbital Hubbard model”, Phys. Rev. B **93**, 085144 (2016) and cited references; A. Mukherjee *et al.*, “Parallelized Traveling Cluster Approximation to Study Numerically Spin-Fermion Models on Large Lattices”, Phys. Rev. E **91**, 063303 (2015). See also S. Dong *et al.*, “BaFe₂Se₃: A High T_c Magnetic Multiferroic with Large Ferrielectric Polarization,” Phys. Rev. Lett. **113**, 187204 (2014); K. Al-Hassanieh *et al.*, “Spin Andreev-like Reflection in Metal-Mott Insulator Heterostructures”, Phys. Rev. Lett. **114**, 066421 (2015).
- [3] N. Sivadas, M. W. Daniels, R. H. Swendsen, S. Okamoto, and D. Xiao, Magnetic ground state of semiconducting transition metal trichalcogenide monolayers, Phys. Rev. B **91**, 235425 (2015). See also S. Calder, L. Li, S. Okamoto, Y. Choi, R. Mukherjee, D. Haskel, and D. Mandrus, “Spin-orbit driven magnetic insulating state with Jeff=1/2 character in a 4d oxide”, Phys. Rev. B **92**, 180413(R) (2015); M. Ochi, R. Arita, N. Trivedi, and S. Okamoto, “Strain-induced topological transition in SrRu2O6 and CaOs2O6”, Phys. Rev. B **93**, 195149 (2016).
- [4] A.E. Taylor, R. Morrow, R.S. Fishman, S. Calder, A.I. Kolesnikov, M.D. Lumsden, P.M. Woodward, and A.D. Christianson, “Exchange Interactions and the Origin of the Spin Gap in Sr₂ScOsO₆”, Phys. Rev. B (RC) **93**, 220408 (2016). See also J. Ma *et al.*, “Strong Competition between Orbital-ordering and Itinerancy in a Frustrated Spinel Vanadate”, Phys. Rev. B (RC) **91**, 020407 (2015); I. K'ezsm'arki, U. Nagel, S. Bord'acs, R.S. Fishman, J.H. Lee, H. T. Yi, S.-W. Cheong, and T. R~o~om, “Optical diode effect at Spin-Wave Excitations in the Room-Temperature Multiferroic BiFeO₃”, Phys. Rev. Lett. **115**, 127203 (2015); J.H. Lee and R.S. Fishman, “Giant Spin-Driven Ferroelectric Polarization in BiFeO₃ at Room Temperature”, Phys. Rev. Lett. **115**, 207203 (2015).

Moments study of anharmonicity of vibrational modes in solids

Murray Daw, Dept of Physics & Astronomy, Clemson University

Keywords: vibrational modes, anharmonicity, Raman spectra, graphene, clathrates

Project Scope

We are implementing a practical moments formalism for evaluating the anharmonicity of vibrational modes in complex materials based on first-principles electronic structure calculations. The first stage of the project is complete, involving analytic studies of simple anharmonic systems. The second stage --- in progress --- involves implementation of the moments method for semi-empirical potentials and application to some interesting examples. The third stage --- begun this summer --- implements the method with a first-principles electronic structure code and also tackles some problems.

Since the last TCMPI meeting, we have implemented the moments method for semi-empirical potentials. This was accomplished by writing a wrapper to *LAMMPS*, not taking advantage of any particular knowledge of individual potentials, so that the calculations can be done with any potential available for *LAMMPS*. We are currently in the process of applying this wrapper (*Jazz*) to some applications that will be discussed below. We are also experimenting with a similar driver for *Quantum Espresso*, which will allow us to perform similar calculations based on that first-principles electronic structure code.

The moments method is an approximation based on low-order moments of the Liouvillian operator, which is the time-evolution operator for a classical dynamical system. Beginning with the harmonic force constant matrix, the normal modes are found, indexed here by an index α (often a wave-vector and branch). The two lowest moments of the power spectrum of the displacement-displacement autocorrelation

$$\mu_{2,\alpha} = \frac{\langle A_\alpha^2 \rangle}{\langle A_\alpha^2 \rangle} = - \frac{\langle A_\alpha \ddot{A}_\alpha \rangle}{\langle A_\alpha^2 \rangle} \quad \mu_{4,\alpha} = \frac{\langle \ddot{A}_\alpha^2 \rangle}{\langle A_\alpha^2 \rangle}$$

give a simple measure of the temperature-dependent dynamics of the system [Ref. 1]. The angle brackets indicate ensemble averages, which are accomplished by standard Metropolis Monte Carlo. The amplitude A_α of each mode is determined by projection onto the harmonic normal modes. The energy differences for the Metropolis algorithm, as well as the accelerations in each mode, are obtained from some available source of energies and forces. In some of the work we have done, these are provided by semi-empirical potentials (through *LAMMPS*). In current and future work, by an off-the-shelf first-principles code such as *Quantum Espresso*. From the moments, we obtain the temperature-dependent frequency and lifetime of each mode by [Pub. 1]

$$\omega_\alpha = \sqrt{\mu_{2,\alpha}} \quad \tau_\alpha = \frac{\sqrt{2}}{\omega_\alpha \sqrt{\gamma_{4,\alpha} - 1}} \quad \gamma_{4,\alpha} = \frac{\mu_{4,\alpha}}{(\mu_{2,\alpha})^2}$$

The wrapper for *LAMMPS* is in Python to take advantage of the recently implemented Python interface for *LAMMPS*. We have carried out two major calculations using this wrapper and discuss those here --- flexural modes in graphene, and anomalously short-lived modes in

clathrates. We have also begun a study of the anharmonicity of the radial breathing mode (RBM) in carbon nanotubes, that is already showing some interesting results. These calculations can take advantage of multiple processors to improve the Monte Carlo sampling. (*LAMMPS* itself is run in serial mode.)

The driver for *Quantum Espresso* is currently under development. It is being implemented as an integrated driver, much as other extensions of the code have been done. We are testing that code on the same clathrates that were done with the *LAMMPS* wrapper.

Recent Progress: Anharmonicity of flexural modes in graphene

Graphene, like any membrane, is expected to have long-wavelength, out-of-plane (so-called “flexural”) modes. If the membrane is stress-free, the dispersion of those modes should be quadratic in wavenumber (that is, $\omega \propto k^2$) when the harmonic approximation holds. Anharmonicity may modify the dispersion relation. The effect of anharmonicity on the dispersion relation of the long-wavelength flexural modes was considered in the continuum limit by E. Mariani and F. von Oppen [Ref. 2] (“MvO” below). Renormalized by the coupling to in-plane modes, the frequency ω of a flexural mode with wave-vector k at temperature T is given by

$$\omega = \alpha(T, k) k^2 \quad \alpha(T, k) = \alpha_0 \left[1 + \frac{k_c^2}{k^2} \right]^{1/4}$$

where the wave-vector scale $k_c \propto T^{1/2}$. At low temperatures, this approaches the quadratic relation expected, while at higher temperatures the dispersion should go like $k^{3/2}$. With the moments method, using two different Tersoff potentials for graphene (one optimized for graphene), we have calculated the temperature-dependent frequency of the flexural modes. We find detailed agreement with the non-linear continuum theory up to about 200K and wave-vector of 0.4 \AA^{-1} and outside of that range there is some deviation that is probably attributable to the breakdown of the perturbation upon which the continuum theory is based.

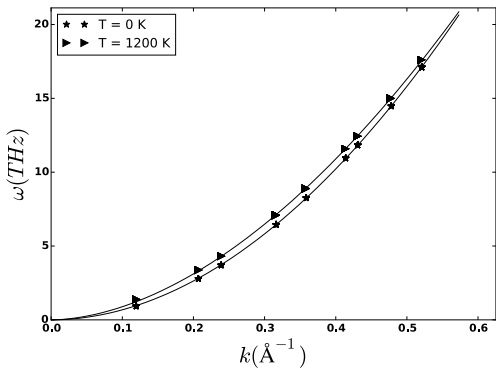


Figure 1: The dispersion of the flexural modes, calculated using the moments method at two temperatures ($T=0\text{K}$ and 1200K). The points are the results of our calculations, and the lines are simple power-law fits.

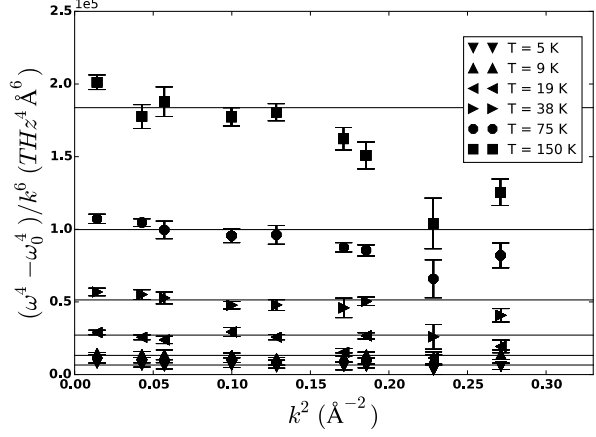


Figure 2: Plot of $(\omega^4 - \omega_0^4)/k^6$ vs. k^2 at low temperatures. This is a replotting of the calculations from Figure 1 (including more temperatures) to emphasize the dependence on temperature and wave-vector. Points are the results of our calculations, and the horizontal lines are simple fits.

In Fig. 1, the dispersion of the flexural modes at different temperatures is shown as points, as calculated by our method on a periodic cell of 1152 atoms. Clearly the effect is present but subtle. Using a simple power law fit (the lines in the figure) the lower temperature is best fit by a quadratic, as expected, and the higher temperature by $k^{1.8}$, which is approaching the continuum result.

To make the analysis more precise, we note that a little rearrangement of the dispersion obtained by MvO gives $\frac{\omega^4 - \omega_0^4}{k^6} = \alpha_0 \beta T$, where ω_0 is the low-temperature frequency (dependent on k , of course). This simple relation is plotted in Fig. 2, where we see that the relation predicted by MvO holds for T up to about 200K and k up to 0.4 \AA^{-1} . The continuum calculation is based on a perturbation in T and k , so it is expected to have some limitations on validity, but MvO did not discuss any attempt to determine that range, so this makes the first determination published.

The importance of these results [Pub. 4] is many-fold. First, this is a subtle test of the validity of the moments approach. The shift in frequency because of the inter-modal coupling is small but can be picked up by the technique. The non-linear continuum calculation is quite general in its way, but does not include a robust potential. Our atomistic, moments calculation is very different in approach, in that it depends so much on the semi-empirical potential. It is gratifying to see the agreement where expected. Second, it is helpful to be able to place limits on the approximations assumed by the non-linear continuum theory. The lifetimes of these modes has also been analyzed and is discussed further in the publication [Pub. 4].

Recent Progress: Short-lived modes in clathrates

We have found in two different Si- and Ge-based clathrates (Clathrate-I and Clathrate-II) some modes that are anomalously short-lived. These calculations of lifetime were done using the moments method with Tersoff potentials for Si and Ge (there are several for Si). These results are shown in Fig. 3, where the quality factor $Q = \omega\tau$ is presented in a scatterplot vs. the low-temperature frequency.

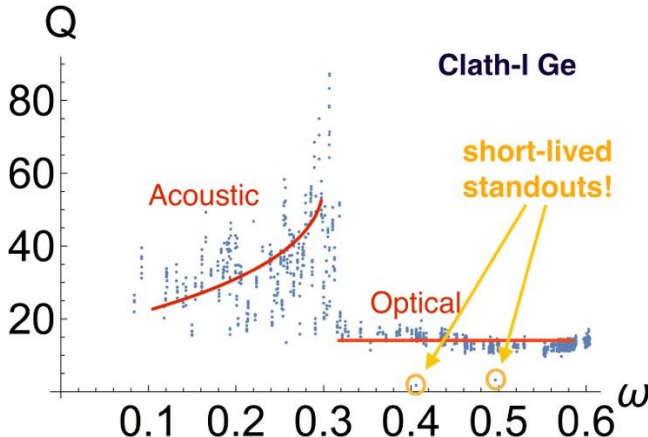


Figure 3: A scatterplot of the quality factor against frequency for the normal modes in a 368 Ge atoms in Clathrate-I structure at $T=300\text{K}$. The two anomalously short-lived standouts are high symmetry A_{1g} modes. These results are limited by the quality of the semi-empirical potentials, as discussed in the text.

Clearly there are some modes that stick out as being very short-lived. These modes are high-symmetry modes (A_{1g} , which are at the zone center in the Brillouin Zone and transform like the identity representation under point group operations). Because these modes are high symmetry, they couple through third- and fourth-order couplings to many modes in the lattice, and so it is not surprising that these would show stronger anharmonicity than other modes. These modes are Raman-active, and so should be looked for in Raman spectra. Temperature-dependent characteristics of these anomalously short-lived modes would be: (1) short lifetime, meaning a broad feature, maybe so broad as to be confused with background, (2) large shift in frequency. The latter characteristic might make it challenging to identify these modes in experimental spectra. First-principles calculations have been very successful in direct comparison to Raman spectra in many solids; however, these calculations are almost always based on harmonic theory, which do not take into account the possible temperature-dependent shift in frequency. A scan of the literature of experiments available on these materials shows that there are many occasions where the harmonic first-principles calculation agrees for the large majority of observable modes, but that certain modes --- in particular, A_{1g} modes --- are sometimes missing where the harmonic theory predicts or are observed where no mode is predicted to occur. These misidentifications have so far not seemed to have drawn much attention. Based on our work with semi-empirical potentials, as well as the argument, based on symmetry, that these modes couple ubiquitously, we raise the question whether these misidentifications can be cleared up by recognizing that these modes will display much stronger anharmonicity than most modes. However, our results so far have been based on semi-empirical potentials, and the details of these calculations appear to depend sensitively on the parameterizations of the potentials, so we do not have confidence in the individual results. For these reasons, we are using these materials as the target problem for the development of our *Quantum Espresso* driver.

Future Plans

- Complete development of the driver for *Quantum Espresso* (a first-principles electronic structure code).
- Investigate the Si- and Ge-based clathrates with this driver.
- Use semi-empirical potentials to investigate the anharmonicity of radial breathing modes of carbon nanotubes, which have been observed in some circumstances to display some degree of anharmonicity.

References

1. D. Dickel and M. S. Daw, "Improved calculation of vibrational mode lifetimes in anharmonic solids. Part I: Theory", Computational Materials Science, v47, pp 698-704 (2010); and 'Part II: Numerical Results", v49, pp 445-449 (2010).
2. E. Mariani and F. von Oppen, Phys Rev Lett, v100 a076801 (2008).

Publications on this grant since the last TCMPI meeting

1. Y. Gao, D. Dickel, D. Harrison, and M. Daw, "Improved calculation of vibrational mode lifetimes in anharmonic solids - Part III: Extension to Fourth Moment", Computational Materials Science, v89, p12 (2014).
2. Y. Gao and M. Daw, "Testing the fourth moment approximation of vibrational mode lifetimes in FCC Lennard-Jonesium", Modeling and Simulation in Materials Science and Engineering, v22, a075011 (2014).
3. Y. Gao, H. Wang, and M. Daw, "Calculations of lattice vibrational mode lifetimes using *Jazz*: a Python wrapper for *LAMMPS*", Modeling and Simulation in Materials Science and Engineering, v23, a045002 (2015).
4. H. Wang and M. Daw, "Effects of anharmonicity on flexural modes in graphene using atomistic calculations", (submitted).

Time-dependent phenomena in correlated materials

Principal Investigator: Adrian Feiguin
Department of Physics, Northeastern University
a.feiguin@northeastern.edu

Project Scope:

Strongly correlated electronic materials, also referred-to as “quantum materials”, are systems where several phases compete producing extremely complex many-body states. Although a single phase may dominate the ground state, competing instabilities are often hidden at higher energies, which can be accessible with intense ultrafast pulses of light. A pulse of electromagnetic radiation will reshape the energy distribution of the many-body spectrum, reordering the relevance of the states, and in the case of a time-dependent electric field, switching rapidly from one to another. Experimentalists can probe the system’s dynamics by shaking it with a pulse of light, allowing them to access states present in the energy spectrum which are not accessible via finite-temperature experiments. These types of non thermal states often contain coexisting orders that are not usually present in the standard ground or thermal states, making a remarkable difference in the way the system evolves after photoexcitation.

In addition, manipulating properties of materials via light has opened a realistic and reliable route to the possibility of studying selected emergent states in complex systems such as super-conductors, organic charge-transfer solids, Mott and charge density wave insulators, and others. Using resonant and intense non-resonant ultrafast pulses of electromagnetic radiation, remarkable experimental outcomes have been observed. Excellent examples include: photo-induced phase transitions, real-space scanning of molecular orbitals, control over dissociation of molecules, study of ionic and electronic motion, melting of ordered states like in superconductors, as well as the analysis of magnetic and charge order.

The present project aims at studying models and time-dependent processes to understand light-matter interaction in strongly correlated materials, and the interplay between electronic, orbital, vibrational, and spin degrees of freedom. The time-scales involved in the creation and recombination of excitons, or the relaxation of the system after a perturbation, will be dictated by the the way light couples to the different excitations, and how these excitations exchange energy and momentum. Our research will advance our understanding of these processes (related to photochemistry, opto-electronics, and light-harvesting applications), and the interpretation of different equilibrium and time-resolved spectroscopies.

The method of choice to study time-dependent phenomena is the time-dependent density matrix renormalization group (tDMRG), which was co-developed by the PI, and has had a remarkable success expanding our knowledge of correlation effects to the time-domain.

Recent progress:

Anomalous pump-driven spectral transfer in 1D spin-full Mott Insulators:

In strongly correlated systems the rigid-band picture --used to understand the phenomenology of semiconductors-- fails dramatically: excitations depend drastically on the electronic density, and the spectrum changes dynamically as the system is excited out of equilibrium. In this work, we study the response of a Mott insulating Hubbard chain to pulse of radiation, and its spectral properties as it is driven out of equilibrium.

One dimensional Hubbard chains fall into the class of models called “integrable”, and possess an extensive number of local integrals of motion that constrain the dynamics of the excitations. For that reason, it is known that after a pump or a quench, the system relaxes to a state that is non-thermal. Another property of this model is that its low energy physics is described by Luttinger liquid theory: In a Luttinger liquid the elementary excitations are collective density fluctuations that carry only either spin (“spinons”) or charge (“holons”). These excitations have different dispersions, and do not carry the same quantum numbers as

the original “bare” fermions. This leads to the spin-charge separation picture, in which a fermion injected into the system separates (“fractionates”) into an holon and a spinon, each of them carrying a share of the fermion’s quantum numbers. The phenomenon of spin-charge separation, and fractionation of particles more generally, is an important and intriguing concept in strongly-correlated systems.

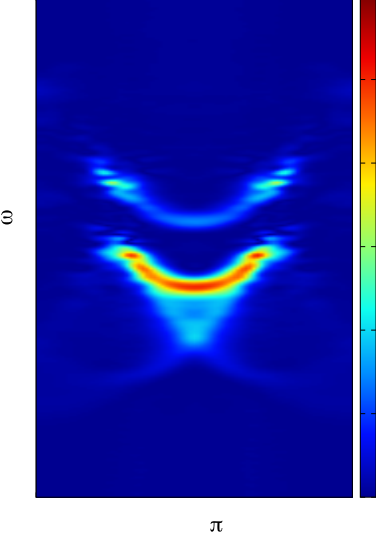


Figure 1: Angle resolved photoemission spectrum of a Mott insulating Hubbard chain after a pump. The upper Hubbard band is populated due to the creation of Hubbard excitons (doublons). The spinon band remains very coherent, while the charge is highly excited.

Due to these two defining phenomena, one could devise a protocol to excite individual excitations (spin or charge) independently, and study their dynamics and mechanisms of relaxation. By pumping with light, or by a sudden quench of parameters in the Hamiltonian we can observe the emergence of excitations in the Mott gap which, for the case of weak interactions, “melt” the gap completely. We have identified intra and inter-band transitions, and we analyzed the role of spin and charge separation comparing to zero-temperature, and finite-temperature results in equilibrium. In addition, we have observed that the spectrum is clearly non-thermal, with charge being excited at high energies, but spin remaining very “cold”. We have introduced integrability breaking terms in the model through second-neighbor repulsion, and verified that spin-charge separation dominates the behavior of the system, yielding essentially similar results.

Unconventional pairing phases in a monochromatically tilted optical lattice: controlling the condensate

It has been theoretically shown that new exotic interactions and correlated hopping terms can be effectively generated by external electromagnetic fields. These ideas have opened a new line of research, termed ‘Floquet engineering’. Indeed, both bosonic and fermionic Hubbard models are currently experimentally investigated in cold-atomic gases, opening the possibility to explore new exciting physics out of equilibrium.

We have studied the one-dimensional attractive fermionic-Hubbard model under the influence of a periodic driving potential with the time-dependent density matrix renormalization group method. The driving introduces a phase in the condensate and we show that the system can be driven in an unconventional paired state characterized by a condensate made of Cooper pairs with a finite center-of-mass momentum similar to a Fulde-Ferrell state. Our results in both, the laboratory and the rotating reference frames, demonstrate that the momentum of the condensate can be finely tuned by changing the ratio between the amplitude and the frequency of the driving. In particular, by quenching the above ratio to the value giving suppression of the tunneling and putting the Coulomb interaction strength to zero, we are able to “freeze” the condensate. We have studied the effects of different initial conditions, and compared our numerical results to those obtained from a time-independent Floquet theory in the large frequency

regime. Our work offers the possibility of engineering and controlling unconventional paired states in fermionic condensates.

Planned activities:

Our planned activities for the second year focuses in the following directions:

Pump-driven phase transitions: A particular problem of great relevance concerns the competing phases in the phase diagram of cuprate superconductors. It is conjectured that the pseudogap phase is indeed a symmetry broken one. Moreover, experiments suggest an instability toward charge density waves (CDW) and that the instability toward superconductivity and CDW are caused by the same interaction and hence are intertwined. The simplest system that possesses both instabilities is the t - J model on 2-leg ladders. One elegant way to determine the magnitude and symmetry of the superconducting instabilities is by performing a numerical phase sensitive experiment. We will study the effects of pumping with light by starting in the paired phase, in the proximity of a CDW state, and viceversa. We will study the transient effects, the properties of the final quasi-thermal state, and analyze the non-equilibrium spectrum and correlations. This project will not only help us understand the competition and interplay between both orders, but also guide the interpretation of time-resolved experiments. Our results may indicate a new way of experimentally studying this transition by conducting time-resolved pump-probe phase sensitive experiments with SQUIDS, and looking for giant superconducting responses in the Josephson current.

We have developed a code to study non-equilibrium effects after pumping a t - J ladder sandwiched in a SQUID geometry using the tDMRG method. We are currently investigating the proximity effects on the equilibrium phase diagram of the system, and the robustness of the different phases, through the behavior of the Josephson current.

Orbital degeneracy in the dynamics of one-dimensional systems: As previously mentioned, a hallmark of one-dimensional physics is the presence of spin-charge separation. In addition, in multi-orbital materials one also finds an orbital degree of freedom that could lead to another class of excitations called “orbitons”. By bombarding the material with high energy photons, one can promote an electron from its ground state to another orbital with a different symmetry. This excitation, much the same as a spin-flip in a spin chain, would propagate as an independent excitation. Moreover, the orbitons will generally be much heavier than the spinons or holons, and in principle should be clearly distinguishable.

We propose studying the full dynamical response of a multi-orbital model with orbital degeneracy, and charge fluctuations: a 2-band Hubbard model, on chains (and possibly ladders), and consider the interplay between spin, orbital, and also charge degrees of freedom, at intermediate values of the Coulomb and Hund couplings. One particular problem that we will address is whether one could find a regime similar to the spin-incoherent Luttinger liquid, in which the orbital degree of freedom is incoherent.

Publications:

DOE Support explicitly acknowledged as “U.S. Department of Energy, Office of Basic Energy Sciences, grant DE-SC0014407.”

1. “Competition between Kondo effect and RKKY physics in graphene magnetism”
Andrew Allerdt, A. E. Feiguin, and S. Das Sarma.
Phys. Rev. Lett. (under review).

2. “Unveiling the internal entanglement structure of the Kondo singlet”
Chun Yang and A. E. Feiguin
Phys. Rev. Lett. (under review).
3. “Anomalous pump-driven spectral transfer in 1D spin-full Mott Insulators”
Alberto Nocera, A. E. Feiguin (in preparation).
4. “Unconventional pairing phases in a monochromatically tilted optical lattice”
Alberto Nocera, A. E. Feiguin (in preparation)

Competing Orders in Correlated Materials: Impact of Disorder and Non-Equilibrium Perturbations

Principal Investigator: Rafael M. Fernandes

School of Physics and Astronomy, University of Minnesota, Minneapolis, MN 55455

rfernand@umn.edu

Keywords: Competing phases, unconventional superconductivity, non-equilibrium physics, disordered systems, quantum phase transitions

Program Scope

The goal of this program is to explore, understand, and ultimately control the competing electronic ordered states ubiquitously present in correlated materials, with particular emphasis in unconventional superconductors, such as iron-based and copper-based materials. While on the one hand the competition with different types of magnetic, orbital, and charge order limits the transition temperatures of these unconventional superconductors, on the other hand the enlarged ground-state degeneracy associated with these multiple many-body instabilities can give rise to unusual inhomogeneous correlated normal states, such as electronic smectic and nematic phases. To achieve the aforementioned goals, the PI employs a multi-faceted theoretical approach consisting of: (i) The investigation of relatively unexplored regimes with the potential to unveil novel behaviors – in particular, the study of competing phases taken out of equilibrium to determine under which conditions the transition temperatures of iron-based and copper-based materials can be enhanced by optical pulses. (ii) The embracement of realistic features of correlated materials in their microscopic descriptions – in particular, the investigation of the impact that disorder, in its various forms, has on emergent inhomogeneous states present in the phase diagrams of unconventional superconductors. (iii) The promotion of synergy with established and novel experimental probes (with particular emphasis on scanning tunneling microscopy and ultrafast spectroscopy) not only by using data as input of theoretical models, but also by providing concrete guidance for experiments.

Recent Progress

Magnetic degeneracy in iron-based superconductors – A unique feature of the iron-based superconductors is the existence of competing magnetic ground states near the onset of superconductivity. The PI and his collaborators investigated several distinct aspects of this rich problem. In collaboration with the student Xiaoyu Wang and the postdoc Jian Kang, a microscopic theory was developed in Ref. 9 demonstrating that the itinerant character of the magnetism in these systems leads not only to the usual single- \mathbf{Q} orthorhombic stripe magnetic ground state, but also to two other tetragonal double- \mathbf{Q} magnetic states. In particular, our results showed that deviations from perfect nesting favor the double- \mathbf{Q} over the single- \mathbf{Q} phase – in agreement with experiments, which observe the former only in optimally hole-doped iron pnictides. In collaboration with the neutron scattering group led by Ray Osborn (Argonne), it was shown in Ref. 3 that the double- \mathbf{Q} state realized in one of these hole-doped materials is the non-uniform charge-spin density-wave, an unusual collinear superposition of two spin density-waves with

different ordering vectors. The possibility of vestigial phases emerging from the two possible types of double- \mathbf{Q} phases – namely, the charge-spin density-wave and the non-collinear spin-vortex crystal – was demonstrated in Ref. 4, together with Steven Kivelson (Stanford) and Erez Berg (Weizmann). Similarly to the nematic phase that arises from the partial melting of the single- \mathbf{Q} stripe phase, it was shown that unusual types of electronic orders, displaying charge order and chiral order, arise due to the partial melting of double- \mathbf{Q} phases (see Fig. 1). Finally, in collaboration with the groups led by Igor Mazin (Naval Lab), Roser Valenti (Frankfurt), and Peter Hirschfeld (Florida), in Ref. 6 the PI showed that the peculiar magnetic degeneracy of the compound FeSe, obtained by first-principle calculations, leads not only to a suppression of long-range magnetic order, but also to an enhancement of the nematic transition temperature.

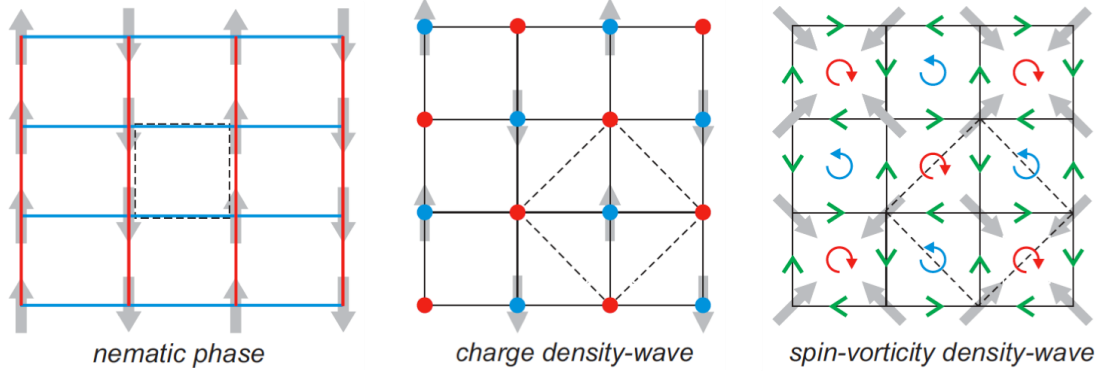


Figure 1: Magnetic states of the pnictides and their vestigial phases: the orthorhombic nematic phase (vestige of the stripe magnetic phase), the charge density-wave (vestige of the charge-spin density-wave), and the chiral spin-vorticity density-wave (vestige of the spin-vortex crystal). From Ref. 4.

Interplay between spin and orbital degrees of freedom in iron pnictides

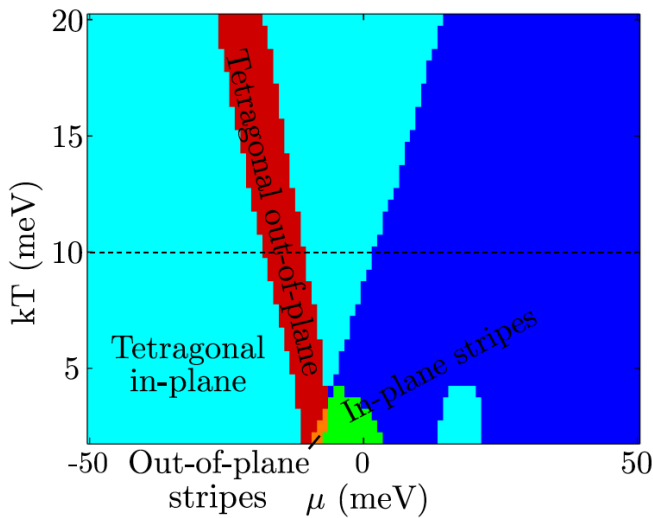


Figure 2: Theoretical temperature-chemical potential phase diagram for the magnetic ground state of the iron pnictides, as well as the spin orientation. While electron-doping favors single- \mathbf{Q} magnetic stripes, hole-doping favors double- \mathbf{Q} tetragonal magnetic phases. From Ref. 5.

The impact of the sizable spin-orbit coupling on the normal state properties of the iron pnictides was studied theoretically by the PI in Ref. 5 (in collaboration with the group led by Brian Andersen, at Copenhagen, and with the postdoc Jian Kang) and in Ref. 10 (in collaboration with Oskar Vafek, at Florida State). In Ref. 5, it was shown via diagrammatic calculations that the spin-orbit coupling, combined with the Hund's coupling, is responsible for the magnetic anisotropy observed experimentally (see Fig. 2), including the spin-reorientation found in hole-doped iron pnictides. In Ref. 10, a microscopic model was solved to show how one can unambiguously distinguish the

signatures of spin-orbit coupling and nematic order in the electronic spectrum of these systems. Even in the absence of spin-orbit coupling, the PI showed in Ref. 2 (in collaboration with the group led by Brian Andersen, at Copenhagen, and with the postdoc Jian Kang) that the intricate interplay between the d_{xz} , d_{yz} , and d_{xy} orbitals with the spin degrees of freedom is essential to stabilize a nematic phase prior to the onset of long-range magnetic order.

Anisotropic transport in strongly correlated systems – The in-plane resistivity anisotropy is the prime experimental tool employed to probe nematic phases.

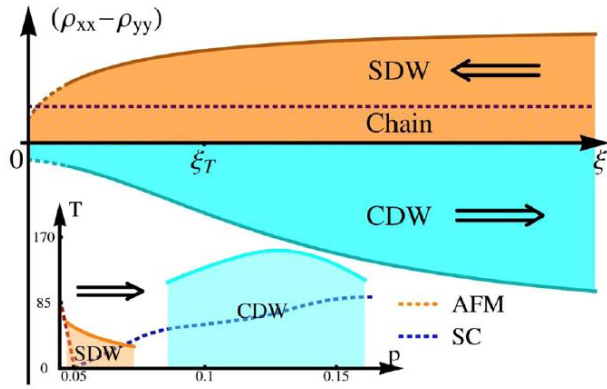


Figure 3: Scattering by anisotropic spin (SDW) and charge (CDW) fluctuations promote different signs of the in-plane resistivity anisotropy $\rho_{xx}-\rho_{yy}$, yielding a non-monotonic doping dependence of the latter across the phase diagram of the cuprates (inset). From Ref. 7.

In collaboration with the postdoc Michael Schütt, in Ref. 7 the PI employed a Boltzmann-equation approach to study the resistivity anisotropy of underdoped cuprates arising from the scattering by anisotropic spin and charge fluctuations. It was found that the two contributions favor anisotropies of opposite signs (see Fig. 3), explaining the experimentally observed non-monotonic dependence of the resistivity anisotropy on the doping concentration. More recently, in collaboration with the postdoc

Michael Schütt and Jörg Schmalian (Karlsruhe), the memory-function approach was used to study the AC conductivity anisotropy of iron-based superconductors. The main result is that the anisotropy in the width of the Drude peak contains not only the trivial contribution from the scattering rate anisotropy, but also an additional contribution, of opposite sign, arising from the optical mass anisotropy. A consequence of this behavior is the sign-change of the anisotropy in the Drude peak width as temperature is lowered.

Impact of disorder in unconventional superconductors – Elucidating what makes unconventional superconductors so robust against non-magnetic disorder remains a main challenge in the field. In collaboration with the postdoc Jian Kang, the PI developed in Ref. 1 a variational approach to study the impact of weak disorder on the pairing state promoted by quantum critical antiferromagnetic fluctuations. In particular, besides the effect of disorder on the quasi-particle spectral weight, this model also took into account the feedback effect of disorder on the electronically driven pairing interaction. It was found that the suppression rate of T_c with impurity scattering is always smaller than the value predicted by the conventional Abrikosov-Gor'kov formalism, being the smallest precisely at the quantum critical point (see Fig. 4). On a related topic, in collaboration with the STM group led by Abhay Pasupathy and with Andrew Millis (both at Columbia), the PI developed and applied a model that allows one to extract the momentum-dependence of the impurity potential by combining ARPES and STM data.

The application to NbSe₂ revealed the key role played by the electron-phonon coupling in promoting the charge density-wave transition of this superconducting material.

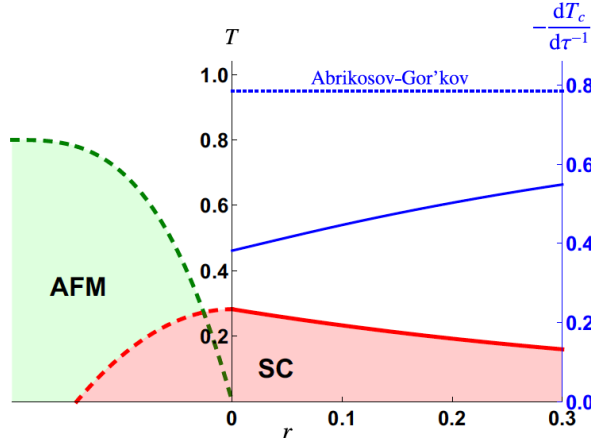


Figure 4: The calculated suppression rate of the transition temperature T_c with respect to a weak non-magnetic scattering rate τ^{-1} is always smaller than the Abrikosov-Gor'kov value, in the case of pairing promoted by quantum critical antiferromagnetic fluctuations. From Ref. 1.

Future Plans

Impact of non-equilibrium phonons on correlated systems – Together with the postdocs Michael Schütt and Peter Orth, and in collaboration with Alex Levchenko (Wisconsin), the PI will investigate the impact of non-equilibrium phonons on various electronic orders observed in cuprates and iron pnictides. Both optical and acoustic phonon modes will be studied, with particular emphasis on the latter. Special consideration will be given to the parameter regime in which different ordered states with superconductivity. The non-equilibrium behavior of different types of superconducting order parameters after interaction with a ultrafast laser pump will also be investigated.

Disorder effects in nematic phases – In collaboration with the student Tianbai Cui, the PI will explore the impact of rare regions and of Griffiths effects near a nematic quantum phase transition that emerges as a vestige of a spin density-wave transition. In this case, the rare regions play fundamentally different roles for the parent and the vestigial phases, since they support long-range nematic order but only quasi-long-range magnetic order. The goal will be to establish whether these effects can split the simultaneous magnetic-nematic first-order quantum phase transition obtained in the clean case.

Unbiased approaches to competing phases – The PI will perform, in collaboration with the student Xiaoyu Wang and the group led by Erez Berg (Weizmann), Quantum Monte Carlo simulations of the two-band spin-fermion model. The appeal of this model is the absence of the fermionic sign-problem, which allows one to probe the interplay between magnetism and superconductivity for systems of moderate sizes and at low temperatures. The emphasis of the study will be not only to establish the role of the Fermi surface geometry to the onset of an unconventional superconducting state, but also to compare quantitatively the QMC results with various analytical field-theoretical approximations that have been developed over the past two decades to understand the spin-fermion model.

Publications

A list of ten selected publications follows below.

1. J. Kang and R. M. Fernandes. “Robustness of quantum critical pairing against disorder.” *Phys. Rev. B* **93**, 224514 (2016).
2. M. H. Christensen, J. Kang, B. M. Andersen, and R. M. Fernandes. “Spin-driven nematic instability of the multi-orbital Hubbard model: Application to iron based superconductors.” *Phys. Rev. B* **93**, 085136 (2016).
3. J. M. Allred, K. M. Taddei, D. E. Bugaris, M. J. Krogstad, S. H. Lapidus, D. Y. Chung, H. Claus, M. G. Kanatzidis, D. E. Brown, J. Kang, R. M. Fernandes, I. Eremin, S. Rosenkranz, O. Chmaissem, and R. Osborn. “Double-Q spin-density wave in iron arsenide superconductors.” *Nature Phys.* **12**, 493 (2016).
4. R. M. Fernandes, S. A. Kivelson, and E. Berg. “Vestigial chiral and charge orders from bidirectional spin-density waves: Application to the iron-based superconductors.” *Phys. Rev. B* **93**, 014511 (2016).
5. M. H. Christensen, J. Kang, B. M. Andersen, I. Eremin, and R. M. Fernandes. “Spin reorientation driven by the interplay between spin-orbit coupling and Hund’s rule coupling in iron pnictides.” *Phys. Rev. B* **92**, 214509 (2015).
6. J. K. Glasbrenner, I. I. Mazin, Harald O. Jeschke, P. J. Hirschfeld, R. M. Fernandes, and R. Valenti. “Effect of magnetic frustration on nematicity and superconductivity in iron chalcogenides.” *Nature Phys.* **11**, 953 (2015).
7. M. Schütt and R. M. Fernandes. “Antagonistic in-plane resistivity anisotropies from competing fluctuations in underdoped cuprate.” *Phys. Rev. Lett.* **115**, 027005 (2015).
8. C. J. Arguello, E. P. Rosenthal, E. F. Andrade, W. Jin, P. C. Yeh, N. Zaki, S. Jia, R. J. Cava, R. M. Fernandes, A. J. Millis, T. Valla, R. M. Osgood Jr., and A. N. Pasupathy. “Quasiparticle interference, quasiparticle interactions, and the origin of the charge density-wave in 2H-NbSe₂.” *Phys. Rev. Lett.* **114**, 037001 (2015).
9. X. Wang, J. Kang, and R. M. Fernandes. “Magnetic order without tetragonal-symmetry-breaking in iron arsenides: Microscopic mechanism and spin-wave spectrum.” *Phys. Rev. B* **91**, 024401 (2015).
10. R. M. Fernandes and O. Vafek. “Distinguishing spin-orbit coupling and nematic order in the electronic spectrum of iron-based superconductors.” *Phys. Rev. B* **90**, 214514 (2014).

Thermal and thermoelectric phenomena in novel materials and systems of disordered and interacting electrons

Principal investigator: Professor Alexander Finkel'stein

Department of Physics and Astronomy, Texas A&M University

College Station, TX 77843-4242

finkelstein@physics.tamu.edu

Project Scope

The project focuses on the theoretical analysis of thermal transport in systems where the heat transport is special. Of particular interest are systems which exhibit elements of the non-Fermi liquid behavior owing to disorder or a strong interaction of conducting electrons with the collective excitations describing fluctuations.

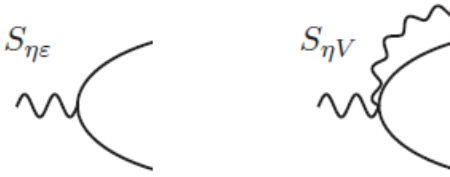
Recent Progress

Below we describe the progress made in the past year in studying thermal transport and understanding the status of the Wiedemann-Franz Law (WFL).

1. Heat Diffusion in the Disordered Electron Gas

The PI, in collaboration with his former postdoc Georg Schwiete (from September 2016 a faculty at the University of Alabama) studied the thermal conductivity of the disordered two-dimensional electron gas. We analyzed the heat density - heat density correlation function concentrating on the scattering processes induced by the Coulomb interaction in the sub-temperature energy range. In two dimensions, these scattering processes are at the origin of logarithmic corrections violating the WFL.

The heat density - heat density correlation function was chosen for the following reasoning: the conservation of energy strongly constrains the general form of the heat density - heat density correlation function. One cannot get correct expressions satisfying energy conservation for this correlation function if the vertices associated with the interaction part of the Hamiltonian are ignored; see e.g., the right term in the figure below. (Because of such vertices, the balance of various terms in the case of the heat density - heat density correlation function turns out to be rather different from that for the correlation functions of other conserved quantities such as the density - density or spin density - spin density correlation functions.)



By contrast, with the use of the heat *current* - heat *current* correlation function it was possible to obtain the correct logarithmic corrections for the heat conductivity even when using incomplete expressions for the heat current. This allowed the authors of one of the papers on thermal transport to claim that the agreement was accidental.

The long-range Coulomb interaction requests for a peculiar care in the case of the heat transport. The principle of gauge invariance has to be implied for identifying the heat density and heat current. Although this has been already discussed, we illuminated this point further by stressing the connection with the field theoretic construction of the Belinfante energy-momentum tensor on the level of the three-dimensional conservation law. While we were interested in heat transport in a two-dimensional electron system, the natural definition of a local conservation law connecting heat density and heat current requires a three-dimensional setting. The reason is that a part of the energy of the system is stored in the electromagnetic field, and this field is not restricted to the two-dimensional plane. In order to define transport of heat in two dimensions, we devised a specific projection procedure.

After sorting out the fundamental problems of the analysis of the thermal transport in a two-dimensional system with long-range Coulomb interaction, we concentrated on calculating logarithmic corrections to the heat conductivity. We focused our attention on the *sub-temperature* energy range, which is beyond the scope of the usual Renormalization Group (RG) analysis. The main difference between the RG interval $(1/\tau, T)$ and sub-temperature energy range is that, while the transitions described by the standard RG procedure are virtual, the sub-temperature range deals with the *on-shell* scattering. For the analysis of the electric conductivity, the sub-temperature processes can be neglected. Thermal conductivity constitutes an important exception. Here, the low-energy scattering processes induced by the long-range Coulomb interaction yield logarithmic corrections which compete with the RG corrections. Moreover, just the corrections caused by the *on-shell* scattering violate the WFL: the sub-temperature processes in the diffusive limit lead to an *increase* of the thermal conductivity as compared to the electric one. Loosely speaking, in the diffusive case with long-range Coulomb interaction, electrons can use the energy $\sim T$ from a remote region to facilitate heat transfer.

The knowledge of the heat density - heat density correlation function of the correct form allows one to extract the heat conductivity out of it. Our analysis showed how the terms violating the WFL become compatible with the general form of the heat density-heat density correlation function. We thereby demonstrated the consistency of our results with the general scheme for the

calculation of a correlation function of the density of a conserved quantity, which in the discussed case was the energy.

2. Theory of Thermal Conductivity in the Disordered Electron Liquid

The fact that the terms violating the WFL are logarithmic in temperature points toward the possibility that this “law” is violated in an extended electron system even at T=0 (for constrained systems this violation is undisputable, because the current and heat relaxation occur in different regions). Still, one can imagine that the RG-corrections may intervene and eliminate the violating terms in the limit T=0. To check this point, we combined the RG-treatment with terms originated from the sub-temperature energy range.

This calculation demands a two-stage procedure: the logarithmic corrections originating from energies in the RG-interval can be absorbed into the scale-dependent RG charges. Once all RG corrections are taken into account, one may find the sub-temperature correction to the thermal conductivity using parameters determined by the current scale of the RG procedure. We included both the Coulomb interaction and scale-dependent Fermi-liquid type interactions arising in the triplet channels. We observed, however, that the sub-temperature corrections to the thermal conductivity remained unaffected by any renormalizations. With this result at hand, we applied the theory to the metallic side of the metal-insulator transition in Si-MOSFETs. The unrenormalized correction to the heat conductivity reveals itself in the fact that maxima of the curves of the “thermal resistance” R_k are all shifted on the same quantity of logarithmic variable $\eta = -0.0785$. (R_k is constructed for different sheet resistances R using the ideal Lorentz ratio, so that $R_k=R$ if the WFL holds.)

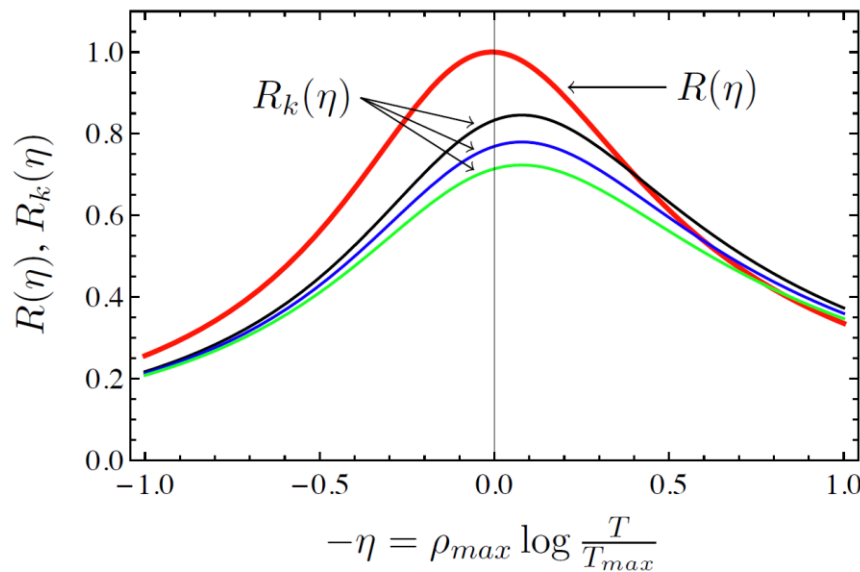


Figure: "Thermal resistance" R_k alongside with the resistance R (red curve). Both quantities, R_k and R , are presented in dimensionless units. In the discussed theory, the maxima R_k are shifted

from the maximum of R by the same value of the logarithmic variable η . (Only the parts of the R_k -curves that lie below the red curve R are physical.)

Future plans: We plan to extend the analysis of disordered electron systems to thermo-power. We also plan to consider the so-called non-Fermi-liquid systems near a quantum critical point. Here, however, one should be cautious, because these systems can be relatively clean. In the clean systems, unlike the dirty one, the dominant fact is that the heat current is not a conserved quantity. As a result, inelastic scattering processes may *decrease* the thermal conductivity (as compared to the electric one), while in the diffusive limit the sub-temperature corrections lead to an *increase* of the thermal conductivity.

Other Directions

Together with my PhD student Wei Zhao, we work on the properties of the flexural phonons in graphene in the presence of random scattering.

Together with my former PhD student Konstantin Tikhonov, we work on tunneling in a p-n junction in the presence of strong spin-orbit.

Publications:

G. Schwiete, A. M. Finkel'stein, "Heat diffusion in the disordered electron gas"

Phys. Rev. B 93, 115121 (2016). Comments: 23 pages, 12 figures.

G. Schwiete, A. M. Finkel'stein, "Theory of Thermal Conductivity in the Disordered Electron Liquid" JETP, Vol. 122, p.567 (2016). Comments: Special JETP issue dedicated to the 85th birthday of Prof. L. V. Keldysh; 8 pages, 1 figure.

Theoretical description of pump-probe experiments in ordered materials

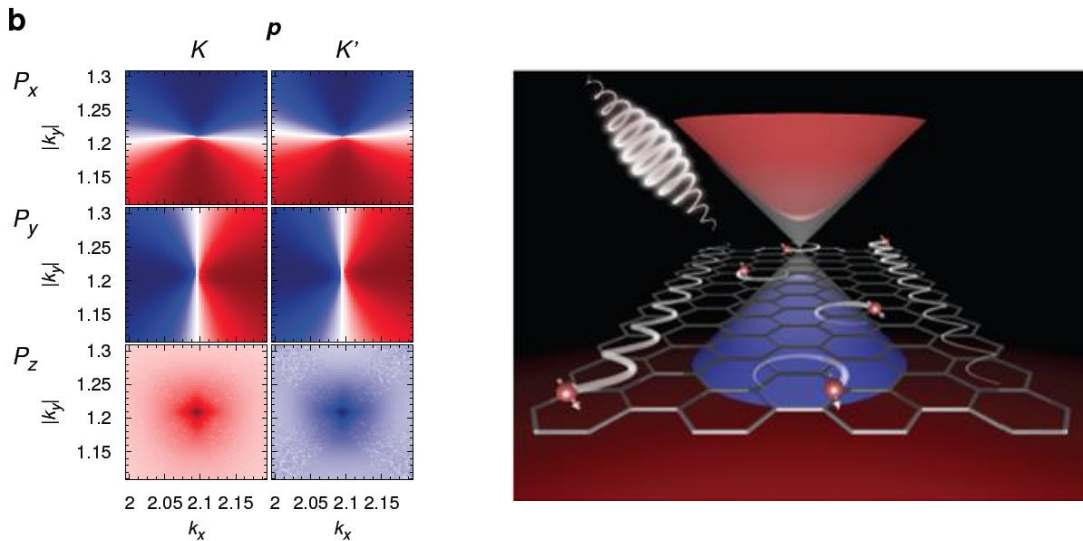
Principal investigator: J. K. Freericks
Department of Physics
Georgetown University
Washington D.C., 20057, USA
freericks@physics.georgetown.edu

Project scope

In recent years, we have developed a research program that has focused on understanding the behavior of pump/probe experiments on quantum materials. Early work focused on the normal phase, while current work is focusing on ordered phases. In particular, we have been examining the properties of superconductors and of charge-density-wave insulators. The main experiment we are trying to describe is time-resolved and angle-resolved photoemission spectroscopy. We also are spending time “peeling the onion” of many-body dynamics to understand better how many-body systems relax in the time domain. Finally, we are investing some effort into developing new methods for solving the many-body problem starting from a Keldysh perspective, which involves directly solving for the dynamics in time, rather than in frequency.

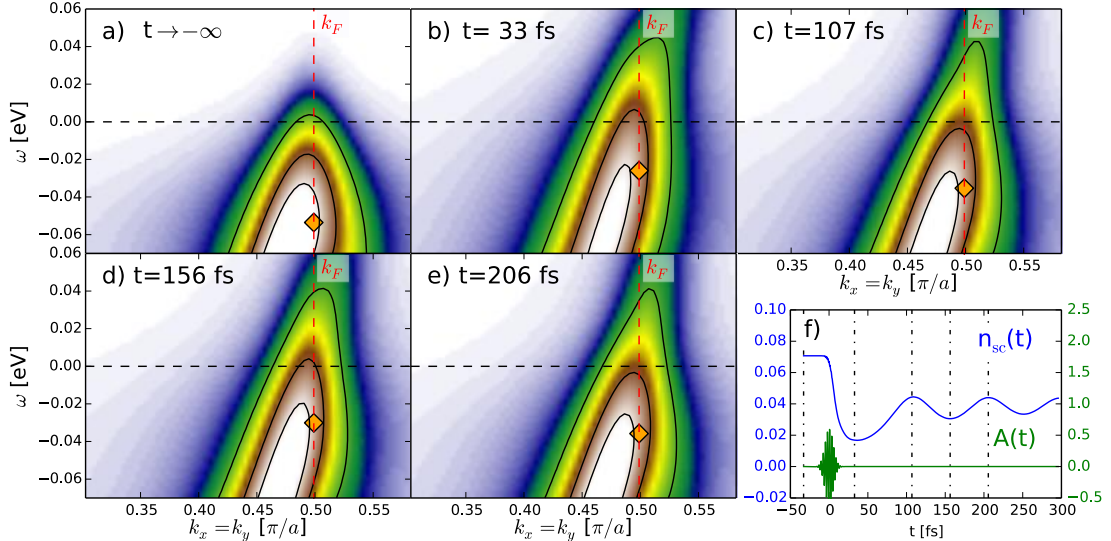
Recent Progress

Generating Floquet states in Graphene



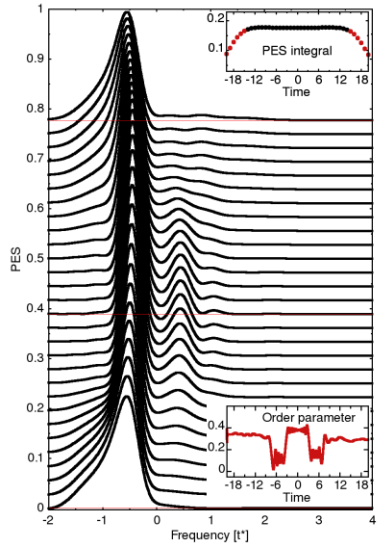
On the left, we show a pseudospin texture of graphene during excitation by a circularly polarized ultrashort light pulse. The change in sign of the texture in the z direction for the two k points indicates a nontrivial topology for the state. The photoemission experiment is depicted graphically on the right. In this research, we showed how circularly polarized light can open gaps in the topologically protected regions of the Brillouin zone. While this general principal was already known from Floquet theory, when one applies a pulse to the system, the electric field is not periodic, so it was not obvious how rapidly the Floquet-like behavior would set in. We found it does so very rapidly, and hence should be able to be observed directly in these systems.

Observing the Higgs mode in superconductors



The Anderson-Higgs mode in superconductors has long been known not to couple linearly to an electric field. But, because it does couple to higher-order in the field, it can be excited in a nonequilibrium experiment. In this work, we show how one can see this behavior by examining the photoemission spectra of a superconductor after a pulse hits it, shown with different snapshots in time in the above figure. Note how the peak position at the Fermi wavevector, denoted by the orange diamond, oscillates at the Higgs mode frequency, and is the direct observation of Higgs physics within the superconductor (shown in the blue curve in the final panel).

Pumping a quantum critical CDW insulator



The Falicov-Kimball model provides an all electronic model for a charge-density-wave insulator. It has a unique quantum critical point with a zero-temperature metal-to-insulator transition occurring at a critical value of U . When this quantum-critical CDW is pumped, it has an ultra-efficient conduction channel which rapidly equilibrates the electrons and does not allow them to be excited. As a result, even if one drives the system at a high fluence, the pump pulse both excites and de-excites electrons so much that very few remain excited at the end of the pulse, as shown in the waterfall plot to the left (delay time increases from bottom to top).

Microscopic origin of the many-body relaxation time

We examined the exact equation of motion for how a momentum population relaxes after a pump and were able to show that the relaxation depends crucially on the average time dependence of the self-energy and we also could show that once one uses the same Wigner distribution function or the Green's function and the self-energy, which is often done in hot-electron models, that the system no longer relaxes. Finally, we also discovered that the relaxation rate is not given simply by the imaginary part of the self-energy, but is more complicated. Unfortunately, we have not yet been able to unravel precisely how it behaves.

Rigorous results about the Hubbard model spectra and eigenvalues

We started a project to understand the spectra and the eigenvalues of the Hubbard model, motivated by the question of whether the gap fills in in the insulating phase as the temperature increases. While we have not yet fully solved this problem, we have provided compelling evidence that the Mott insulating phase will actually have infinite bandwidth, which could play a role in high temperature transport, since these states at high energy have extremely long relaxation times, and so can carry substantial current.

Time-Evolved Wilson Molecule Algorithm (TEWMA)

We are working on developing a novel computational algorithm that can solve the many-body impurity problem in both equilibrium and nonequilibrium. The method is different from other techniques and is based primarily on directly solving for the time evolution of the impurity problem and employing simplifications because the time-evolved wavefunction does not evolve through the entire Hilbert space, but is rather restricted in where it can move.

Future work for 2016-2017

The main project we are working on for the Fall of 2016 is to develop the Time-Evolved Wilson Molecule Algorithm (TEWMA) for both equilibrium and nonequilibrium situations. If successful, the approach will be more accurate than continuous-time quantum Monte Carlo methods and will not require numerical analytic continuation. We also are working on developing the theory for time-resolved Raman scattering and extending the ordered phase work to d-wave superconductors and to competing superconducting-charge-density-wave orders. Finally, we want to continue the smaller projects we have on understanding the microscopic nature of relaxation in the time-domain and on understanding the mathematical properties of the solutions to the Hubbard model.

Publications supported by DOE 2015-2016

- [1] M. A. Sentef, M. Claassen, A. F. Kemper, B. Moritz, T. Oka, J. K. Freericks, and T. P. Devereaux, Theory of Floquet band formation and local pseudospin textures in pump-probe photoemission of graphene, *Nature Commun.* **6**, 7047 (2015). Doi: 10.1038/ncomms8047
- [2] G. R. Boyd, V. Zlatic', and J. K. Freericks, Ubiquity of Linear Resistivity at Intermediate Temperature in Bad Metals, *Phys. Rev. B* **91**, 075118 (2015). Doi: 10.1103/PhysRevB.91.075118.
- [3] Veljko Zlatic', Greg Boyd and Jim K. Freericks, Universal thermopower of bad metals, *J. Phys.: Conf. Ser.* **592**, 012056 (2015). Doi: 10.1088/1742-6596/592/1/012056.
- [4] A. F. Kemper, M. A. Sentef, B. Moritz, J. K. Freericks, and T. P. Devereaux, Amplitude mode oscillations in pump-probe photoemission spectra of electron-phonon mediated superconductors, *Phys. Rev. B* **92**, 224517 (2015). Doi: 10.1103/PhysRevB.92.224517
- [5] J. K. Freericks, H. R. Krishnamurthy, M.A. Sentef, and T.P. Devereaux, Gauge invariance in the theoretical description of time-resolved angle-resolved pump/probe photoemission spectroscopy, *Physica Scripta* **2015 T165**, 014012 (2015) (conference proceedings for FQMT2013). Doi: 10.1088/0031-8949/2015/T165/014012.

[6] J. K. Freericks, Khadijeh Najafi, A. F. Kemper, and T. P. Devereaux, Nonequilibrium sum rules for the Holstein model, in *Femtosecond electron imaging and spectroscopy: Proceedings of the conference on femtosecond electron imaging and spectroscopy, FEIS 2013, December 9-12, 2013*

Key West, FL, USA edited by Martin Berz, Phillip M. Duxbury, Kyoko Makino, and Chong-Yu Ruan, pp. 83--95, Advances in Imaging and Electron Physics, **191**, series editor Peter W. Hawkes, (United Kingdom, Academic Press, 2015). Doi:10.1016/bs.aiep.2015.03.012

[7] O. P. Matveev, A. M. Shvaika, T. P. Devereaux, and J. K. Freericks, Nonequilibrium response of an electron mediated charge-density-wave-ordered material to a large dc electric field, *Phys. Rev. B* **93**, 045110 (2016). Doi: 10.1103/PhysRevB.93.045110

[8] O. P. Matveev, A. M. Shvaika, T. P. Devereaux, and J. K. Freericks, Nonequilibrium dynamical mean-field theory for the charge-density-wave phase of the Falicov-Kimball model, *J. Supercond. Nov. Magn.* **29**, 581-585 (2016). Doi: 10.1007/s10948-015-3304-2

[9] Alexander Kemper and James Freericks, Relationship between Population Dynamics and the Self-Energy in Driven Non-Equilibrium Systems, *Entropy* **18**, 180 (2016). Doi: 10.3390/e18050180.

[10] A. F. Kemper, H. R. Krishnamurthy, and J. K. Freericks, The role of average time dependence on the relaxation of excited electron populations in nonequilibrium many-body physics, *to appear in Fortschritte der Physik* (conference proceedings for FQMT15) (2016).

[11] J. K. Freericks, J. R. Cohn, P. G. J. van Dongen, and H. R. Krishnamurthy, Infinite single-particle bandwidth of the Mott-Hubbard insulator, *Int. J. Mod. Phys. B* **30**, 1642001 (2016). Doi: 10.1142/S0217979216420017.

[12] J. K. Freericks, O. P. Matveev, A. M. Shvaika, and T. P. Devereaux, Theoretical description of pump/probe experiments in nesting induced charge density wave insulators, *Proc. SPIE* **9835**, Ultrafast Bandgap Photonics, 98351F (2016). Doi: 10.1117/12.2223335.

[13] O. P. Matveev, A. M. Shvaika, T. P. Devereaux, and J. K. Freericks, Time-domain pumping a quantum-critical charge-density-wave-ordered material, *submitted to Phys. Rev. B* (2016).

[14] J. K. Freericks, O. P. Matveev, W. Shen, A. M. Shvaika, and T. P. Devereaux, Theoretical description of pump/probe experiments in electron mediated charge-density-wave insulators, *submitted to Physica Scripta* (2016).

[13] J. D. Rameau, S. Freutel, M. A. Sentef, A. F. Kemper, J. K. Freericks, I. Avigo, M. Ligges, L. Rettig, Y. Yoshida, H. Eisaki, J. Schneeloch, R. D. Zhong, Z. J. Zhu, G. D. Gu, P. D. Johnson, and U. Bovensiepen, Time-resolved boson emission in the excitation spectra of $\text{Bi}_2\text{Sr}_2\text{CaCu}_2\text{O}_{8+x}$, *submitted to Nature Commun.* (2016)

Odd-Parity Superconductors: Nematic, Chiral and Topological

Liang Fu (MIT)

Keywords: topological insulator, topological superconductor, Majorana fermion, Weyl fermion

Project Scope

The goal of this project is to predict/propose and study odd-parity superconductors in spin-orbit-coupled materials. Recently it has been recognized that strong atomic spin-orbit coupling plays an essential role in new quantum phases of matter such as topological insulators, Weyl semimetals, and now odd-parity (e.g., p-wave) superconductors. In a 2010 PRL, the PI and Berg proposed that the doped topological insulator $Cu_xBi_2Se_3$, a superconductor with $T_c=3.8K$, has an odd-parity pairing symmetry due to inter-orbital triplet pairing in a strong spin-orbit-coupled normal state. A series of recent experiments, including NMR, specific heat, magnetoresistance, and torque magnetometry, has provided clear evidence of odd-parity spin-triplet superconductivity in $Cu_xBi_2Se_3$ as well as $Sr_xBi_2Se_3$ and $Nb_xBi_2Se_3$. Remarkably, the superconducting state is found to spontaneously break rotational symmetry of the crystal, leading to a nematic superconductor where rotational symmetry breaking is caused by superconductivity [1], a new state of matter unseen before.

This newly-discovered nematic superconducting state which breaks rotational symmetry is a competing state to the widely-studied chiral superconducting state which breaks time-reversal symmetry. Both states arise from a superconducting order parameter with degenerate components at T_c , with the difference that this order parameter is real in the nematic state, but complex in the chiral state.

Remarkably, both nematic and chiral superconductors with odd-parity pairing symmetry are topological superconductors, belonging respectively to time-reversal-invariant (class DIII) and time-reversal-breaking (class D) categories of the topological classification. The PI and his collaborators have shown [1,2,3] that these superconducting states host topologically protected Majorana fermion excitations, either on the surface or in the bulk. Therefore, odd-parity superconductors in naturally-occurring quantum materials provide a route to itinerant Majorana fermions in two and three dimensions, which are very difficult to realize in quantum devices.

Recent Progress

Over the past year, the PI and his student Vlad Kozii and postdoc Jorn Venderbos have extensively studied novel physical properties of this newly-discovered nematic superconductor phase in doped Bi_2Se_3 . In Ref.[2], we showed that spin-orbit-coupling is crucial for stabilizing the nematic superconducting state, as opposed to the familiar chiral state. We also found [1,2] that the gap structure of nematic superconductors is anisotropic in momentum space due to the interplay of spin-orbit-coupling, crystal anisotropy and the nematic direction. A recent low-temperature

specific heat measurement of $\text{Cu}_x\text{Bi}_2\text{Se}_3$ under a rotating magnetic field by Yoshi Maeno (Kyoto), arXiv:1602.08941, found a twofold oscillation which onsets at the upper critical field H_{c2} and persists down to 1.5% of H_{c2} . This is the first direct measurement of the gap structure in a nematic superconductor, and the results agree well with theoretical prediction [1].

In Ref.[4], we showed that the in-plane upper critical field of nematic superconductor shows a distinctive crystal anisotropy that is strongly temperature dependent. This serves as a powerful technique for detecting nematic superconductivity. In Ref.[5], the PI collaborated with Lu Li (Michigan) on torque measurements on $\text{Nb}_x\text{Bi}_2\text{Se}_3$. As the external field is rotated in the ab-plane, the torque shows a dominant twofold symmetry in the superconducting state, contrary to the 12-fold symmetry in the normal state. This is the first experiment probing the pairing symmetry of $\text{Nb}_x\text{Bi}_2\text{Se}_3$ and finding evidence for nematic superconductivity.

In addition to nematic superconductors, the PI's group recently studied chiral superconductors with odd-parity pairing symmetry. In the presence of strong spin-orbit coupling, the gap structures of chiral superconductors are generally non-unitary, i.e., states with opposite spin polarizations have different gaps. Based on a thorough symmetry and topology classification of non-unitary gap structures, the PI's group found [3] that 3D chiral superconductors typically host point nodes that are spin-non-degenerate (contrary to spin-degenerate point nodes in the A phase of superfluid He-3). In this case, nodal quasiparticles are Majorana fermions, i.e., identical to their own antiparticles. The PI has identified the heavy fermion superconductor $\text{PrOs}_4\text{Sb}_{12}$ as a promising candidate for realizing chiral superconductivity with Majorana nodal quasiparticles.

Future Plans

The PI will continue to study novel properties of nematic superconductors including the vortex state, coupling to strain, and Andreev states near impurities. He plans to work closely with experimental colleagues working on neutron scattering, thermal conductivity, and STM to fully characterize this new phase of matter. He will also explore the hallmark of topological superconductivity, Majorana fermions in (Cu, Nb, Sr)-doped Bi_2Se_3 , which have so far remained elusive.

The PI will continue to identify promising candidates for chiral superconductors with Majorana quasiparticles. He plans to develop theory of Kerr rotation and thermal Hall conductivity for 3D time-reversal-breaking superconductors. He will work closely with experimental colleagues to find distinctive signatures of non-unitary gap structures and Majorana nodal quasiparticles.

References

1. L. Fu, "Odd-parity topological superconductor with nematic order: Application to $\text{Cu}_x\text{Bi}_2\text{Se}_3$ ", *Phys. Rev. B* 90, 100509(R) (2014).
2. J. Venderbos, V. Kozii, and L. Fu, "Odd-parity superconductors with two-component order parameters: nematic and chiral, full gap and Majorana node", arXiv:1512.04554

3. V. Kozii, J. Venderbos, and L. Fu, “Three-Dimensional Majorana Fermions in Chiral Superconductors”, arXiv:1607.08243
4. J. Venderbos, V. Kozii, and L. Fu, “Identification of nematic superconductivity from the upper critical field”, arXiv:1503.03406
5. Tomoya Asaba, B.J. Lawson, Colin Tinsman, Lu Chen, Paul Corbae, Gang Li, Y. Qiu, Y.S. Hor, Liang Fu, Lu Li, “Rotational Symmetry Breaking in a Trigonal superconductor Nb-doped Bi₂Se₃”, arXiv:1603.04040

Publications

1. E. Tang and L. Fu, “Strain-Induced Helical Flat Band and Interface Superconductivity in Topological Crystalline Insulators”. *Nature Physics* 10, 964, (2014).
2. X. Qian, J. Liu, L. Fu and J. Li, “Quantum Spin Hall Effect and Topological Field Effect Transistor in Two-Dimensional Transition Metal Dichalcogenides”, *Science* 346, 1344 (2014).
3. T. H. Hsieh, J. Liu and L. Fu, “Topological Crystalline Insulators and Dirac Octets in Anti-perovskites”, *Phys. Rev. B* 90, 081112(R) (2014).
4. L. Fu, “Odd-parity topological superconductor with nematic order: Application to Cu_xBi₂Se₃”, *Phys. Rev. B* 90, 100509(R) (2014).
5. L. Lu, Z. Wang, D. Ye, L. Ran, L. Fu, J. D. Joannopoulos and M. Soljačić, 2015. “Experimental observation of Weyl points”, *Science* 349, 622 (2015).
6. L. Lu, C. Fang, L. Fu, S. G. Johnson, J. D. Joannopoulos and M. Soljačić, 2016. “Symmetry protected Topological Photonic Crystals in Three Dimensions”, *Nature Physics* 12, 337 (2016).
7. J. Venderbos, V. Kozii, and L. Fu, “Odd-parity superconductors with two-component order parameters: nematic and chiral, full gap and Majorana node”, arXiv:1512.04554
8. V. Kozii, J. Venderbos, and L. Fu, “Three-Dimensional Majorana Fermions in Chiral Superconductors”, arXiv:1607.08243
9. J. Venderbos, V. Kozii, and L. Fu, “Identification of nematic superconductivity from the upper critical field”, arXiv:1503.03406
10. Tomoya Asaba, B.J. Lawson, Colin Tinsman, Lu Chen, Paul Corbae, Gang Li, Y. Qiu, Y.S. Hor, Liang Fu, Lu Li, “Rotational Symmetry Breaking in a Trigonal superconductor Nb-doped Bi₂Se₃”, arXiv:1603.04040

Theory of Fluctuations in Strongly-Correlated Materials

Principal investigator: Professor Victor Galitski

Address: Department of Physics, University of Maryland, College Park, MD 20742

Phone: 1-301-405-6107

E-mail: galitski@umd.edu

1. Project Scope

The main general focus of the project is to explore the interplay between fluctuation phenomena and strong correlations in quantum materials, including superconductors. The specific goals of the projects are the following:

- (i) To develop a theory of heterostructures involving topological insulators and magnetic materials.
- (ii) To extend the theory of topological Kondo insulators to strongly fluctuating regimes, where the mean field theory breaks down, and to guide experiments that would probe and exploit the interplay between strong correlations and topological physics in heavy-fermion compounds.
- (iii) To advance the theory of competing orders in high-temperature superconductors, in particular, that of quantum dynamics and coupled collective modes.
- (iv) To develop a non-perturbative theory of quantum fluctuations in superconductors, with the focus on the interplay between Aslamazov-Larkin-type fluctuations and phase fluctuations (including solitons) of the order parameter.
- (v) To develop theories of Casimir effect in strongly correlated materials and critical systems.

2. Recent Progress

Below are some highlights of progress made in the past year:

2.1 Amperean superconducting pairing in topological heterostructures

In recent paper, "Amperian pairing at the surface of topological insulators," (<http://arxiv.org/abs/1603.04081>, to be published in Phys. Rev. Lett.), the PI and his postdocs, Dmitry Efimkin (currently at the Univ of Texas, Austin) and Mehdi Kargarian, proposed an experimental platform to realize a new type of a superconductor - dubbed "Amperian superconductor." The basic idea, pioneered earlier by Prof. Patrick Lee and collaborators in the context of exotic, hypothetical spin liquid states of matter, is that magnetic-like forces there (i.e. current-current like interactions similar to law) lead to attraction for particles moving in the same direction (as well known, two co-moving current-carrying wires attract each other). This leads to pairing and superconductivity of co-moving fermions (in sharp contrast to conventional Cooper pairing, where opposite-moving electrons pair). In conventional metals, this effect is negligible because magnetic forces are extremely weak. The PI has shown that in strongly spin-orbit-coupled materials, in particular topological insulators, coupled to magnetic fluctuations the same effect

appears and is extremely strong. A recent experiment (to be published) has observed superconductivity in a topological heterostructure of the kind proposed in this work.

2.2 Strain-induced enhancement of topological Kondo insulating behavior in Samarium hexaboride to room temperature

One of the main challenges in studying and using topological Kondo insulators, predicted by the PI, is that the topological state appears only at low temperatures in the SmB₆ compound under natural conditions. To increase the relevant energy scales is clearly of great importance. It is known that high-pressure can suppress the topological insulating

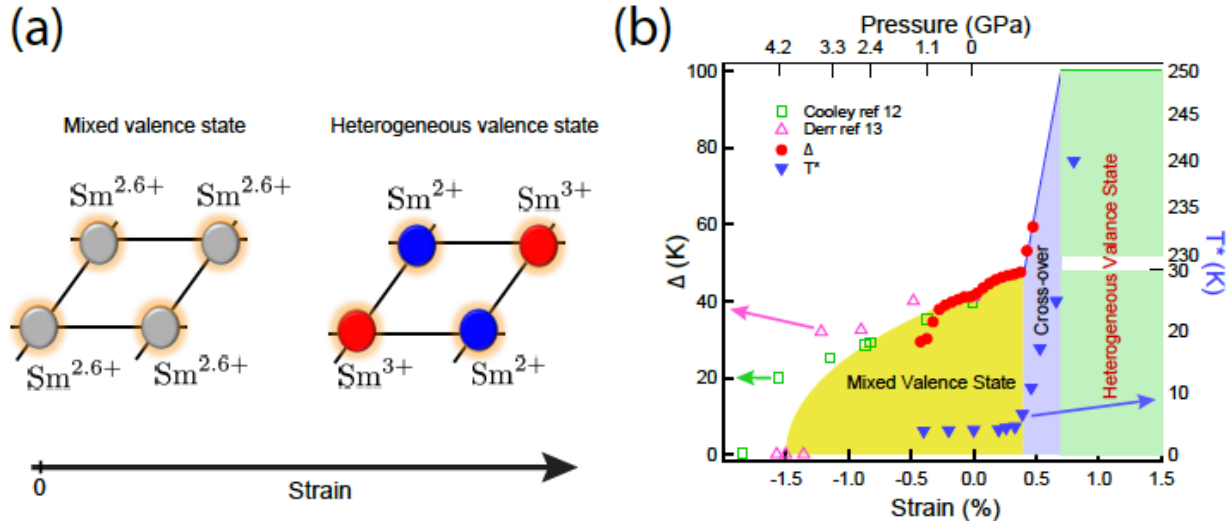


FIG. 1: Temperature-strain phase diagram (a) A cartoon illustration of strain-induced transition from temporal fluctuating mixed-valence state to spatially heterogeneous hetero-valence state. (b) A reconstructed experimental phase diagram of SmB₆ under strain with data from the work of J. Xia, V. Galitski and collaborators as well as pressure data from earlier works [J. C. Cooley et al., Phys. Rev. Lett. **74**, 1629 (1995) and J. Derr et al., Phys. Rev. B **77**, 193107 (2008)]. The left axis corresponds to the Derr et al. bandgap data (purple triangles), the Cooley et al. bandgap data (green squares), and new Xia et al. bandgap data (red circles). The right axis corresponds to the characteristic temperature, where surface-dominated transport commences, which is shown in blue.

state and eventually destroy the gap. This led the PI and collaborators to propose that perhaps tensile strain can have the opposite effect. The idea is that samarium hexaboride under natural conditions exists in the strongly-fluctuating mixed valence regime and by using strain one can move the system towards a less-fluctuating, more mean-field like state with a larger hybridization gap. A detailed theory of strain-induced hybridization enhancement has been developed. In a recent experiment led by PI's collaborator Prof. Jing Xia (a manuscript, co-authored with Prof. Zach Fisk and the PI, is currently under review), a weak tensile strain (a few percent) was applied to SmB₆ and surprisingly led to a huge enhancement of the gap essentially to room temperature. This is a very important discovery, which may have implications on both fundamental aspects of strongly-correlated materials and applications of topological materials.

2.3 Hybridized Higgs modes in the hole-doped cuprate superconductors

In Phys. Rev. B **92**, 184511 (2015), the PI and his group members have studied collective modes in the high-temperature hole-doped cuprates with co-existing competing orders - superconductivity and bond-density wave. It is known that fluctuations of the modulus of the order parameter in a conventional superconductor lead to a mode that is a condensed matter equivalent to the famous Higgs boson in high-energy physics. However, unlike the latter, the superconducting Higgs mode is overdamped (coexists with the single electron excitation continuum) and hence is not actually observable. The key idea of this PI's work is that if two orders co-exist, the coupled fluctuations of their order parameters - hybridized Higgs modes - lead to a stable Higgs collective mode, which is pushed down in energy and becomes long-lived and experimentally detectable.

2.4 Anomalous Coulomb Drag in Bilayers due to the Formation of Excitons

In Phys. Rev. Lett. **116**, 046801 (2016), the PI and his postdoc, Dr. Efimkin, showed that the recent experiments that observed anomalous Coulomb drag in electron-hole bilayers can be explained by formation of fluctuating excitons. It is well-known that excitons - bound states of electrons and holes - would strongly enhance the drag effect in bi-layers. However, exciton condensation would lead to too strong an effect that has not actually been observed. The PI has shown that what likely is observed is the formation of uncondensed excitons that form a classical gas as opposed to a superfluid.

3. Future Plans

The work in the next reporting period will build on the successes of this year's research. In particular, the following will be major foci of PI's research:

1. Now that the Amperian superconductor, predicted by the PI, may have been experimentally discovered (see Sec. 2.1 above), the PI intends to study in depth the properties of this new type of a superconductor (critical current, transport, Meissner effect, etc.). Even the most basic understanding of this type a material is currently missing and the PI will fill this gap to motivate more experiments.
2. Now that the topological Kondo insulating behavior has been extended to high-temperature (see Sec. 2.2 above), the PI will develop a quantitative theory of this phenomenon, which will be based no the study of Kondo fluctuations and how they are suppressed under strain. Applications to other mixed-valence materials will be considered.
3. The PI also collaborates with Andrea Cavalleri's group in Hamburg, that is involved in experimental research of enhancing high-temperature superconductivity by photoexcitation. The PI visited Prof. Cavalleri in February with an invited Colloquium on the topic and Cavalleri and his group members are scheduled to visit the PI in the coming year. A particular focus of PI's current work in this direction is (unpublished at this stage) proposal to look for signatures of the proximity effect in driven systems. The main controversy behind the Cavalleri et al experiments is whether they actually have seen "superconductivity" or the data have an alternative explanation. The PI has proposed a setup to unambiguously resolve

this issue - by coupling a driven system to a non-driven one and looking for signatures of leakage of non-equilibrium superconductivity in the latter. The PI will develop a theory of this phenomenon.

References (September 2015 – July 2016)

- [1] D. K. Efimkin and V. Galitski, "Anomalous Coulomb Drag in Electron-Hole Bilayers due to the Formation of Excitons," *Physical Review Letters* **116**, 046801 (2016)
- [2] M. Kargarian, D. K. Efimkin, and V. Galitski, "Amperian pairing at the surface of topological insulators," arXiv:1603.04081, to be published in *Physical Review Letters* (2016)
- [3] H. M. Hurst, D. K. Efimkin, and V. Galitski, "Transport of Dirac electrons in a random magnetic field in topological heterostructures," *Physical Review B* **93**, 245111 (2016)
- [4] J. Hofmann, A. M. Lobos, and V. Galitski, "Parity effect in a mesoscopic Fermi gas," *Physical Review A* **93**, 061602 (2016)
- [5] M. Neupane *et al.*, "Gigantic surface life-time of an intrinsic topological insulator revealed via time-resolved (pump-probe) ARPES," *Physical Review Letters* **115**, 116801 (2015)
- [6] Z. M. Raines, V. G. Stanev, and V. M. Galitski, "Hybridization of Higgs modes in a bond-density-wave state in cuprates," *Physical Review B* **92**, 184511 (2015)
- [7] M. Dzero, M. G. Vavilov, K. Kechedzhi, and V. Galitski, "Non-universal weak antilocalization effect in cubic topological Kondo insulators," *Physical Review B* **92**, 165415 (2015)
- [8] T. A. Sedrakyan, V. M. Galitski, and A. Kamenev, "Topological spin ordering via Chern-Simons superconductivity," arXiv:1606.08473 (submitted to *Physical Review Letters*)
- [9] S. Ganeshan, A. V. Gorshkov, V. Gurarie, and V. M. Galitski, "Exactly soluble model of boundary degeneracy," arXiv:1604.02089 (submitted to *Physical Review B*)
- [10] A. Stern, M. Dzero, V. M. Galitski, Z. Fisk, and J. Xia, "Kondo insulator SmB₆ under strain: surface dominated conduction at room temperature," submitted to *Science*

Midwest Integrated Center for Computational Materials



Director: Giulia Galli,
University of Chicago & ANL, gagalli@uchicago.edu

The Midwest Integrated Center for Computational Materials (MICCoM: <http://miccom-center.org/>) develops and disseminates interoperable computational tools - encompassing open source software, data, simulation templates, and validation procedures - that enable the user community to simulate and predict properties of **functional materials for energy conversion processes**. The Center represents a partnership, based at Argonne National Laboratory (ANL), with the University of Chicago (UC), Northwestern University (NU), the University of Michigan (UM), the University of California at Davis (UCD), and Notre Dame University (ND).

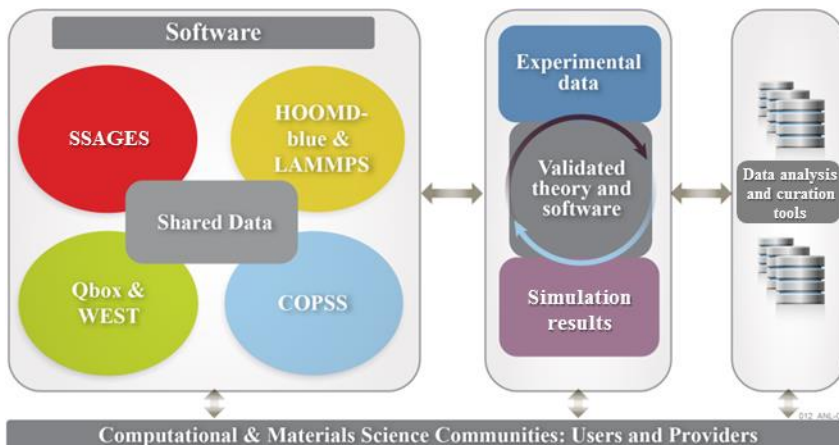


Figure 1 Summary of MICCoM activities and goals. The four circles on the left represent the codes that are made

The Center's design principle has been conceived under the premise that, in order to accelerate the discovery of innovative functional materials, it is not sufficient to compute the properties of the end product; it is critical to **simulate and validate the assembly processes that take place during synthesis and fabrication**.

In addition, in order to

design materials relevant to energy technologies, it is essential that the basic mass, charge, and energy **transport phenomena** involved in energy storage and conversion processes be understood and predicted in **heterogeneous materials**, inclusive of **defects and interfaces**. Most of these phenomena, e.g. electron transport, are inherently quantum mechanical and require a first-principles treatment. Others, such as ionic transport, occur at the molecular scale. Hence one of MICCoM's goal is the coupling of electronic-structure methods to dynamical descriptions of matter, thereby providing the means to capture all the relevant length and time scales of importance to a material's performance.

The multi-scale approach adopted by MICCoM is summarized in Figure 1. The Center is developing methods and delivering and maintaining codes to carry out electronic structure calculations based on Density Functional Theory (DFT) and first principles molecular dynamics (FPMD)-- the Qbox code, and to compute excited state electronic properties

within many body perturbation theory (MBPT)-- the WEST code; software to compute transport coefficients from first principles, integrated with FPMD is being built using Qbox & WEST as bases. These transport coefficients serve as inputs to continuum-particle codes (COPSS) that will predict the effect of applied fields on a material's structure and performance. Within a client-server strategy, we plan to couple quantum (Qbox) and classical Molecular Dynamics (MD), and Monte Carlo (MC) codes (LAMMPS and HOOMD-blue) through a suite of advanced generalized-ensemble sampling techniques (SSAGES), which will in turn operate in tandem with continuum codes. This integrated approach will enable simulations of assembly processes of nano- or meso-building blocks of arbitrary shapes, with designer electronic properties; it will also enable ab initio based calculations of the free energy of **complex materials, both at equilibrium and far from equilibrium**.

MICCoM open source software is already productive on a wide range of computers and **optimized for leadership systems**; it is designed and will be maintained to facilitate and accelerate the incorporation of new, innovative algorithms, proposed both by MICCoM researchers and by the scientific community.

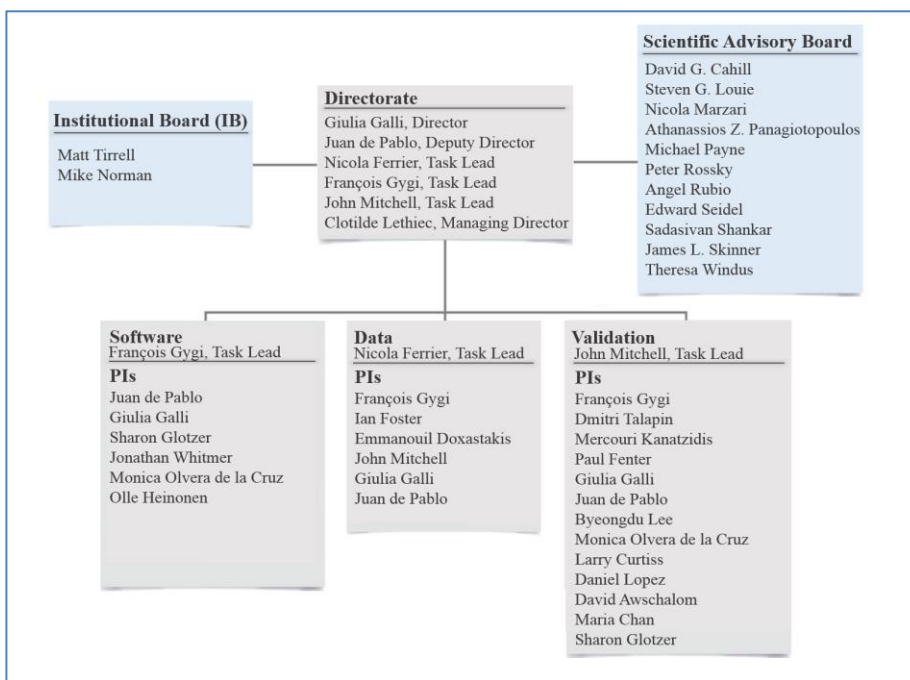


Figure 2 Management structure of the center.

of nanostructured multi-phase assemblies by annealing processes out of equilibrium to create. However the generality of the methods being implemented, and the architecture of the software and validation strategies developed, will facilitate transferability to **broader classes of systems** and hence to different design problems.

In addition to software development and distribution, a key objective of MICCoM is the **systematic validation** of the codes to be distributed and their ability to predict purposely generated experimental data. Controlled experimental synthesis, along with materials characterization performed at the Advanced Photon Source (APS), provide concrete

The materials efforts of the Center are addressing **three representative classes of systems and properties**, with the following objectives: (a) Optimization of assembly of solids of nanoparticles and of their transport properties; (b) Optimization of interfacial ion organization and transport at interfaces between solids and aqueous solutions; (c) Design

platforms for rigorous assessment of MICCoM software. The storage and integration of the results of the interoperable codes and of **data** and metadata is planned through the use of the NIST Curator software installed on MICCoM servers, and data collection through the NIST Dspace Repository. Moreover data analysis software will be made available to the community.

The center is organized in a three-task structure focused on software, validation strategies and data, as indicated in Fig.2, which also shows MICCoM management structure.

PUBLICATIONS

Elastic properties of common Gay–Berne nematogens from density of states (DOS) simulations, Hythem Sidky and Jonathan K. Whitmer, *Liquid Crystals* (2016), accepted.

Implementation and Validation of Fully-Relativistic GW Calculations: Spin-Orbit Coupling in Molecules, Nanocrystals and Solids, Peter Scherpelz, Marco Govoni, Ikutaro Hamada, and Giulia Galli, *J. Chem. Theory Comput.* (2016), accepted.

Elastic response and phase behavior in binary liquid crystal mixtures, Hythem Sidky and Jonathan K. Whitmer, *Soft Matter* 12, 4489-4498 (2016).

Photoelectron spectra of aqueous solutions from first principles, Alex P. Gaiduk, Marco Govoni, Robert Seidel, Jonathan Skone, Bernd Winter, and Giulia Galli, *J. Am. Chem. Soc.* 138, 6912-6915 (2016).

Lattice Boltzmann simulation of asymmetric flow in nematic liquid crystals with finite anchoring, Rui Zhang, Tyler Roberts, Igor S. Aranson and Juan J. de Pablo, *J. Chem. Phys.* 144, 084905 (2016).

SEMICONDUCTOR NANOSTRUCTURES BY SCIENTIFIC DESIGN

PI: Giulia Galli

Institute for Molecular Engineering, University of Chicago, gagalli@uchicago.edu

PROJECT SCOPE

Functional nanostructured systems have long been recognized as a promising platform for the development of materials with target properties. This project is focused on the **development and application of first principles methods** to predict the **opto-electronic and charge transport properties of nanostructured semiconductors**. Systems of interest include materials for solar and thermal energy conversion, with main focus on group IV, and IV-VI compounds.

In the last few years we developed and applied methods to predict the structural and opto-electronic properties of semiconducting nanostructures and nanostructured solids. In a progression of increasingly complex systems and properties, we investigated **isolated nanoparticles** (NPs), the role of surface chemistry and termination in determining their electronic properties, the interplay between quantum confinement and surface structure and morphology and the influence of specifically engineered, metastable core geometries. We then moved to more realistic environments and studied the structural and electronic properties of **nanoparticles embedded in solid matrices**, with focus on the role of interfaces, and of **nanostructured solids**, e.g. **inorganic clathrates**, including atomistic defects.

While our early studies were mostly based on Density Functional Theory (DFT), more recent ones used many body perturbation theory (MBPT) for the electronic properties, while relying on DFT in first principles molecular dynamics simulations (MD) and for the optimization of structural properties. In particular we developed **methods, algorithms and codes to compute efficiently and accurately emission and absorption spectra** by solving approximate forms of the Dyson and Bethe Salpeter Equation (BSE); we focused on the G_0W_0 approximation and the statistically screened BSE.

Recently, we started exploring models to describe ionic and electronic transport properties of nanostructured solids with parameters derived from first principles, as any design of semiconductor nanostructures for use in energy conversion processes needs to include **predictive calculations of charge and heat transport properties**. Some of the models turned out to be useful to qualitatively predict trends of mobilities, e.g. in solar perovskite and clathrate materials and for a qualitative understanding of charge transport at interfaces between nanoparticles and matrices. However it has become increasingly clear that a more serious effort anchored within first principles theories is necessary to describe electron and hole transport in materials for energy applications, in order to define descriptors for the design of semiconductor nanostructures with optimal solar and thermal energy conversion properties.

The main objectives of our ongoing work and future activities are the development of efficient and accurate first principles methods to describe **hopping and band transport**

processes in assemblies of nanoparticles and nanostructured solids and the application of these methods to **realistic configurations of semiconducting nanostructures obtained by first principles molecular dynamics** at room temperature. We are focusing on assemblies of Si and Ge NPs, and PbSe/PbS. Our choice of systems is motivated by their potential application as components in both photovoltaic and thermoelectric materials.

RECENT PROGRESS

Last year we **completed the first release of the WEST code** (<http://www.west-code.org/>) for large-scale GW calculations. WEST is based on algorithms that do not require the explicit calculation of virtual orbitals, are based on the spectral decomposition of dielectric matrices (and hence do not require any explicit diagonalization and storage of the dielectric matrix) and make use of full frequency integration. We carried out a parallel implementation of the algorithm, summarized in Fig. 1, which takes advantage of separable expressions of both the single particle Green's function and the screened Coulomb interaction. In addition we generalized the applicability of GW calculations to DFT wavefunctions obtained not only with semi-local but also with hybrid functionals. Further releases and optimizations of the GW and BSE methods in the WEST code, in particular the coupling of WEST to ab initio molecular dynamics and to continuum simulation codes were moved to MICCoM's support (<http://miccom-center.org/>) on October 1st, 2015.

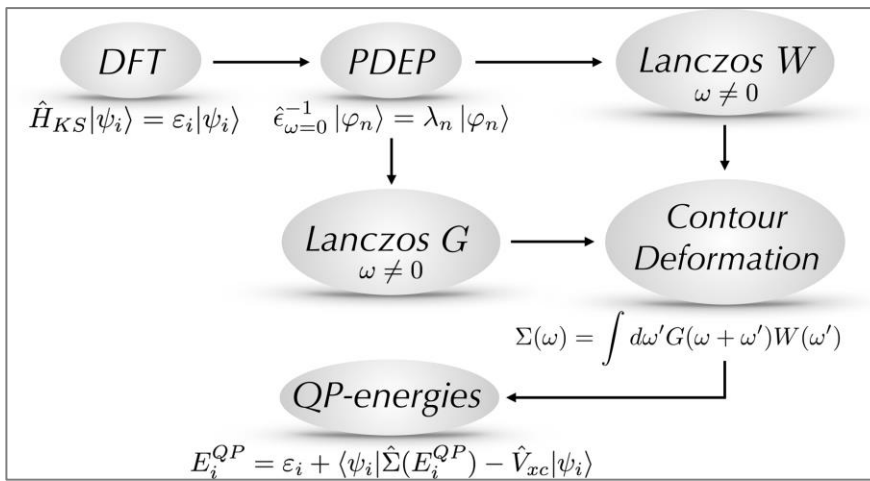


Figure 1 Schematic representation of the steps involved in the calculation of quasiparticle (QP) energies, within the GoWo approximation, as implemented in the WEST code. The Kohn-Sham energies (ε) and occupied orbitals (ψ) computed at the DFT level are input to the PDEP algorithm, which is used to iteratively diagonalize the static dielectric matrix (ϵ^{-1}) at zero frequency. The set of eigenvectors $\{\varphi\}$ constitutes the basis set used to compute both G and W at finite frequencies with the Lanczos algorithm. The frequency integration is carried out using the contour deformation technique.

with thousands of electrons including defective solids, and nanoparticles with several hundreds atoms.

Our studies based on many body perturbation theory (MBPT) led us to understand how to **derive novel range separated hybrid functionals** with non-empirical parameters. These were tested on opto-electronic properties of solids and molecular crystals with excellent

In addition to releasing WEST, we completed a **comprehensive validation of the method used in the code**, encompassing calculations of ionization potentials and electron affinities of various molecules and of band gaps for several crystalline and disordered semiconductors. Finally, we **applied the newly developed technique to GW calculations of systems of unprecedented size**,

results compared to experiments and other methods, and were also used for Si NPs. Work is in progress to routinely use these non-empirical range separated functionals as a starting point of G_0W_0 calculations. In particular, we plan to use them to obtain electronic properties (single particle energies, wavefunctions and total energies) that will serve as input to transport calculations.

Using DFT and MBPT calculations we studied two phenomena relevant to the use of nanoparticle-based devices for solar energy conversion: **blinking and multi-exciton generation (MEG)**, with focus on Si NPs for the former. We explored high-pressure phases of Si and Ge NP cores to obtain structures with optimal gaps for solar absorption and possibly high MEG efficiencies.

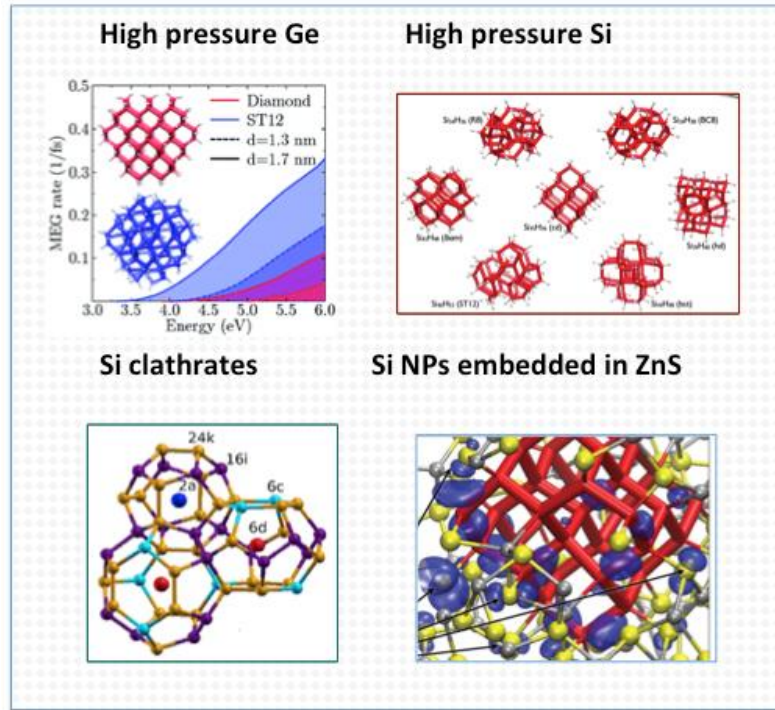


Figure 2 Summary of the major class of systems recently studied in this project, including isolated Ge and Si nanoparticles (NPs, upper panels), NPs embedded in solid matrices and Si-based clathrates (lower panels).

visible range by strain engineering. We also found that upon light absorption, excited electron and hole states are spatially separated in the material, with low probability of charge recombination. Work is in progress to analyze other Si based clathrates, including clathrate superlattices.

FUTURE PLANS

Building on our work on opto-electronic properties, we plan to develop methods for first principles calculations of charge transport properties of solids and nanostructures, and to apply these methods to the study of specific systems of interest to solar and thermoelectric applications. The main questions we seek to answer include:

The exploration of isolated NPs was followed by that of nanostructured solids, composed of either embedded NPs or naturally nanostructured clathrates (see Fig.2, where our main investigations are summarized).

In the case of naturally nanostructured silicon, we predicted a new promising material for solar energy conversion, namely a **Si-based clathrate, composed entirely of Earth abundant elements**. Our predictions were confirmed by experiments. In particular, we found that the type-I clathrate $K_8Al_8Si_{38}$ exhibits a quasi-direct band gap of ~ 1.0 eV, which may be tuned to span the IR and

- **What is the main mechanism (or are there competing mechanisms) of electronic and hole transport in inorganic nanostructured solar cells** composed of semiconducting nanoparticles, as a function of NP size, ligands capping the NPs (type, density and morphology), distance between NPs and interfaces with contacts utilized in experimental devices?
- **What is the main mechanism (or are there competing mechanisms) of electronic and hole transport in perovskite solar cells and how is transport affected by the presence of substitutional halogens and Schottky defects?**
- Can we dope **Si-based inorganic clathrates** so as to increase their Seebeck coefficient and hence increase their thermoelectric figure of merit?
- How is charge transport affected by the formation of **superlattices of clathrates or of chalcogenide materials?**

PUBLICATIONS

1. *Nonempirical range-separated hybrid functionals for solids and molecules*, Jonathan Skone, Marco Govoni, and Giulia Galli, Phys. Rev. B 93, 235106 (2016).
2. *Design of defect spins in piezoelectric aluminum nitride for solid-state hybrid quantum technologies*, Hosung Seo, Marco Govoni, and Giulia Galli, Sci. Rep. 6, 20803 (2016).
3. *Surface Dangling Bonds Are a Cause of B-Type Blinking in Si Nanoparticles*, Nicholas Brawand, Márton Vörös and Giulia Galli , Nanoscale 7, 3737 (2015).
4. *Large scale GW calculations*, Marco Govoni and Giulia Galli, J. Chem. Theory Comput. 11, 2680 (2015).
5. *Perovskites for Solar Thermoelectric Applications: a First Principle Study of $CH_3NH_3AlI_3$ ($A=Pb$ and Sn)*, Yuping He and Giulia Galli, Chem. Mat. 26, 5394-5400 (2014).
6. *Ab initio optoelectronic properties of silicon nanoparticles: Excitation energies, sum rules, and Tamm-Dancoff approximation*, Dario Rocca, Márton Vörös, Adam Gali and Giulia Galli, J. Comp. Theor. Chem. 10, 3290 (2014).
7. *A Nanostructured Clathrate Phonon Glass: Beyond the Rattling Concept*, Yuping He and Giulia Galli, Nanoletters 14, 2920 (2014).
8. *Germanium nanoparticles with non-diamond core structures for solar energy conversion*, Márton Vörös, Stefan Wippermann, Bálint Somogyi, Adam Gali, Dario Rocca, Giulia Galli, and Gergely T. Zimanyi , J. Mater. Chem. A 2, 9820 (2014).
9. *Si-Based Earth Abundant Clathrates for Solar Energy Conversion*, Yuping He, Fan Sui, Susan M. Kauzlarich and Giulia Galli , Energy Environ. Sci. 7, 2386 (2014).
10. *Solar nanocomposites with complementary charge extraction pathways for electrons and holes: Si embedded in ZnS*, Stefan Wippermann, Márton Vörös, Adam Gali, Francois Gygi, Gergely Zimanyi and Giulia Galli, Phys. Rev. Lett. 112, 068103 (2014).
11. *GW calculations using the spectral decomposition of the dielectric matrix: Verification, validation, and comparison of methods*, Tuan Anh Pham, Huy-Viet Nguyen, Dario Rocca and Giulia Galli , Phys. Rev. B 87, 155148 (2013).
12. Spectral representation analysis of dielectric screening in solids and molecules, Amandeep Kaur, Erik R. Ylvisaker, Deyu Lu, Tuan Anh Pham, Giulia Galli and Warren E. Pickett, Phys. Rev. B 87, 155144 (2013).
13. *Dimensionality and heat transport in Si-Ge superlattices*, Ivana Savic, Davide Donadio, Francois Gygi and Giulia Galli , Appl. Phys. Lett. 102, 073113 (2013).
14. *High pressure core structures of Si nanoparticles for solar energy conversion*, Stefan Wippermann, Márton Vörös, Dario Rocca, Adam Gali, Gergely Zimanyi and Giulia Galli Phys. Rev. Lett. 110, 046804 (2013).

NON-EQUILIBRIUM EFFECTS IN CONVENTIONAL AND TOPOLOGICAL SUPERCONDUCTING NANOSTRUCTURES

Principal investigator: Leonid Glazman

Department of Physics, Yale University, 217 Prospect St., New Haven, CT 06511,
leonid.glazman@yale.edu

Co-Investigator and PI on the sub-contract from Yale University: Alex Kamenev

Department of Physics, University of Minnesota, 116 Church St., Minneapolis, MN 55455,
kamenev@physics.umn.edu

Project Scope

In this program, we concentrate on quantum kinetic phenomena in conventional and topological superconducting nanostructures. A special focus is placed on the quasiparticles kinetics and its effect on the coherent dynamics of the superconducting order parameter. Understanding the kinetics is important for a broad array of basic and applied problems of superconductivity emerging in the development of devices of the future quantum information technology. The two major directions in developing the superconducting qubits aim, respectively, at perfecting the conventional-superconductor qubits, and building devices carrying Majorana states. The non-equilibrium quasiparticles limit the coherence times of the conventional superconducting qubits, which raises the problem of quasiparticles trapping. Advancing the diffusion and trapping theory is a part of current effort. The electron transport spectroscopy of Majorana states in engineered p-wave superconducting structures relies on the understanding of quasiparticles tunneling, which is another major part of the current theoretical effort.

Recent Progress

Quasiparticles kinetics in mesoscopic superconductors

Superconducting quantum circuits have made rapid progress in realizing increasingly sophisticated quantum states and operations with high fidelity. Excitations of the superconductor, quasiparticles, can limit their performance by causing relaxation and decoherence. The relaxation rate is approximately proportional to the quasiparticles density in the vicinity of Josephson junctions comprising a qubit. Operating at 20mK or lower temperature, superconducting aluminum in thermal equilibrium should have no more than one quasiparticle for the volume of the Earth. However, a substantial background of quasiparticles has been observed in various devices from single electron or Cooper-pair transistors, kinetic inductance detectors to superconducting qubits. A detailed understanding of the generation mechanism and dominant relaxation processes will eventually be necessary to suppress this small background of quasiparticles and continue the improvement of these devices. Relaxation is enhanced by the presence in a superconductor of regions with suppressed gap. Such regions may be created artificially, by normal-metal traps in contact with the superconductor, or appear naturally, as cores of vortices induced by a weak magnetic field.

Quasiparticle trapping by a single vortex line is a basic property of a superconductor. In a film, the corresponding rate is characterized by a trapping power P which has the same units as the

diffusion constant D . We developed a theory which allowed the experimental group of Prof. Schoelkopf (Yale University) to extract P from measurements of the T_1 time of a transmon qubit. (The theoretical and experimental findings were published in a joint *Nature Communications* paper [1].) The theory predicts the recovery rate of T_1 after a pulse flooding the qubit with quasiparticles. The recovery of T_1 to its steady-state value is determined by the rate at which quasiparticles are evacuated from the Josephson junction. That process involves the quasiparticles diffusion and subsequent trapping by vortices, which are controllably introduced in a field-cooled device. If the vortex number is small, trapping (rather than diffusion) presents the bottleneck for the relaxation of the population of quasiparticles. Under these conditions, increasing the vortex number one by one should lead to a step-like increase in the recovery rate of T_1 , each step increasing the rate proportionally to P . The measurements indeed revealed the step-like increase of the net trapping rate with the number of introduced vortices (controlled by the magnetic field applied during the cooling of the qubit). The small-number steps are of equal height, see Fig. 1. The found single-vortex trapping power was $P \approx 0.06 \text{ cm}^2/\text{s}$. The smallness of the ratio $P/D \sim 0.01$ implies that a quasiparticle can diffuse through a vortex with only a small ($\sim 1\%$) probability to be trapped. The order of magnitude of the measured P is in agreement with a crude estimate of the trapping power $P \sim \square^{-1} \square^{-1}$ in terms of the superconducting coherence length \square and energy relaxation time \square of an electron entering the normal core of a vortex with energy close to the nominal gap value. At present, there is no theory of quasiparticles trapping in a vortex core, which would go beyond the simple estimate.

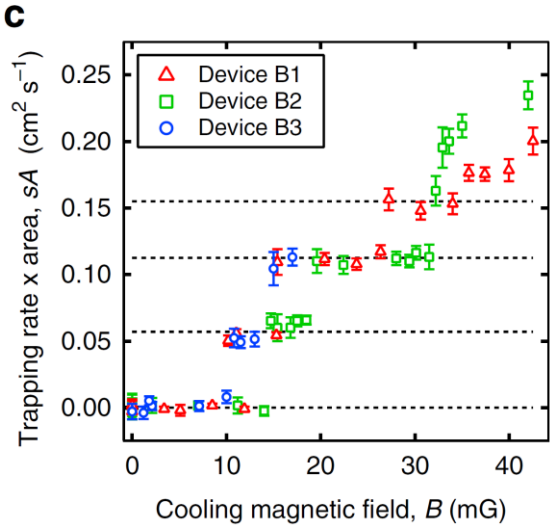


Fig. 1. The quasiparticles trapping rate after subtracting a zero-vortex background and multiplying by the total area of the device, as a function of magnetic field B for Devices B1, B2 and B3. Dashed lines are guides to the eye showing the discrete steps associated with 0, 1, 2 and 3 vortices (adapted from Ref. [1]).

Results of Ref. [1] did show that vortices are less effective for trapping than normal-metal pads in tunnel contact with the superconductor. The effect of such traps on the recovery rate of T_1 after an injection of quasiparticles was studied in our recent preprint [2]. We found, unexpectedly, that such traps become less effective at low temperatures. A part of our predictions has been already confirmed in the ongoing experiments.

While the quasiparticles relaxation channels are reasonably well understood, the uncontrolled sources of non-equilibrium quasiparticles remain a mystery. Our joint effort with the experimental group of Prof. Michel Devoret revealed a strong bunching effect in the time-resolved rate of generation [3]. The origin of this effect is still not known.

Majorana resonances in multiple Andreev reflections

In the conventional theory of the Josephson effect, the dissipative current across a junction at zero temperature requires an application of bias exceeding a threshold, $e|V| > \Delta_L + \Delta_R$, defined by the superconducting gaps in the leads (L and R). At smaller biases, the dissipative current is associated with multiple Andreev reflections (MAR); the lower the bias, the higher the order n of MAR ($n \geq 2$). The MAR current scales as n -th power of the transmission coefficient of the junction, if transmission is weak. Therefore, usually MAR is hard to observe in tunnel junctions. The presence of sub-gap states may lead to resonances strongly enhancing the MAR current. The $n = 2$ resonances occur at such biases which align the discrete sub-gap level in one electrode with the singularity of the density of states in the opposite one. The $n = 2$ resonance for the Majorana mid-gap state (residing in the lead R) occurs at $eV = \pm\Delta_L$.

The presence of a robust peak in the differential conductance at $eV = \pm\Delta_L$ may help to identify Majorana states formed at the ends of magnetic atoms chains deposited on a surface of a conventional superconductor. The existing experimental evidence for Majorana bound states largely relies on measurements of the tunneling conductance. While the conductance into a Majorana state is in principle quantized to $2e^2/h$, observation of this quantization has been elusive, presumably due to temperature broadening in the normal-metal lead. In Ref. [4], we propose to use a superconducting lead instead, whose gap strongly suppresses thermal excitations. For a wide range of tunneling strengths and temperatures, a Majorana state is then signaled by symmetric conductance peaks at $eV = \pm\Delta_L$ of a universal height $G = [4 - \pi]2e^2/h$. These peaks differ qualitatively from those appearing due to the conventional Andreev levels with accidentally zero energy: in scanning by a superconducting tip, Majorana states appear as spatial conductance plateaus while for the trivial Andreev bound states the conductance varies with the local wave function, see Fig. 2. The Majorana conductance drops only far from the bound state, where the natural broadening of the square-root singularity in the density of states of the tip exceeds the tunneling width of the Majorana state.

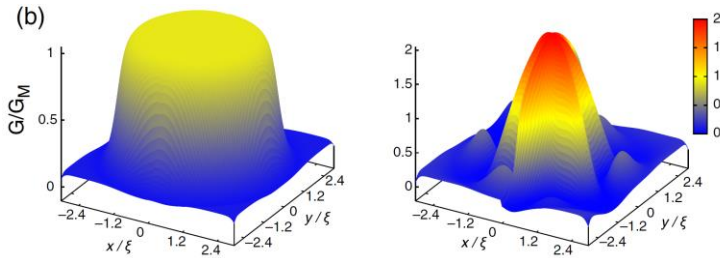


Fig. 2. Spatial conductance maps for Majorana (left) and Andreev (right) states. The Majorana state gives rise to a conductance plateau, whereas the Andreev state exhibits a pattern reflecting the spatial structure of the corresponding wave function (adapted from Ref. [4]).

Conductance of a proximitized nanowire in the Coulomb blockade regime

We identified [5] the leading processes of electron transport across finite-length segments of proximitized nanowires and built a quantitative theory of their two-terminal conductance. In the presence of spin-orbit interaction, a nanowire can be tuned across the topological transition point by an applied magnetic field. Due to a finite segment length, electron transport is controlled by the Coulomb blockade. Upon increasing of the field, the shape and magnitude of the Coulomb blockade peaks in the linear conductance are defined, respectively, by Andreev reflection, single-electron tunneling, and resonant tunneling through the Majorana modes emerging after the

topological transition. Our theory provided the framework for the analysis of experiments with proximitized nanowires [such as reported in S. M. Albrecht *et al*, *Nature* (London) **531**, 206 (2016)] and identified the signatures of the topological transition in the two-terminal conductance. We explained quantitatively the experimental results obtained in Prof. C.M. Marcus group (Niels Bohr Institute) for wire segments which were too short for the topological transition, and pinpointed the difficulties in the interpretation of the data for longer segments in which the topological transition is possible.

Future Plans

We continue our theoretical investigation of effects of quasiparticles on the coherence of the superconducting nanostructures. The two closest aims are building a microscopic theory of quasiparticles trapping by vortices in type-II superconductors, and a full theory of normal-metal traps which would account for the electrodynamics of the hybrid nanostructure, along with the quasiparticle kinetics.

Our closest goal in the investigation of voltage-biased Josephson junctions is to address the recently emerged puzzle of the fractional Josephson effect. It was observed in a spin-Hall edge states setting, which preserves the time-reversal symmetry [R.S. Deacon *et al*, arXiv:1603.09611]. We anticipate the electron interaction with magnetic impurities (which nominally does not break the time-reversal symmetry) may explain the observation.

In the investigation of the conductance of proximitized wires, we are focused on extending our transport theory on the case of high conductance of the junctions connecting the wire segment to the normal-state leads.

References

- [1] “Measurement and Control of Quasiparticle Dynamics in a Superconducting Qubit,” by Chen Wang, Yvonne Y. Gao, Ioan M. Pop, Uri Vool, Chris Axline, Teresa Brecht, Reinier W. Heeres, Luigi Frunzio, Michel H. Devoret, Gianluigi Catelani, Leonid I. Glazman, and Robert J. Schoelkopf, *Nature Communications*, **5**, 5836 (2014).
- [2] “Non-Poissonian Quantum Jumps of a Fluxonium Qubit due to Quasiparticle Excitations,” by Uri Vool, Ioan M. Pop, Katrina Sliwa, Baleegh Abdo, Chen Wang, Teresa Brecht, Yvonne Y. Gao, Shyam Shankar, Michael Hatridge, Gianluigi Catelani, Mazyar Mirrahimi, Luigi Frunzio, Robert J. Schoelkopf, Leonid I. Glazman, and Michel H. Devoret, *Phys. Rev. Lett.*, **113**, 247001 (2014).
- [3] “Normal-metal quasiparticle traps for superconducting qubits,” by R.-P. Riwar, A. Hosseinkhani, L. D. Burkhardt, Y. Y. Gao, R. J. Schoelkopf, L. I. Glazman, and G. Catelani, preprint arXiv:1606.04591 (2016).
- [4] “Robust Majorana Conductance Peaks for a Superconducting Lead,” by Yang Peng, Falko Pientka, Yuval Vinkler-Aviv, Leonid I. Glazman, and Felix von Oppen, *Phys. Rev. Lett.*, **115**, 266804 (2015).
- [5] “Conductance of a proximitized nanowire in the Coulomb blockade regime,” by B. van Heck, R. M. Lutchyn, and L. I. Glazman, *Phys. Rev. B*, **93**, 235431 (2016).

Simulation of Correlated Lattice and Impurity Systems out of Equilibrium

Principal investigator: Professor Emanuel Gull

Department of Physics, University of Michigan

Ann Arbor, MI 48109

egull@umich.edu

Project Scope

The main goal of this project is the simulation of properties of lattice and impurity models in strongly non-equilibrium situations using numerically exact continuous-time quantum Monte Carlo methods. The focus for the first years was on obtaining the time dependent quantum dynamics of impurities after a quantum quench from an initially decoupled system, and involved the development and application of bold-line quantum Monte Carlo codes. Over the last year, we have developed the ‘inchworm’ quantum Monte Carlo method and extended it to the Keldysh contour, so that we can now simulate the time-dependent behavior of quenches from an equilibrium / thermal state.

One of the goals of the project is the development of reliable and efficient methods for computing the Green’s function and spectral function of quantum impurities, with the aim

of providing impurity solvers for the non-equilibrium dynamical mean field theory.

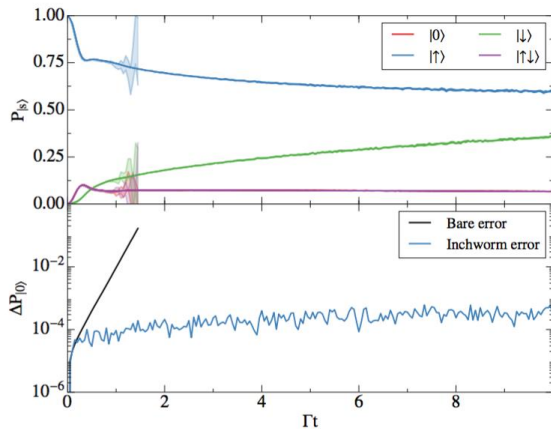


Figure 2. Top panel: population dynamics of the Anderson impurity model in the Kondo regime following a coupling quench from a fully magnetized state at $U = -2\epsilon = 8\Gamma$ and $\beta\Gamma = 50$. The bare hybridization expansion result (Fig. 1(a)) is shown for times $\Gamma t < 1.5$, along with the Inchworm result (Fig. 1(c)) up to $\Gamma t = 10$. Bottom panel: Error estimate of data in upper panel showing an exponential increase of the error as a function of time due to the dynamical sign problem in the bare method, and a roughly constant error in the inchworm method.

quantities is quadratic as a function of time, rather than exponential, making times accessible that are orders of magnitude bigger than what we could previously simulate. A typical example is illustrated in the panel above: where previously times of about 1 were accessible (in units of the coupling density), our new methods can easily access times up to 10. This allows us to simulate the slow dynamics of certain processes, e.g. the spin relaxation in the Kondo regime. Efficient parallelization and scaling on large computers

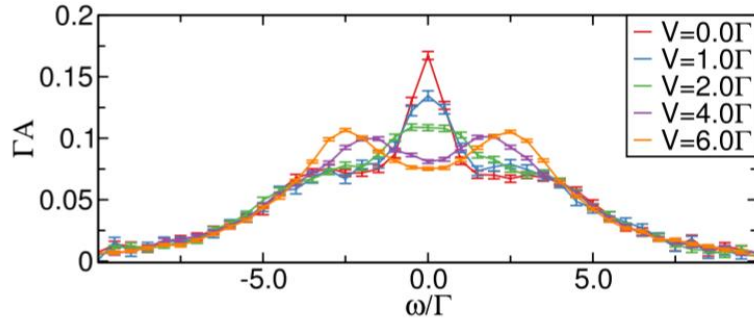
Recent Progress

Below are some highlights of progress made in the past 3 years

Taming the Dynamical Sign Problem in Real-Time Evolution of Quantum Many-Body Problems – This project is based on the causal nature of some expansions on the Keldysh contour: using an efficient resummation, a numerical algorithm can be formulated such that at any time, information obtained at previous times can be reused. As a consequence, the numerical simulation effort for single-time

give additional speed advantages compared to previous methods. The method can give access to the non-equilibrium Green's function, as illustrated in the panel on the right, where the spectral function of a system after a quench is shown as a function of diagram expansion order.

With a new extension of this method to the Keldysh contour containing the equilibrium branch, we can now also do quenches out of equilibrium states. Recent advances have allowed us to do not just static properties and currents, but the full two-time dependent Green's function.



problem. Among the numerically exact methods able to obtain spectra is the bold-line continuous-time quantum Monte Carlo method. An auxiliary lead formalism has allowed us to obtain spectral functions after a quench, and to observe the slow formation of a Kondo peak after a quantum quench. The graph on the left shows a typical example of a steady-state spectral function: as a voltage applied to a Kondo system is gradually increased, the characteristic Kondo peak is suppressed and gradually split into two peaks for large voltages. The observation of this behavior as a function of real time is shown in the figure on the right: for weak voltage (equilibrium), the system (which is initially in a decoupled state) gradually attenuates to half filling and, on a much longer time scale, builds up Kondo correlations and the Kondo peak. As a

Green's functions from real-time bold-line Monte Carlo: spectral properties of the non-equilibrium Anderson impurity model

— Obtaining spectral functions after a quantum quench is a longstanding

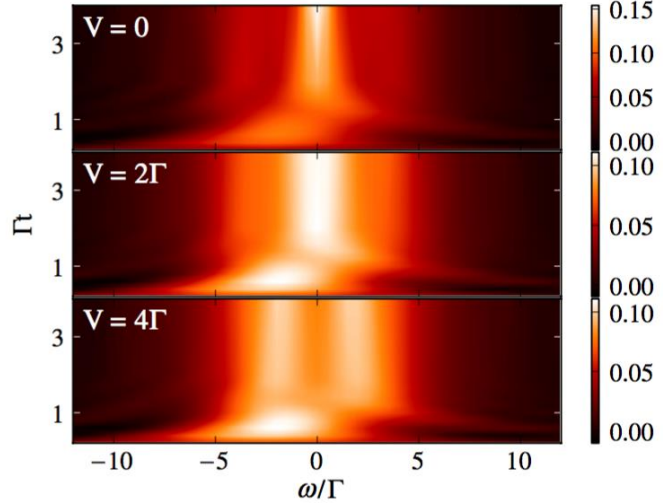


FIG. 2 (color online). The time evolution of the spectral function $A_{\text{aux}}(\omega)$ shown at several voltages, obtained from bold-CTQMC calculations using the double-probe auxiliary lead formalism, with $\eta = 10^{-3}\Gamma$.

small voltage is applied, that buildup gets suppressed and no peak appears. Rather, the sharp peak is replaced by a broadened hump. Finally, a very large voltage leads to a buildup of two split peaks away from zero frequency.

Green's functions from real-time bold-line Monte Carlo – Obtaining spectral functions for interacting many-body systems is one of the big challenges of the field. The analytic continuation of data obtained in an imaginary time formalism suffers from an uncontrolled exponential amplification of noise and errors. We developed an auxiliary lead formalism that allows probing of spectral functions similar to the probing of an STM lead and thereby directly imaging the density of states at a given frequency. An example spectral function evolution after a quench is given below.

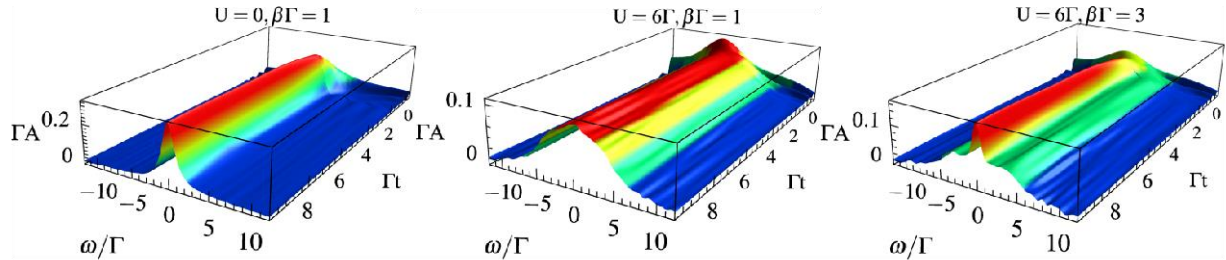


Figure 5. The dependence of the probed Spectral function $A(t) \propto -\frac{1}{t} = \{G^R(t)\}$ on time and frequency, as obtained from the auxiliary current method for an initially decoupled quantum dot at $\Omega_c = 10\Gamma$. At $U = 0$ and $\beta\Gamma = 1$ (left), a simple Lorentzian shape develops. At $U = 6\Gamma$ and $\beta\Gamma = 1$ (center), the interaction distorts and widens the spectrum. At $U = 6\Gamma$ and $\beta\Gamma = 3$ (right), the spectral profile typical to the Kondo problem develops, exhibiting a central Kondo peak between two lower Hubbard peaks.

Voltage quench dynamics of a Kondo system – When a quantum dot in the mixed valence regime is exposed to a voltage quench, the current exhibits short equilibration times and saturates upon the decrease of temperature at all times, indicating Kondo behavior both in the transient regime and in steady state. The time-dependent current saturation temperature matches the Kondo temperature at small times or small voltages; a substantially increased value is observed outside of linear response regime. Using our newly developed numerical methods we were able to predict behavior of the current/voltage characteristics of these dots far outside the equilibrium regime that should be experimentally observable. An example is given in the figure above that shows the transient current normalized to its value at zero temperature, which shows behavior similar to a quantum dot exposed to a magnetic field.

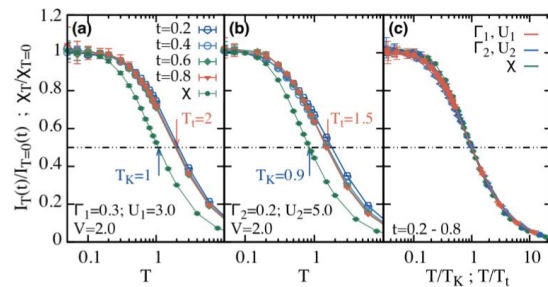


FIG. 3. Normalized transient current $I_T(t)/I_{T=0}(t)$ and static magnetic susceptibility $\chi_T/\chi_{T=0}$ as a function of temperature T for a set of times at $V = 2$, $\epsilon_d = 0$, $D = 5$ and (a) $\Gamma = 0.3$, $U = 3$; (b) $\Gamma = 0.2$, $U = 5$. Dashed line: value of $1/2$. Vertical arrows: crossing points T_K (susceptibility) and T_t (current). (c) $I_T(t)/I_{T=0}(t)$ and $\chi_T/\chi_{T=0}$ [all points from panels (a) and (b)] rescaled as a function of T/T_K and T/T_t correspondingly.

When a quantum dot in the mixed valence regime is exposed to a voltage quench, the current exhibits short equilibration times and saturates upon the decrease of temperature at all times, indicating Kondo behavior both in the transient regime and in steady state. The time-dependent current saturation temperature matches the Kondo temperature at small times or small voltages; a substantially increased value is observed outside of linear response regime. Using our newly developed numerical methods we were able to predict behavior of the current/voltage characteristics of these dots far outside the equilibrium regime that should be experimentally observable. An example is given in the figure above that shows the transient current normalized to its value at zero temperature, which shows behavior similar to a quantum dot exposed to a magnetic field.

Future plans

With the progress achieved over the last years we are now in a very good position to start investigating non-equilibrium dynamical mean field theory. This, as well as the physics of quenches out of correlated states, is the goal of the next projects.

Publications acknowledging this grant

1. Voltage Quench Dynamics of a Kondo System, Andrey E. Antipov, Qiaoyuan Dong, and Emanuel Gull, Phys. Rev. Lett. 116, 036801 – Published 19 January 2016
2. Taming the Dynamical Sign Problem in Real-Time Evolution of Quantum Many-Body Problems, Guy Cohen, Emanuel Gull, David R. Reichman, and Andrew J. Millis, Phys. Rev. Lett. 115, 266802 – Published 23 December 2015
3. Solutions of the Two-Dimensional Hubbard Model: Benchmarks and Results from a Wide Range of Numerical Algorithms, J. P. F. LeBlanc, Andrey E. Antipov, Federico Becca, Ireneusz W. Bulik, Garnet Kin-Lic Chan, Chia-Min Chung, Youjin Deng, Michel Ferrero, Thomas M. Henderson, Carlos A. Jiménez-Hoyos, E. Kozik, Xuan-Wen Liu, Andrew J. Millis, N. V. Prokof'ev, Mingpu Qin, Gustavo E. Scuseria, Hao Shi, B. V. Svistunov, Luca F. Tocchio, I. S. Tupitsyn, Steven R. White, Shiwei Zhang, Bo-Xiao Zheng, Zhenyue Zhu, and Emanuel Gull, Phys. Rev. X 5, 041041 – Published 14 December 2015
4. Mechanisms of finite-temperature magnetism in the three-dimensional Hubbard model, Daniel Hirschmeier, Hartmut Hafermann, Emanuel Gull, Alexander I. Lichtenstein, and Andrey E. Antipov, Phys. Rev. B 92, 144409 – Published 9 October 2015
5. Green's functions from real-time bold-line Monte Carlo, Guy Cohen, David R. Reichman, Andrew J. Millis, and Emanuel Gull, Phys. Rev. B 89, 115139 – Published 31 March 2014
6. Green's Functions from Real-Time Bold-Line Monte Carlo Calculations: Spectral Properties of the Nonequilibrium Anderson Impurity Model, Guy Cohen, Emanuel Gull, David R. Reichman, and Andrew J. Millis, Phys. Rev. Lett. 112, 146802 – Published 9 April 2014

High-performance First-Principles Molecular Dynamics for Predictive Theory and Modeling

Principal investigator: Francois Gygi, Department of Computer Science, University of California Davis, Davis CA 95616 fgygi@ucdavis.edu

Co-Investigators: Giulia Galli, University of Chicago gagalli@uchicago.edu, E. Schwegler, Lawrence Livermore National Laboratory schwegler1@llnl.gov

Project Scope

This project focuses on the development of a robust infrastructure for large-scale, high-performance first-principles molecular dynamics (FPMD) simulations, and its use in investigations of materials relevant to energy conversion processes. FPMD simulations combine a quantum-mechanical description of electronic structure (typically at the level of Kohn-Sham theory) with the statistical description provided by molecular dynamics (MD) simulations. New algorithms and scalable implementations are developed in this project for i) efficient computations of electronic structure using hybrid density functionals, ii) computation of spectroscopic properties (Raman, infrared and sum-frequency generation spectra), and iii) improved statistical sampling methods. The software is used in investigations of aqueous solutions and liquid/solid interfaces. The algorithms are implemented in the Qbox code[1], a plane-wave, pseudopotential implementation of FPMD distributed under a GPL open-source license.

Hybrid DFT FPMD simulations

Most current FPMD simulations are carried out within the framework of density functional theory (DFT) using local or semi-local (GGA) approximations of exchange and correlation. This level of theory is however unable to describe liquids and aqueous solutions with sufficient accuracy. Hybrid DFT functionals include a fraction of non-local Hartree-Fock exchange, which improves accuracy at the cost of a much higher computational effort. We have developed algorithms that reduce the computational cost of hybrid DFT simulations. These algorithms exploit the localization properties of Kohn-Sham orbitals (according to Kohn's nearsightedness principle). In particular, the recursive subspace bisection (RSB) algorithm provides a representation of wave functions in terms of orbitals localized in specified domains, while keeping a controlled accuracy. When coupled with an efficient parallel implementation[10], this approach enables FPMD simulations using hybrid DFT functionals. Our FPMD simulations of solvated ions in water[19] have shown that the study of the electronic properties of anions in water requires the use of hybrid functionals, with additional many body perturbation theory calculations[16], in order to properly describe the correct alignment of their energy levels with those of water.

Vibrational spectroscopy

Vibrational spectroscopy is an ideal tool to probe the complex structure of hydrogen-bonded systems, in particular ice, water and aqueous solutions. However, the interpretation of experimental spectra is usually not straightforward, due to complex spectral features associated with different bonding configurations present in these systems. Therefore, accurate theoretical predictions are required to assign spectral signatures to specific structural properties and hence

to fully exploit the potential of vibrational spectroscopies. We are developing algorithms and scalable implementations to include on-the-fly computations of vibrational spectra during FPMD simulations.

Applications include computations of vibrational properties of water under pressure, infrared, Raman[18], and sum-frequency generation (SFG) spectra of liquids, and vibrational spectra of solvated ions.

Verification and Validation

We are developing software and reference data[2] to ensure a proper verification and validation (V&V) of our simulation infrastructure.

New norm-conserving pseudopotentials: The FPMD implementation used in this project relies on the availability of pseudopotentials. In order to guarantee a high accuracy of computed results, we have developed an optimization approach for the generation of accurate norm-conserving pseudopotentials[6]. The resulting potentials (available for H to Bi) closely reproduce structural properties of hundreds of solids computed using all-electron methods[4]. Norm-conserving potentials offer the advantage of simplicity of implementation, a feature that is critical to implementations on large-scale parallel computers.

FPMD simulation analysis: We are also developing various data processing strategies for the analysis of FPMD simulations, in particular in the aim of characterizing the approach to equilibrium in an MD simulations.

Recent Progress

Hybrid DFT molecular dynamics with controlled accuracy – We have demonstrated that the recursive subspace bisection method can be used to accelerate hybrid DFT simulations in inhomogeneous systems such as liquid/solid or solid/solid interfaces, while preserving control of the approximation error[9]. The resulting method allows for efficient FPMD hybrid DFT simulations of these systems.

Vibrational spectroscopy: sum-frequency generation spectra

We have developed a first-principles framework to compute sum-frequency generation (SFG) vibrational spectra of semiconductors and insulators[5]. The method is based on Density Functional Theory and the use of Maximally Localized Wannier functions to express the response to electric fields, and it includes the effect of electric field gradients at surfaces. In addition, it includes quadrupolar contributions to SFG spectra, thus enabling the verification of the dipolar approximation, whose validity determines the surface specificity of SFG spectroscopy.

Computations of the density and compressibility of water and ice

We have determined the equilibrium density and compressibility of water and ice from first-principles molecular dynamics simulations using gradient-corrected (PBE) and hybrid (PBE0) functionals and the Qbox code[7]. Both functionals predicted the density of ice to be larger than that of water, by 15 (PBE) and 35% (PBE0). The PBE0 functional yielded a lower density of both ice and water with respect to PBE, leading to better agreement with experiment for ice but not for liquid water. Approximate inclusion of dispersion interactions on computed molecular-

dynamics trajectories led to a substantial improvement of the PBE0 results for the density of liquid water, which, however, resulted to be slightly lower than that of ice.

Computations of photoelectron spectra

The computation of photoelectron spectra in liquids and solutions requires accurate calculations of *absolute* quasiparticle energies of both solvent and solute. The GW approximation can be used for such calculations, and requires electronic orbitals computed during molecular dynamics simulations, obtained using hybrid-DFT exchange-correlation functionals. We have investigated the photoelectron spectrum of a simple aqueous solution of NaCl [14]. First-principles simulations were performed using hybrid functionals and many-body perturbation theory at the G_0W_0 level, starting with wave functions computed in FPMD simulations. We found excellent agreement between theory and experiments for the positions of both the solute and solvent excitation energies on an absolute energy scale and for peak intensities. The best comparison was obtained using wave functions obtained with dielectric-dependent self-consistent and range-separated hybrid functionals. Our computational protocol opens the way to accurate, predictive calculations of the electronic properties of electrolytes, of interest to a variety of energy problems.

Future Plans

We will pursue the development of integrated vibrational spectroscopy calculations in FPMD simulations with a focus on making implementations more efficient on future DOE leadership-class platforms such as ANL Theta and Aurora. Efficient use of these resources will enable vibrational spectroscopy studies of large systems (>1000 atoms).

The increasing size of FPMD simulations coupled with the availability of more powerful computers raises issues of management of large datasets. We will develop data compression algorithms based on localized representations of orbitals in order to facilitate archival and sharing of FPMD results.

We will pursue the development of accurate norm-conserving pseudopotentials by including multiple criteria (in addition to structural properties) in the optimization procedure. This is expected to yield robust potentials for use in spectroscopy and quasiparticle energy computations.

Publications

1. Qbox first-principles molecular dynamics code, <http://qboxcode.org>
2. Web standards for electronic structure calculations <http://quantum-simulation.org>
3. A. P. Gaiduk, M. Govoni, R. Seidel, J. Skone, B. Winter, and G. Galli, “Photoelectron spectra of aqueous solutions from first principles”, *J. Am. Chem. Soc. Comm.* **138**, 6912 (2016).
4. K. Lejaeghere, et al. "Reproducibility in density functional theory calculations of solids." *Science* **351**.6280 (2016): aad3000.
5. Q. Wan, and G. Galli, “First-principles framework to compute sum-frequency generation vibrational spectra of semiconductors and insulators”, *Phys. Rev. Lett.* **115**, 246404 (2015).
6. M. Schlipf and F. Gygi, “Optimization Algorithm for the Generation of ONCV Pseudopotentials”, *Comput. Phys. Comm.* **36**, 196 (2015).
7. A. P. Gaiduk, F. Gygi and G. Galli, “Density and Compressibility of Liquid Water and Ice from First-Principles Simulations with Hybrid Functionals”, *J. Phys. Chem. Lett.* **6**, 2902 (2015).

8. E. Boulard, D. Pan, G. Galli, Z. Liu, and W. L. Mao, "Tetrahedrally coordinated carbonates in Earth's lower mantle", *Nature Commun.* 6, 6311 (2015).
9. W. Dawson and F. Gygi. "Performance and Accuracy of Recursive Subspace Bisection for Hybrid DFT Calculations in Inhomogeneous Systems." *Journal of chemical theory and computation* **11**.10 (2015): 4655-4663.
10. W. Dawson and F. Gygi, "Optimized Scheduling Strategies for Hybrid Density Functional Theory Electronic Structure Calculations", *Proceedings of the International Conference for High Performance Computing, Networking, Storage and Analysis (Supercomputing '14)* (pp. 685-692). IEEE Press (2014).
11. T. A. Pham, D. Lee, E. Schwegler, and G. Galli, "Interfacial Effects on the Band Edges of Functionalized Si Surfaces in Liquid Water", *J. Am. Chem. Soc.* 136, 17071 (2014).
12. Dipolar Correlations in Liquid Water, Cui Zhang and Giulia Galli, *J. Chem. Phys.* 141, 084504 (2014)
13. Q. Wan, L. Spanu, F. Gygi, and G. Galli, "Electronic Structure of Aqueous Sulfuric Acid from First-Principles Simulations with Hybrid Functionals", *J. Phys. Chem. Lett.* 5(15), 2562 (2014).
14. A. P. Gaiduk, C. Zhang, F. Gygi, and G. Galli, "Structural and electronic properties of aqueous NaCl solutions from ab initio molecular dynamics simulations with hybrid density functionals", *Chem. Phys. Lett.* 604, 89 (2014).
15. P. Huang, T. A. Pham, G. Galli, and E. Schwegler, "Alumina(0001)/Water Interface: Structural Properties and Infrared Spectra from First-Principles Molecular Dynamics Simulations", *J. Phys. Chem. C* 118, 8944 (2014).
16. T. A. Pham, C. Zhang, E. Schwegler, and G. Galli, "Probing the electronic structure of liquid water with many-body perturbation theory", *Phys. Rev. B* 89, 060202(R) (2014).
17. S. Wippermann, M. Vörös, A. Gali, F. Gygi, G. Zimanyi and G. Galli, "Solar nanocomposites with complementary charge extraction pathways for electrons and holes: Si embedded in ZnS", *Phys. Rev. Lett.* 112, 068103 (2014).
18. Q. Wan, L. Spanu, G. Galli and F. Gygi, "Raman spectra of liquid water from ab initio molecular dynamics: vibrational signatures of charge fluctuations in the hydrogen bond network", *J. Chem. Theory Comput.* 9, 4124 (2013).
19. C. Zhang, T. A. Pham, F. Gygi and G. Galli, "Electronic structure of the solvated chloride anion from first principles molecular dynamics", *J. Chem. Phys- Comm.* 138, 181102 (2013).

Quantum Quench Dynamics – Crossover Phenomena in Non-Equilibrium Correlated Quantum Systems

Principal Investigator: Stephan Haas, Department of Physics & Astronomy, University of Southern California, Los Angeles, CA 90089-0484, shaas@usc.edu

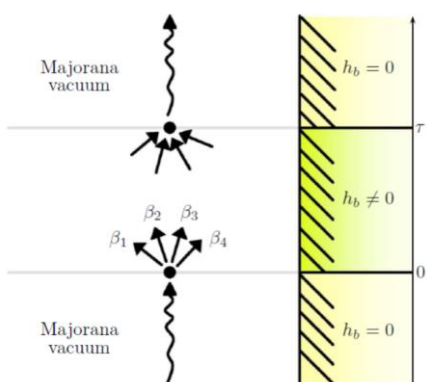
Collaborators: Hubert Saleur (Saclay, France), Stefan Kettemann (Jacobs University, Germany)

Project Scope

In this project we are developing analytical and numerical tools to study the interplay between interactions, dimensionality, fluctuations and disorder in quantum impurity systems. One of our goals is to study the transient dynamics following a quench, i.e. the sudden change in a control variable of the model Hamiltonian, which offers a unique way to examine the system's spatial, temporal and energetic structure. For example, we are investigating how crossover scales, i.e. given by Kondo couplings, are affected by disorder. We are interested in a wide range of phenomena, such as the effects of static disorder on dynamical screening of magnetic impurities, or the influence of a fully time-fluctuating bath environment on the dephasing of system qubits. Many of these systems hold the promise of fascinating counterintuitive behavior, such as e.g. the possibility of asymptotic unitary time evolution in specifically conditioned system-bath Hamiltonians. From a technical point of view, we are generalizing the strong-coupling real-space renormalization group method to probe the quench dynamics of higher-dimensional quantum impurity systems, we are developing a super-symmetric formalism to analyze scaling functions of disordered quantum impurity spin chains, and we are devising a master equation approach that includes the effects of a fully fluctuating environment. This way, we can address a very broad spectrum of transient phenomena in quantum impurity systems, with disorder ranging from the quenched to the annealed limit.

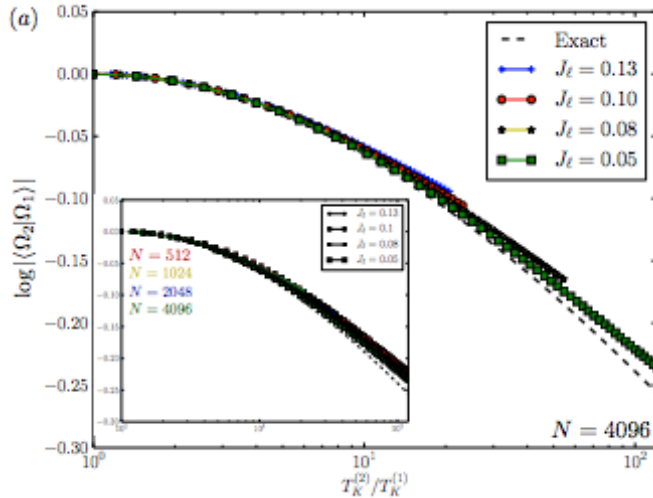
Recent Progress

Crossover Physics in Quenched Quantum Impurity Systems: We have developed a general framework to tackle analytically local quantum quenches in integrable impurity systems, combining a mapping onto a boundary problem with a form factor approach to boundary-condition-changing operators. Using this approach, we were able to compute two central quantities of interest: the Loschmidt echo and the distribution of the work done during the quantum quench. Our results display an interesting crossover characterized by the energy scale T_b of the impurity corresponding to the Kondo temperature. We studied in detail the non-interacting case as a paradigm and



benchmark for more complicated integrable impurity models, and checked our results using numerical methods. The calculated time evolution of the Loschmidt echo was found to be in beautiful agreement with independent numerical studies of equivalent lattice models. Applying the same formalism to the Kondo case is a bit more involved, since the form factors are more complicated in this case. However, the Kondo problem is not fundamentally different from the case we treated.

Exact Overlaps in the Kondo Problem: It is well known that the ground states of a Fermi liquid with and without a single Kondo impurity have an overlap which decays as a power law of the system size, expressing the Anderson orthogonality catastrophe. Ground states with two different values of the Kondo couplings have, however, a finite overlap in the thermodynamic limit. This overlap, which plays an important role in quantum quenches for impurity systems, is a universal function of the ratio of the corresponding Kondo temperatures, which is not accessible using perturbation theory nor the Bethe ansatz. Using a strategy based



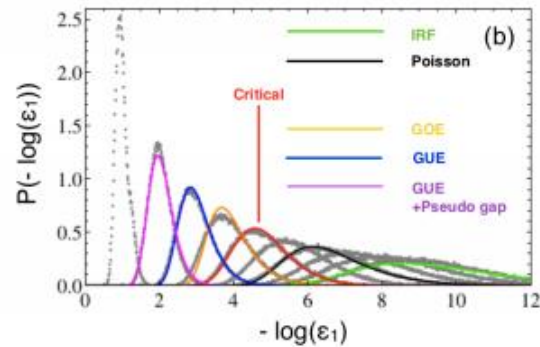
on the integrable structure of the corresponding quantum field theory, we have worked out an exact formula for this overlap, which was checked against extensive density matrix renormalization group calculations. Note that the comparison shown in the figure between numerical and field theory results does not involve any free parameter. Here we compare measures of the overlap in the free-fermion case, modeled by a spinless non-interacting resonant level Hamiltonian, tunnel-coupled with parameter J_1 to two metallic reservoirs with $N = 4096$ sites each. The dashed line is the analytical result, with $T_K \propto J^2$. Inset: finite size scaling.

Full counting statistics in the not-so-long-time limit: The full counting statistics of charge transport is the probability distribution $p_n(t_m)$ that n electrons have flown through the system in measuring time t_m . The cumulant generating function (CGF) of this distribution $F(x, t_m)$ has been well studied in the long-time limit $t_m \rightarrow \infty$, however there are relatively few results on the finite measuring time corrections to this. In recent work, we obtained the leading finite-time corrections to the CGF of interacting Fermi systems with a single transmission channel at zero temperature but driven out of equilibrium by a bias voltage. We conjectured that the leading finite-time corrections are logarithmic in t_m with a coefficient universally related to the long time limit. We provided detailed numerical evidence for this with reference to the self-dual interacting resonant level model. This model further contains a phase transition associated with the fractionalization of charge at a critical bias voltage. This transition manifests itself technically as branch points in the CGF. We provided numerical results of the dependence of the CGF on measuring time for

model parameters in the vicinity of this transition, and thus identified features in the time evolution associated with the phase transition itself.

Many-Body Localization Quantum Phase Transitions: we applied the real space renormalization technique to analyze a novel class of localization transitions in disordered quantum systems. We were particularly interested in how long-range interactions between the quantum degrees of freedom affect such transitions. This is for example relevant for interacting surface defects, i.e., randomly placed atoms on semiconductor or metal surfaces. More precisely, we studied the anisotropic Heisenberg model with long-range interactions, decaying with a power α , which are generated by placing spin sites at random positions along a chain. The real space renormalization method permits a large-scale finite-size analysis of systems with up to 256 spins, along with a disorder average over up to 300,000 realizations.

Analyzing the distribution of the first excitation energy from the ground state, we identified a critical power-law decay where the distribution function becomes critical, separating an insulator phase at larger α where the distribution is Poissonian, and a metallic state at smaller α , where it follows the Wigner surmise. In this figure, we show the distribution functions of the lowest excitation gap for various decay exponents α . Here the distribution functions are fitted by various analytical functions that are known from random matrix theory. These include the IRFP (infinite randomness fixed point) as $\alpha \rightarrow \infty$, Poisson (localized) for $\alpha > \alpha_c$, a critical distribution function at $\alpha = \alpha_c$, and the Wigner surmise for $\alpha < \alpha_c$.



Small quench dynamics as a probe for trapped ultra-cold atoms: Furthermore, we studied finite systems of bosons and fermions described by the Hubbard model, which can be realized by ultra-cold atoms confined in optical lattices. The ground states of these systems typically exhibit a coexistence of compressible superfluid and incompressible Mott insulating regimes. We have analyzed such systems by studying the out-of-equilibrium dynamics following a weak sudden quench of the trapping potential. In particular, we have shown how the temporal variance of the site occupations reveals the location of spatial boundaries between compressible and incompressible regions. We have demonstrated the feasibility of this approach for several models using numerical simulations. We first considered integrable systems, hard-core bosons (spin-less fermions) confined by a harmonic potential, where space separated Mott and superfluid phases coexist. Then, we analyzed a non-integrable system, a J-V - V' model with coexisting charge density wave and superfluid phases. We found that the temporal variance of the site occupations is a more effective measure than other standard indicators of phase boundaries such as a local compressibility. Finally, in order to make contact with experiments, we proposed a consistent estimator for such temporal variance. Our numerical experiments have shown that the phase boundary is correctly spotted using as little as 30 measurements. Based on these results, we were able to argue that analyzing

temporal fluctuations is a valuable experimental tool for exploring phase boundaries in trapped atom systems.

Future Plans

We are continuing our study of quenches of quantum systems towards non-equilibrium steady states, such as states carrying a DC current in quantum dots. Our past work has shown strong numerical evidence of the existence of $1/t$ universal corrections to the DC current and noise (in fact, the full counting statistics), and we are currently working to justify this result analytically and explore its range of validity across various models. Needless to say, the existence and universality of $1/t$ corrections is fascinating physically, and opens the door to powerful new methods of analysis of numerical data.

We are also currently working on the understanding of crossovers in ordinary quantum quenches, such as the crossover in the entanglement between two conductors when a weak link is suddenly turned on between them. It is then expected that the corresponding physics is universal on scales of the order of a Kondo temperature, but very little evidence for this exists so far. Our work is based on analytical calculations using the form-factor technique (generalizing our previous work on the Loschmidt echo) as well as on direct numerical calculations. We are also working on similar problems in the disordered case - such as the infinite disorder phase of random XX spin chains - where the existence of a single crossover scale is also suspected. The problem will have direct applications to the physics of disordered Kondo systems.

Publications

1. Crossover physics in the non-equilibrium dynamics of quenched quantum impurity systems, R. Vasseur, K. Trinh, S. Haas, H. Saleur, Phys. Rev. Lett. 110, 240601 (2013).
2. Many Body Localization Transition in Random Quantum Spin Chains with Long-Range Interactions, N. Moure, S. Haas and S. Kettemann, Eur. Phys. Lett. 111, 27003 (2015).
3. Exact overlaps in the Kondo problem, S. L. Lukyanov, H. Saleur, J. L. Jacobsen, R. Vasseur, Phys. Rev. Lett. 114, 080601 (2015).
4. Phase Diagram of Electron Doped Dichalcogenides M. Rösner, S. Haas, T. O. Wehling, Phys. Rev. B 90, 245105 (2014).
5. Valley Plasmonics in the Dichalcogenides, R.E. Groenewald, M.R. Rösner, G. Schönhoff, S. Haas, and T.O. Wehling, Phys. Rev. B 93, 205145 (2016).
6. Full counting statistics in the not-so-long-time limit, S. T. Carr, P. Schmitteckert, H. Saleur, Phys. Scr. T 165, (2015).
7. Interplay of screening and superconductivity in low-dimensional materials, G. Schönhoff, M. Rösner, R. Groenewald, S. Haas, and T. O. Wehling, <http://arxiv.org/pdf/1605.07489v1.pdf>
8. Small quench dynamics as a probe for trapped ultracold atoms, S. Yeshwanth, M. Rigol, S. Haas, and L. Campos Venuti, Phys. Rev. A 91, 06363 (2015).

Symmetry in Correlated Quantum Matter

Principal investigator: Michael Hermele

**Department of Physics, University of Colorado Boulder
Boulder, CO 80309**

Keywords: topological phases of matter, strongly correlated materials

Project Scope

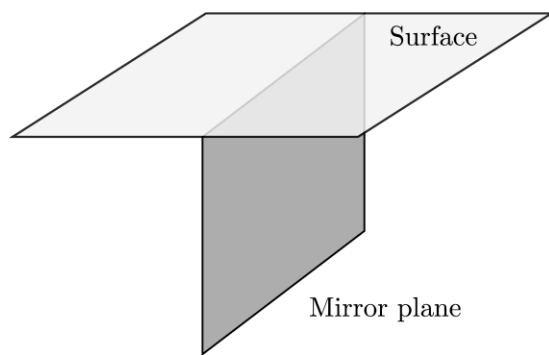
The over-arching goal of this project is to elucidate the role symmetry plays in correlated quantum matter. This includes both the role symmetry plays at the microscopic level, and its role in the universal properties of quantum phases of matter – both are significant in the physics of correlated materials. Selected specific issues addressed by recent and current work include: 1) Solving the problem of classifying symmetry protected topological phases with point group symmetry and identifying some physical properties of such states. 2) Developing theories of symmetry fractionalization in three-dimensional topologically ordered phases and for non-symmorphic crystalline symmetry. 3) Identification of quantum spin liquid states that can be realized in systems of novel magnetic degrees of freedom, and development of theories of their properties.

Recent Progress

Below are some highlights of progress made from the beginning of this project in August 2015. A comprehensive publication list for the past two years, also including work supported by the PI's previous DOE BES grant that ended in April 2015 (DE-FG-02-10ER46686), is included below.

Topological phases protected by point group symmetry. The PI, with Hao Song (former graduate student), Sheng-Jie Huang (graduate student) and Liang Fu, solved the problem of classifying symmetry protected topological (SPT) phases protected by crystalline point group symmetry, without making any assumptions about the strength of interactions. SPT phases are generalizations of

topological insulators to symmetries beyond charge conservation and time reversal, and to include states that have no band theory description. Developing a theory of point group SPT (pgSPT) phases is important because the



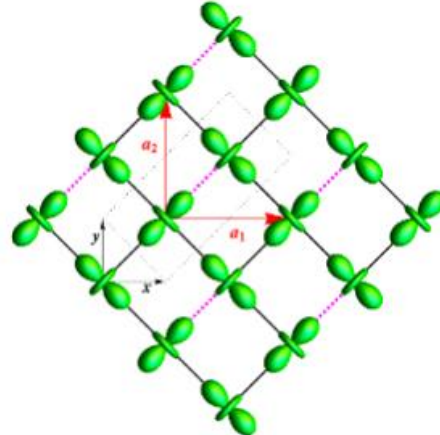
Topological phases protected by mirror symmetry in three dimensions can be reduced to lower-dimensional states located on the mirror plane.
(From #7 in publication list, arXiv:1604.08151.)

protecting symmetries occur in real solids, so that pgSPT phases may be realized in materials. Indeed, this has already been successful with topological crystalline insulators, which have been found in SnTe following the prediction of Hsieh *et. al.* Our work lays the foundation for efforts to realize beyond-band-theory pgSPT states in materials, and to predict associated physical properties.

Our approach applies in arbitrary spatial dimension, for bosonic and fermionic systems, and is based on a physically transparent reduction to lower-dimensional topological phases with internal symmetries. We showed that, surprisingly, pgSPT phases can always be thought of as stacks and arrays of such lower-dimensional states, and this provides a useful window into physical properties and provides clues about realization. This work has been submitted to *PRX*.

Symmetry fractionalization in three dimensions. The PI and Xie Chen developed a theory of symmetry fractionalization in three dimensions, for phases such as Z2 quantum spin liquids. The crucial new contribution is to understand the fractional action of symmetry on vortex-loop-like excitations, which we understood in terms of dimensional reduction to 2d. This work, which has been submitted to *PRB*, may be expected to lead to new insights into types and properties of three-dimensional spin liquid phases.

Non-symmorphic symmetry fractionalization. The PI, with S. Parameswaran and S. B. Lee, developed a theory of crystal symmetry fractionalization for non-symmorphic space groups, focusing on a particular example of a Z2 spin liquid on the 2d Shastry-Sutherland lattice. One outcome is a set of signatures of such symmetry fractionalization that can be used in numerical simulations. There may be applications to quantum magnets with non-symmorphic symmetry, which we are considering. Our work has been submitted to *PRB*.



An orbital order pattern with non-symmorphic space group symmetry. One of the models for non-symmorphic symmetry fractionalization studied in #8 of the publication list (arXiv:1605.08042) is based on this pattern.

Theory of quantum kagome ice. The PI and Yi-Ping Huang (graduate student) have developed a theory of quantum kagome ice as a Z2 quantum spin liquid. Quantum kagome ice is an apparent spin liquid state reported in recent numerical simulations of Roger Melko and collaborators, in a model of dipolar-octupolar doublets on the kagome lattice, study of which was inspired by prior studies of the PI, Huang and former postdoc Gang Chen (which were supported by the PI's previous DOE BES grant). Assuming quantum kagome ice is a Z2 spin liquid, we have identified which Z2 spin liquid it is most likely to be, and worked out some of its physical properties having to do with symmetry fractionalization, that can be computed in future numerical simulations, to confirm or rule out our theory. A manuscript on this work is being finalized for submission.

Future Plans

Realization and properties of topological phases protected by point group symmetry. The PI will build on the classification of point group symmetry protected topological phases to identify particularly promising examples of such states, to explore and suggest possible realizations of these states, and to elucidate their properties. Approaches will include developing bulk and surface field theories of these states, and connecting these field theories to microscopic models. Another approach we will pursue exploits the fact that point group SPT phases can be thought of as stacks and arrays of lower-dimensional phases, to explore the possibility of engineering such states in heterostructures or arrays of quantum wires. We will also consider the properties of topological crystal defects (*i.e.* dislocations and disclinations) in point group SPT phases.

Topological phases protected by space group symmetry. The PI will work to extend the classification of point group SPT phases to describe strongly interacting topological phases protected by full space group symmetry. This is expected to be especially fruitful in the case of non-symmorphic symmetries.

Symmetry enriched topological phases with point group symmetry. The PI will extend the classification of point group SPT phases to topological phases with exotic bulk excitations (*i.e.* anyons), such as gapped quantum spin liquids and fractional Chern insulators. This work may lead to new examples of such states and new insights into their properties.

Publications

This publication list covers the period August 2014 – July 2016, and includes works submitted (publicly available on the arXiv). Note that this project began in August 2015; for this reason, the publication list also includes publications supported under the PI's previous DOE BES project (DE-FG-02-10ER46686) that ended in April 2015 (denoted by *).

1. L. Wang, A. Essin, M. Hermele and O. Motrunich, *Numerical detection of symmetry-enriched topological phases with space-group symmetry*, Physical Review B **91**, 121103(R) (2015).*
2. J.-A. Yang, Y.-P. Huang, M. Hermele, T. Qi, G. Cao and D. Reznik, *High-energy electronic excitations in Sr₂IrO₄ observed by Raman scattering*, Physical Review B **91**, 195140 (2015).*
3. Y. Cao, Q. Wang, J. A. Waugh, T. J. Reber, H. Li, X. Zhou, S. Parham, S.-R. Park, N. C. Plumb, E. Rotenberg, A. Bostwick, J. D. Denlinger, T. Qi, M. A. Hermele, G. Cao and D. S. Dessau, *Hallmarks of the Mott-metal crossover in the hole-doped pseudospin-1/2 Mott insulator Sr₂IrO₄*, Nature Communications **7**, 11367 (2016).*
4. G. Chen, K. R. A. Hazzard, A. M. Rey and M. Hermele, *Synthetic-gauge-field stabilization of the chiral-spin-liquid phase*, Physical Review A **93**, 061601(R) (2016).*
5. X. Chen and M. Hermele, *Bosonic topological crystalline insulators and anomalous symmetry fractionalization via the flux-fusion anomaly test*, arXiv:1508.00573, submitted to PRX.
6. X. Chen and M. Hermele, *Symmetry fractionalization and anomaly detection in three-dimensional topological phases*, arXiv:1602.00187, submitted to Physical Review B.
7. H. Song, S.-J. Huang, L. Fu and M. Hermele, *Topological phases protected by point group symmetry*, arXiv:1604.08151, submitted to PRX.
8. S. B. Lee, M. Hermele and S. A. Parameswaran, *Fractionalizing glide reflections in two-dimensional Z2 topologically ordered phases*, arXiv:1605.08042, submitted to Physical Review B.

Quantitative Studies of the Fractional Quantum Hall Effect

Principal investigator: Professor Jainendra Jain

Department of Physics, 104 Davey Lab, Penn State University, University Park, PA 16802

jkj2@psu.edu

Project Scope

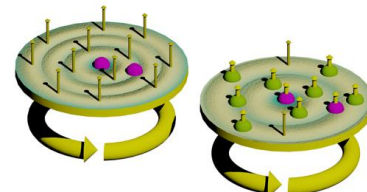
The objective of this program is to achieve an understanding of the fractional quantum Hall effect (FQHE) at a detailed quantitative level. Certain topological properties of candidate fractional quantum Hall states can be described through an effective field theory. However, the effective field theory does not tell us whether the fractional quantum Hall state will actually occur in nature for a realistic interaction, and it also does not provide quantitative predictions for many experimentally measurable quantities such as excitation gaps or spin polarization. Such quantitative comparisons with experiments are crucial for substantiating our understanding of the FQHE and can also reveal new puzzles. Fortunately, the FQHE is a strongly correlated system where it has been possible to make progress toward a quantitative understanding.

Recent Progress

All publications supported by DOE during the period 2014-2016 are listed at the end. We highlight some of the prominent results here.

Unconventional FQHE: In [1], we have made a convincing case that certain delicate FQHE states, such as that at 4/11, do not subscribe to any known type of FQHE but signify a new underlying structure. The actual wave function for this state is an open problem, but it is topologically distinct from the more obvious candidates.

FQHE for bosons: We have studied FQHE of bosons in anticipation of its realization in cold atom systems [6,13,15]. We have proposed that the quasiholes of a FQHE state can be conveniently captured and manipulated by the insertion of a few test bosons in the system. In particular, we have proposed [6] that it should be possible to measure the relative angular momentum of a pair of test bosons, which should have a fractional value under appropriate conditions. A measurement of fractional relative angular momentum will serve as a direct evidence for fractional statistics. Experimentalists are interested in pursuing our proposal. We have also shown [15] how two bosons can be put into topologically distinct qubits inside a non-Abelian state, but that would require an exquisite control over the interaction.

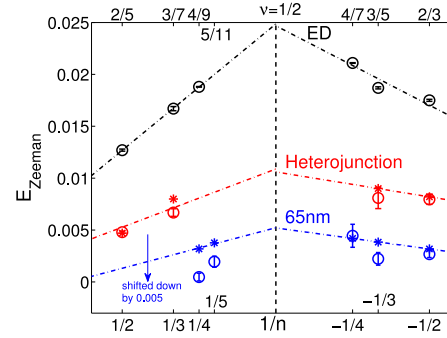


FQHE in graphene: We have focused on FQHE in graphene for three reasons. One, finite thickness corrections are negligible for graphene FQHE, and it may therefore offer an

opportunity for a more accurate comparison between theory and experiment than GaAs based quantum wells (where the finite width of the quantum well leads to significant quantitative corrections). In [16], we evaluate the phase diagram of spin polarization for FQHE in graphene. Secondly, experiments have suggested a surprising possibility that FQHE in the $n=1$ Landau level of graphene may involve the spin degree of freedom up to very high magnetic fields. We showed in [19] that, in contrast to the $n=0$ Landau level, the FQHE states in the $n=1$ Landau level of graphene are fully spin polarized even at zero Zeeman energy. This conclusion ought to be experimentally testable. Finally, graphene has now begun to show extensive FQHE, and may replace GaAs based systems in the future.

Effect of Landau level mixing: The article [4], which is primarily an experimental article, showed that the spin phase transitions are a very sensitive tool for studying the breaking of particle hole symmetry due to Landau level mixing. In particular, this article found that the spin phase transitions at filling factors $3/5$ and $7/5$ occur at very different values of the Zeeman energy, even though particle hole symmetry within the lowest Landau level would predict the same values. In [21], we have

studied this issue in a diffusion Monte Carlo approach, which treats Landau level mixing in a non-perturbative fashion, and found excellent agreement with experiments. (In the attached figure, the colored circles are from our theory including both finite thickness and Landau level mixing corrections and stars are from experiments. The black circles are from an ideal theory that assumes zero thickness and no Landau level mixing.)



Luttinger theorem for composite fermions: Composite fermions form a Fermi sea at half filling. Slightly away from half filling, there is an ambiguity regarding the size of the composite fermion Fermi sea: It can be equal to the number of electrons or the number of holes in the lowest Landau level. Experimental measurements of the Fermi wave vector of composite fermions found that the answer is closer to the smaller of the two numbers. In [17] we evaluated the Fermi wave vector from the microscopic theory and found that the result is consistent with experiments. Our work also suggests a slight violation of the Luttinger theorem, which states that the area of the Fermi sea is equal to the number of particles.

Fractionally charged skyrmions: For sufficiently low Zeeman energies, the lowest energy excitation at filling factor 1 is not a spin reversed electron but a skyrmion. Similar physics was proposed also at $1/3$, but under much more restrictive conditions. In Ref. [18], which is a joint theory-experiment collaboration, we showed that the smallest skyrmion exists in the excitation spectrum for a much larger range of parameters, and identified certain sub-Zeeman energy modes with these skyrmions. We found excellent agreement between the predicted and the measured binding energies of the skyrmion.

Future Plans

I briefly describe my plans for the near future.

Fixed phase diffusion Monte Carlo studies of FQHE: My student Yuhe Zhang has developed a fixed phase diffusion Monte Carlo code to study the role of finite width and Landau level mixing on various quantities. We have recently applied this method to the issue of spin polarization transitions in FQHE, and found that corrections due to finite width and Landau level mixing can be significant. Yuhe Zhang will study many other quantities with this approach, including excitation gaps and collective mode energies, the competition between Pfaffian and antiPfaffian for the 5/2 FQHE, and the phase transition from a FQHE state into a crystal phase with increasing Landau level mixing. We will also extend the fixed phase diffusion Monte Carlo method to treat graphene.

Density functional theory for composite fermions: We will develop a density functional theory for fractional quantum Hall effect, to treat systems in the presence of a non-uniform external potential. To this end we will need an accurate exchange correlation potential for which we will employ the composite fermion theory. The density functional theory will be used to determine the density profile at the edges of FQHE states, and also the density modulation of the composite fermion Fermi sea when exposed to a periodic potential (motivated by recent Princeton experiments that create such a potential by realizing a Wigner crystal in a nearby layer). We will also look for solutions containing stripes and bubble crystals.

Publications supported by DOE during 2014-2016

1. "The Enigmatic 4/11 State: A Prototype for Unconventional Fractional Quantum Hall Effect," Sutirtha Mukherjee, Sudhansu S. Mandal, Y.-H. Wu, Arkadiusz W'ojs, J. K. Jain, Phys. Rev. Lett. 112, 016801 (2014).
2. "A note contrasting two microscopic theories of the fractional quantum Hall effect," J. K. Jain, Indian Journal of Physics 88, 915-929 (2014).
3. "Collective excitations of a system of coupled relativistic and non-relativistic two-dimensional electron gases," A. C. Balram, J. A. Hutasoit, and J. K. Jain, Phys. Rev. B 90, 045103 (2014).
4. "Spin-Polarization of Composite Fermions and Particle-Hole Symmetry Breaking," Yang Liu, S. Hasdemir, D. Kamburov, A. W'ojs, J.K. Jain, L.N. Pfeiffer, K.W. West, K.W. Baldwin, and M. Shayegan, Phys. Rev. B 90, 085301 (2014) [5 pages].
5. "Possible realization of a chiral p-wave paired state in a two component system," Sutirtha Mukherjee, J. K. Jain, and Sudhansu S. Mandal, Phys. Rev. B 90, 121305(R) (2014) [Rapid Communications].
6. "Fractional angular momentum in cold atom systems," Y. Zhang, G. J. Sreejith, N. D. Gemelke, and J. K. Jain, Phys. Rev. Lett. 113, 160404 (2014). [Selected as an Editor's Suggestion.]

7. "Theoretical investigation of edge reconstruction in the $v = 5/2$ and $7/3$ fractional quantum Hall states," Yuhe Zhang, Ying-Hai Wu, Jimmy A. Hutasoit, and Jainendra K. Jain, Phys. Rev. B. 90, 165104 (2014) [17 pages].
8. "Long-Range Spin Triplet Helix in Proximity Induced Superconductivity in Spin-Orbit-Coupled Systems," Xin Liu, J. K. Jain and C.-X. Liu, Phys. Rev. Lett. 113, 227002 (2014).
9. "Single-Fluxon Controlled Resistance Switching in Centimeter-Long Superconducting Gallum- Indium Eutetic Nanowires," Weiwei Zhao, J. L. Bischof, J. Hutasoit, X. Liu, T. C. Fitzgibbons, J. R. Hayes, P. J. A. Sazio, C.-X. Liu, J. K. Jain, J. V. Badding, and M. H. W. Chan, Nano Lett. 15, 153-158 (2015).
10. "Fractional Quantum Hall Effect of Composite Fermions in Multi-Component Systems," A. C. Balram, C. T'oke, A. Wojs and J. K. Jain, Phys. Rev. B 91, 045109 (2015) [25 pages].
11. "Fractional topological phases in generalized Hofstadter bands with arbitrary Chern numbers," Ying-Hai Wu, J. K. Jain and K. Sun, Phys. Rev. B 91, 041119(R) (2015) [Rapid Communications].
12. "Composite fermion theory of exotic fractional quantum Hall effect," J. K. Jain, Annu. Rev. Condens. Matter Phys. 6, 39-62 (2015).
13. "Emergent Fermi Sea in a System of Interacting Bosons," Y.-H. Wu and J. K. Jain, Phys. Rev. A 91, 063623 (2015) [7 pages].
14. "Zero-field dissipationless chiral edge transport and the nature of dissipation in the quantum anomalous Hall state, Cui-Zu Chang, Weiwei Zhao, Duk Y. Kim, Peng Wei, J. K. Jain, Chaoxing Liu, Moses H. W. Chan, and Jagadeesh S. Moodera, Phys. Rev. Lett. 115, 057206 (2015).
15. "Creating and manipulating non-Abelian anyons in cold atom systems using auxiliary bosons," Y. Zhang, G. J. Sreejith and J. K. Jain, Phys. Rev. B 92, 075116 (2015) [15 pages].
16. "Fractional Quantum Hall Effect in Graphene: Quantitative Comparison between Theory and Experiment," Ajit C. Balram, Csaba T'oke, A. Wojs, and J. K. Jain, Phys. Rev. B 92, 075410 (2015) [13 pages].
17. "Luttinger theorem for the strongly correlated composite fermion liquid," A. C. Balram, C. T'oke and J. K. Jain, Phys. Rev. Lett. 115, 186805 (2015).
18. "Fractionally charged skyrmions in the fractional quantum Hall effect," Ajit C. Balram, U. Wurstbauer, A. Wojs, A. Pinczuk, and J. K. Jain, Nature Commun. 6, 9981(2015).
doi:10.1038/ncomms9981.
19. "Spontaneous polarization of composite fermions in graphene $n = 1$ Landau level," A. C. Balram, C. T'oke, A. Wojs and J. K. Jain, Phys. Rev. B 92, 205120 (2015).
20. "Robustness of topological surface states against strong disorder observed in Bi₂Te₃ nanotubes," Renzhong Du, Hsiu-Chuan Hsu, Ajit C. Balram, Yuewei Yin, Sining Dong, Wenqing Dai, Weiwei Zhao, DukSoo Kim, Shih-Ying Yu, Jian Wang, Xiaoguang Li, Suzanne E. Mohney, Srinivas Tadigadapa, Nitin Samarth, Moses H. W. Chan, Jainendra. K. Jain, Chao-Xing Liu, and Qi Li, Phys. Rev. B 93, 195402 (2016).
21. "Landau level mixing and particle hole symmetry breaking for spin transitions in fractional quantum Hall effect," Y. Zhang, A. Wojs, J. K. Jain, submitted (arXiv:1606.03485).

Targeted Band Structure Design and Thermoelectrics Materials Discovery Using High-Throughput Computation

Principal investigator: Anubhav Jain
Energy Technologies Area, Lawrence Berkeley National Laboratory
Berkeley, CA 94720
ajain@lbl.gov

Project Scope

This project aims to (i) generate large simulation data sets of electronic structure and transport, (ii) apply statistical analysis and data mining techniques to these data sets to understand how the electronic band structures of materials can be rationalized and controlled, and (iii) design and discover new thermoelectric materials. Sub-projects include developing and benchmarking theoretical tools (e.g., density functional theory and related methods) for accurate band structure and transport calculations, developing a high-throughput computing environment capable of executing millions of calculations at national supercomputing centers, establishing relevant chemical and structural descriptors that are predictive of features of the band structure, and working with experimental partners to identify and optimize new thermoelectric materials.

Recent Progress

Below are some highlights from the initial year of funding:

Database of electronic transport coefficients – We calculated a database of electronic transport properties (currently ~50,000 records) based on solving the Boltzmann transport equations (using the BoltzTraP software) using density functional theory band structures from the Materials Project (MP) database. The data includes computations of electronic conductivity, Seebeck coefficient, power factor, and electronic contribution to thermal conductivity. A manuscript (in preparation) will distribute the full data set publicly. We validated the transport calculations versus known experimental data, investigating two broad issues in accuracy. The first class of problems stem from the underlying band structure, for example due to well-known accuracy problems with GGA/GGA+U band gaps. A second class of problems originates in the electronic transport theory; the most severe of these is the constant relaxation time approximation used by BoltzTraP code. In the case of the Seebeck coefficient, discrepancies between theory and experiment largely originate from issues in the underlying band structure, whereas for the electronic conductivity, the constant power factor approximation is the dominant source of error. These results, plus a broader analysis of the electronic transport data set, were published in Journal of Materials Chemistry C.

Identification and experimental verification of YCuTe₂ thermoelectric material – The database of electronic transport properties discussed in the previous section, and including further calculations such as minimum thermal conductivity via the Cahill model, was used to identify materials in the database with promising thermoelectric properties that remain unexplored by the thermoelectrics community. One of these materials,

YCuTe_2 , was targeted due to (i) reasonable thermoelectrics possibility in the calculation database (zT reaching $\sim 1.0\text{-}1.5$, depending on assumptions made), (ii) known low thermal conductivities of copper chalcogenides and potential for liquid-like Cu phonon scattering mechanisms, and (iii) a good match to the synthesis capabilities of our collaborators (Snyder group at Northwestern).

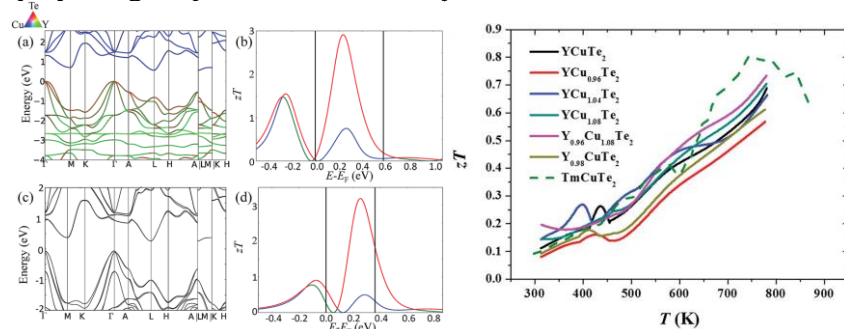


Figure 1 Projected band structure (top-left) and band structure with spin-orbit effects included (bottom-left) of YCuTe_2 . Spin-orbit coupling breaks the degeneracy between Gamma and A points, such that the attainable zT is expected to reach 1.5 (top-center) in the absence of spin-orbit coupling but only ~ 1.0 with its inclusion (bottom-center). The experimental zT of ~ 0.75 (right) is lower than the theoretical prediction due to insufficient carrier concentration. This material represents a new thermoelectrics candidate identified by high-throughput computational screening.

Experimental synthesis and characterization of this material confirmed a zT reaching as high as 0.75 (Figure 1). In particular, a very low lattice thermal conductivity of $0.43 \text{ W m}^{-1} \text{ K}^{-1}$ was measured in experiments. Further computational characterization of the YCuTe_2 material is ongoing to understand the origin of low thermal conductivity and to probe whether targeted dopants might enhance the carrier concentration to further improve zT . The results of this study were published in the Journal of Materials Chemistry A.

Data mining analysis of electronic structure – Preliminary work has been initiated towards the use of data mining techniques to understand electronic structure. The database of 50,000 compounds for electronic transport was used to uncover broad trends, such as the fact that oxide materials tend to have lower power factors than sulfides, selenides, and tellurides, even after fully controlling for factors such as the relaxation time and doping level (Figure 2). Thus, there exists some fundamental property of oxide band structures that make them poorer thermoelectrics; understanding these reasons more clearly could help in designing exceptions to the rule and developing earth-abundant oxide thermoelectrics.

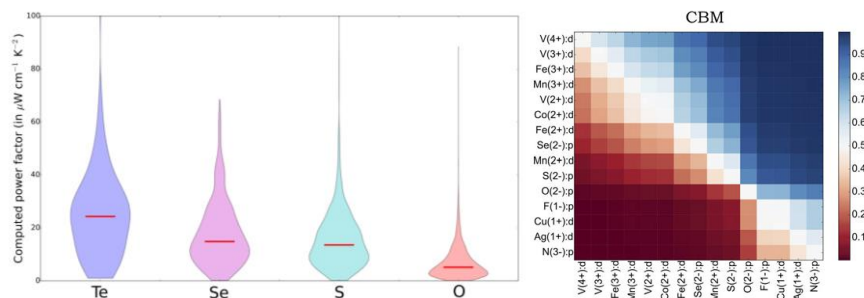


Figure 2 Left: Violin plots depicting the distribution of computed maximum power factor under a fixed relaxation time approximation across compounds in the MP database, separated by anion type. The red lines indicate the median computed power factor for different anions. The distribution of power factors for tellurides tends to be higher than that for selenides and sulfides, which are in turn higher than those of oxides. Right:

Pairwise probability for the ionic orbital listed to the left to have a greater contribution to a band edge (in this case, conduction band minimum) than the ionic orbital listed at the bottom. This can be used to predict how compositional substitution can affect band character.

One contribution towards more rationally designing electronic properties would be to better understand how orbital interactions give rise to the band structure of materials and to be able to predict what types of interactions will dominate the band edges, which are most responsible for transport properties. Differences in orbital character of the valence and conduction bands will furthermore be major factors in determining valley degeneracy and band gap. In one sub-study, we used machine learning techniques to predict the orbital character of the valence band and conduction band in arbitrary materials (Figure 2). Integration of the results of this study with the thermoelectrics screening should yield better insights into chemistry-based differences in thermoelectrics performance.

Open source software toolkit development – We developed and extended several open-source software tools that will help enable high-throughput computing and data mining for the broader materials research community:

- **FireWorks** is a workflow software for high-throughput calculations primarily authored by PI Jain and that was initially funded by the Materials Project center. In the past year, there have been 284 new commits to FireWorks. Major features include (i) support for Argonne Leadership Computing Facility via the Cobalt job submission manager, allowing calculations to run on some of the largest DOE supercomputers (ii) new reporting features that generate statistical reports on jobs and workflows, and (iii) an “introspection” option that can help identify parameters responsible for failing jobs. More information on FireWorks, including source code download, is available at [<http://pythonhosted.org/FireWorks>].
- **MatMethods** is a new open-source software developed in the past year that contains explicit workflows for calculating the properties of materials (currently focusing on DFT and related methods; extensions for classical molecular dynamics are being developed by collaborators). MatMethods contains specific workflows for computing the band structure, spin-orbit coupling effects, hybrid functional band gaps, ab initio molecular dynamics, elastic properties of materials, and optical properties of materials – all fully automatically and scalable to million of workflows and deployable on a range of computing environments. More information, including the source code, is available at [<http://pythonhosted.org/MatMethods>].
- **MatMiner** is a new open-source software initiated in the past year that is intended to make it possible for materials scientists to quickly and easily employ data mining to understand materials property data. The core features of MatMethods are (i) loading data from a variety of platforms (e.g., Materials Project, the Citrination platform, MongoDB databases, etc.) into the Pandas statistical data format, (ii) development of a library of descriptors that can be used to relate crystal structure input properties to output properties, (iii) integration with the scikit-learn library for machine learning, and (iv) visualization and data analysis tailored to materials science applications. The source code of MatMiner can be found at: [<http://www.github.com/hackingmaterials/MatMiner>].

Future Plans

Develop more accurate methodologies and software for electronic transport calculations

– We have recently begun pursuing two strategies for more accurate calculation of electronic transport properties in high-throughput. The first strategy is to employ functionals expected to produce more accurate results than GGA/GGA+U. The second strategy is to develop a new method for computing electronic transport properties that is capable of including realistic scattering models based on calculated data (e.g., polar optical scattering) and that avoids many limitations of the constant relaxation time model; preliminary results indicate much greater accuracy than the standard BoltzTraP code.

Develop a library of descriptors that can be used to build predictive models of how crystal structure and composition influences band structure

– We have begun developing a library of compositional descriptors that can be used for data mining purposes within the MatMiner library. Structural descriptors, and in particular local environment analysis, are currently in the benchmarking phase. These descriptors will make it possible to employ statistical learning and data mining techniques to extract insights from the large database of electronic structure and transport properties.

Continue screening / search for new thermoelectric materials and expanding the database of electronic transport properties

– Calculation of electronic structure and transport, as well as identification of promising thermoelectrics materials, is ongoing and will continue into the future.

Publications

1. Chen W., Pohls J.-H., Hautier G., Broberg D., Bajaj S., Aydemir U., Gibbs Z.M., Zhu H., Asta M., Snyder G.J., Meredig B., White M.A., Persson K.A., Jain A., Understanding Thermoelectric Properties from High-Throughput Calculations: Trends, Insights, and Comparisons with Experiment, *J. Mater. Chem. C*, 2016, 4, 4414-4426
2. Aydemir U., Pohls J.-H., Zhu H., Hautier G., Bajaj S., Gibbs Z.M., Chen W., Li G., Ohno S., Broberg D., Kang S.D., Asta M., Ceder G., White M.A., Persson K., Jain A., Snyder G.J., YCuTe2: A Member of A New Class of Thermoelectric Materials with CuTe4-Based Layered Structure, *J. Mater. Chem. A*, 2016, 4, 2461-2472
3. Jain A., Hautier G., Ong S.P., Persson K., New opportunities for materials informatics: Resources and data mining techniques for uncovering hidden relationships, *J. Mater. Res.*, 2016, 31, 977-994

Mapping and Manipulating Materials Transformation Pathways and Properties

Principal investigator: Duane D. Johnson

Ames Laboratory, and Dept. of Materials Science & Engineering, Iowa State University

Ames, IA 50011-1015

ddj@ameslab.gov

Project Scope

Our primary goal is to explore, explain, and control the unique properties and phase transformation in complex materials, particularly correlated, responsive properties involving alloying, chemical disorder and defects, magnetic (paramagnetic and non-collinear spin) correlations, applied fields, and electronic effects, such as Fermi-surface and dispersion driven phenomena. To design multicomponent materials and tailor their functionality, and guide synthesis and characterization, we are developing and applying unique electronic-structure-based, thermodynamic techniques to quantify stability and properties by mapping *global solid-solid transformations* (e.g., between competing long-range order (LRO) states) and *local structural instabilities* (e.g., short-range order (SRO) or order-disorder transitions). Applications are mainly on novel, complex multicomponent alloys and responsive materials, such as shape-memory alloys, high-entropy alloys, nanoalloy catalysts, iron-arsenide superconductors and topological insulators. Examples of phenomena studied include: (i) properties and transformation paths in shape-memory alloys, with newly predicted structures; (ii) stability and SRO in high-entropy alloys, including ordering transitions; (iii) stabilizing topological systems and identifying new properties, like Dirac node arcs; (iv) alloying and magnetic effects in Fe-As systems, such as spin waves, Lifshitz transitions, and quantum critical phenomena.

We are advancing thermodynamic linear-response theory to predict SRO involving coupled *electronic, chemical, magnetic, and structural* fluctuations in complex N-component systems. We are mapping solid-solid transformation pathways (enthalpies and barriers) between states, including by extending *solid-state nudged-elastic band* methods to incorporate magneto-volume collapse and chemical disorder. With magnons included we can address, e.g., doped-BaFe₂As₂; magnets with magneto-structural transitions; and skyrmion-type systems. Jointly, these methods *uniquely assess global and local stability between competing structures and synthesis routes*, revealing opportunities to manipulate properties. These innovative methods *predict and interpret origins of properties* in coupled, complex materials to tailor functionality.

Recent Progress

Below are some highlights of progress made in the past 2 years (a more comprehensive publication list is appended at the end).

Short-Range Order and Incipient Long-Range Order in High-Entropy Alloys – We use Green's function KKR-CPA electronic-structure methods to address thermodynamics in ordered, partially disordered and fully disordered systems. Relative stability and order-disorder phase transitions (chemical and magnetic) are determined by formation enthalpies. Interestingly, thermodynamic linear-response theory can be done analytically using the homogeneous disordered state as a reference (Landau-like theory), and the resulting second-order variations

of the free-energy [the chemical stability matrix, $S^{\lambda\mu}(\mathbf{q};T)$] for λ - μ pair-exchange for an ordering wave with periodicity \mathbf{q} on the underlying Bravais lattice. This energy cost can be numerically evaluated for any number of alloying components (i.e., an N-component alloy, such as high-entropy alloys), including with magnetic disorder. The eigenvectors and eigenvalues of $S^{\lambda\mu}(\mathbf{q};T)$ reveal all competing chemical ordering (or clustering, $\mathbf{q}=(000)$) modes, including low-energy (favorable) modes, similar to phonons that reveal low-energy vibrational modes. The temperature-dependence is weak, and arises from Fermi factors. Eigenvectors describe the allowed low-energy order, predicting competing phases and energy scales. [1]

Analytically, $S^{\lambda\mu}(\mathbf{q};T)$ determines the $N(N-1)/2$ distinct Warren-Cowley pair correlations, i.e., $\alpha_{\lambda\mu}^{-1}(\mathbf{q},T) = \left[(\delta_{\lambda\mu} - c_\mu) \left(\delta_{\lambda\mu} + \frac{c_\mu}{c_N} \right) \right] - (k_B T)^{-1} (\delta_{\lambda\mu} - c_\mu) S^{\lambda\mu}(\mathbf{q};T)$. Hence, $S^{\lambda\mu}(\mathbf{q};T)$ reveals the short-range order (SRO) in an N-component alloy. For $N>3$, a single pair correlation typically dictates SRO, but multiple Warren-Cowley SRO parameters will exhibit the same peak, due to the above inversion and probability conservation. Hence, pair correlations do not necessarily distinguish the dominant interactions that drive SRO and phase transitions, but we can! [1]

Figure 1 (top) gives the relative global stability of $\text{Al}_x(\text{CoCrFeNi})_{1-x}$ high-entropy alloys ($N=5$) from formation enthalpies for A1 (fcc) and A2 (bcc) phases calculated using KKR-CPA (MECCA2.0 code). For A1, the SRO is clustering (segregation) tendency; for A2, SRO is B2 like driven by Al-Ni interactions, **Figure 1** (bottom). [1] The two-phase (A1+A2) region is observed, and shows competing effects. Our work was highlighted in Nature News (*Nature* 533, 306–307 (2016) [10.1038/533306a](https://doi.org/10.1038/533306a)). These electronic-structure-based thermodynamic calculations were used to develop improved semi-empirical potentials for use in LAMMPS molecular dynamics code to assess mechanical responses of high-entropy alloys and their dynamics, which are useful for technological applications. [2]

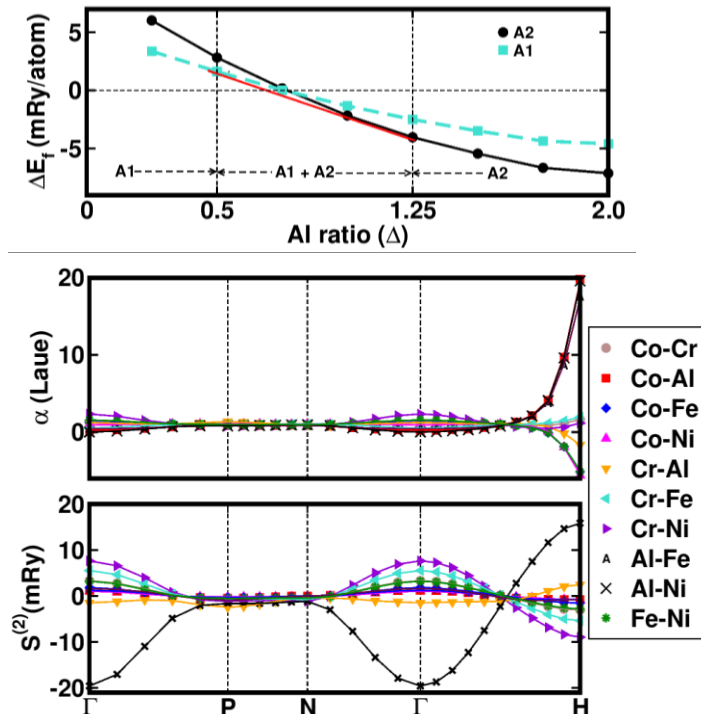


Figure 1 For $\text{Al}_x(\text{CoCrFeNi})_{1-x}$ high-entropy alloys ($N=5$), with $x=\Delta/5$.

(top) KKR-CPA calculated formation enthalpy for A1 and A2 phases, with a two-phase (A1+A2) region from $0.5 < \Delta < 1.25$, which matches experiment well.

(bottom) For A2 phase, $N(N-1)/2=10$ unique Warren-Cowley SRO parameters in Laue units calculated at 10% above the spinodal temperature. For $S^{\lambda\mu}(\mathbf{q})$ in lower plot, positive values indicate the favorable modes that will go unstable. As is clear, the Al-Ni pair is driving order with an $H=(111)$ mode, indicating B2-type short-range order. NOTE: Besides Al-Ni, both the Al-Co and Al-Fe also exhibit a correlation in the Warren-Cowley pair correlations at H , not due to physics.

Transformation Pathways and Transition States in Shape-Memory System – We have developed the first complete atomic-scale view of structural transformations responsible for shape-memory effect in Nitinol (Ni-Ti) alloys, which “remember” their original shape and respond to heat to produce desirable shape changes. Despite its industrial popularity, the underlying physics and atomistic mechanics have remained unclear for 50 years. The shape-memory effect is controlled by transformations mostly between high-temperature (austenite) and low-temperature (martensite) structures. To elucidate the path of shape change, structures, and transition states, we employed a generalized solid-state nudged elastic band (GSS-NEB) method that properly handles the mechanics of solid-solid transformations,[3] co-developed earlier with G. Henkelman (U. of Texas – Austin) and now a worldwide standard.

Identifying the origin of this technologically useful effect provides vital information for synthesizing and designing new shape-memory materials. Predicted transformations include a previously unidentified stable austenite structure (not B2), kinetically-limited intermediate R' structures, and B19' martensitic variants.[3,4,5] We predicted a new structure for austenite, a “phonon glass” hexagonal-like structure with large isotropic displacements with broad distribution of sizes correlated over $\sim 3\text{\AA}$, [4] which appears B2 (on average) in diffraction. The displacements are up to 20% of the average B2 lattice constant, much larger than the Lindeman criterion for melting! Overall, the calculated latent heat, diffraction, phonon density of states all agree well with experiments. We continue to apply these techniques to other critical systems, e.g., Ti [6], chosen for 2016 Physical Review B *Kaleidoscope*.

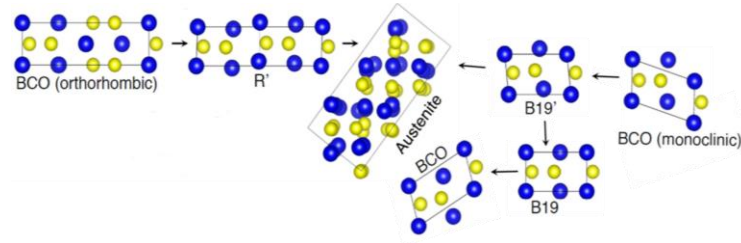


Figure 2a. NiTi shape-memory transitions [Ni, yellow; Ti, blue]: Body-Centred Orthorhombic (BCO) groundstate, R' phases, new austenite (hex-like phonon-glass) structure, and martensite (BCO) variants.

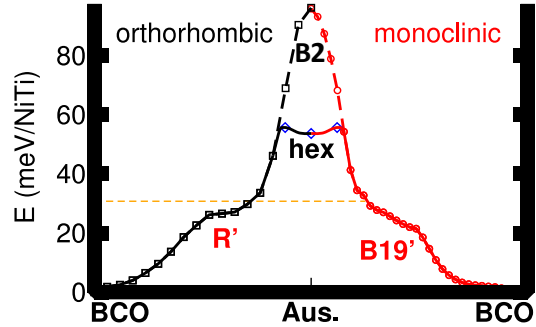


Figure 2b. Austenite-to-Martensite minimum enthalpy pathways (MEP) for transitions. B2 is unstable. The small Aus.-to-Mart. barrier gives observed hysteresis. MEP slope gives driving force for transformations, so, R' is a sluggish transformation, as observed. The angle for B19' is between 90–110 degrees along MEP, as observed. BCO-to-BCO MEP involves multiple martensite variants, as observed, with a twinned martensite at the transition state.

Transformation Pathways in Magnetic Systems with Pressure – We extended the proper GSS-NEB method to address correctly magneto-structural transitions, controlled by non-conserved order parameters, wrong in all other NEB and related methods.[7,8] We applied this to pressure-induced bcc-to-hcp transformations in Fe, explaining all experimental results, and showing that not all pressures used are hydrostatic. All the codes are available [4,7,8].

We have applied these electronic-structure methods to broad classes of other systems to support ongoing BES-funded programs, such as discovering *Dirac Node Arcs* [9]; predicting

Lifshitz transitions and alloying in Fe-As superconductors [10-11]; *line-compound catalyst* [12,13]; *Devil's staircase ordering* on wetting layer [14]; *spin gapless semiconductors* [15]; and we develop methods [4,7,16-21] to predict accurate structural and thermodynamic properties.

Future Plans

Chemical SRO and Incipient LRO in Multisublattice Complex Systems – We are extending the electronic-structure-based thermodynamic techniques to general multisublattice, partially ordered systems, e.g., non-groundstate Fe-As systems, ferroelectrics, and caloric materials. Coding and testing is underway.

Magnons – in collaboration with Bill Shelton (LSU), we will add spin-spin linear-response (*magnon*) *susceptibility* capabilities to MECCA2.0. Besides revealing direct electronic origins for phenomena, magnetic SRO pre-define supercells needed below Curie/Neél temperatures, eliminating supercell “guesswork” required with other methods unable to address symmetric high-temperature states with disorder. This can be combined atomic SRO.

Publications

1. P. Singh, A.V. Smirnov, and D.D. Johnson, "Atomic Short-Ranged Order and Incipient Long-Range Order in High Entropy Alloys," **Phys. Rev. B** **91**, 224204-12 (2015). [10.1103/PhysRevB.91.224204](https://doi.org/10.1103/PhysRevB.91.224204)
2. A. Sharma, P. Singh, D.D. Johnson, Peter K. Liaw, and G. Balasubramanian, "Atomistic clustering-ordering and high-strain deformation of $\text{Al}_{0.1}\text{CrCoFeNi}$ high-entropy alloys," **Nature Scientific Reports** (2016). *In Press*
3. N.A. Zarkevich and D.D. Johnson, "Shape-memory transformations of NiTi: minimum-energy-pathways between austenite, martensites, and kinetically-limited intermediate states," **Phys. Rev. Letts.** **113**, 265701-5 (2014). [10.1103/PhysRevLett.113.265701](https://doi.org/10.1103/PhysRevLett.113.265701)
4. N.A. Zarkevich and D. D. Johnson, "Stable atomic structure of NiTi austenite," **Phys. Rev. B** **90**, 060102-4(Rapid) (2014). [10.1103/PhysRevB.90.060102](https://doi.org/10.1103/PhysRevB.90.060102)
5. N. A. Zarkevich and D.D. Johnson, "Nudged-Elastic Band method using double-climbing images: finding transition states in complex energy landscapes," **J. Chem. Phys.** **142**, 024106 (2015). [10.1063/1.4905209](https://doi.org/10.1063/1.4905209)
6. N.A. Zarkevich and D.D. Johnson, "Titanium α - ω transformations pathway and a predicted metastable structure," **Phys. Rev. B** **93**, 0201104(R)-5 (2016). [10.1103/PhysRevB.93.020104](https://doi.org/10.1103/PhysRevB.93.020104)
7. N.A. Zarkevich and D.D. Johnson, "Magneto-structural transformations via a solid-state nudged elastic band method: Application to iron under pressure," **J. Chem. Phys.** **143**, 064707-7 (2015). [10.1063/1.4927778](https://doi.org/10.1063/1.4927778)
8. Nikolai A. Zarkevich and D.D. Johnson, "Coexistence pressure for a martensitic transformation from theory and experiment: Revisiting the bcc-hcp transition of iron under pressure," **Phys. Rev. B** **91**, 174104-9(2015). [10.1103/PhysRevB.91.174104](https://doi.org/10.1103/PhysRevB.91.174104)
9. Yun Wu, Lin-Lin Wang, Eundeok Mun, D. D. Johnson, Daixiang Mou, Lunan Huang, Yongbin Lee, S. L. Bud'ko, P.C. Canfield, Adam Kaminski, "Dirac Node Arcs in PtSn_4 ," **Nature Physics** (2016), 6-pgs. [10.1038/nphys3712](https://doi.org/10.1038/nphys3712)
10. S.N. Khan, Aftab Alam, and D.D. Johnson, "Fermi surfaces and phase stability of $\text{Ba}(\text{Fe}_{1-x}\text{M}_x)\text{As}_2$ ($\text{M}=\text{Co}, \text{Ni}, \text{Cu}, \text{Zn}$)," **Phys. Rev. B** **89**, 205121 (2014). [10.1103/PhysRevB.89.205121](https://doi.org/10.1103/PhysRevB.89.205121)
11. S.N. Khan and D. D. Johnson, "Lifshitz transition and chemical instabilities in $\text{Ba}_{1-x}\text{K}_x\text{Fe}_2\text{As}_2$ superconductors," **Phys. Rev. Lett.** **112**, 156401-5 (2014). [10.1103/PhysRevLett.112.156401](https://doi.org/10.1103/PhysRevLett.112.156401)
12. Raghu V. Maligal-Ganesh, Chaoxian Xiao, Tian Wei Goh, Lin-Lin Wang, Jeffrey Gustafson, Yuchen Pei, Duane D. Johnson, Shiran Zhang, Franklin (Feng) Tao, and Wenyu Huang, "A Ship-in-a-Bottle

- Strategy to Synthesize Encapsulated Intermetallic Nanoparticles Catalysts: exemplified for furfural hydrogenation," **ACS Catalysis** **6**, 1754-1763 (2016). [10.1021/acscatal.5b02281](https://doi.org/10.1021/acscatal.5b02281)
- 13. Teck L. Tan, Lin-Lin Wang, Jia Zhang, Duane D. Johnson, and Kewu Bai, "Platinum Nanoparticle During Electrochemical Hydrogen Evolution: Adsorbate Distribution, Active Reaction Species, and Size Effect," **ACS Catalysis** **5**, 2376-2383(2015). [10.1021/cs501840c](https://doi.org/10.1021/cs501840c)
 - 14. Lin-Lin Wang, D. D. Johnson, and M. C. Tringides, " C_{60} -Induced Devil's Staircase Reconstructions on Pb/Si(111) Wetting Layer," **Phys. Rev. B** **92**, 245405-6(2015). [10.1103/PhysRevB.92.245405](https://doi.org/10.1103/PhysRevB.92.245405)
 - 15. Lakhan Bainsla, A.I. Mallick, M. Manvel Raja, A.A. Coelho, A.K. Nigam, D.D. Johnson, Aftab Alam, and K.G. Suresh, "Evidence of spin gapless semiconductor behavior in the equiatomic quaternary Heusler CoFeCrGa alloy," **Phys. Rev. B** **92**, 045201-5 (2015). [10.1103/PhysRevB.92.045201](https://doi.org/10.1103/PhysRevB.92.045201)
 - 16. N.A. Zarkevich, E.H. Majzoub, and D.D. Johnson, "Anisotropic thermal expansion in molecular solids: theory and experiment on LiBH₄," **Phys. Rev. B** **89**, 134308-7 (2014). [10.1103/PhysRevB.89.134308](https://doi.org/10.1103/PhysRevB.89.134308)
 - 17. Aftab Alam, S.N. Khan, A.V. Smirnov, D.M. Nicholson, and D.D. Johnson, "Green's function multiple-scattering theory with a truncated basis set: an augmented-KKR formalism," **Phys. Rev. B** **90**, 205102-7 (2014). [10.1103/PhysRevB.90.205102](https://doi.org/10.1103/PhysRevB.90.205102)
 - 18. Lin-Lin Wang, Teck L. Tan, and Duane D. Johnson, "Configurational Thermodynamics of Alloyed Nanoparticles with Adsorbates," **Nano Letters** **14**, 7077-7084 (2014). [10.1021/nl503519m](https://doi.org/10.1021/nl503519m)
 - 19. Lin-Lin Wang, Teck L. Tan, and Duane D. Johnson, "*Nanoalloy Electrocatalysis: Simulating Cyclic Voltammetry from Configurational Thermodynamics with Adsorbates*," **Phys. Chem. Chem. Phys.** **17**, 28103-28111 (2015), invited themed volume "*Recent advances in the chemical physics of nanoalloys*". [10.1039/C5CP00394F](https://doi.org/10.1039/C5CP00394F)
 - 20. Vitalij K. Pecharsky, Jun Cui, and D.D. Johnson, "(Magneto)caloric refrigeration: *Is there light at the end of the tunnel?*" **Phil. Trans. R. Soc. A** **374**: 20150305 (2016) 11 pages. [10.1098/RSTA.2015.0305](https://doi.org/10.1098/RSTA.2015.0305)
 - 21. Prashant Singh, M. K. Harbola, M. Hemanadhan, A. Mookerjee, and D. D. Johnson, "Better Band Gaps with Asymptotically-Corrected Local-Exchange Potentials," **Phys. Rev. B** **93**, 085204 (2016). [10.1103/PhysRevB.93.085204](https://doi.org/10.1103/PhysRevB.93.085204)

Network for ab initio many-body methods: development, education and training

Principal investigator: Paul R. C. Kent, Oak Ridge National Laboratory, kentpr@ornl.gov

Co-PIs: Anouar Benali, Argonne National Laboratory

David M. Ceperley, University of Illinois at Urbana Champaign

Miguel A. Morales, Lawrence Livermore National Laboratory

Luke Shulenburger, Sandia National Laboratories

Website: <http://www.qmcpack.org>

Project Scope

The primary goal of this project is to advance the theory, implementation and practical application of high-accuracy ab initio many body quantum Monte Carlo (QMC) methods. We therefore aim to accelerate the discovery and characterization of advanced materials, particularly those were existing methods such as density functional theory are known to be unreliable in practice. The project is organized around developers and users of the open-source QMC package QMCPACK. The project specifically supports methods development and applications, aims to foster the collaborations among developers and users, and to educate new computational materials scientists. The intended outcomes include software, efficient workflows, and data repositories as well as scientific applications.

Recent Progress

Below are two highlights of recent progress applying QMC to materials that challenge conventional electronic structure methods. Our experience applying QMC to these materials helps focus the tools and methods development that are essential to improve the applicability and accuracy of QMC techniques.

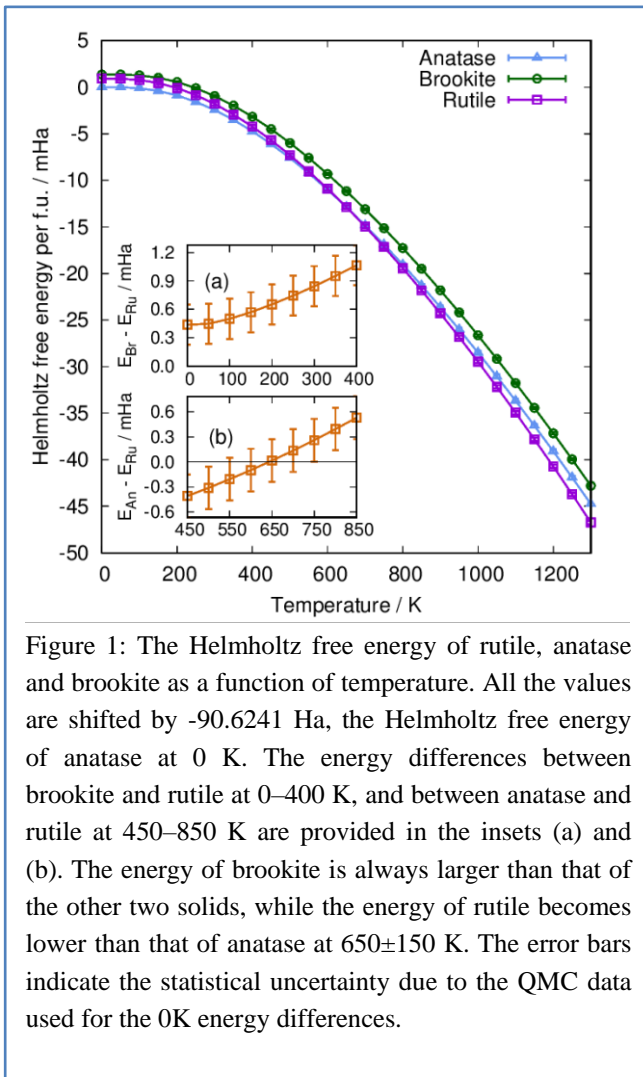
Phase stability of TiO₂ polymorphs – Titanium dioxide, TiO₂, has multiple applications in catalysis, energy conversion and memristive devices because of its electronic structure. Most of these applications utilize the naturally existing phases: rutile, anatase and brookite. Despite the simple form of TiO₂ and its wide uses, there is long-standing disagreement between theory and experiment on the energetic ordering of these phases that has never been resolved. Standard local and hybrid DFTs generally disagree with experiment, giving anatase as the lowest energy structure. Solving this disagreement is an important demonstration of the role we hope QMC can provide, and is an important step to predicting the phase stability and properties of more complex and less well characterized oxides.

We performed the first analysis of phase stability at zero temperature using fixed node diffusion Quantum Monte Carlo (DMC) method. We optimized the nodal surface via using orbitals from DFT+U calculations with the U chosen to produce the lowest variational DMC energy. We also took care to converge the convergable technical details of the calculations – time step error and supercell size. This methodology has been shown by us and other QMC practitioners to give highly accurate results when compared to experimental results for many challenging oxides including FeO, superconducting cuprates, VO₂, and MnO₂.

Surprisingly our QMC calculations find that anatase is the most stable phase at 0K, consistent with many previous mean-field calculations. However, when we also include the effects of temperature by calculating the Helmholtz free energy including both internal energy and vibrational contributions from density functional perturbation theory based quasi harmonic phonon calculations, rutile becomes the most stable phase at elevated temperatures. For all finite temperatures, brookite is the least stable phase.

The fact that our QMC obtains anatase as the most stable phase at 0K suggests that commonly used density functionals might be qualitatively correct in giving this energetic ordering between anatase and rutile: it should not be automatically assumed that these calculations are in error, and we caution against using prediction of rutile as most stable at 0K to validate new electronic structure methods.

There are two sources of systematic error remaining in our zero-temperature QMC calculations that prevents them from being exact. First, the calculations are subject to the fermion sign problem and the error that results from using fixed node DMC. Ideally the nodal structure of the trial wave functions would be more fully optimized in QMC, and we are working to add this capability to QMCPACK in a robust form. Second, because we utilize pseudopotentials we must be concerned with the fundamental accuracy of the pseudopotential construction and the locality errors that result when evaluated in DMC. We expect considerable error cancellation because all of the polymorphs have, by definition, exactly the same composition. The locality error can be reduced by more accurate trial wave functions, e.g. using methods inspired by quantum chemistry. Finally, the results for finite temperatures would presumably be more accurate if QMC methods could be used for the lattice dynamics; however, this is at present not possible.



Nature of the interlayer interaction in bulk and few-layer phosphorus – There is the large interest in understanding and correctly describing the nature of the weak interlayer interaction in layered systems such as few-layer graphene, transition metal dichalcogenides and few-layer phosphorene. Phosphorene displays a high and anisotropic carrier mobility and a robust band gap that depends sensitively on the in-layer strain. Progress in device fabrication indicates clearly that phosphorene holds technological promise. However, because the fundamental band gap depends sensitively on the number of layers, understanding the nature of the interlayer interaction is particularly important.

We studied the nature of the interlayer interaction in layered black phosphorus using fixed node DMC, which treats covalent and dispersive interactions on the same footing. The methods has previously been shown to accurately predict the binding energies of graphite, while chemical accuracy is attainable for small van der Waals (vdW) molecular complexes. Unlike in true vdW systems, we find that the interlayer interaction in few-layer phosphorene is associated with a significant charge redistribution between the in-layer and interlayer region, caused by changes in the nonlocal correlation of electrons in adjacent layers. Consequently, the resulting interlayer interaction can not be described properly by DFT augmented by semilocal vdW correction terms, and thus the designation “van der Waals solids” is strictly improper for systems including few- layer phosphorene. We also tested several nonlocal DFT functionals designed to capture van der Waals effects and have found that the tested formulations do not quantitatively reproduce the charge reorganization found using DMC. Our results may be used as benchmarks for developing more sophisticated DFT functionals that should provide an improved description of nonlocal electron correlation in layered systems. In particular, we note that one nonlocal vdW functional, vdW-DF2, was able to qualitatively but not quantitatively capture the charge redistribution, suggesting an important avenue for further functional development.

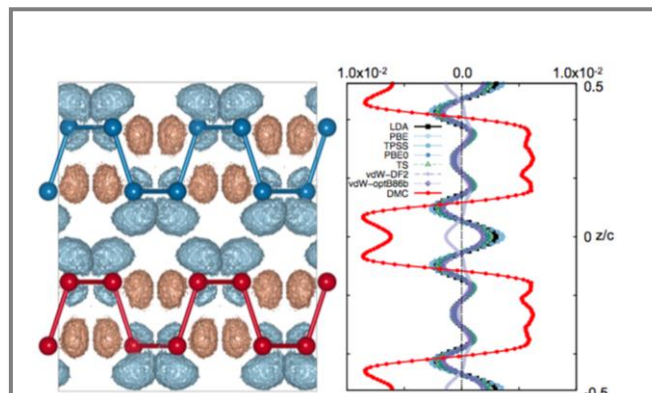


Figure 2. (Left) Charge reorganization induced by the interaction of black phosphorous layers. (Right) Large qualitative differences in charge transfer between density functional theory predictions and QMC (red), from Shulenburger et al. Nano Letters **15** 8170 (2015).

Future Plans

Applying QMC to more complex and strongly correlated materials – We aim to establish QMC techniques applicable to materials that are fully self-consistent and that are not dependent on a mean-field starting point. This will enable QMC to be applied with greater confidence to materials and phenomena where well-established methods are unreliable – such as the strongly correlated materials or materials containing heavy elements. Fully optimized wavefunctions can already be made in QMC for some small molecules, but much greater robustness is required for wide application to solids and large systems. Associated with these developments, we will be able to better characterize and therefore improve pseudopotentials, because high quality wavefunctions will be obtainable. Finally, we have implemented several force algorithms, currently for the all electron case, and will extend these to pseudopotential solids. This will enable studies of complex solids and defects where there is uncertainty in the geometry, and improve options for validating our predictions by enabling comparison of internal coordinates with x-ray and microscopy data.

Recent Publications

1. Y. Luo, A. Benali, L. Shulenburger, J. T. Krogel, O. Heinonen, and P. R. C. Kent. "Phase Stability of TiO_2 Polymorphs from Diffusion Quantum Monte Carlo". Submitted to New Journal of Physics (2016).
2. M. Ceriotti, W. Fang, P. G. Kusalik, R. H. McKenzie, A. Michaelides, M. A. Morales, T. E. Markland, "Nuclear Quantum Effects in Water and Aqueous Systems: Experiment, Theory, and Current Challenges", Chemical Reviews (2016) , DOI: 10.1021/acs.chemrev.5b00674
3. A. Benali, L. Shulenburger, J. T. Krogel, X. Zhong, P. R. C. Kent, O. Heinonen, "Quantum Monte Carlo analysis of a charge ordered insulating antiferromagnet: the Ti_4O_7 Magneli phase". Phys. Chem. Chem. Phys., **18**, 18323 (2016),
4. R. Nazarov, L. Shulenburger, M. Morales, and Randolph Q. Hood, "Benchmarking the pseudopotential and fixed-node approximations in diffusion Monte Carlo calculations of molecules and solids", Phys. Rev. B **93**, 094111 (2016).
5. R. C. Clay, M. Holzmann, D. M. Ceperley, M. A. Morales, "Benchmarking density functionals for hydrogen-helium mixtures with quantum Monte Carlo: Energetics, pressures and forces", Phys. Rev. B **93**, 035121 (2016).
6. J. T. Krogel, "Nexus: a modular workflow management system for quantum simulation codes", Computer Physics Communications **198** 154 (2016).
7. J. McMinis, M. A. Morales, D. M. Ceperley, J. Kim, "The Transition to the Metallic State in Low Density Hydrogen", J. Chem. Phys. **143** 194703 (2015).
8. S. Root, L. Shulenburger, R. W. Lemke, D. H. Dolan, T. R. Mattsson, and M. P. Desjarlais, "Shock Response and Phase Transitions of MgO at Planetary Impact Conditions", Phys. Rev. Lett. **115**, 198501, (2015). Editor's Suggestion.
9. L. Shulenburger, A. D. Baczewski, J. Guan, Z. Zhu, D. Tomanek, "The Nature of the Interlayer Interaction in Bulk and Few-Layer Phosphorus", Nano Letters **15** 8170 (2015).
10. G. Medders, A. Götz, M. Morales, P. Bajaj and F. Paesani, "On the representation of many-body interactions in water", J. Chem. Phys. **143**, 104102 (2015)

Emergence of High Tc Superconductivity out of Charge and Spin Ordered Phases

Principal Investigator: Dr. Eun-Ah Kim

Department of Physics, Cornell University, Ithaca, NY 14853

Eun-ah.kim@cornell.edu

Project Scope

Recent evidence of new forms of charge and spin orders in cuprate largely demystified the pseudogap region, and puts us in a moment of opportunity. The scope of this project is to investigate the mechanisms and roles of charge/spin orders in two classes of high Tc superconductors: I. cuprates and II. Fe-based superconductors(Fe-SC's). Our approach is a symmetry-guided "middle-up/down approach": applying symmetry and quantum field theory based perspective to experimental data and using the results as input to microscopic models that will be studied through a combination of numerical methods. The theoretical advances will be in synergetic relation with rapidly developing experimental discoveries on the subject.

Recent Progress

Topological superconductivity in Metal/Quantum-spin-ice Heterostructure [1]:

The original proposal to achieve superconductivity by starting from a quantum spin-liquid (QSL) and doping it with charge carriers, as proposed by Anderson in 1987, has yet to be realized. Here we propose an alternative strategy: use a QSL as a substrate for heterostructure growth of metallic films to design exotic superconductors (Fig1). By spatially separating the two key ingredients of superconductivity, i.e., charge carriers (metal) and pairing interaction (QSL), the proposed setup naturally lands on the parameter regime conducive to a controlled theoretical prediction. Moreover, the proposed setup allows us to "customize" electron-electron interaction imprinted on the metallic layer. The QSL material of our choice is quantum spin ice well-known for its emergent gauge-field description of spin frustration. Assuming the metallic layer forms an isotropic single Fermi pocket, we predict that the coupling between the emergent gauge-field and the electrons of the metallic layer will drive topological odd-parity pairing. We further present guiding principles for materializing the suitable heterostructure using ab initio calculations and describe the band structure we predict for the case of $\text{Y}_2\text{Sn}_{2-x}\text{Sb}_x\text{O}_7$ grown on the (111) surface of $\text{Pr}_2\text{Zr}_2\text{O}_7$. Using this microscopic information, we predict topological odd-parity superconductivity at a few Kelvin in this heterostructure, which is comparable to the T_c of the only other confirmed odd-parity superconductor Sr_2RuO_4 .

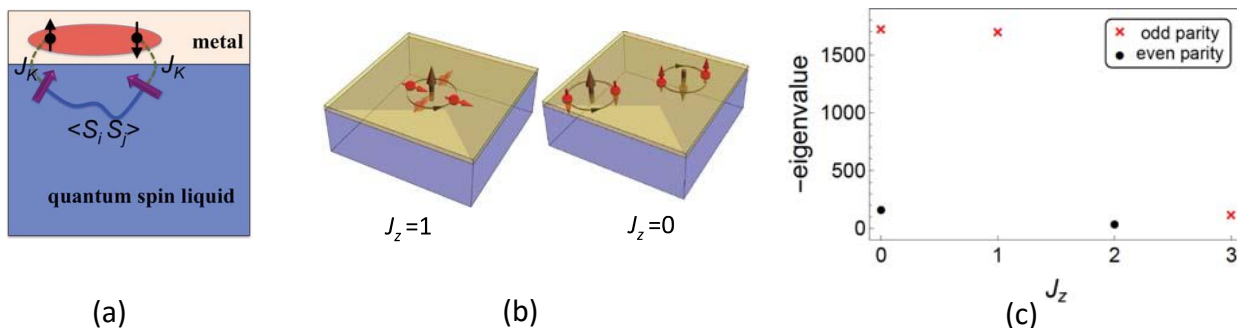


Figure 1 (a) The setup. (b) Two odd parity channels. (c) Negative eigenvalues of pairing vertex matrix [1].

Cold-spots and glassy nematicity in underdoped cuprates [2]:

There is now copious direct experimental evidence of various forms of (short-range) charge order in underdoped cuprate high temperature superconductors, and spectroscopic signatures of a nodal-antinodal dichotomy in the structure of the single-particle spectral functions. In this context, we analyze the Bogoliubov quasiparticle spectrum in a superconducting nematic glass(Fig2(a)). The coincidence of the superconducting "nodal points" and the nematic "cold-spots" on the Fermi surface naturally accounts for many of the most salient features of the measured spectral functions (from angle-resolved photoemission) (Fig 2b-d) and the local density of states (from scanning tunnelling microscopy)(Fig 3 (a-b)). Moreover, the cold spots protected in nematic glass reproduces the characteristic shape of optical conductivity consisting of a sharp peak at $\omega=0$ superposed with a broad peak at $\omega \sim \omega_{\text{peak}}$.

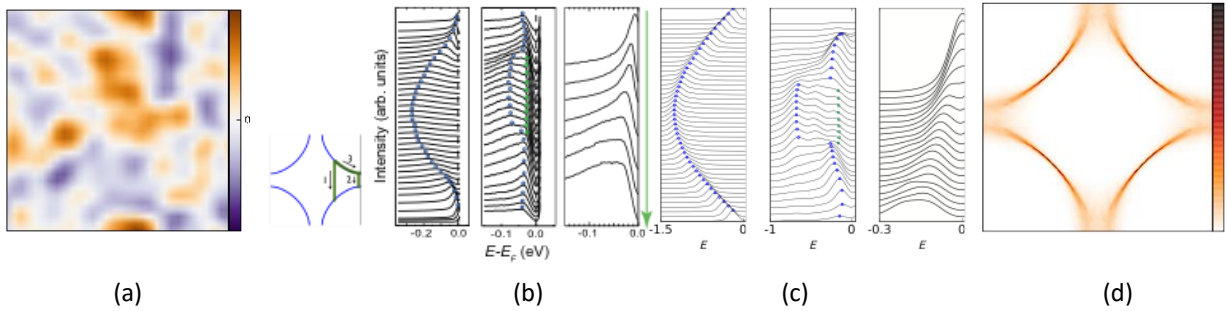


Figure 2 Spectroscopic features of glassy nematic. (a) A representative configuration of the nematic order parameter field. (b) Energy distribution curves reproduced from He et al (Science 2011) along different paths in k -space as shown in the left. (c) EDC's computed along the same paths in k -space se in (b). (d) $A(k,\omega)$ of the superconducting nematic glass at a fixed energy showing nodal-antinodal dichotomy.

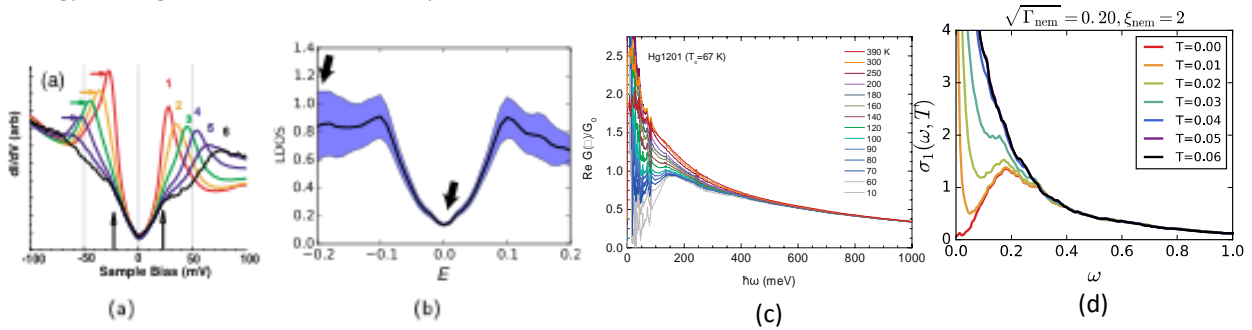


Figure 3 (a-b) Local density of states measured at multiple locations on the surface: (a) Results of STM measurements on Bi-2212 reproduced from McElroy et al (PRL 2005). Different curves represent tunneling spectra measured at different locations of the sample. (b) Computed for a superconducting nematic glass; the solid black curve and the shaded region indicate the spatially aver- aged DOS and spatial standard deviation of LDOS, respectively. (c) Optical conductivity from Mirzaei et al (PNAS 2013). (d) Optical conductivity calculated for the superconducting nematic glass.

Detection of a Cooper Pair Density Wave in $\text{Bi}_2\text{Sr}_2\text{CaCu}_2\text{O}_{8+\chi}$ [3]:

A finite momentum paired state with modulated superconducting order parameter has been long sought after. There have been growing interest in such a pair density wave state as a broken symmetry state associated with cuprate pseudogap phase since the notion was sharpened in Berg et al (PRL 2007) the PI co-authored. Using Scanning Josephson Tunneling Microscopy (SJTM) we have been able to detect the modulation of Cooper pair density for the first time. Fourier

analysis of images from SJTM (Fig 4 (a-b)) reveal direct signature of a Cooper-pair density modulation at wavevectors $Q_p \sim (0.25, 0) 2\pi/a, (0, 0.25) 2\pi/a$ (Fig 4(c)) in $\text{Bi}_2\text{Sr}_2\text{CaCu}_2\text{O}_8$. The amplitude of these modulations is $\sim 5\%$ of the homogeneous condensate density.

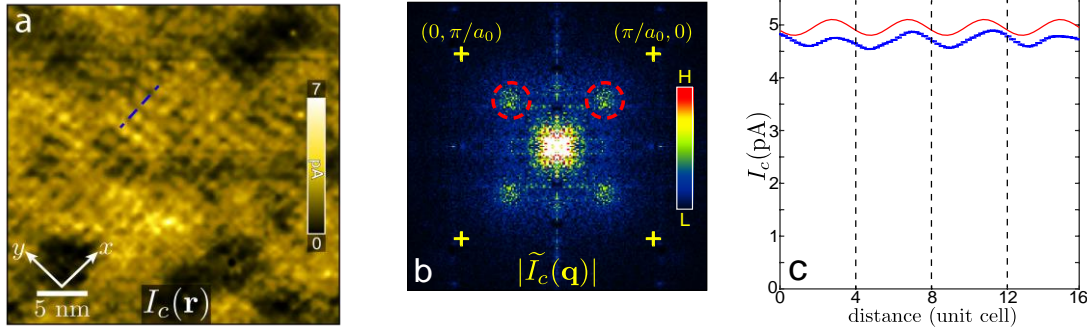


Figure 4 Cooper Pair Density wave. (a)Scanned $I_c(\mathbf{r})$ image in 35 nm X 35 nm field of view.(b) Magnitude of Fourier transform of $I_c(\mathbf{r})$ in a, $|I_c(\mathbf{q})|$ (crosses at $\mathbf{q}=(\pi/a_0,0);(0,\pi/a_0)$). Maxima due to modulations in $I_c(\mathbf{r})$ (dashed red circles) occur at $Q_p=(0.25,0)2\pi/a_0;(0,0.25)2\pi/a_0$. (c) Measured values of $I_c(\mathbf{r})$ along the dashed blue line in a (blue dots); statistical error bars are defined as variance of I_c transverse to dashed line. Fine red line shows the global amplitude and Q_p of modulations in $I_c(\mathbf{r})$, as determined from the magnitude and central Q_p value of the maxima in b.

Commensurate $4a_0$ -period Charge Density Modulations throughout the $\text{Bi}_2\text{Sr}_2\text{CaCu}_2\text{O}_{8+x}$ Pseudogap Regime [4]: Theories based upon strong real space (r -space) electron-electron interactions have long predicted that unidirectional charge density modulations (CDM) with four-unit-cell ($4a_0$) periodicity should occur in the hole-doped cuprate Mott insulator. Experimentally, however, increasing the hole density p is reported to cause the conventionally-defined wavevector Q_A of the CDM to evolve continuously as if driven primarily by momentum-space (k -space) effects. Here we introduce phase-resolved electronic structure visualization for determination of the cuprate CDM wavevector. Remarkably, this new technique reveals a virtually doping independent locking of the local CDM wavevector at $|Q_0| = 2\pi/4a_0$ throughout the underdoped phase diagram of the canonical cuprate $\text{Bi}_2\text{Sr}_2\text{CaCu}_2\text{O}_8$ (Fig 5). These observations have significant fundamental consequences because they are orthogonal to a k -space (Fermi-surface) based picture of the cuprate CDM but are consistent with strong-coupling r -space based theories. Our findings imply that it is the latter that provide the intrinsic organizational principle for the cuprate CDM state.

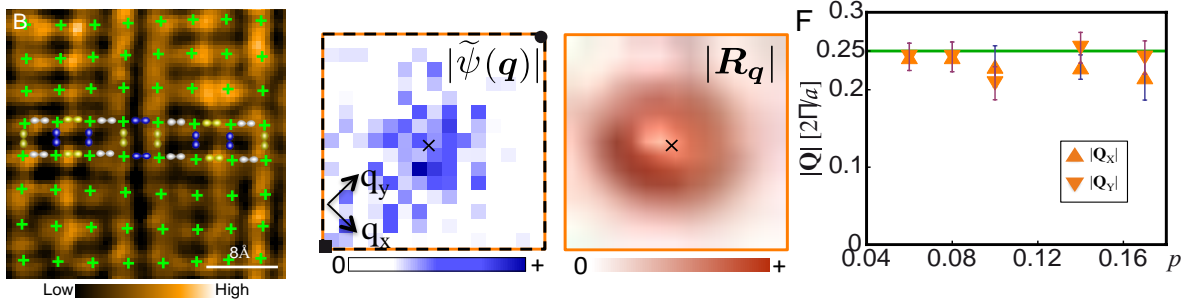


Figure 5. Doping independent commensurate CDW. (a)Typical measured R-map data in the charge ordered phase. The overlay shows how d-symmetry form factor affects each oxygen sites. (b)Fourier transform amplitude showing a broad peak associated with the modulations at hole doping level $p=0.06$. (c)Demodulation residue R_q shows clear isolated minima at $(0,2\pi/4a)$. (d) Doping dependence of phase optimized Q selected by demodulation residue.

Future Plans

The understanding we gained from Ref[1] and [2] gave the PI a new springboard to approach issues in FeSe. Also with increasing number of frustrated quantum spin systems the PI is well-positioned to further the idea of predictively designing superconductors using spin-fluctuation of quantum spin-liquid. Planed topics of study include:

- **Quantum paramagnetic nematicity and superconductivity of FeSe:** Observed nematicity in bulk FeSe has been puzzling the community due to the absence of accompanying magnetic order. Spin fluctuation scenario predict d-wave with nodes but evidence is against nodal gap structure. Motivated by strong inelastic neutron spectra indicating active and anisotropic magnetic fluctuations we plan to develop a microscopic model for the quantum paramagnetic nematic state and investigate the consequence of magnetic fluctuations in such state in superconductivity.
- **Properties of an emergent 1D superconductor defined at a nematic domain wall in FeSe:** It is experimentally well established the FeSe develop superconductivity from a strongly nematic state with definite nematic domains. With the availability of the nematic domain imaging one could also investigate the domain wall state. With lower symmetry on the domain wall irreducible representations of C_{4v} symmetry group can mix in on the domain wall and define an emergent 1D superconducting state which can be exotic.
- **Nematic quantum critical fluctuations as a mechanism of pairing in v=5/2 quantum Hall state:** With increasing theoretical interest in nematic quantum critical fluctuations as meditor of superconducting pairing in the context of high T_c superconductors we plan to investigate longest standing paired state with nearby nematic state, namely half-filled Landau levels. We plan to use recently developed two parameter expansion to study the renormalization group flow of coupling to nematic order parameter field and to gauge fluctuation. In particular we will study how these flow will influence superconducting instability.

List of Publications

- [1] *Topological Superconductivity in Metal/Quantum-Spin-Ice Heterostructures*, Jian-Huang She, Choong H. Kim, Craig J. Fennie, Michael J. Lawler, Eun-Ah Kim, arXiv:1603.02692, under review at Nature Materials.
- [2] *Cold-spots and glassy nematicity in underdoped cuprates*, Kyungmin Lee, Steven A. Kivelson, Eun-Ah Kim, Phys. Rev. B 94, 014204 (2016).
- [3] *Detection of a Cooper Pair Density Wave in Bi₂Sr₂CaCu₂O_{8+x}*, M. H. Hamidian, S. D. Edkins, Sang Hyun Joo, A. Kostin, H. Eisaki, S. Uchida, M. J. Lawler, E. -A. Kim, A. P. MacKenzie, K. Fujita, Jinho Lee, J. C. Séamus Davis, Nature 532, 343 (2016)
- [4] Commensurate 4a₀-period Charge Density Modulations throughout the Bi₂Sr₂CaCu₂O_{8+x} Pseudogap Regime, A. Mesaros, K. Fujita, S.D. Edkins, M.H. Hamidian, H. Eisaki, S. Uchida, J.C. Davis, M. J. Lawler and Eun-Ah Kim, under review at Proceedings of National Academy of Sciences.

Correlation Effects and Magnetism in Actinides: Elements and Compounds

Principal investigator: Professor Gabriel Kotliar

Department of Physics and Astronomy, Rutgers, the State University of New Jersey
Piscataway, NJ 08854

kotliar@physics.rutgers.edu

Project Scope

Actinides compounds in general and Pu in particular pose a significant challenge to electronic structure theory. Addressing this challenge is the primary goal of the current program. Renewed interest in actinide research arises as the search for more efficient and safer (higher thermal conductivity and higher melting point) nuclear fuels continues. Besides their relevance to national security, they are also extremely important for basic science. Because of their unique combination of large f-electron bandwidth, large spin orbit coupling, sizable crystal field effects, and strong local Coulomb matrix elements (such as the Hubbard interaction and Hund's coupling), they give rise to unique extreme phenomena such as large volume collapses among the phases of Pu and the highest superconducting transition temperature among the heavy fermion compounds in PuCoGa_5 .

It has been recognized long time ago that the f-electrons in actinides are close to an electronic localization-delocalization transition which can be induced by various factors such as pressure, temperature, and alloying. To describe these unique properties, the approach taken by the Principal Investigator (PI) is to develop gradually the electronic structure tools needed to tackle this kind of materials, while at the same time using them to generate physical pictures of the phenomena that guide us in understanding these systems. During the process of the current program our theoretical approach has been tested against experiments. Photoemission spectra, XAS spectra, phonon spectra and spin excitation spectra has been measured in several materials and compared against theoretical calculations, and we are reaching a point where satisfactory agreement for multiple properties has been achieved. This presents a unique scientific opportunity to elucidate important problems which have been open over many years, such as understanding and predicting the energetics and the physics of multiple phases of Pu and Am and deriving the emergent properties of the Pu 115's from a microscopic theory.

Our series of most recent works have been towards further understanding of cerium and plutonium systems including modeling of the electronic properties of a complex phase with several atoms per unit cell and the nontrivial topological properties of a compound. The spin fluctuation spectra of Pu was predicted and is in good agreement with experimental measurements. Important methodological advances enable the determination of structural properties using both LDA+DMFT and LDA+Gutzwiller methods. We have made progress in the technical developments for simulating finite temperature effects and began exploring techniques for carrying out molecular

dynamics of correlated models, with the view towards understanding properties of actinides.

Recent Progress

We highlight some of the accomplishments briefly as follows.

Site-selective correlation effects in α -Plutonium The PI, in collaboration with the theory group at Los Alamos and Rutgers, presented electronic-structure calculations of the full 16-atom per unit cell α -phase structure within the framework (LDA+DMFT). Our calculations demonstrate that Pu atoms sitting on different sites within the α -Pu crystal structure have a strongly varying site dependence of the localization delocalization correlation effects of their 5f electrons and a corresponding effect on the bonding and electronic properties of this complicated metal. In short, α -Pu has the capacity to simultaneously have multiple degrees of electron localization/delocalization of Pu 5f electrons within a pure single-element material.

Plutonium based topological insulators The PI in collaboration with Profess K. Haule and postdoc X. Deng carried out LDA+DMFT revealed the electronic structure of PuB_6 , one of the several binary compounds formed in plutonium-boron systems, of which most properties are still unknown. A small hybridization gap shows up in a pronounced quasiparticle peak, as shown in the left-up panel in Figure 1. It has mixed-valent ground state with f-occupancy of Pu site around 5.3 (left-down panel of Figure 1). The band inversion at X-point between bands with Pu-d and Pu-f characters, gives rise to nontrivial topological properties. We computed the resulting topological protected

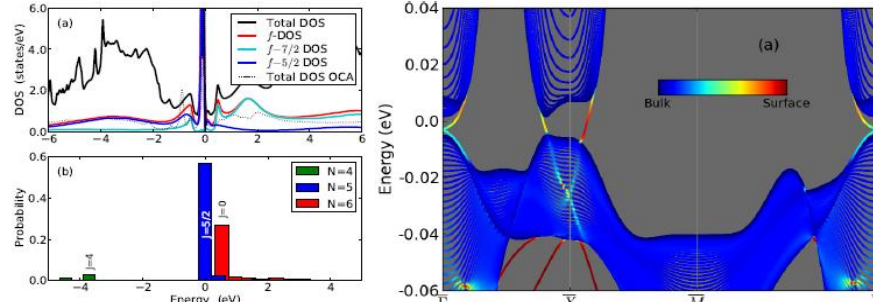


Figure 1: The spectra (left-up), the valence-histogram (left-down) and the quasiparticle surface states of PuB_6 (right) computed using LDA+DMFT method.

surface states of PuB_6 as shown in the right of Figure 1. PuB_6 has also a very high melting temperature and we proposed that it has ideal solid state properties for a nuclear fuel material, because of the high thermal conductivity

of the topologically protected surface states. This study provides a 5f analog of the 4f system SmB_6 and a novel playground for studying the interplay of correlation effects and topological order as well as the applications of topological surface states in nuclear fuel materials.

Spin Fluctuations in δ -plutonium In this joint study of both theory and experiment, neutron spectroscopy and LDA+DMFT method are used to investigate plutonium, the prototypical material at the brink between bonding and nonbonding configurations. Our study reveals that the ground state of plutonium is governed by valence fluctuations, that is, a quantum mechanical superposition of localized and itinerant electronic configurations as recently predicted by dynamical mean field

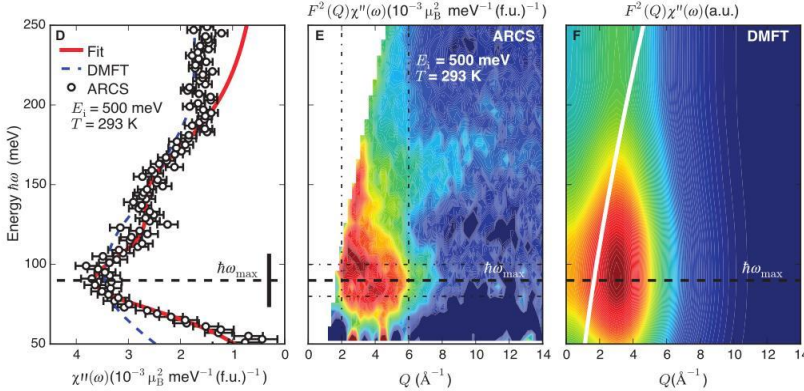


Figure 2: The dynamical magnetic susceptibility of δ -Pu. (Left), the measured and computed dynamical magnetic susceptibility are in good agreement. And the full energy and momentum dependence of the magnetic scattering observed in experiment (middle) is in good agreement with the one computed using LDA+DMFT method (right).

theory. Notably our computed dynamical magnetic susceptibility and magnetic form factor using LDA+DMFT method in excellent agreement with neutron spectroscopy as shown in Figure 2. Our results not only resolve the long-standing controversy between experiment and theory on plutonium's magnetism but also suggest an improved understanding of the effects of such an electronic dichotomy in complex materials.

Phase Diagram and Electronic Structure of Plutonium In order to accelerate LDA+DMFT calculations of actinide materials, we began a renewed exploration of slave bosons and Gutzwiller solvers. We develop a new implementation of the Gutzwiller approximation (GA) in combination with the density functional theory, which enables us to study complex 4f and 5f systems beyond the reach of previous approaches. We calculate from first-principles the zero-temperature phase diagram and electronic structure of Pr and Pu, finding good agreement with the experiments. Our study of Pr indicates that its pressure-induced volume-collapse transition would not occur without change of lattice structure-contrarily to Ce. Our study of Pu shows that the most important effect originating the differentiation between the equilibrium densities of its allotropes is the competition between the Peierls effect and the Madelung interaction, and not the dependence of the electron correlations on the lattice structure. With this new method, we are able to describe quite accurately the zero-temperature equilibrium properties for various phase of plutonium, such as the equilibrium volumes, bulk modulus and the energy differences.

Future Plans

We plan to explore many fascinating phenomena in actinide systems which are now accessible to theoretical treatment, from the following directions.

Orbital and Site Selectivity: A Key for Understanding the Physical Properties of Elemental Plutonium Phases Strong site-orbital differentiation is a natural consequence of the proximity to the localization transition. We demonstrated the site-differentiation of correlation effects in α -Pu. In δ -Pu, our preliminary quantum Monte Carlo runs, revealed an unexpected feature of orbital differentiation in the f-electron self energies. The origin of this feature and its consequence to the optic and thermoelectric properties are to be studied for deeper understanding of Pu.

Valence and Spin Fluctuations in Pu 115 Actinide compounds in the 115 and related structures represent a flexible and fertile ground for exploring a bewildering variety of strong correlation phenomena in actinide materials. These materials continue to be a great source of interest, due to their exotic properties, and because they provide a point of comparison for elemental Pu. We will study the physical properties of the actinides in the 115 and 215 structures. We will calculate the angle resolved photoemission spectra of the Pu 115 compound. We will also investigate the proximity to potential valence instabilities.

Equation of State, Photoemission and f-Valence in Am under Pressure Right after plutonium in the periodic table, Americium metal is an important elemental solid of relevance to the nuclear industry and use to applications such as smoke detectors. We propose to revisit the equation of state in Am system under pressure and the AmIII to AmIV transition using state of the art LDA+DMFT techniques with advanced impurity solvers. The more accurate CTQMC impurity solvers and the more accurate LAPW basis now in use in our group will enable us to obtain more precise spectra, valence histograms and 5f average valence. We will compare the results with those from the more approximate LDA+RISB methods.

Publications

1. Site-selective electronic correlation in α -plutonium metal, Jian-Xin Zhu, R.C. Albers, K. Haule, G. Kotliar and J.M. Wills, *Nature Communications* 4, 2644 (2013)
2. Plutonium hexaboride is a correlated topological insulator, X. Deng, K. Haule and G. Kotliar, *Phys. Rev. Lett.* 111, 176404 (2013)
3. The valence-fluctuating ground state of plutonium, Marc Janoschek, Pinaki Das, Bismayan Chakrabarti, Douglas L. Abernathy, Mark D. Lumsden, John M. Lawrence, Joe D. Thompson, Gerard H. Lander, Jeremy N. Mitchell, Scott Richmond, Mike Ramos, Frans Trouw, Jian-Xin Zhu, Kristjan Haule, Gabriel Kotliar and Eric D. Bauer, *Science Advances*, Vol. 1, no. 6 (2015)
4. Temperature-dependent electronic structures, atomistic modeling and the negative thermal expansion of δ -Pu, *Philosophical Magazine Letters* 94,620 (2014)
5. Phase Diagram and Electronic Structure of Praseodymium and Plutonium, Nicola Lanatà, Yongxin Yao, Cai-Zhuang Wang, Kai-Ming Ho and Gabriel Kotliar, *Phys. Rev. X* 5, 011008 (2015)
6. Interplay of spin-orbit and entropic effects in Cerium, Nicola Lanatà, YongXin Yao, Cai-Zhuang Wang, Kai-Ming Ho, and Gabriel Kotliar, *Phys. Rev. B* 90, 161104(R) (2014)
7. Finite-Temperature Gutzwiller Approximation from Time-Dependent Variational Principle, Nicola Lanatà, Xiaoyu Deng, Gabriel Kotliar, *Phys. Rev. B* 92, 081108(R) (2015)
8. Mott transition in a metallic liquid - Gutzwiller molecular dynamics simulations, Gia-Wei Chern, Kipton Barros, Cristian Batista, Joel Kress and Gabriel Kotliar, arxiv: 15090.05860

Non-collinear magnetism and dynamic effects in Dzyaloshinskii-Moriya magnets

Principal investigator: Professor Alexey Kovalev

Department of Physics and Astronomy, University of Nebraska-Lincoln

Lincoln, NE 68588

alexey.kovalev@unl.edu

Project Scope

The primary goal of this proposal is to obtain a general understanding of effects related to spin-orbit interactions in the context of equilibrium and nonequilibrium thermodynamics in mesoscale and nanoscale magnetic systems with ferromagnetic, antiferromagnetic, and non-collinear ordering. To this end, we will advance our fundamental knowledge about magnetism and phase transitions in systems with Dzyaloshinskii-Moriya interactions that are driven out of equilibrium by applying temperature gradients, microwave fields, and/or electric and magnetic fields. Pure spin and energy currents mediated by magnons can then be induced in such systems where low dissipation (ideally non-dissipative) transport without generation of Oersted fields becomes possible. The proposed research program has three major objectives: (1) understand effects of Dzyaloshinskii-Moriya interactions on spin and energy transport phenomena and magnetic order parameter dynamics in systems with and without magnetic textures such as domain walls, skyrmions, and magnetic vortices by developing a hydrodynamic description of such systems combined with diagrammatic and linear response approaches; (2) understand dynamic effects in the context of novel emergent phases in magnets with Dzyaloshinskii-Moriya interactions; (3) assess the feasibility of novel ultra-low-power spintronic devices that combine logic and memory functionalities by employing theoretical descriptions of spin and energy currents and their interplay with magnetic order parameter dynamics.

Recent Progress

Stability of skyrmion lattices and symmetries of quasi-two-dimensional chiral magnets – the PI, in collaboration with Utkan Güngörđü (postdoc), Rabindra Nepal (graduate student), Oleg Tretiakov, and Kirill Belashchenko have considered the most general form of the quasi-2D free energy with Dzyaloshinskii-Moriya interactions (DMI) constructed from general symmetry considerations reflecting the underlying system. We predict that the skyrmion phase is robust and it is present even when the system lacks the in-plane rotational symmetry (see Figure 1). In fact, the lowered symmetry leads to increased stability of vortex-antivortex lattices with fourfold symmetry and in-plane spirals, in some instances even in the absence of an external magnetic field. Our results relate different hexagonal and square cell phases to the symmetries of materials used for realizations of skyrmions. This will give clear directions for experimental realizations of hexagonal and square cell phases, and will allow engineering of skyrmions with unusual properties. We have also found striking differences in gyrodynamics induced by spin currents for isolated skyrmions and for crystals where spin currents can be induced by

charge carriers or by thermal magnons. Under certain conditions, isolated skyrmions can move along the current without a side motion which can have implications for realizations of magnetic memories. The paper has been published in Physical Review B.

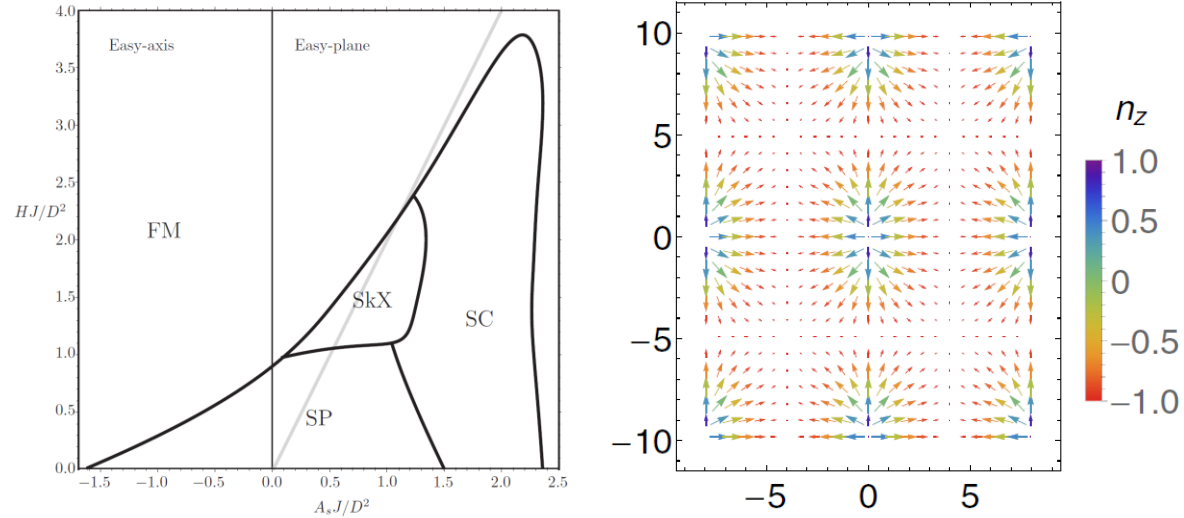


Figure 1 Left: Zero temperature phase diagram for the Rashba+Dresselhaus DMI with C₂v symmetry ($D_R/D_D = 5$). SkX (skyrmion) phase is only present in the easy-plane region of the phase diagram. The gray line separates the aligned and the tilted regions of the FM phase, whereas SkX and SP (spiral) phases are not affected by this line. Right: A typical normalized spin density for SC phase with four-fold symmetry. The skyrmions are noticeably elongated reflecting C₂v symmetry.

Magnon-mediated spin Nernst effect in antiferromagnets – the PI, in collaboration with Vladimir Zyuzin (postdoc) have considered transport of magnons with non-trivial momentum Berry curvature.

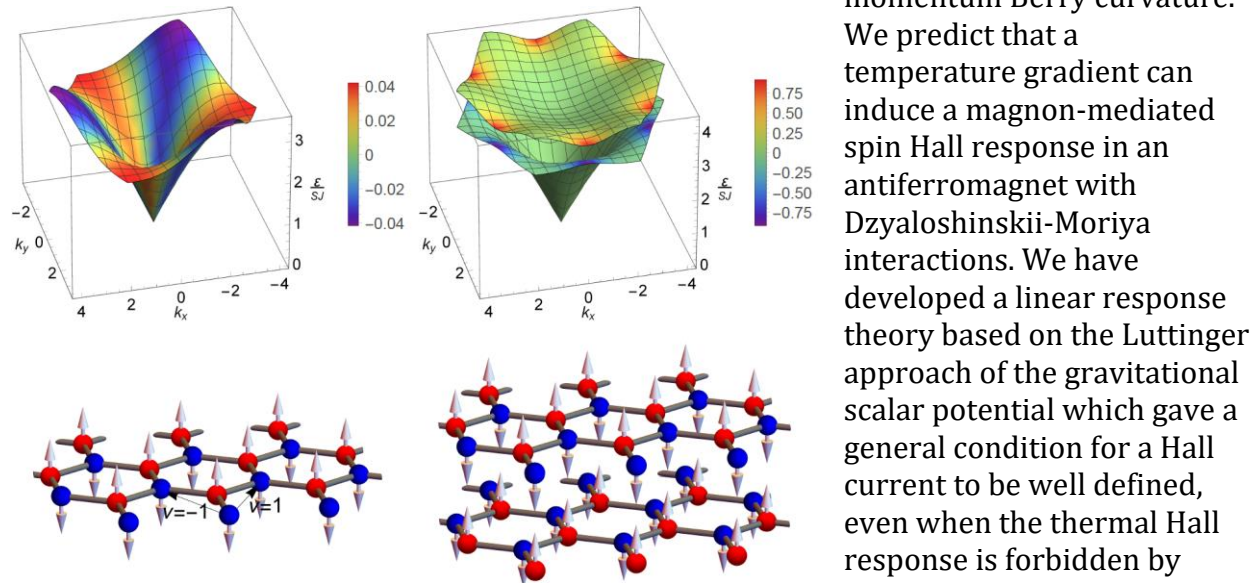


Figure 2 Left: Magnon spectrum of a single layer antiferromagnet (black arrows correspond to v sign convention of DMI), with schematics of the lattice and Neel order in z-direction in the bottom. Right: Magnon spectrum of antiferromagnet on a bilayer honeycomb lattice. In both cases the distribution of the Berry curvature over the Brillouin zone is plotted by the color distribution on top of the spectrum for one of the degenerate subbands.

have considered single and bi-layer honeycomb antiferromagnets with antiferromagnetic interlayer coupling where the nearest neighbor exchange interactions and the second nearest neighbor Dzyaloshinskii-Moriya interactions were present (see Figure 2). We have showed that both models possess the magnon edge states in the finite geometry and discussed their role for the spin Nernst effect. For a single layer, we observe an interplay between the Berry curvature due to the lattice topology and Dzyaloshinskii-Moriya interactions and find that the Berry curvature is not of the monopole type, contrary to a ferromagnet on a honeycomb lattice. From our analysis, we conclude that the spin Nernst effect can be present in antiferromagnets that are invariant under (i) a global time reversal symmetry (e.g., Figure 2, right) or under (ii) a combined operation of time reversal and inversion symmetries (e.g., Figure 2, left). In both cases the thermal Hall effect is zero while the spin Nernst effect should change sign with the reversal of the Neel vector in the latter case but not in the former case. The paper has been submitted to Physical Review Letters.

Spin torque and Nernst effects in Dzyaloshinskii-Moriya ferromagnets – the PI, in collaboration with Vladimir Zyuzin (postdoc) have considered transport of magnons with non-trivial momentum Berry curvature and non-equilibrium magnon-mediated spin torques. We have predicted that a temperature gradient can induce a magnon-mediated intrinsic torque in systems with a nontrivial magnon Berry curvature. With the help of a microscopic linear response theory of nonequilibrium magnon-mediated torques and spin currents we have identified the interband and intraband components that manifest in ferromagnets with Dzyaloshinskii-Moriya interactions. To illustrate and assess the importance of such effects, we have applied the linear response theory to the magnon-mediated spin Nernst and torque responses in a kagome lattice ferromagnet. The paper has been published in Physical Review B. As a follow up, we will consider the same effect by employing the Onsager reciprocity principle. This should lead to studies of the effect of energy pumping by magnetization dynamics. We can directly obtain this energy pumping effect by considering the wave packet approach and Berry phase corrections to the Dzyaloshinskii-Moriya tensor.

Theory of magnon motive force in chiral ferromagnets – the PI, in collaboration with Utkan Güngörđü (postdoc) have considered magnon motive force induced by the magnetization dynamics. We have predicted that magnon motive force can lead to temperature dependent, nonlinear chiral damping in both conducting and insulating ferromagnets. We estimate that this damping can significantly influence the motion of skyrmions and domain walls at finite temperatures. We also find that in systems with low Gilbert damping moving chiral magnetic textures and resulting magnon motive forces can induce large spin and energy currents in the transverse direction. The effect of magnon spin accumulation induced by magnon motive force has also been studied with the help of the diffusion equation. The paper has been published in Physical Review B.

Magnetoelectric domain wall dynamics and its implications for magnetoelectric memory – the PI, in collaboration with K. Belashchenko, O. Tchernyshyov, and O. A. Tretiakov have considered domain wall dynamics in an antiferromagnetic magnetoelectric in the presence of electric and magnetic fields. It is found that the domain wall mobility has a maximum as a function of the electric field due to the gyrotropic coupling and domain wall precession. A small in-plane shear strain blocks the domain wall precession and allows control over the Walker breakdown. This substantially raises the maximum velocity

of the domain wall, making it comparable to ferromagnetic counterparts. The paper has been published in Applied Physics Letters.

Future Plans

Magnon-mediated transport of spin and energy in magnon topological insulators – the PI will study magnon-mediated spin and energy transport phenomena in magnets with Dzyaloshinskii-Moriya interactions. This will include ferromagnets, antiferromagnets, and magnets with non-collinear order. Such studies are strongly related to recent developments in realizations of magnonic analogs of topological insulators. We will use linear response and diagrammatic methods to further develop our recent results on the spin Nernst effect. We will also put our findings in the context of the spin Seebeck effect related phenomena.

Thermal torques and Onsager reciprocity in insulating magnets – the PI will study how magnetization (or magnetic order) dynamics can be affected by energy and magnon currents in insulating ferromagnets, antiferromagnets, and magnets with non-collinear order. We will build on our recent studies of magnon-mediated spin torques in Dzyaloshinskii-Moriya ferromagnets. Here the Berry phase corrections should play an important role. We will also study the Onsager reciprocal effect by which energy can be pumped by the dynamics of the order parameter in a magnet. Similar energy pumping phenomena have been recently reported in the context of conducting Dzyaloshinskii-Moriya ferromagnets.

Stability of skyrmion lattices and skyrmion dynamics – the PI will study realizations of unconventional skyrmions and their stability in systems with spin-orbit interactions, building on our recent studies of how symmetry can affect the skyrmion lattice. Studies of skyrmion lattices can shed the light on fundamental questions related to the nature of phase transitions in such systems. We plan to perform Monte Carlo simulations as well as study magnetization dynamics (e.g., skyrmion dynamics) with atomistic micromagnetic simulations. Both approaches will complement our analytical studies.

Publications

1. A. A. Kovalev, V. Zyuzin, “Spin torque and Nernst effects in Dzyaloshinskii-Moriya ferromagnets,” Phys. Rev. B 93, 161106(R) (2016).
2. U. Güngördü, R. Nepal, O. A. Tretiakov, K. Belashchenko, A. A. Kovalev, “Stability of skyrmion lattices and symmetries of quasi-two-dimensional chiral magnets,” Phys. Rev. B 93, 064428 (2016).
3. K. D. Belashchenko, O. Tchernyshyov, Alexey A. Kovalev, O. A. Tretiakov, “Magnetolectric domain wall dynamics and its implications for magnetoelectric memory,” Appl. Phys. Lett. 108, 132403 (2016).
4. U. Güngördü, A. A. Kovalev, “Theory of magnon motive force in chiral ferromagnets”, Phys. Rev. B 94, 020405(R) (2016).
5. K. D. Belashchenko, A. A. Kovalev, M. van Schilfgaarde, “Theory of spin loss at metallic interfaces”, under review for Physical Review Letters.
6. V. Zyuzin, A. A. Kovalev, “Magnon spin Nernst effect in antiferromagnets”, under review for Physical Review Letters.

Toward High-Accuracy Point Defect Calculations in Materials Using the Quasiparticle-Self-consistent GW Method.

Walter R. L. Lambrecht, Department of Physics, Case Western Reserve University

Keywords: GW method, lattice dynamics, point defects, semiconductors

Project Scope

The project's main goal is to develop a "cut-and-paste" approach to construct the GW self-energy in real-space for defect systems from those of the perfect crystal and the near neighborhood of the point defect, thus enabling quasiparticle self-consistent (QS)GW calculations for large supercells. Additional goals are to better understand the limitations of the QSGW approach itself for strongly correlated and ionic materials and to develop methodology to go beyond these limitations, for example by including lattice polarization effects. We have also worked on lattice dynamical effects in halide perovskites.

Recent Progress

Description of new methodology: In the linearized muffin-tin orbital (LMTO) implementation of the quasiparticle self-consistent (QS) GW method, we have a real space representation of the self-energy operator, or rather its hermitian energy-independent average $\Sigma_{ij} = \text{Re}[\Sigma_{ij}(E_i) + \Sigma_{ij}(E_j)]/2$ available, where i, j are the independent-particle eigenstates. These can be expanded in Bloch-function basis states (MTOs) and eventually in local atom-centered orbitals, so we have a $\Sigma_{R,L;R'+T,L'}$ where R are sites in the unit cell, L represents angular momenta and envelop function decay constants κ , and T is a lattice vector. The basic idea of our methodology is to construct the $\Sigma_{R,L;R'+T,L'}$ for a large system like a supercell with a defect from the $\Sigma_{R,L;R'+T,L'}$ for smaller systems. We achieve this by means of a *self-energy editor*, constructed by our collaborator Mark van Schilfgaarde. As a first step, this self-energy editor can construct the $\Sigma_{R,L;R'+T,L'}$ for a perfect crystal supercell from that of the primitive cell. Second, we can replace the Σ for the defect atom itself and/or its near neighbors from those of a small defect containing cell while keeping those farther away the same as in a perfect crystal, or we can simply neglect the $\Sigma_{R,L;R'+T,L'}$ elements for atoms connecting to the defect atom $R=R_{\text{defect}}$. At the interface between both regions we can average the two types of $\Sigma_{R,L;R'+T,L'}$ matrix blocks. With this versatile tool, we can now explore how to construct a reasonable Σ for the supercell with a defect without actually having to carry out a time consuming GW calculation for the large system. We can also limit the range of sites $R'+T$ to explore how long-ranged Σ is required for a desired accuracy. For a small enough supercell we can eventually carry out the fully self-consistent QSGW calculation and compare with the approximate schemes to prove the validity of the latter. However, we can then expand to even larger cells to reduce the supercell finite size effects and improve the accuracy of the defect calculation at little extra cost. We are in the process of testing this strategy.

Illustrative examples: As first exam example we studied the As_{Ga} antisite in GaAs. This is a well-known defect closely related to the EL2 defect. First we constructed a minimal defect cell of 8 atoms from the primitive 2 atom zinc blende cell with 1 antisite defect. This could still be easily calculated at the QSGW level. We then constructed a 64 atom supercell for the same defect and constructed the Σ for this cell from that of the primitive perfect crystal cell for all atoms except the defect atom itself. The latter is taken from the 8 atom cell. In Fig. 1 we illustrate the band structure of the 64 atom cell in the LDA and this approximate cut-and-paste QSGW method. In the LDA (relativistic all electron band structure) the band gap of GaAs is significantly underestimated (0.60 eV) and as a result the defect level band structure is hardly recognizable. The defect level band in fact moves below the VBM. Once the approximate Σ is added, the band gap is increased to 1.83 eV and a defect band emerges in the middle of the gap. This is in fact the a_1 state formed from the As dangling bonds surrounding the antisite forming a bonding state with the As_{Ga} site. One may also recognize a second defect band just at the edge of the CBM which is the t_2 -like excited state of the defect. In future work we will explore the more interesting aspects of this defect, namely the distorted metastable state that occurs when one electron is excited to the t_2 -state. However, the potential of the methodology is already clear here.

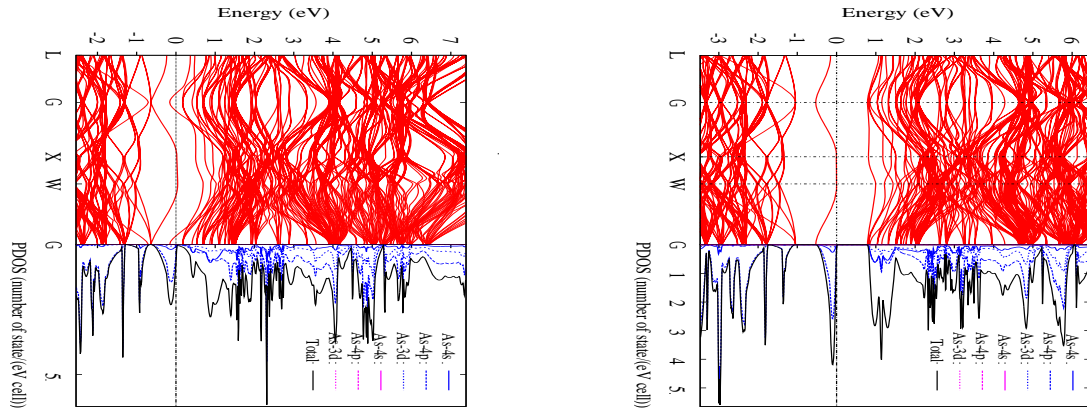


Figure 1: As_{Ga} in GaAs 64 atom supercell band structure and DOS, left LDA and right LDA+ Σ constructed with cut-and-paste approach from perfect crystal Σ and 8 atom defect Σ .

Our second example (not shown here) is a ZnGe antisite in ZnGeN_2 . Here we performed a fully self-consistent calculation for a 32 atom defect cell and subsequently used it to model the Σ in a 128 atom cell. We found that the defect level structure is similar to what we obtained in LDA. The GW correction simply increases the gap and acceptor-like defect levels near the VBM shift slightly deeper into the gap. This is consistent with our earlier findings that the GW- Σ in this

material mostly shifts only the conduction bands up but does not significantly change the VBM nor the acceptor like levels close to it.

Supercell size effects: In the course of developing the above methodology, we also reviewed and improved our procedures for dealing with finite size effects in the defect supercells. Specifically, we developed a method for determining the so-called alignment potential. For a charged defect, the potential near a defect falls off as q/cr but we found that in some cases the charge here should be taken as an effective charge rather than the nominal charge. This is because the net charge of a defect consists both in the nuclear charge density which is localized delta-function-like and an electronic charge density from the defect wave function which can be delocalized if the defect is a shallow defect. We applied our approach in a study of native defects in ZnGeN₂ [1] in which we also studied the concentrations of defects and Fermi level pinning by the dominant defects, which turn out to be the ZnGe⁻¹ acceptor and GeZn⁺² donor states.

Lattice polarization effects in QSGW: It has recently been pointed out that in ionic materials, the lattice polarization to the screening also affects the screened Coulomb interaction W in the GW method. In our study [2] of the band structure of V₂O₅, we found that the QSGW method strongly overestimates the band gap. Because it also has quite large LO-TO splittings, we hypothesized that the lattice polarization effect could be an important factor in this overestimate of the band gap. In that paper, we estimated the effect as a reduction factor of W by a factor $\epsilon^\infty/\epsilon^0$ using direction averaged dielectric constants. However, this approach is not theoretically satisfactory because it applies the same correction factor to $W(q,\omega)$ for all q and ω , whereas this effect should only affect the $q \rightarrow 0$ and $\omega \rightarrow 0$ limits. A more complete implementation of this effect following the approach of Botti and Marques, [3] was implemented in the FP-LMTO QSGW code including a proper treatment of the anisotropy and tested for various materials. An important problem here is that the formalism applied does not itself provide a good measure of the range of q that is affected. Although we made some estimates of this, which indicate that the effect is significantly smaller than previously assumed, we are still working on this problem by carrying out additional calculations of $\epsilon(q)$ including lattice relaxation compared to purely electronic screening. Meanwhile it already appears that in V₂O₅ the lattice polarization effect is much smaller than we thought and instead excitonic effects need to be taken into account. This will be pursued in our recently submitted renewal proposal. Meanwhile, we have already studied additional aspects of V₂O₅, in particular doping of the split-off conduction band, as occurs in NaV₂O₅, leads to the formation of magnetic moments and antiferromagnetic ordering. Our calculations[4] predict a transition to ferromagnetic ordering for doping slightly less than half filling of the split-off band. Our interest in this system stems from the possibility to exfoliate V₂O₅ to atomically thin layers and thereby gaining unprecedented control over the doping of this material, combined with its unique structure consisting of 1D chains within the 2D layers.

Lattice dynamics in halide perovskites: Halide perovskites have recently attracted great attention in photovoltaics. From a fundamental point of view they exhibit a number of interesting phenomena: a combination of ionic bonding with intra-cluster covalent bonding, strong lattice dynamical effects on the dielectric constants because of the large LO-TO splittings, various types of instabilities via soft phonons. As part of this project, we have studied the lattice dynamics and electronic band structure in this family of materials. We have studied the role of soft-phonons in the phase transitions of CsSnX_3 , the phonons and Raman spectra in monoclinic CsSnCl_3 , the electronic band structure in CsGeX_3 and CsSiX_3 halides and the phonons and Raman spectra of the CsGeX_3 compounds. See publication list below. We have shown that there is a distinct distortion mode for the Pb and Sn families of these halides from the Ge and Si ones: the former distort by octahedral rotation soft-phonon modes and eventually form edge-sharing octahedral structures, while the latter undergo a ferro-electric rhombohedral distortion.

Future Plans

In our recently submitted renewal proposal we propose to further test our newly developed cut-and-paste self-energy editor approach and apply it to interesting point defect cases. As a second direction of research, we plan to study effects beyond the random phase approximation screening in QSGW, in particular the role of electron-hole interaction effects in the screening. We plan to do this via the bootstrap kernel approach.[5] We also propose to combine dynamical mean field theory (DMFT) in the Hubbard-I approximation with QSGW, which would allow us to include multiplet splittings of the strongly localized f-states of rare-earth elements. We plan to apply these approaches primarily to strongly correlated oxides such as V_2O_5 and f-electron materials, such as rare-earth nitrides and rare-earth impurities in semiconductors. Combining these new approaches with the lattice polarization effect still under study will allow us to obtain a more complete picture of effects beyond standard GW on the electronic structure of these materials.

References

1. D. Skachkov, A. P. Jarroenjitchai, L.-y Huang, W. R. L. Lambrecht, *Native point defects and doping in ZnGeN_2* , Phys. Rev. B **93**, 155202 (2016)
2. C. Bhandari, W. R. L. Lambrecht, and M. van Schilfgaarde, *Quasiparticle self-consistent GW calculations of the electronic band structure of bulk and monolayer V_2O_5* , Phys. Rev. B **91**, 125116 (2015)
3. S. Botti and M. A. L. Marques, *Strong Renormalization of the Electronic Band Gap due to Lattice Polarization in the GW Formalism*, Phys. Rev. Lett. **110**, 226404 (2013)
4. C. Bhandari and W. R. L. Lambrecht, *Electronic and magnetic properties of electron-doped V_2O_5 and NaV_2O_5* , Phys. Rev. B **92**, 125133 (2015).
5. W. Chen, A. Pasquarello, *Accurate band gaps of extended systems via efficient vertex corrections in GW*, Phys. Rev. B **92**, 041115 (2015).

Publications

1. L.-y. Huang and W. R. L. Lambrecht, *Lattice dynamics in perovskite halides $CsSnX_3$ with $X=I, Br, Cl$* , Phys. Rev. B **90**, 195201 (2014).
2. L.-y. Huang and W. R. L. Lambrecht, *First-principles calculations of phonons and Raman spectra in monoclinic $CsSnCl_3$* , Phys. Rev. B **91**, 075206 (2015).
3. C. Bhandari, W. R. L. Lambrecht, and M. van Schilfgaarde, *Quasiparticle self-consistent GW calculations of the electronic band structure of bulk and monolayer V_2O_5* , Phys. Rev. B **91**, 125116 (2015).
4. T. Cheiwchanchamgij and W. R. L. Lambrecht, *Fully opposite spin polarization of electron and hole bands in DyN and related band structures of GdN and HoN* , Phys. Rev. B **92**, 035134 (2015).
5. C. Bhandari and W. R. L. Lambrecht, *Electronic and magnetic properties of electron-doped V_2O_5 and NaV_2O_5* , Phys. Rev. B **92**, 125133 (2015).
6. D. Skachkov, A. P. Jarroenjitichai, L.-y. Huang, W. R. L. Lambrecht, *Native point defects and doping in $ZnGeN_2$* , Phys. Rev. B **93**, 155202 (2016).
7. L.-y. Huang and W. R. L. Lambrecht, *Electronic band structure trends of perovskite halides: Beyond Pb and Sn to Ge and Si* , Phys. Rev. B **93**, 195211 (2016).
8. L.-y. Huang and W. R. L. Lambrecht, *Vibrational spectra and non-linear optical coefficients of rhombohedral $CsGeX_3$ halide compounds with $X=I, Br, Cl$* , submitted to Phys. Rev. B (2016).
9. C. Bhandari, W. R. L. Lambrecht, and M. van Schilfgaarde, *Lattice polarization effects on the screened Coulomb interaction of the GW approximation*, in preparation for Phys. Rev. B (2016)

STRUCTURE AND DYNAMICS OF MATERIAL SURFACES, INTERPHASE INTERFACES AND FINITE AGGREGATES

Principal Investigator: Professor Uzi Landman, Uzi.Landman@physics.gatech.edu
School of Physics, Georgia Institute of Technology, Atlanta, GA 30332-0430

PROJECT SCOPE

The research program emphasizes the development and implementation of computational and simulation methodologies of predictive capabilities, and their use as tools of discovery in a broad range of materials problems of fundamental and technological interest, with a focus on nanoscale systems, where “small is different”. Topics of our research and educational program include:

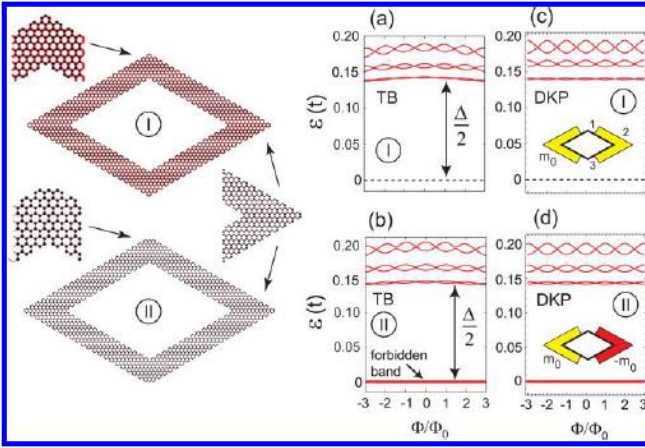
1. First-principles explorations of bottom-up growth of atomically precise graphene nanostructures, including segmented graphene nanoribbons, sGNRs. Investigations (using electronic structure, Greens function transport and relativistic quantum field theory models) of topological effects in graphene nanostructures, including transport in atomically precise sGNRs.
2. Computational explorations (using exact diagonalization) of the properties of confined electrons exhibiting highly correlated states; semiconducting, metal, and graphene quantum dots (QDs) at field-free conditions and under the influence of magnetic fields.
3. Nanoscale systems exhibiting unique structures, organizations, stabilities, reactivities, and dynamics, which endow them with unique physical and chemical properties. These systems are made of varied constituent units and under differing conditions, including investigations of nanocrystallites with superatom electronic-shell structure stabilities, self-assembled into ordered superlattices, and exhibiting collective response mechanisms to varying pressure and temperature conditions, and unique optical response and transport characteristics.

RECENT PROGRESS (see references, [R#], in the reference list, below)

1. Graphene Nanorings (GNRGs): Topological effects investigated with tight-binding (TB) and a position-dependent Dirac formulation [R1]. Analysis of energy spectra of graphene nanorings (GNRGs) calculated with TB calculations and with the use of a relativistic quantum field (RQF) theoretical formulation of a Dirac-Kronig-Penney (DKP) model revealed fundamentally distinct physical regimes: namely, quantum field theoretical ones involving position-dependent or constant masses depending solely on the materials’ shape and edge termination, unlike the massless neutrino-like quasiparticle in 2D graphene sheets. These predicted signatures could be tested in systems prepared with atomic precision (using the methodology employed for graphene nanoribbons), and in nanopatterned artificial graphene..

We illustrate these concepts and the employment of RQF theoretical approaches through applications to GNRGs, with the polygonal rings viewed as made of connected graphene-nanoribbon (GNR) fragments – here we consider armchair GNRs, denoted as aGNRs. The excitations of an infinite aGNR are described by the 1D massive Dirac equation, with a constant mass term $\phi(x) \equiv \phi_0 = \Delta/2 \equiv |t_1 - t_2|$, where the two (in general) unequal hopping parameters $t_1(N^W, t)$ and $t_2 = -t$ are associated with an effective 1D tight-binding problem; N^W is the number of carbon atoms specifying the width of the nanoribbon and $t = 2.7$ eV. We recall that armchair graphene nanoribbons fall into three classes: (I) $N^W = 3l$ (semiconducting, $\Delta > 0$), (II) $N^W = 3l + 1$ (semiconducting, $\Delta > 0$), and (III) $N^W = 3l + 2$ (metallic $\Delta = 0$), $l = 1, 2, 3, \dots$.

GNRGs with semiconducting arms exhibit a particle-hole (particle-antiparticle) gap, as indeed we find for a rhombic armchair graphene ring with a width of $N^W = 12$ carbon atoms having type-I corners (see TB results in Fig. 1a). Surprisingly, a rhombic armchair graphene nanoring of the *same width* $N^W = 12$, but having corners of type-II, exhibits a “*forbidden*” band (with $\epsilon \sim 0$) in the middle of the gap region [see TB results in Fig. 1b)].



the Higgs fields (position-dependent mass) $\phi(x)$ employed in the DPK modeling. $\phi(x)$ is approximated by step-like functions $m_i^{(n)}$, $n=1,2$; i counts the three regions of each half of the rhombus. The non-zero (constant) variable-mass values of $\phi(x)$ are indicated by yellow (red) color when positive (negative). Note the two-membered braided bands and the “forbidden” band [within the gap, in (b) and (d)]. The twofold forbidden band with $\epsilon \sim 0$ appears as a straight line due to the very small amplitude oscillations of its two members. $t=2.7$ eV is the hopping parameter. The edge terminations of both the inside and outside sides of the ring are armchair.

The behavior of rhombic armchair graphene rings with type-II corners can be explained through analogies with RQF theoretical models, describing single zero-energy fermionic solitons with fractional charge, or their modifications when forming soliton/anti-soliton systems. The scalar (mass) field equation of motion gives a Z_2 kink soliton $\phi_k(x)$, which in turn yields a fermionic soliton solution when substituted in the generalized Dirac equation. We find that the DPK model applied to the rhombic ring reproduces [see Fig. 1(d)] the TB spectrum of the type-II rhombic ring (including the forbidden band) when considering alternating masses $\pm m_0$ associated with each half of the ring [see inset in Fig. 1(d)]. The transition zones between the $-m_0$ and $+m_0$ segments (here two of the four corners of the rhombic ring) are referred to as the domain walls, in analogy with the physics of polyacetylene.

The strong localization of a fraction of a fermion at the domain walls (two of the rhombus’ corners), characteristic of fermionic solitons and of soliton/anti-soliton pairs, is clearly seen in the TB density distributions (modulus of single-particle wave functions) displayed in Fig. 2(a). The sublattice component of the tight-binding wave functions localizes at the odd numbered corners (1 & 3). These alternating localization patterns are faithfully reproduced [see Fig. 2(b)]

by the upper, ψ_u , and lower, ψ_l , spinor components of the continuum DPK model. The soliton-antisoliton pair in Fig. 2(b) generates an $e/2$ charge fractionization at each of the odd-numbered corners, which is similar to the $e/2$ fractionization familiar from polyacetylene.

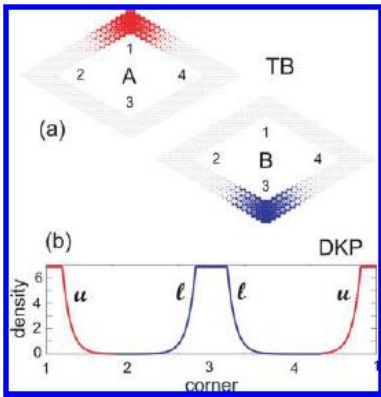
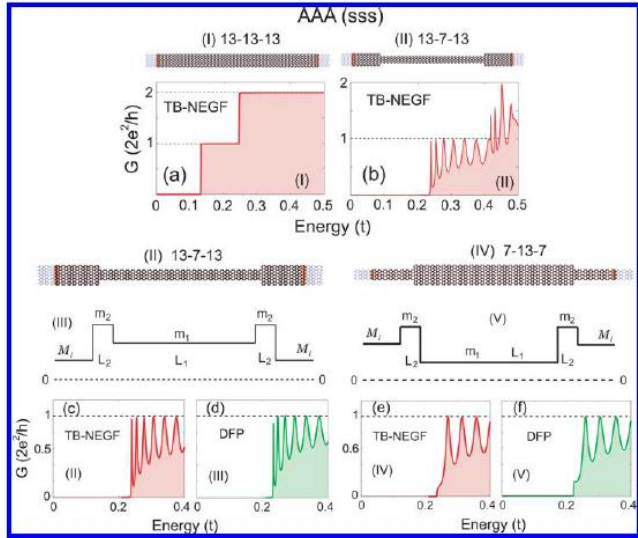


Fig. 2. Wave functions for an excitation belonging to the “forbidden” solitonic band. (a) A-sublattice (red) and B-sublattice (blue) components of the TB state with energy $\epsilon = -0.280 \times 10^{-4}$ at zero magnetic flux, belonging to the forbidden solitonic band of the type-II nanoring with $N^W=12$ [see Fig. 1(b)]. (b) Upper (red) and lower (blue) spinor components for the corresponding state (forbidden band) according to the DPK spectrum [see Fig. 1(d)], reproducing the TB behavior of the type-II nanoring with $N^W=12$, $m_0 = 0.15t/v_F^2$. The TB and DPK wave functions for all states of the solitonic band are similar to those displayed here. The wave functions here represent a pair of solitons.

The absence of a forbidden band (i.e., solitonic excitations within the gap) in the spectrum of the type-I aGNRG [see TB spectrum in Fig. 1(a)] indicates that here the corners do not act as topological domain walls. Nevertheless, here too, direct correspondence between the TB and DKP spectra is achieved by using a variable Higgs field defined as $\varphi(x) = m_i^{(n)}(x)$ with $m_1^{(n)} = m_3^{(n)} = 0$ and $m_2^{(n)} = m_0 = 0.15t/v_F^2$ [see the schematic inset in Fig. 1(c) and the DKP spectrum plotted in the same figure].

2. Interplay of relativistic and nonrelativistic transport in atomically precise segmented graphene nanoribbons

[R1&2]. This work focused on manifestations of relativistic and/or nonrelativistic quantum behavior, explored through tight-binding calculations of electronic states, the non-equilibrium Green's function transport theory, and a newly developed Dirac continuum model that absorbs the valence-to-conductance energy gaps as position-dependent masses, including topological-in-origin mass-barriers at the contacts between segments.



both a semiconducting central constriction and semiconducting leads (13-7-13 and 7-13-7). For the systems shown here all the segments have armchair edge termination (hence, AAA), and all have width corresponding to semiconducting GNRs [hence (sss)]. (III, V) Schematics of the mass barriers used in the Dirac- Fabry-Pérot (DFP) modeling, with the dashed line denoting the zero mass. The physics underlying such a junction is that of a massive relativistic Dirac fermion impinging upon the junction and performing multiple reflections (above $m_1 v_F^2$) within a particle box defined by the double-mass barrier. (c,e) TB-NEGF conductance as a function of the Fermi energy of the *massive* Dirac electrons in the leads. (d) DFP conductance reproducing [in the energy range of the $1G_0$ step, see (b)] the TB-NEGF result in (c). (f) DFP conductance reproducing the TB-NEGF result in (e).

The electronic conductance has been found to exhibit Fabry-Pérot (FP) oscillations associated with formation of a quantum box (resonant cavity) in the junction. Along with the familiar optical FP oscillations (with equal spacing between neighboring peaks) that we find for massless electrons in GNRs with metallic armchair central segments, we find other FP categories. In particular, our calculations reveal: **(a)** A *massive relativistic FP pattern* exhibiting a valence-to-conduction gap and unequal peak spacing, associated with semiconducting armchair nanoribbon central segments, irrespective of whether the armchair leads are metallic or semiconducting (Fig..3). **(b)** A *massive non-relativistic FP pattern* with $1/L^2$ peak spacings, but with a vanishing valence-to-conduction gap. This is the pattern expected for carriers in usual semiconductors described by the (nonrelativistic) Schrödinger equation, and it is associated with zigzag nanoribbon central segments (for both zigzag or metallic armchair leads are used).

Perfect quantized conductance steps were found only for uniform GNRs (Fig. 3a). This behavior obtained through TB-NEGF calculations is reproduced by the 1D continuum fermionic Dirac-Fabry-Pérot (DFP) interference theory, with an effective position-dependent mass term to absorbing the finite-width (valence-to-conduction) gap in armchair nanoribbon segments, as well as the interfacial barriers between GNR segments forming junctions. For zigzag nanoribbon segments the mass term in the Dirac equation reflects the nonrelativistic Schrodinger-type behavior of the excitations, and it is much larger than the particle mass in semiconducting arm-

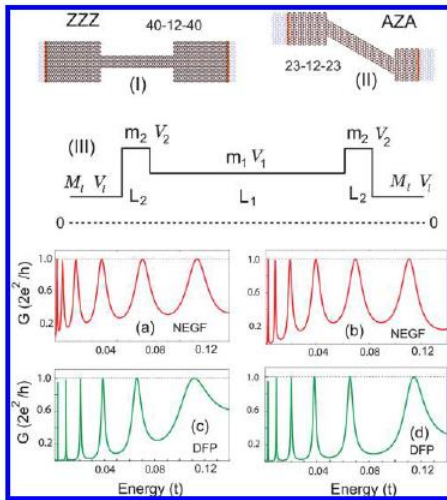


Fig. 4. Conductance for ZZZ (all-zigzag edge termination, left) and AZA (armchair-zigzag-armchair edge termination, right) segmented GNR junctions. See corresponding lattice diagrams in (I) and (II). The 3-segment GNRs are denoted as $N_1^W - N_2^W - N_1^W$, with N_L^W ($L = 1, 2$) being the number of carbon atoms specifying the width of the ribbon segments. The armchair leads in the AZA junction are metallic ($N_1^W = 23$ class III aGNR). (a) & (b) TB-NEGF conductance for the ZZZ and AZA junction, respectively. (c) & (d) DFP conductances reproducing the TB-NEGF ZZZ junction result in (a), and in (d) for the AZA junction (in b). The Fabry-Pérot patterns in (a) and (b) are very similar, manifesting control by the central segment. According to the continuum relativistic DFP analysis, the physics underlying such patterns is that of a massive nonrelativistic Schrödinger fermionic carrier performing multiple reflections within a cavity defined by a double-mass barrier [see diagram in (III)].

chair terminated GNR segments. In the zigzag GNR segments (always characterized by a vanishing valence-to-conduction energy gap), the mass corresponds simply to the carrier mass, whereas in the aGNR segments the carrier mass endows the segment also with a valence-to-conduction energy gap, according to Einstein's relativistic energy relation.

PLANNED ACTIVITIES

Atomically precise segmented graphene nanoribbons (sGNRs), rings and dots – structures, spectra and transport in sGNRs, made of armchair or zigzag terminations (and their combinations), including multiple-armed junction configurations, will be explored with first-principles calculations, non-equilibrium Greens function transport techniques, the generalized Dirac equation that includes spatially varying mass terms (scalar field) and matrix-transfer transport method. . These studies will include magnetic field-free conditions as well as magnetoresistance calculations. Additionally we will explore sGNRs with embedded graphene rings and dots, as elements in graphene-based circuitry. Aharonov-Bohm effects on the transport in such hybrid configurations will be explored.

Highly-correlated states in 2D multi-quantum-dots (MQDs) – Correlated states of electrons in 2D semiconductor MQDs will be explored with the use of configuration interaction (CI) exact diagonalization of the microscopic Hamiltonian, for field-free conditions and as a function of applied magnetic field, as well as the dependencies on detuning between the QDs. The formation of electron Wigner-molecules and development of spin states (in particular antiferromagnetic ordering) and mapping onto Heisenberg and t-J Hamiltonian spin-chain and spin-cluster models will be investigated in the context of the use of MQDs as quantum computing logic gates.

Atomically precise 3D nanocrystals – A first-principles strategy for the prediction of atomic arrangements in 3D metal (e.g. Au, Ag, Pd and their alloys) nanocrystallites will be developed, and their electronic superatom shell stability, optical spectra (TDDFT) and self-assembly will be investigated. The mechanical response of 2D and 3D superstructures will be explored.

SELECTED REFERENCES (including the ones cited above; see Annual Reports)

1. “Transport, Aharonov-Bohm, and topological effects in graphene molecular junctions and graphene nanorings”, C. Yannouleas, I. Romanivsky, U. Landman, J. Phys. Chem. C **119**, 11131 (2015).
2. “Interplay of relativistic and nonrelativistic transport in atomically precise segmented graphene nano-ribbons”, C. Yannouleas, I. Romanivsky, U. Landman, Scientific Reports (Nature) **5**, 7893 (2015).
3. “Structure sensitivity in the nonscalable regime: catalyzed ethylene hydrogenation on supported Pt nanoclusters”, A. S. Crampton, et al., Nature Comm., Article Number: 10389 (2016). DOI:10.1038/ncomms10389.
4. “The interaction of water with $Mn_4O_4^{+}$ clusters: deprotonation and structural transformations”, S. M. Lang, T. M. Bernhardt, D. M. Kiawi, J. M. Bakker, R.N. Barnett, U. Landman Angew. Chem. Int. Ed. **127**, 15328 (2015).
5. “Highly correlated fermionic ultracold atoms and electrons in double wells: Microscopic exact and t-J modeling” B. B. Brandt, C. Yannouleas, U. Landman, Phys. Rev. A (2016).

Strongly correlated electronic systems: local moments and conduction electrons.

Patrick Lee, MIT

Superconductivity, Weyl, semimetals, photovoltaic

Project Scope

In the past two years we have focused our attention on two topics. The first concerns Weyl semimetals, their transport properties and their interaction with light. We came up with a semiclassical explanation of the linear magneto-resistance which has been found experimentally in this class of materials. [P1] We also found a number of unusual phenomena when the Weyl semimetal is exposed to light. Examples include the generation of anomalous Hall effect, [P2] a transition between type I and type II Weyl cones [P4] and the spontaneous production of current in materials which break inversion and mirror symmetry. [P6] A second topic is the theory of superconductivity at very low density. Here we are inspired by the recent revival of interest in the superconductivity in doped SrTiO₃, either in the bulk or at heterostructure interface. We find that at the lowest density, the Fermi energy is only 10 Kelvin, much lower than any optical phonon frequency so that the conventional BCS theory of pairing via phonon exchange cannot apply. The acoustic phonon also does not work because the coupling constant is much less than unity. We propose that exchange of plasmon may be the only viable mechanism for superconductivity in the lowest density bulk samples. [P5]

Recent Progress

A. Transport and optical properties of Weyl semimetals.

In the past several years there have been great interests in a new class of materials called Weyl semimetals. [1] There are three dimensional materials where there exist linearly dispersing bands which cross without any band gap. They can be thought of as three dimensional analog of graphene. Their existence requires materials which break either inversion or time reversal symmetry and each Weyl point is a monopole source or sink of Berry's curvature. Interesting phenomena such as Fermi arc surface states and chiral anomaly in magneto-transport have been predicted. A large number of materials which harbor Weyl points has been discovered and many of the predictions verified. [2] One puzzling observation has been that large linear magneto-resistance seems to be ubiquitous in this class of materials. [3] This often masks the more fanciful effects such as the negative magnetoresistance due to chiral anomaly. The phenomenon of linear magnetoresistance itself has a long history. There has been very few viable proposals, but the best known one by Abrikosov does not apply because it requires a large field so that the zeroth Landau level is occupied. We propose a model of electrons moving in a slowly

varying potential and found that by careful studies of the drift motion of the guiding center, linear magnetoresistance can be obtained. [P1] There is independent evidence that disorder scattering is mainly forward in these materials, justifying our model of a smooth random potential.

A second direction we pursued is the interaction of light with the Weyl semi-metals. We find that laser light pushes the position of the Weyl points in momentum space in such a way that the chirality no longer cancels, resulting in a photoinduced anomalous Hall effect, ie. by shining circularly polarized light on these materials, a Hall conductivity can be produced without any applied magnetic field. [P2]

Very recently, we took this approach one step further and showed that when inversion symmetry and mirror symmetry are broken, the Weyl semimetals exhibit a large photocurrent, ie. circularly polarized light produces a spontaneous current without any applied voltage. [P6] As seen in Fig. 1 the tilting of the Weyl cone (which is generic with these broken symmetry) turns out to play a crucial role. The linear dispersion of the Weyl system offers two important advantages. First the photon energy can be very low and limited only by the position of the chemical potential relative to the node energy, which can be a few to tens of meV in practice. Second electron velocity is independent of the electron density and is large, thus giving a large current even when the chemical potential is small. As a result, this effect may be observable even at room temperature and may have practical application as detectors in the terahertz range.

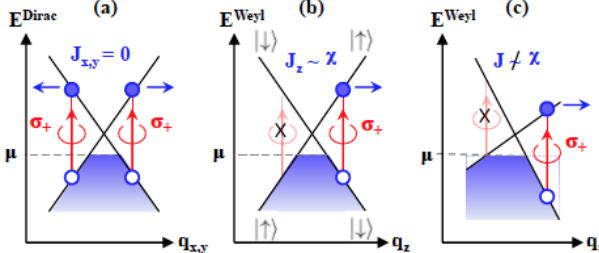


FIG. 1. Schematics of photocurrent generations in Dirac and Weyl systems. Circularly polarized photons propagating along the z -axis induce spin-flip vertical transitions denoted by the red arrows. (a) In a 2D ideal Dirac system, the excitations are symmetric about $\vec{q} = 0$ at each Dirac node and thus the photocurrent vanishes. (b) In a 3D Weyl system with an upright crossing spectrum, the extra dimension allows an asymmetric particle-hole excitation along q_z and creates a chirality-dependent photocurrent from each Weyl cone. However, the chiral currents from a monopole and an anti-monopole negate each other, yielding no net current. (c) In the presence of tilt along some direction q_t , asymmetric excitations can happen when the system is doped away from the neutrality. The resultant photocurrent is not just determined by the node chirality and the total current is generically non-zero.

B. Superconductivity at very low densities.

The BCS theory very successfully explains superconductivity in metals. The essential attraction between electrons, according to this theory, is generated by exchange of phonons, which have a characteristic frequency ω_D . A crucial condition for the applicability of the theory is the ‘retardation’ condition, namely that $\omega_D \ll \epsilon_F$, where ϵ_F is the Fermi energy. This condition holds in almost all known conventional superconductors and seems to be a universal property.

An outstanding exception is doped strontium titanate (SrTiO_3). Free charge carriers in this material are achieved by inducing oxygen vacancies or doping with elements such as La or Nb. Superconductivity is typically observed at temperatures lower than a few hundreds of Millikelvins. The transition temperature exhibits a dome shape as a function of carrier concentration, which extends to surprisingly low densities. Recently it has been reported that superconductivity extends to densities as low as $n_{3D} = 5 \times 10^{17} \text{ cm}^{-3}$ where the Fermi energy is $\epsilon_F \sim 1 \text{ meV}$. [4] In this situation ϵ_F is certainly not greater than ω_D , and therefore BCS theory does not apply. The natural question is therefore, why is strontium titanate superconducting at such a low density?

We find that almost all of the previous work on SrTiO_3 failed to address this question. After exhausting any possible mechanism using optical or acoustic phonons, we propose that the only viable mechanism is the exchange of plasmons. [P5] Due to the very large dielectric constant, the plasma frequency is smaller than the Fermi energy, in contrast to most conventional metals. By assuming a local reduction of the dielectric constant, we can account for the doping dependence of the transition temperature.

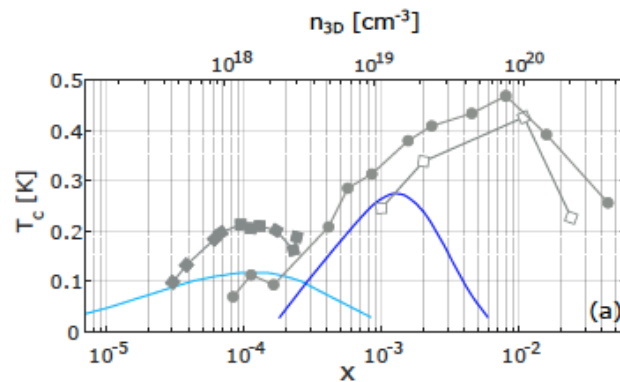


FIG. 2 Superconducting transition temperature vs doped electron concentration in SrTiO_3 . Dots are data from [4] and blue lines are theory curves from P5.

Future Plans

We plan to further pursue both topics in the near future. In the Weyl semimetals we plan to collaborate closely with Nuh Gedik at MIT to experimentally test our proposals on the anomalous Hall effect as well as the photo-current effect. Once the material is identified (and we have several candidates), we will carry out detailed calculations of the photo-current direction and amplitude and its dependence on the incident direction of the light. We will also continue to explore other unusual effect related to the unique properties of the Weyl spectrum.

For superconductivity we are intrigued by another class of superconductors at low densities. These are the half-Heusler compounds, a typical example being YPtBi which has a T_c of 1.6K and a density of 10^{19} cm^{-3} . [5] These are noncentro-symmetric materials, with the possibility of band inversion like a topological insulator. Spin-orbit coupling is strong. We do not think the plasmon mechanism is at play here, but strong coupling effect must be present. For example, the coherence length is only 15mm, which is comparable to the spacing between electrons. At the same time, the current interests in topological insulators have focused attention on many small band gap semi-conductors. These typically have dielectric constant near 100 and are promising places to look for plasmon induced pairing when doped.

References

1. X.G. Wan, A.M. Turner, A. Vishwanath, and S.Y. Savrasov, “*Topological semimetal and Fermi-arc surface states in the electronic structure of pyrochlore iridates*” Phys. Rev. B **83**, 205101 (2011).
2. Z. K. Liu, B. Zhou, Y. Zhang, Z. J. Wang, H. M. Weng, D. Prabhakaran, S.-K. Mo, Z. X. Shen, Z. Fang, X. Dai, Z. Hussain, and Y. L. Chen, “*Discovery of a Three-Dimensional Topological Dirac Semimetal*”, Na₃Bi” Science **343**, 864-867 (2014).
3. T. Liang, Q. Gibson, M. N. Ali, M. Liu, R. J. Cava and N. P. Ong, “*Ultrahigh mobility and giant magnetoresistance in the Dirac semimetal Cd₃As₂*”, Nat.Mater. **14**, 280–284 (2015).
4. X. Lin, G. Bridoux, A. Gourgout, G. Seyfarth, S. Krämer, M. Nardone, B. Fauqué, and K. Behnia, “*Critical Doping for the Onset of a Two-Band Superconducting Ground State in SrTiO₃-δ*”, Phys. Rev. Lett. **112**, 207002 (2014).
5. Y. Nakajima, R. Hu, K. Kirshenbaum, A. Hughes, P. Syers, X. Wang, K. Wang, R. Wang, S. Saha, D. Pratt, J. W. Lynn and J. Paglione, “*Topological RPdBi half-Heusler semimetals: a new family of non-centrosymmetric magnetic superconductors*”, arXiv:1501.04096 (2015).

Publications

- P1. J.C. Song, G. Rafael and P.A. Lee Author, “*Linear magnetoresistance in metals: guiding center diffusion in a smooth random potential*” Phys. Rev. B **92**, 180204 (2015).
- P2. C.K. Chan, P.A. Lee, K. S. Burch, J.H. Han, Y. Ran, “*When chiral photons meet chiral fermions: Photoinduced anomalous Hall effects in Weyl semimetals*”, Phys. Rev. Lett. **116**, 026805 (2016).
- P3. F.Mahmood, C.K.Chan, Z. Alpichshev, D. Gardner, Y. Lee, P. A. Lee, and N. Gedik, “*Selective scattering between Floquet-Bloch and Volkov states in a topological insulator*”, Nature Physics **12**, 306–310 (2016).
- P4. C.K. Chan, Y.T. Oh, J.H. Han, and P. A. Lee, “*Type-II Weyl cone transitions in driven semimetals*”, arXiv:1605.05696v1 (2016).

- P5. J. Ruhman and P. A. Lee, “*Superconductivity at very low density: the case of strontium titanate*”, arXiv:1605.01737 (2016).
- P6. C.K. Chan, N. Linder, G. Refael and P.A. Lee, “*Photocurrents in Weyl semimetals*”, To be published.

Design of functional materials based on new principles of disorder

Andrea J. Liu, Department of Physics and Astronomy, University of Pennsylvania

Keywords: functional materials, scaling theory, jamming, disordered solids, glasses

Project Scope

Central to the theory of equilibrium phase transitions is the fact that the free energy can be written in a scale-invariant form that captures scaling exponent relations. Our work shows that for the jamming transition, the elastic energy is the relevant free energy and can be expressed in a scale-invariant form consistent with known exponent relations. This result places jamming in the context of the theory of critical phenomena, suggesting the potential for a theoretical description of the non-equilibrium jamming transition on par with that of Ising criticality. It also provides powerful support for the idea that the observed commonality in the mechanical and thermal response of disordered solids can be understood as a manifestation of universality associated with the critical jamming transition [1].

The jamming transition marks the onset of rigidity in athermal sphere packings, and was originally proposed as a zero-temperature transition [1] for soft repulsive spheres in a non-equilibrium “jamming phase diagram” [2] of varying packing density and applied shear. Many studies have documented behaviors characteristic of critical phenomena near the jamming transition, including power-law scaling and scaling collapses of numerous properties with the expression of quantities in terms of scaling functions, diverging length scales, and finite-size scaling. Theories have been developed to individually understand and relate some of these power laws, but a unified scaling theory has been lacking.

The critical-point scaling ansatz introduced by Widom in the 1960s was a key advance in the theory of critical phenomena that set the stage for the development of the renormalization group. The ansatz writes the state functions near continuous equilibrium phase transitions in terms of power-law ratios of the control parameters. By positing a scaling function for the free energy, it exploits the fact that quantities such as the specific heat, magnetization and susceptibility are derivatives of the free energy to derive not only relations among their scaling exponents, but among their scaling functions. Thus, the scaling ansatz provides a unified and comprehensive description of systems exhibiting what later was realized to be an emergent scale invariance.

Recent Progress

We have recently developed a unified scaling theory for the jamming transition in terms of the fields originally identified by the jamming phase diagram [2], namely density and shear. The fact that the jamming transition can be described by a scaling ansatz is powerful evidence of the existence of criticality at the jamming transition. Unlike most systems exhibiting dynamical scale invariance, we find that a jammed system can also be viewed as a material whose critical properties are determined by a state function, analogous to those at thermodynamic critical points.

We introduce a scaling ansatz [3] for the elastic energy of a sphere packing just above the jamming transition to develop a unified theory of the scaling exponents and scaling functions for the energy, excess packing fraction, shear strain, pressure, shear stress, bulk modulus, shear modulus and system size. Our theory yields scaling relations that relate the singular behavior of all of these quantities to only three independent scaling exponents, which can be extracted from known numerical and theoretical results. It predicts new exponents for the shear stress and shear strain. Most importantly, however, our scaling theory shows how the jamming transition can be understood in the context of the theory of critical phenomena.

We consider d -dimensional jammed packings of soft frictionless spheres at temperature $T = 0$ with packing fraction φ . Note that the packing fraction at the jamming transition, $\varphi_{c,\Lambda}$, varies from one member of the ensemble Λ to the next. For each packing, we characterize the distance above the transition by $\Delta\varphi \equiv \varphi - \varphi_{c,\Lambda}$ [1]. Systems are further characterized by the average number of interacting neighbors per particle (the contact number, Z), which satisfies $Z \geq Z_{\min}$ where $Z_{\min} = 2d - (2d - 2)/N$ approaches the isostatic value $Z_{\text{iso}} \equiv 2d$ in the thermodynamic limit [1]. A key quantity is the excess contact number (the number of contacts per particle in excess of the minimum value), namely $\Delta Z = Z - Z_{\min}$. For a given protocol for preparing jammed states, the mean dimensionless energy density E of a sphere packing will depend on ΔZ and $\Delta\varphi$ as well as the shear strain ε and the system size N . We define ε relative to the strain of the as-quenched state.

Our scaling ansatz [4] is:

$$E(\Delta Z, \Delta\varphi, \varepsilon, N) = \Delta Z^\zeta E_0 \left(\frac{\Delta\varphi}{\Delta Z^{\beta_\varphi}}, \frac{\varepsilon}{\Delta Z^{\beta_\varepsilon}}, N \Delta Z^\psi \right) \quad [1]$$

where the scaling exponents ζ , β_φ , β_ε and ψ are to be determined. Eq. 1 is set up so that the leading singular part of the elastic energy in the thermodynamic limit is proportional to ΔZ^ζ . The excess packing fraction $\Delta\varphi$ and shear strain ε represent components of the same strain tensor (compression and shear respectively) but are allowed to scale differently. This would seem natural, since they are different “relevant directions” in the jamming phase diagram. The different exponents lead to different scaling properties for the bulk and shear moduli, B and G [1].

We proceed by calculating derivatives of the energy (Eq. [1]) with respect to $\Delta\varphi$ and ε to obtain scaling expressions for the pressure p and the residual shear stress s . Similarly, the bulk modulus B and shear modulus G are second derivatives of the energy. The four exponents for p , s , B and G can therefore be related to the four exponents in Eq. [1] via scaling relations. In addition, we derive a fifth scaling relation connecting shear stress to pressure via system size. Thus, by using previous theoretical or numerical results to obtain 3 of the 8 exponents, the remaining 5 can be determined from the scaling relations. Of these, two are new to the literature; one is verified in Fig. 1 and the other has recently been verified by others [4]. These results validate the scaling ansatz.

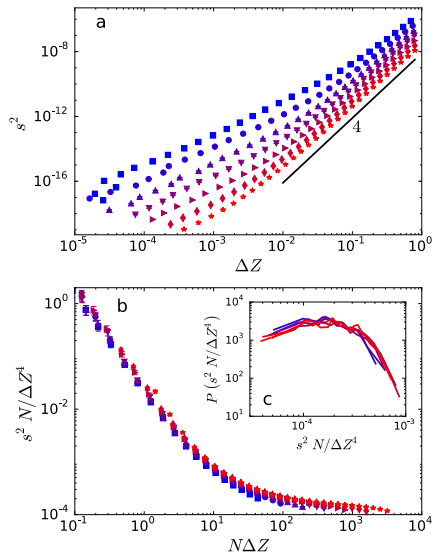


Fig. 1. Scaling collapse of the residual shear stress. (a) s^2 as a function of ΔZ . (b) s^2 scaled using the predicted exponents. The excellence of the collapse verifies these exponents. (c) Probability distribution of $s^2 N/\Delta Z^4$ for systems at fixed $N\Delta Z$ and $p/\Delta Z^2$. This also collapses as predicted.

Our preliminary results show that the shear-jammed state is fundamentally different, even in the thermodynamic limit, because it has an anisotropic structure. This leads to different scaling of the shear modulus, which jumps discontinuously at the jamming transition, in contrast to the isotropically-jammed state, where it rises continuously from zero at the jamming transition. The important question is whether the shear-jamming transition belongs to a different universality class due to anisotropy, or whether it is fundamentally the same as the isotropic jamming transition.

We are also using real-space renormalization group approaches to study the jamming transition. We start with the covariance matrix $C = \langle u_{i\alpha} u_{j\beta} \rangle$, where $u_{i\alpha}$ is the α -component of the displacement of particle i from its equilibrium position. This matrix C is the inverse of the dynamical matrix D . We can therefore add together the displacements of nearby particles to obtain a coarse-grained displacement and invert to obtain the coarse-grained dynamical matrix. The idea is then to rescale the resulting dynamical matrix to understand how its behavior flows with coarse-graining.

References

1. A. J. Liu and S. R. Nagel, *The jamming transition and the marginally-jammed solid*, Annual Reviews of Cond. Mat. Phys. **1**, 347 (2010).

The fact that the jamming transition can be described by a scaling ansatz implies that the jamming transition exhibits emergent scale invariance, and that the tools of the theory of equilibrium critical phenomena, such as coarse-graining and rescaling to study renormalization group flows, should be applicable. The scaling ansatz is therefore an important step towards a complete theoretical description of the jamming transition capable of systematically including friction, non-spherically-symmetric potentials, three-body interactions and other features of the real world, to understand the extent of universality in the mechanical properties of disordered solids.

Future Plans

Our first step will be to consider the effects of anisotropy. Spheres with frictional interactions are able to jam at much lower densities than those without friction when subjected to an external shear stress, leading to a so-called ‘‘shear-jammed’’ state [5]. Until recently, it was thought that friction was necessary for shear jamming. However, recent studies have shown that shear jamming of frictionless particles is possible for finite systems [5].

2. A. J. Liu and S. R. Nagel, *Jamming is not just cool anymore*, Nature **396**, N6706, 21 (1998).
3. C. P. Goodrich, A. J. Liu and J. P. Sethna, *Scaling ansatz for the jamming transition*, PNAS (in press, 2016).
4. H. Yoshino, F. Zamponi, *Shear modulus of glasses: Results from the full replica-symmetry-breaking solution*. Phys. Rev. E **90**, 022302 (2014).
5. D. Bi, J. Zhang, B. Chakraborty and R. P. Behringer, *Jamming by shear*, Nature **480**, 355358 (2011).

Publications (August 2014-July 2016)

1. C. P. Goodrich, A. J. Liu and S. R. Nagel, *Contact nonlinearities and linear response in jammed particulate packings*, Phys. Rev. E **90**, 022201 (2014).
2. C. P. Goodrich, S. Dagois-Bohy, B. P. Tighe, M. van Hecke, A. J. Liu and S. R. Nagel, *Jamming in finite systems: stability, anisotropy, fluctuations and scaling*, Phys. Rev. E **90**, 022138 (2014).
3. E. D. Cubuk, S. S. Schoenholz, J. M. Rieser, B. D. Malone, J. Rottler, D. J. Durian, E. Kaxiras and A. J. Liu, *Identifying structural flow defects in disordered solids using machine learning methods*, Phys. Rev. Lett. **114**, 108001 (2015).
4. M. L. Manning and A. J. Liu, *A random matrix definition of the boson peak*, Europhys. Lett. **109**, 36002 (2015).
5. D. M. Sussman, C. P. Goodrich, A. J. Liu and S. R. Nagel, *Disordered surface vibrations in jammed sphere packings*, Soft Matter **11**, 2745-2751 (2015).
6. C. P. Goodrich, A. J. Liu and S. R. Nagel, *The principle of independent bond-level response: tuning by pruning to exploit disorder for global behavior*, Phys. Rev. Lett. (2015).
7. S. S. Schoenholz, E. D. Cubuk, D. M. Sussman, E. Kaxiras and A. J. Liu, *A structural approach to relaxation in glassy liquids*, Nature Physics **12**, 469 (2016).
8. D. M. Sussman, C. P. Goodrich and A. J. Liu, *Spatial structure of states of self stress in jammed systems*, Soft Matter **12**, 3982 (2016).
9. A. L. Graves, S. Nashed, E. Padgett, C. P. Goodrich, A. J. Liu and J. P. Sethna, *Pinning susceptibility: the effect of dilute, quenched disorder on jamming*, Phys. Rev. Lett. **116**, 235501 (2016).
10. E. D. Cubuk, S. S. Schoenholz, E. Kaxiras and A. J. Liu, *Structural properties of defects in glassy liquids*, J. Phys. Chem. B **120**, 6139-6146 (2016).

Theory of Materials Program at the Lawrence Berkeley National Laboratory

Principal Investigator:

Prof. Steven G. Louie – Physics Department, UC Berkeley, and Materials Sciences Division, LBNL, Berkeley, CA 94720 (sglouie@berkeley.edu)

Co-Principal Investigators:

Prof. Marvin L. Cohen – Physics Department, UC Berkeley, and Materials Sciences Division, LBNL, Berkeley, CA 94720 (mlcohen@berkeley.edu)

Prof. Dung-Hai Lee -- Physics Department, UC Berkeley, and Materials Sciences Division, LBNL, Berkeley, CA 94720 (dhlee@berkeley.edu)

Prof. Jeffrey B. Neaton – Physics Department, UC Berkeley, and The Molecular Foundry and Materials Sciences Division, LBNL, Berkeley, CA 94720 (jbneaton@lbl.gov)

Dr. Lin-Wang Wang – Materials Sciences Division, LBNL, Berkeley, CA 94720
(lwwang@lbl.gov)

Project Scope

The goal is to understand and compute material properties and behaviors, covering complex materials, nanostructures, reduced-dimensional materials, and strongly correlated electron systems. Novel materials and new concepts are explored. Studies include: superconductivity and mechanisms; excited states in novel materials; methodology developments; symmetry and topological phases; and transport phenomena. A variety of theoretical techniques are employed, ranging from first-principles electronic structure calculations to new conceptual and computational frameworks suitable for complex materials/nanostructures and strongly interacting electron systems. Emphasis is on investigation of realistic systems employing microscopic first-principles approaches, including many-electron effects. Model systems are also examined. Close collaboration with experimentalists is maintained. Another emphasis is to push theory beyond the Landau paradigm. New phenomena, new phases, and new organization principles may be discovered. Equally important is the development of computational methods suitable for increasingly complex materials and strongly correlated materials.

Recent Progress

Activities since the last PI Meeting in 2014 covered advances on two-dimensional (2D) crystals, topological phases, molecular junctions, nanostructures, superconductors, photovoltaics, strongly correlated systems, and new theoretical and computational methods. Since July 2014, fifty papers have been published acknowledging this Program including 1 *Science*, 4 *Nature* “family”, 5 *Phys. Rev. Letters*, 8 *Nano Letters*, 1 *PNAS*, etc. articles. The work has led to formulation of new concepts, prediction of novel phenomena, and explanation of experiments for a range of materials. Some selected results are:

- *Discovery of electron supercollimation in graphene and 2D Dirac fermion materials using 1D disorder*
- *Tuning and control of charge transport and rectification in molecular junctions*
- *Theory of underdoped superconducting cuprates as topological superconductors*
- *Development of range-separated hybrid functional for electronic structure calculations*
- *Methods for calculating transport at molecular interfaces*

- *Prediction of tunable magnetism and half-metallicity in hole-doped monolayer GaSe*
- *Theory and magneto-optical spectroscopy of SU(4) symmetry breaking in epitaxial graphene*
- *Mechanism of large electron-phonon interactions from FeSe phonons in a monolayer*
- *Theory of topological phase transition*
- *Efficient methods and algorithms for: a) self-consistent GW calculations, b) classical force field simulations, and real-time Time Dependent Density Functional Theory*
- *New method for automated construction of maximally localized Wannier functions*
- *Discovery of massless excitons in 2D crystals*
- *Theory of interplay of bias-driven charging and the vibrational Stark effect in molecular junctions*
- *Proposal for a bulk material based on monolayer FeSe on SrTiO₃ high T_c superconductor.*

Future Plans

Planned activities are focused in: 1) superconductivity and mechanisms; 2) excited-state properties of novel materials; 3) theoretical and methodological developments; 4) symmetry and topological phases; and 5) transport phenomena. Areas 1 & 4 concern with understanding and/or discovery of new phases and new classes of materials with novel properties. Areas 2 & 5 concern with excited-state (spectroscopic) and transport properties of materials and nanostructures. Area 3 concerns with developments of theoretical and computational methods that would allow accurate and predictive studies. Some selected projects include:

- *Superconductivity mechanisms in Fe-based superconductors*
- *Exploration of 3D heterostructures to enhance superconductivity*
- *High T_c superconductivity in H-S and H-P systems*
- *Optoelectronic phenomena in quasi 2D materials and those with defects*
- *Controlling plasmons in metallic transition metal dichalcogenides layers and related quasi-2D materials.*
- *Method for Wannier representation of Z₂ topological insulators*
- *Explore difference between Landau-like and topological phase transitions*
- *Temperature dependent topological phase diagrams and electron-phonon interactions*
- *Diffusive transport properties of halide perovskites and topological materials*
- *Methods and their applications to transport phenomena through nanoscale heterogeneous interfaces*
- *Photophysics & excitons of materials with nontrivial band topology*

Publications (selected from July 2014-present)

Primary Publications

- S. K. Choi, C.H. Park, and S.G. Louie, "Electron Supercollimation in Graphene and Dirac Fermion Materials Using One-Dimensional Disorder Potentials," Phys. Rev. Lett. 113, 026802 (2014).
- T. Kim, Z.-F. Liu, C. Lee, J. B. Neaton, and L. Venkataraman, "Charge transport and rectification in molecular junctions formed with carbon-based electrodes," Proc. Natl. Acad. Sci. 111, 10928 (2014).
- Y.M. Lu, T. Xiang and D-H. Lee, "Underdoped superconducting cuprates as topological superconductors", Nature Physics **10**, 634 (2014).

- Z.-F. Liu, S. Wei, H. Yoon, O. Adak, I. Ponce, Y. Jiang, W.-D. Jang, L. M. Campos, L. Venkataraman, and J. B. Neaton, "Control of single-molecule junction conductance of porphyrins via transition metal center," *Nano Lett.* **14**, 5365 (2014).
- I. Tamblyn, S. Refaelly-Abramson, J. B. Neaton, and L. Kronik, "Simultaneous Determination of Structures, Vibrations, and Frontier Orbital Energies from a Self-Consistent Range-Separated Hybrid Functional," *J. Phys. Chem. Lett.* **5**, 2734 (2014).
- Z.-F. Liu and J. B. Neaton, "Energy-dependent resonance broadening in symmetric and asymmetric molecular junctions from an ab initio non-equilibrium Green's function approach", *J. Chem. Phys.* **44**, 131104 (2014).
- J. Lischner, G. K. Palsson, D. Vigil-Fowler, S. Nemsak, J. Avila, M. C. Asensio, C. S. Fadley, and S. G. Louie, "Satellite Band Structure in Silicon Caused by Electron-Plasmon Coupling," *Phys. Rev. B* **91**, 5113 (2015).
- T. Cao, Z. Li, and S. G. Louie, "Tunable Magnetism and Half-Metallicity in Hole-Doped Monolayer GaSe," *Phys. Rev. Lett.* **114**, 236602 (2015).
- L.Z. Tan, M. Orlita, M. Potemski, J. Palmer, C. Berger, W.A. de Heer, S. G. Louie, and G. Martinez, "SU(4) symmetry breaking revealed by magneto-optical spectroscopy in epitaxial graphene," *Phys. Rev. B* **91**, 5122 (2015).
- S. Coh, M. L. Cohen, and S. G. Louie, "Large electron-phonon interactions from FeSe phonons in a monolayer," *New J. of Phys.* **17**, 073027 (2015).
- Y. Sakai, S. Saito, and M. L. Cohen, "Electronic properties of B-C-N ternary kagome lattices," *Phys. Rev. B* **91**, 165434 (2015).
- H. Oh, S. Coh, and M. L. Cohen, "Calculation of the specific heat of optimally K-doped BaFe₂As₂," *J. Phys.: Condens. Matter* **27**, 335504 (2015).
- L. Tsui, H.-C. Jiang, Y.-M. Lu and D.H. Lee, "Quantum phase transitions between a class of symmetry protected topological states", *Nuclear Physics B*, 330-359 (2015).
- M. Kotiuga, P. Darancet, C. R. Arroyo, L. Venkataraman, and J. B. Neaton, "Adsorption-Induced Solvent-Based Electrostatic Gating of Charge Transport through Molecular Junctions," *Nano Lett.* **15**, 4498 (2015)
- L.W. Wang, "Full self consistent solution of the Dyson equation using a plane wave basis set" *Phys. Rev. B*, **91**, 125135 (2015).
- C. Barrett, and L.W. Wang, "A double charge model for classical force field simulations" *Phys. Rev. B*, **91**, 235407 (2015).
- Z. Wang, S.S. Li, and L.W. Wang, "An efficient real-time time-dependent DFT method and its applications to ion-2D material collision" *Phys. Rev. Lett.* **114**, 063004 (2015).
- L. Shi, K. Xu, and L.W. Wang, "A comparative study of ab initio nonradiative recombination rate calculations under different formalisms", *Phys. Rev. B* **91** 205315 (2015).
- J. Wang, Y. Zhang, L.W. Wang, "Systematic approach for simultaneously correcting the band-gap and p-d separation errors of common cation III-V or II-VI binaries in density functional theory calculations within a local density approximation", *Phys. Rev. B* **92**, 045211 (2015).
- Y. Chen, Y. Xie, S.A. Yang, H. Pan, F. Zhang, M. L. Cohen, and S. B. Zhang, "Nanostructured carbon allotropes with Weyl-like loops and points." *Nano Letters* **15**, 6974 (2015).
- J. I. Mustafa, S. Coh, M. L. Cohen, and S. G. Louie, "Automated construction of Maixmally localized Wannier functions: Optimized projection functions method." *Phys. Rev. B* **92**, 165134 (2015).
- D. Y. Qiu, T. Cao, and S.G. Louie, "Nonanalyticity, Valley Quantum Phases, and Lightlike Exciton Dispersion in Monolayer Transition Metal Dichalcogenides: Theory and First-Principles Calculations," *Phys. Rev. Lett.* **115**, 176801 (2015).
- C. Barrett, L.W. Wang, "A systematic fitting procedure for accurate force field models to reproduce ab initio phonon spectra of nanostructures". *Comp. Phys. Comm.* **200**, 27 (2016).
- Y. Li, P. Zolotavin, P. Doak, L. Kronik, J. B. Neaton, and D. Natelson, "Interplay of Bias-Driven Charging and the Vibrational Stark Effect in Molecular Junctions." *Nano Lett.* **16**, 1104 (2016)).
- G. Li, T. Rangel, Z.-F. Liu, V. R. Cooper, and J. B. Neaton, "Energy level alignment of self-assembled linear chains of benzenediamine on Au(111) from first principles," *Phys. Rev. B* **93**, 125429 (2016).
- J. Ma and L.W. Wang, "Using Wannier functions to improve solid band gap predictions in density functional theory," *Scientific Reports* **6**, 24924 (2016).
- D. Y. Qiu, F. H. da Jornada, and S. G. Louie, "Screening and many-body effects in two-dimensional crystals: Monolayer MoS₂," *Phys. Rev. B* **93**, 235435 (2016).
- S. Coh, D.-H. Lee, S. G. Louie, and M. L. Cohen, "Proposal for a bulk material based on a monolayer FeSe on SrTiO₃ high-temperature superconductor," *Phys. Rev. B* **93**, 245138 (2016).

Secondary Publications

- S. Y. Wang, L.Z. Tan, W. Wang, S. G. Louie, and N. Lin, "Manipulation and Characterization of Aperiodical Graphene Structures Created in a Two-dimensional Electron Gas," *Phys. Rev. Lett.* **113**, 196803 (2014).
- L. Zhang, K. Liu, A.B. Wong, J. Kim, X. Hong, C. Liu, T. Cao, S. G. Louie, F. Wang, and P. Yang, "Three-dimensional Spirals of Atomic Layered MoS₂," *Nano Lett.* **14**, 6418 (2014).
- M. M. Ugeda, A. J. Bradley, S.-F. Shi, F. H. da Jornada, Y. Zhang, D. Y. Qiu, W. Ruan, S.-K. Mo, Z. Hussain, Z.-X. Shen, F. Wang, S. G. Louie, and M. F. Crommie, "Giant bandgap renormalization and excitonic effects in a monolayer transition metal dichalcogenide semiconductor," *Nature Materials* **13**, 1091 (2015).
- J. Lischner, T. Bazhirov, A. H. MacDonald, M. L. Cohen, and S. G. Louie, "First-principles theory of electron-spin fluctuation coupling and superconducting instabilities in iron selenide," *Phys. Rev. B* **91**, 020502(R) (2015).
- F. Wang, S. A. Kivelson and D.H. Lee, "Nematicity and quantum paramagnetism in FeSe" *Nature Physics* **11**, 959 (2015).
- D. A. Egger, Z.-F. Liu, J. B. Neaton, and L. Kronik, "Reliable Energy Level Alignment at Physisorbed Molecule-Metal Interfaces from Density Functional Theory," *Nano Lett.* **15**, 2448 (2015)
- B. Capozzi, J. Xia, O. Adak, E. J. Dell, Z.-F. Liu, J. C. Taylor, J. B. Neaton, L. M. Campos, and L. Venkataraman, "Single-molecule diodes with high rectification ratios through environmental control," *Nature Nanotechnology* **10**, 522 (2015)
- Z. Gui, L.W. Wang, and L. Bellaiche, "Electronic properties of electrical vortices in ferroelectric nanocomposites from large-scale ab-initio computations", *Nano Lett.* **15**, 3224 (2015).
- L. Dou, A.B. Wong, Y. Yu, M. Lai, N. Kornienko, S. W. Eaton, A. Fu, C.G. Bischak, J. Ma, T. Ding, N. S. Ginsberg, L.W. Wang, A. P. Alivisatos, and P. Yang, "Atomically Thin Two-dimensional Organic-inorganic Hybrid Perovskites", *Science* **349**, 1518 (2015).
- J. Zheng, Y. Hou, Y. Duan, X. Song, Y. Wei, T. Liu, J. Hu, H. Guo, Z. Zhou, L. Liu, Z. Chang, X. Wang, D. Zherebetsky, Y. Fang, Y. Li, K. Xu, L.W. Wang, Y. Wu, F. Pan, "Janus solid-liquid interface enabling ultra-high charging and discharging rate for advanced lithium-ion batteries", *Nano Lett.* **15**, 6102 (2015).
- J. H. Yang, L. Shi, L.W. Wang, S. H. Wei, "Non-radiative carrier recombination enhanced by two-level process: a first-principle study", *Science Report* **6**, 21712 (2016).
- J. Lischner, S. Nemšák, G. Conti, A. Gloskovskii, G. K. Pálsson , C. M. Schneider, W. Drube, S. G. Louie, and C. Fadley, "Accurate determination of the valence band edge in hard x-ray photoemission spectra using GW theory," *J. Appl. Phys.* **119**, 165703 (2016) .

CHARGE CARRIER HOLES CORRELATIONS AND NON-ABELIAN PHYSICS IN NANOSTRUCTURES, QUANTUM HALL EFFECT AND HYBRID SUPERCONDUCTOR/SEMICONDUCTOR STRUCTURES.

Principal Investigator: Yuli Lyanda-Geller, yuli@purdue.edu

Department of Physics and Astronomy, Purdue University West Lafayette IN 47907

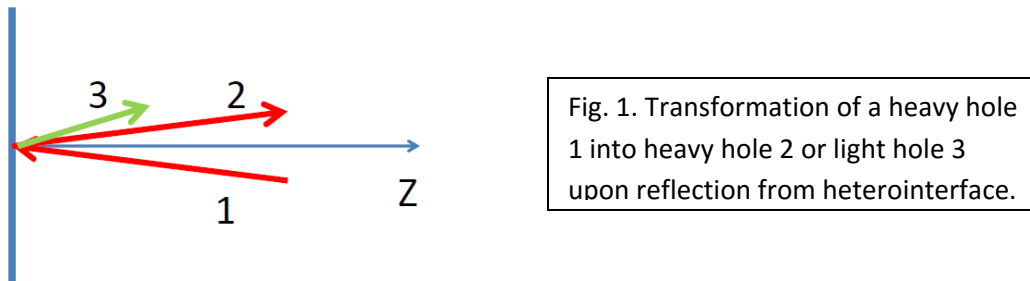
Project Scope.

The project goal is to uncover new non-Abelian effects and states with non-Abelian statistics in charge carrier hole systems. We investigate Fractional Quantum Hall states at and around crossings in spectra of single-particle hole states arising due to strong angular momentum-orbital interactions of Luttinger holes. Methods of investigating systems with strong coupling of spin and orbital degrees of freedom and coupling of in-plane and out of plane motion are developed. Understanding edge states in quantum Hall charge carrier hole systems are central to potential realization of Majorana Fermions, parafermions and Fibonacci anyons in hole settings.

Recent Progress

Magnetic field spectral crossings of Luttinger holes in quantum wells

Over several decades, understanding spectra of holes in spin 3/2 degenerate valence band in a magnetic field has been a challenging problem. In quantum wells, the problem becomes even more non-trivial due to a strong coupling of spin, in-plane motion of holes and their motion in the direction of spatial quantization. We have achieved significant progress in understanding quantization of the magnetic field spectrum of quantum well holes described by Luttinger Hamiltonian. The principal result is finding numerous crossings between various hole levels, including those in the ground state of holes. Our results account for coupling of cyclotron motion with spatial quantization and spin, which represents the crucial effect of mutual transformation between heavy and light holes upon reflection from hetero-boundaries.



These effects were largely omitted by researchers earlier. We found an analytical method to include these effects non-perturbatively, which significantly affects the spectrum compared to inclusion of perturbative admixture of hole states.

The results further include:

- Determination of g-factors of holes in a high magnetic field.

- Determination of cyclotron mass. Proof that for high Landau indices the cyclotron mass coincides with in-plane hole mass in the absence of magnetic field.
- Theory of Dresselhaus spin-orbit interactions in a high magnetic field including non-trivial k_z^3 term.
- Effects of anisotropy (warping) have been fully accounted.
- Analysis of the origin of beats in Shubnikov-De Haas oscillations, which arise from Luttinger terms alone, in the absence of Dresselhaus and Rashba interactions.

Hole spectra in quantum wells and wires

We derived hole spectra in quantum wells and wires[1,3]. These spectra define both topological phenomena, such as Majorana zero modes in proximitized wires and non-Abelian fractional quantum Hall effect states of holes, and spintronic effects such as generation and manipulation of spin currents. The new understanding of spectra accounts for mutual transformation of heavy and light holes Fig.1, that changes hole mass, spin-orbit constants and g-factors.

The treatment of low-dimensional holes has been controversial for a long time. The majority of authors treats holes like electrons: if the motion of particles is quantized in direction z in a well of width d, their Hamiltonian is solved by replacing momentum p_z by zeros and p_z^2 by its expectation value in the ground state, $(\hbar\pi/d)^2$, and spin-orbit and Zeemann terms are found by using a perturbation theory. However, this approach for holes is flawed. The Luttinger Hamiltonian terms proportional to $[J_z J_x]p_x p_z$ and to $[J_z J_y]p_y p_z$, which are neglected in this approach, transform heavy holes into light holes and couple in-plane motion with motion along the growth direction of the quantum well or wire, as shown in Fig.1. Although this effect can be evaluated perturbatively by including off-diagonal terms linear in p_z , it then requires summation of an infinite number of terms, which are parametrically all the same [1]. We therefore employed an alternative non-perturbative approach known since the work by Nedorezov, which was seldom used in the past and almost ignored over the past two decades. Our most important results for theorists and experimentalists alike are:

We determined g-factor of holes. For decades, both experimental physicists and theorists have been convinced that the only contribution to the hole g-factor in quantum wells and wires comes from a direct Zeemann coupling between the magnetic field and angular momentum of holes. We showed the existence of the strong orbital contribution, resolving a long-standing experimental puzzle.

We derived *the Rashba and Dresselhaus spin-orbit constants* for hole quantum wells and wires. Their values are strongly affected by mutual transformation of holes.

We derived *new σ_z spin-orbit coupling*. This new contribution to spin-orbit interaction in quantum wells and wires is of interest for spin currents and spin relaxation and dephasing of holes in two dimensional hole gas, but plays detrimental role for Majorana fermions in wires. Ways to suppress this term have been found.

Theory of the fractional quantum Hall effect in hole systems [2].

One of the principal goals of the proposed research has been the prediction and understanding of new states of matter for charge carrier holes, particularly new Fractional Quantum Hall effect

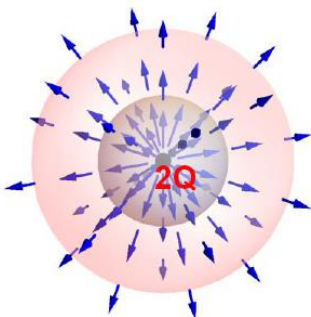


Fig 2. Spherical shell configuration for modeling hole quantum Hall effect, accounting for correlations of radial motion, angular motion and spin, that describe heavy to light hole transformations

states. We proposed a new method of mapping states of holes confined to a finite width quantum well in a perpendicular magnetic field to states in a spherical shell geometry, Fig. 2. Holes wavefunctions are four-spinors and their in-plane and z-direction degrees of freedom are inseparable, making the treatment of Coulomb interactions very challenging. For electrons, the in-plane and z-direction motion are independent, so it is possible to use the Haldane technique of homogeneous states with translationally invariant wavefunctions for a finite number of electrons on a sphere in a monopole magnetic field. This method cannot be applied to holes, hence we apply the spherical shell geometry. We calculated two-hole pseudopotentials including corrections due to Landau level mixing as well as and three-hole pseudopotentials and their irreducible components, and used them in exact diagonalization of finite size hole systems. Evaluating Coulomb interactions matrix elements for holes is much more complex than for electrons. While the electron wavefunction on the sphere

in the absence of spin-orbit coupling has a single component, the hole wavefunction has 16 components (4 angular momenta and 4 spin states). Interaction matrix elements contain summation over all angular momenta and spin states of two pairs of states and integration over two radial coordinates. There are 65536 "electron-like" matrix elements for holes instead of a single matrix element for electrons. This makes modeling for holes a computationally intensive task.

Compared to electrons, holes have smaller cyclotron energy and stronger Landau level mixing by Coulomb interactions. Near crossings in single-hole spectra, a single quantum well hole system mimics the physics of electron bilayers. Around crossings, ratio of interaction and cyclotron energies can change significantly with a magnetic field, and interaction pseudopotentials can be easily tuned. Therefore, hole systems are much more controllable than electron systems. We have shown that these features make hole system promising for observation of non-Abelian excitations and transition between non-Abelian and Abelian states. In particular, we applied our spherical shell method for study of the quantum Hall effect at filling factor $v=1/2$.

Non-Abelian matter in the fractional quantum Hall effect of holes at $v=1/2$

Recently, a unique fractional quantum Hall effect of holes at half-filling of the ground state of holes in magnetic field has been observed by Shayegan's group. For electrons, $v=1/2$ state does not exist in single-layer systems. Heterostructure quantum wells with 250-300 Å width, which were part of these studies, are not expected to be transformed into two narrow triangular wells at heteroboundaries, and it is highly probable that a single-quantum well physics is responsible for the observed state.

Using calculated pseudopotentials, we considered a system of 8, 10, 12, 14 and 16 holes at $v=1/2$ filling factor. Exact diagonalization shows an angular momentum $J=0$ ground state separated by a gap from the continuum of states, a clear indication of an incompressible state. We have demonstrated that in the presence of mixing of hole levels in a magnetic field the overlap of the wavefunction of the state of holes with the Moore-Read Pfaffian state is up to 0.7 and the overlap

of excitation wavefunctions reaches 0.6, raising the possibility that charge carrier hole excitations at $v=1/2$ present an example of non-Abelian matter. We also tested whether it is possible that the $v=1/2$ state represents the Halperin 331 state. The overlap of the calculated hole wavefunctions with the wavefunction of the 331 state found by Haldane and Rezayi is ~ 0.17 in the broad range of fields around the crossing in the hole spectra, making the 331 state highly unlikely.

Majorana zero modes in charge carrier hole quantum wires [3]

In search of Majorana zero modes in hybrid superconductor-semiconductor structures, the key problem is achieving significant strength of p-pairing due to spin-orbit interactions. We have demonstrated that hole GaAs and InSb systems exhibit stronger p-pairing compared to electron systems. While InSb electrons have strong spin-orbit coupling constants γ , the characteristic spin-orbit energy $E_{so} = \gamma^2 m$ is also defined by the electron mass m , which is very small in InSb. In hole InSb and GaAs systems, spin-orbit constants are comparable, but masses are bigger. We found optimal conditions for realization of Majorana fermions in quantum well-based nanowires. The combination of values of g-factor, chemical potential, and strength of spin-orbit interactions, as well as favorable conditions for superconducting proximity effect due to surface defect levels inside the semiconductor bandgap, makes these systems a promising experimental setting.

We have advanced an understanding of the criterion for realizing Majorana modes and topological superconductivity in hybrid settings with spin-orbit interactions. Spin-orbit effects in hole wires lead to momentum-dependent Zeemann fields in all three spatial directions. This situation can also take place in electron settings. We have demonstrated that zero energy Majorana mode in this case exists despite the Bogoliubov-De Gennes equation cannot have real solutions, and no choice of the phase of the superconducting order parameter can decouple real and imaginary parts of the BdG wavefunctions.

Future Work. We will extend investigation of the fractional quantum Hall effect to a larger number of holes in exact diagonalization studies, use density matrix renormalization group method, and analyze non-Abelian nature of quantum Hall states in hole systems by evaluating an entanglement entropy. We will study how gate voltage and in-plane magnetic fields affect edge states. Their control can lead to creation of helical domain walls between various phase boundaries hosting non-Abelian quasiparticles. We will explore the possibility to control hole edge states in order to generate and manipulate Fibonacci anyons.

Publications

- [1] G.E. Simion and Y.B. Lyanda-Geller, Magnetic field spectral crossings of Luttinger holes in quantum wells, *Physical Review B*. **90**, 195410 (2014).
- [2] G.E. Simion and Y.B. Lyanda-Geller, Non-Abelian $v=1/2$ quantum Hall state in Γ_8 Valence Band Hole Liquid, ArXiv:1603.03308
- [3] J. Liang and Y. Lyanda-Geller, Majorana Fermions in charge carrier hole quantum wires, ArXiv:1603.03750.

Correlation between electron transport and antiferromagnetic ordering

Principle Investigator: Dr. Allan H. MacDonald (macd@physics.utexas.edu)

Co-Principle Investigator: Dr. Qian Niu (niu@physics.utexas.edu)

Keywords: antiferromagnetism, noncollinear, anomalous Hall effect, orbital magnetization, spin torque

Project Scope

This project involves theoretical research on a variety of related topics connected mainly to the interplay between electron and phonon transport and different types of electronic order. Three important themes of this work are i) the interrelationship between order in spin and valley space and the integer and fractional quantum Hall effect in graphene, ii) the idea of Berry curvature in momentum space and its relationship to Hall transport effects and to magnetic order, and iii) the relationship between phonon angular momentum and magnetic order.

Recent Progress

Detailed below are our recent works mostly under theme ii) of the project, specifically on exploring the correlation between electric fields or currents and antiferromagnetic ordering. Antiferromagnets have so far played a more modest role in spintronics than ferromagnets, partly because their order parameters are not approximately conserved quantities, and partly because their order is less easily detected and manipulated. There are, however, a number of advantages of antiferromagnets over ferromagnets application-wise. For example, since antiferromagnetic order parameters couple to external magnetic fields rather weakly, spintronic devices based on antiferromagnets can be much more robust against external magnetic fields than their ferromagnetic counterparts. Another benefit of using antiferromagnets is that their resonance frequency is proportional to the square root of the product of antiferromagnetic exchange coupling and uniaxial anisotropy, and can therefore be much higher than that of ferromagnets, whose resonance frequency at small magnetic fields is only proportional to the uniaxial anisotropy and independent of exchange coupling. As such, devices based on magnetization dynamics of antiferromagnets can potentially operate at much higher frequencies, i.e., faster, than those based on ferromagnets. One major goal of our recent work is to find new ways to detecting and manipulating different antiferromagnetic orders.

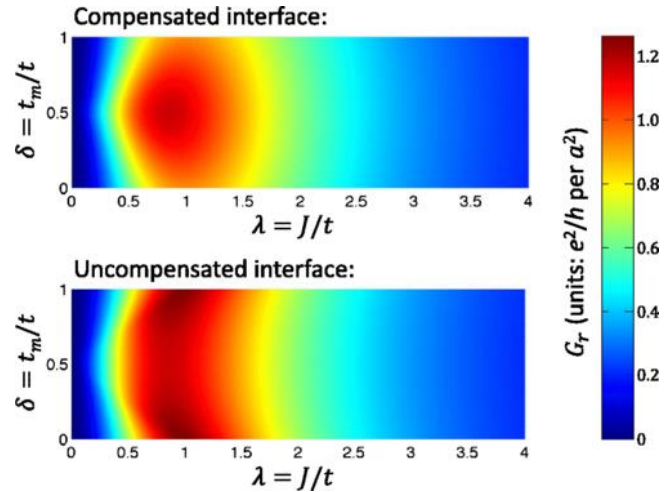
(a) Spin pumping and spin-transfer torques in antiferromagnets

Spin pumping and spin-transfer torques are key elements of coupled dynamics of magnetization and conduction electron spin, which have been widely studied in various ferromagnetic materials. Recent progress in spintronics suggests that a spin current can

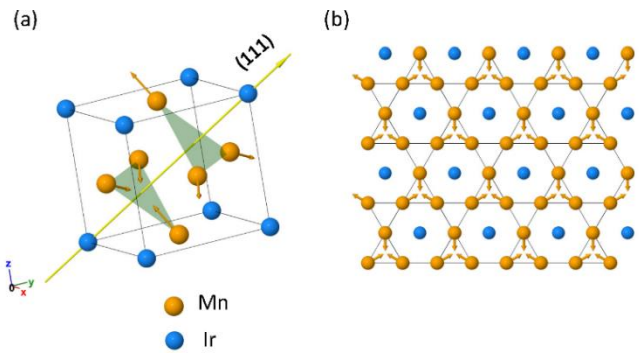
significantly affects the behavior of an antiferromagnetic material [1], and the electron motion becomes adiabatic when the staggered field varies sufficiently slowly [2]. However, pumping from antiferromagnets and its relation to current-induced torques is yet unclear. In a recent study, we have solved this puzzle analytically by calculating how electrons scatter off a normal metal-antiferromagnetic interface. The pumped spin and staggered spin currents are derived in terms of the staggered field, the magnetization, and their rates of change. We find that for both compensated and uncompensated interfaces, spin pumping is of a similar magnitude as in ferromagnets; the direction of spin pumping is controlled by the polarization of the driving microwave. Via the Onsager reciprocity relations, the current-induced torques are also derived, the salient feature of which is illustrated by a terahertz nano-oscillator.

(b) Anomalous Hall effect arising from noncollinear antiferromagnetism.

Shortly after Edwin Hall discovered the Hall effect, voltage perpendicular to current direction when conductors are exposed to a magnetic field, he discovered that a similar effect, now known as the anomalous Hall effect, occurs in ferromagnetic conductors that does not require a magnetic field and is often larger. Although the origin of the Hall effect, Lorentz forces on moving charges, was understood soon after the effect's discovery, our understanding of the anomalous Hall effect in terms of magnetic ordering and spin-orbit coupling started to take shape only after a half-century of progress in quantum physics and is still evolving [3]. Technologically, the importance of the anomalous Hall effect lies in that it provides a convenient way of detecting the order parameter direction of magnetic materials using electrical measurements. Conventionally the anomalous Hall effect was assumed to exist only in ferromagnets with a nonzero total magnetization. However, in a recent work we theoretically predicted that the anomalous Hall effect can exist in certain antiferromagnets with



Spin mixing conductance G_r as a function of λ and δ , standing for rescaled hopping and s - d type exchange coupling in the antiferromagnet, respectively, for compensated and uncompensated N/AF interfaces.



(a) The structure and noncollinear antiferromagnetic order of Mn_3Ir . (b) Single (111) layer of Mn_3Ir . The magnetic Mn atoms form a kagome lattice.

noncollinear magnetic order that is stable at room temperature, e.g. Mn₃Ir. This prediction has recently been verified experimentally in a closely related material Mn₃Sn [4]. As we pointed out above one major challenge of utilizing antiferromagnets in spintronic devices is the difficulty of detecting the order parameter direction. The anomalous Hall effect in antiferromagnets shown by this work can then be used as an effective indicator of antiferromagnetic order parameter directions and suggests great technological potential.

(c) Magneto-optical effects of noncollinear antiferromagnets

Magneto-optical Kerr effect (MOKE) refers to the change in the polarization of a linearly polarized light upon reflection by a material surface. MOKE is essentially determined by the off-diagonal optical conductivity, whose zero-frequency limit is just the Hall conductivity. Therefore MOKE is closely related to the anomalous Hall effect and is normally found in magnetic materials with nonzero magnetization such as ferromagnets and ferrimagnets. Using first-principles density functional theory, we demonstrated large magneto-optical Kerr effect in high-temperature noncollinear antiferromagnets Mn₃X(X=Rh,Ir,Pt), in contrast to conventional wisdom. The calculated Kerr rotation angles are large, being comparable to that of transition-metal magnets such as bcc Fe. The large Kerr rotation angles and ellipticities are found to originate from the lifting of band double degeneracy due to the absence of spatial symmetry in the Mn₃X noncollinear antiferromagnets which together with the time-reversal symmetry would preserve the Kramers theorem. Our results indicate that Mn₃X would provide a rare material platform for exploration of subtle magneto-optical phenomena in noncollinear magnetic materials without net magnetization.

Future Plans

We will continue to explore the interaction between the antiferromagnetic order parameters with external perturbations, aiming at effective detection and manipulation of antiferromagnetic orders. For example, orbital magnetization from itinerant electrons always goes side by side with the anomalous Hall effect. One can naturally expect that in noncollinear antiferromagnets with nonzero anomalous Hall effect, there will be accompanying orbital magnetization. Indeed, our preliminary first-principles calculations indicated that the orbital magnetization of the noncollinear antiferromagnet Mn₃Ir is much larger than the net spin magnetization due to canting. The orbital magnetization can thus serve as a handle for detecting and manipulating the noncollinear antiferromagnetic order through its coupling to magnetic fields.

Separately, since we now know that the anomalous Hall effect in certain noncollinear antiferromagnets can be used to read the magnetic configuration through electrical measurements, it would be very desirable if the antiferromagnetic order parameters can be switched between different directions by electric currents as well, so that one can have an all-electric reading and writing logic device based on antiferromagnets. We are currently studying

the current-induced spin-orbit torque in metallic noncollinear antiferromagnets such as Mn₃Sn, focusing on nontrivial differences between the noncollinear antiferromagnets and collinear antiferromagnets or ferromagnets. We are also interested in the possibility of generating self-oscillation through the current-induced spin-orbit torque.

References

1. R. Cheng and Q. Niu, *Dynamics of antiferromagnets driven by spin current*, Phys. Rev. B **89**, 081105(R) (2014).
2. R. Cheng and Q. Niu, *Electron dynamics in slowly varying antiferromagnetic texture*, Phys. Rev. B **86**, 245118 (2012).
3. N. Nagaosa, J. Sinova, S. Onoda, A. H. MacDonald, and N. P. Ong, *Anomalous Hall effect*, Rev. Mod. Phys. **82**, 1539 (2010).
4. S. Nakatsuji, N. Kiyohara, and T. Higo, *Large anomalous Hall effect in a non-collinear antiferromagnet at room temperature*, Nature **527**, 212-215 (2015).

Publications

Put the 2-year (August 2014 – July 2016) list of publications SUPPORTED BY BES here using Times New Roman 10 pt. If more than 10 publications, list only the 10 most relevant.

1. R. Cheng, J. Xiao, Q. Niu, and A. Brataas, *Spin Pumping and Spin-Transfer Torques in Antiferromagnets*, Phys. Rev. Lett. **113**, 057601 (2014).
2. H. Chen, Q. Niu, and A. H. MacDonald, *Anomalous Hall effect arising from noncollinear antiferromagnetism*, Phys. Rev. Lett. **112**, 017205 (2014).
3. W. Feng, G.-Y. Guo, J. Zhou, Y. Yao, and Q. Niu, *Large magneto-optical Kerr effect in noncollinear antiferromagnets Mn₃X (X=Rh, Ir, Pt)*, Phys. Rev. B **92**, 144426 (2015).
4. "Enhanced spin Seebeck effect signal due to spin-momentum locked topological surface states", Jiang, Zilong; Chang, Cui-Zu, Masir, Massoud R; Tang, Chi; Xu, Yadong; Moodera, Jagadeesh S., MacDonald, Allan H.; Shi, Jing, Nat. Comm. **7** (May 2016).
5. "SU(3) Quantum Hall Ferromagnetism in SnTe", Li, Xiao; Zhang, Fan; MacDonald, Allan H., Phys. Rev. Lett. **116**, 026803 (Jan 2016).
6. "SU(3) and SU(4) singlet quantum Hall states at n=2/3", Wu, Fengcheng; Sodemann, Inti; MacDonald, Allan H.; Jolicoeur, Thierry, Phys. Rev. Lett. **115**, 166805 (Oct 2015).
7. "Spontaneous layer-pseudospin domain walls in bilayer graphene", Li, Xiao; Zhang, Fan; Niu, Qian; MacDonald, Allan H., Phys. Rev. Lett. **113**, 116803 (Sept 2014).
8. "Origin of band gaps in graphene on hexagonal boron nitride", Jung, Jeil; DaSilva, Ashley M; MacDonald, Allan H; Adam, Shaffique, Nat. Comm. **6**, 6308 (Feb 2015).
9. "Valley contrasting chiral phonons in monolayer hexagonal lattices", Zhang, Lifa; Niu, Qian, Phys. Rev. Lett. **115**, 115502, (Feb 2015).
10. "Quantum Anomalous Hall Effect in Graphene Proximity Coupled to an Antiferromagnetic Insulator", Qiao, Zhenhua; Ren, Wei; Chen, Hua; Bellaiche, L.; Zhang, Zhenyu; MacDonald, Allan H.; Niu, Qian; Phys. Rev. Lett. **112**, 116404 (Jan 2015).

Structure and Electronic Properties of Dirac Materials

Principal investigator: Eugene Mele

Department of Physics and Astronomy, University of Pennsylvania, Philadelphia PA 19104

mele@physics.upenn.edu

Project Scope

The field of van der Waals heterostructures is driven by the idea that the electronic behavior of a stack of two dimensional materials can be exquisitely sensitive to their layer-layer interactions at the atomic level. This concept has been demonstrated in proof-of-principle experiments on graphene-derived materials and related systems. These successes highlight a fundamental challenge: atomic level sensitivity necessitates atomic level control of interfaces that support a desired functionality. This is inevitably complicated by strain, bend and orientational epitaxy of two deformable lattices. Our research project seeks to understand how electronic physics in single- and few-layer two dimensional forms of matter is controlled by topological lattice defects in the former and by stacking order in the latter. Using single layer graphene as the prototype we study lateral confinement of electronic states on grain boundaries and at topological structures that are designed to deflect an atomically thin two dimensional material into the third dimension. In multilayer graphenes we study the electronic signatures of uniform and nonuniform stacking patterns. Here layer-layer interactions are used to tune the low energy semimetallic properties by producing laterally confined transport channels and in some cases by inducing optical anisotropies that are impossible in strictly two dimensional forms of matter.

Highlights

1. Topological defects in single-layer graphene

(a) *Topological states and transport signatures in single layer graphene* [ref 1]

Electronic states confined to zero-angle grain boundaries in single-layer graphene are analyzed using topological band theoretic arguments. These boundaries embed odd-membered rings of bonds in the covalent network which lifts the two sublattice (chiral) symmetry usually associated with the appearance of topological states at the charge neutrality point. Nonetheless we find that robust zero modes occur in the projected bulk gaps of these structures and we provide a topological analysis of the symmetries that protect them. These features are studied by numerical calculations on a tight-binding lattice and by analysis of the geometric phases in the k-projected bulk ground states.

(b) *Bend versus stretch in graphene kirigami* [ref 2]

The three-dimensional shapes of graphene sheets produced by nanoscale cut-and-join kirigami are studied by combining large-scale atomistic simulations with continuum elastic modeling. Lattice segments are selectively removed from a graphene sheet, and the structure is allowed to close by relaxing in the third dimension. Although this material is known to be very stiff with respect to in-plane strains we find that the relaxed structures are quantitatively understood as shapes optimize their bending energies. This generically

produces smoothly modulated landscapes in contrast to the sharp ridge-and-plateau motif encountered in macroscopic lattice kirigami. The microscopic basis for this unexpected result was identified. The surface shapes and their interactions are well described by a new set of microscopic kirigami rules that resolve the competition between bending and stretching energies at the nanoscale and for the case of graphene provide a new route to controllably writing strain patterns that can ultimately couple shape to electronic motion.

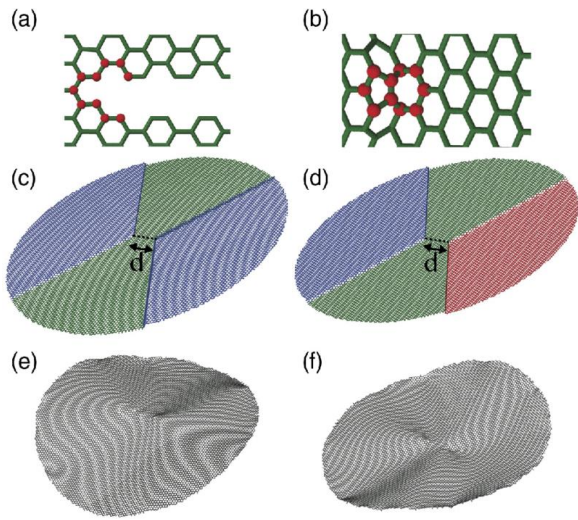


Figure 1 Kirigami on a honeycomb lattice is generated by removing a strip of atoms and reconnecting the undercoordinated sites to generate a pair of compensating dislocations at the terminations of the “branch cut”. This reconstructed network relaxes by a vertical deflection into the third dimension. An inextensible medium (c-d) does not allow any in plane strain so the reconstruction is a ridge and plateau motif where all the Gaussian curvature is confined within its dislocation cores. Graphene is also very in-plane stiff, but its relaxed structures (e-f) smoothly distribute the Gaussian curvature so as to minimize the bending energy at the expense of incurring some nonzero strain energy.

2. Stacking walls and textures in graphene bilayers

(a) Confined modes at AB/BA domain walls in bilayer graphene [ref 3]

Electronic states confined at domain walls in electrostatically gapped bilayer graphene are studied by analyzing their four-and two-band continuum models, by performing numerical calculations on the lattice, and by using quantum geometric arguments. The continuum theories reveal distinct electronic properties of boundary modes localized near domain walls produced by interlayer electric field reversal, by interlayer stacking reversal, and by simultaneous reversal of both quantities. Interfacial modes are associated with topological transitions and gap closures in the bulk Hamiltonian parameter space. The important role played by intervalley coupling effects not directly captured by the continuum model is studied using lattice calculations for specific domain wall structures.

(b) Stacking textures in bilayer graphene [ref 4]

We study a family of spatially varying strain-optimized two-dimensional stacking textures in bilayer graphene. We find that stacking patterns that minimize the strain energy and smoothly connect inequivalent ground states with local AB and BA interlayer registries are composed of primitive two-dimensional twisted textures of the interlayer displacement field. These textures are obtained by matching complex-analytic and anti-analytic representations of the two dimensional displacement field on a boundary line. We construct and display these strain optimized stacking textures for bilayer graphene, examine their interactions, and explicitly develop the composition rules for these elementary defects that provide a unified description of more complex stacking textures, including globally twisted graphenes and extended one-dimensional domain walls.

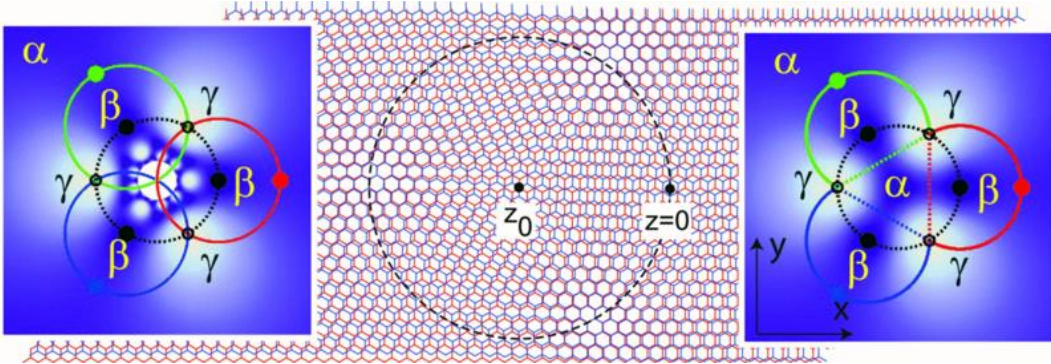


Figure 2 Illustration of a nontrivial strain-optimized stacking texture in bilayer graphene. The wire frame rendering (center) shows the lattice structure as the two layers evolve from local BA stacking (β) at $z=x+iy=0$ to AB stacking (α) in the far field. The strain-minimized structure is derived by matching a representation of the exterior displacement field as a complex-antianalytic function to an interior complex-analytic function on the dashed boundary. This solution realizes every possible local stacking configuration somewhere in the texture, e.g. the highest energy AA stacked structure occurs at three vertices (γ) on the matching boundary. The colored lines map the trajectories of three distinct domain walls that isolate local α and β stacked regions. The density plot on the right gives the potential energy density of the local stacking configuration.

3. Three dimensional topological semimetals

(a) *Three dimensional Dirac semimetals in nonsymmorphic crystal lattices* [ref 5,6]

We show that pseudorelativistic physics of electrons at a Fermi point described by a massless Dirac equation can be realized in three dimensional (3D) materials. Unlike the situation for massless Weyl fermions which require either a T- or P- broken state matter, these new Dirac systems are both T- and P- invariant and support fourfold rather than twofold point degeneracies at the Fermi energy. The Dirac point can be understood as the merger of two Weyl points of opposite handedness where their annihilation is prevented by the space group symmetry of the medium. We provide criteria necessary to identify space groups that protect this behavior and, as an example, present density functional calculations of β -cristobalite BiO_2 which exhibits well developed Dirac singularities at its Fermi points[5]. This type of singularity is a robust symmetry-enforced property as it cannot be removed without changing the space group of the medium. This can be contrasted with the weaker situation where an accidental band crossing can occur near a band inversion, protected by axial rotational symmetry but removable by a continuous evolution to the band uninverted state.

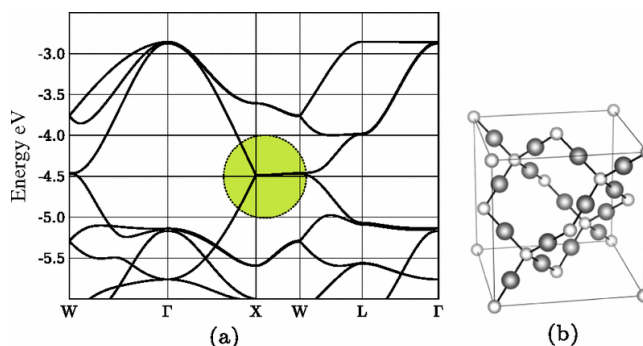


Figure 3 Demonstration of a predicted material realization of a three dimensional Dirac semimetal (DSM). BiO_2 in the β cystobalite structure (b) occurs in an nonsymmorphic space group (227) that hosts four dimensional irreducible representations in its double groups at the X-points. This represents a fourfold point degeneracy in a T- and P- invariant crystal that is lifted linearly in momentum in all directions around the Dirac point [1]. Similar behavior in the related space group 74 predicted in a family of distorted spinels [6].

Project Plans

Boundary modes from curvature and strain

Our work on the role of lattice stretch and strain in graphene kirigami (Section 2b) provides a strategy for using Gaussian curvature to produce strain patterns on demand in single layer graphene. Strain couples to electronic motion through a valley-antisymmetric gauge field and there has been progress in identifying the special nonuniform strain pattern that provides a proxy for a uniform (albeit enormously strong) pseudomagnetic field. However strain-induced *nonuniform* pseudofields are more generic and potentially much more useful. In particular pseudofield patterns that embed *sign changes* can host topologically protected transport channels on their interior nodal lines. We are developing structural models for these patterns, exploring how they can be realized by kirigami, and carrying out numerical simulations of ballistic transport along these topological networks.

Proximitized chirality and magnetoelectric response

Weak coupling between proximitized two dimensional materials can break lattice symmetries and induce new physical effects. We are inspired by the recent experimental observation ("Chiral Atomically Thin Films" Nature Nanotechnology 11, 520–524 (2016)) showing that a twisted graphene bilayer (t-BLG) is a chiral medium that supports circular dichroism (CD), i.e. differential absorption of right- and left- handed circularly polarized light. This requires a dynamic magnetoelectric susceptibility, an intrinsically 3D response that is forbidden by symmetry in single layer graphene and indeed in any stacked variant that retains mirror symmetries. We have discovered that some (though not all) linear AB/BA domain walls can support this physics *localized in the wall* giving perhaps the simplest illustration of the effect and possibly even clarifying the mechanism for CD in t-BLG. We are exploring this through theory and computation of the frequency dependent magnetoelectric coupling in domain walls and in topological semimetals.

Plasmon propagation and scattering in two dimensional electronic materials

Domain walls and grain boundaries in two dimensional electronic materials can host 1D charge modes that produce significant changes of the local conductivity even if the underlying structural change is small. We are investigating the dynamics of plasmon scattering from these so called "electronic boundaries" in the context of deep subwavelength optics in a family of two dimensional materials.

Publications

- [1] M. Phillips and E.J. Mele "Zero Modes on Zero Angle Grain Boundaries in Graphene" Physical Review B 91, 125404 (2015)
- [2] Bastien F.Grosso and E.J. Mele "Bending Rules in Graphene Kirigami" Physical Review Letters 115, 19550 (2015)
- [3] Fan Zhang, A.H. MacDonald and E.J. Mele "Valley Chern numbers and boundary modes in gapped bilayer graphene" Proc. Nat. Acad. Sci. 110 10546 (2013).
- [4] X. Gong and E.J. Mele "Stacking textures and singularities in bilayer graphene" Physical Review B 89, 121415 (2014).
- [5] S.M. Young, S. Zaheer, J.C.Y. Teo, C.L. Kane, E.J. Mele, and A.M. Rappe "Dirac Semimetal in Three Dimensions" Phys. Rev. Lett. 108, 140405 (2012)
- [6] J.A. Steinberg, S.M. Young, S. Zaheer, C.L. Kane, E.J. Mele and A.M. Rappe "Bulk Dirac Points in Distorted Spinels" Phys. Rev. Lett. 112, 036403 (2014)

Surface and Interface Physics of Correlated Electron Systems

A. J. Millis , Department of Physics, Columbia University
ajm2010@columbia.edu

Project Scope: Our group develops and applies new theoretical methods for the grand-challenge problem of understanding and controlling the behavior of materials with strongly correlated electron properties. The ultimate aim is to design structures that give rise to new (or enhanced versions of known) behavior. Reaching this goal requires development and benchmarking of new theoretical methods and applying existing methods to predict materials properties and to determine the effectiveness of different modalities of control of many body properties. In the area of methods development our main effort is creating, implementing and benchmarking new methods for solving the equations of dynamical mean field theory, which is by now the method of choice for combining physical and chemical realism with the quantum mechanics of strongly correlated electrons. In applications we focus on geometric and electrostatic control: situations such as surfaces, interfaces and epitaxially strained films where the local electronic structure and charge balance can be controlled. We have predicted new quantum states of matter created by heterostructuring, have shown that our methods predict nontrivial properties in detail, and have begun to study the defects that complicate the behavior of quantum-designed structures.

Recent Research Highlights:

Methods development: The dynamical mean field methodology provides an approximation to the NP-hard quantum many-body problem in terms of the solution of a simpler problem (a ‘quantum impurity model’) plus a self-consistency condition. Although simpler than the full infinite system quantum many-body problem, quantum impurity models are still true interacting quantum models and are formidably difficult to solve. The continuous-time quantum Monte Carlo method, which the PI helped develop, solves the problem for situations such as the one-band Hubbard model which possess a high degrees of point

symmetry and/or a simple interaction structure, but is inadequate for the many physically relevant cases where multiple orbitals and low point symmetry lead to severe sign problems. An alternative is the exact diagonalization method, which approximates the continuous bath of the impurity model by a finite number of states. Heretofore the exponential growth of Hilbert space with system size means that exact diagonalization method has been limited to models with no more than 12 sites, meaning that in a problem with 4 correlated orbitals the bath would be approximated by two bath orbitals per correlated orbital. **Ara Go**, an

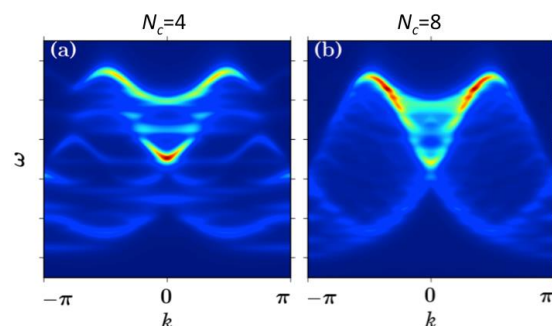


Figure 1: Spectral function of one dimensional Hubbard model computed via cluster dynamical mean field methodology using new exact diagonalization methodology with 4 and 8 correlated orbitals, revealing spinon and holon bands in agreement with exact results

outstanding postdoc supported by the grant, has developed a new exact diagonalization-based solver that uses active space and dynamically adjustable basis ideas from quantum chemistry to exploit the nontrivial Hilbert-space sparsity structure of impurity models (interactions only on a small subset of sites). Developing an appropriate active space for the excited state manifold needed for Greens function calculation was particularly challenging, but now we can now easily study much larger systems 40-50 orbitals including up to 8 correlated orbitals and 4-5 bath sites per correlated orbital, qualitatively improving the capabilities of the method and in particular enabling studies of the full d manifold in low symmetry situations, enabling treatment of challenge problems including Co on graphene or Cu 111 surface, orbitally degenerate situations with strong spin-orbit coupling (ruthenates, irridates, osmates etc) and corrections to the single-site DMFT approximation for nickelates, titanates, vanadates and other important materials. We have benchmarked the method on the one dimensional Hubbard model (see Figure 1). The algorithm and benchmarking are now being prepared for publication and the method is being applied to pyrochlore irridates and other systems where strong spin-orbit coupling leads to a severe sign problem. We are also collaborating with other groups to develop new methods based on matrix product methods (ref 6 below and in press, collaboration with Schollwoeck) and hybrid quantum computing (Troyer, Bauer; Phys Rev X in press 2016).

We have also conducted extensive studies of the formal structure of the DFT+DMFT methodology including the key issue of the choice of underlying DFT functional and have benchmarked the method on key model systems (refs 4,5,9).

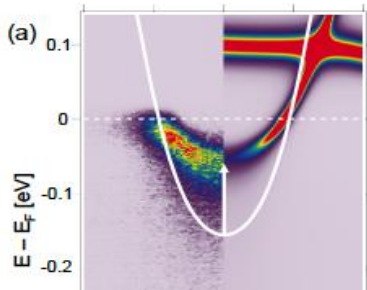


Figure 2 Experiment (left half) and DFT+DMFT theory (right half) for electron dispersion in LaNiO_3 . Band theory shown as white line. From Ref. 7

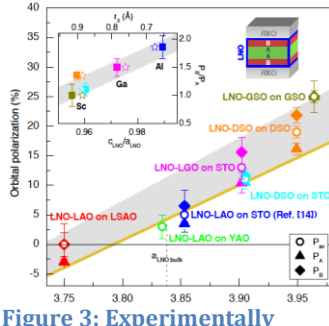


Figure 3: Experimentally determined orbital polarization of Ni sites in strained LaNiO_3 superlattices, from Wu et al PRB 88 125254.

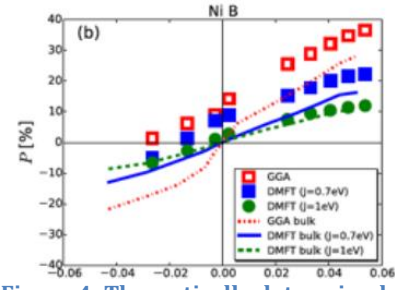


Figure 4: Theoretically determined orbital polarization of LaNiO_3 based superlattices, from DFT+DMFT calculations (blue and green symbols) and band theory, compared to strained bulk materials

Theory-Experiment collaboration. With the Schlom and Shen groups (Cornell, not funded by this project) and E. Nowadnick (funded by the grant in prior years) we completed a significant study of the accuracy of the DFT+DMFT method for predicting the many-body electronic structure of a non-trivial material. We showed that with proper attention to the double counting correction the method quantitatively predicts the electron dispersion (Fig 2) and the orbital polarization in observed (Fig 3) in nickelate superlattices (fig 4). The results give new insights into the effectiveness of the different mechanisms for controlling electronic properties, including strain, octahedral rotations and charge transfer.

Materials Prediction. As discussed previously, we predicted that a superlattice consisting of alternating layers of LaNiO₃ (metal) and LaTiO₃ (Mott Insulator) would become completely insulating, due to a large charge transfer from the Ni to the Ti sites (ref 1). Our predictions, both the insulating nature and the charge transfer, have now been verified by Cao and Chakhalian (Nature Communications 7 10418 (2016)).

With a student, Z. He, initially supported by the grant, we have shown how epitaxial strain in thin films can be used to control electronic phase behavior using as an example the rare earth nickelates (ref 3). We predict that appropriate choice of substrate can induce Jan-Teller order not observed in bulk materials.

We have also obtained first results on the use of superlattices to design novel ferroelectrics and multiferroics, with band gaps in technologically useful regimes. In this work analysis of the different density functionals was crucial (ref 9). This work will continue.

Planned Research:

New Impurity Solvers: we will exploit Ara Go's newly developed impurity solver and the solver under development with the Schollwoeck group to obtain many body phase diagrams and spectra for materials with strong spin-orbit coupling and for beyond single-site DMFT physics of layered materials. Anticipated significant results include the first controlled cluster DMFT studies of layered vanadates and ruthenates, providing a crucial test of the validity of the single-site DMFT approximation to realistic multiorbital systems with strong Hunds coupling and new insights into the regimes where topologically nontrivial phases may occur in iridates and related systems. We will also obtain the first controlled estimates of the dynamical scales associated with nontrivial multiorbital impurity models, in particular Co on Cu 111 and on graphene.

Novel ferroelectrics and multiferroics. The classic ferroelectrics rely on a structural instability associated with an empty d-shell (e.g. the Ti in BaTiO₃). We have realized that the strong Hunds coupling associated with transition metal d-shell means that a half-filled d-shell or half-filled t_{2g} subshell will may have a similar structural instability, accompanied by the magnetic properties of the high-spin d state, thus, a multiferroic. Charge transfer in superlattices can lead to many new realizations of this physics and the variety possible materials means that it may be possible to design systems with band-gaps in the solar range or other desirable properties.

Lattice effects and the metal-insulator transition. In very recent work (stimulated by interaction with the Schlom experimental group at Cornell) we have realized that the combination of orbital ordering and volume change associated with most Mott metal-insulator transitions has remarkable consequences for epitaxial films and superlattices. The pinning of the in-plane lattice parameters by the epitaxial constrain means that in general a material cannot satisfy both the volume and octrahedral distortion constraints associated with metal-insulator transitions, so transitions observed in bulk can be strongly

suppressed or strongly enhanced by appropriate epitaxy. We will develop a general theory of this effect and apply it to design systems with controlled metal-insulator transitions.

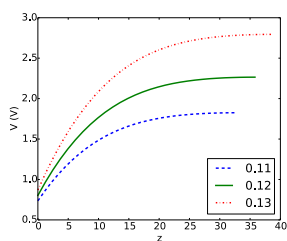


Figure 5: Potential profile of depletion layer of SrTiO_3 due for values $Q=0.11, 0.12, 0.13$ of charge transfer to FeSe monolayer, showing robust doping of FeSe independent of details, from Ref 10

Monlayer FeSe : One of the most exciting recent discoveries is the finding of very high transition temperature superconductivity in monolayer films of FeSe grown on SrTiO_3 and other substrates. Experimentally a key issue is the electron-doping level. A strong coupling from dipole active substrate phonons has been proposed. Building on our recent Schottky theory of the doping of these materials we will develop a theory of dipolar phonon superconductivity and investigate other physical effects in these important materials

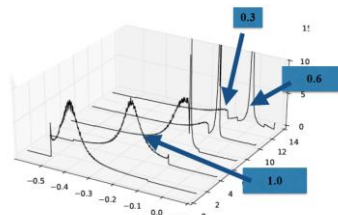


Figure 6: Electron spectral function of FeSe computed from theory of dipolar substrate phonons

Publications

1. "Engineering Correlation Effects via Artificially Designed Oxide Superlattices", Hanghui Chen, Andrew J. Millis, and Chris A. Marianetti, PRL **111**, 116403 (2013).
2. "Charge transfer across transition metal oxide interfaces: emergent conductance and new electronic structure", Hanghui Chen, Hyowon Park, Andrew J. Millis, Chris A. Marianetti, Phys. Rev. **B90**, 245138 (2014).
3. "Strain Control of Electronic Phase in Rare Earth Nickelates", Zhuoran He and Andrew J. Millis, Phys. Rev. **B91**, 195138 (2015).
4. "Density functional plus dynamical mean-field theory of the spin-crossover molecule $\text{Fe}(\text{phen})_2(\text{NCS})_2$ ", Jia Chen, C. Marianetti and A. J. Millis, PR **B91** 241111 (2015).
5. "Density functional versus spin-density functional and the choice of correlated subspace in multivariable effective action theories of electronic structure", Hyowon Park, Andrew J. Millis, and Chris A. Marianetti, Phys. Rev. **B92** 035146 (2015).
6. "Imaginary-time matrix product state impurity solver for dynamical mean-field theory", F. Alexander Wolf, Ara Go, Ian P. McCulloch, Andrew J. Millis, Ulrich Schollwoeck, Phys. Rev. **X5**, 041032 (2015)
7. "Quantifying electronic correlation strength in a complex oxide: a combined DMFT and ARPES study of $\text{LaNiO}_{3.3}$ ", E. A. Nowadnick, J. P. Ruf, H. Park, P. D. C. King, D. G. Schlom, K. M. Shen, A. J. Millis, Phys. Rev. **B92**, 245109 (2015).
8. "Antisite defects at oxide interfaces", Hanghui Chen and Andrew Millis, PR **B93**, 104111 (2016).
9. "Comparative study of exchange-correlation functionals for accurate predictions of structural and magnetic properties of multiferroic oxides", Hanghui Chen and A. J. Millis, Phys. Rev. **B93**, 205110 (2016).
10. Y Zhou and A. J. Millis, Phys. Rev. **B93**, 224506(2016)

Optical, transport phenomena, and interaction effects in novel low-dimensional electron systems

Principal Investigator: Dr. Eugene Mishchenko

Department of Physics, University of Utah

Salt Lake City, UT 84112

mishch@physics.utah.edu

Project scope

Progress of modern day condensed matter physics is to a large extent ensured by the synthesis of new materials. In particular, of special interest are those materials that support chiral electron states, i.e. the states whose properties depend on the direction of electron propagation. Such states exist in a variety of practical realizations: conventional two-dimensional electron gas with spin-orbit interaction, Dirac fermions in graphene and topological insulators, metallic carbon nanotubes, direct-gap semiconducting (such as MoS₂) monolayers, Weyl semimetals. Within this research project we investigate physics of such chiral electron systems. Through a variety of specific problems concerning transport, optical phenomena, and many-body effects, we try to accomplish our main objective, to look for features common to various chiral systems.

Among particular projects addressed are: i) theory of excitons and depolarization effect in metallic carbon nanotubes with the account for the Luttinger liquid dynamics, ii) interaction corrections to the ac conductivity of graphene, iii) possibility of existence of non-RPA polarization waves, iv) resonant impurity-induced states in mono- and bilayer graphene, the latter of particular interest for applications due to the possibility of being gate-controlled, v) collective excitations in various chiral electron systems, vi) optical response of many-body systems, vii) effective interaction (including spin coupling) of impurities on graphene. This project relies significantly upon our previous broad expertise in spin-polarized transport, and many-body effects in low-dimensional systems, both 2D and 1D. The methods to be employed include diagrammatic technique, Luttinger liquid theory, self-consistent approximations, hydrodynamics of electron liquid, DFT calculations. Both analytical as well as numerical approaches are utilized. In particular, to study the depolarization effect in nanotubes we combine the conventional diagrammatic technique with the methods of bosonization, as each method is not sufficient on its own. Another example involves resonant adatoms in graphene known to be strong and attractive: its renormalization due to electron-electron interaction is expected to be so significant as to even reverse the very sign of the coupling. Numerical methods are used to help determine induced charges in the host layer, together with the method of self-consistent non-linear screening. A new research direction is the investigation of the effective indirect spin coupling between adatoms (such as hydrogen) deposited on graphene, as a function of both the strength of the potential (non-spin) coupling of such adatoms with the carbon lattice of the graphene host, as well as the geometry of the adatom configuration. In particular, we study the sensitivity of such indirect spin exchange to the positions of adatoms on the same vs. opposite carbon sublattices.

Recent progress

Suppression of diffusion of hydrogen adatoms on graphene by effective adatom interaction

Diffusion of hydrogen on graphene is a problem of major interest for a number of applications. Hydrogen adatoms are believed to be resonant graphene dopants. Consequently, they have been shown (by us, as well as by other investigators) to experience long-range effective interaction with other adatoms, mediated by the conduction electrons. We have shown that such interaction has a profound effect on the mobility of adatoms. The most prominent feature of this long-range interaction is its sign reversal when the two adatoms reside on opposite sublattices compared with the same-sublattice occupancy. As a result of this interaction, when several adatoms are present in the sample, hopping of adatoms between sites belonging to different sublattices involves significant energy changes. Different inelastic mechanisms facilitating such hopping – coupling to phonons and conduction electrons – have also been considered. It was estimated that the diffusion of hydrogen adatoms is rather slow, amounting to roughly one hop to a nearest neighbor per millisecond. In arriving at this result we have used a variety of theoretical techniques: 1) the non-perturbative treatment of the effective strong hydrogen-electron coupling, 2) the Golden Rule-type calculations of the inelastic hopping of hydrogen adatoms mediated by flexural phonons and conduction electrons of graphene, 3) DFT calculations of the potential barrier for hydrogen atom hopping between nearest neighbor carbon atoms, see Fig. 1.

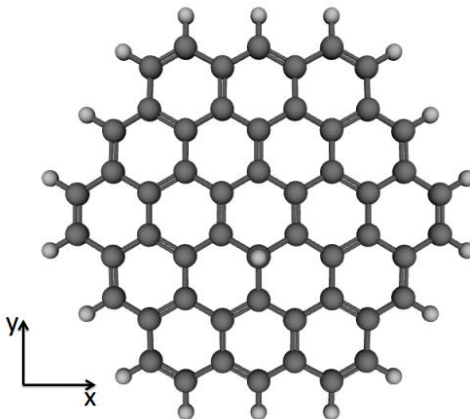


FIG. 1. Hydrogenated circumcoronene $C_{54}H_{18} + H$ is a system amenable to DFT calculations of the potential barrier for hydrogen adatom hopping between different carbon sites of graphene.

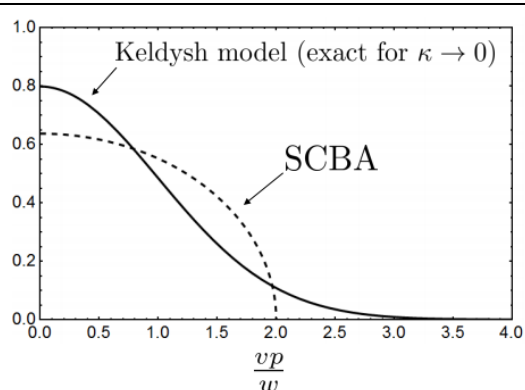


Fig. 2: Full spectral weight at zero energy in the limit of infinite correlation radius of disorder ($\kappa \rightarrow 0$). Solid line - Keldysh model, dashed line - SCBA with full disorder correlator.

Weyl semimetals with long-range disorder: density of states and magnetotransport

We have studied the density of states and magnetotransport properties of disordered Weyl semimetals, focusing on the case of a strong long-range disorder. To calculate the disorder-averaged density of states close to nodal points, we treated exactly the long-range random potential fluctuations produced by charged impurities (the so-called Keldysh model), while the short-range component of disorder potential is included systematically and controllably with the help of a diagram technique. We found that for energies close to the degeneracy point, long-range potential fluctuations lead to a finite density of states, see

Fig. 2. In the context of transport, we discussed that a self-consistent theory of screening in magnetic field may conceivably lead to non-monotonic low-field magnetoresistance.

Plasmonics: plasmons and plasmon-mediated energy transfer in multi-connected geometries

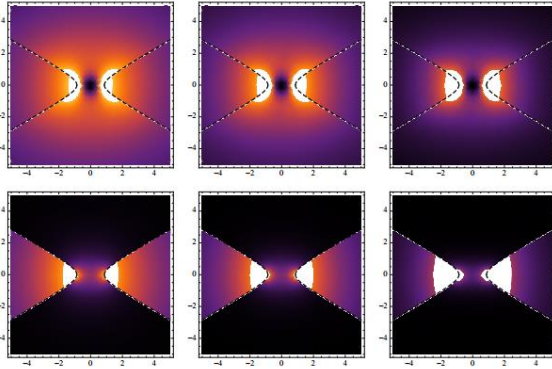


Fig. 3: Density plot of the field intensity of the plasmon modes in the geometry of two symmetric hyperbolic wedges. The upper row corresponds to symmetric modes with progressively (from left to right) decreasing wavelength. While the fields of individual hyperbolas are disconnected along the x-axis, they overlap along the y-axis. The lower row corresponds to antisymmetric modes. The field of individual hyperbolas overlap, predominantly, along the y-axis.

The two central issues of the contemporary plasmonics are manipulation and focusing of light on subwavelength scales, and plasmon-mediated energy transfer.

We have developed a theory of surface plasmon spectra of a single and double metallic hyperbola. The spectrum consists of two branches: symmetric, low-frequency branch, and antisymmetric high-frequency branch. The frequency width of the plasmon band increases with decreasing the angle between the asymptotes of the hyperbola. For the simplest multi-connected geometry of two hyperbolas separated by an air spacer the plasmon spectrum contains two low-frequency branches and two high-frequency branches, see Fig. 3. Most remarkably, the lower of two low-frequency branches exists at $\omega \rightarrow 0$. We have studied how the complex structure of the plasmon spectrum affects the energy transfer between two emitters located on the surface of the same hyperbola and on the surfaces of different hyperbolas.

Planned activities (2016-2017)

- 1) *Retardation effects in hyperbolic structures.* We will continue our work on the properties and transport of plasmons in single- and multi-connected structures. In particular, we are interested in calculating the transmission and reflection rates of plasmons propagating along the surfaces of hyperbolic metallic wedges. In our recent work we have studied plasmon properties in a double-wedge geometry in the electrostatics approximation while neglecting the retardation effects. That approach suffered from a number of limitations. Most importantly, dispersionless character of a (electrostatics) surface plasmon makes the problem of scattering ill defined. In particular, such plasmons lack group velocity and associated with it energy flux. At present we are working on the plasmon scattering problem with the effects of retardation taken into account. Since Maxwell's equations do not admit separation of variables in the elliptic/hyperbolic coordinates, approximate solutions are being sought within the WKB approach. The second question we are trying to address is the amount of radiative losses that such plasmon scattering entails.

2) *Electron-mediated effective spin interaction in graphene.* In our previous works we developed a theory of long-range coupling between strong potential impurities or adatoms on graphene lattice and applied it to phonon-assisted transport of adatoms on graphene. Of particular importance was the fact that the interaction is strongly sensitive to whether the two adatoms resided on the same or different carbon sublattices. We now begin extending our approach to electron-mediated interaction of impurities that have localized spins. We plan to develop a theory that determines the sign of the effective spin-spin super-exchange coupling depending on the strength of the potential part of the adatom-electron coupling. In particular, we are interested in determining the type of magnetic structures (ferro- or anti-ferromagnetic ordering) should be expected under various conditions.

Publications

1. J. Talbot, S. LeBohec, E. G. Mishchenko, *Suppression of diffusion of hydrogen adatoms on graphene by effective adatom interaction*, Phys. Rev. B **93**, 115402 (2016).
2. L. Shan, E. G. Mishchenko, M. E. Raikh, *Plasmon spectrum and plasmon-mediated energy transfer in a multi-connected geometry*, Phys. Rev. B **93**, 085435 (2016).
3. D. A. Pesin, E. G. Mishchenko, A. Levchenko, *Density of states and magnetotransport in Weyl semimetals with long-range disorder*, Phys. Rev. B **92**, 174202 (2015).
4. R. C. Roundy, M. C. Prestgard, A. Tiwari, E. G. Mishchenko, and M. E. Raikh, *Manifestation of two-channel nonlocal spin transport in the shapes of Hanle curves*, Phys. Rev. B **90**, 115206 (2014).
5. E. G. Mishchenko and O. A. Starykh, *Equilibrium currents in chiral systems with nonzero Chern number*, Phys. Rev. B **90**, 035114 (2014).
6. S. LeBohec, J. Talbot, and E. G. Mishchenko, *Attraction-repulsion transition in the interaction of adatoms and vacancies in graphene*, Phys. Rev. B **89**, 045433 (2014).
7. E.G. Mishchenko, *Dipole-induced localized plasmon modes and resonant surface plasmon scattering*, Phys. Rev. B **88**, 115436 (2013).

Variable spins in electronic structure quantum Monte Carlo and the fixed-phase approximation

Principal investigator: Lubos Mitas

Department of Physics, North Carolina State University, Raleigh, NC 27695-8202

lmitas@ncsu.edu

Project Scope:

The key goal of the project is to expand applicability of quantum Monte Carlo (QMC) methods in real space for many-body electronic structure calculations of strongly correlated quantum systems. The focus is on two important aspects: studies of fixed-node errors in simple metallic systems and treating electronic spins as quantum variables [1-7]. We briefly sketch the progress for the variable spins in QMC that we have achieved very recently [3-5].

Recent Progress:

Electronic structure quantum Monte Carlo (QMC) calculations are routinely done with particle spins being assigned as fixed labels, up or down. Since spins commute with Hamiltonians without explicit spin terms, the problem simplifies to spatial-only solution of the stationary Schrodinger equation. We have succeeded in overcoming this limitation and our new approach [4,5] represents, for the first time, an independent method that is able to recover $\sim 95\%$ of the correlations with explicitly many-body, spinor-based, wave functions that directly compares with traditional basis set approaches such as Configuration Interaction, while it is applicable to significantly larger systems. In the following we briefly describe the key aspects of this new method that is further elaborated in Refs. [4,5].

Fixed-phase and fixed-node methods. Let us first consider a many-electron Hamiltonian $H = T + V$, where V denotes electronic, ionic (local) and possibly other interactions while T is the total kinetic energy. When the desired eigenstate is real the stochastic methods of solutions are well-known and are mostly based on the familiar fixed-node approximation as have been described in many QMC reviews. This time, our focus is on cases with inherently complex wave functions so that we write any eigenstate as $\Psi = \rho \exp(i\Phi)$, where $\rho(\mathbf{R}) \geq 0$ is a non-negative amplitude and $\Phi(\mathbf{R})$ is a phase. Here by $\mathbf{R} = (\mathbf{r}_1, \dots, \mathbf{r}_N)$ we denote a set of spatial coordinates of N fermionic particles. If we substitute Ψ into the imaginary-time Schrödinger equation we get the following real and imaginary components

$$-\partial_\tau \rho = \left[T + V + \frac{1}{2} (\nabla \Phi)^2 \right] \rho$$

and

$$-\partial_\tau \Phi = [T\Phi - \rho^{-1} \nabla \rho \cdot \nabla \Phi]$$

The imaginary part describes a conservation of the phase flow. The real part is the relation that provides the eigenvalue, ie, its solution converges to the desired eigenstate amplitude in the limit $\lim_{\tau \rightarrow \infty} \rho(\tau)$.

The generalization of the fixed-node for the complex wave functions is the so-called fixed-phase approximation. This is given by replacing the exact phase by the trial phase $\phi \rightarrow \phi_T$ where the trial function is written as $\Psi_T = \rho_T \exp(i\Phi_T)$. The fixed-phase and fixed-node methods are

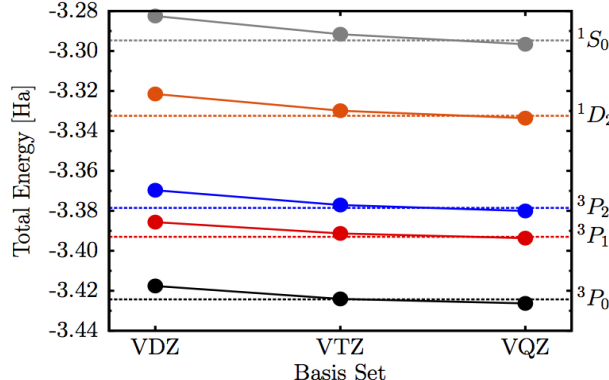
closely related. In particular, the fixed-node is the special case of the fixed-phase as has been shown before (see for example, Refs. [3,4] and references therein). In general, they also provide similar accuracy in most cases as our very recent study shows [3]. Note that the fixed-node is variational for arbitrary non-negative and symmetric amplitude $\rho(\mathbf{R})$. The fixed-phase method is actually commonly used by QMC practitioners in another setting, for example, in sampling the Brillouin zone of periodic systems by twist-averaging.

The treatment of spins as quantum variables in QMC is done in two-component spinor formalism. The determinantal part of the wave function is written as an antisymmetric product of one-particle spinors that are given as

$$\chi(r, s) = \phi^\uparrow(r)\chi^\uparrow(s) + \phi^\downarrow(r)\chi^\downarrow(s)$$

where $\chi^{\uparrow,\downarrow}(s)$ are corresponding spin functions. The spin s is treated as continuous (periodic) variable in the interval $(0, 2\pi)$ and the spin functions are chosen as $\chi^\uparrow(s) = \exp(+is)$, $\chi^\downarrow(s) = \exp(-is)$. Note that this implies an overcomplete representation [4-5] that enables us to use continuous sampling of spins similarly to the ordinary spatial variables.

Figure 1. Total valence energies for the lowest multiplets of the Pb atom with the explicit spin-orbit interaction. The calculations are carried out in two-component formalism. Plotted are Configuration Interaction energies as a function basis set size (points, full lines) and fixed-phase spin-orbit DMC energies (dashed lines). The energies are converged to ~ 3 mHa ($= 0.1$ eV).



linear combination of Slater determinants with the distinction that these are determinants of single-particle spinors

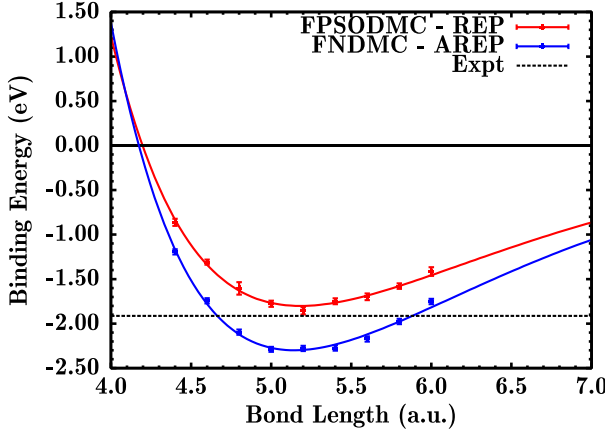
$$\Psi_T(\mathbf{R}, \mathbf{S}) = \sum_k c_k \det_k[\{\chi_j(\mathbf{r}_i, s_i)\}] \exp[U(\mathbf{R})]$$

where $\mathbf{R} = (\mathbf{r}_1, \mathbf{r}_2, \dots)$ and $\mathbf{S} = (s_1, s_2, \dots)$ are spatial and spin coordinates, respectively.

The next problem we have to address is the treatment of atomic cores in heavy atoms. We build

upon our previous work on nonlocal pseudopotentials (PP) since the spin-orbit operator is just another case of inherent nonlocality. This is well suited for calculations of real systems with

Figure 2. Binding curves of Sn_2 in diffusion Monte Carlo without (FNDMC) and with explicit spin-orbit (FPSODMC) with 44 valence electrons, compared with experiment.



$[(W\Psi_T)/\Psi_T]$. This approximation has the same scaling as the fixed-phase, ie, it converges to the exact energy/eigenstate proportionally to the square of the trial wave function error. Consequently, in practice, these two errors appear together as a single systematic bias. We were able to decrease this bias below ~ 0.1 eV in the tests mentioned below.

Spin-orbit tests. Testing of the method was done, for example, on total energies of atomic cases in two-component spinor formalism using independent calculations by Configuration Interaction (CI) method for cross-checking. CI gives essentially exact results for small systems such as Pb atom with $6s^26p^2$ valence space. We found excellent agreement with our fixed-phase spin-orbit DMC (FPSODMC) for this (Fig. 1) and other systems such as Bi, Tl atoms, PbH and PbO molecules [5]. Another system we want to mention is the tungsten atom since it nicely demonstrates the importance of *both* spin-orbit as well as the electron correlation. It is an interesting case due to the fact that the isovalent Cr and Mo atoms have the ground-state occupations d^5s^1 whereas the ground state of W is d^4s^2 . Qualitatively, d^4 occupation is favored due to the lower energy in the $j = 3/2$ channel; however, it turns out that this is not enough, and correlations have to be captured very accurately as well, otherwise one obtains incorrect ground state! We used a relativistic PP with 14 electrons in valence space with two different trial wave functions, COSCI (complete open shell CI) and CISD (singles doubles CI). Only after including important configurations from CISD the trial function has sufficiently accurate phase to predict the correct ground state [5]. We also find that almost all states with spin-orbit present are inherently multi-reference due lower symmetries. The total angular momentum J becomes the only good quantum number in high-symmetry systems such as atoms and molecules, implying much stronger mixing of states, in general. The last example we present here is a seemingly

heavy atoms since both scalar relativistic and spin-orbit effects can be accurately represented by pseudopotentials as it is routinely done in quantum chemical calculations. In particular, the commonly used pseudopotential that contains projectors on lm states of the spatial angular momentum is generalized to jlm_j projectors on atomic eigenstates of one-particle total angular momentum J . It is well-known, however, that the nonlocality is problematic in projection (diffusion Monte Carlo) methods since such algorithms are local in the many-particle space. Here we use experience from our treatment of nonlocal operators and we employ the so-called locality approximation. That means that we replace the one-particle nonlocal operator W by its projection that relies on the accurate trial function: $W \rightarrow \text{Re}$

“simple” molecule of Sn_2 . Interestingly, already for elements such as tin (4th row), the spin-orbit impact on the binding of this molecule is changed by almost 0.5 eV (!), in excellent agreement with experiment Fig. 2 [4]. Corrections by 1 eV or more in the 5th row are common [4,5].

Future plans:

We plan to apply the developed method to several challenges that involve 5th row atoms in 2D and 3D systems. One is the impact of spin-orbit on the ground and excited states in oxides with 5th row elements. This could possibly include some perovskites that feature both ordinary and topological electronic phases. One example of such class of systems are iridium compounds that have been studied very intensely over that last decade or so. Despite the effort, many of the questions regarding the nature of the electronic states in these systems remain open. Similar challenges exist in 2D materials that involve 5th row elements. Clearly, study of these materials using many-body wave function QMC methods that recover $\sim 95\%$ of the correlations has a potential to offer new insights into the physics of these systems.

Publications (2015-2016):

- [1] M. C. Bennett, C. Melton, A. Kulahlioglu, and L. Mitas, Fixed-node errors in 4d and 5d molecular systems, to be published
- [2] M.C. Bennett, A. Kulahlioglu, and L. Mitas, A Quantum Monte Carlo Study of benzene and bis(benzene) Mo and W, arXiv: 1607.XXXXX, submitted to CPL
- [3] C. A. Melton, L. Mitas, Fixed-node and fixed-phase approximations and their relationship to variable spins in quantum Monte Carlo, arXiv: 1605.03813, in Recent Progress in quantum Monte Carlo, edited by S. Tanaka, P.-N. Roy and L. Mitas, ACS, (2016), in press
- [4] C. A. Melton, M. C. Bennett, L. Mitas, Quantum Monte Carlo with variable spins, J. Chem. Phys. **144**, 244113 (2016)
- [5] C. A. Melton, M. Zhu, S. Guo, A. Ambrosetti, F. Pederiva, L. Mitas, Spin-orbit interaction in electronic structure quantum Monte Carlo, Phys. Rev. A **93**, 042502 (2016)
- [6] A. Ambrosetti, P. L. Silvestrelli, F. Pederiva, L. Mitas, and F. Toigo, Repulsive Atomic Fermi Gas with Rashba Spin-Orbit Coupling: a Quantum Monte Carlo Study, Phys. Rev. A **91**, 053622 (2015)
- [7] K. M. Rasch, L. Mitas, [Fixed-node diffusion Monte Carlo method for lithium systems](#), Phys. Rev. B **92**, 045122 (2015)

Nonequilibrium phenomena in Topological Insulators

Principal investigator: Professor Aditi Mitra
Department of Physics, New York University, New York, NY 10003
aditi.mitra@nyu.edu

Project Scope

The primary goal of this program is to explore nonequilibrium phenomena in topological insulators (TIs). Within this broad topic, the current focus has been to study a new kind of topological insulator known as Floquet topological insulator (FTI) which is a system that shows topological properties on the application of a time-periodic perturbation. However a time-periodic perturbation also drives the system out of equilibrium, so that standard assumptions made for TIs, do not apply to FTIs. Thus it is unclear what the topological quantum number of Floquet Hamiltonians really mean, and what would be the outcome of measuring topologically relevant observables. The PI's DOE funded research clarifies the meaning of FTIs by fully accounting for the inherently nonequilibrium nature of these systems, and their sensitivity to external dissipation. The outcome of the research include predictions for photoemission spectra, dc and optical Hall conductivity, edge state occupation, and the entanglement properties of FTIs. The results also show that Floquet systems coupled to a reservoir can lead to nonequilibrium non-Gibbsian steady states that can be characterized by a net entropy production rate, and that a reservoir can be engineered to make the FTI more coherent than a finite temperature Gibbs state. Thus the research shows when FTIs can behave as regular TIs, and in what ways they can be startlingly different. The project's goal in the coming years is to understand the role of interactions.

Recent Progress

Below are some highlights of progress made in the past 2 years.

Quasi-energy level occupation for a closed and open system and the corresponding photoemission spectra: In Ref [1] the PI and her research group and an external collaborator (Dr. Oka) studied the steady-state electron distribution function of FTIs under two conditions: one when the system is closed, and the second when the system has a dissipative coupling to a phonon bath. Predictions were made for the photoemission spectra. It was found that near the vicinity of the topological gaps where the periodic drive in the form of a circularly polarized laser is off-resonant, the reservoir can produce an effective cooling. In contrast, in the vicinity of resonances in the quasi-energy spectrum, the reservoir cannot efficiently cool the system, and enhanced photo-carriers appeared as bright spots in the photoemission spectra. It was also found that the matrix elements for higher photon absorption and emission processes are rapidly suppressed, so that only 2-4 Floquet bands were visible in the photoemission spectra for reasonable laser amplitudes.

dc and optical Hall conductivity and bulk-boundary correspondence:

In Refs [2], [3] the DOE funded research explored the consequence of the quasi-energy band occupations on the dc and optical Hall conductivity. Using a Kubo formula approach, it was shown exactly how the time-dependent Berry curvature (see Fig. 1) and the electron distribution function (see Fig. 2) enter in the dc and optical Hall conductivity.

It was found that for the off-resonant laser, the dc Hall conductance for the dissipationless i.e., closed system, was quite close (almost 80% to the quantized limit) and coupling to the reservoir produced cooling, thereby allowing the system to further approach the ideal limit. In contrast for resonant lasers where anomalous edge states appear in the Floquet zone boundaries, the conductance for the closed system was suppressed from the ideal limit. This behavior was understood by noting that the resonant laser creates population inversion in selected regions of momentum space causing Berry curvatures to cancel (Fig 2). It was also found that for the resonant laser, coupling to the reservoir in fact did not further cool the system, and the dc conductance was further reduced.

The bulk-edge correspondence in TIs requires that all transport can be understood in two complementary ways, one is in terms of a bulk Kubo formula calculation discussed above that completely neglects boundaries and leads. The second is in terms of transport purely along edge modes. It was found that the results of the bulk calculation of Ref [2] can also be justified purely by noting how the edge modes are occupied (see Figs. 3 and 4 and Ref [4]). In particular edge-states arising from resonant processes were occupied at a very high effective temperature, and therefore were ineffective in dc transport. Most of the conductance could be accounted for by the edge states arising from off-resonant processes which were at a low effective temperature.

Reservoir induced coherence and steady-state entropy production in open Floquet systems:

Periodically driven open systems cannot in general be described by an effective temperature, even when the bath is ideal. The DOE funded research in Ref [5] showed that the lack of detailed balance can be characterized via a steady-state entropy production rate. This is the entropy that the system releases to the reservoir. It was found that a stronger coupling to the reservoir increases the entropy production rate and also increases the system coherence. This is because the system maintains its purity by releasing the excess entropy into the surroundings. The enhanced purity of the system density matrix opens up the possibility of engineering the reservoir in order to drive the system into completely pure states known as dark states.

Entanglement properties of Floquet Chern Insulators: For conventional TIs arising from static Hamiltonians, it is known that an entanglement cut in the ground state wave function hosts edge-states that mimic the edge states in spatial boundaries. This observation is key to using entanglement to explore topological invariants in interacting systems where numerical methods such as matrix product states make it easier to access the entanglement directly. In Ref [6] the PI and her research group explored how this well understood fact concerning the entanglement in static TIs carry over to FTIs. In particular the entanglement properties of a state which is initially a half-filled ground state of graphene, but is unitarily evolved in time with a time-dependent Hamiltonian corresponding to graphene irradiated by a circularly polarized laser was studied. The laser parameters were chosen to correspond to several representative Floquet Chern insulator phases. The entanglement properties of this unitarily evolved state was compared with the entanglement properties the Floquet eigenstate, ie, the ground state of the Floquet Hamiltonian where one of the Floquet bands is fully occupied. It was found that the true states arising from unitary time evolution show a volume law for the entanglement entropy, whereas the Floquet states show an area law (see Fig. 5). The latter arises because the Floquet states are ground states of a short-ranged Hamiltonian (the Floquet Hamiltonian) with a gap.

The physics was a lot richer when the entanglement spectrum (ES), which is the spectrum of the reduced density matrix, was studied (see Fig 6). For the Floquet Chern insulator, qualitative differences were found in the ES of the off-resonant and on-resonant laser. While the ES can be separated between a bulk and an edge contribution both for the Floquet state and the unitarily evolved state, for the unitarily evolved state, the bulk ES is a measure of the excitation density of the Floquet bands. Thus a resonant laser resulted in closing of the entanglement gap and therefore a lack of topological protection of some of the edge states. An analytic theory was developed to argue that only edge states corresponding to off-resonant processes appear in the ES, whereas edge states due to resonant processes are absent as they hybridize with bulk states.

Future Plans

Superconducting instabilities in periodically driven systems- As a first step towards understanding the role of interactions in periodically driven systems, the PI and graduate student Mr. Hossein Dehghani are exploring the onset of superconductivity in these systems.

Symmetry protected interacting Floquet topological phases in one dimension- Along with graduate student Mr. Daniel Yates, the PI is exploring one dimensional periodically driven systems that host Majorana edge modes. The goal is to understand the stability of the Majorana modes when interactions are present.

Floquet system coupled to a quantum bath – As a generalization of the PI's previous work on understanding the role of a classical Markovian bath on stabilizing nonequilibrium states in FTIs, the PI is now exploring what happens when the bath is quantum.

Publications

- [1]. Hossein Dehghani, Takashi Oka, and Aditi Mitra, Dissipative Floquet Topological Systems, Phys. Rev. B 90, 195429 (2014).
- [2]. Hossein Dehghani, Takashi Oka, and Aditi Mitra, Out of equilibrium electrons and the Hall conductance of a Floquet topological insulator, Phys. Rev. B 91, 155422 (2015).
- [3]. Hossein Dehghani and Aditi Mitra, Optical Hall conductivity of a Floquet Topological Insulator, Phys. Rev. B 92, 165111 (2015).
- [4]. Hossein Dehghani and Aditi Mitra, Occupation probabilities and current densities of bulk and edge states of a Floquet topological insulator, Phys. Rev. B 93, 205437 (2016).
- [5]. Hossein Dehghani and Aditi Mitra, Floquet topological systems in the vicinity of band crossings: Reservoir induced coherence and steady-state entropy production, Phys. Rev. B 93, 245416 (2016).
- [6]. Daniel J. Yates, Yonah Lemonik, and Aditi Mitra, Entanglement properties of Floquet Chern insulators, arXiv:1602.02723, in review at PRL.

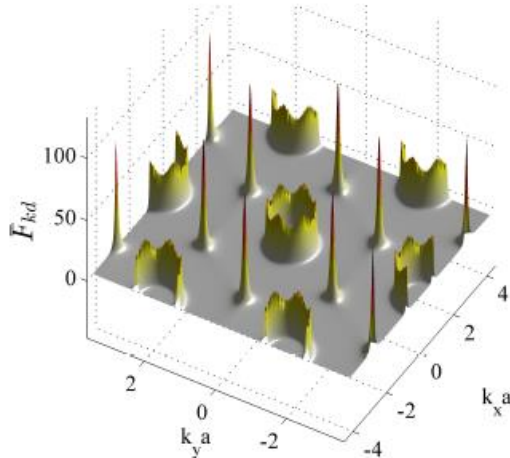


Figure 1: Time averaged Berry curvature for a phase of the Floquet Chern Insulator corresponding to Chern number =3.

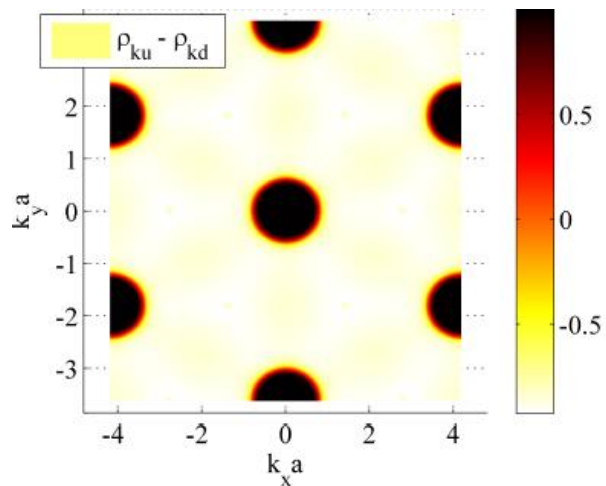


Figure 2: Contour plot for the population difference between the two Floquet bands for the closed system and for the phase shown in Figure 1.

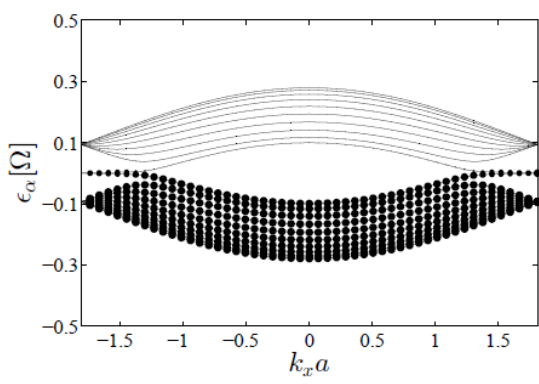


Figure 3: Occupation probability indicated by size of the circles for an off-resonant laser and Chern number=1. The edge states are occupied at a low effective temperature.

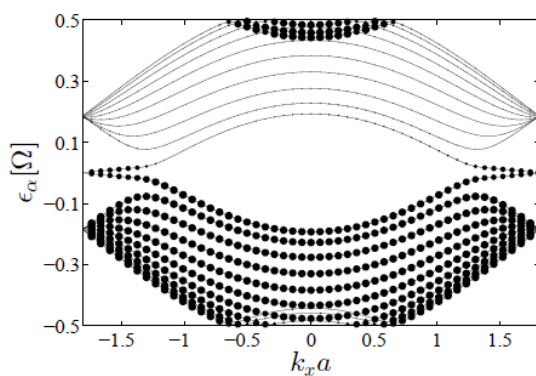


Figure 4: Occupation probability indicated by size of the circles for a resonant laser and Chern number=3. Of the 3 pairs of chiral edge-states, one is occupied at a low effective temperature, while the other two pairs are at a high effective temperature.

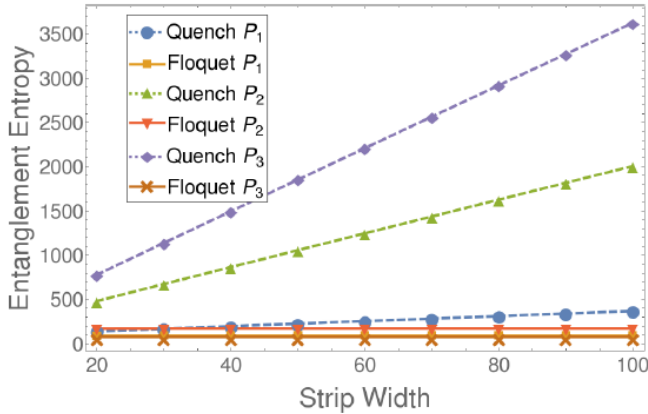


Figure 5: Entanglement entropy for the Floquet eigenstate and for the unitarily evolved state. The former shows area law while the latter shows volume law.

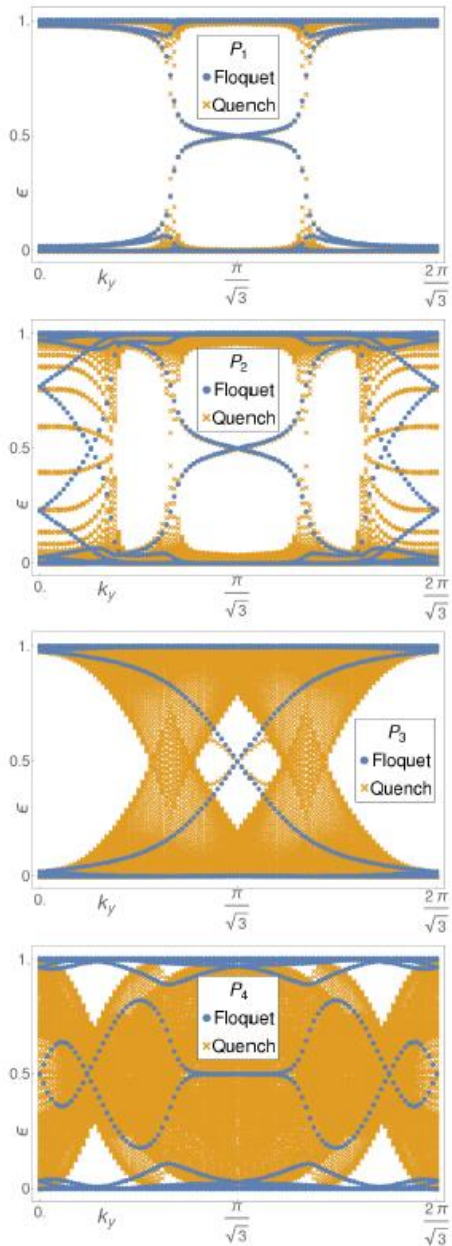


Figure 6: Entanglement spectrum for four different phases of the Floquet Chern insulator for the Floquet eigenstate and the unitarily evolved state. For the latter, edge-states coexist with bulk excitations that can ruin their topological protection.

Non-Equilibrium Physics at the Nanoscale

Principal investigator: Dirk K. Morr
Department of Physics, University of Illinois at Chicago, IL 60607
dkmorr@uic.edu

Project Scope

The goal of this program is to discover and understand novel non-equilibrium phenomena at the nanoscale. The PI investigates the form of non-equilibrium charge, spin and excitonic energy transport in a wide range of materials and systems, including unconventional superconductors, strongly correlated heavy fermion materials, topological insulators and superconductors, quantum critical materials, and light-harvesting biological complexes. Exploring the properties of these systems out-of-equilibrium provides unprecedented opportunities to gain insight into the effects of strong correlations and the nature of topological states. The complexity of these systems allows for the emergence of novel transport functionalities, such as the creation of spin-diodes, or the formation of states with a topologically protected quantized conductance. In turn, the discovery of such novel out-of-equilibrium properties provide new markers for the detection of strongly correlated and topological phases.

Recent Progress

Below is a selection of four examples, highlighting the accomplishments of the PI's research program over the last year.

Charge Transport as a Probe for Topological Superconductors

Majorana states in topological superconductors hold unprecedented potential as a novel platform for quantum computing. The PI, together with S. Rachel and M. Vojta (Technical University Dresden) recently explored propagating Majorana states which emerge at the edges of magnetic islands placed on *s*-wave superconductors with a Rashba spin-orbit interaction. Such systems possess a large number of topological states, which differ in

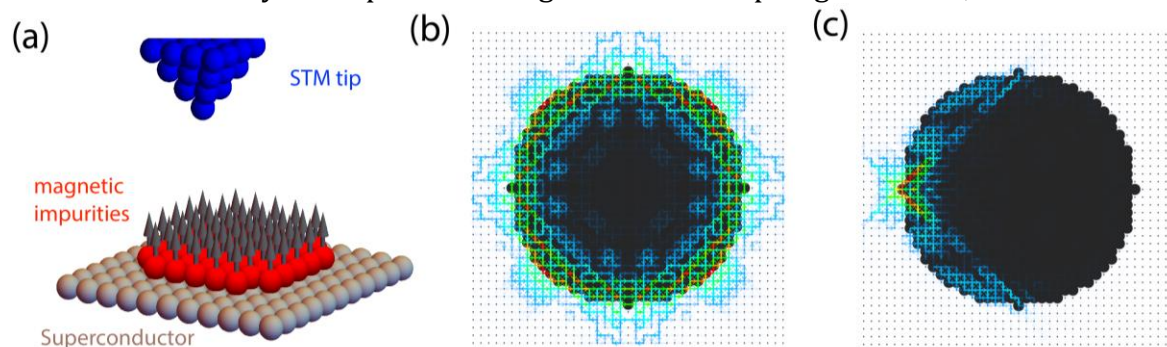


Figure 1: (a) Probing topological edge states via scanning tunneling spectroscopy. (b) Supercurrent in the topological $C = 2$ phase (the magnetic island is shown in black). (c) Transformation of normal current entering from the STM tip into Cooper pairs.

their Chern number, C . For a dense island of magnetic atoms, there exist two topological phases with $C = 2$ and $C = -1$. The PI showed that the topological edge states carry a supercurrent [Fig.1(b)] whose chirality reflects the sign of the Chern number. Moreover, the PI demonstrated that the differential conductance measured via scanning tunneling spectroscopy (STS) [Fig.1(a)] is quantized in these topological phases, and given by the quantum of conductance times the magnitude of the Chern number. In contrast, the conductance is not quantized in the topologically trivial phase with $C = 0$. These phases show different characteristics of how the normal current entering the system from the STM tip is converted into Cooper pairs [Fig.1(c)]. Since these results are robust against disorder in the magnetic island, they imply that charge transport can identify topological phases and provide direct insight into their Chern numbers, which is of great importance for the use of Majorana modes in quantum computation.

Josephson Scanning Tunneling Spectroscopy in Unconventional Superconductors

The development of Josephson Scanning Tunneling Spectroscopy (JSTS) in a series of recent groundbreaking experiments has opened the possibility to gain unprecedented insight into the nature of superconducting order parameters. While it was argued that the

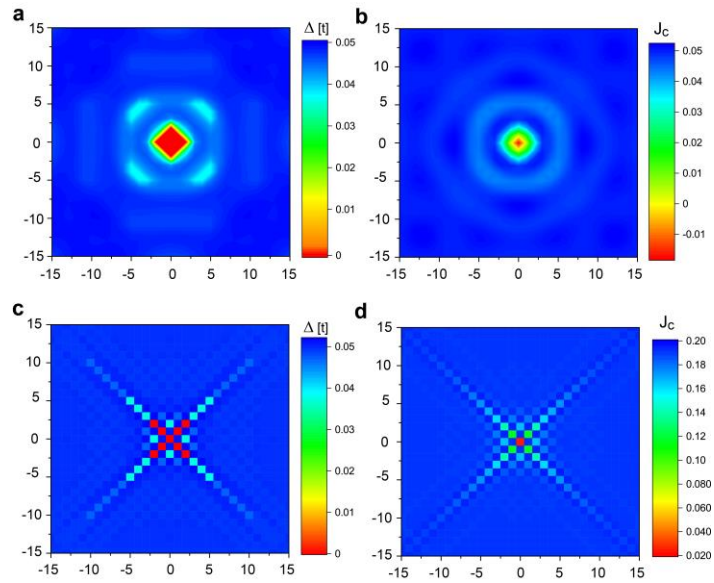


Figure 2: Spatial variations of (a),(c) the superconducting order parameters, and (b),(d) J_c for a magnetic (a),(b) and potential (c),(d) defect.

spatial variations in the Josephson current J_c reflect those of the superconducting order parameter, a theoretical understanding of this effect is still lacking. In collaboration with M. Graham (a graduate student in the PI's group), the PI developed a theory for JSTS in conventional and unconventional superconductors to address this important question. For an s -wave superconductor, the PI showed that the spatial oscillations in J_c [Fig.2b and d] reflect those of the order parameter [Fig.2a and c] both for magnetic defects [Fig.2a and b], which induce Shiba states, as well as for non-magnetic defects [Fig.2c and d]. This establishes that JSTS provides direct insight into the

spatial form of the superconducting order parameter, which is of great importance for the exploration of unconventional iron based and heavy fermion superconductors.

Shot Noise Tunneling Spectroscopy

The current development of shot noise tunneling spectroscopy (SNTS) holds unprecedented potential to provide spatially resolved insight into the transport properties of correlated and topological materials that are not accessible through current measurements. The PI, together with M. Rezaei (a graduate student in the PI's group) has therefore developed a theory for SNTS in metallic, topological and correlated materials. For metallic systems [Figs. 3(a),(b)] and topological insulators [Figs. 3(c),(d)], the PI

demonstrated that the spatial structure of the shot noise measured by the STS tip [Figs. 3(b),(d)] is similar to that of the current flowing through the system [Figs. 3(a),(c)]. Thus

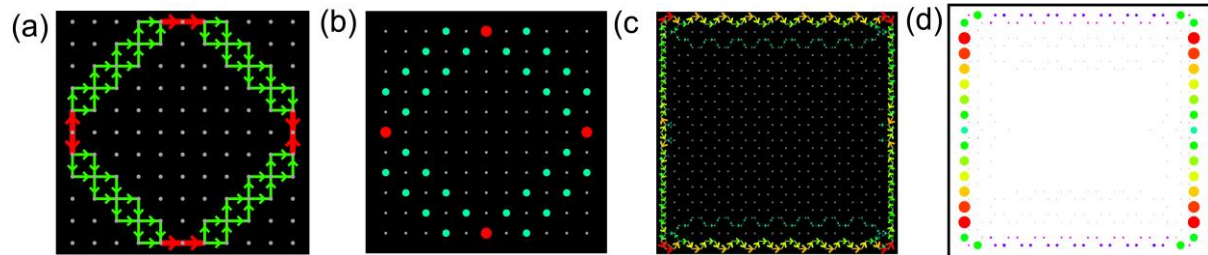


Figure 3: Spatial form of (a),(c) current flow, and (b),(d) shot noise measured via STS, for (a),(b) a metal, and (c),(d) a two-dimensional topological insulator.

SNTS can spatially image current paths with near atomic resolution, providing unprecedented insight into a system's transport properties. Moreover, the PI showed that the Fano factor associated with STS current and noise measurements exhibits a nontrivial spatial structure which reflects the complex non-local correlations in the system.

The Equivalent Resistance from the Quantum to the Classical Limit

The PI, together with S. Sarkar and D. Kroeber (two graduate students in the PI's group) has generalized the notion of an equivalent resistance to the entire range from classical to quantum transport by introducing the concept of transport equivalent networks (TENs).

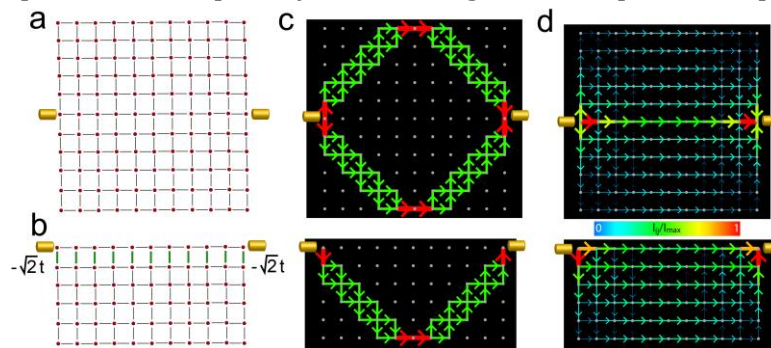


Figure 4: (a),(b) Transport equivalent networks, which possess "identical" local current patterns in the entire range from (c) quantum to (d) classical.

Two networks [Figs.4a,b] are said to be transport equivalent if, for a given bias and gate voltage, the same net current flows through them. The PI demonstrated that transport equivalence persist even in the presence of electron-electron or electron-phonon interactions. As a system can be tuned from the quantum to the classical transport limit by increasing

the interaction strength, two networks that are transport equivalent in the quantum limit, remain transport equivalent over the entire range up to the classical limit. The global transport equivalence is reflected in the close similarity of local transport properties given by the spatial current patterns [Figs.4c,d]. As a result, it is possible to map transport equivalent quantum networks onto equivalent classical resistor networks. The concept of TENs can be extended to networks of polymers, molecules, or even light-harvesting biological complexes, providing exciting new opportunities for the creation of novel transport functionalities.

Future Plans

The planned activities for the next year will extend in several directions. First, the PI will extend his work on Josephson Scanning Tunneling spectroscopy to iron-based and cuprate superconductors. Of particular interest is here the question of whether JSTS can be employed to unambiguously identify the symmetry of unconventional superconductors, an

issue which is still not settled in some of the iron-based materials. Second, the PI will investigate to what extent shot noise spectroscopy can provide insight into the Kondo screening process of single Kondo impurities, and in heavy fermion materials, and how quantum interference between different tunneling paths affects the Fano factor. Of particular interest is to what extent SNTS can spatially detect changes in current patterns that are induced by defects. This study will complement the PI's ongoing research project on non-equilibrium charge transport in heavy fermion materials. Third, the PI will continue the investigation of transport phenomena in topological superconductors. In particular, the PI intends to explore how the induced superconducting order parameter varies between the different topological non-trivial and trivial phases, and whether signatures of these changes can be detected in charge or heat transport. Fourth, the PI will continue his collaboration with the group of J.C. Davis on investigating quasi-particle interference (QPI) in the quantum critical heavy fermion material YbRh_2Si_2 . Of particular interest here are the effects of quantum critical fluctuations on the QPI spectrum. The PI also plans to develop a theory for shot noise tunneling spectroscopy in this material.

Publications

1. "Equivalent Resistance from the Quantum to the Classical Limit", S. Sarkar, D. Kröber, and D.K. Morr, submitted to *Nature Physics* (2016).
2. "Theory of Scanning Tunneling Spectroscopy: from Kondo Impurities to Heavy Fermion Materials", D.K. Morr, invited review article for a special focus issue on *Strongly Correlated Electron Systems* in *Reports on Progress in Physics*, in press (2016).
3. "Microscopic Origin of the Neutron Spin Resonance in Heavy Fermion Superconductor $\text{Ce}_{1-x}\text{Yb}_x\text{CoIn}_5$ ", Y. Song, J.S. Van Dyke, I. K. Lum, B. D. White, L. Shu, A. Schneidewind, P. Cerm, Y. Qiu, M. B. Maple, D. K. Morr, and P. Dai, submitted to *Nat. Comm.* (2015).
4. "Differential Conductance and Defect States in the Heavy Fermion Superconductor CeCoIn_5 ", J. S. Van Dyke, J. C. Davis, and D.K. Morr, *Phys. Rev. B* **93**, 041107 (R) (2016), Rapid Communication.
5. "Controlling the Flow of Spin and Charge in Nanoscopic Topological Insulators", J. Van Dyke and D. K. Morr, *Phys. Rev. B* **93**, 081401(R) (2016), Rapid Communication.
6. "Crossover from Quantum to Classical Transport", D. K. Morr, *Contemporary Physics* **57**, 19 (2016); invited review article.
7. "Magnetic f -Electron Mediated Cooper Pairing Mechanism in the Heavy Fermion Superconductor CeCoIn_5 ", J. Van Dyke, F. Massee, M. P. Allan, J. C. Davis, C. Petrovic, and D.K. Morr, *PNAS* **111**, 11663 (2014).
8. "Lifting the Fog of Complexity", D.K. Morr, *Science* **343**, 382 (2014).
9. "Quantum Transport and Energy Flow Patterns in Photosynthesis under Incoherent Excitation: A Non-Equilibrium Green's Function Analysis", K. M. Pelzer, T. Can, S. K. Gray, D. K. Morr, and G. S. Engel, *J. Phys. Chem. B* **118**, 013054 (2014).
10. "Current Patterns, Dephasing and Current Imaging in Graphene Nanoribbons", J. Mabillard, T. Can and D. K. Morr, *New J. Phys.* **16**, 013054 (2014).

Materials Theory

Principal Investigator: J. R. Morris (morrisj@ornl.gov)

Co-investigators: V. R. Cooper, M. H. Du, L. R. Lindsay, D. S. Parker

Scope

This project employs state-of-the-art theory to explore novel phenomena and material properties in order to guide materials design and discovery. In conjunction with extensive collaborations with ORNL and external experimental and theoretical groups, we investigate a wide range of material functionality, including magnetism, transport (electrical and thermal), optical transitions and weak interactions. Specific materials that are investigated include those with unconventional thermal transport properties, halide and chalcohalide based photovoltaic (PV) and photodetector materials, transparent conductors, luminescent materials, novel magnetic and superconducting materials, and materials and interfaces where van der Waals interactions are important. A critical aspect of this project is the examination of unconventional material behaviors thereby revealing hidden chemical trends that govern complex collective phenomena. We use these capabilities to aid the discovery of new materials and systems with targeted properties which will have impacts in multiple areas of condensed matter physics and materials science relevant to energy applications.

Recent Progress

Recent progress includes: (1) the prediction of unusual phonon scattering mechanisms and thermal transport behaviors in novel materials;^{1,2,3,4,5,6,7,8,9} (2) the development of important understanding of carrier transport and ion migration in emerging lead halide perovskite solar cell materials^{10, 11, 12, 13, 14} and the investigation of lead-free (Ge-, Sn-, and Bi-based) halides, chalcohalides, oxyhalides, and oxides as potential solar absorber materials, hole transport materials, radiation detection materials, or transparent conducting materials;^{15,16,17,18,19} (3) the development of new luminescent materials based on transition metal and rare-earth activators and excitons (stable at room temperature) for energy efficient lighting, imaging, and photodetection;^{20,21,22,23,24,25} (4) the investigation of metallic hydrides as potential high- T_c superconductors based on strong electron-phonon coupling;²⁶ (5) and the prediction of a new structural phase in mercury dihalides using van der Waals functionals. We focus on a few selected results below.

Novel phonon scattering mechanisms and unconventional thermal transport behavior

Lattice thermal conductivity is a fundamental physical property that governs the performance of a wide range of materials relevant to energy efficiency, such as thermoelectrics, thermal barrier coatings, and thermal interface and heat dissipation materials. We have pioneered the development of theoretical methods for thermal conductivity calculations via the coupling of interatomic forces derived from density functional theory (DFT) with a full solution of the Peierls-Boltzmann transport equation with *no adjustable parameters*. We have developed new insights into thermal transport and have demonstrated that old ‘rules of thumb’ used to understand thermal conductivity are insufficient as they neglect critical phonon scattering phase space effects arising from fundamental conservation conditions.

For example, we recently demonstrated that optic phonon bandwidth plays a critical role in determining the ability of optic phonons to scatter heat-carrying acoustic phonons in Li_2X ($\text{X}=\text{O}, \text{S}, \text{Se}, \text{Te}$) materials.¹ Without consideration of this feature one would expect significantly higher thermal conductivity in these compounds when comparing phonon dispersion features with other systems (Fig. 1), e.g., the high thermal conductivity material GaN. Also, we found the surprising behavior of thermal conductivity *decreasing* with increasing pressure despite increasing sound velocities in a class of compound materials.⁵ This behavior has not been found experimentally or theoretically in any material unless approaching a pressure induced phase transition as thermal conductivity typically increases with increasing pressure. Furthermore, we demonstrated that CdO alloyed with small concentrations of MgO has increased thermal conductivity at higher temperatures despite increased phonon-disorder scattering.⁶ These examples contradict conventional wisdom, and demonstrate that dispersion properties, i.e., the acoustic-optic frequency gap, bunching of acoustic branches, and the optic phonon bandwidth, play a pivotal role in determining thermal conductivity and its behavior with varying external parameters (e.g., temperature and pressure).

Halide perovskites and related halide optoelectronic materials

Halide perovskite solar cells have recently undergone rapid development. The power conversion efficiency of $\text{CH}_3\text{NH}_3\text{PbI}_3$ -based solar cells has exceeded 20%. $\text{CH}_3\text{NH}_3\text{PbI}_3$ has many unusual properties which have not been observed in conventional inorganic PV materials, such as the coexistence of long carrier diffusion lengths and high defect densities as well as significant ion migration (which leads to device polarization). We have systematically investigated the electronic structure, dielectric properties, and defect properties of

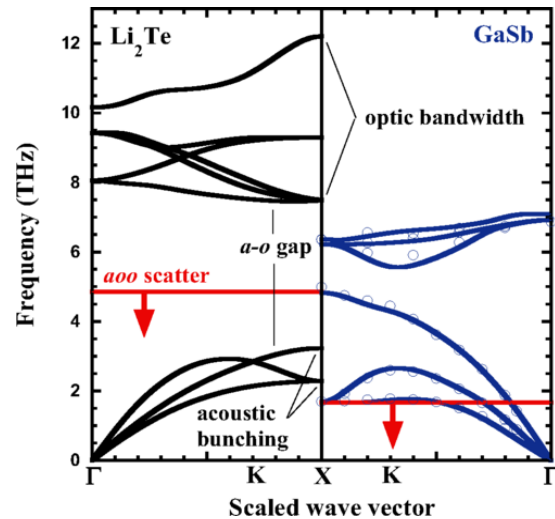


Figure 1. Calculated phonon dispersions for Li_2Te and GaSb . The red lines correspond to the calculated optic bandwidth for each material. Given conservation of energy, only acoustic phonons below these lines can participate in acoustic+optic+optic (*aoo*) scattering.

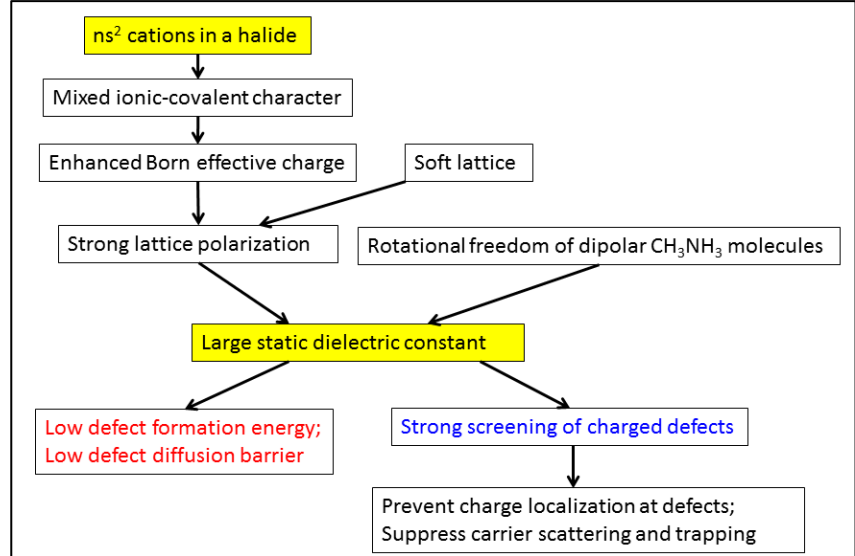


Figure 2. A flow chart that illustrates the effects of the ns^2 ion (Pb^{2+}) on the performance of the $\text{CH}_3\text{NH}_3\text{PbI}_3$ solar cell.

$\text{CH}_3\text{NH}_3\text{PbI}_3$.^{10,11,12,13,14} The key understanding of these fundamental material properties is summarized in Figure 2.

The large static dielectric constant of $\text{CH}_3\text{NH}_3\text{PbI}_3$ promotes defect formation; however, it also strongly screens charged defects and impurities, making them less harmful to carrier transport.¹⁰ This explains the coexistence of long carrier diffusion lengths and high defect densities. Low defect formation energies further lead to low diffusion barriers of iodine ions and certain other impurities, thus causing degradation.¹⁴ As shown in Figure 2, many important properties of $\text{CH}_3\text{NH}_3\text{PbI}_3$ are connected. The centerpiece is the large dielectric constant, which originates from the chemistry of Pb^{2+} [or more generally the chemistry of the ns^2 ions (the ions with the outermost electron configuration of ns^2)].

The important role of the ns^2 ions in carrier transport in $\text{CH}_3\text{NH}_3\text{PbI}_3$ prompted us to search for new halide optoelectronic materials with ns^2 ions, including CsGeI_3 , Bi chalcohalides, and Bi oxyhalides.^{15,16} Based on calculated electronic structure and defect properties, we proposed potential applications for these compounds: *p*- CsGeI_3 as a hole transport material in dye-sensitized TiO_2 solar cells; *n*-type BiSeBr and *p*-type BiSI and BiSeI as solar absorber materials; BiSeBr and BiSI as room-temperature γ -ray detection materials; BiOBr as a *p*-type transparent conducting material.

Metallic hydride superconductors

The recent discovery of superconductivity with $T_c = 203$ K in sulfur hydrides under high pressures has re-invigorated interest in electron-phonon coupling (the likely source of this high T_c) as a route to higher T_c . We sought to theoretically study metallic hydrides, with the hopes of finding similar T_c behavior *at ambient pressure*. Many such hydrides are semiconducting and therefore not superconducting, but we settled on TiH_2 , previously known to be metallic. Our electronic structure calculation (Figure 3) depicts a peak in the density-of-states precisely at the Fermi level, suggestive of strong electron-phonon coupling.

From calculations of the Eliashberg function $\alpha^2 F(\omega)$ and the associated electron-phonon coupling constant λ , we find a λ of 0.87 in the cubic phase and an associated superconducting T_c of 7 K.²⁶ This T_c , while significant, is much lower than in the sulfur hydrides due to the lack of significant H *s* states at the Fermi level and the weak H atom electron-phonon coupling. However, this need not be generally true – it should be possible to discover metallic hydrides with stronger H electron-phonon coupling. An example of such coupling is the Pd hydrides and deuterides PdH_x and PdD_x , which show T_c values exceeding 10 K.

Van der Waals interactions

The ability to simulate the subtle energetic differences between the effects of crystal packing, hydrogen-bonded networks and dispersion dominated interactions is one of the most important criteria for computational crystal structure predictions. The key challenge from theory is the ability

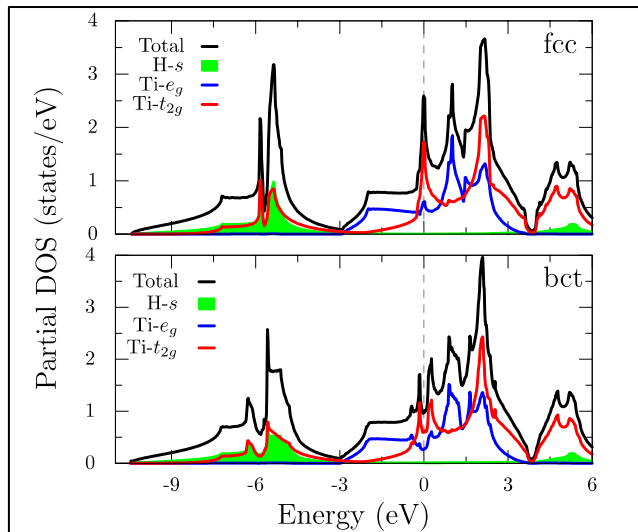


Figure 3. The calculated densities-of-states for cubic (top) and tetragonal (bottom) TiH_2 . Note the peak precisely at the Fermi energy in the cubic phase.

of 0.87 in the cubic phase and an associated superconducting T_c of 7 K.²⁶ This T_c , while significant, is much lower than in the sulfur hydrides due to the lack of significant H *s* states at the Fermi level and the weak H atom electron-phonon coupling. However, this need not be generally true – it should be possible to discover metallic hydrides with stronger H electron-phonon coupling. An example of such coupling is the Pd hydrides and deuterides PdH_x and PdD_x , which show T_c values exceeding 10 K.

to model covalent and non-covalent interactions on the same footing. For example, the difference in crystal energies of the hydrogen bonded network and the stacked structure for a typical molecular crystal could be as small as 2 kJ/mol making standard local and semi-local exchange correlation functionals used in DFT incapable of predicting the relative stability of these systems. Recent developments of a non-local correlation functional (i.e., the van der Waals density functional – vdW-DF) now make it possible to account for non-covalent interactions with chemical accuracy (on the order of a few kJ/mol). Even more important, new exchange functionals that pair with vdW-DF, such as the C09 functional designed by the PI Cooper, make it possible to model materials with significant covalent bonding, thus providing a framework for a general purpose functional. Given the diversity of the forms of bonding exhibited by the mercury dihalides, HgX_2 (where $X=F, Cl, Br, I$), and the significant role of dispersion forces in some cases, this class of material provides an ideal testbed for examining the performance of the vdW-DF-C09 functional. Here, HgF_2 is a dense solid, $HgCl_2$ and $HgBr_2$ are molecular crystals and HgI_2 is a layered material. We find that the vdW-DF-C09 successfully reproduces the experimental results available for HgX_2 . Surprisingly, our calculations also suggest that the $PbCl_2$ -type structure is a competitive alternative for HgF_2 at low temperatures. This result is consistent with a similar compound, PbF_2 and is in direct contradiction to GGA calculations which show a preference towards the fluorite structure for both PbF_2 and HgF_2 (Figure 4). Furthermore, it has recently been shown that this $PbCl_2$ -type polymorph is far more stable than the fluorite structure above 5 GPa. We raise the question of whether low temperatures may induce this transition as well, inviting an experimental assessment of the fluoride at low temperatures and a more expansive elucidation of the phase diagram for the mercury dihalides. Nevertheless, these results provide strong indication that the new functional is indeed a general purpose functional capable of exploring materials that range from dense structures to sparse matter.

Future Plans

We will continue the work on (1) the development of modern thermal conductivity calculations and apply them to novel energy materials, (2) the study of unconventional hybrid inorganic-organic halide perovskite PV materials and the search of new halide optoelectronic materials, (3) the investigation of fundamental electronic and optical transitions in transition-metal and rare-earth dopants and their associated defects in wide-gap luminescent materials for energy-efficient lighting and optical imaging, (4) magnetism and high- T_c superconductivity, (5) the investigation and the design of van der Waals solids with electronic, optical, and magnetic functionalities. In particular, we will explore the spin-phonon response in layered pnictides. This work will build on recent developments that now incorporate spin within the non-local vdW-DF correlation term. The goal is to understand how important spin in the local correlation term are for understanding the spin-phonon coupling within these materials. This work will also utilize connections with Quantum Monte Carlo simulations through an INCITE award to assess the accuracy and limitations of the vdW-DF method.

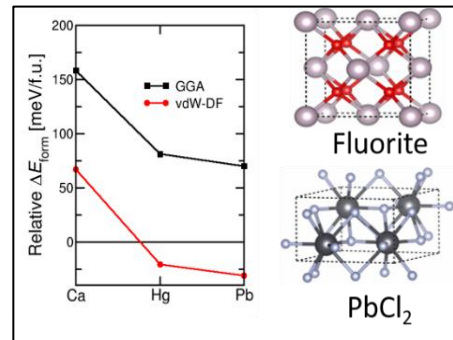


Figure 4 (left) Relative formation energy for the fluorite structure versus the $PbCl_2$ -type structure for CaF_2 , HgF_2 and PbF_2 employing both the vdW-DF-C09 (red) and PBE (black) exchange-correlation functionals. Negative energies indicate a preference towards the formation of the $PbCl_2$ structure type. (right) Structure models of the two crystal-types explored.

Partial list of publications, 2014-2016:

- ¹ S. Mukhopadhyay, L. Lindsay, and D. S. Parker, Optic phonon bandwidth and lattice thermal conductivity: The case of Li₂X (X=O, S, Se, Te), *Physical Review B* 93, 224301 (2016).
- ² P. Jiang, L. Lindsay, and Y. K. Koh, Role of low-energy phonons with mean-free-paths >0.8 μm in heat conduction in silicon, *Journal of Applied Physics* 119, 245705 (2016).
- ³ Y. Kuang, L. Lindsay, S. Shi, X. Wang, and B. Huang, Thermal conductivity of graphene mediated by strain and size, *International Journal of Heat and Mass Transfer* 101, 772 (2016).
- ⁴ Y. Kuang, L. Lindsay, S. Q. Shi, and G. P. Zhen, Tensile strains give rise to strong size effects for thermal conductivities of silicene, germanene and stanene, *Nanoscale* 8, 3760 (2016).
- ⁵ L. Lindsay, D. A. Broido, J. Carrete, N. Mingo, and T. L. Reinecke, Anomalous pressure dependence of thermal conductivities of large mass ratio compounds, *Physical Review B* 91, 121202(R) (2015).
- ⁶ L. Lindsay and D. S. Parker, Calculated transport properties of CdO: Thermal conductivity and thermoelectric power factor, *Physical Review B* 92, 144301 (2015).
- ⁷ Y. Kuang, L. Lindsay, and B. Huang, Unusual enhancement in intrinsic thermal conductivity of multi-layer graphene by tensile strain, *Nano Letters* 15, 6121 (2015).
- ⁸ I. Jo, M. T. Pettes, L. Lindsay, E. Ou, A. Weathers, A. L. Moore, Z. Yao, and L. Shi, Reexamination of basal plane thermal conductivity of suspended graphene samples measured by electro-thermal micro-bridge methods, *AIP Advances* 5, 053206 (2015).
- ⁹ G. D. Mahan, L. Lindsay, and D. A. Broido, The Seebeck coefficient and phonon drag in silicon, *Journal of Applied Physics* 116, 245102 (2014).
- ¹⁰ M. H. Du, “Efficient carrier transport in halide perovskites: theoretical perspectives”, *Journal of Material Chemistry A*, 2, 9091 (2014).
- ¹¹ H. Shi and M. H. Du, “Shallow halogen vacancies in halide optoelectronic materials”, *Physical Review B* 90, 174103 (2014).
- ¹² M. H. Du, “Density functional calculations of native defects in CH₃NH₃PbI₃: Effects of spin-orbit coupling and self-interaction error”, *Journal of Physical Chemistry Letters*, 6, 1461 (2015).
- ¹³ B. Yang, J. Keum, O. S. Ovchinnikova, A. Belianinov, S. Chen, M. H. Du, I. N. Ivanov, C. M. Rouleau, D. B. Geohegan, and K. Xiao, “Deciphering halogen competition in organometallic halide perovskite growth”, *Journal of American Chemical Society*, 138, 5028 (2016).
- ¹⁴ D. Yang, W. Ming, H. Shi, L. Zhang, and M. H. Du, “Fast diffusion of native defects and impurities in perovskite solar cell material CH₃NH₃PbI₃”, *Chemistry of Materials* 28, 4349-4357 (2016).
- ¹⁵ W. Ming, H. Shi, M. H. Du, “Large dielectric constant, high acceptor density, and deep electron traps in perovskite solar cell material CsGeI₃”, *Journal of Materials Chemistry A*, in press.
- ¹⁶ W. Ming, H. Shi and M. H. Du, “Bismuth chalcogenides and oxyhalides as optoelectronic materials”, *Physical Review B*, 93, 104108 (2016).
- ¹⁷ Y. Li, D. J. Singh, M. H. Du, Q. Xu, L. Zhang, W. Zheng, Y. Ma, “Design of ternary alkaline-earth metal Sn(II) oxides with potential good p-type conductivity”, *Journal of Materials Chemistry C*, 4, 4592 (2016).
- ¹⁸ J. Sun, H. Shi, M. H. Du, T. Siegrist, and D. J. Singh, “Ba₂TeO as an optoelectronic material: First-principles study”, *Journal of Applied Physics*, 117, 195795 (2015).
- ¹⁹ H. Shi, B. Saparov, D. J. Singh, A. S. Sefat, and M. H. Du, “Ternary chalcogenides Cs₂Zn₃Se₄ and Cs₂Zn₃Te₄: Potential p-type transparent conducting materials”, *Physical Review B*, 90, 184104 (2014).

²⁰ M. H. Du, "Chemical trend of electronic and optical properties of ns² ions in halides", Journal of Material Chemistry C, 2, 4784 (2014).

²¹ H. Shi and M. H. Du, "Discrete electronic bands in semiconductors and insulators: Potential high-light-yield scintillators", Physical Review Applied, 3, 054005 (2015).

²² H. Shi, M. H. Du, and D. J. Singh, "Li₂Se as a neutron scintillator", Journal of Alloys and Compounds, 647, 906 (2015).

²³ Y. Wu, H. Shi, B. C. Chakoumakos, M. Zhuravleva, M. H. Du, and C. L. Melcher, "Crystal structure, electronic structure, temperature-dependent optical and scintillation properties of CsCe₂Br₇", Journal of Materials Chemistry C, 3, 11366 (2015).

²⁴ M. H. Du, "Using DFT methods to study activators in optical materials", ECS Journal of Solid State Science and Technology 5, R3007 (2016) (invited review article).

²⁵ H. Wei, M. H. Du, L. Stand, Z. Zhao, H. Shi, M. Zhuravleva, and C. L. Melcher, "Scintillation properties and electronic structure of intrinsic and extrinsic mixed elpasolites Cs₂NaREBr₃I₃ (RE = La, Y)", *Physical Review Applied* 5, 024008 (2016).

²⁶ K.V. Shanavas, L. Lindsay, and D. S. Parker. "Electronic structure and electron-phonon coupling in TiH₂." *Scientific Reports* 6, 28102 (2016).

Designing allostery-inspired response in mechanical networks

Principal investigator: Professor Sidney Nagel

Department of Physics and the James Franck and Enrico Fermi Institutes

The University of Chicago

Chicago, IL 60615

srnagel@uchicago.edu

Project Scope

The proposed work builds on the new concept of bond-level independence of properties in disordered matter. This concept arose from the original jamming paradigm for creating out-of-equilibrium disordered solids. This project will address the question: How does disorder provide new potentialities for the behavior of a material that would be absent in a crystalline material of the same composition?

In order to elaborate on novel ideas about bond-level independence of properties in disordered materials, this work will address the possibility of creating new classes of mechanical meta-materials with applications everywhere from functional nano-scale materials to large-scale architectural disordered networks. Such flexibility for tuning the mechanical properties of disordered matter raises a host of questions that need to be addressed. The theoretical formalism and algorithms that we have developed are useful in a number of contexts. They can be used to tune bulk properties such as the elastic moduli of a material. This allows a new form of material design that is based on using unique features of disordered materials. As we will show below, these ideas also allow the design of more local, targeted, responses. The network design rules that will emerge will have potential impact on building of structural materials to create novel flexible functionality.

The marginally jammed solid at the jamming transition represents an extreme limit of disorder that is an opposite pole from a perfect crystalline order. At that transition there is no length scale over which one can average in order to regain solid elastic behavior. It is thus an extreme limit of a solid. As one compresses the packing above the threshold, elastic behavior re-emerges on long length scales. The idea that jamming is one extreme pole of rigid matter allows a new way of understanding materials that cannot be easily classified as crystals or glasses. Poly-crystalline materials have regions that are highly ordered separated by grain boundaries that are highly deformed. This research will explore to what extent such materials can be analyzed from the point of view of a jammed solid in order to understand the low shear strengths of such samples.

Memory formation, the ability to encode and read out a series of inputs, is a fundamental property of matter. There are a myriad of ways in which this occurs. Some are especially relevant to disordered matter, in which certain classes of memory can be stored in its geometric packing structure. The issue of memory formation raises another set of questions at the heart of how the complex energy landscape is organized and how it can

be manipulated to store information in a disordered solid. The proposed project will seek to understand the degree to which multiple memories can be stored in a single system and create a holistic understanding of how inputs can be used to create a desired response. This work will impact the broad area of memory formation in matter.

Recent Progress

We have performed computer simulations of particles with finite-ranged repulsive interactions at different packing fractions and with long-range interactions as a function of density. We can transform these packings into equivalent networks of springs. Starting with these networks and using our theoretical formulations and algorithms, we have been investigating what properties can be tuned into the material in order to create novel functionality. These include properties such as variable Poisson ratio, allosteric interactions and memory retention.

The ability to tune the response of mechanical networks has significant applications for designing meta-materials with unique properties. For example, we have already shown that the ratio G/B of the shear modulus G to the bulk modulus B can be tuned by over 16 orders of magnitude by removing only 2% of the bonds in an ideal spring network [1]. Such a pruning procedure allows one to create a network that has a Poisson ratio ν anywhere between the auxetic limit ($\nu = -1$) and the incompressible limit ($\nu = +1/(d - 1)$ in d dimensions). In another example, the average coordination number of a network controls the width of a failure zone under compression or extension [2]. Both these results are specific to tuning the global responses of a material. However, many applications rely on targeting a local response to a local perturbation applied some distance away. For example, allostery in a protein is the process by which a molecule binding locally to one site affects the activity at a second distant site [3]. Often this process involves the coupling of conformational changes between the two sites [4]. Disordered networks generically do not exhibit this behavior. However, we have found that such networks can be tuned to develop a specific allosteric structural response by pruning bonds.

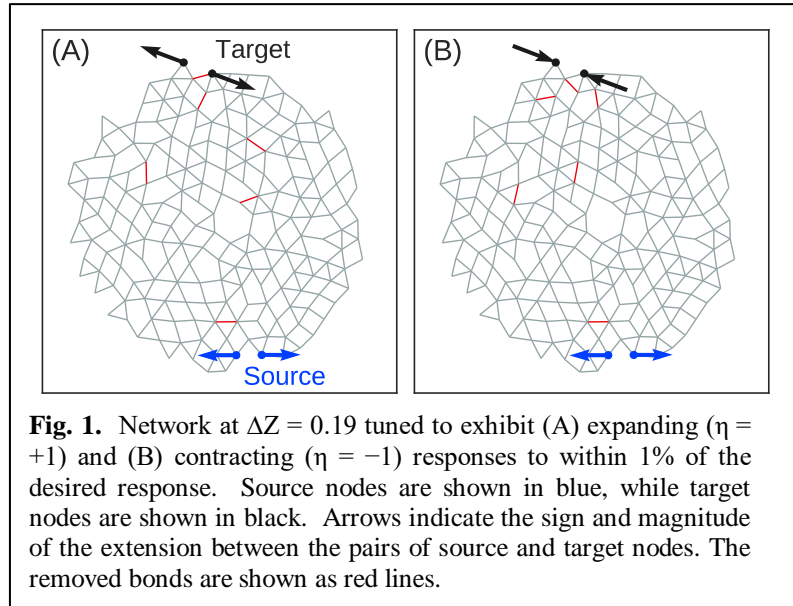
We have introduced a formalism for calculating how each bond contributes to the mechanical response anywhere in the network to an arbitrary applied source strain. This allows us to develop algorithms to control how the strain between an arbitrarily chosen pair of target nodes responds to the strain applied between an arbitrary pair of source nodes. In the simplest case, bonds are removed sequentially until the desired target strain is reached. For almost all of the initial networks studied, only a small fraction of the bonds need to be removed in order to achieve success. As was the case in tuning the bulk and shear moduli, we can achieve the desired response in a number of ways by pruning different bonds. We have extended our approach to manipulate multiple targets simultaneously from a single source, as well as to create independent responses to different locally applied strains in the same network.

We demonstrate the success of this method by reproducing our theoretical networks in macroscopic physical systems constructed in two dimensions by laser cutting a planar sheet and in three dimensions by using 3D printing technology. Thus, we have created a new class of mechanical meta-materials with specific allosteric functions.

Our central result is the ease and precision with which allosteric conformational responses can be created with only minimal changes to the network structure. This finding can be viewed as a first step towards understanding why allosteric behavior is so common in biopolymers [5]. It has been emphasized that the ability to control allosteric responses in folded proteins could lead to significant advances in drug design [6, 7]. While much work has focused on identifying, understanding and controlling pre-existing allosteric properties, the question of how to introduce new allosteric functions is relatively unexplored [8].

We applied our tuning approach to networks with free boundaries in both two and three dimensions. We characterized the connectivity of our networks by the excess coordination number $\Delta Z \equiv Z - Z_{\text{iso}}$ where Z is the average number of bonds per node and $Z_{\text{iso}} \equiv 2d - d(d + 1)/N$ is the minimum number of bonds needed for rigidity in a network with free boundary conditions [9]. For each trial, a pair of source nodes was chosen randomly on the network's surface, along with a pair of target nodes located on the surface at the opposing pole. The response of each network was tuned by sequentially removing bonds until the difference between the actual and desired strain ratios, η and η^* respectively, was less than 1%.

To demonstrate the ability of our approach to tune the response, we show results for $\eta = \pm 1$. Note that $\eta > 0 (< 0)$ corresponds to a larger (smaller) separation between the target nodes when the source nodes are pulled apart. Figure 1 shows a typical result for a 2-dimensional network: in Fig 1(A), the strain ratio has been tuned to $\eta = +1$ with just 6 (out of 407) bonds removed; Figure 1(B) shows the same network tuned to $\eta = -1$ with a different set of 6 removed bonds. The red lines in each figure indicate the bonds that were pruned.



Remarkably few bonds need to be removed in order to achieve strain ratios of $\eta = \pm 1$. In

two dimensions only about 5 bonds out of about 400 were removed on average ($\sim 1\%$); similarly, in three dimensions only about 4 bonds out of about 740 were removed on average ($\sim 0.5\%$). The failure rate is less than 2% for strain ratios of up to $|\eta| = 1$ in two dimensions and less than 1% in three dimensions. Therefore, not only does our algorithm allow for precise control of the response, it also works the vast majority of the time.

Future Work

Further work needs to be done to understand why removing specific bonds achieves the desired response. Our method of identifying the elements of the stress basis associated with individual bonds indicates that these stress states are fundamental to this understanding. The dependence on network size and node connectivity also needs to be understood in greater detail. The limits of our algorithm are not yet known, including the number of targets that can be controlled and the number of independent responses that can be tuned for networks of a given size and coordination. To understand experimental systems ranging from proteins to the macroscopic networks we have fabricated, we must extend the theory to include temperature, dynamics, pre-stress, bond bending, and nonlinear effects due to finite strains. Our approach provides a starting point for addressing these issues.

References

1. “The principle of independent bond-level response: tuning by pruning to exploit disorder for global behavior,” Carl P. Goodrich, Andrea J. Liu, and S. R. Nagel [1] *Phys. Rev. Lett.* **114**, 225501 (2015). arXiv 1502.02953
2. “The role of rigidity in material failure,” Michelle M. Driscoll, Bryan Gin-ge Chen, Thomas H. Beuman, Stephan Ulrich, S. R. Nagel, and Vincenzo Vitelli [1] *PNAS* accepted (2016). arXiv:1501.04227 [SEP]
3. “A chemical perspective on allosteric,” A. A. S. T. Ribeiro, V. Ortiz *Chemical Reviews* **116**, 6488–6502 (2016). [SEP]
4. “Local motions in a benchmark of allosteric proteins” M. D. Daily, J. J. Gray *Proteins: Structure, Function and Bioinformatics* **67**, 385–399 (2007). [SEP]
5. “Is allosteric an intrinsic property of all dynamic[1]proteins?” K. Gunasekaran, B. Ma, R. Nussinov *Proteins: Structure, Function and Bioinformatics* **57**, 433–443 (2004). [SEP]
6. “Allostery in disease and in drug discovery” R. Nussinov, C. J. Tsai *Cell* **153**, 293–305 (2013). [SEP]
7. “Allosteric sites: Remote control in regulation of protein activity” E. Guarnera, I. N. Berezovsky *Current Opinion in Structural Biology* **37**, 1 (2016).
8. “Controlling allosteric networks in proteins” N. V. Dokholyan *Chemical Reviews* **116**, :6463 (2016).
9. “Finite-size scaling at the jamming transition.” C. R. Goodrich, A. J. Liu, S. R. Nagel *Physical Review Letters* **109**, 095704 (2012).

Condensed Matter Theory

Lead PI – Mike Norman

Co-PIs – Olle Heinonen, Alex Koshelev, Peter Littlewood, Ivar Martin, Kostya Matveev
Materials Science Division, Argonne National Laboratory, Argonne, IL 60439

Project Scope

Condensed matter theory research programs are carried out in the areas of superconductivity, magnetism, and low dimensional systems, with a desire to make a major impact in a number of important endeavors, including the understanding of high temperature cuprate and pnictide superconductors, other transition metal compounds with novel properties such as quantum spin liquids and charge density waves, topological properties of metallic and nanostructured magnets, quantum phase transitions in strongly correlated electron systems, and transport in quantum wires, quantum dots, and spintronic devices.

Recent Progress

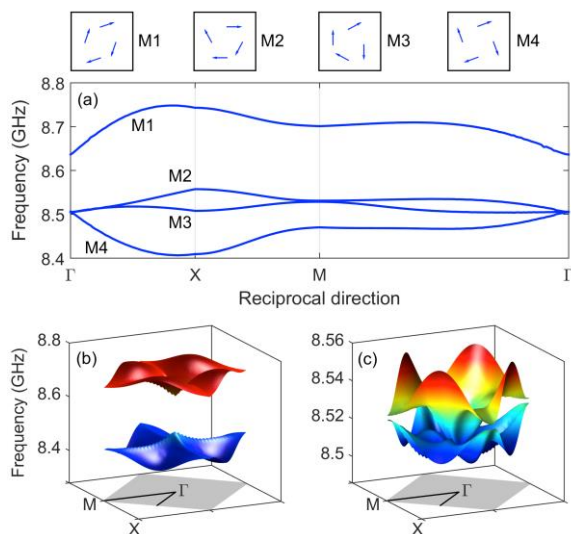


Fig. 1 - (a) Band structure of the vortex state. The insets show the magnetization vector configuration of the unit cell for each band. The FBZ surface plots of M1/M2 and M3 are shown in (b) and (c), respectively.

reconfigurable and tunable magnonic crystals that can be used as metamaterials for spin-wave-based applications at the nanoscale.

Artificial spin ices as reconfigurable magnonic crystals. Artificial square spin ices are composed of magnetic nano-elements arranged on a two-dimensional square lattice, such that there are four interacting magnetic elements at each vertex, leading to frustration. Using a semi-analytical approach, we showed that square ices exhibit a rich spin-wave band structure that is tunable both by external fields and the configuration of individual elements. Internal degrees of freedom can give rise to equilibrium states with bent magnetization at the element edges leading to characteristic excitations; in the presence of magnetostatic interactions these form

separate bands analogous to impurity bands in semiconductors. We used micromagnetic simulations to corroborate our semi-analytical approach. Our results show that artificial square ices can be viewed as

Second Harmonic Generation in Iridium Oxides. Iridates are thought to be a spin-orbit analog of cuprates, and along this line, second harmonic generation (SHG) has been detected and proposed to be due to orbital currents, as speculated for cuprates by Varma. In a rather exhaustive study, we have classified all sources of second harmonic generation that could occur in the iridates, and identified the appropriate multipole order parameter. We found that of the three possible magnetic ground states allowed by space group symmetry in Sr_2IrO_4 , two of the three generate an SHG signal. In the +++, state (here, the sign refers to that of the ferromagnetic moment in each of the four IrO_2 planes per unit cell), where one has a net ferromagnetic moment due to canting,

the order parameter is actually that of the ferromagnetic moment, with the SHG signal due to a coupling of two electric dipole transitions to one magnetic dipole transition. The other +--- state, with no net ferromagnetic moment, has an SHG signal due to inversion breaking (with the SHG signal due to coupling of three electric dipole transitions), the order parameter being due to a toroidal dipole or magnetic quadrupole. In neither case is it necessary to invoke orbital currents. The actual magnetic ground state of Sr_2IrO_4 , though, is the +--- state, which has no SHG signal. Therefore, if the SHG signal is due to magnetism, this implies that the laser pump used in the measurement has induced a non-equilibrium magnetic state.

Magneto-transport of nearly antiferromagnetic metals due to hot-spot scattering: Multiple-band electronic structure and proximity to an antiferromagnetic (AF) instability are key properties of iron-based superconductors. We explored the influence of scattering by the AF spin fluctuations on transport of multiple-band metals above the magnetic transition. A salient feature of this scattering is that it is strongly enhanced at the Fermi surface locations where nesting is perfect (“hot lines”). In the paramagnetic state, the enhanced scattering rate near the hot lines leads to anomalous behavior of the electronic transport in a magnetic field. We explored this behavior by analytically solving the Boltzmann transport equation. Our approach accounts for return scattering events and is more accurate than the relaxation-time approximation. The magnetic field dependences are characterized by two different field scales: the lower scale is set by the hot line width, and the higher scale is set by the total scattering amplitude. Conventional magneto-transport behavior is limited to magnetic fields below the lower scale. In the wide range between these two scales, the longitudinal conductivity has a linear dependence on the magnetic field and the Hall conductivity has a quadratic dependence. The predicted behavior is qualitatively consistent with the magneto-transport data in several compounds such as $\text{Ba}[\text{As}_{1-x}\text{P}_x]_2\text{Fe}_2$ and $\text{FeTe}_{0.5}\text{Se}_{0.5}$.

Wigner crystals. We studied one-dimensional quantum systems near the classical limit described by the Korteweg-deVries (KdV) equation. An important example of such a system is a one-dimensional Wigner crystal that emerges in quantum wires when the electron density is small. The elementary excitations near this limit are solitons and phonons. The classical description breaks down at long wavelengths, where quantum effects become dominant. We noticed that some exactly solvable models, such as the Lieb-Liniger model and the quantum Toda model, exhibit the same crossover. Using the known results for these models, we have been able to obtain analytic expressions for the spectra of the elementary excitations in the entire classical-to-quantum crossover. We further argued that the results obtained for exactly solvable models are universally applicable to all quantum one-dimensional systems with a well-defined classical limit described by the KdV equation, including the 1D Wigner crystals. We also showed that the ultimate quantum fate of the classical KdV excitations is to become fermionic particles and holes. Our results can be tested by measuring the dynamic structure factor of these systems.

Physics of quasicrystals. Crystallization is one of the most familiar, but hardest to analyze, phase transitions. The principal reason is that crystallization typically occurs via a strongly first-order phase transition, and thus a rigorous treatment would require

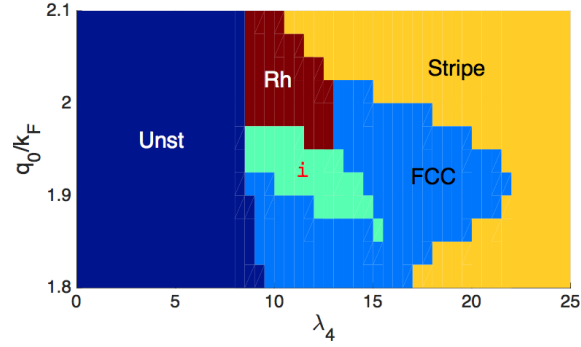


Fig. 2 - Variational phase diagram for $T = 0.1 E_F$ as a function of the local repulsion strength λ_4 and the ionic ordering vector q_0 . At small values of λ_4 (Unst), the fourth order GL terms become negative, signaling the need to consider higher order stabilizing terms. The icosahedral quasicrystal is denoted as i.

comparing energies of an infinite number of possible crystalline states with the energy of the liquid. A great simplification occurs when the crystallization transition happens to be weakly first order. In this case, *weak crystallization theory*, based on a GL expansion, can be applied. In its standard form, however, weak crystallization theory cannot explain the existence of a majority of the observed crystalline and quasicrystalline states. In our work, we have extended the weak crystallization theory to the case of metallic alloys. We identified a singular effect of itinerant electrons on the form of the weak crystallization free energy. It is geometric in nature, generating a strong dependence of the free energy on the angles between the ordering wave vectors of the ionic density. This leads to stabilization of the FCC, rhombohedral (Rh), and icosahedral quasicrystalline (i) phases, which are absent in a generic theory with only local interactions.

Vacancies in oxides. Using LDA+U, DMFT, and cluster methods, we have studied the energetics and spectroscopy of vacancies in the prototypical oxides LaAlO_3 and SrTiO_3 . In the latter, we find that depending on strain and carrier density, the O vacancy can change from a double donor to a single donor (which then has a moment). The observation of carrier density- and O vacancy-dependent magnetism is consistent with non-linear optical Kerr measurements by the Crooker group at Los Alamos, and with the gating of the magnetism by the Levy group at Pittsburg.

Future Plans

Artificial spin ices. Some of our preliminary results on artificial spin ices indicate that in the presence of Dzyaloshinskii-Moriya interactions that can arise, for example, by depositing the spin ice islands on a spin-orbit scatterer such as Pt, the magnonic bands attain a non-zero Chern number. This would imply that there are lower-dimensional edge modes with specific chiralities that are topologically protected. The possibility to manipulate and control such modes by reconfiguring the magnetization opens intriguing new avenues in the area of magnonics.

XMR in semimetals. In collaboration with Wai Kwok's group, we are looking into the nature of the novel transport properties of LaSb that were identified by Cava's group. We have found that the transport scattering rate inferred from the residual resistivity of this material is over a factor of 30 smaller than the scattering rate inferred from the Dingle temperature from quantum oscillation studies. This implies a strong suppression of backscattering, despite the fact that there is little evidence for any topological character to this material. The goal then is to understand what is causing this suppression, and relate this to the nature of the extreme magneto-resistance.

Wigner crystals. We plan to study the decay of solitons in a 1D Wigner crystal. Unlike the spectra of elementary excitations, the lifetimes cannot be obtained by studying exactly solvable models, as it is the deviations from exact integrability that give rise to finite decay rates. We will develop an approach in which the soliton is treated as a mobile impurity in a Luttinger liquid. We expect that the decay rate will grow with energy, but remain small at relevant energy scales.

Enhancing materials properties by irradiation. Motivated by the observed transient enhancement of superconductivity in several materials upon irradiation with high intensity pulses of THz light, we will analyze the Cooper instabilities in strongly driven electron-phonon systems. The light-induced non-equilibrium state of phonons should result in a simultaneous increase of the coupling constant and the scattering. The competition between these two effects could lead to an enhanced superconducting transition temperature in a broad range of parameters. This work may pave a new way for engineering high-temperature light-induced superconducting states.

Oxides. With a U Chicago student, A. Edelman, we have modeled the crossover from strong- to moderate coupling of the Frohlich polaron in SrTiO_3 which has recently been observed by

ARPES and tunneling (Hwang, SLAC). We will use this fit to see whether the strongly coupled optical phonon in SrTiO₃ can explain the anomalous low carrier density superconductivity.

Select Publications (2015-2016)

1. Broken vertex symmetry and finite zero-point entropy in the artificial square ice ground state, S. Gliga, A. Kakay, L. Heyderman, R. Hertel, O. Heinonen, Phys. Rev. B **92**, 060413 (2015).
2. Reconfigurable spin wave band structure of artificial square spin ice, E. Iacocca, S. Gliga, R.L. Stamps, O. Heinonen, Phys. Rev. B **93**, 134420 (2016).
3. Generation of magnetic skyrmion bubbles by inhomogeneous spin-Hall currents, O. Heinonen, W. Jiang, H. Somaily, S.G.E. te Velthuis, A. Hoffmann, Phys. Rev. B **93**, 094407 (2016).
4. Dynamic response of an artificial square spin ice, M.B. Jungfleisch, W. Zhang, E. Iacocca, J. Sklenar, J. Ding, W. Jiang, S. Zhang, J.E. Pearson, V. Novosad, J.B. Ketterson, O. Heinonen, A. Hoffmann, Phys. Rev. B **93**, 100401 (2016).
5. Nanoscale skyrmions in a non-chiral metallic multiferroic: Ni₂MnGa, C. Phatak, O. Heinonen, M. de Graef, A. Petford-Long, Nano Letters **16**, 441 (2016).
6. Vector optical activity in the Weyl semimetal TaAs, M.R. Norman, Phys. Rev. B **92**, 241116 (2015).
7. Ferromagnetic domain behavior and phase transition in bilayer manganites investigated at the nanoscale, C. Phatak, A.K. Petford-Long, H. Zheng, J.F. Mitchell, S. Rosenkranz, M.R. Norman, Phys. Rev. B **92**, 224418 (2015).
8. Dichroism as a probe for parity-breaking phases of spin-orbit coupled metals, M.R. Norman, Phys. Rev. B **92**, 075113 (2015).
9. Linear dichroism and the nature of charge order in underdoped cuprates, M.R. Norman, Phys. Rev. B **91**, 140505 (2015).
10. Emergence of coherence in the charge-density wave state of 2H-NbSe₂, U. Chatterjee, J. Zhao, M. Iavarone, R. Di Capua, J.P. Castellan, G. Karapetrov, C.D. Malliakas, M.G. Kanatzidis, H. Claus, J.P.C. Ruff, F. Weber, J. vanWezel, J.C. Campuzano, R. Osborn, M. Randeria, N. Trivedi, M.R. Norman, S. Rosenkranz, Nature Comm. **6**, 6313 (2015).
11. Fate of classical solitons in one-dimensional quantum systems, M. Pustilnik and K.A. Matveev, Phys. Rev. B **92**, 195146 (2015).
12. Decay of Bogoliubov excitations in one-dimensional Bose gases, Z. Ristivojevic and K.A. Matveev, Phys. Rev. B **94**, 024506 (2016).
13. Weak crystallization theory of metallic alloys, I. Martin, S. Gopalakrishnan, E. Demler, Phys. Rev. B **93**, 235140 (2016).
14. Nematic quantum liquid crystals of bosons in frustrated lattices, G. Zhu, J. Koch, I. Martin, Phys. Rev. B **93**, 144508 (2016).
15. 1/f^a noise and generalized diffusion in random Heisenberg spin systems, K. Agarwal, E. Demler, I. Martin, Phys. Rev. B **92**, 184203 (2015).
16. Electronic properties of 8-Pmmn borophene, A. Lopez-Bezanilla, P.B. Littlewood, Phys. Rev. B **93**, 241405 (2016).
17. Preface: Special Topic on Materials Genome, C.L. Phillips, P. Littlewood, APL Materials **4**, 053001 (2016).
18. Spectroscopic properties of oxygen vacancies in LaAlO₃, O.A. Dicks, A.L. Shluger, P.V. Sushko, P.B. Littlewood, Phys. Rev. B **93**, 134114 (2016).
19. Plentiful magnetic moments in oxygen deficient SrTiO₃, A. Lopez-Bezanilla, P. Ganesh, P.B. Littlewood, APL Materials **3**, 100701 (2015).
20. Magnetism and metal-insulator transition in oxygen-deficient SrTiO₃, A. Lopez-Bezanilla, P. Ganesh, P.B. Littlewood, Phys. Rev. B **92**, 115112 (2015).

Symmetry Effects on the Interplay between Strong Correlation and Spin-Orbit Coupling

Principal investigator: Warren E. Pickett
Department of Physics, University of California Davis
Davis CA 95616
wepickett@ucdavis.edu

Project Scope

Our recent work, and that of others as well, has demonstrated that the interplay of strong correlations and large spin-orbit coupling (SOC) can lead to new physical phases, some with topological character of the electronic state being the most exciting. In a few different contexts, we have found that the effect of even rather weak SOC can be magnified by strong interactions. However, In our several studies of (001) interfaces and thin film overlayers of perovskite transition metal oxides (viz. LaAlO_3 on a SrTiO_3 substrate), broken charge and spin symmetry phases were common but SOC was never a factor.[1] The suggestion that buckled bilayer honeycomb lattices of open-shell 3d ions, produced by (111) layer growth of 5d-based perovskites, provides a new vista for strong interaction-large SOC-broken symmetry interplay, which has led us to turn our attention to such systems.[2-6] Many of these findings have been reported.[7-9] Symmetry in itself is found to be a central consideration. Although sometimes couched in terms of global (space group; magnetic order) terms, it seems that sometimes it is the local symmetry of an open-shell ion that is crucial: large Hubbard U encourages (Jahn-Teller) distortions, lowering symmetry; SOC produces large orbital moments, thus large magnetocrystalline anisotropy and enhanced effects of SOC. A second honeycomb lattice system that contains a Chern phase in its generalized phase diagram is the ferromagnetic Ising Mott insulator $\text{BaFe}_2(\text{PO}_4)_2$,[10] where U(Fe) is so large as to make the Chern phase inaccessible.[10,11] In both systems the crucial interplay is among large interaction, strong SOC, and symmetry.

This project addresses a number of DOE/BES priorities. Electronic correlations are addressed specifically: most of the applications are to strongly correlated materials, but there are several other characteristics that modulate the effects of strong interactions. We address materials design (MGI), not in a high throughput manner such as several groups are doing well, but in making applications to atomic layer-by-layer grown materials that experimentalists are gaining experience with. Several competing energy scales make the systems we study less amenable to high throughput approaches. Another aspect of our design vision is to replace oxides with nitrides, for hole transport reasons.[12,13] Phenomena studied include magnetism, quantum phase transitions, thermoelectric behavior, and occasionally having superconducting potential in mind. Topological characters of Hamiltonians (of real materials) are being given priority in this project. Design/prediction of topological insulators and semimetals is an active area for us, and understanding their origins in real materials is one focus. Our discovery of a large Chern number phase is driving us to pursue a more thorough understand of topological indices.

Recent Progress

Below are some highlights of progress over the past 2-3 years, including a breakthrough on predicted Chern insulators, reported in a submitted manuscript.[5,11]

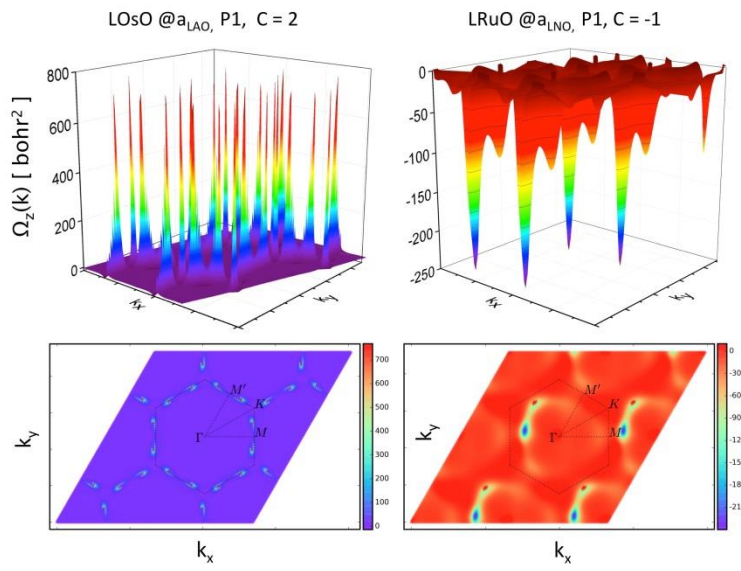
Buckled honeycomb lattices of 3d ions. The PI, in collaboration with Pentcheva's group (Univ. of Duisburg-Essen) involving exchange visits, initially studied the SrTiO_3 bilayer encased in LaAlO_3 , "a three-orbital strongly correlated generalization of graphene" (subtitle of our paper). Restricted to a symmetric honeycomb lattice, a ferromagnetic Dirac-point semimetal (Weyl semimetal) phase was found for the ground state. Allowing inversion symmetry breaking, the system was driven to a charge-ordered multiferroic (ferromagnetic, ferroelectric) state. Applying the same density functional theory for correlated materials (DFT+U) to the nickelate bilayer (LaNiO_3), again a Mott insulating ferromagnetic phase was obtained, but in addition the possibility of strain-controlled orbital engineering was demonstrated.

Aiming at determining whether a Chern insulating state (quantum Hall state without applied magnetic field) can be designed in this system, a study of the entire $3d$ series of transition metal atoms was carried out. In three cases, the Dirac point, Weyl insulator phase was obtained when threefold symmetry was imposed, however all three preferred symmetry-broken (charge ordered) and normal (Mott) insulating ground states. It was however discovered that in relaxing from the Weyl semimetal state to the Mott insulator, some of them passed through a Chern insulating phase.[4,11] It was clear that a combination of too large Hubbard U (and resulting Jahn-Teller distortion) and too small SOC strength, were limiting factors in achieving the quantum anomalous Hall phase.

The most promising direction was not difficult to find: moving to $4d$ or perhaps $5d$ ions would decrease U and increase SOC, both of which should be helpful for supporting a Chern phase. We performed a study of the Mn and Fe columns of transition metal series. At the same time, to assess the effect of strain, the substrate (LaAlO_3 what actually used) was taken to have the lattice constant of both LaAlO_3 and LaNiO_3 , differing by 1.8%. In short: Chern insulating states have been obtained for both bilayer LaOsO_3 and bilayer LaRuO_3 , each requiring a particular strain (different for the two cases). A collaboration with an experimental group is being formed to follow up on our predictions.

Chern phase in the generalized phase diagram of the ferromagnetic Mott insulator $\text{BaFe}_2(\text{PO}_4)_2$. Almost two years ago our collaboration with Kwan woo Lee's group (Korea University) had shown this honeycomb lattice compound, which is electronically two dimensional, to be an unusual ferromagnetic Mott insulator. Its spin $S=2$ ion induces, surprisingly for a 3d element, a large $0.7\mu\text{B}$ orbital moment (essentially $L=1$), accounting both for the extremely large magnetocrystalline anisotropy (Ising nature) and the observed Curie-Weiss moment. In work submitted, it is demonstrated that this compound would be a Chern insulator if U would have been less than 3.5 eV; the large U makes the Mott gap larger than that for which band entanglement can be sustained, given the modest strength of spin-orbit coupling in iron. In this incipient Chern phase a puzzling behavior is found: the Chern number

changes by three, or even by six, through complexes of 1-3 bands. Only changes by multiples of three are obtained. Already C=3 it a very large Chern number for a real material; the prospect of C=6 or more is truly exciting, and as already mentioned, truly puzzling at present, as there is little understanding of what it is in the electronic structure, or the Hamiltonian, that determines the magnitude of the Chern number.



Colorplots of the Berry curvature (top, perspective view; bottom, top view) of the two designed quantum anomalous Hall insulators (Chern insulators). Left side: buckled bilayer of LaOsO_3 ; with Chern number of 2; right side, buckled bilayer of LaRuO_3 with Chern number of -1. The differing Chern numbers indicate differing Hall current (by a factor of two) and different direction of the current (sign of the Chern number). The characters of the Berry curvature are very different: concentrated in the sharp peaks in the osmate, while more diffuse in the zone in the ruthenate.

Charge-ordering: where's the charge?

The phenomenon of charge-ordering [14-16] has presented longstanding interest in materials research. Charge order accounts for insulating phases where average ionic charges would indicate unfilled band and hence conduction. We have accumulated several examples (not listed in the references) in which insulating states are characterized by ‘charge-ordered’ ions that have identical local charges. From our quantitative studies, the concept of charge-ordering is robust, but must be understood in more general terms. The charge of ‘charge order’ is not an ionic attribute – a Ni^{2+} has the same charge density as a Ni^{3+} ion – rather it is a characteristic of an ion in its local environment. “Charge states” can be quantified in terms of Wannier functions: a Ni^{2+} site is the center of eight occupied ‘3d’ WFs, while a Ni^{3+} site hosts only seven. This behavior has been quantified for several cases (YNiO_3 , CaFeO_3 , AgNiO_2 , V_4O_7 , AgO , $\text{La}_4\text{Ni}_3\text{O}_8$, $\text{La}_3\text{Ni}_2\text{O}_6$).

Future Plans.

1. Study the mixed osmate-ruthenate buckled bilayer and determine whether there is a Chern insulating state as strain is varied (the osmate and ruthenate are individually Chern insulators, but with different strains).
2. Work with experimentalists in attempting to verify our designed Chern phases in transition metal oxide honeycomb lattice layers.
3. Pursue a deeper understanding of the origin of the large Chern numbers (jumping by 3 and sometimes 6 through a band complex) in $\text{BaFe}_2(\text{PO}_4)_2$. Study the Ru analog.

Selected Publications

1. R. Pentcheva, R. Arras, K. Otte, V. G. Ruiz Lopez, and W. E. Pickett, Termination control of electronic phases in oxide thin films and interfaces: $\text{LaAlO}_3/\text{SrTiO}_3(001)$, Phil. Trans. Roy. Soc. A 370, 4904 (2012).
2. D. Doennig, W. E. Pickett, and R. Pentcheva, Massive Symmetry Breaking in $\text{LaAlO}_3/\text{SrTiO}_3(111)$ Quantum Wells: a Three-Orbital, Strongly Correlated Generalization of Graphene, Phys. Rev. Lett. 111, 126804 (2013).
3. D. Doennig, W. E. Pickett, and R. Pentcheva, Confinement-driven Transitions between Topological and Mott Phases in $(\text{LaNiO}_3)_N/(\text{LaAlO}_3)_M(111)$ Superlattices, Phys. Rev. B 89, 121110 (2014).
4. D. Doennig, W. E. Pickett, and R. Pentcheva, Design of Chern and Mott Insulators in Buckled 3d-oxide Honeycomb Bilayers, Phys. Rev. B 93, 165145 (2016).
5. H. Guo, S. Gangopadhyay, R. Pentcheva, and W. E. Pickett, Wide Gap Chern Mott Insulating Phases achieved by Design (submitted, 2016).
6. M.-C. Jung, Y.-J. Song, K.-W. Lee, and W. E. Pickett, Octahedral Rotations, Hybridization, and Correlation in Insulating Antiferromagnetic Perovskite NaOsO_3 , Phys. Rev. B 87, 115119 (2013).
7. H. B. Rhee and W. E. Pickett, Strong Interactions, Narrow Bands, and Dominant Spin-orbit Coupling in Mott Insulating Quadruple Perovskite $\text{CaCo}_3\text{V}_4\text{O}_{12}$, Phys. Rev. B 90, 205119 (2014).
8. Y.-J. Song, K.-H. Ahn, K.-W. Lee, and W. E. Pickett, Unquenched eg1 Orbital Moment in the Mott Insulating Antiferromagnet KO_3O_4 , Phys. Rev. B 90, 245117 (2014).
9. K.-W. Lee and W. E. Pickett, Organometallic-like localization of 4d-derived spins in an Inorganic conducting niobium suboxide, Phys. Rev. B 91, 195152 (2015).
10. Y.-J. Song, K.-W. Lee, and W. E. Pickett, Large Orbital Moment and Spin-orbit Enabled Mott Transition in the Ising Fe Honeycomb Lattice of $\text{BaFe}_2(\text{PO}_4)_2$, Phys. Rev. B 92, 125109 (2015).
11. Y.-J. Song, K.-H. Ahn, W. E. Pickett, and K.-W. Lee, Following the Chern Insulator to Mott Insulator Transition in High Chern Number Ferromagnetic $\text{BaFe}_2(\text{PO}_4)_2$, submitted (2016).
12. A. S. Botana, V. Pardo, and W. E. Pickett, Nitride Multilayers as a Platform for Parallel Two-dimensional Electron-Hole Gases: $\text{MgO}/\text{ScN}(111)$, Phys. Rev. B 93, 085125 (2016).
13. A. S. Botana, V. Pardo, and W. E. Pickett, Thermoelectric Device at the Nanoscale: All-3d Electron-Hole Bilayers in $\text{CrN}/\text{MgO}(111)$ Multilayers, submitted (2015).
14. W. E. Pickett, Y. Quan, and V. Pardo, Charge States of Ions, and Mechanisms of Charge-Ordering Transitions, J. Phys.: Condens. Matter 26, 274203 (2014).
15. Y. Quan and W. E. Pickett, Analysis of charge states in the mixed valence ionic insulator AgO , Phys. Rev. B 91, 035121 (2014).
16. A. S. Botana, V. Pardo, W. E. Pickett, and M. R. Norman, Charge Ordering in $\text{Ni}^{1+}\text{Ni}^{2+}$ Nickelates: $\text{La}_4\text{Ni}_3\text{O}_8$ and $\text{La}_3\text{Ni}_2\text{O}_6$, Phys. Rev. B(RC) (2016, in press).

Emergent properties of highly correlated electron materials

Principal investigator: Professor Srinivas Raghu

Department of Physics, Stanford University and SLAC National Accelerator Laboratory
Stanford, CA 94305

sraghu@stanford.edu

Project Scope

The primary goal of this program has been to explore robust low energy properties of correlated electron materials in the context of effective model systems. These effective models include simplified Hamiltonians and effective field theories and involve far fewer microscopic degrees of freedom than are present in an actual system. This in turn allows us to identify well-controlled solutions to the theory in various limits and to extract the qualitative, robust features present in such solutions that may carry over to real materials. Specific issues that have been addressed in this project in the past two years include: 1) superconductivity near a metallic quantum critical point, 2) phenomenology of the magnetic field tuned superconductor to insulator transition, 3) physics of a half-filled Landau level 4) phenomenology of heavy fermion materials, and 5) study of quantum materials and unconventional superconductivity.

Recent Progress

Below are some highlights of progress made in the past 2 years (a more comprehensive publication list is appended below the highlights).

Superconductivity near a metallic quantum critical point – The problem of superconductivity near quantum critical points (QCPs) remains a central topic of modern condensed matter physics. Near a QCP, there is a competition between two offsetting effects. First, near criticality, the order parameter mediates strong, long-ranged attractive interactions (the range is set by the correlation length, which diverges at the QCP). Second, the order parameter leads to a much greater quasiparticle scattering and decay rate, which undermines a Landau Fermi liquid description. This in turn invalidates BCS theory and all estimation of pairing scales that follow from it. In recent work, the PI, in collaboration with Gonzalo Torroba (former Stanford postdoc, now faculty member at Bariloche) and Huajia Wang (former Stanford student, now postdoc at UIUC) addressed these competing effects in the context of a solvable model of a metallic quantum critical point. We showed that the two effects - namely the enhanced pairing and the destruction of Landau quasiparticles - can offset one another, resulting in stable "naked" quantum critical points without superconductivity. However, the resulting quantum critical metal exhibits strong superconducting fluctuations on all length scales. The result was established using a large N theory in $d=3-\epsilon$ spatial dimensions ($\epsilon \ll 1$). While this is certainly an artificial limit when it comes to actual quantum materials, the solutions obtained shed considerable light on the nature of superconductivity near quantum critical

points. Our theory interpolates from one extreme, where the superconducting scale far overpowers the effects of quasiparticle destruction, to another extreme where quasiparticle destruction and non-Fermi liquid behavior overpower the low energy dynamics, leading to a naked, quantum critical point without a superconducting dome (See Fig. 1). A multicritical point, where superconductivity just begins to develop at the quantum critical point, separates these extreme limits. The multicritical point is somewhat exotic, and related to the Kosterlitz-Thouless transition of the 2d XY model. While it remains to be seen whether such solutions reflect the actual behavior of quantum materials, the theory studied here leads to testable experimental predictions and signatures in numerical treatments of the problem.

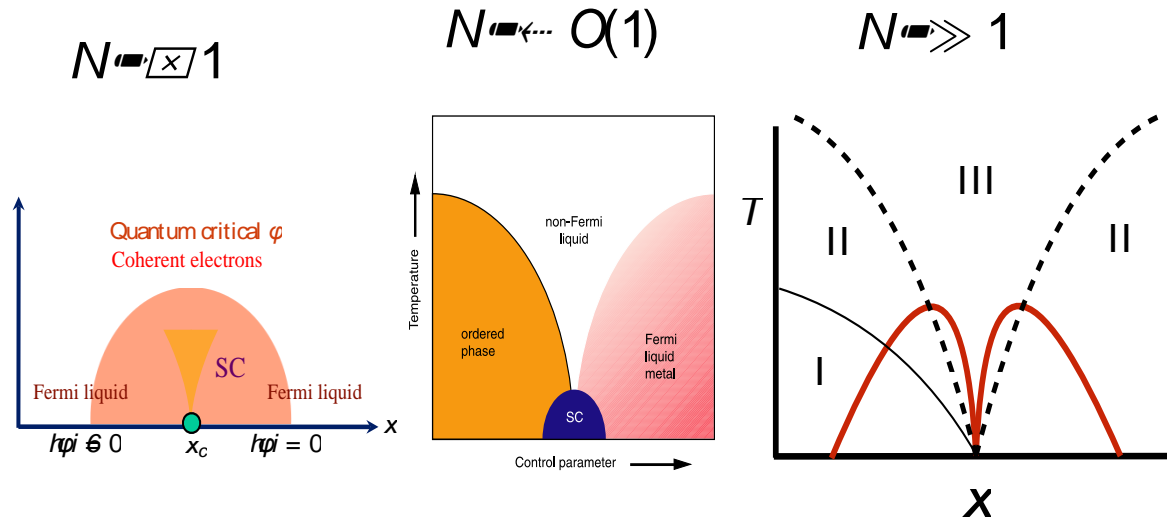


Figure 1. Our theory has two small parameters, $1/N$ and ϵ . Their ratio, $N\epsilon$, however is arbitrary. In our analysis, we find that when $N\epsilon \ll 1$, superconductivity overwhelms non-Fermi liquid behavior, whereas in the opposite limit, when $N\epsilon \gg 1$, non-Fermi liquid behavior dominates, resulting in a “naked” quantum critical point. When this ratio $N\epsilon$ is of order unity, one has a situation where enhanced superconductivity arises out of a normal state without well-defined quasiparticles.

Magnetic field tuned superconductor-insulator transition in two dimensions – the PI, in collaboration with former postdoctoral scholar Michael Mulligan (now faculty member at UC Riverside) has been investigating universal properties associated with the two dimensional magnetic field-tuned superconductor-insulator (SIT) quantum phase transition. In several thin films including InOx thin films, where disorder is strong, a magnetic field tuned SIT has been observed, with the critical resistance at the SIT being close to the Cooper pair quantum of resistance, namely $h/4e^2$. This value of resistance is consistent with the notion of self-duality at the transition. However, in thin films where the disorder is somewhat less, instead of a direct SIT with self-duality, a stable metallic phase has been observed. Building on an influential theory of the SIT ‘dirty boson’ description, we suggested that the metallic region is analogous to the composite Fermi liquid observed about half-filled Landau levels of the two-dimensional electron gas. The analog of the fermion here is a bound state of a Cooper pair and a vortex. Such a charge/flux composite exhibits Fermi statistics, and is a natural low energy degree of freedom in the vicinity of a self-dual SIT. The formulation of the SIT and related metallic phase transition in terms of fermionic variables enables a natural explanation not just of

the existence of a metallic phase, but also of a self-dual SIT, which in the language of fermions amounts to a particle-hole symmetry. Thus, direct SIT with self-duality maps onto a quantum Hall plateau transition with (disorder averaged) particle-hole symmetry. Our fermionic approach to the SIT also leads to several computational projects involving the study of the superconductor-insulator transition all of which are ongoing. Lastly, the fermionic description may enable an understanding of an unconventional insulating phase known as the Hall insulator, which persists in the vicinity of the SIT and the quantum Hall to insulator transition. More broadly, the hypothesis that composite fermions underlie both the description of both quantum Hall transitions and SITs leads to a number of testable predictions as the two systems complement and inform one another.

Emergent particle-hole symmetry of the half-filled Landau level -

The PI, with Michael Mulligan (former Stanford postdoc, now faculty member at UC Riverside) and Matthew Fisher (KITP, UCSB) investigated the possibility that particle hole symmetry in the lowest Landau level at half filling arises as an emergent low energy symmetry. Specifically, we started with the traditional approach to

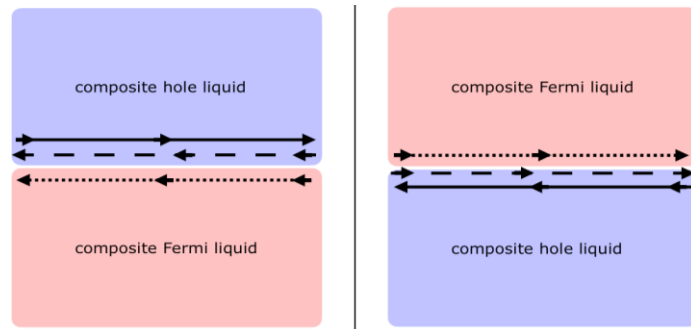


Figure 3. The left side of the figure depicts the CFL in the lower half-plane and the CHL in the upper half-plane. The right side shows the particle-hole transformed version of the left half. Chiral edge present at the boundary between a CFL and vacuum is denoted by the short dashed line. The chiral field corresponding to the edge of a CHL is shown by the long dashed line. At the interface between the CFL and CHL, there is also a chiral charged edge mode equivalent to the edge mode of a filled Landau level. This mode ϕ_{LL} is denoted by the solid line.

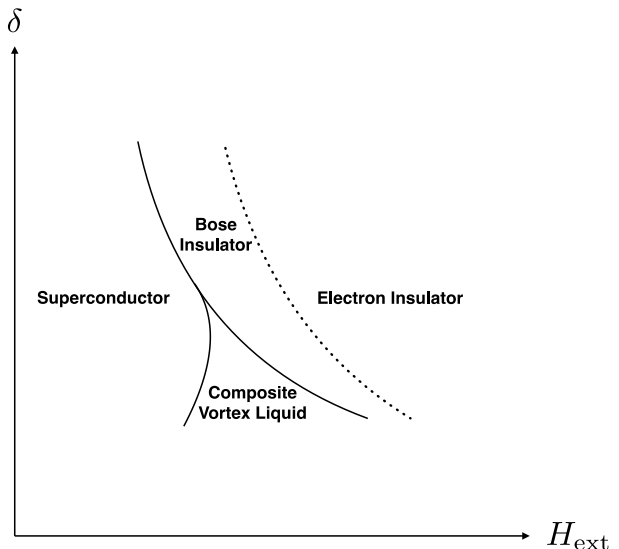


Figure 2. Conjectured $T=0$ phase diagram in the vicinity of a SIT as a function of external field and disorder. The solid lines denote phase transitions, while the dashed line denotes the boundary (either phase transition or crossover) between a Bose insulator of Cooper pairs and an electron insulator. A similar phase diagram obtains for a 2D Electron gas in the quantum Hall regime with the following relabeling: Superconductor \leftrightarrow Integer quantum Hall effect, Bose insulator \leftrightarrow Hall insulator, and composite vortex liquid \leftrightarrow composite Fermi liquid.

the half-filled Landau level – an effective field theory known as the composite Fermi liquid pioneered by Halperin, Lee and Read. In this theory composite fermions arise when flux is attached to electrons in a half-filled Landau level and particle-hole symmetry is manifestly broken. However, an equivalent starting point is one where one starts with a filled Landau level, depletes electrons (or equivalently, adds holes) to the point of half-filling. One then attaches flux to the holes, and the resulting composite hole description – which also breaks particle-hole symmetry – is another viable description of the half-filled Landau level. In recent

work, we constructed a particle-hole symmetric theory by studying a system consisting of alternating quasi-one-dimensional strips of composite Fermi liquid (CFL) and composite hole liquid (CHL), both of which break particle-hole symmetry (Figure 3). When the CFL and CHL strips are identical in size, the resulting state is manifestly invariant under the combined action of a particle-hole transformation with respect to a single Landau level (which interchanges the CFL and CHL) and translation by one unit, equal to the strip width, in the direction transverse to the strips. Gauge invariance requires the existence of gapless edge modes at the interface between the CFL and CHL. Out of these modes, we constructed a neutral Dirac fermion coupled to an emergent U(1) gauge field. Thus, at distances long compared to the strip width, we demonstrated that the system is described by a Dirac fermion coupled to an emergent gauge field, with an anti-unitary particle-hole symmetry, precisely the form conjectured by Son to be the low energy description of a particle-hole symmetric half-filled Landau level.

Future Plans

Non-Fermi liquids – The PI will develop theory of superconductivity near a quantum critical point focusing on finite temperature correlations and crossovers using methods of finite size scaling. He will also complement the analytic studies with phenomenological studies of experiments investigating quantum critical metals such as the cuprates and ruthenates, and will consider signatures of scaling laws in numerical simulations.

Superconductor-insulator and quantum Hall transitions – The PI is currently studying these transitions using DMRG techniques. On the phenomenological side, the PI is studying quantum oscillation signatures of half-filled Landau levels, and is constructing a theory of the Hall insulator phase. Finally from the standpoint of effective field theory, the PI is working on examples of renormalization group fixed points with *finite disorder strength*, which exhibit diffusive metal behavior in 2 spatial dimensions. Such a proposal goes against the wisdom of the scaling theory of localization, which argues against the presence of diffusion in two spatial dimensions. If realized, such a diffusive metal fixed point would ultimately describe the behavior of half-filled Landau levels and metallic phases in the vicinity of SIT, when both disorder and interactions lead to important effects.

Unconventional superconductivity – The PI has been focusing on heavy fermion superconductors where ferromagnetism and superconductivity both coexist. In the past, the PI has written a paper on the material UCoGe. In the future, the PI will consider the behavior of URhGe, which exhibits ferromagnetism and superconductivity at ambient pressure. The PI will study the effect of Lifshitz transitions on the superconductivity of this material.

Publications

1. S. Lederer, W. Huang, E. Taylor, S. Raghu, and C. Kallin, “Suppression of spontaneous currents in Sr_2RuO_4 by surface disorder,” Phys. Rev. B **90**, 134521 (2014).
2. H. Watanabe, S. Parameswaran, S. Raghu, and A. Vishwanath, “Anomalous Fermi liquid phase in metallic skyrmion crystals”, Phys. Rev. B **90**, 045145 (2014).

3. S. Riggs, M. Shapiro, A. Maharaj, S. Raghu, E. Bauer, R. Baumbach, P. Giraldo-Gallo, M. Wartenbe, and I.R. Fisher, "Evidence for a nematic component to the hidden order parameter in URu_2Si_2 from differential elastoresistance measurements", *Nature Comm.* **6**, 6425 (2015).
4. A. Maharaj, P. Hosur and S. Raghu, "Crisscrossed stripe order from interlayer tunneling in hole-doped cuprates," *Phys. Rev. B* **90**, 125108 (2014).
5. A. Liam Fitzpatrick, S. Kachru, J. Kaplan, S. Raghu, G. Torroba, and H. Wang, "Enhanced pairing of quantum critical metals near $d=3+1$," *Phys. Rev. B* **92**, 045118 (2015).
6. P. Hlobil, A. Maharaj, M. Shapiro, I. Fisher, and S. Raghu, "Elastoconductivity as a probe of broken mirror symmetries," *Phys. Rev. B* **92**, 035148 (2015).
7. W. Cho, C. Platt, R. Mackenzie, and S. Raghu, "Spin-triplet superconductivity in a weak-coupling Hubbard model for the quasi-one-dimensional compound $\text{Li}_{0.9}\text{Mo}_6\text{O}_{17}$," *Phys. Rev. B* **92**, 134514 (2015).
8. S. Raghu, G. Torroba, and H. Wang, "Metallic quantum critical points with finite BCS couplings," *Phys. Rev. B* **92**, 205104 (2015) [Editor's selection].
9. M. Mulligan and S. Raghu, "Composite fermions and the field-tuned superconductor-insulator transition," *Phys. Rev. B* **93**, 205116 (2016).
10. A. Cheung and S. Raghu, "Topological properties of ferromagnetic superconductors," *Phys. Rev. B* **93**, 134516 (2016).
11. C. Platt, W. Cho, R. McKenzie, R. Thomale, and S. Raghu, "Spin-orbit coupling and odd-parity superconductivity in the quasi-one-dimensional compound $\text{Li}_{0.9}\text{Mo}_6\text{O}_{17}$," *Phys. Rev. B* **93**, 214515 (2016)
12. M. Mulligan, S. Raghu, and M.P.A. Fisher, "Emergent particle-hole symmetry in the half-filled Landau level," *Phys. Rev. B* [Editor's selection], In press.

Theoretical and Computational Studies of Functional Nanomaterials

Principle Investigator: Talat S. Rahman

Department of Physics, University of Central Florida, Orlando, Florida 32816

Project Scope

Our work focuses on understanding structure-function relationship in nanomaterials so as to enable the long term goal of rational material design. We are particularly interested in understanding factors that control the magnetic and optical properties of these materials and their response to ultrafast external fields. We thus develop and apply techniques which provide accurate description of excited and bound states, correlation effects and non-adiabatic, non-equilibrium behavior of nano-scale systems. Our efficient Density Functional Theory + Dynamical Mean-Field Theory (DFT+DMFT) algorithm allows proper incorporation of electron-electron interaction. While our density matrix version of Time-Dependent Density Functional Theory (TDDFT) makes feasible examination nonlinear effects (e.g. trions, biexcitons, exciton-plasmon and plasmon-phonon coupled states) in nanostructures. For out-of-equilibrium phenomena we construct exchange-correlation functionals by merging DMFT and TDDFT. Our systems of interest include transition metal nanoalloys and dichalcogenides and magnetic nanoparticles.

Recent Progress

A. Further developments in techniques beyond DFT

In the past several years we have developed three codes that we continue to refine. One is our density matrix based formulation of time dependent density functional theory (DM-TDDFT) which can be applied efficiently to examine multiple excitations and time evolution of nanoscale systems of interest, in-equilibrium and out-of-equilibrium. The other is our DMFT+DFT code in which the single impurity problem in DMFT involves finding of the single-electron Green's function for the given site/orbital by treating the rest of the electrons in the system as a bath. Here the approximate Iterative Perturbation Theory (IPT) solver, in which the expression for the single-electron self-energy is a function of second order in the local Coulomb repulsion parameter and chosen such that the resulting self-energy satisfies known limiting cases (such as the high-frequency and large-Coulomb repulsion limits), has been supplemented by the more accurate one based on the Quantum Monte Carlo (QMC) method.

Non-adiabatic exchange correlation kernel for strongly correlated systems (TDDFT+DMFT): We have proposed a new method for examining spectral properties and out-of-equilibrium response of strongly-correlated electron systems through the merger of time-dependent density functional theory (TDDFT) and dynamical mean-field theory (DMFT). The key element in the theory- the exchange-correlation kernel – is obtained from the expression in DMFT for the two-particle susceptibility and the electron self-energy for a multi-orbital effective Hubbard Hamiltonian.

B. Some highlights of applications of DFT based methods to systems of interest

1. Bound-state dynamics during the ultrafast response of the bilayer MoS₂-WS₂

We have used our DM-TDDFT approach [1] to calculate the binding energies of coupled electron and hole states -excitons, trions and biexcitons - in monolayer MoS₂ and WS₂ and bilayer MoS₂-WS₂ systems excited by an ultrafast laser pulse. Our results are in a good agreement with

experimental data [2-13], confirming the experimental finding that the electrons and holes form strongly-bond states in mono- and bi-layer transition-metal dichalcogenides (Table 1). As the next step, we have performed time-resolved study of the dynamics of electrons and holes, including formation and dissociation of bound states. In particular, we find that the experimentally-observed [12] ultrafast (50fs) inter-layer MoS₂ to WS₂ hole migration in MoS₂-WS₂ may be attributed to unusually large delocalization of the hole state which extends far into the inter-layer region (Fig. 1). We have also calculated the exciton radiative lifetimes in the three systems (Table 2), and show that these times are longer than the inter-layer hole migration time, which makes the process of the charge separation in MoS₂-WS₂ feasible. In addition, we have also analyzed the process of exciton dissociation in presence of external field, and found that the dissociation happens in rather weak fields for all three systems (Table 2), which have applications in photovoltaic devices.

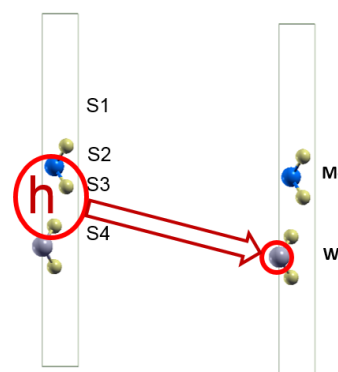
Table 1. Exciton, trion and biexciton binding energies (meV) from DM-TDDFT (screened Slater exchange-correlation (XC) kernel). Experimental results are presented in parenthesis.

System	exciton	trion	biexciton
1L MoS ₂	361 (220-570) ^{2,3}	40(18-40) ⁴⁻⁶	25(40,60) ⁷
1L WS ₂	410 (320-700) ⁸⁻¹⁰	47(30) ¹⁰	44(65) ¹⁰
MoS ₂ -WS ₂	180 (~100) ^{11,12}	12	10

Table 2. Exciton radiative lifetimes (ps) at 3 temperatures and critical field E for exciton dissociation from TDDFT + many-body calculations

System	T=0	T=4K	T=300K	E (V/nm)
1LMoS ₂	0.164	6.2 (5) ¹³	467 (850) ¹³	0.005
1LWS ₂	0.150	3.2	239	0.035
MoS ₂ -WS ₂	6.010	104	7800	0.001

Fig.1 Scheme showing mechanism of the inter-layer hole migration in MoS₂-WS₂ (see the text).



2. Development of the TDDFT+DMFT approach for strongly correlated materials

We have performed a thorough analysis of the structure of the TDDFT XC kernel obtained from the DMFT charge susceptibility of the one-band Hubbard model for different values of the on-site electron-electron Coulomb repulsion parameter. [14] We solve the DMFT equations using the numerically exact Quantum Monte Carlo solver. In particular, we find an analytical expression for the kernel as function of frequency, which is a generalization of the kernel for the homogeneous electron gas proposed 30 years ago by Kohn and Gross.[15] We show that strong electron-electron correlations lead

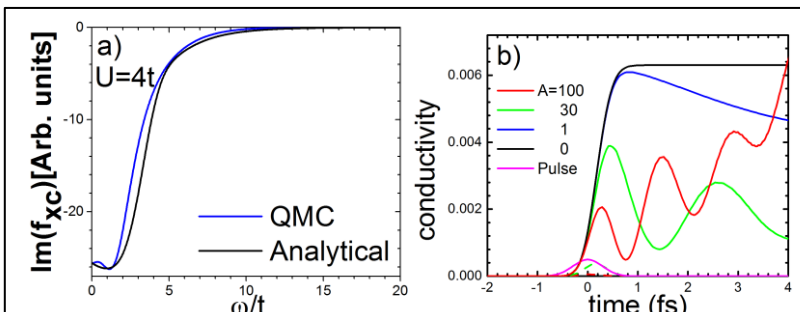
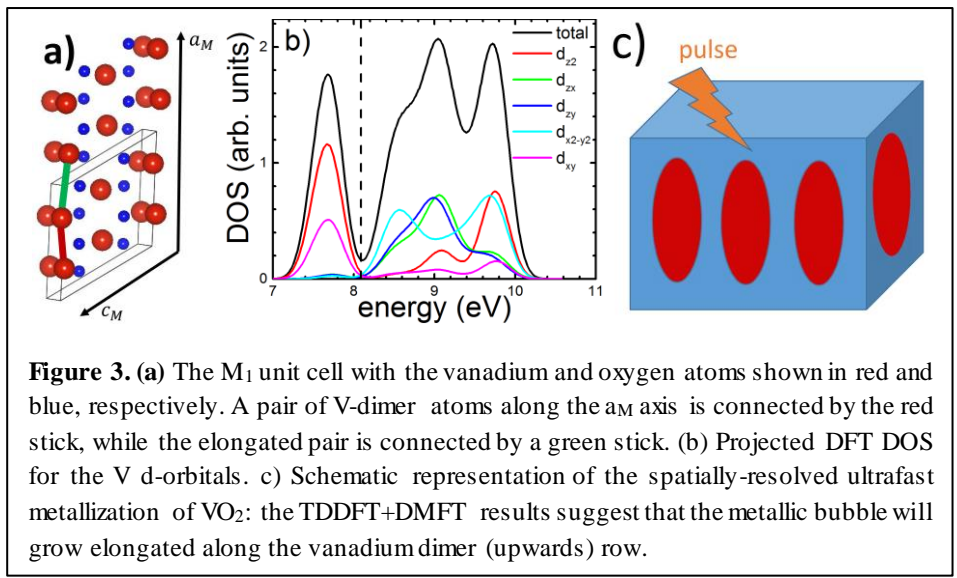


Figure 2. a) The QMC and analytical fitting for the imaginary parts of the XC kernels at U=4t. b) Time-dependence of the conductivity in the case of YTiO₃ excited by a 0.8fs homogeneous Gaussian laser pulse (field $E_0 = 0.1\text{eV}/\text{Bohr}$). The results correspond to U=4eV and to different XC kernels.

to an extra exponentially-decaying pre-factor in the Kohn-Gross kernel. The results for the exact numerical and analytically-fitted kernels are in a rather good agreement for different values of U (the case of U=4t is shown in Fig.2a), though the work on further improvement of the analytical formula for the kernel is in progress. We applied the obtained kernel to study the time-dependent conductivity in the Mott insulator YTiO_3 after the system was excited by an fs laser pulse. We find that a strong overlap of the charge orbitals may lead to beats in the time-dependent electric conductivity in YTiO_3 (Fig.2b, the orbital overlap is quantified by a dimensionless parameter A). This feature can be tested experimentally and can help verify the quantitative details of the structure of the XC kernel used in our formulation. Finally, we generalized the TDDFT+DMFT formalism for application to nonlinear response. Currently, we are using this approach to analyze the nonlinear ultrafast response of several correlated materials: VO_2 , V_2O_3 and MnO .

3. Nonhomogeneous ultrafast electrons dynamics in monoclinic VO_2 : application of TDDFT+DMFT

We have applied the TDDFT+DMFT approach to examine the ultrafast spatially-resolved breakdown of the insulating M_1 phase in VO_2 . In particular, we examined the processes of nucleation and possible spinodal decomposition of the excited metallic and insulating domains. The electron-driven scenario of the insulator-to-metal transition (IMT) was considered, i.e. it was assumed that during the IMT the M_1 lattice structure did not transform to the stable insulating rutile one, which is valid at times of order or below a few hundred femtoseconds. We find that the system is initially metallized preferentially along the vanadium-dimer C_R axis, with subsequent growth of C_R -elongated metallic bubbles. This behavior is determined by a specific dimer-chain alignment of the vanadium atoms that mainly contributes electron charges to the ultrafast response (the M_1 lattice structure and the DFT vanadium-atom d-orbital densities of states relevant to the dynamics are shown in Figs. 2a and 2b, respectively). We also find that the time-dependent bubble radius along C_R axis is approximately 2.5 times larger than that perpendicular to it (for a qualitative picture, see Fig. 2c). Further, even for such short times the dynamics of the system is significantly affected by memory effects - the time-resolved electron-electron interactions. We also analyze the implications of the nonhomogeneous femtosecond response for the general feature of the ultrafast charge response in VO_2 [16-18] and consequent monoclinic-to-rutile phase transformation.



transition (IMT) was considered, i.e. it was assumed that during the IMT the M_1 lattice structure did not transform to the stable insulating rutile one, which is valid at times of order or below a few hundred femtoseconds. We find that the system is initially metallized preferentially along the vanadium-dimer C_R axis, with subsequent growth of C_R -elongated metallic bubbles. This behavior is determined by a specific dimer-chain alignment of the vanadium atoms that mainly contributes electron charges to the ultrafast response (the M_1 lattice structure and the DFT vanadium-atom d-orbital densities of states relevant to the dynamics are shown in Figs. 2a and 2b, respectively). We also find that the time-dependent bubble radius along C_R axis is approximately 2.5 times larger than that perpendicular to it (for a qualitative picture, see Fig. 2c). Further, even for such short times the dynamics of the system is significantly affected by memory effects - the time-resolved electron-electron interactions. We also analyze the implications of the nonhomogeneous femtosecond response for the general feature of the ultrafast charge response in VO_2 [16-18] and consequent monoclinic-to-rutile phase transformation.

References:

- [1] A. Ramirez-Torres, V. Turkowski, and T.S. Rahman, Phys. Rev. B **90**, 085419 (2014).
- [2] K.F. Mak et al., Phys. Rev. Lett. **105**, 136805 (2010).
- [3] F. Wu et al., Phys. Rev. B **91**, 075310 (2015)
- [4] K.F. Mak et al., Nature Mat. **12**, 208 (2013)

- [5] C. H. Lui, Phys. Rev. Lett 113, 166801 (2014)
- [6] C. Zhang et al., Phys. Rev. B **89**, 205436 (2014)
- [7] E.J. Sie et al., **92**, 125417 (2015)
- [8] E.J. Sie et al., Nature Mat. 14, 290 (2015)
- [9] A. Chernikov et al., Phys. Rev. Lett. 115, 126802 (2015)
- [10] G. Plechinger et al., Physica Status Solidi (RRL) 9, 457 (2015).
- [11] X. Hong et al., Nature Nanotech. 9, 682 (2014)
- [12] Q. Liu et al., Phys. Rev. Lett. 114, 087402 (2015)
- [13] Palummo et al., NanoLett. 15, 2794 (2015).
- [14] S.R. Acharya, V. Turkowski, and T.S. Rahman (submitted).
- [15] E. Gross, W. Kohn, Phys. Rev. Lett. **55**, 2850 (1985).
- [16] D. Wegkamp, et al., Phys. Rev. Lett. **113**, 216401 (2014).
- [17] V.R. Morrison, et al., *Science* 346, 445 (2014).
- [18] B.T. O'Callahan, et al., Nature Comm. **6**, 6849 (2015).

Selected Publications from DOE Grant: DE-FG02-07ER46354 (2015-2016)

1. M. Alcántara Ortigoza, M. Aminpour, and T.S. Rahman, "Revisiting the surface properties of Mg(0001) thin films and their effect on adatom binding energy and self-diffusion," Surface Science, **632**, 14-19 (2015). DOI:10.1016/j.susc.2014.09.005
2. A. Kabir, V. Turkowski, and T.S. Rahman, "A DFT + Nonhomogeneous DMFT approach for finite systems," J. Phys. Condens. Matt. **27**,125601 (2015). DOI: 10.1088/0953-8984/27/12/125601
3. A. Ramirez-Torres, D. Le, and T.S. Rahman, "Effect of monolayer supports on the electronic structure of single layer MoS₂," IOP Conference Series: Materials Science and Engineering **76**, 012011 (2015). DOI: 10.1088/1757-899X/76/1/012011.
4. E Ridolfi, D Le, T S Rahman, E R Mucciolo and C H Lewenkopf, "A tight-binding model for MoS₂ monolayers," J. Phys.: Condens. Matt. **27** 365501 (2015). DOI: 10.1088/0953-8984/27/36/365501
5. S. Hong and T. S. Rahman, "Geometric and electronic structure and magnetic properties of Fe-Au nanoalloys: insights from ab initio calculations," Phys. Chem. Chem. Phys. **17**, 28177 (2015). DOI: 10.1039/C5CP00299K
6. A. Kabir, J. Hu, V. Turkowski, R. Wu, R. Camley, and T. S. Rahman, "Magnetic anisotropy of L1₀ FePt nanoparticles," Phys. Rev B **92**, 054424 (2015). DOI:10.1103/PhysRevB.92.054424
7. M. Alcantara Ortigoza, M. Aminpour, and T. S. Rahman, "Friedel oscillations responsible for stacking fault of adatoms: The case of Mg(0001) and Be(0001)," Phys. Rev. B **91**, 115401 (2015). DOI: 10.1103/Physrevb.91.115401
8. D. Le, A. Barinov, E. Preciado, M. Isarraraz, I. Tanabe, T. Komesu, C. Troha, L. Bartels, T.S. Rahman, and P.A. Dowben, "Spin-Orbit Coupling in the Band Structure of Monolayer WSe₂," Journal of Physics: Condensed Matter (Fast Track) **27**, 182201 (2015). DOI: 10.1088/0953-8984/27/18/182201
9. P. Patoka, G. Ulrich, A.E. Nguyen, L. Bartels, P.A. Dowben, V. Turkowski, T.S. Rahman, P. Hermann, B. Kästner, A. Hoehl, G. Ulm, and E. Rühl, "Nanoscale plasmonic phenomena in CVD-grown MoS₂ monolayer revealed by ultra-broadband synchrotron radiation based nano-FTIR spectroscopy and near-field microscopy", Optics Express 24, 1154 (2016).
10. S. R. Acharya, V.Turkowski, and T. S. Rahman, "Towards building the TDDFT theory for strongly correlated materials," submitted (2016).

Physical Analysis of the Bulk Photovoltaic Effect for Solar Harvesting Materials

Principal investigator: Professor Andrew M. Rappe
Department of Chemistry, University of Pennsylvania
rappe@sas.upenn.edu

Project Scope

The primary goal of this program is to understand and design bulk photovoltaic effect (BPVE) materials. These materials are noncentrosymmetric, and they support a quantum ballistic light-induced current. Greater understanding of this effect can allow for power generation in single, easily fabricated materials.

In our previous DOE-supported work, we have identified the shift current mechanism as the origin of BPVE and have implemented accurate and efficient *ab initio* calculations of shift current [1-7]; however, further investigations are necessary to unlock the potential of shift current BPVE materials for future devices. The behavior of shift current in thin films and inhomogeneous samples, its modification due to applied external (electric, magnetic, and strain) fields, and its fundamental efficiency limits have all not been fully explored.

Understanding of these issues is crucial for the discovery and engineering of PV devices that exceed the Shockley-Queisser limit, and are also of fundamental scientific interest. Despite a wide and growing set of known ferroelectric semiconductors, the materials design research into shift current has mainly been limited to perovskite oxides. There is therefore a need to study new types of ferroelectric semiconductors, including organic and hybrid materials, layered 2D materials, and topological materials for BPVE applications.

We propose to build on these foundations by expanding our research along three distinct directions. 1) We will study new physics of shift currents by considering shift currents in previously unexplored contexts: magnetic effects, coherence effects, and its connection to band topology. 2) We will develop new methodologies for calculating shift current under realistic operating conditions. 3) we will consider new materials classes for shift current BPVE. These will include materials based on perovskite ferroelectrics, as well as those outside this material class, including two-dimensional materials and conjugated polymers.

Recent Progress

Below, we highlight progress made in the past award period. A more comprehensive publication list is appended at the end of this document.

Material design of new shift current materials

We have developed design principles for shift current materials, including the nanolayering and dimensional reduction, band gap manipulation, and wavefunction manipulation by cation selection.

We find that nanolayering with Ni ions and O vacancies can enhance the BPVE in PbTiO₃ by up to a factor of 43. Our first-principles calculations show that this enhancement is driven by

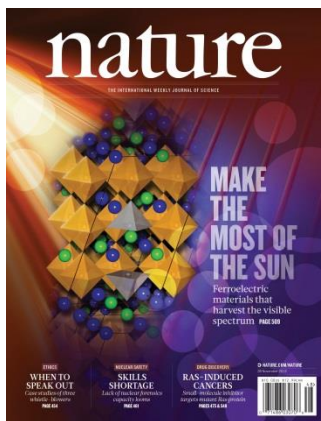


Figure 1: By alloying polar KNbO_3 and light-absorbing BaNiO_2 , this team developed single-phase materials that combine visible light absorption and strong inversion symmetry breaking. This material opens the door to a new class of semiconducting ferroelectrics as bulk photovoltaic effect light absorbers. [16]

rotation, Zn doping into KNbO_3 combined with charge compensation at the A-sites, and the introduction of low-lying intermediate bands through Bi^{5+} substitution as guidelines to design materials with stronger BPVE performance than prototypical ferroelectric oxides. [3,8] These results show that band gap engineering using solid solutions is a viable strategy for increasing the power conversion efficiency of ferroelectric light absorbers. [10]

We have also proposed a materials design strategy for high BPVE based on manipulation of wavefunction characters. We found that perovskite oxides with $d^{10}s^0$ cations lead to conduction bands composed of cation s orbitals and O p orbitals, which will enhance the BPVE response. Three materials were proposed: PbNiO_3 , $\text{Mg}_{1/2}\text{Zn}_{1/2}\text{PbO}_3$, and LiBiO_3 . They all have the LiNbO_3 structure and low band gaps, and their BPVE responses are dramatically enhanced by as much as an order of magnitude over previous materials, demonstrating the potential for high-performing bulk photovoltaics. [2]

Extension to shift current theory

Our work in the previous grant cycle has resulted in the discovery of new physical phenomena related to the shift current BPVE. We predict the linear bulk photovoltaic *spin* current in antiferromagnetic materials. [6] For example, Fe_2O_3 has antiferromagnetic ordering of the Fe ions, and the spin-up and spin-down sublattices are related by a glide plane. Thus, the charge current cancels, and pure spin current arises from these two sublattices under unpolarized light illumination. This effect does not depend on spin-orbit effects or require inversion symmetry breaking, distinguishing it from previously explored phenomena.

Coulomb interactions. [1] In comparison, dimensional reduction results in larger BPVE response in the alkali-metal chalcogenides for a different reason. These materials have one-dimensional As-S or As Se chains which contribute the carrier transport, resulting in increased joint density of states near the band gap energy. We studied the BPVE response of the polar compounds LiAsS_2 , LiAsSe_2 , and NaAsSe_2 , and found that the magnitudes of the photovoltaic responses in the visible range for these compounds exceed the maximum response obtained for BiFeO_3 by 10–20 times. In addition to the density of states enhancement, we find correlations between the high shift

current response and the presence of p states at both the valence and conduction band edges, as well as the dispersion of these bands, while also showing that high polarization is not a requirement. [5]

We studied band gap manipulation via a variety of techniques in perovskite materials. In the broadly explored BiFeO_3 , which has a large band gap, the shift current response is confined to energies greater than peak solar irradiation. We find that, in materials such as KNbNO and KNbO_3 , there is a comparable shift current with that of the but at a much lower photon energy. We assessed polarization

In addition, we have made connections between the fields of BPVE and topological insulators by showing that materials close to a band inversion topological phase transition have enhanced shift current responses. [7] We find that the bulk photocurrent reverses direction across the band inversion transition, and that its magnitude is enhanced in the vicinity of the phase transition. These results are demonstrated with first principles DFT calculations of BiTeI and CsPbI₃ under hydrostatic pressure, and explained with an analytical model, suggesting that this phenomenon remains robust across disparate material systems.

Future Plans

New physics of shift current

In GaAs, the observed deflection of the photocurrent in a magnetic field in GaAs is not consistent with a purely shift current explanation. The ballistic current, which arises from inelastic scattering, has been advanced as a possible explanation for this phenomenon. While first-principles methodology has enabled the calculation of shift currents, no such theoretical framework for the calculation of ballistic photocurrents is presently available. To address these unexplained ballistic current experimental observations, we propose to develop a theoretical framework to enable the first-principles calculation of the ballistic photocurrent, and to place it on the same theoretical footing as the shift current. In doing so, we will obtain a clearer picture of the following two alternatives: (i) Can the defect contribution to the ballistic current be simply understood as shift current in the presence of defects? (ii) Is an asymmetric carrier distribution necessary for the description of the ballistic current?

Computing shift current under operating conditions

To obtain a deeper understanding of shift current in real devices under operating conditions, we propose to develop a set of new methodological tools based on a real-space description of shift current. This will allow description of a number of issues germane to real devices, such as open-circuit voltages and efficiency limits, the effects of nanostructuring, and of spatial inhomogeneities. To address these challenges, we propose to use the Wannier function representation, which allows us to identify different spatial contributions to the shift current. This will further reveal structure-function relationships in inhomogeneous materials that will guide the design of new materials and enable optimization of their performance as potential solar cells. This Wannier approach will be supplemented by an explicit description of external electric fields and electrodes. The former will be treated by the Berry-phase approach in DFT, which has found success in describing dielectric and piezoelectric properties from first principles. We will treat electrodes explicitly by making use of the Green's function formalism of the shift current and the Landauer transport picture. We will apply this perturbation theory to the set of localized states of a nanoscale system, thereby obtaining its shift current. In this way, we can calculate the shift current from the Green's functions of a nanoscale system, modeled using an electrode/polar/electrode computational setup.

New classes of materials for polar PV

Building upon our earlier work on alkali-metal chalcogenides, we will continue our investigation into the shift current response of low dimensional materials. We propose to study

noncentrosymmetric single-layer TMD materials such as the hexagonal phases of MoS₂, MoSe₂, and WS₂, as well as ferroelectric polymers. We expect the high density of states due to the reduction of dimension in these materials will enhance their BPVE performance. We will use these materials as building blocks of more complex structures such as heterogeneous stacks of TMDs, epitaxially strained TMDs, densely packed organic crystals, and functionalized polymer chains. The study of BPVE in these materials will help us understand the relationship between the structure and the shift current response from a more fundamental point of view, providing more explicit materials design principles for higher BPVE performance in polar materials.

Publications

- [1] Wang, F., Young, S. M., Zheng, F., Grinberg, I. & Rappe, A. M. *Nat Commun* **7**, 10419 (2016).
- [2] Young, S. M., Zheng, F. & Rappe, A. M. *Phys. Rev. Applied* **4**, 54004 (2015).
- [3] Wang, F., Grinberg, I., Jiang, L., Young, S. M., Davies, P. K. & Rappe, A. M. *Ferroelectrics* **483**, 1(2015).
- [4] Wang, F. & Rappe, A. M. *Phys. Rev. B* **91**, 165124 (2015).
- [5] Brehm, J. A., Young, S. M., Zheng, F. & Rappe, A. M. *The Journal of Chem. Phys.* **141**, 204704 (2014).
- [6] Young, S. M., Zheng, F. & Rappe, A. M.. *Phys. Rev. Lett.* **110**, 57201 (2013).
- [7] Tan, L. Z. & Rappe, A. M. *Phys. Rev. Lett.* **116**, 237402 (2016).
- [8] Jiang, L., Grinberg, I., Wang, F., Young, S. M., Davies, P. K. & Rappe, A. M. *Phys. Rev. B* **90**, 75153 (2014).
- [9] Brehm, J. A., Bennett, J. W., Schoenberg, M. R., Grinberg, I. & Rappe, A. M. *The Journal of Chemical Physics* **140**, 224703 (2014).
- [10] Wang, F., Grinberg, I. & Rappe, A. M. *Phys. Rev. B* **89**, 235105 (2014).
- [11] Brehm, J. A., Takenaka, H., Lee, C.-W., Grinberg, I., Bennett, J. W., Schoenberg, M. R. & Rappe, A. M. *Phys. Rev. B* **89**, 195202 (2014).
- [12] Steinberg, J. A., Young, S. M., Zaheer, S., Kane, C., Mele, E. & Rappe, A. M. *Phys. Rev. Lett.* **112**, 36403 (2014).
- [13] Huon, A., Lang, A. C., Saldana-Greco, D., Lim, J. S., Moon, E. J., Rappe, A. M., Taheri, M. L. & May, S. J. *Applied Physics Letters* **107**, 142901 (2015).
- [14] Chen, F., Goodfellow, J., Liu, S., Grinberg, I., Hoffmann, M. C., Damodaran, A. R., Zhu, Y., Zalden, P., Zhang, X., Takeuchi, I., Rappe, A. M., Martin, L. W., Wen, H. & Lindenberg, A. M. *Adv. Mater.* **27**, 6371–6375 (2015).
- [15] Xu, R., Liu, S., Grinberg, I., Karthik, J., Damodaran, A. R., Rappe, A. M. & Martin, L. W. *Nat. Mater.* **14**, 79 (2015).
- [16] Grinberg, I., West, D. V., Torres, M., Gou, G., Stein, D. M., Wu, L., Chen, G., Gallo, E. M., Akbashev, A. R., Davies, P. K., Spanier, J. E. & Rappe, A. M. *Nature* **503**, 509–512 (2013).
- [17] Kocia, L., Young, S. M., Kholod, Y. A., Fayer, M. D., Gordon, M. S. & Rappe, A. M. *Chemical Physics* **422**, 175–183 (2013).
- [18] Jablonski, M. L., Liu, S., Winkler, C. R., Damodaran, A. R., Grinberg, I., Martin, L. W., Rappe, A. M. & Taheri, M. L. *ACS Appl. Mater. Interfaces* **8**, 2935–2941 (2016).
- [19] Zheng, F., Saldana-Greco, D., Liu, S. & Rappe, A. M. *J. Phys. Chem. Lett.* **6**, 4862–4872 (2015).
- [20] Zheng, F., Tan, L. Z., Liu, S. & Rappe, A. M. *Nano Lett.* **15**, 7794–7800 (2015).
- [21] Liu, S., Zheng, F., Koocher, N. Z., Takenaka, H., Wang, F. & Rappe, A. M. *J. Phys. Chem. Lett.* **6**, 693 (2015).
- [22] Zheng, F., Takenaka, H., Wang, F., Koocher, N. Z. & Rappe, A. M. *J. Phys. Chem. Lett.* **6**, 31–37(2015).
- [23] Shi, J., Grinberg, I., Wang, X. & Rappe, A. M. *Phys. Rev. B* **89**, 94105 (2014).
- [24] Liu, S., Grinberg, I. & Rappe, A. M. *Appl. Phys. Lett.* **103**, 232907 1-4 (2013).
- [25] Liu, S., Grinberg, I., Takenaka, H. & Rappe, A. M. *Phys. Rev. B* **88**, 104102 1-7 (2013).
- [26] Takenaka, H., Grinberg, I. & Rappe, A. M. *Phys. Rev. Lett.* **110**, 147602 (2013).
- [27] Liu, S., Grinberg, I. & Rappe, A. M. *J. Physics.: Condens. Matter* **25**, 102202 1-6 (2013).

Extending the reach of computational-theoretical methods to materials at the energy frontier

Principle investigator: Fernando A. Reboredo

Materials Science and Technology Div., Oak Ridge National Lab., Oak Ridge TN, 37830
reboredofa@ornl.gov

Co-PI's G. Malcolm Stocks, Markus Eisenbach and Jaron T. Krogel

Project Scope

The overarching goal of this program is to significantly improve our description and understanding of electronic correlations and magnetic interactions in an *ab initio many-body* framework. The design of new materials for clean energy requires us to overcome obstacles in the current theoretical approach so that we can describe the physical, chemical and electronic properties of materials with an accuracy comparable to experimental characterization and in large physically-relevant systems. A priority in this program is to develop and improve new theories and implement them in computer codes taking advantage of current high performance computers (HPC). Many relevant properties of correlated oxides, but also semiconductors, polymers, and magnets, are currently beyond the accuracy obtainable with the state-of-the-art approaches based on Density Functional Theory (DFT). Accordingly, we are following an alternative route using the highly-accurate Quantum Monte Carlo (QMC) and/or improved DFT approximations (e.g. for finite temperature). Since a significant fraction of the theoretical research in materials is currently based on DFT approximations, the results provided by our research will quantify the errors of these approximations. Since higher performance/high-capacity computers are becoming available to a larger group of researchers, we are now providing an alternative Monte Carlo based approach to reach the required accuracy for energy applications.

Examples of Recent Progress

Transition-metal-oxide (TMO) interfaces and superlattices exhibit properties that are not present in either of the constituent materials [1,2]. Identifying the origin of such properties typically requires a combination of experiments and theoretical calculations. Predictive capability beyond the usual approximations of Density Functional Theory (DFT) is required because suitable parameter-free exchange-correlation potentials for TMOs have not so far been possible.

Quantum Monte Carlo (QMC) solutions of the full many-electron problem in solids have become practical for bulk oxides and have provided unique values for defect formation energies [3–5]. Applications of QMC to complex structures such as TMO interfaces and superlattices have until recently been hampered by computer limitations. As an example of the work performed by our team, we compare QMC calculations with extensive calculations of site-specific O-vacancy formation energies in a $(\text{LaFeO}_3)_2/(\text{SrFeO}_3)$ superlattice using a wide range of available exchange-correlation functions [local density

approximation (LDA) with and without generalized gradient corrections (GGA) plus a hybrid functional; and LDA and GGA supplemented by a Hubbard U (LDA+U, GGA+U)] [6]. There is a large variation in the resulting O-vacancy formation energies at the four distinct O sites, making it impossible to reach a definitive conclusion about the relative stability of distinct O vacancies within DFT without experimental input. We also report Diffusion Monte Carlo (DMC) [7] calculations for site-specific O-vacancy formation energies obtaining parameter-free values that allow a direct account of the experimental data. Further examination of the results shows that the various theoretical schemes result in different electron localization around the TM atoms compared with the DMC results. The net conclusion is that DMC calculations are now in position to make substantial contributions to understand the properties of complex-oxide structures.

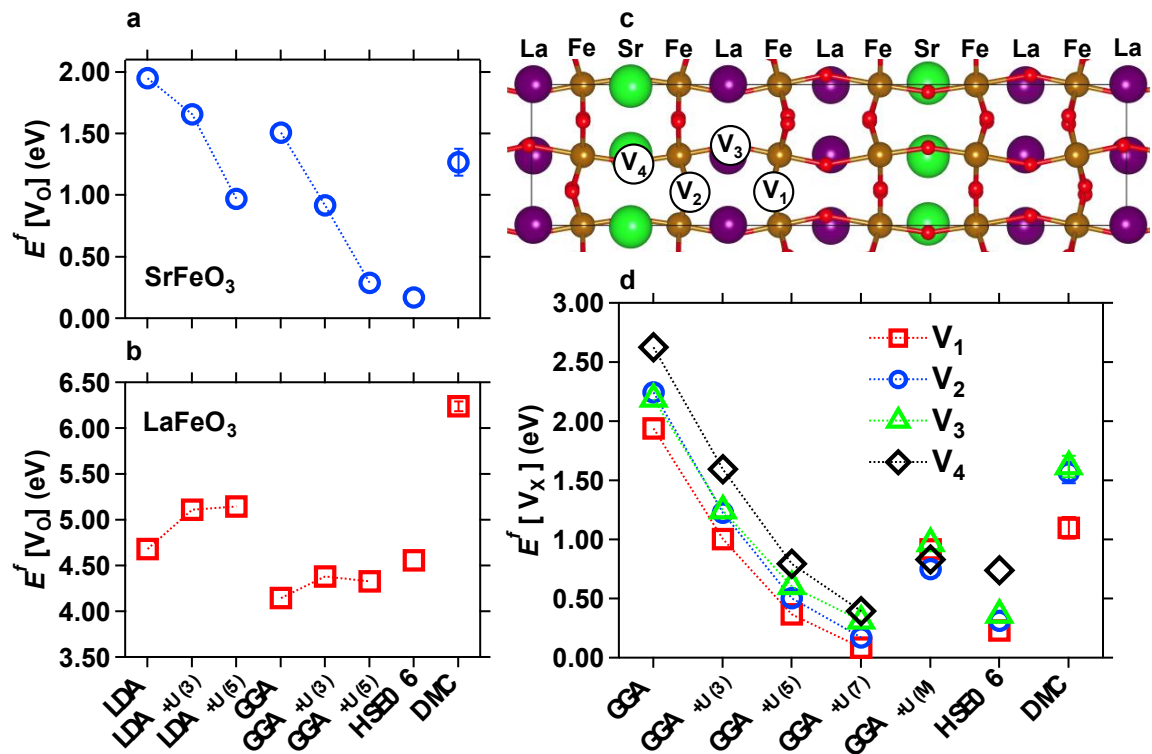


Figure 1. Formation energy of the oxygen vacancy calculated with DFT approximations and DMC under oxygen rich conditions for (a) SrFeO_3 and (b) LaFeO_3 . (c) Schematic illustration of the oxygen vacancy in the FeO_2 layers that are in the LaFeO_3 (V_1) and $\text{La}_{0.5}\text{Sr}_{0.5}\text{FeO}_3$ (V_2) units, in the LaO layer (V_3) and in the SrO layer (V_4) in the $(\text{LaFeO}_3)_2/\text{(SrFeO}_3)$ superlattice. (d) Formation energy for V_1 , V_2 , V_3 and V_4 under oxygen rich conditions for each vacancy.

First Principles Calculations of Ordering Transitions in Alloys: Understanding phase transitions and specific heat in alloys is of fundamental importance in material science. [8-11] The design of new materials relies on the knowledge of the thermodynamic properties of the different phases. Due to the size of the configuration space, a standard method is to fit models (such as cluster expansion) to first principles DFT calculations for small, representative cells. The advances in available computational resources have made it possible to consider directly the order-disorder transition in solid solution alloys

without resorting to fitting to models or the need to resort to mean field theories. The performance of our real space, Locally Self-consistent Multiple Scattering code (LSMS) on DOE's leadership computing facilities [12] has enabled us to conduct Monte-Carlo simulations, where each move's energy calculations consist of a full first principles DFT result, thus the changes in the electronic state due to changes in the atomic order are naturally taken into account. We calculate the ordering transition from a high temperature disordered A2 phase to an ordered B2 phase in Cu_{0.5}Zn_{0.5}. The Wang-Landau Monte Carlo algorithm obtains the microcanonical entropy of the system for all energies in a pre-selected energy window and we record the atomic configurations that contribute to the Monte-Carlo walk to analyze the order parameters of the system. In our calculation of a 250 atom supercell with 600,000 samples with atoms on fixed lattice sites, we find the phase transition at 870K as compared to an experimental value of 750K. Yet the decay of the short-range order parameter above T_c is in very good agreement with the experimentally observed results. [13]

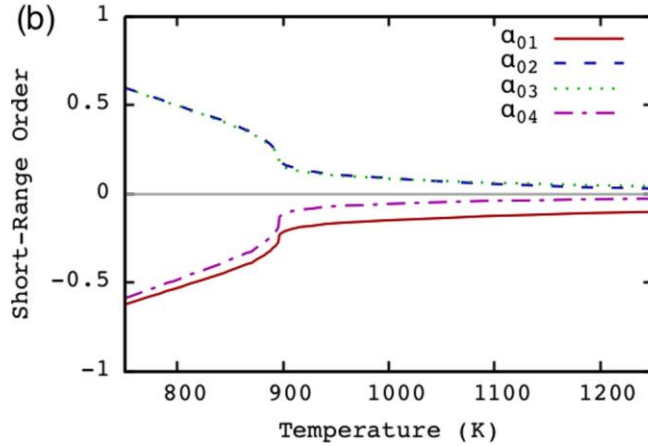


Figure 2: Short range order parameter in CuZn for the first four nearest-neighbor shells.

Simulation of Spin-Orbit Coupling of Phonon and Magnon Dynamics: The simulation of magnetic devices requires an understanding of transfer of energy and torque between the crystal lattice and the magnetic subsystem. Thus the dynamic simulation has to take both the movement of the atoms and the magnetic moments into account. This requires a Hamiltonian that contains both the usual molecular dynamics terms of kinetic energy and the interatomic potential as well as a Heisenberg exchange term for the spin dynamics, where the exchange parameter depends on the atomic positions. This conventional approach can successfully describe the thermalization of a magnetic system that is coupled to a spin thermostat, but due to the symmetry of the Hamiltonian is unable to break collinear magnetic order when the thermostat is coupled to the lattice. We extend this model by including a local anisotropy term that accounts for the effects of spin-orbit coupling that couples the spin to the lattice movements. Thus the atomic movements will enable the breaking of the rotational spin symmetry of the Hamiltonian and we have demonstrated that this will allow the thermal equilibration of the magnetic moments by coupling to the atomic lattice. [14]

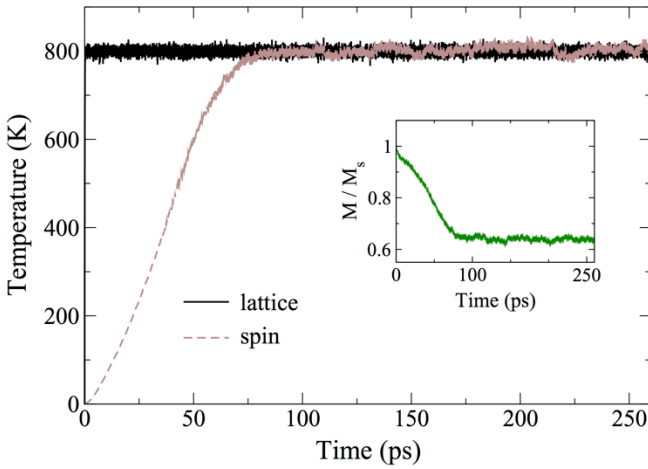


Figure 3: Thermal relaxation in combined molecular and spin dynamic simulation with spin-orbit local anisotropy term. The lattice subsystem is coupled to a heat bath at 800K.

References:

- [1] H. Y. Hwang, Y. Iwasa, M. Kawasaki, B. Keimer, N. Nagaosa, and Y. Tokura, *Nat. Mater.* **11**, 103 (2012).
- [2] G. Rijnders, *Nat. Mater.* **13**, 844 (2014).
- [3] E. Ertekin, L. K. Wagner, and J. C. Grossman, *Phys. Rev. B* **87**, 155210 (2013).
- [4] J. A. Santana, J. T. Krogel, J. Kim, P. R. C. Kent, and F. A. Reboredo, *J. Chem. Phys.* **142**, 164705 (2015).
- [5] C. Mitra, J. T. Krogel, J. A. Santana, and F. A. Reboredo, *J. Chem. Phys.* **143**,
- [6] V. I. Anisimov, J. Zaanen, and O. K. Andersen, *Phys. Rev. B* **44**, 943 (1991).
- [7] W. Foulkes, L. Mitas, R. J. Needs, and G. Rajagopal, *Rev. Mod. Phys.* **73**, 33 (2001).
- [8] Khan, S. N. and M. Eisenbach, *Phys. Rev. B* **93**, 024203 (2016). PTS 59577.
- [9] Khan, S. N., J. B. Staunton, and G. M. Stocks. *Phys. Rev. B* **93**, 54206 (2016).
- [10] Troparevsky, M. C., J. R. Morris, P. R. C. Kent, A. R. Lupini and G. M. Stocks, *Phys. Rev. X* **5**, 011041 (2015). 10.1103/PhysRevX.5.011041
- [11] M. Claudia Troparevsky, James R. Morris, Markus Daene, Yang Wang, Andrew R. Lupini, and G. Malcolm Stocks JOM, Vol. 67, No. 10, 2015 DOI: 10.1007/s11837-015-1594-2
- [12] Eisenbach, M., J. Larkin, J. Lutjens, S. Rennich, and J. H. Rogers, book chapter in *Big Data Technology and Applications*, Springer, March 2016. PTS 60799.
- [13] Khan, S. N., J. B. Staunton, and G. M. Stocks. *Phys. Rev. B* **93**, 54206 (2016).
- [14] Perera, D., M. Eisenbach, D. M. Nicholson, G. M. Stocks, and D. P. Landau, *Phys. Rev. B* **93**, 060402 (2016). PTS 55590.

PUBLICATIONS

Santana, J. A., J. T. Krogel, P. R. C. Kent, F. A. Reboredo, "Cohesive energy and structural parameters of binary oxides of groups IIA and IIIB from diffusion quantum Monte Carlo," *J. Chem Phys.* **144**, 174707 (2016), PTS 61154.

Yiu, Yuen, A. A. Aczel, G. E. Granroth, D. L. Abernathy, M. B. Stone, W. J. L. Buyers, J. Y. Y. Lin, G. D. Samolyuk, G. M. Stocks, and S. E. Nagler, "Light atom quantum oscillations in UC and US," *Phys. Rev. B* **93**, 014306 (2016). PTS 58066.

Petrie, J. R., C. Mitra, H. Jeen, W. S. Choi, T. L. Meyer, F. A. Reboredo, J. W. Freeland, G. Eres, H. N. Lee, "Strain control of oxygen vacancies in epitaxial strontium cobaltite films," *Adv. Func. Mat.* **26** (10) 1564-1570. (2016) PTS 54953.

Mathis, J. E., J. J. Lieffers, C. Mitra, F. A. Reboredo, Z. Bi, C. A. Bridges, M. K. Kidder, M. P. Panthanaman, "Increased photocatalytic activity of TiO₂ mesoporous microspheres from codoping with transition metals and nitrogen," *Ceram. Intl.* **42** (2) 3556-3562, Part B. (2016) PTS 58378.

Jan Korringa Obituary

By: Faulkner, J. Sam; Stocks, G. Malcolm
Physics Today, **69**, 4 (70-71) April 2016

Krogel, J. T., J. A. Santana, and F. A. Reboredo, "Pseudopotentials for quantum Monte Carlo studies of transition metal oxides," *Phys. Rev. B* **93**, 075143. (2016), PTS 55330.

Eisenbach, M., J. Larkin, J. Lutjens, S. Rennich, and J. H. Rogers, "GPU Acceleration of the Locally Selfconsistent Multiple Scattering Code for First Principles Calculation of the Ground State and Statistical Physic of Materials," book chapter in *Big Data Technology and Applications*, Springer, March 2016. PTS 60799.

Khan, S. N., J. B. Staunton, and G. M. Stocks, "Statistical physics of multicomponent alloys using KKR-CPA," *Phys. Rev. B* **93**, 054206 (2016). PTS 60838.

Gonis, A., X.-G. Zhang, M. Däne, G. M. Stocks, and D. M. Nicholson, "Reformulation of density functional theory for *N*-representable densities and the resolution of the *v*-representability problem," *J. Phys. Chem. Solids* **89**, 23-31 (2016). PTS 61423.

Perera, D., M. Eisenbach, D. M. Nicholson, G. M. Stocks, and D. P. Landau, "Reinventing atomistic magnetic simulations with spin-orbit coupling," *Phys. Rev. B* **93**, 060402 (2016). PTS 55590.

Jin Li, C. He, L. Meng, H. Xiao, C. Tang, X. Wei, J. Kim, N. Kioussis, G. M. Stocks, and J. Zhong. "Two-dimensional topological insulators with tunable band gaps: Single-layer HgTe and HgSe," *Sci. Reports* 5, 14115. September 2015. PTS 60956

A. Pramanick, A. Glavic, G. Samolyuk, A. A. Aczel, V. Lauter, H. Ambaye, Z. Gai, J. Ma, A. D. Stoica, G. M. Stocks, S. Wimmer, S. M. Shapiro, and X.-L. Wang. "Direct *in situ* measurement of coupled magnetostriuctural evolution in a ferromagnetic shape memory alloy and its theoretical modeling," *Phys. Rev. B* **92**, 134109. October 2015. PTS 60957

B. Radhakrishnan, D. M. Nicholson, M. Eisenbach, C. Parish, G. M. Ludtka, and O. Rios. "Alignment of iron nanoparticles in a magnetic field due to shape anisotropy," *J. Mag. Mag. Mat.* **394**, 481-480. November 2015. PTS 54057

T. Egami, M. Ohja, O. Khorgolkhuu, D. M. Nicholson, and G. M. Stocks. "Local Electronic Effects and

Irradiation Resistance in High-Entropy Alloys," *JOM* **67** (10) 2345-2349. October 2015 PTS 56502

M. C. Troparevsky, J. R. Morris, M. Daene, Y. Wang, A. R. Lupini, and G. M. Stocks. "Beyond Atomic Sizes and Hume-Rothery Rules: Understanding and Predicting High-Entropy Alloys," *JOM* **67** (10) 2350-2363. October 2015. PTS 59635

Chandrima Mitra, J. Krogel, J. A. Santana, and F. A. Reboreda. "Many-body ab initio diffusion quantum Monte Carlo applied to the strongly correlated oxide NiO," *J. Chem Phys.* **143** (16) 164710. October 2015. PTS 56928

Khan, S. N. and M. Eisenbach, "Density-functional Monte-Carlo simulation of CuZn order-disorder transition," *Phys. Rev. B* **93**, 024203 (2016). PTS 59577.

Next Generation Photon and Electron Spectroscopy Theory

Principal investigator: John J. Rehr, Dept. of Physics, University of Washington, Seattle, WA 98195-1560, jjr@uw.edu

Keywords: XAS, XPS, GW/BSE, Cumulant, Spectral Function

Project scope

The primary goal of our DOE BES Grant is to develop next generation theories for photon and electron spectroscopies, covering a broad spectrum from the visible to x-ray energies for materials throughout the periodic table. Over the years, our research has led to highly successful codes such as FEFF [1], which are used worldwide to interpret x-ray spectra from synchrotron x-ray sources. One of the challenges in this effort is the need to understand excited states and correlation effects in complex materials. Our recent progress has focused on cumulant-based Green's function methods [2] which go beyond the conventional GW and TDDFT approaches. In particular we have recently developed the particle-hole cumulant approach for inelastic losses in x-ray absorption (XAS) and photoemission spectra (XPS) [3]. We have also developed improved algorithms for GW/Bethe-Salpeter Equation (GW/BSE) calculations [4], and for treating correlation effects in *d*- and *f*-electron materials. These techniques have led to breakthroughs in quantitative treatments of inelastic losses, satellites, and other excited state properties.

Recent progress

Cumulant expansion methods: The cumulant expansion for the one-electron Green's function was the main topic of our 2014 presentation, and has spurred considerable interest in the electronic structure community [2]. Our recent progress has extended this effort in several respects [3]. Briefly, this powerful many-body approach is based on an exponential representation of the Green's function in the time-domain $G(t)=G_0(t)e^{C(t)}$, and is advantageous compared to the conventional Dyson equation $G=G_0+G_0\Sigma G$. Here $G_0(t)$ is the independent particle Green's function, Σ is the one-electron self-energy, and many-body effects are embedded in the cumulant $C(t) = \int \beta_k(\omega) (e^{i\omega t} - i\omega t - 1) / \omega^2 d\omega$. The kernel $\beta_k(\omega) = |\text{Im } \Sigma_k(\omega + \varepsilon_k)|$ can be obtained from the GW approximation for the self-energy $\Sigma = iGW$ which reflects the dominant excitations in the system. One of the key signatures of many-body correlation effects is the satellite structure in the one-electron spectral function $A_k(\omega) = (1/\pi) |\text{Im } G_k(\omega)|$, which can be directly measured in XPS. Many body interactions generally replace the sharply defined one-particle states k , for which $A_k(\omega) = \delta(\omega - \varepsilon_k)$, by a broadened quasi-particle peak and a series of satellites. While the GW approximation gives good quasi-particle properties, it usually gives a poor approximation for the satellites. Remarkably, the cumulant approach builds in dynamic vertex corrections, and gives a good description of both the quasi-particle peak *and* the multiple-satellite structure in $A_k(\omega)$, consistent with experiment. Nevertheless, the physics of x-ray

absorption spectra (XAS) involves particle-hole excitations, for which the one-particle cumulant approach is inadequate.

Particle-hole Cumulant Approach for Inelastic Losses: Physically the satellites in x-ray spectra arise from the excitations of the system due to the sudden creation of a core-hole and a photoelectron. These losses are dominated by plasmons and particle-hole excitations, i.e., neutral bosonic excitations, which can be treated on a common footing within the quasi-boson approximation of Hedin. Phonon contributions to the cumulant expansion can be treated similarly. Physically the excitation energies correspond to peaks in the electron energy loss function $L(\omega) = (1/\pi) |\text{Im } \epsilon^{-1}(\omega)|$. Three types of losses can be distinguished: *intrinsic losses* from excitations due to the sudden creation of a core-hole (c); *extrinsic losses* due to excitations by the propagating photoelectron (k); and additionally, *interference terms* between these processes that reduce the losses. A proper description of these properties requires a particle-hole Green's function G_K analogous to the BSE, where $K=(c,k)$ labels an excited core state. Again the formalism simplifies with a time-dependent formalism, and our generalization introduces a particle-hole cumulant $C_K(t)$, for which $G_K(t) = G_{K0}(t)e^{C_K(t)}$. The approach yields a total spectral function $A_K(\omega)$ (see Fig. 1) but with the kernel $\beta_k(\omega)$ replaced by a renormalized excitation amplitude $\gamma_K(\omega)$. Explicit calculations of $\gamma_K(\omega)$ are then carried out by partitioning the excitations into extrinsic, intrinsic, and interference terms $\gamma_K = \gamma_c + \gamma_k + \gamma_{ck}$, so that $C_K = C_c + C_k + C_{ck}$. As a consequence, inelastic losses in XPS and XAS can be calculated (Fig. 2) in terms of a convolution $\mu(\omega) = \int A_K(\omega') \mu_0(\omega - \omega') d\omega'$ of the quasi-particle spectrum $\mu_0(\omega)$ and $A_K(\omega)$. This can be implemented *ex post facto* with various treatments of $\mu_0(\omega)$. A key advance made possible by this development is an improved treatment of the various many-body amplitude reduction effects in x-ray spectra due to inelastic losses [3]. Heretofore these effects, which are typically of order 10-20% of the quasi-particle strength, have either been neglected or approximated by smooth background factors, leading to semi-quantitative accuracy in theoretical simulations. Of the three types of losses, the intrinsic losses are treated using the hole-cumulant C_c , which is calculated using a real-time, time-dependent density functional (TDDFT) approach. The corresponding excitation spectrum $\beta_c(\omega)$ is given by the Fourier transform of the transient, oscillatory, response of the charge density fluctuations due to the suddenly created core-hole. Remarkably, this approach can also account for the strong charge-

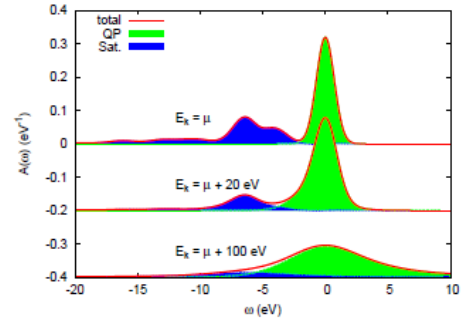


Fig. 1: CeO₂ spectral function (red) with quasiparticle (green filled) and satellite (blue filled) contributions [3].

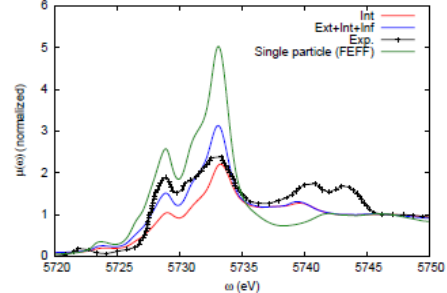


Fig. 2: Ce L₃ XAS of CeO₂: note that the near edge is dominated by intrinsic excitations, but that interference effects are also important [3].

transfer excitations in some correlated d - and f - electron systems. This development illustrates the advantages of real-time approaches for calculations of both excited states and spectra. In contrast, the extrinsic losses are calculated using the electron cumulant C_k with a kernel $\beta_k(\omega)$ obtained with the GW approximation. Finally the interference terms C_{ck} are of critical importance. They are opposite in sign to the extrinsic and intrinsic contributions and reduce the satellites while transferring spectral weight back to the quasi-particle peak; if neglected the calculated inelastic losses would be much too strong. While their calculation is technically difficult depending on both local and extended contributions, we have developed reasonable approximations.

Improved treatments of core level x-ray spectra: We have also made significant advances in improving our codes. In particular we have extended our core-level GW/BSE code OCEAN for more efficient calculations of a variety of core-spectra in large systems, including XAS, XES, and both non-resonant and resonant inelastic x-ray scattering spectra [4]. The calculations use a basis of particle-hole states taken from DFT (e.g., ABINIT or QuantumEspresso), coupled with the NIST Bethe-Salpeter equation solver (NBSE). Our new implementation includes improvements in efficiency and parallelization, yielding about a ten-fold increase in calculable system size, up to several thousand atoms. We have also extended the real-space Green's function (RSGF) approach in FEFF to include Hubbard model corrections in d - and f -electron systems.

Future Plans

We plan to continue our development of next generation theoretical methods and their implementation in our spectroscopy codes, FEFF, OCEAN and RTXAS. Work is currently in progress to extend the cumulant approach to include self-consistency and off diagonal contributions, with applications to a variety of materials. Our efforts will include extensions of the retarded cumulant method to include finite temperature corrections; the investigation of various approximations to the screened coulomb interaction and their effects on total energies; and the development of a unified description of intrinsic, extrinsic and interference effects. In addition, we plan to continue the development of our real-space multiple scattering code FEFF and its interface to our other codes, focusing on improved treatments of many-body excitations with Green's function techniques such as the cumulant methods and Hubbard-I corrections. Our aim is to develop a simultaneous treatment of both localized and extended electronic states, to obtain an improved treatment of excited states and spectra.

References

1. For recent reviews see e.g. Joshua J. Kas, Kevin Jorissen and John J. Rehr, *Real-Space Multiple-Scattering Theory of X-ray Spectra*, in *X-Ray Absorption and X-Ray Emission Spectroscopy Theory and Applications*, Jeroen A. van Bokhoven and Carlo Lamberti (eds), (Wiley, New York, 2015).

2. Jianqiang Sky Zhou, J. J. Kas, Lorenzo Sponza, Igor Reshetnyak, Matteo Guzzo, Christine Giorgetti, Matteo Gatti, Francesco Sottile, J. J. Rehr, and Lucia Reining, *Dynamical effects in electron spectroscopy*, J. Chem. Phys. **143**, 184109 (2015).
3. J.J. Kas, J. J. Rehr and J. B. Curtis, *Particle-hole cumulant approach for inelastic losses in x-ray spectra*, Phys. Rev. B (in press, July 2016); arXiv:1604.06829.
4. K. Gilmore, John, E.L. Shirley, D. Prendergast, C.D. Pemmaraju, J.J. Kas, F.D. Vila, J.J. Rehr, *Efficient implementation of core-excitation Bethe-Salpeter equation calculations*, Comput. Phys. Comm. **197**, 109 (2015).

Publications

1. J. J. Kas, J. J. Rehr, and L. Reining, *Cumulant expansion of the retarded one electron Green's function*, Phys. Rev. B **90**, 085112 (2014).
2. S. M. Story, J. J. Kas, F. D. Vila, M. J. Verstraete, and J. J. Rehr, *Cumulant expansion for phonon contributions to the electron spectral function*, Phys. Rev. B **90**, 195135 (2014).
3. J. J. Kas, J. J. Rehr, and S. A. Chambers, *Real time cumulant approach for charge transfer satellites in x-ray photoemission spectra*, Phys. Rev. B **91**, 121112(R) (2015).
4. Vitova, Tonya; Green, Jennifer; Denning, Robert; Löble, Matthias; Kvashnina, Kristina; Kas, Joshua; Jorissen, Kevin; Rehr, John; Malcherek, Thomas; and Denecke, Melissa, *Polarization Dependent High Energy Resolution X-ray Absorption Study of Dicesium Uranyl Tetrachloride*, Inorg. Chem. **54**, 174 (2015).
5. C. Vorwerk, K. Jorissen, J. Rehr, and T. Ahmed, *Real-space multiple-scattering Hubbard model calculations for d-and f-state materials*, J. Synchrotron Radiat. **22**, 1042 (2015).
6. K. Gilmore, John Vinson, E.L. Shirley, D. Prendergast, C.D. Pemmaraju, J.J. Kas, F.D. Vila, J.J. Rehr, *Efficient implementation of core-excitation Bethe-Salpeter equation calculations*, Comput. Phys. Comm. **197**, 109 (2015).
7. Jianqiang Sky Zhou, J. J. Kas, Lorenzo Sponza, Igor Reshetnyak, Matteo Guzzo, Christine Giorgetti, Matteo Gatti, Francesco Sottile, J. J. Rehr, and Lucia Reining, *Dynamical effects in electron spectroscopy*, J. Chem. Phys. **143**, 184109 (2015).
8. R. Thomas, J. Kas, P. Glatzel, M. Al Samarai, F.M.F. de Groot, R. Alonso, and J. Mori, *Resonant Inelastic X-ray Scattering of molybdenum oxides and sulfides*, J. Phys. Chem. C **119**, 2419 (2015).
9. J.J. Kas, J. J. Rehr and J. B. Curtis, *Particle-hole cumulant approach for inelastic losses in x-ray spectra*, Phys. Rev. B (in press, July 2016); arXiv:1604.06829.

Percolative Metal-Insulator Transition in the Perovskite Oxides

Principal Investigator: Sashi Satpathy

Department of Physics, University of Missouri, Columbia, MO 65211

satpathys@missouri.edu

Project Scope

The overall goal of this project is to understand and develop a theoretical description of the physics of the correlated oxides and their interfaces and the emerging phenomena in these systems. During the past two years, we have studied two main topics within this broad area of research, viz., (i) The percolative Mott metal-insulator transition (MIT), ubiquitous in the correlated oxides and (ii) The control of the Rashba effect in the spin-orbit coupled systems, including oxide surfaces. In addition, we have studied the consequences of strong spin-orbit coupling such as the origin of the Dzyaloshinskii-Moriya interaction in MnSi, the prototypical material for the skyrmion spin ordered state.

Recent Progress

1) Percolative Metal-Insulator Transition in the Oxides – The Mott metal-insulator transition (MIT) is a ubiquitous phenomenon in the correlated electron systems and has been observed in many perovskite materials such as LaMnO_3 , LaTiO_3 , etc. The Mott transition comes in two varieties, viz., band-width driven, where the MIT occurs as the relative strength of the band-width as compared to the Coulomb repulsion (W/U) is changed, for example, by applying pressure, and the second one, the dopant driven, where addition of carriers to a half-filled band leads to the transition. Theoretically, Mott insulators exist only at half filling; addition of a single carrier would turn the system into a metallic state (Nagaoka Theorem). However, in many oxide systems, the transition has been observed to occur only when the carrier concentration exceeds a significant, non-zero critical value. Even when the carrier concentration is fixed at half filling, changing the band-width does not simply produce a transition from a single-phase metallic to an insulating state, as the Hubbard model would suggest, but rather, a phase separation can occur due to the presence of additional interactions such as the Jahn-Teller interaction. With increasing bandwidth with external pressure, a mixed-phase state may be produced consisting of intermixed metallic and insulating puddles and the system would then conduct if the volume of the metallic region exceeds the percolation threshold. Similarly also, the doping-driven MIT may also be percolative depending on the energetics of the system. For example, the standard Hubbard model has been shown to exhibit phase separation as carrier concentration is changed from half filling. The goal of this work is to understand the Mott metal-insulator transition observed in the correlated oxide materials and connect our theory work to the experimental results in the literature. The results presented below are for the pressure-induced, band-width driven MIT taking LaMnO_3 (LMO) as the example.

Percolative MIT in LMO -- We showed that the pressure-induced metal-insulator transition (MIT) in LaMnO_3 is fundamentally different from the Mott-Hubbard transition and is percolative in nature, with the measured resistivity obeying the percolation scaling laws. In this work, we solved a model Hamiltonian which included the electron kinetic energy, as well as both Coulomb and Jahn-Teller interactions using the Gutzwiller variational method to treat the correlation effects. We found two main results: First, the MIT is driven by a competition between electronic correlation and the electron-lattice

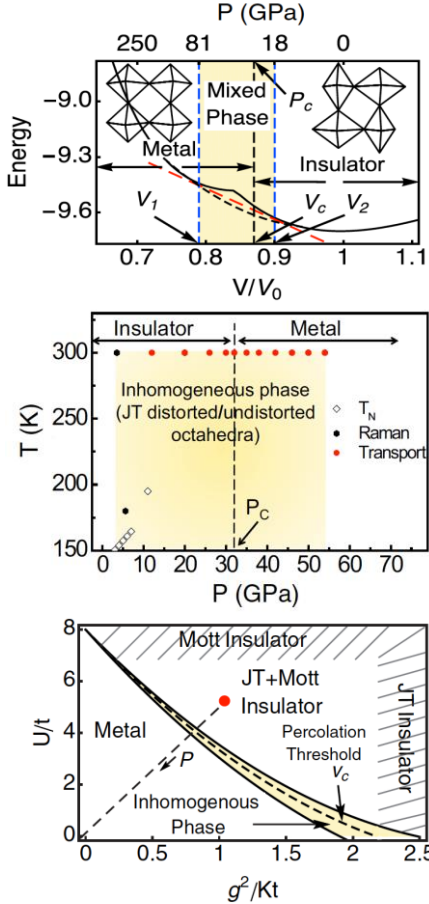


Fig. 1: Top, Energy as a function of volume computed for LMO, indicating regions of JT distorted and undistorted octahedra and the coexistence of a mixed phase (shadow region). Percolative conduction is predicted to begin, when the metallic fraction exceeds the percolation threshold, $v_c = 0.29$. The middle figure shows the experimental confirmation of the predicted results. The bottom figure shows the calculated phase diagram [From Refs. 1 and 2].

undistorted octahedra (Fig 1). The existence of the mixed phase means that conduction occurs by percolation and the MIT occurs when the metallic volume fraction, steadily increasing with pressure, exceeds the well-known percolation threshold $v_c = 0.29$. Our experimental collaborators (Baldini and coworkers) confirmed the theoretical predictions by measuring the high-pressure resistivity close to the MIT, which, quite remarkably, followed the well-known percolation scaling laws, and, in addition, the temperature dependence followed the Efros-Shklovskii variable-range hopping behavior, expected for granular materials. Our work established

the percolative nature of the MIT in LMO. More details may be found in Refs. 1 and 2.

2) Rashba Effect in the perovskite oxides

(a) Oxide Surfaces -- We studied the Rashba effect at the oxide surfaces and the 2D material, Black Phosphorous to illustrate the possibility of an anisotropic Rashba effect. The Rashba effect describes the momentum dependent spin splitting of the electron states at surfaces, commonly described by the Hamiltonian $H_R = \alpha_R(k_y\sigma_x - k_x\sigma_y)$, and is the combined result of the spin-orbit interaction and the inversion-symmetry breaking. Control of the Rashba effect by an applied electric field is at the heart of a class of proposed spintronics devices for manipulating the electron spin and as such the effect has been well studied for semiconductors. Polar oxides are expected to have a much larger Rashba effect owing to the presence of high Z elements and a two-dimensional electron gas (2DEG) formed by the polar catastrophe at the surface. In our earlier work (Ref. 3), we studied the Rashba effect for the oxide surfaces, taking the specific example of KTaO_3 (KTO) using density-functional theory (DFT), and showed that the Rashba effect is quite strong and can be tuned by an applied electric field, using

interaction, an issue that has been long debated in the literature, and, Second, that the calculated energy as a function of volume indicated via the Maxwell construction, the formation of a mixed or inhomogeneous phase of interspersed insulating and metallic regions close to the MIT, consisting, respectively, of Jahn-Teller distorted and

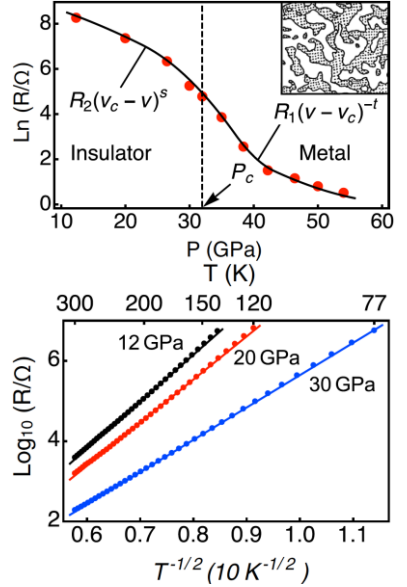


Fig. 2: Confirmation of the mixed phase in LMO: Top, Measured resistance close to the MIT (red dots) and the percolation scaling laws (full line). The temperature dependence (bottom) follows the Efros-Shklovskii variable range hopping behavior [From Ref. 1].

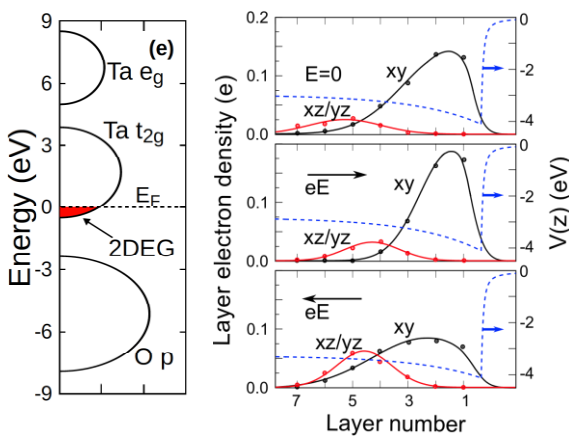


Fig. 3: The 2DEG at the KTO surface and its manipulation by an electric field as obtained from DFT, leading to the field tuning of the surface-sensitive Rashba effect [From Ref. 3].

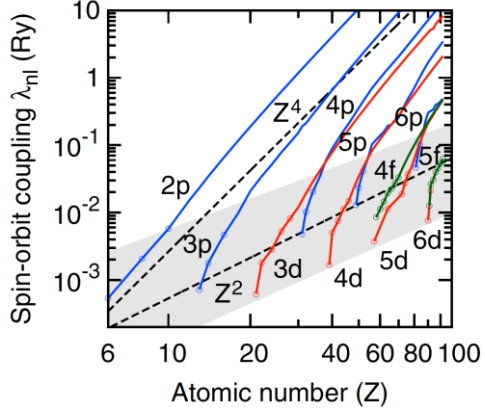


Fig. 4: A pedagogical figure, showing the Z^2 dependence of the spin-orbit coupling for the outermost (valence) electrons in the solid (indicated by shaded area). The hydrogenic, text-book Z^4 dependence is obeyed only if we stay within a particular series such as 2p. [From Ref. 4].

developed an expression for the magnitude of the anisotropic effect. Details are given in Ref. 4.

3) Other Works: Other notable works in the past two years where the spin-orbit interaction plays a central role consisted of (i) The origin of the Dzyaloshinskii-Moriya interaction in MnSi, a prototypical material for the observation of the skyrmion state (Ref. 7) and (ii) The study of the RKKY interactions in the spin-polarized electron gas (Ref. 8).

it to draw the 2DEG out to the surface or push it deeper into the bulk, thereby controlling the surface-sensitive phenomenon.

Analytical results obtained with a tight-binding model (Ref. 5) unraveled the interplay between the various factors affecting the Rashba effect such as the strengths of the spin-orbit interaction and the surface-induced asymmetry. From the tight-binding model, we derived the expressions for the Rashba coefficients in both limits of weak and strong SOI by using the perturbative Löwdin downfolding of the full tight-binding Hamiltonian. The d electron systems offer a rich system for manipulating the Rashba effect, not only because the magnitude of the effect can be strong owing to the large atomic numbers Z

(Fig. 4), but also because the orbital characters and their energies are sensitive to external forces such as strain, which can be used for tailoring the effect.

(b) Anisotropic Rashba effect – The newly discovered, graphene-inspired 2D materials such as BP offer a platform for studying the anisotropic Rashba effect; the anisotropy gives a novel twist to the Rashba effect and could have important consequences in spintronics applications as well. From DFT calculations of BP, we proposed the anisotropic Rashba effect (Fig. 5), which may be quite common in solids, occurring whenever there is a strong band mass anisotropy. We

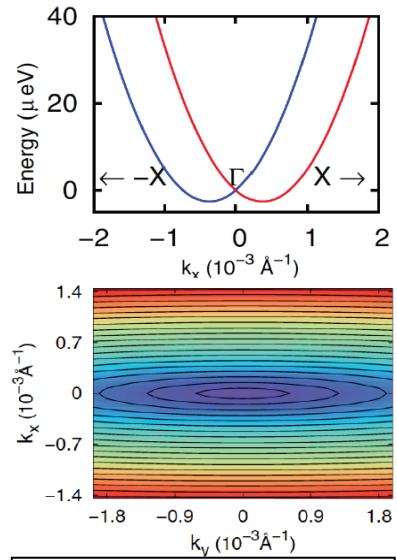


Fig. 5: Momentum-dependent spin splitting of the conduction bands in Black Phosphorous showing the Rashba effect (top) and its anisotropy (bottom) [From Ref. 4].

Future Plans

1) Spin-Orbit Entangled Mott Insulators in the 5d Oxides: There is considerable current interest on the physics of 5d materials owing to the presence of both strong spin-orbit and Coulomb interactions, which leads to the novel Mott-Hubbard physics, where the strong spin-orbit coupling plays an essential role in the formation of the Mott insulating state. Examples are the Iridates such as Sr_2IrO_3 , where the strong SOI splits the 5d-derived t_{2g} states into spin-orbit entangled $J_{\text{eff}} = 3/2$ and $1/2$ states. The Hubbard U term further splits the spin-orbit entangled $J_{\text{eff}} = 1/2$ state into a lower and an upper Hubbard band, producing thereby a Mott insulator. In this project, we will study the electronic structure of the 5d systems using the Gutzwiller as well as density-functional methods. Of particular interest is the development of spin-rotational invariant methods for the simultaneous treatment of the spin-orbit and Coulomb interactions.

2) Doped Mott Insulators: The doping of the Mott insulators within the Hubbard model has been actively studied by a variety of techniques. However, largely unexplored are models that include important interactions relevant to a large number of oxides such as the Jahn-Teller coupling, even though the doped Mott insulators have been experimentally studied for a long time. We have gained considerable insight by studying the band-width controlled metal-insulator transition in LaMnO_3 as was already described above. In this project, we will study the doping-driven Mott metal-insulator transition in the oxides such as LaTiO_3 . Although metallic conduction is expected as soon as dopants are introduced in the half-filled Mott insulating state (Nagaoka Theorem), experiments show otherwise, viz., that the insulating state continues until a critical amount of doping ($x_c \sim 0.05 - 0.25$) is introduced into the system. Our work will result in a deeper understanding of the dopant-driven Mott transitions in solids.

Selected Publications

1. M. Sherafati, M. Baldini, L. Malavasi, and S. Satpathy, Percolative Metal-Insulator Transition in LaMnO_3 , *Phys. Rev. B* 93, 024107 (2016)
2. M. Baldini, T. Muramatsu, M. Sherafati, H-K Mao, L. Malavasi, P. Postorino, S. Satpathy, and V. V. Struzhkin, Inhomogeneity-driven colossal magneto-resistance in compressed LaMnO_3 , *Proc. Natl. Acad. Sciences* 112, 10869 (2015)
3. K. V. Shanavas and S. Satpathy, Electric Field Tuning of the Rashba Effect in the Polar Perovskite Structures, *Phys. Rev. Letts.* 112, 086802 (2014)
4. Z. S. Popovic, J. M. Kurdestany, and S. Satpathy, “Electronic Structure and Anisotropic Rashba Spin-Orbit Coupling in Monolayer Black Phosphorus,” *Phys. Rev. B* 92, 035135 (2015)
5. K. V. Shanavas, Z. S. Popovic, and S. Satpathy, Theoretical model for Rashba Spin-Orbit Interaction in d Electrons, *Phys. Rev. B* 90, 165108 (2014)
6. K. V. Shanavas and S. Satpathy, Effective tight-binding model for MX_2 under electric and magnetic fields, *Phys. Rev. B* 91, 235145 (2015)
7. K. V. Shanavas and S. Satpathy, “Electronic structure and the Dzyaloshinskii-Moriya interaction in MnSi ,” *Phys. Rev. B* 93, 195101 (2016)
8. M. Valizadeh and S. Satpathy, RKKY Interaction for the Spin Polarized Electron Gas, *Int. J. Mod. Phys. B* 29, 1550219 (2015)
9. S. Kissinger and S. Satpathy, “A free-electron model for the Dirac bands in graphene,” *Phys. Rev. B* (Submitted)

Quantum Monte Carlo Studies of Multiband Hubbard Models

Principal Investigator: Professor Richard Scalettar
Department of Physics, University of California, Davis
Davis, CA 95616
scalettar@physics.ucdavis.edu

Project Scope

This project involves exploring the physics of multiband Hubbard models and, in addition to that global goal, has three more specific objectives: (i) the exploration of how electrons behave at the interface between different materials, for example, how magnetism in one might penetrate into another; (ii) the development of an understanding of the “Knight shift anomaly,” a phenomenon which occurs at low temperatures in a class of solids known as heavy fermion materials, in which the response of the electrons to the nuclear spin is no longer proportional to the magnetic susceptibility; and (iii) the study of solids represented by “depleted lattices” in which a regular array of sites is removed.

Recent Progress

Below are highlights of progress in the last year. A publication list follows.

Superconductivity and Nematic Fluctuations - In contrast to bulk FeSe, which exhibits nematic order and low temperature superconductivity, in atomic layers of FeSe the situation is reversed, with high temperature superconductivity appearing along with suppression of nematic order. To investigate this phenomenon, the PI studied, in collaboration with Philipp Dumitrescu, Maksym Serbyn, and Ashvin Vishwinath of UC Berkeley, a minimal electronic model of FeSe, with interactions that enhance nematic fluctuations. We developed a determinant quantum Monte Carlo algorithm with parallel tempering, which proved to be an efficient source of global updates and allowed us to access the region of strong interactions. Over a wide range of intermediate couplings, we observed superconductivity with an extended s-wave order parameter, along with enhanced, but short ranged, $q=(0,0)$ ferro-nematic order.

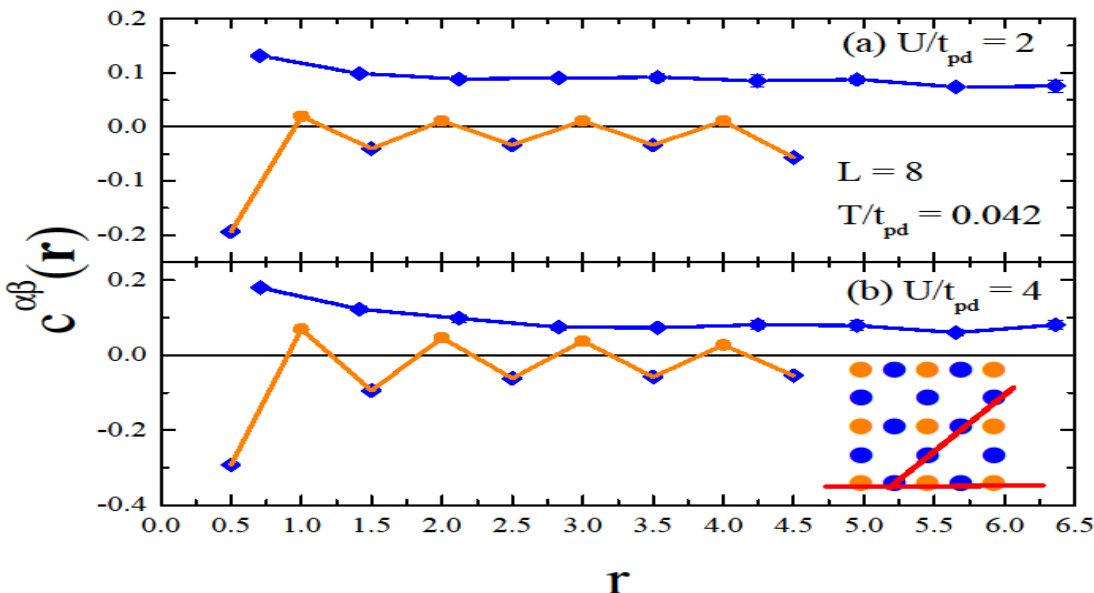
Magnetism on Quasicrystalline Lattices-

The Periodic Anderson Model (PAM) is widely studied to understand strong correlation physics and especially the competition of antiferromagnetism and singlet formation. Together with an undergraduate and graduate student, the PI extended QMC work on lattices with uniform numbers of neighbors to geometries in which the conduction electron sites can have variable coordination z . This situation is relevant both to recently discovered magnetic quasicrystals and also to magnetism in doped heavy fermion systems. Our key results are the presence of antiferromagnetic order at weak interorbital hybridization V_{fd} , and a delay in singlet formation to larger values of V_{fd} on sites with

larger z. The staggered magnetization tends to be larger on sites with higher z, providing insight into the behavior to be expected in crown, dice, and CaVO lattices.

Nuclear Magnetic Resonance Relaxation Rates at a QCP - Heavy fermion systems, and other strongly correlated electron materials, often exhibit a competition between antiferromagnetic (AF) and singlet ground states. Using exact Quantum Monte Carlo (QMC) simulations, the PI examined, with a visiting graduate student from Brazil and his supervisors, the effect of impurities in the vicinity of such AF-singlet quantum critical points (QCP), through an appropriately defined "impurity susceptibility." Our key finding was a connection, within a single calculational framework, between AF domains induced on the singlet side of the transition, and the behavior of the nuclear magnetic resonance (NMR) relaxation rate $1/T_1$. We showed that local NMR measurements provide a diagnostic for the location of the QCP which agrees remarkably well with the vanishing of the AF order parameter and large values of the impurity susceptibility. We connected our results with experiments on Cd-doped CeCoIn₅.

Ferromagnetism on a Depleted (Lieb) Lattice- The noninteracting electronic structures of tight binding models on bipartite lattices with unequal numbers of sites in the two sublattices have a number of unique features, including the presence of spatially localized eigenstates and flat bands. When a uniform on-site Hubbard interaction U is turned on, Lieb proved rigorously that at half filling the ground state has a non-zero spin. The PI, with the same Brazilian group as above, used exact Determinant Quantum Monte Carlo simulations to quantify the nature of magnetic order on such a lattice, as well as the projected density of states, and the compressibility. We determined the conditions under which the system is metallic or a ferromagnetic insulator.



Caption: Spatial dependence of spin-spin correlation functions in the Lieb lattice geometry.

Future Plans

Our immediate plans are to extend the above work in two ways: First, we will study itinerant electron models of disordered heavy fermions rather than their strong coupling (spin) limit. Second, we will collaborate with Prof. Curro's NMR group to model directly their data on the extent of AF regions and the effect of disorder on NMR spectra.

Publications

1. Superconductivity and Nematic Fluctuations in a model of FeSe monolayers: A Determinant Quantum Monte Carlo Study, P.T. Dumitrescu, M. Serbyn, R.T. Scalettar, and A. Vishwanath, Phys. Rev. B, to appear.
2. Magnetic Correlations in a Periodic Anderson Model with Non-Uniform Conduction Electron Coordination, N. Hartman, W.-T. Chiu, and R.T. Scalettar, Phys. Rev. B93, 235143 (2016).
3. Impurities near an Antiferromagnetic-Singlet Quantum Critical Point, T. Mendes, N. Costa, G. Batrouni, N. Curro, R.R. dos Sandos, T. Paiva, and R.T. Scalettar, Phys. Rev. Lett., submitted.
4. Ferromagnetism beyond Lieb's theorem, N.C. Costa, T. Mendes-Santos, T. Paiva, R.R. dos Santos, and R.T. Scalettar, Phys. Rev. B, submitted.

STRONGLY CORRELATED ELECTRONS

Principal investigator: Pedro Schlottmann

Department of Physics, Florida State University, Tallahassee, FL 32306

schlottmann@physics.fsu.edu

Project Scope

The research in this program is on aspects of heavy fermions, quantum criticality, magnetism and topological Kondo insulators. Here I briefly report on three projects. (1) A renormalization group (RG) study of a two pocket model that opens the possibility to a superconducting dome around the QCP in quantum critical heavy fermion systems. This requires the transfer of pairs of electrons between the pockets and commensurability of the nesting vector with the lattice. (2) In the case of incommensurate nesting, commensurate and incommensurate spin-density waves appear close to the QCP of heavy fermions, but no superconductivity. (3) SmB₆ is a strong topological Kondo insulator. Recent studies confirmed this for the electrical conductivity below 5 K. We have studied the Landau quantization and spin-momentum locking for the states in the Dirac cones.

Recent Progress

(1) Quantum criticality of heavy fermions

The nesting of the Fermi surfaces of an electron and a hole pocket separated by a nesting vector \mathbf{Q} and the interaction between electrons gives rise to itinerant AFM. The order is gradually suppressed by mismatching the nesting and a quantum critical point (QCP) is obtained as $T_N \rightarrow 0$.

Properties of the QCP have been studied within the Hertz-Millis-Moriya theory, in which all the fermionic degrees of freedom are eliminated at the expense of bosonic fields (spinwaves) [1]. They can alternatively be treated within a renormalization group (RG) approach of the fermionic Hamiltonian. We had proposed a fermionic nested two-pocket model (Schlottmann, Phys. Rev. B **59**, 12379 (1999) and **68**, 125105 (2003)), that reproduces many of the non-Fermi liquid (NFL) properties, namely, the mass enhancement, logarithmic dependence of the specific heat, T-linear dependence of the resistivity, the linewidth of the quasi-particles, the crossover from Fermi liquid to NFL as a function of T and a tuning parameter δ (mismatch of the Fermi surfaces), and the amplitude of the de Haas-van Alphen oscillation through a modified Lifshitz-Kosevich expression.

The above two-pocket model has been extended to include electronic Umklapp processes, i.e. two-electron transfers between pockets. In the case the vector \mathbf{Q} is commensurate with the lattice (Umklapp with $\mathbf{Q} = \mathbf{G}/2$) a superconducting dome above the QCP may arise without destroying the NFL properties in the specific heat and the linewidth of the quasi-particles, i.e. the electrical resistivity [2]. A schematic of the phase diagram and the T and δ dependence of the specific heat are shown in Fig. 1. The extended model is similar to the one studied by Chubukov (Physica C **469**, 640 (2009)) for a 2D Fermi surface in the context of the Fe pnictides.

The stable superconducting phase is S⁺, which for the proper choice of model parameters gives rise to a superconducting dome above the QCP. It is necessary to assume that the pair transfer amplitude decreases with the Fermi surface mismatch between the two pockets. Since the SDW order and S⁺ compete for the same portion of the Fermi surface, the dome is split into two

regions, one is purely S^+ and in the other one SDW coexists with superconductivity (see right panel of Fig. 1), in agreement with NMR experiments for CeIn_3 , $\text{CeCu}_2(\text{Si}_{0.98}\text{Ge}_{0.02})_2$ and CeRhIn_5 .

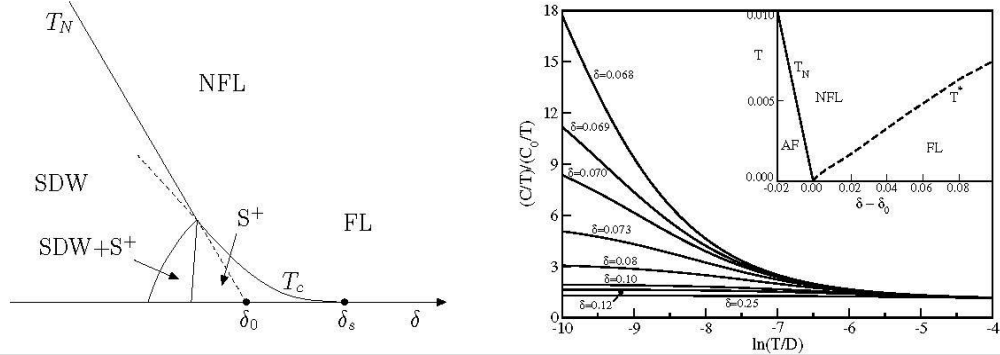


Fig.1 *Left panel*: Schematic phase diagram showing the SDW, the S^+ superconducting (starting at δ_s) and the possible coexistence of the phases. The dashed lines are the extrapolations of (a) the SDW boundary into the mixed phase (ending at δ_0 at $T=0$) and (b) the S^+ phase into the AF phase, respectively. The SDW and S^+ phases compete for the same portion of the Fermi surface. The NFL and FL regimes are also indicated. *Right panel*: C/T as a function of $\ln(T)$ for various values of δ and a Hubbard-like interaction with the S^+ phase suppressed. At intermediate T , C/T follows a logarithmic dependence and saturates at very low T . The crossover from NFL to FL as T is reduced depends on the value of $\delta > \delta_0$. The estimated crossover temperature is denoted T^* and shown in the inset, together with the Néel temperature, T_N . The OCP is at $\delta = \delta_0$ for $T=0$.

(2) Commensurate and incommensurate spin-density waves

In the case where the vector \mathbf{Q} is not commensurate with the lattice the analysis of the extended two-pocket model is more complicated. There are now eight phases that need to be considered, namely, commensurate and incommensurate spin and charge density waves and four superconducting phases, two of them with modulated order parameter of the Fulde-Ferrell-Larkin-Ovchinnikov (FFLO) type. In contrast to FFLO here the modulation is not with the magnetic field but with the parameter $\alpha = |\mathbf{Q} \cdot \mathbf{G}/2|$. The implementation of the renormalization group technique is

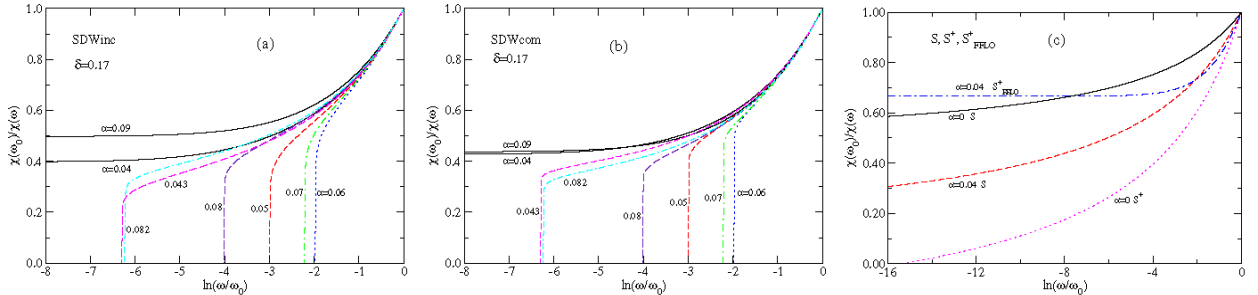


Fig.2: Inverse of the density correlation functions and superconductivity normalized to their value at $\omega_0=0.1$. *Left panel (a)*: Incommensurate SDW, *middle panel (b)*: Commensurate SDW for $\delta_0 = 0.17$, $D=10$, and $v_0=u_0=p_{a0}=p_{b0}=0.12$. The subindex 0 indicates the initial value of the interaction before renormalization. The QCP is at $\delta_0 = 0.155$ and $\alpha=0$. The different curves correspond to different values of α . Re-entrant long-range SDW order is induced in the range $0.042 < \alpha < 0.083$, where both the commensurate and incommensurate SDW responses diverge. *Right panel (c)*: Superconductivity ($w_0 = 0.7$ and $p_{c0} = 0.12$) is strongly suppressed by α and only can occur if $\alpha < T_c \sim 0$, where T_c is the superconducting transition temperature for $\alpha=0$. All superconductivity correlation functions remain finite for $\alpha > T_c$. Different correlation functions have to be used for $\alpha = 0$ because the FFLO phases cannot be realized (all phases are homogeneous). The S^+ correlation for $\alpha=0$ yields superconductivity at low T and gives rise to a superconducting dome around the QCP.

more complicated in this case and requires a numerical integration of the differential equations, especially for the susceptibilities corresponding to the eight forms of order [8].

The phase diagram has been studied as a function of the mismatch of the Fermi surfaces and the magnitude of α . For repulsive interactions the responses to charge-density waves are always finite and CDWs (either commensurate or incommensurate) are not favored. On the other hand, commensurate and incommensurate spin-density waves can be induced by increasing α , giving rise to a re-entrant phase (see Fig. 2). Both SDW order parameters are driven by the same set of diverging vertices. The phase diagram also shows a Fermi liquid and a non-Fermi liquid phase. A finite value of the parameter α , on the other hand, quenches all forms of superconducting order.

(3) The strong topological Kondo insulator SmB₆

SmB₆ has been predicted to be a strong topological Kondo insulator (TKI) and experimentally it has been confirmed that for temperatures below 4 K the electrical conductivity only takes place at the surfaces of the crystal. The indirect semiconductor gap of about 54 K freezes out all the conducting states at low T. However, the static susceptibility, the 16 meV magnetic excitation intensity measured by inelastic neutron scattering, the intensity of the Raman transition and the NMR relaxation rate display temperature dependences up to an energy scale of 20 to 30 K, which are then clearly not related to the appearance of the topological surface states. These features have been attributed to magnetic exciton bound states proposed by Riseborough [Phys. Rev. B **68**, 235213 (2003)]. The "in-gap" bulk states do not contribute to the electrical conductivity but to the magnetic properties. There are then two energy scales, one related to the bulk and one associated to the surface states (see Fig.3).

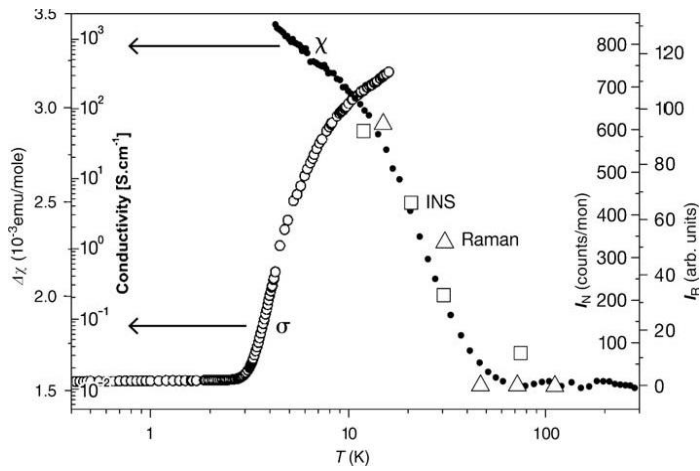


Fig.3: The contribution of the 'in-gap' state to the susceptibility ($\Delta\chi$) (solid circles), the T-dependence of the 16 meV magnetic excitation intensity measured by inelastic neutron scattering I_N (open squares), and the intensity of the Raman transition I_R (open triangles) compared to electrical conductivity data (open small circles). While the surface states contributing to the conductivity are active below 4 K, the 'in-gap' states are formed at much higher T. (Figure adapted from Alekseev et al, Physica B **186-188**, 384 (1993)) [4].

Quantum oscillations and ARPES measurements revealed several Dirac cones on the (001) and (101) surfaces of the crystal. We considered four models for surface Dirac cones (related to the standard Dirac dispersion, weak and strong Kondo topological insulators) with an additional parabolic dispersion and studied the Landau quantization and the expectation value of the spin of the electrons [11]. The Landau quantization is quite similar in all four cases and would give rise to similar de Haas-van Alphen oscillations. The spin-momentum locking, on the other hand, differs dramatically. Without the additional parabolic dispersion the spins are locked in the plane of the surface. The parabolic dispersion, however, produces a gradual canting of the spins out of the surface plane.

The NMR Korringa relaxation and Knight shift of ^{11}B nuclei in the topological Kondo insulator SmB_6 have been discussed. A relaxation into the topological surface states is only possible in the extreme dirty limit. In a strong magnetic field the clean 2D electron gas has a discrete energy spectrum as a consequence of the Landau quantization. For the more realistic case of a surface with a low concentration of defects (dirty limit) the scattering of the electrons leads to a broadening of the Landau levels and hence to a finite density of states. We also explored the possibility of microwave transitions among the surface states. This experiment is presently being carried out at the Magnetlab.

Future Plans

- To extend the study of pre-critical fluctuations to the quantum critical point in heavy fermion systems considering the Anderson lattice, i.e. two hybridized bands.
- Further study of the magnetic properties of the topological Kondo insulator SmB_6 .
- Quantum criticality in ferromagnetic Kondo systems has recently been observed in Yb based compounds. I plan to investigate the quantum criticality of the Kondo lattice with *ferromagnetic* Heisenberg exchange using field-theoretical and RG techniques.
- To continue the study of a boson and fermion mixture confined to a 1D trap interacting via a repulsive δ -function potential.
- To continue providing theoretical support to experimental groups through collaborations.

Selected Recent Publications

1. **P. Schlottmann**, Non-Fermi liquid behavior in heavy fermion systems, in *Handbook of Magnetic Materials*, ed. K.H.J. Buschow (Elsevier, Amsterdam, 2014), vol. 23, Chapter 2, p. 86
2. **P. Schlottmann**, Spin-density waves and the superconductivity dome in heavy electron systems with nested Fermi surfaces, Phys. Rev. B **89**, 014511 (2014).
3. S. Ghosh, S. Datta, H. Zhou, M.J.R. Hoch, C.R. Wiebe, **P. Schlottmann**, and S. Hill, Spin cluster excitations in the rare earth kagomé system $\text{Nd}_3\text{Ga}_5\text{SiO}_{14}$, Phys. Rev. B **90**, 224405 (2014).
4. **P. Schlottmann**, NMR relaxation in the topological Kondo insulator SmB_6 , Phys. Rev. B **90**, 165127 (2014).
5. B. Zeng, Q.R. Zhang, D. Rhodes, Y. Shimura, D. Watanabe, R.E. Baumbach, **P. Schlottmann**, T. Ebihara, and L. Balicas, CeCu_2Ge_2 : Challenging our understanding of quantum criticality, Phys. Rev. B **90**, 155101 (2014).
6. **P. Schlottmann** and A.A. Zvyagin, Threshold singularities in a Fermi gas with attractive potential in one-dimension, Nuclear Physics B **892**, 269 (2015).
7. L.J. Zhu, S.H. Nie, P. Xiong, **P. Schlottmann** and J.H. Zhao, Orbital two-channel Kondo effect in epitaxial ferromagnetic $\text{L1}_0\text{-MnAl}$ films, Nature Communications **7**, 10817 (2016).
8. **P. Schlottmann**, Commensurate and incommensurate spin-density waves and the superconductivity dome in heavy electron systems, Phys. Rev. B **92**, 045115 (2015).
9. J.C. Wang, S. Aswartham, Feng Ye, J. Terzic, H. Zheng, Daniel Haskel, Shalinee Chikara, Yong Choi, **P. Schlottmann**, Radu Custelcean, S.J. Yuan, and G. Cao, Decoupling of the antiferromagnetic and insulating states in Tb-doped Sr_2IrO_4 , Phys. Rev. B **92**, 214411 (2015).
10. S.J. Yuan, S. Aswartham, J. Terzic, H. Zheng, H.D. Zhao, **P. Schlottmann** and G. Cao, From $J_{\text{eff}}=1/2$ insulator to p -wave superconductor in single-crystal $\text{Sr}_2\text{Ir}_{1-x}\text{Ru}_x\text{O}_4$ ($0 < x < 1$), Phys. Rev. B **92**, 245103 (2015).
11. **P. Schlottmann**, Quantum oscillations in the surface states of topological Kondo insulators, Philosophical Magazine (2016), DOI: 10.1080/14786435.2016.1178405.

Theoretical Studies in Very Strongly Correlated Matter

PI: Sriram Shastry

Physics Department, University of California Santa Cruz,

sriram@physics.ucsc.edu

Project Renewal Date: September 1, 2016

Project Scope:

The proposal relates to developing a reliable methodology for calculating various physical properties of models with very strong interactions, where the familiar Feynman-Dyson perturbation theory fails. These include the t-J model and the large U Hubbard and Anderson models. Existing reliable techniques for these problems- such as the Dynamical Mean Field Theory-[G1] are largely numerical, and work in high dimensions. A new analytical framework for this demanding many-body problem has been proposed by the PI in 2011 [P-1], applicable in general dimensions and with general coupling constants. The project aims at establishing practical and controlled calculational schemes based on this approach, and applying them to unravel the physics of important strongly correlated problems, including High Tc superconductors. The schemes that have emerged have recently been tested quantitatively against DMFT in high dimensions, paving the way for applications to the physically interesting case of low dimensions.

The proposal also focusses on different transport quantities of interest in strongly correlated matter, including the longitudinal and Hall conductivity and the thermopower, both in the static limit and at finite frequencies. We propose extension of the high T expansion from thermodynamic variables, to dynamical variables such as the Greens functions and the optical conductivity by developing appropriate rules for symbolic programming to high orders

The proposal contains projects pertaining to important issues in quantum integrable systems, in providing theoretical models and calculations in frustrated magnetic systems such as TmB₄ relating to recent experiments [P-2].

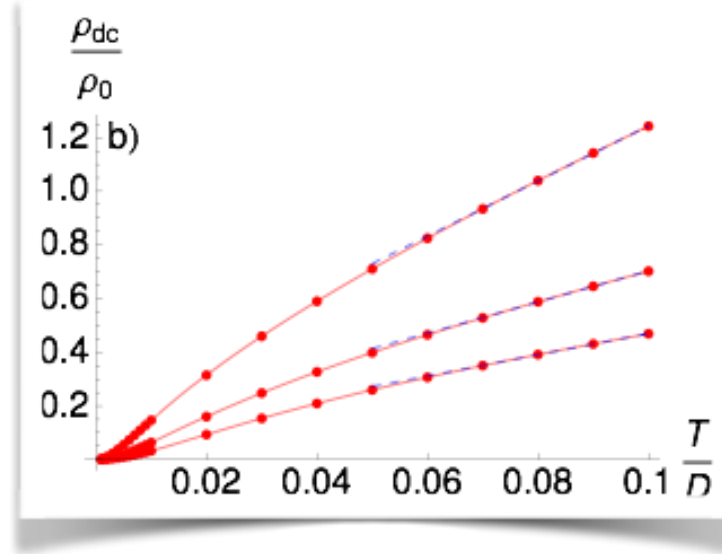
Recent Progress:

Large U Anderson Impurity Model and DMFT comparison and a rescaled scheme

The general formalism developed by the PI is called the extremely correlated Fermi liquid theory (ECFL). Here one of the main methods for calculation involves a systematic expansion in a parameter λ . This parameter is the Fermionic analogue of the inverse spin 1/(2S) in theories of quantum magnetism, where one expands the objects of interest, involving quantum spins, in terms of Bosons representing spin waves. The classical limit $S \rightarrow \infty$ parallels the limit of free (un-projected) Fermions at $\lambda=0$, while the extreme quantum limit of $S \rightarrow 1/2$ is analogous to Gutzwiller projected electrons [P-3] having $\lambda=1$. In recent works [P-4, P-5] (reported earlier), the PI and collaborators have compared the results from a systematic $O(\lambda^2)$ expansion of the ECFL theory with the numerically exact solution of the Anderson impurity problem (using the Wilson numerical renormalization group) and the $U=\infty$ Hubbard model using DMFT. The comparison is overall impressive since detailed features characteristic of strong correlations,

such as the lower Hubbard band and the particle hole asymmetry, are captured by the theory very well. It is also unexpected as well as impressive, that a low (second) order expansion already captures many interesting features of a very sophisticated numerical theory. The main problem with this version of ECFL is that the computed quasiparticle weight Z is too large as (the particle density) $n \rightarrow 1$, and therefore the spectral functions agree with the exact results only if we scale the frequencies with Z .

Very recently the PI and Perepelitsky have presented a method [P-6], termed the **rescaled scheme**, for overcoming the difficulty with the magnitude of Z . The resolution of the problem, through a high energy cutoff, is somewhat intuitive and further work is planned to establish it more firmly. However the results of [P-6] (for the $d \rightarrow \infty$ t-J or infinite U Hubbard model) are already very interesting. We find a Z that becomes very small near half filling, the spectral functions and self energy are captured very well. The resulting electron spectral functions can be then used to compute the electrical resistivity of the model and compared with the recent computation of the resistivity in DMFT [G-2]. The latter is an important result, since the computation is technically very demanding and requires great precision. We find that the our computation (see Figure below) is quantitatively similar to that in [G-2], with a tiny Fermi liquid (quadratic in T) regime, followed by **two** linear regimes separated by a knee.



aid an intuitive understanding of the physics.

In the figure, the three curves are at $\delta = 0.75, 0.8, 0.85$ from top to bottom, D is half the band width, and ρ_0 is the Mott-Ioffe-Regel resistivity.

The theory of [P-6] also gives pictorial insights into the destruction of the Fermi liquid by heating. It yields a single particle self-energy, which departs significantly from the Fermi liquid expectation, by developing a strong asymmetry between particles and holes. The formalism helps us to put the results in terms of simple formulas that can

λ -Expansion Diagrams to high order.

In [P-7] Edward Perepelitsky and the PI have formulated rules for enumerating the λ -expansion in the t-J model in any dimension, in a form that is amenable to high order computation by symbolic programs. This expansion contains terms that are identical to the Feynman series, but also includes diagrams beyond it, arising from the fact that the theory deals with non canonical objects. Indeed the Schwinger equations of motion, originally used by the PI in [P-1], lead to exactly these terms. The advantage of the diagrams is that we can write down diagrams to the n^{th}

order, without enumerating all the $(n-1)^{\text{th}}$ order diagrams, unlike in the Schwinger technique—thereby enabling the application of Monte Carlo type techniques [G-3] for high order summations.

Planned Research:

Analytical methods in low order ECFL: broken symmetry solutions, superconductivity and magnetic states.

Having established useful results in high dimension, we are proceeding to use the analytical (rescaled) second order ECFL theory in 2-dimensions with a non zero super exchange J , to compute the properties of the tJ model. The various broken symmetry solutions are being looked at. We plan to locate the phase diagram, and to compute various physical quantities that can be compared directly with experiments.

Computational ECFL for high orders in lambda:

We plan to use the Monte Carlo method in order to sum the high order diagrams in the λ -expansion established recently in [P-7]. Since the range of λ is bounded between 0 and 1, this expansion is quite promising. This work will help provide a numerical alternative to the analytical methods above.

Spectral shapes, study of dispersion features

We plan to study the Angle Resolved Photo emission (ARPES) derived spectral functions and the energy dispersion and its subtle features, such as the low energy kinks. We will compare our theoretical computations with experimental results.

Magneto transport studies using ECFL and High T expansions

The Hall constant in strongly correlated matter has several unexplained features, including their magnitude, frequency dependence and T dependence. It is also a very accessible quantity through high field experiments. We plan on computing the Hall constant using the analytical theory. We are also pursuing the high T expansion for obtaining transport variables, where our group has developed symbolic programs for generating high order terms.

Thermoelectric studies in correlated matter

We plan to study the challenging and technologically important Seebeck coefficient in strongly correlated matter. We also plan on a collaboration with other experts in this area.

Quantum Integrable systems and Frustrated Magnetism

We plan to devote some effort to the study of frustrated magnets such as TmB_4 , which are currently intensely studied. These form the so called Shastry-Sutherland lattice and have mobile electrons with interesting charge transport, in addition to magnetic moments. They exhibit non-trivial magneto resistance and magnetization plateaux, which lack theoretical understanding.

The PI has a long standing interest in quantum integrable models, such as the 1-d Hubbard model, the Haldane Shastry model, and more recently in finite dimensional matrix models. Some effort in this direction is planned.

(PI) Relevant Publications:

[P-1] "Extremely Correlated Fermi Liquids", B. S. Shastry, arXiv:1102.2858 (2011), Phys. Rev. Letts. 107, 056403 (2011).

[P-2] "Hysteretic magnetoresistance and unconventional anomalous Hall effect in the frustrated magnet TmB₄", S. S. Sunku, T. Kong, T. Ito, P.C. Canfield, B. S. Shastry, P. Sengupta and C. Panagopolous, arXiv:1602.02679., Phys. Rev. B 93, 174408 (2016).

[P-3] "Theory of extreme correlations using canonical Fermions and path integrals", B. S. Shastry, arXiv:1312.1892 (2013), Ann. Phys. 343, 164-199 (2014).

[P-4] "Extremely Correlated Fermi Liquid study of the U = ∞ Anderson Impurity Model", B. S. Shastry, E. Perepelitsky and A. C. Hewson, arXiv:1307.3492 [cond-mat.str-el], Phys. Rev. B 88, 205108 (2013).

[P-5] "Extremely correlated Fermi liquid theory meets Dynamical mean-field theory: Analytical insights into the doping-driven Mott transition", R. Zitko, D. Hansen, E. Perepelitsky, J. Mravlje, A. Georges and B. S. Shastry, arXiv:1309.5284 (2013), Phys. Rev. B 88, 235132 (2013).

[P-6] "Low energy physics of the t-J model in d = ∞ using Extremely Correlated Fermi Liquid theory: Cutoff Second Order Equations", B. S. Shastry and E. Perepelitsky", arXiv:1605.08213.

[P-7] "Diagrammatic λ series for extremely correlated Fermi liquids", E. Perepelitsky and B. S. Shastry, arXiv: 1410.5174, Ann. Phys. 357, 1 (2015). doi:10.1016/j.aop.2015.03.010

References:

[G-1] A. Georges et al., Rev. Mod. Phys. **68**, 13 (1996).

[G-2] X. Deng, J. Mravlje, R. Zitko, M. Ferrero, G. Kotliar, and A. Georges, Phys. Rev. Letts. 110, 086401 (2013).

[G-3] N. Prokofiev and B. Svistunov, Phys. Rev. Letts. **99**, 250201 (2007).

Novel Fractional Quantum Hall Effect and New Topological Phase in Interacting Systems

Principle investigator: Dr. Donna N. Sheng

California State University Northridge

Northridge, CA 91330

donna.sheng@csun.edu

Project Scope

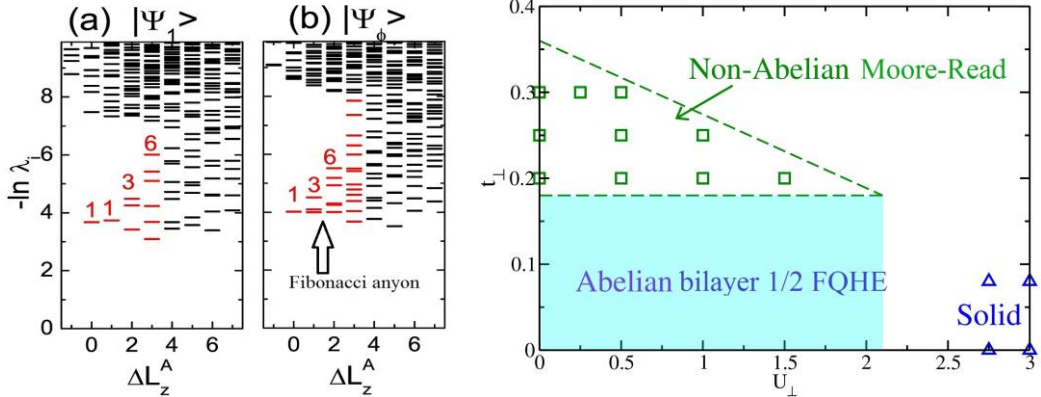
The project involves theoretical (numerical) study of the topological physics in strongly interacting systems. We identify relevant theoretical models which have the potential to host these topological phases, at the same time they are also realistic for condensed matter or optical lattice experiments. By developing and applying advanced computational methods, we determine the quantum phase diagrams for such systems and characterize the nature of different quantum phases and transitions. Based on our theoretical modeling, we validate theoretical proposes and develop theoretical understanding for these complex correlated systems. We also predict and suggest experimental researches searching for new topological states of matter. We have made important progress in the following areas: (a) Identifying and characterizing non-Abelian phases in experimental fractional quantum Hall effect (FQHE) systems; establishing the new mechanism for realizing non-Abelian FQHE by tuning the tunneling of two component systems; suggesting new experiments for their detections; (b) Identifying spontaneous integer quantum Hall effect (IQHE) in fermionic Hubbard model and FQHE in bosonic Hubbard model with time-reversal symmetry, which realize the interaction induced topological physics without a topological band; (c) Developing efficient computational methods for identifying and characterizing topological states of matter and applying them to characterize new states of matter; (d) Identifying different topological phases in lattice models with nontrivial topological bands.

Recent Progress

Characterizing 12/5 FQHE as the Non-Abelian Read-Rezayi state and establishing tunneling induced non-Abelian Moore-Read from bilayer 1/2 FQHE:

We investigate the nature of the FQHE at filling factor 13/5, and its particle-hole conjugate state at 12/5, with the Coulomb interaction, and address the issue of possible

competing states. Based on large-scale density-matrix renormalization group (DMRG) calculations in spherical geometry, we present evidence that the physics of the Coulomb ground states (GS) at these filling numbers is captured by the $k=3$ parafermion Read-Rezayi (RR_3) state. By performing a finite-size scaling analysis of the GS energies for $12/5$ with different shifts, we find that the RR_3 state has the lowest energy among different competing states in the thermodynamic limit. We find the fingerprint of the topological order in the FQHE $12/5$ and $13/5$ states based on their entanglement spectrum and topological entanglement entropy, both of which strongly support their identification with the RR_3 state. Furthermore, by considering the shift-free infinite-cylinder geometry, we expose two topologically-distinct GS sectors, one identity sector and a second one matching the non-Abelian sector of the Fibonacci anyonic quasiparticle, which serves as the smoking gun evidence for the RR_3 state at $12/5$ and $13/5$.



Caption: The left panel: the smoking gun evidence for the RR_3 state at filling factor $13/5$. The right panel: the phase diagram of bilayer $\nu=1/2$ FQHE for topological band systems.

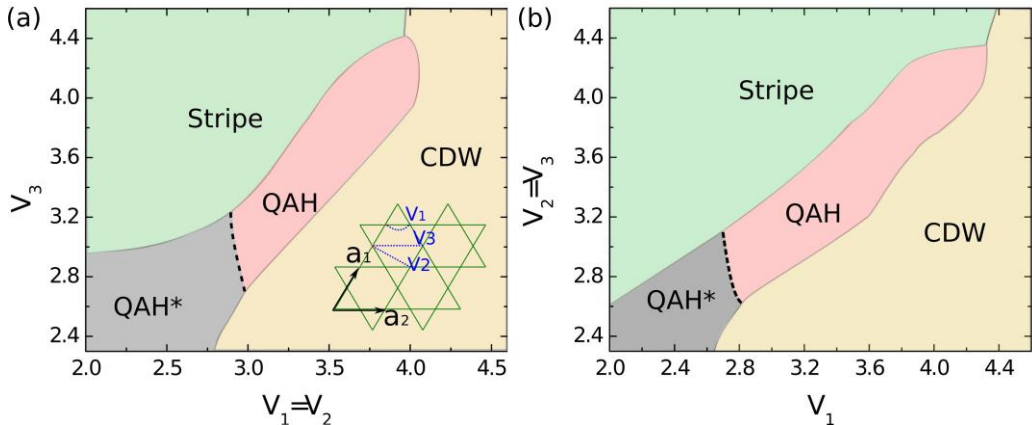
The multi-component quantum Hall systems with the presence of internal degrees of freedom provide a fertile ground for the emergence of the exotic quantum liquid physics.

Here we investigate the possibility of non-Abelian topological order in the half-filled FQHE bilayer systems driven by tunneling effect between two layers. By means of the state-of-the-art DMRG, we unveil “finger print” evidences of a non-Abelian Moore-Read Pfaffian state emergent in the intermediate tunneling regime, including the ground state degeneracy on torus geometry and entanglement spectroscopy (orbital-cut entanglement spectrum and topological entanglement entropy) on spherical geometry, respectively. Remarkably, the phase transition from previously identified Abelian Halperin-331 state to non-Abelian Moore-Read Pfaffian state is determined to be

continuous, which belongs to the Ising universality class. Our results not only provide “proof-of-principle” demonstration of realizing non-Abelian state through coupling different degrees of freedom, but also open up the possibility in FQHE bilayer systems for chiral p-wave pairing mechanism. We suggest specific experimental measurements for discovering non-Abelian state in such systems.

Identifying spontaneous IQHE in fermionic and bosonic Hubbard models with time-reversal symmetry

Non-interacting topological states of matter can be realized in band insulators with intrinsic spin-orbital couplings as a result of the nontrivial band topology. In recent years, the possibility of realizing novel interaction-driven topological phase has attracted a lot of research activities, which may significantly extend the classes of topological states of matter. Here, we explore the fermionic Hubbard model and report a new finding of an interaction-driven spontaneous quantum Hall effect (QHE) (Chern insulator) emerging on Kagome lattice. By means of DMRG, we expose universal properties of the IQHE including time-reversal symmetry spontaneous breaking and quantized Hall conductance. By accessing the ground state in large systems, we demonstrate the robustness of the IQHE against finite-size effects. Moreover, we map out a phase diagram and identify two competing charge density wave (CDW) phases by varying interactions, where transitions to the QHE phase are determined to be of the first order. Our study provides a “proof-of-the-principle” demonstration of interaction-driven QHE without the requirement of external magnetic field or magnetic doping, and we provide theoretical understanding of the emerging physics based on mean-field theory.



Caption: Phase diagram of extended fermionic Hubbard model on Kagome lattice in the interaction parameter plane, obtained by DMRG calculations on cylinder geometry.

We have also showed an interaction-driven topological phase emerging in an extended

Bose-Hubbard model on Kagome lattice, where the non-interacting band structure is topological trivial with zero Berry curvature in the Brillouin zone. By means of an unbiased DMRG technique, we identify that the groundstate in a broad parameter region is equivalent to a bosonic 1/2 FQHE state, based on the characterization of universal properties including groundstate degeneracy, edge excitations and anyonic quasiparticle statistics. Our work paves a way of finding interaction induced topological phases at the phase boundary of conventionally ordered solid phases.

Symmetry protected topological (SPT) phase for interacting bosons:

We study the interacting bosons in topological Hofstadter bands with Chern number two as a potential system for hosting the SPT. SPT states are short-range entangled states distinctly different from a long-range entangled topological phase. However, SPT states can have protected gapless boundary excitations, which enrich the strongly correlated physics. Using exact diagonalization, we demonstrate that bosonic IQHE state emerges at integer boson filling factor $v=1$ of the lowest Chern band with evidences including a robust spectrum gap and quantized topological Hall conductance two. Moreover, the robustness of BIQH state against different interactions and next-nearest neighbor hopping is investigated. The strong nearest neighbor interaction would favor a charge density wave. When the onsite interaction decreases, the boson IQHE state undergoes a continuous transition into a superfluid state. Without next-nearest neighbor hopping, the ground state is possibly in a metallic Fermi-liquid-like phase. Experimental observations of the SPT phase may be possible from cold atom Rb systems with tunable magnetic flux by further controlling the magnitude of hopping.

Future direction: By identifying the inter-tunneling induced non-Abelian phase in our current work (14), we are at the stage that we can examine many realistic multi-component systems to identify other promising candidates with nontrivial topological nature. Computational studies are under way for $1/5+1/5$, $1/3+1/3$ and other total filling numbers for different Landau levels. We will also study open issues about non-Abelian FQHE in 2D graphene and its bilayers, as well as the surfaces of topological insulators using our newly developed DMRG codes. We are also exploring topological phases in cold atom systems, where topological bands can be realized through gauge flux. We will also study the charge pump, charge polarization and density correlation functions, where the nature of quantum system can be revealed through these experimental accessible measurements. Other direction is to further develop computational method for detecting topological phases, and calculating modular matrix. We are combining our current DMRG codes with tensor network approach for more efficient calculations.

Publications

1. Wei Li, D. N. Sheng, C. S. Ting, Yan Chen, “Interaction driven quantum phase transition in fractional quantum spin Hall effects”, Phys. Rev. B **90**, 081102(R) (2014).
2. W. Zhu, S. S. Gong, F. D. M. Haldane, D. N. Sheng, “The Fractional Quantum Hall States at $\nu=13/5$ and $12/5$ and their Non-Abelian Nature”, Phys. Rev. Lett. **115**, 126805 (2015).
3. Wen-Jun Hu, Shou-Shu Gong, Wei Zhu, D. N. Sheng, “Competing Spin Liquid States in the Spin-1/2 Heisenberg Model On Triangular Lattice”, Phys. Rev. B **92**, 140403 (2015).
4. W. Zhu, S. S. Gong, D. N. Sheng, L. Sheng, “Possible non-Abelian Moore-Read state in double-layer bosonic fractional quantum Hall system”, Phys. Rev. B **91**, 245126(2015).
5. W. Zhu, S. S. Gong, F. D. M. Haldane, D. N. Sheng, “Topological Characterization of Non-Abelian Moore-Read State using Density-Matrix Renormalization Group”, Phys. Rev. B **92**, 165106 (2015).
6. Shou-Shu Gong, Wei Zhu, Leon Balents, D. N. Sheng, “Global Phase Diagram of Competing Ordered and Quantum Spin Liquid Phases on the Kagome Lattice”, Phys. Rev. B **91**, 075112 (2015).
7. Wen-Jun Hu, Wei Zhu, Yi Zhang, Shoushu Gong, Federico Becca, D. N. Sheng, “Variational Monte Carlo study of a chiral spin liquid in the extended Heisenberg model on the Kagome lattice”, Phys. Rev. B **91**, 041124(R) (2015).
8. W. Zhu, S. S. Gong, D. N. Sheng, “Chiral and Critical Spin Liquids in Spin-1/2 Kagome Antiferromagnet”, Phys. Rev. B **92**, 014424 (2015).
9. Shou-Shu Gong, Wei Zhu, D. N. Sheng, “Quantum phase diagram of the spin-1 J1-J2 Heisenberg model on the honeycomb lattice”, Phys. Rev. B **92**, 195110 (2015).
10. Tian-Sheng Zeng, W. Zhu, D. N. Sheng, “Bosonic integer quantum Hall states in topological bands with Chern number two”, Phys. Rev. B **93**, 195121 (2016).

11. W. Zhu, S. S. Gong, and D. N. Sheng, “Interaction-driven fractional quantum Hall state of hard-core bosons on Kagome lattice at one-third filling”, Phys. Rev. B **94**, 035129 (2016).
12. W. Zhu, S. S. Gong, T. S. Zeng, L. Fu, D. N. Sheng, “Interaction-Driven Spontaneous Quantum Hall Effect on Kagome Lattice”, *arXiv:1604.07512, submitted to Phys. Rev. Lett.*
13. Deng, H. Geng, Wei Luo, Wei Chen, L. Sheng, D. N. Sheng, D. Y. Xing, “Robust AC Quantum Spin Hall Effect without Participation of Edge States”, *arXiv:1606.08301, submitted to Phys. Rev. Lett.*
14. W. Zhu, Z. Liu, F. D. M. Haldane, and D. N. Sheng, “Fractional Quantum Hall Bilayers at Half-Filling: Tunneling-driven Non-Abelian Phase”, to be submitted (2016).

Many-Body Theory of Energy Transport and Conversion at the Nanoscale

Principal Investigator: Charles A. Stafford
Department of Physics, University of Arizona
1118 E. 4th Street, Tucson, AZ 85721
staffordphysics92@gmail.com

Program Scope

This project addresses the fundamental challenge of understanding quantum systems far from equilibrium, while simultaneously exploring the potential of nanostructured materials for applications in energy-conversion technologies. The main focus of the project is quantum thermoelectrics. The enhancement of thermoelectricity due to electron wave interference in nanostructures will be investigated in both the linear and nonlinear regimes. To elucidate the local quantum mechanisms responsible for thermoelectricity, the project will investigate local thermoelectric probes of nonequilibrium quantum systems. Fundamental research on the nonequilibrium many-body theory of nanostructures will be conducted in parallel, to enable the applied research on nanoscale energy conversion. The local properties of interacting quantum systems far from equilibrium will be investigated using nonequilibrium Green's functions (NEGF), including the development of new nonperturbative approximations to describe local heat dissipation.

Recent Progress

Local thermoelectric probes of nonequilibrium quantum systems - Recent advances in thermal microscopy,^{1–3} where spatial and thermal resolutions of 10nm and 15mK, respectively, have been achieved,³ raise a fundamental question, “On how short a length scale can a statistical quantity like temperature be meaningfully defined?” In prior work,⁴ we provided a physically motivated and mathematically rigorous definition of an electron thermometer as an open third terminal in a thermoelectric circuit. We then developed a realistic model of a scanning thermal microscope (SThM) with atomic resolution, including an analysis of the factors limiting both spatial and thermal resolution. We also showed that the local temperature of a nonequilibrium system so defined satisfies a fluctuation-dissipation theorem.⁵

In collaboration with Justin Bergfield, Mark Ratner, and Massimiliano Di Ventra, we investigated the local electron temperature distribution in graphene nanojunctions subject to an applied thermal gradient. Using a realistic model of a scanning thermal microscope, we predict quantum temperature oscillations whose wavelength is related to that of Friedel oscillations (see Fig. 1). Experimentally, this wavelength can be tuned over several orders of magnitude by gating/doping, bringing quantum temperature oscillations within reach of the spatial resolution of existing measurement techniques for the first time.

In collaboration with Justin Bergfield, a generalization of Büttiker’s voltage probe concept for nonzero temperatures was developed. An explicit analytic expression for the thermoelectric correction to an ideal quantum voltage measurement was derived, and interpreted in terms of

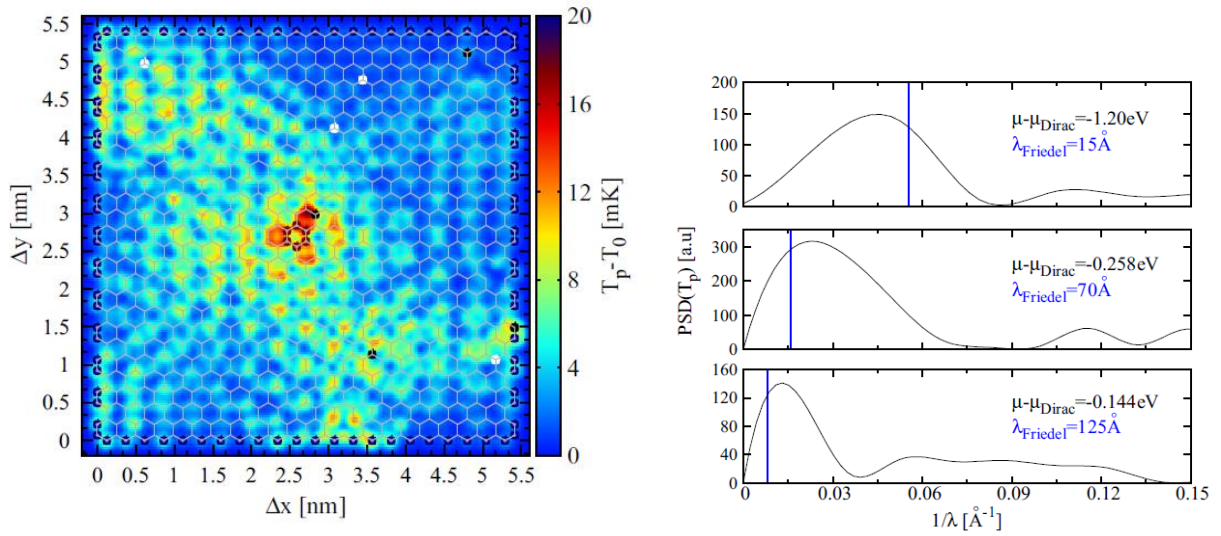


FIG. 1. Left panel: Simulated temperature distribution of a disordered graphene nanofragment contacted by an atomically-sharp hot needle at the center. Right panel: Power spectrum of graphene nanoribbon temperature distributions for three different gate voltages, indicating the existence of long-wavelength thermal oscillations near the Dirac point.

local Peltier cooling/heating within the nonequilibrium system. The thermoelectric correction was found to be large (up to $\pm 24\%$ of the peak voltage) in a prototypical ballistic quantum conductor (graphene nanoribbon). The effects of measurement non-ideality were also investigated. Our findings have important implications for precision local electrical measurements.

In collaboration with Abhay Shastray, the properties of cold spots in nonequilibrium quantum systems were investigated. A new definition of local entropy of a nonequilibrium quantum system was introduced. It was shown that the local nonequilibrium entropy is always less than or equal to the entropy of a local equilibrium distribution satisfying the same constraints, leading to a proof of the *third law of thermodynamics* for nonequilibrium systems: the local entropy must approach zero as the local temperature as measured by a thermoelectric probe goes to zero.

In collaboration with Abhay Shastray, it was shown that a local measurement of temperature and voltage for a quantum system in steady state, arbitrarily far from equilibrium, with arbitrary interactions within the system, is unique when it exists. A necessary and sufficient condition for the existence of a solution is derived. We find that a positive temperature solution exists whenever there is no net population inversion. However, when there is a net population inversion, we may characterize the system with a unique negative temperature (see Fig. 2). Our results strongly suggest that a local temperature measurement without a simultaneous local voltage measurement, or vice-versa, is a misleading characterization of the state of a nonequilibrium quantum electron system. These results provide a firm mathematical foundation for voltage and temperature measurements far from equilibrium.

Local thermodynamics of an interacting system far from equilibrium - It was shown that

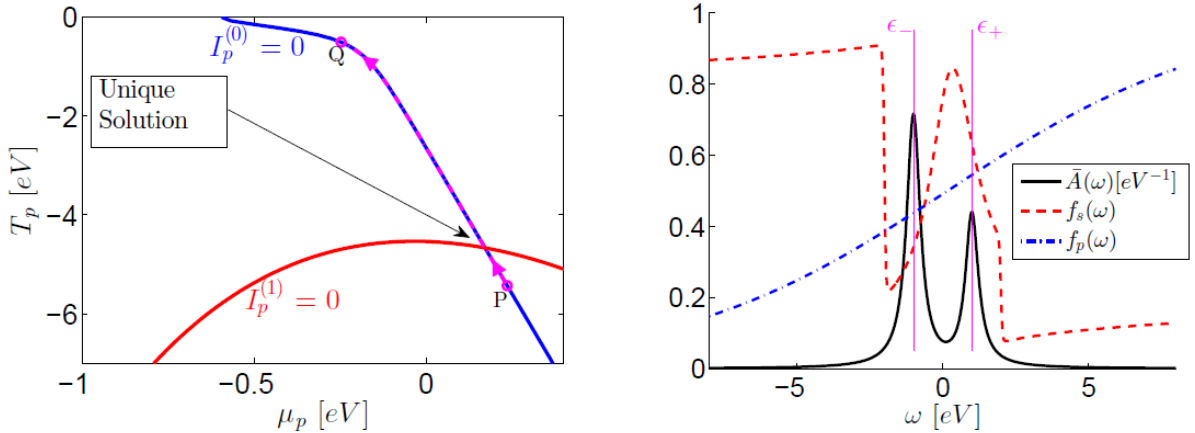


FIG. 2. Equilibration of a thermoelectric probe with a strongly-driven two-level quantum system. Left panel: Curves along which the electric current $I_p^{(0)}$ and heat current $I_p^{(1)}$ into the probe vanish. Right panel: The local spectrum $\bar{A}(\omega)$, local nonequilibrium distribution $f_s(\omega)$, and probe distribution $f_p(\omega)$ corresponding to the unique negative temperature solution on the left.

the local temperature defined by a scanning thermoelectric probe is consistent with the zeroth, first, second, and third laws of thermodynamics, provided the probe-system coupling is weak and broad band. For non-broadband probes, the local temperature obeys the Clausius form of the second law and the third law exactly, but there are corrections to the zeroth and first laws that are higher-order in the Sommerfeld expansion. The corrections to the zeroth and first laws are related, and can be interpreted in terms of the error of a nonideal temperature measurement. These results also hold for systems at negative absolute temperature.

Control of exciton transport using quantum interference - In collaboration with Mark Lusk, Lincoln Carr, and Jeramy Zimmerman, it was shown that quantum interference can be employed to create an exciton transistor. An applied potential gates the quasiparticle motion and also discriminates between quasiparticles of differing binding energy. When implemented within nanoscale assemblies, such control elements could mediate the flow of energy and information. Quantum interference can also be used to dissociate excitons as an alternative to using heterojunctions. Selected entanglement measures are shown to distinguish regimes of behavior which cannot be resolved from population dynamics alone.

Future Plans

Local heat and energy flow in nonequilibrium quantum systems - Like the well-known persistent electric currents that flow in closed quantum systems ranging from small cyclic organic molecules to mesoscopic metal and semiconductor rings, driven open quantum systems exhibit quantum mechanical eddy currents. It is clear from the definitions of the local currents that eddies of the local energy current must also exist in these systems, and it is an interesting open question whether such eddy currents are related to the quantum oscillations of the local temperature predicted by the PI and collaborators, as well as by other investigators. The relationship, if it exists, cannot be one-to-one, since quantum thermal oscillations also exist in simply connected (e.g., one-dimensional) systems. Perhaps even more interesting is whether local quantum enhancements of thermoelectricity can be explained in terms of such thermal eddy

currents.

Local entropy of nonequilibrium quantum systems - A formula for the local entropy of a nonequilibrium system of independent fermions was postulated by the PI and Ph.D. student Abhay Shastry in the current reporting period. This formula satisfies important limiting cases: (i) It gives the correct global entropy for a nonequilibrium system, and (ii) it gives the correct local entropy for an equilibrium system. It was shown that this formula satisfies the maximum entropy principle and the third law of thermodynamics. The extent to which the first law of thermodynamics can be formulated locally in terms of differentials of this local entropy will be investigated. A fundamental derivation of the formula will be sought, and its extension to interacting systems will be pursued, where entanglement entropy will compete with the entropy of mixing.

Emergence of Fourier's law of heat transport in quantum systems - The PI and collaborator Justin Bergfield have argued qualitatively that the classical picture of diffusive propagation of heat emerges in quantum systems not due to intrinsic scattering mechanisms that wash out quantum wave effects, but rather through coarse-graining of the measured temperature distribution itself. This qualitative picture will be tested/confirmed quantitatively by studying quantum heat propagation in two-dimensional systems. Preliminary results indicate that the classical Fourier law of heat transport indeed emerges from coarse graining without the introduction of any intrinsic scattering processes.

Photon thermometer - The apparent temperatures of electrically biased single-molecule junctions inferred from the spectrum of photons emitted can exceed 2000K, far exceeding the conditions for junction stability. The "photon temperature" of such a junction will be defined by that of black body radiation surrounding the junction which causes the net power absorbed by the junction to equal that radiated. A nonequilibrium Green's function calculation of the junction radiation problem will carried out, with the goal of explaining the apparent temperatures of electrically biased junctions in terms of the thermalized photons reemitted from the surroundings of the junction.

References

1. A. Majumdar, "Scanning thermal microscopy," *Annu. Rev. Mater. Sci.* **29**, 505–585 (1999).
2. Y.-J. Yu, M. Y. Han, S. Berciaud, A. B. Georgescu, T. F. Heinz, L. E. Brus, K. S. Kim, and P. Kim, "High-resolution spatial mapping of the temperature distribution of a joule self-heated graphene nanoribbon," *Appl. Phys. Lett.* **99**, 183105 (2011).
3. K. Kim, W. Jeong, W. Lee, and P. Reddy, "Ultra-high vacuum scanning thermal microscopy for nanometer resolution quantitative thermometry," *ACS Nano* **6**, 4248–4257 (2012).
4. J. P. Bergfield, S. M. Story, R. C. Stafford, and C. A. Stafford, "Probing Maxwell's demon with a nanoscale thermometer," *ACS Nano* **7**, 4429–4440 (2013).
5. J. Meair, J. P. Bergfield, C. A. Stafford, and P. Jacquod, "Local Temperature of Out-of-Equilibrium Quantum Electron Systems," *Phys. Rev. B* **90**, 035407 (2014).

Publications

1. J. P. Bergfield and C. A. Stafford, [Thermoelectric Corrections to Quantum Voltage Measurement](#), Physical Review B **90**, 235438 (2014).
2. Lan Gong, J. Bürki, Charles A. Stafford, Daniel L. Stein, [Lifetimes of Metal Nanowires with Broken Axial Symmetry](#), Physical Review B **91**, 035401 (2015).

3. Justin P. Bergfield, Mark A. Ratner, Charles A. Stafford, Massimiliano Di Ventra, [Tunable Quantum Temperature Oscillations in Graphene Nanostructures](#), Physical Review B **91**, 125407 (2015).
4. Abhay Shastray and Charles A. Stafford, [Cold spots in quantum systems far from equilibrium: local entropies and temperatures near absolute zero](#), Physical Review B **92**, 245417 (2015).
5. Mark T. Lusk, Charles A. Stafford, Jeramy D. Zimmerman, and Lincoln D. Carr, [Control of exciton transport using quantum interference](#), Physical Review B **92**, 241112(R) (2015).
6. Charles A. Stafford, [Local temperature of an interacting quantum system far from equilibrium](#), Physical Review B **93**, 245403 (2016).
7. Abhay Shastray and Charles A. Stafford, [Temperature and voltage measurement in quantum systems far from equilibrium](#), arXiv:1603.00096, submitted to Phys. Rev. B.

Non-equilibrium Relaxation and Aging Scaling of Driven Topological Defects in Condensed Matter

Principal Investigator: Uwe C. Täuber (tauber@vt.edu)

Co-Principal Investigator: Michel Pleimling (pleim@vt.edu)

Department of Physics (MC 0435), Virginia Tech

Robeson Hall, 850 West Campus Drive, Blacksburg, Virginia 24061

Keywords: driven topological defects, type-II superconductors, skyrmions, non-equilibrium relaxation, aging scaling

Project Scope

Technical applications of type-II superconductors, especially high- T_c compounds, in external magnetic fields require an effective flux pinning mechanism to reduce Ohmic losses due to flux creep and flow. Consequently, the properties of interacting vortex lines subject to strong thermal fluctuations and point-like or extended disorder have been a major research focus in condensed matter physics. Supported through DOE-BES, we have developed efficient and versatile Monte Carlo and Langevin molecular dynamics algorithms, based on an elastic line representation of the magnetic vortices, and studied in detail the dynamical relaxation features towards the equilibrium vortex or Bose glass phases following sudden temperature and magnetic field changes. We have thus identified unique dynamical signatures that distinguish samples with point pinning centers and extended columnar defects. Our current research efforts aim at several crucial and novel extensions: (1) We investigate the relaxation kinetics and possible aging scaling of driven vortex matter towards or from non-equilibrium stationary states following temperature, magnetic field, and driving current quenches. (2) We intend to further clarify the decisive effects of pinning center geometry on vortex relaxation dynamics by exploring samples with extended planar defects. (3) Our Langevin numerical approach has been modified to describe the kinetics of relaxing and driven skyrmion topological defects in two-dimensional magnets. Our goal is to propose specific experimental set-ups amenable to probing the different dynamical regimes, and stimulate the development of new tools for material characterization and optimization.

Recent Progress

Relaxation dynamics of vortex lines following magnetic field and temperature quenches

After having achieved a good understanding of relaxation processes in vortex systems where the initial state is characterized by randomly distributed straight flux lines, we recently focused on situations where the system is brought out of equilibrium by sudden field or temperature quenches. Employing an elastic line model and performing Langevin molecular dynamics simulations we are bringing a previously equilibrated system out of equilibrium by either suddenly changing the temperature or by instantaneously altering the magnetic field which is reflected in adding or removing flux lines to or from the system. The subsequent aging properties are investigated in samples with either randomly distributed point-like or extended columnar defects, which allows to distinguish the complex relaxation features that result from either type of pinning centers. One-time observables such as the radius of gyration and the fraction of

pinned line elements are employed to characterize steady-state properties, and two-time correlation functions such as the vortex line height autocorrelations and their mean-square displacement are analyzed to study the non-linear stochastic relaxation dynamics in the aging regime.

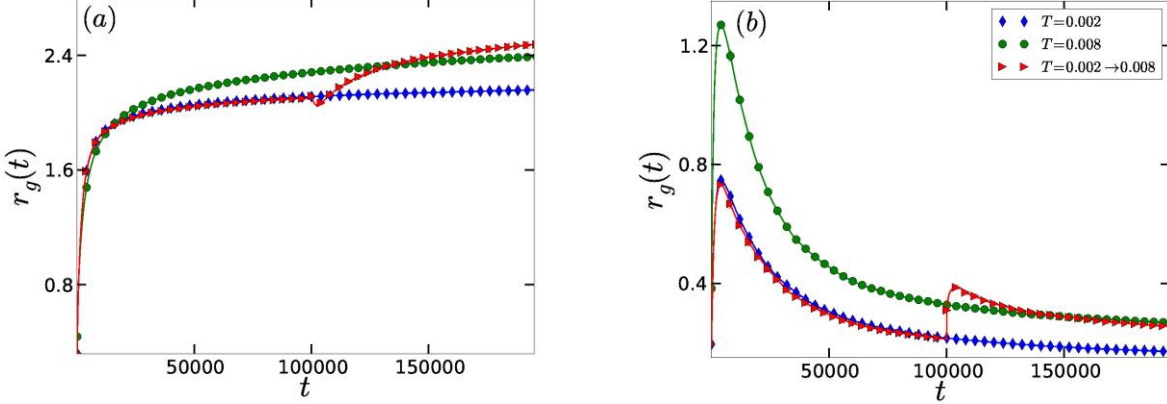


Fig. 1: Relaxation of the gyration radius in systems of interacting vortex lines with (a) point disorder or (b) columnar defects, when the temperature is either held fixed or instantaneously raised (data averaged over 1000 realizations). Systems with columnar defects require a longer relaxation time for the radius of gyration at higher temperatures than that at lower temperatures, asserting that thermal fluctuations resist the straightening of vortex lines as they become localized at columnar pinning centers.

Current quenches in disordered type-II superconductors

We have also investigated the relaxation dynamics of magnetic vortex lines in type-II superconductors following rapid changes of the external driving current. A system of flux vortices in a sample with randomly distributed point-like defects is subjected to an external current of appropriate strength for a sufficient period of time so as to be in a moving non-equilibrium steady state. The current is then instantaneously lowered to a value that pertains to either the moving or pinned regime. The ensuing relaxation of the flux lines is studied via one-time observables such as their mean velocity and radius of gyration. We have in addition measured the two-time flux line height autocorrelation function to investigate dynamical scaling and aging behavior in the system, which in particular emerge after quenches into the glassy pinned state. For quenches within the moving regime, we have studied the effects of the vortex-vortex repulsive interactions on the relaxation kinetics of the vortices by performing drive quenches in the system with the interactions initially absent or in effect. In both cases, drive quenches within the moving phase result in fast exponential relaxation of the system from one non-equilibrium steady state to another, as evidenced by the rapid temporal evolution of one-time observables. For our study on drive quenches from the moving to the pinned regime, in stark contrast to quenches within the moving regime, the relaxation of the system after the quench is much slower, which is seen in the non-exponential, logarithmic time evolution of the radius of gyration and fraction of pinned line elements. This indicates that the system fails to reach a steady state when quenched into the pinned regime on time scales that are on the order of the simulation duration. The two-time height autocorrelations show breaking of time translation invariance, accompanied by dynamical scaling, evidence for aging in the system, as we quench it from a moving non-equilibrium steady state into a pinned, glassy one.

Future Plans

Quenches onto the depinning threshold and critical aging

Our recent investigation of relaxation processes in driven vortex matter focused on parameter changes within the moving phase as well as on the coarsening that follows quenches from the moving steady state into the glassy equilibrium phase. Of special interest are also quenches from the moving phase onto the critical depinning regime. At zero temperature, elastic strings driven through disordered media undergo a non-equilibrium continuous phase transition at the critical driving force that separates the pinned from the moving phase. Signatures of this dynamical critical point should clearly be observable at sufficiently low temperatures in the vicinity of the depinning threshold. Since critical correlations are governed by a diverging correlation length, dynamical features in this regime presumably display a higher degree of universality than coarsening kinetics in the respective glassy phases. For example, one would expect the same critical scaling in the aging kinetics of flux lines that either interact with localized point pins or are subject to a continuous disorder landscape, in contrast to the noticeable distinctions that we described for the relaxation dynamics and pinning time distributions deep inside the vortex glass. With the correlation length taking over the role of the coarsening scale, we anticipate a reduction of complexity in the observed kinetics and dynamical scaling features. Yet the freezing into a vortex glass phase of magnetic flux lines in the presence of uncorrelated disorder remains manifestly different from the Bose glass transition, *i.e.*, their localization to extended columnar defects. We intend to identify and characterize these distinctions in detailed studies of various dynamical observables in the critical aging regime.

Non-equilibrium relaxation of magnetic flux lines subject to planar defects

In many high-temperature superconductors such as the cuprates, twin boundaries are abundant, and in conjunction with random point defects (oxygen vacancies) serve as natural pinning centers for flux lines. Recent work argued that planar defects destabilize the Bragg glass phase and induce a distinct, novel planar glass state. Numerical simulations as well as various experimental studies established the anisotropy of vortex pinning and transport in twinned superconductors: within the defect planes, thermal flux line fluctuations are enhanced and vortex motion facilitated. Thus flux flow may be channeled along twin or grain boundaries, even when their orientation is tilted with respect to the driving current. Our extensive studies of non-equilibrium aging phenomena of vortex matter in disordered superconductors have demonstrated the paramount influence of the geometry and spatial distribution of pinning centers. We expect that planar defects will further highlight this crucial role and moreover add new characteristic signatures imprinted by twin or grain boundaries on flux line relaxation phenomena. We just started to embark on a series of numerical investigations that will address various aging scenarios of magnetic vortices in systems with both point and extended planar pinning sites. The questions to be addressed in this project group themselves into two categories: (1) what are the signatures of anisotropic non-equilibrium vortex fluctuations in systems with planar defects and (2) what are the relaxation phenomena to and from driven steady states with anisotropic flux transport.

Non-equilibrium kinetics of relaxing and driven skyrmions

Magnetic skyrmions, *i.e.*, particle-like spin textures of nanometer size, have been shown to exist in chiral magnets without inversion symmetry. Skyrmions are topologically protected and form

triangular lattices, similar to vortices in type-II superconductors. Since current-driven transport is of obvious interest in spintronics applications, skyrmion propagation in an applied field has been the subject of both experimental and theoretical studies. These investigations demonstrated that skyrmions only interact weakly with impurities and are set in motion even at ultra-low current densities. A recently derived particle model for skyrmions yields equations of motion in two dimensions that are very similar to those used for the effective two-dimensional description of vortices in type-II superconductors, when the latter are treated as point-like objects. The most important difference resides in the strong effect of the Magnus force on a skyrmion that acts in the direction perpendicular to its velocity. We propose to leverage our comprehensive understanding of the non-equilibrium relaxation and aging properties of vortex matter to gain novel insights into the corresponding phenomena in interacting skyrmion systems. Our starting point will be the particle model, which we will explore by means of Langevin molecular dynamics simulations. These detailed studies of magnetic skyrmion kinetics will provide us with a more complete picture of the complex relaxation processes that take place in condensed matter systems whose dynamics are governed by fluctuating and correlated topological defects.

Publications (2014 – 2016)

1. M. T. Shimer, U. C. Täuber, and M. Pleimling, *Non-equilibrium relaxation and aging scaling of the Coulomb and Bose glass*, Phys. Rev. E **90**, 032111 (2014) [arXiv: 1403.6615].
2. U. Dobramysl, M. Pleimling, and U. C. Täuber, *Pinning time statistics for vortex lines in disordered environments*, Phys. Rev. E **90**, 062198 (2014) [arXiv: 1405.7261].
3. H. Assi, H. Chaturvedi, U. Dobramysl, M. Pleimling, and U. C. Täuber, *Relaxation dynamics of vortex lines in disordered type-II superconductors following magnetic field and temperature quenches*, Phys. Rev. E **92**, 052124 (2015) [arXiv: 1505.06240].
4. M. Pleimling and U. C. Täuber, *Characterization of relaxation processes in interacting vortex matter through a time-dependent correlation length*, J. Stat. Mech. 2015, P09010 (2015) [arXiv: 1507.07283].
5. H. Assi, H. Chaturvedi, U. Dobramysl, M. Pleimling, and U. C. Täuber, *Disordered vortex matter out of equilibrium: a Langevin molecular dynamics study*, accepted for publication in Molecular Simulation (2016) [arXiv: 1509.02227].
6. S. Chen and U. C. Täuber, *Non-equilibrium relaxation in stochastic lattice Lotka-Volterra model*, Phys. Biol. **13**, 025005 (2016) [arXiv: 1511.05114].
7. U. C. Täuber, *Phase transitions and scaling in systems far from equilibrium*, submitted to Annu. Rev. Condens. Matter Phys. (to appear in 2017) [arXiv: 1604.04487].
8. H. Assi, H. Chaturvedi, M. Pleimling, and U. C. Täuber, *Structural relaxation and aging scaling in the Coulomb and Bose glass models*, submitted to Eur. Phys. J. B (2016) [arXiv: 1606.02971].
9. H. Chaturvedi, H. Assi, U. Dobramysl, M. Pleimling, and U. C. Täuber, *Flux line relaxation kinetics following current quenches in disordered type-II superconductors*, submitted to J. Stat. Mech. (2016) [arXiv: 1606.06100].
10. W. Liu and U.C. Täuber, Critical initial-slip scaling for the noisy complex Ginzburg-Landau equation, submitted to J. Phys. A: Math. Theor. (2016) [arXiv: 1606.08263].

Unconventional Metals in Strongly Correlated Systems

Principal Investigator: Senthil Todadri

Department of Physics

Massachusetts Institute of Technology

Cambridge MA 02139 -4307

senthil@mit.edu

Project scope:

A growing number of metals display phenomena that defy textbook paradigms for metallic behavior in electronic systems. These arise due to either strong electron correlations, reduced dimensionality, or disorder effects (or a combination of more than one of these effects). One class of metals (famously in the cuprates) do not fit the Landau fermi liquid paradigm. In many cases the non-fermi liquid state seems optimal for superconductivity to develop on cooling. Our theoretical understanding of such unconventional metals and their superconducting instability is rather primitive. Though many basic questions about such non-Fermi liquid metals are open, there has been slow but steady progress over the years. A major component of the project seeks to develop methods capable of dealing with non-fermi liquid physics and its relation with superconductivity.

Recent progress:

1. Non-fermi liquid metals and superconductivity:

Understanding the vicinity of the electronic Mott metal-insulator transition is fundamental to many phenomena. An old and fundamental question is whether the Mott transition can ever be continuous. A few years back I answered this question in the affirmative and developed a theory for a continuous Mott transition from a Fermi Liquid metal to a spin liquid insulator (T. Senthil, Phys. Rev. B 78, 045109 (2008)). This earlier work was restricted to a single two dimensional plane or to a fully three dimensional system. Inspired by new experiments, very recently in [1] I (with student Liujun Zou) studied the highly nontrivial fate of this transition in a quasi-two dimensional layered materials.

We demonstrated the phenomenon of dimensional decoupling: the system behaves as a three-dimensional metal in the Fermi liquid side but as a stack of decoupled two-dimensional layers in the Mott insulator. We showed that the dimensional decoupling happens at the Mott quantum critical point itself. We derived the temperature dependence of the interlayer electric conductivity in various crossover regimes near such a continuous Mott transition, and discussed experimental implications.

2. Phenomena near optimal doping in the cuprates and the pnictides

Some of the most fascinating phenomena in correlated metals happen in the vicinity of where their low temperature superconducting transition temperature is optimal. In two recent papers I proposed explanations of some new experiments in the cuprates and the pinctides. I also describe below ongoing work (with student Liujun Zou and post-doc Sam Lederer).

A recent experimental observation (Ramshaw et al, Science 2015) of a mass enhancement in high magnetic fields in nearly optimally doped cuprates poses several puzzles. For the suggested nodal electron pocket induced by bidirectional charge order in high field, in Ref . [2] I proposed that the mass enhancement is very anisotropic around the small Fermi surface. The corners of the pocket were proposed to have a big enhancement without any enhancement along the diagonal nodal direction. A natural mechanism for such angle dependent mass enhancement comes from the destruction of the Landau quasiparticle at hot spots on the large Fermi surface at a proximate quantum critical point. The possibility of a divergent cyclotron effective mass was discussed within a scaling theory for such a quantum critical point. Ref . [2] considered both a conventional quantum critical point associated with the onset of charge order in a metal and an unconventional one where an antinodal pseudogap opens simultaneously with the onset of charge order. The latter may describe the physics of the strange metal regime at zero magnetic field.

In ongoing work I am calculating Hall transport in this model, with an eye toward explaining recent experimental measurements by the Taillefer group on nearly optimal cuprates in high magnetic fields.

In Ref. [3] (with D. Chowdhury, J. Orenstein, and S. Sachdev) I presented a theory for the large suppression (Hashimoto et al, Science, 2012) of the superfluid-density, in $\text{BaFe}_2(\text{As}_{\{1-x\}}\text{P}_x)_2$ in the vicinity of a putative spin-density wave quantum critical point at a P-doping, $x=x_c$. We argued that the transition becomes weakly first-order in the vicinity of x_c , and disorder induces puddles of superconducting and antiferromagnetic regions at short length-scales; thus the system becomes an electronic micro-emulsion. We proposed that frustrated Josephson couplings between the superconducting grains suppress the superfluid density. In addition, the presence of 'normal' quasiparticles at the interface of the frustrated Josephson junctions resolves some seemingly contradictory observations between the metallic and the superconducting phases. We proposed experiments to test our theory.

3. Detecting many body entanglement in numerical calculations

In recent years it has become clear that many novel phases of matter may be usefully characterized by theor many body quantum entanglement. In the simple case of gapped topological phases, there is a concept known as the topological entanglement entropy that provides a partial measure of the entanglement. It is challenging to study this numerically though an extrapolation method based on calculations in a cylinder geometry have been frequently used.

In Ref. [4] My student Liujun Zou (with Jeongwan Haah) showed that this protocol might sometimes return spurious answers. Work is ongoing in our group to obtain better numerical signatures of the many body entanglement.

4. Spin and pair density wave glasses

Spontaneous breaking of translational symmetry---known as 'density wave' order---is common in nature. However such states are strongly sensitive to impurities or other forms of frozen disorder leading to fascinating glassy phenomena. In Ref [5] I (with D. Mross) analyzed impurity effects on a particularly ubiquitous form of broken translation symmetry in solids: a Spin Density Wave (SDW) with spatially modulated magnetic order. Related phenomena occur in Pair Density Wave (PDW) superconductors where the superconducting order is spatially modulated. For weak disorder, we find that the SDW / PDW order can generically give way to a SDW / PDW glass---new phases of matter with a number of striking properties, which we introduce and characterize here. In particular, they exhibit an interesting combination of conventional (symmetry-breaking) and spin glass (Edwards-Anderson) order. This is reflected in the dynamic response of such a system, which---as expected for a glass---is extremely slow in certain variables, but---surprisingly---is fast in others. Our results apply to all uniaxial metallic SDW systems where the ordering vector is incommensurate with the crystalline lattice, and to recent proposals of PDW order in the cuprates.

Planned activities:

I am currently studying transport in my proposed model of a small Fermi surface with anisotropic mass enhancement as a possible explanation of phenomena in the cuprates. The general results may also apply to heavy fermion metals and other related systems. I am also currently working to understand the pairing transition and the nature of the paired state of composite fermions in bilayer quantum Hall systems. This is a nice, experimentally relevant test-bed for pairing out of a non-fermi liquid normal state.

Recent publications supported by DOE:

1. Dimensional decoupling at continuous quantum critical Mott transitions,
[Liujun Zou, T. Senthil, arXiv:1603.09359](#)
2. . T. Senthil, [arXiv:1410.2096](#)
3. Phase transition beneath the superconducting dome in BaFe₂(As_{1-x}P_x)₂, [Debanjan Chowdhury, J. Orenstein, Subir Sachdev, T. Senthil](#), Phys. Rev. B 92, 081113(R) (2015)

4. Spurious Long-range Entanglement and Replica Correlation Length,
[Liujun Zou, Jeongwan Haah](#), arXiv:1604.06101.

4. Spin and pair density wave glasses,
[David F. Mross, T. Senthil](#), Phys. Rev. X 5, 031008 (2015).

Orbital-free Quantum Simulation Methods for Applications to Warm Dense Matter

Principal Investigator: Samuel B. Trickey

Dept. of Physics and Dept. of Chemistry, Univ. Florida, Gainesville FL 32611-8435

trickey@qtp.ufl.edu

co-PIs: J.W. Duffy (Physics, Univ. Florida), F. E. Harris (Physics, Univ. Utah),

K. Runge (Materials Science and Eng., Univ. Arizona)

15 July 2016

Project Scope

The motivating physical systems for this project are materials under extreme state conditions: electronic temperature $T_e \approx T_F$ the Fermi temperature and pressures P in the Mbar range. That warm dense matter (WDM) regime (and the states traversed to reach it) includes the thermodynamic trajectory of inertial confinement fusion targets, structure and heat flow of giant planet interiors, and ultra-fast material response in Z-pinchers. Experimental accessibility to WDM is limited and difficult, hence predictive simulation is a high payoff alternative. The motivating technical context is high potential opportunity for major improvement of the predictive capacity and speed of ab initio molecular dynamics (AIMD) simulations.

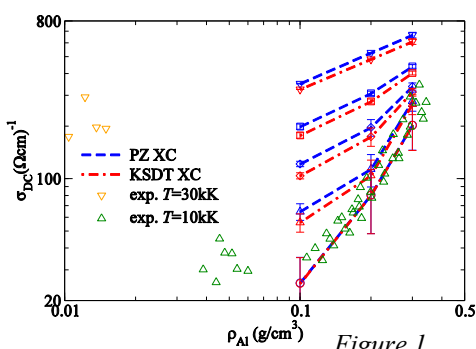
AIMD is the approach of choice because WDM is best treated as a complicated condensed phase regime, not a plasma. Ion thermodynamics in AIMD comes from classical dynamics with forces from quantum electrons in the Born-Oppenheimer approximation. Cost versus accuracy balance makes the Mermin free-energy generalization of ground-state density functional theory (DFT) the best choice for the quantum part. But extension of advanced ground-state DFT methodology into WDM state conditions is challenging. Before this project, there was no well-founded, non-empirical exchange-correlation (XC) free-energy functional. Constraints from formal properties (e.g. scaling, bounds) were little known until the last few years. Thermal occupation of high-energy Kohn-Sham (KS) states exacerbates the unfavorable computational cost scaling (cubic) with T_e and system size. Orbital-free DFT depends only on the density, so it scales with system size. But venerable OF-DFT schemes of Thomas-Fermi type cannot give bound molecules and condensed phases, thus cannot describe WDM. Better non-interacting functionals are required.

Advancing free-energy DFT as a powerful tool for ab initio simulation of WDM thus is a major thrust of this project. Another thrust is OF-DFT to evade the KS computational scaling bottleneck. The third, closely related thrust is foundational: development of the theoretical underpinnings that provide constraints, bounds, and other rigorous results for free-energy DFT approximations. The fourth thrust is

development, implementation, testing, and distribution of open-source simulation software which exploits the advances in the other three thrusts. After progress summaries on these four thrusts, we outline important components of research presently underway or in prospect.

Recent Progress

Free-energy XC functionals – Common practice in AIMD simulations of WDM has been to approximate the XC free energy $\mathcal{F}_{xc}[n;T]$ via a ground-state functional evaluated with the T -dependent density, $E_{xc}[n(T)]$. Recently we showed [3] the strong state-dependence of the validity of this approximation. Figure 1



shows the DC conductivity of low density Al for five values of T_e , from bottom to top 5 kK (circles), 10 kK (triangles up), 15 kK (diamonds), 20 kK (squares), and 30 kK (triangles down). Experimental data are

shown for 10 kK (triangles up) and 30 kK (triangles down). Red symbols are KS calculations with our LSDA free-energy parameterization (KSDT: Publication [14]). Blue symbols are with Perdew-Zunger ground-state LSDA. KSDT gives shifts of as much as 15% *toward experiment*. A 6% range of pressure differences occurs for the deuterium equations of state obtained from the two XC functionals, but the hydrogen principal Hugoniot is insensitive to the explicit T_e dependence in KSDT because of cancellation in the Rankine-Hugoniot equation.

Orbital-free KS kinetic energy and entropy functionals – Publication [5] explored the possibility of expressing the enhancement factor F_s in $\int dr n(r)^{5/3} F_s[n(r)]$, the ground-state non-interacting kinetic energy, solely as a function of powers of the density, following the approximation scheme of Liu and Parr {Phys. Rev. A **55**, 179 (1997)}. It is surprisingly successful for atoms, hence may lead to improved OF-DFT formulations of both ground-state and finite- T_e approximate non-interacting functionals. In publication [10] we began exploration of the disjuncture between constraints on OF-DFT functionals from density cusp conditions and the absence of such cusps in many of the pseudo-densities with which those functionals are used in computation. That study then explored the question of the optimum possible numerical fit of a generalized-gradient-approximation (GGA) non-interacting KE functional, *irrespective* of formal constraints. Significant limits were found, yet the success of our VT84F functional {Phys. Rev. B **88**, 161108(R) (2013)} demonstrates that a useful GGA is possible. See also our comment in publication [6]. There are limits to VT84F, however. In particular, it does not deliver a characterization of the liquid-vapor critical point in aluminum, though a published KS AIMD calculation shows it {Desjarlais, Atom. Proc. Plasmas, CP-1161, K.B. Fournier ed., 32 (2009)}. The KS AIMD calculation is very delicate. We are investigating its sensitivity to parameters, approximate functional choice, etc.

Foundational theory – Publication [4] extended earlier work from this project on scaled variables {Phys. Rev. B **84**, 125118 (2011)} to derive uniform coordinate scaling requirements for interacting system free energy density functionals. Publication [9] studied the use of grand canonical expressions in the fixed particle-number environment (canonical ensemble) of a computer code. The two ensembles agree well at modest, finite particle number but both disagree with the infinite-degree-of-freedom limit. Publications [2] and [7] developed the consequences for the HEG and harmonically confined electrons respectively, of our previous formulation {Phys. Rev. E **87**, 032102 (2013)} of an exact mapping of quantum effects into a classical liquid-like treatment. Unexpected hard-wall behavior was found in the harmonic confinement case. Publication [1] provides a systematic way from DFT to renormalize the Thomas-Fermi potential such that in the field of an ion the electron density is non-singular at the nucleus. Finally, publications [12,18] gave a new recursive procedure for evaluating matrix elements in 3- and 4-body systems. 4-body systems (e.g. Li atom) are of particular interest in understanding the requirements on OF-DFT kinetic energy functionals.

Figure 2

Open-source Software – Publication [13] presented our PROFESS@QuantumEspresso libraries and code. In March 2016, we released version 2. See Fig. 2. It couples PROFESS version 3.0 (with our modifications and patches) with QuantumEspresso version 5.2.1. code. The result enables OF-DFT AIMD simulations in modified QuantumEspresso on the same technical footing (MD algorithms, thermostats, parameters, etc.) as for KS DFT. PROFESS enhancements include our free-energy density functionals. Publication [8] described algorithms and software for high-accuracy evaluation of several commonly encountered Fermi-Dirac integral combinations. Those modules were made available as downloads in

June 2105. In late Dec. 2015, our KSDT XC free energy functional was made available in LibXC version 3.0. However, that implementation will not initialize properly if called in standard LibXC style. On June 15, 2016 we posted an initialization routine, a HOWTO file which explains the extra initialization, and a set of simple test routines to check. And KSDT modules also are available directly from us. All of our software is downloadable from www.qtp.ufl.edu/ofdft under GNU GPL. In collaboration with Profs. Rehr and Seidler (Univ. of Washington) we have installed the KSDT functional in the FEFF9 code and begun to explore the implications for algorithmic stability of calculations in the low density part of the WDM regime.

Investigations Underway and Planned

We have developed and are well into testing a full Kubo-Greenwood (K-G) electrical conductivity package for QuantumEspresso. Release under GPL is expected this Fall. After that, we will be in position to make a thorough study of a scheme we proposed that was recently tried by a group alumnus {Sjostrom and Daligault, Phys. Rev. E **92**, 063304 (2015)}, namely to compute K-G conductivities from OF-DFT AIMD snapshot ion configurations via non-self-consistent evaluation of the KS Hamiltonian from the OF-DFT density at each configuration. A single diagonalization scheme, it is a comparatively fast route to transport coefficients.

Calculations have been completed and analysis is underway of quantum nuclear effects (i.e., beyond the Born-Oppenheimer approximation) for light nuclei, e.g. H and D, in the WDM regime. The methodology is path-integral molecular dynamics for nuclear motion driven by our VT84F OF-DFT functional. The investigation focuses on nuclear temperatures that are low compared to T_e . Initial analysis suggests that the OF-DFT driven PIMD is consistent with what is known for the same state conditions from other, much more costly calculations. Publication is expected by late Fall 2016.

We are well along on construction of substantially more general and accurate XC free energy functionals \mathcal{F}_{xc} than LSDA. These are of GGA form, with constraints familiar both from ground-state GGA XC construction and from free-energy considerations. As regards non-interacting functionals (KS KE and entropy), we have constructed and now are refining correspondingly improved functionals compared to VT84F. A continuing challenge is that the Pauli term part of such a functional must vanish for a two-electron singlet system in its ground state, yet must be non-vanishing for all three and higher number systems. These new non-interacting functionals incorporate density Laplacian dependence, which raises the technical difficulty of rather complicated “kinetic potentials” in the Euler equation and attendant instabilities. Another direction for non-interacting functional development is tunable functionals, built to extrapolate and/or interpolate finite- T_e KS calculations by parametrizing to them while respecting known constraints. On the formal side, we are studying how to resolve the anomalous behavior of OF-DFT functionals that behave well with some types of pseudo-potentials but badly with others. We continue analyzing the formal basis of free-energy DFT as the mean-field context for kinetic theory, electron-electron scattering, and the resulting transport coefficients.

The major computation we are driving to completion is the Al liquid-vapor critical point study, now focused on the XC free energy functional and technical choices. At present it is unclear whether the prior calculations are entirely predictive. We also are collaborating supportively with groups at Univ. Arizona (on complex materials simulations using our methods and software) and Univ. Washington (on LCLS experiments using two-color techniques to probe elevated T_e effects before lattice relaxation occurs).

Since this project began (Fall 2009), we and a few others have moved free-energy DFT substantially along a path of refinement roughly parallel to the celebrated evolution of ground-state DFT. (Before this project there was not even a purely Monte Carlo based LSDA XC free-energy functional.) Free-energy DFT now is at the level of a soundly based, practical methodology for thermodynamics of matter under extreme conditions. The next steps are better functionals rooted in deeper understanding of the theory, along with paradigmatic calculations to illustrate the power and reach of the approach.

Publications (2014 – present)

[All publications and software are available from <http://www.qtp.ufl.edu/ofdft>]

- [1] “Revised Thomas-Fermi Approximation for Singular Potentials”, J.W. Dufty, and S.B. Trickey, Phys. Rev. B, submitted 28 June 2016 (arXiv 1606.09151v1).
- [2] “Finite Temperature Quantum Effects on Confined Charges”, J. Wrighton, J. Dufty, and S. Dutta, Phys. Rev. E, submitted 01 June 2016 (arXiv 1606.00281v1).
- [3] “Importance of Finite-temperature Exchange-correlation for Warm Dense Matter Calculations”, Valentin V. Karasiev, Lázaro Calderín, and S.B. Trickey, Phys. Rev. E **93**, 063207 (2016).
- [4] “Finite Temperature Scaling in Density Functional Theory”, J.W. Dufty and S.B. Trickey, Mol. Phys. **114**, 988 (2016).
- [5] “Study of Some Simple Approximations to the Non-Interacting Kinetic Energy Functional”, Edison X. Salazar, Pedro F. Guarderas, Eduardo V. Ludeña, Mauricio H. Cornejo, and Valentin V. Karasiev, Int. J. Quantum Chem. Online DOI: 10.1002/qua.25179 (2016).
- [6] “Comment on ‘Single-point kinetic energy density functionals: a pointwise kinetic energy density analysis and numerical convergence investigation’, Phys. Rev. B **91**, 045124 (2015)”, S.B. Trickey, V.V. Karasiev, and D. Chakraborty, Phys. Rev. B **92**, 117101 (2015).
- [7] “Finite Temperature Quantum Effects in Many-body Systems by Classical Methods”, J. Wrighton, J. Dufty, and S. Dutta, Adv. Quantum Chem. **72**, 1 (2016).
- [8] “Improved analytical representation of combinations of Fermi-Dirac integrals for finite-temperature density functional calculations”, V.V. Karasiev, D. Chakraborty, and S.B. Trickey, Computer Phys. Commun. **192**, 114 (2015).
- [9] “System-Size Dependence in Grand Canonical and Canonical Ensembles”, D. Chakraborty, J. Dufty, and V.V. Karasiev, Adv. Quantum Chem. **71**, 11 (2015).
- [10] “Frank Discussion of the Status of Ground-state Orbital-free DFT”, V.V. Karasiev and S.B. Trickey, Adv. Quantum Chem. **71**, 221 (2015).
- [11] “Generalized Gradient Approximation Exchange Energy Functional with Correct Asymptotic Behavior of the Corresponding Potential”, J. Carmona-Espíndola, J.L. Gázquez, A. Vela, and S.B. Trickey, J. Chem. Phys. **142**, 054105 (2015).
- [12] Comment on "Compact wave functions for four-electron atomic systems" F.E. Harris, Phys. Rev. A **91**, 026501 (2015).
- [13] “Finite-temperature Orbital-free DFT Molecular Dynamics: Coupling PROFESS and Quantum Espresso”, V.V. Karasiev, T. Sjostrom, and S.B. Trickey, Computer Phys. Commun. **185**, 3240 (2014).
- [14] “Accurate Homogeneous Electron Gas Exchange-correlation Free Energy for Local Spin-density Calculations”, V.V. Karasiev, T. Sjostrom, J.W. Dufty, and S.B. Trickey, Phys. Rev. Lett. **112**, 076403 (2014).
- [15] “Innovations in Finite-Temperature Density Functionals”, V.V. Karasiev, T. Sjostrom, D. Chakraborty, J.W. Dufty, F.E. Harris, K. Runge, and S.B. Trickey, chapter in *Frontiers and Challenges in Warm Dense Matter*, F. Graziani et al. eds., (Springer, Heidelberg, 2014) 61-85.
- [16] “Progress on New Approaches to Old Ideas: Orbital-free Density Functionals”, V.V. Karasiev, D. Chakraborty, and S.B. Trickey, chapter in *Many-Electron Approaches in Physics, Chemistry, and Mathematics*, L. Delle Site and V. Bach eds. (Springer, Heidelberg, 2014) 113-134.
- [17] “Comparative Studies of Density Functional Approximations for Light Atoms in Strong Magnetic Fields”, W. Zhu, L. Zhang, and S.B. Trickey, Phys. Rev. A **90**, 022504 (2014).
- [18] “Atomic Three- and Four-body Recurrence Formulas and Related Summations”, F.E. Harris, Theoret. Chem. Acc. **133**, 1475 (2014).

QUANTUM SIMULATIONS OF ORBITALLY CONTROLLED PHYSICS AND NANOSCALE INHOMOGENEITY IN CORRELATED OXIDES

PI: Nandini Trivedi, The Ohio State University

Keywords: Transition metal oxides, spin-orbit coupling, orbital frustration, orbital entanglement

Project Scope

Sandwiched between the weakly correlated topological insulators and the strongly correlated 3d transition metal oxides, lie 5d compounds that combine both strong spin-orbit coupling (SOC) and correlations on an equal footing. These materials have spurred great interest since they open up new regimes-- spin-orbit coupling enhanced correlations and orbitally controlled Kitaev magnetism. In contrast to the well studied 5d⁵ materials, the effect of strong spin-orbit coupling in 4d⁴ and 5d⁴ systems have been sparsely studied due to expectations that these naturally lead to boring J=0 atomic non-magnetic singlet insulating states. Yet upon allowing for hopping between atoms, we show that the superexchange interactions J_{SE} opposes SOC λ to create local moments on each site [1]. With increasing Hund's coupling, the superexchange interactions switch from supporting antiferromagnetic (AFM) spin interactions to favoring ferromagnetic (FM) spin

interactions. On the other hand, we find that the *orbital* interactions are *frustrated* even in the absence of geometric frustration. By tuning the ratio of J_{SE} to λ we obtain a phase transition at a critical strength from the J=0 singlet to a novel magnetic phase. SOC plays a non-trivial role in generating a triplon condensate [2] of weakly interacting J=1 excitations at $\mathbf{k}=\pi$ regardless of whether the local spin interactions are FM or AFM. With increasing g, the system evolves into a regime with localized spin and orbital moments and the possibility of a second phase transition to orbitally entangled liquid states. The calculations are performed using exact diagonalization, perturbation theory and quantum Monte Carlo methods. We make predictions for materials such as Ca₂RuO₄, double perovskite irridates [3] and honeycomb ruthenates, all of which have transition metal ions in the d⁴ configuration and have been found to show magnetism.

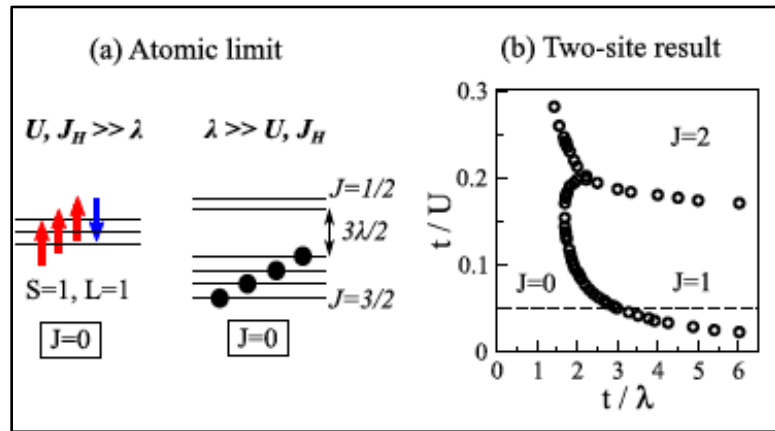
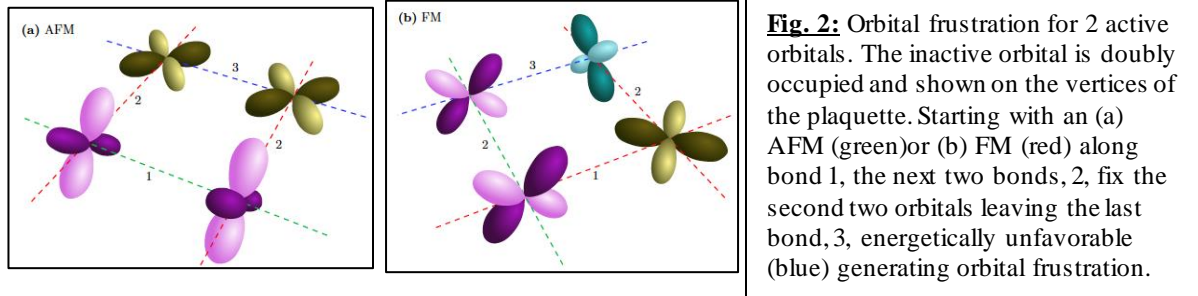


Fig 1: The atomic ground state of d⁴ ions in both $U, J_H \gg \lambda$ and $\lambda \gg U, J_H$ limits is nonmagnetic with $J=0$.
(b) The two-site phase diagram of the d⁴ system calculated by exact diagonalization shows formation of a local moment from the competition of superexchange and SOC.

Recent Progress

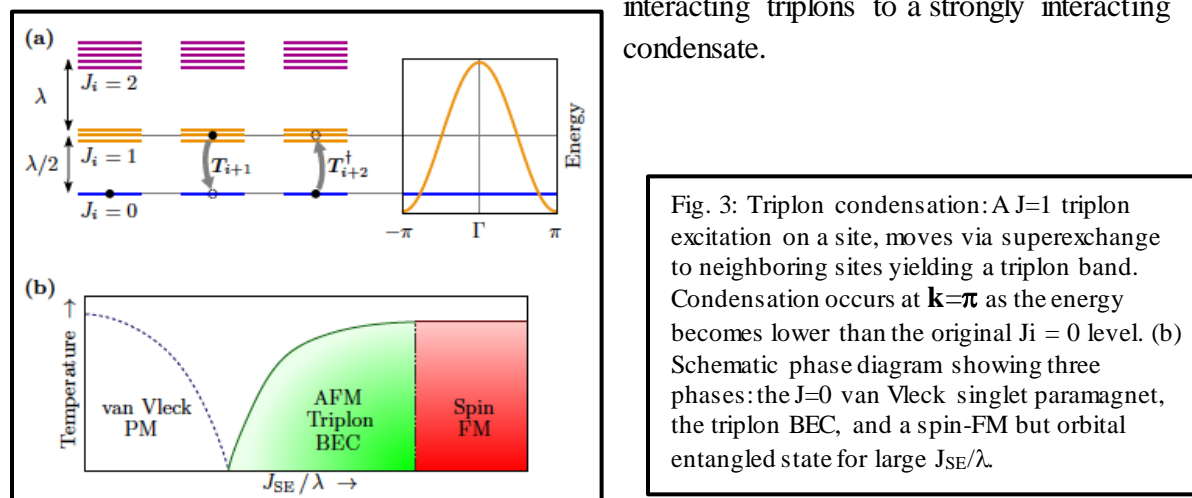
We start with the atomic multi-orbital Hamiltonian with intra and inter-orbital Coulomb interactions and spin-orbital coupling specifically for $(t_{2g})^4$ systems. We next allow hopping between atoms and investigate all cases of orbital geometries-- the idealized fully symmetric case when all orbitals participate in hopping, as well as more realistic cases when one orbital is blocked, for example in a simple cubic lattice, or with two blocked orbitals as for FCC lattices. For each case, we derive the effective spin-orbital superexchange Hamiltonian that competes with spin-orbit coupling to produce strong deviations from the non-magnetic atomic behavior. Our main results are the following:

(1) Upon turning on hopping, local moments are generated on each atom that grow with increasing hopping, a new paradigm beyond the standard Goodenough-Kanamori rules [4].



(2) We derive effective magnetic Hamiltonians for different numbers of active orbitals. The nature of the interaction between these moments is determined by the strength of Hund's coupling: small Hund's coupling leads to the expected antiferromagnetic (AFM) superexchange between the spins while large Hund's coupling leads to ferromagnetic (FM) superexchange interactions between spins. The orbital interactions are frustrated even in the absence of geometric frustration, potentially leading to orbital liquid phases.

(3) By tuning $g = J_{SE}/\lambda$, a phase transition from the $J=0$ singlet to a magnetic phase occurs at a critical point. Close to the transition the magnetic phase is a Bose condensate of weakly interacting $J=1$ triplet excitations [5]. With increasing g there is a crossover from a weakly interacting triplons to a strongly interacting condensate.



Regardless of the local interactions, whether FM or AFM, only AFM condensates that condense at the $\mathbf{k}=\pi$ point are supported. It is remarkable that spin-orbit coupling, even though a single-site effect, can switch the sign the effective spin couplings. To put this in perspective, the sign of Heisenberg spin interactions would not be effectively changed by the presence of single site anisotropy. Yet here we reach the conclusion, unique to spin-orbital coupled systems, that a rotationally invariant single site effect can flip the rotationally invariant superexchange coupling.

(4) In the opposite regime where the superexchange dominates, the spins and orbitals are best described as localized moments. We predict a second phase transition at g_{c2} to orbitally entangled but spin-ordered phases, either FM when Hund's coupling is large or AF for smaller Hund's coupling.

Future Plans

- (1) DMRG calculations of the derived spin-orbital frustrated Hamiltonians and calculations of spin and orbital correlations, entanglement entropy and entanglement spectra.
- (2) Mean field theory and quantum Monte Carlo simulations of orbitally frustrated models.

References

1. G. Khaliullin, *Excitonic Magnetism in Van Vleck-type d4 Mott Insulators*, Phys. Rev. Lett. **111**, 197201 (2013).
2. O. N. Meetei, W. S. Cole, M. Randeria, and N. Trivedi, *Novel magnetic state in d4 Mott insulators*, Phys. Rev. B **91**, 054412 (2015).
3. G. Cao, T. F. Qi, L. Li, J. Terzic, S. J. Yuan, L. E. DeLong, G. Murthy, and R. K. Kaul, *Novel Magnetism of Ir⁵⁺(5d⁴) Ions in the Double Perovskite Sr₂YIrO₆*, Phys. Rev. Lett. **112**, 056402 (2014).
4. D. Khomskii, *Transition metal compounds*, Cambridge (2014)
5. S. Sachdev and R. N. Bhatt, *Bond-operator representation of quantum spins: Mean-field theory of frustrated quantum Heisenberg antiferromagnets*, Phys. Rev. B **41**, 9323 (1990).

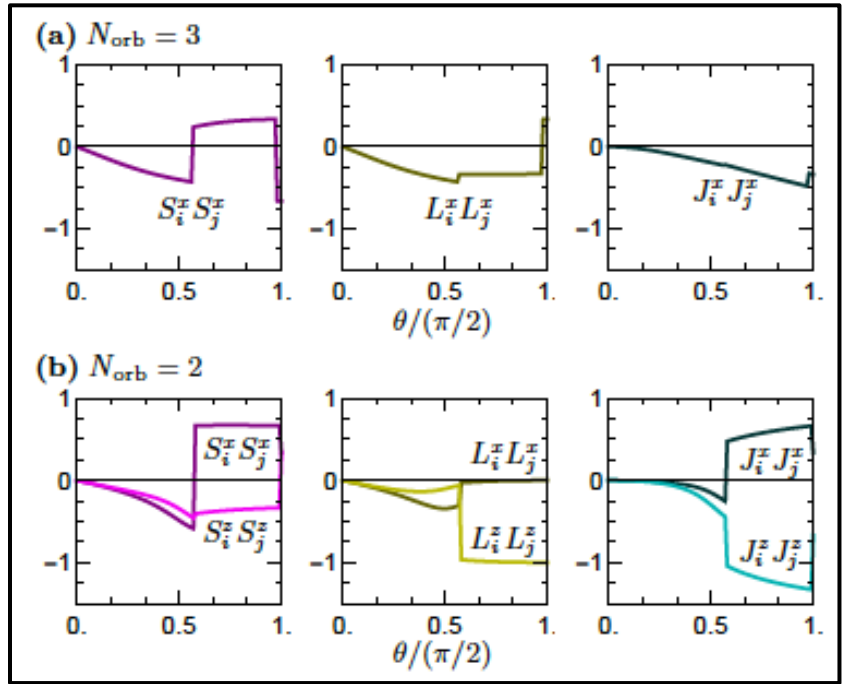


Fig. 4 Angular momentum correlators for the two-site effective Hamiltonian for 3 orbitals and 2 orbital cases (the orbital perpendicular to the direction of hopping blocked) with the parameterization $\lambda = \cos \theta$, $t^2/U = \sin \theta$; $\lambda J_H = 1$, $J_H/U = 0.1$. While the spins are FM, the orbital interactions are frustrated.

Publications

- (1) Panjin Kim, Hosho Katsura, Nandini Trivedi, Jung Hoon Han, *Entanglement and corner Hamiltonian spectra of integrable open spin chains*, arXiv:1512.08597.
- (2) Yen Lee Loh, Mohit Randeria, Nandini Trivedi, Chia-Chen Chang, and Richard Scalettar, *Superconductor-Insulator Transition and Fermi-Bose Crossovers*, Phys. Rev. X, **6**, 021029 (2016).
- (3) U. Chatterjee, J. Zhao, M. Iavarone, R. Di Capua, J.P. Castellan, G. Karapetrov, C.D. Malliakas, M.G. Kanatzidis, H. Claus, J.P.C. Ruff, F. Weber, J. vanWezel, J.C. Campuzano, R. Osborn, M. Randeria, N. Trivedi, M.R. Norman & S. Rosenkranz, *Emergence of coherence in the charge-density wave state of 2H-NbSe₂*, Nat. Comms. DOI: 10.1038/ncomms7313 (2015).
- (4) Daniel Sherman, Uwe S. Pracht, Boris Gorshunov, Shachaf Poran, John Jesudasan, Madhavi Chand, Pratap Raychaudhuri, Mason Swanson, Nandini Trivedi, Assa Auerbach, Marc Scheffer, Aviad Frydman1 and Martin Dressel, *The Higgs mode in disordered superconductors close to a quantum phase transition*, Nat. Phys. **11**, 188 (2015).
- (5) Daniel Sherman, Boris Gorshunov, Shachaf Poran, Nandini Trivedi, Eli Farber, Martin Dressel, and Aviad Frydman, *Effect of Coulomb interactions on the disorder-driven superconductor-insulator transition*, Phys. Rev. B, **89**, 035149 (2014).
- (6) Mason Swanson, Yen Lee Loh, Mohit Randeria, and Nandini Trivedi, *Dynamical Conductivity across the Disorder-Tuned Superconductor-Insulator Transition*, Phys. Rev. X **4**, 021007 (2014).
- (7) Elias Lahoud, O. Nganba Meetei, K. B. Chaska, A. Kanigel, and Nandini Trivedi, *Emergence of a Novel Pseudogap Metallic State in a Disordered 2D Mott Insulator*, Phys. Rev. Lett. **112**, 206402 (2014).

Non-equilibrium thermodynamics in magnetic nanostructures

Principle Investigator: Yaroslav Tserkovnyak

**Department of Physics and Astronomy, University of California, Los Angeles,
CA 90095**

Project Scope

Our work focuses on the geometric gauge fields and related topological aspects in the interactions between collective degrees of freedom (associated with diverse magnetic orders) and itinerant spin-carrying quasi-particles (electrons, magnons, or spinons). We pay special attention to out-of-equilibrium phenomena in thermally biased magnetic systems, the nascent field of *spin caloritronics*. Energy and spin angular momentum is at the core of our investigation, bringing about phenomenological framework based on conservation laws, hydrodynamic continuity, magnetic order, symmetries, and dynamic reciprocities.

Recent Progress

Spin-Nernst effect in a realization of the Haldane model

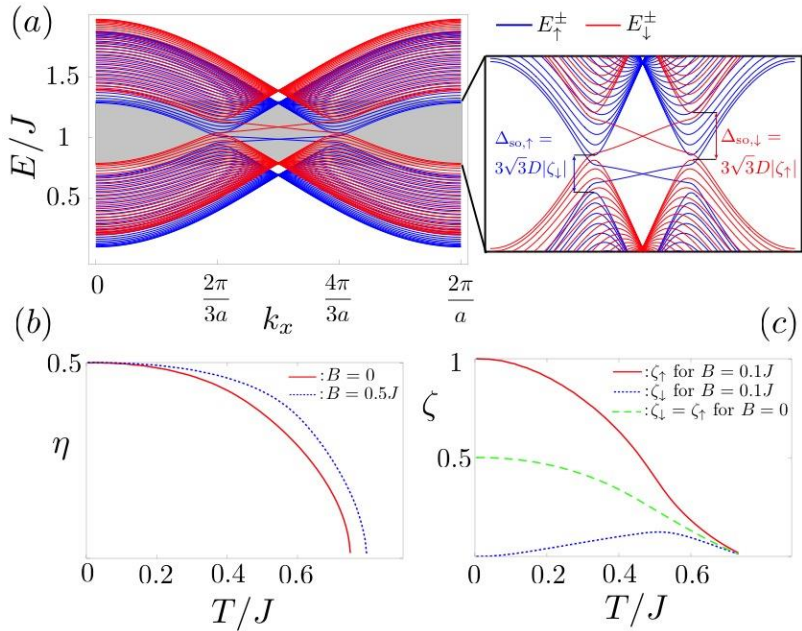


Fig. 1: (a) One-dimensional projection of the Schwinger-boson spectrum in the proposed model. (b) and (c) show the evolution of the mean-field parameters as a function of the temperature.

We studied a spin Hamiltonian for spin-orbit-coupled ferromagnets on the honeycomb lattice, for which a feasible experimental realization was proposed. At sufficiently low temperatures supporting the ordered phase, the effective Hamiltonian

for magnons was shown to be equivalent to the Haldane model for electrons in the honeycomb lattice, which indicates the nontrivial topology of the band and the existence of the associated edge state. At high temperatures comparable to the ferromagnetic-exchange strength, we took the Schwinger-boson representation of spins, in which the mean-field spinon band (Fig. 1) forms a bosonic counterpart of the aforementioned model. The nontrivial geometry of the spinon band can be inferred by detecting the spin Nernst effect (Fig. 2), in which applying a longitudinal temperature gradient generates a transverse spin current.

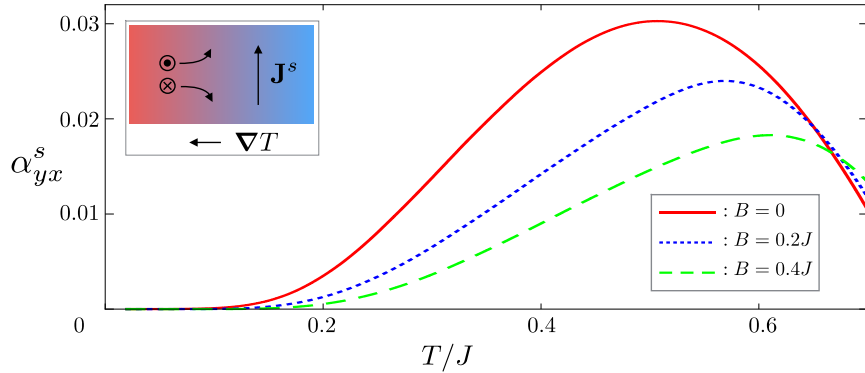


Fig. 2: The spin Nernst conductivity as a function of temperature.

Topological spin-transfer drag mediated by skyrmion diffusion

We studied the spin-transfer drag mediated by the Brownian motion of skyrmions. The essential idea is illustrated in a two-terminal geometry (Fig. 3), in which a thin film of a magnetic insulator is placed in between two metallic reservoirs. An electric current in one of the terminals pumps topological charge into the magnet via a spin-transfer torque. The charge diffuses over the bulk of the system as stable skyrmion textures. By Onsager's reciprocity, the topological charge leaving the magnet produces an electromotive force in the second terminal. The voltage signal decays algebraically with the separation between contacts, in contrast to the exponential suppression of the spin drag driven by non-protected excitations like magnons. We showed how this topological effect could be used as a tool to characterize the phase diagram of chiral magnets and thin films with interfacial Dzyaloshinskii-Moriya interactions.

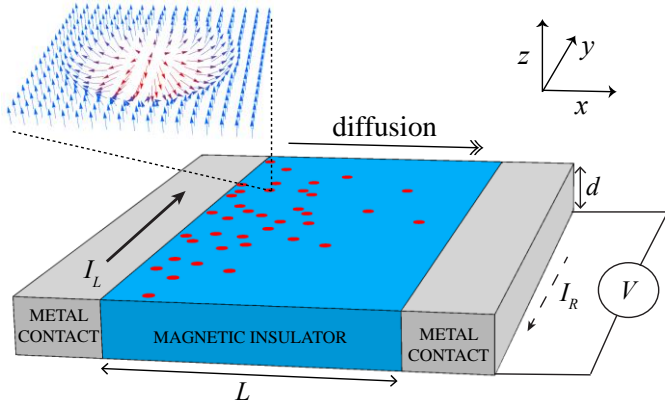


Fig. 3: Scheme for electrical detection and injection of skyrmions.

Gauge fields from curvature in single-layers of transition metal dichalcogenides

We analyzed the dynamics of electrons in corrugated layers of transition metal dichalcogenides (Fig. 4). We found that in these materials, the intrinsic (Gaussian) curvature along with the strong spin-orbit interaction leads to an emergent gauge field associated with the Berry connection of the spinor wave function. We studied in detail the effect of topological defects of the lattice (tetragonal and octogonal disclinations) and the scenarios where they can be identified with effective magnetic monopoles. We suggested that this magnetic field could be detected in an Aharonov-Bohm interferometry experiment by measuring the local density of states in the vicinity of corrugations.

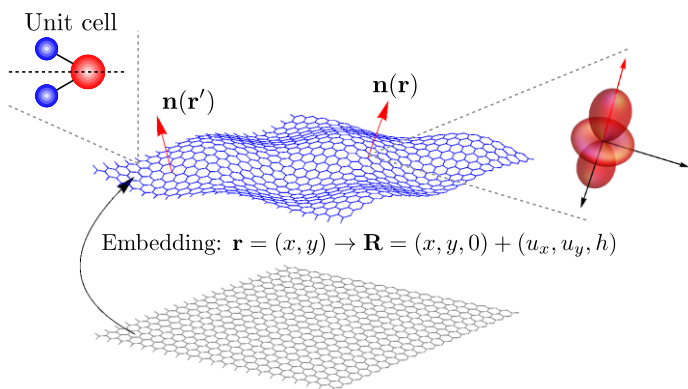


Fig. 4: Transition metal dichalcogenide as a corrugated membrane

Future Plans

Caloritronics in disordered systems and quantum magnets

We plan to extend the magnon-drag paradigm to other spin excitations (spinons, Schwinger bosons) in systems lacking magnetic order. These theoretical tools are also useful to explore spin and heat transport properties in systems with non-conventional magnetic order such as spin liquids.

Thermal transport in skyrmion crystals and related systems

Skyrmions are capable to transport energy, and their dynamics can be manipulated by thermal torques. In a skyrmion crystal, the spin-transfer drag is mediated by the phonon modes of the lattice, providing information about their interactions and setting the basis to characterize the phase diagram of chiral magnets by means of spin and heat transport measurements. These ideas can be extended to related systems such as vortex lattices in type II superconductors.

Spin pumping in transition metal dichalcogenides

We plan to continue to study effects beyond the static regime such as the electromotive forces induced by dynamical corrugations, and reciprocally, the back-action of spin currents on the dynamics of topological defects.

Selected Publications (2016)

- Yaroslav Tserkovnyak, Scott A. Bender, Rembert A. Duine, and Benedetta Flebus, *Bose-Einstein condensation of magnons pumped by the bulk spin Seebeck effect*, Physical Review B **93**, 100402(R).
- B. Flebus, S. A. Bender, Y. Tserkovnyak, and R. A. Duine, *Two-Fluid Theory for Spin Superfluidity in Magnetic Insulators*, Physical Review Letters **116**, 117201.
- Se Kwon Kim, Héctor Ochoa, Ricardo Zarzuela, and Yaroslav Tserkovnyak, *A Realization of the Haldane-Kane-Mele Model in a System of Localized Spins*, arXiv:1603.04827 (submitted to Physical Review Letters).
- Héctor Ochoa, Se Kwon Kim, and Yaroslav Tserkovnyak, *Topological spin drag driven by skyrmion diffusion*, arXiv:1605.02857 (accepted in Physical Review B).
- Héctor Ochoa, Ricardo Zarzuela, and Yaroslav Tserkovnyak, *Emergent gauge fields from curvature in single layers of transition metal dichalcogenides*, arXiv:1605.07326 (submitted to Physical Review Letters).

Strongly Correlated Systems: Further Away from the Beaten Path

Principal Investigator: Alexei M. Tsvelik, Brookhaven National Laboratory, Upton, NY
11973, tsvelik@gmail.com

Co-investigators: R. M. Konik, Wei Ku, Weiguo Yin.

Program Scope

In recent years the activity of our FWP has been focused in a number of different areas which included nonperturbative studies of out-of-equilibrium physics, frustrated magnetism, physics of low dimensional systems. The common features of these activities is that they all point away from traditional well understood physics. In pursuing these activities we have been greatly assisted by the new numerical methods developed in our group and by the past expertise in nonperturbative techniques our group possesses. Our theory group is working in close contact with experimentalists. Out of 35 papers published (1 Science, 2 Nature Comm., 2 PNAC, 1 PRX, 9 PRL, 1 Nano Lett.), 14 were published with experimentalists.

Recent Progress

Fractionalized excitations in real materials: In collaboration with experimental groups in BNL we have studied an f-electron metal $\text{Yb}_2\text{Pt}_2\text{Pb}$ whose magnetic excitations turned out to be one-dimensional and fractionalized (spinons). The theory of this highly unusual phenomenon was developed which quantitatively describes the observations [10].

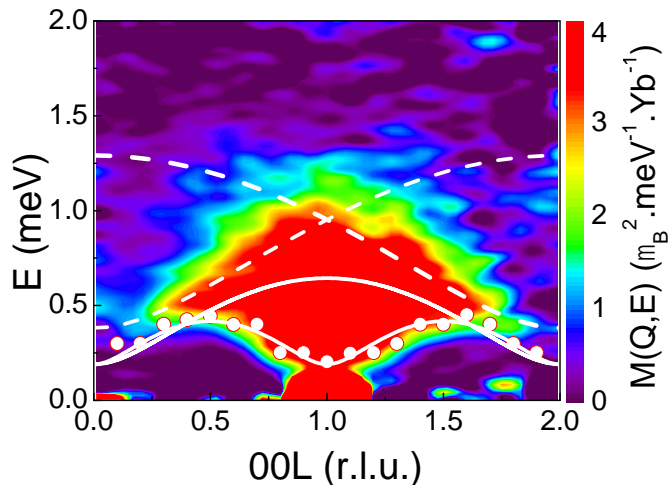


Fig. 1. Spinon continuum in $\text{Yb}_2\text{Pt}_2\text{Pb}$. The solid white lines are lower and upper boundaries of the 2-spinon continuum in the $S=1/2$ XXZ model with a particular value of the Ising-like anisotropy.

Ballistic transport in 1D materials:

Kondo chain was studied in the regime of high spin concentration where the low energy physics

is dominated by the Ruderman-Kittel-Kasuya-Yosida (RKKY) interaction [7,8]. This model has two phases with drastically different transport properties depending on the anisotropy of the exchange interaction. In particular, for the easy plane anisotropy the spins form a spiral configuration (Fig. 2) and the helical symmetry of the fermions is spontaneously broken. In this state the electron spectrum undergoes restructuring so that backscattering requires a spin flip (Fig. 3). This leads to a parametrical suppression of the localization effects.

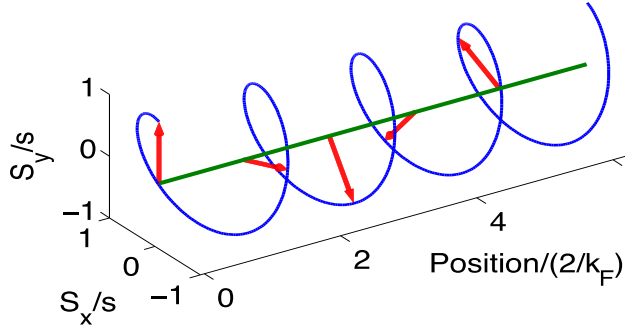


Fig. 2. Spiral configuration of the spins
broken helicity symmetry.

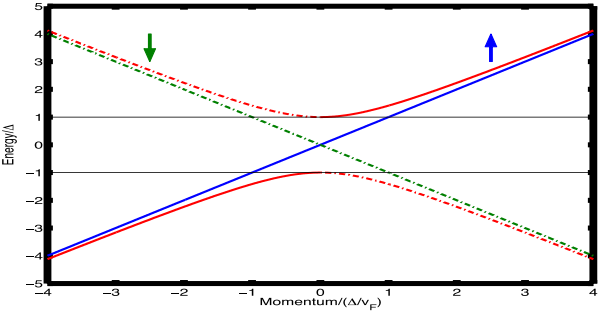
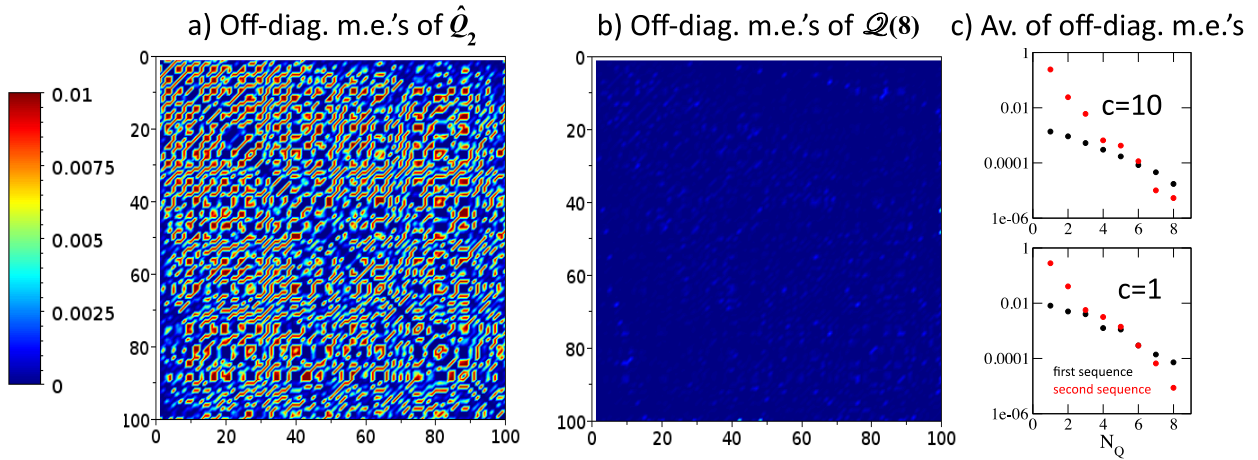


Fig.3. The quasiparticle spectrum in the state with

Towards a theory of quantum KAM in manybody systems:

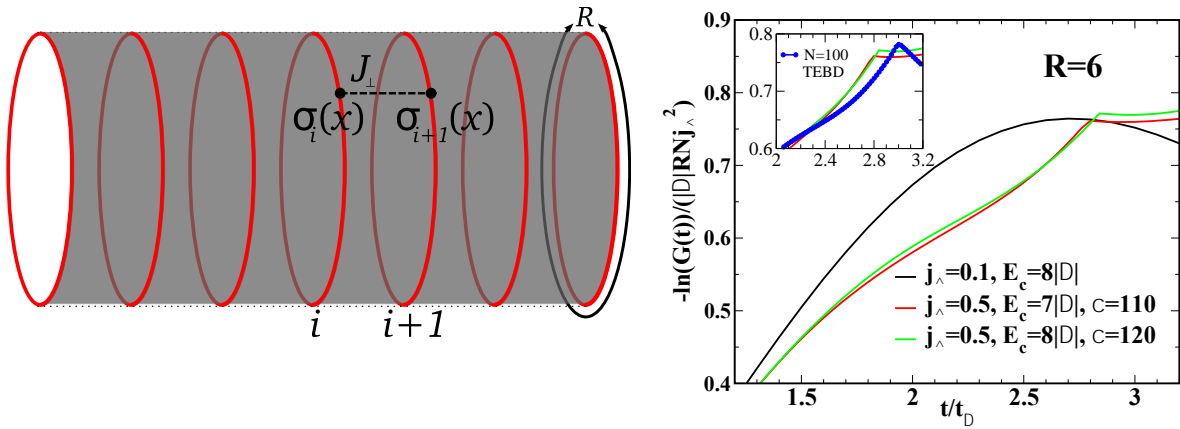


a) The off-diagonal matrix elements of the Lieb-Liniger Hamiltonian with respect to the eigenstates of the Lieb-Liniger model **plus** a one-body potential. The presence of off-diagonal matrix elements show that the original unperturbed Hamiltonian is not a conserved quantity. b) The off-diagonal matrix elements (again with respect to the eigenstates of the perturbed model) of a linear combination of operators conserved in the original Lieb-Liniger model. We thus show that when perturbing a quantum integrable model, it is still possible to construct deformed, nearly conserved operators, so obtaining an analog to the classical KAM theorem. c) We show that by increasing the size of the linear combination of operators in the Lieb-Liniger model we can reduce the size of the off-diagonal matrix elements.

Real time dynamics in a quantum many-body system are inherently complicated and so difficult to predict. There are, however, a special set of systems where these dynamics are theoretically

tractable, integrable models. Such models possess an infinite number of non-trivial conserved quantities. These charges are believed to control dynamics and thermalization in low dimensional atomic gases as well as in quantum spin chains. But what happens when the special symmetries leading to the existence of the extra conserved quantities are broken? Is there any memory of the quantities if the breaking is weak? Here, in the presence of weak integrability breaking, we show that it is possible to construct residual quasi-conserved quantities, so providing a quantum analog to the KAM theorem and its attendant Nekhorochev estimates. We demonstrate this construction explicitly [20] in the context of quantum quenches in one-dimensional Bose gases and argue that these quasi-conserved quantities can be probed experimentally.

Studying non-equilibrium behavior in 2D Strongly Correlated Systems:

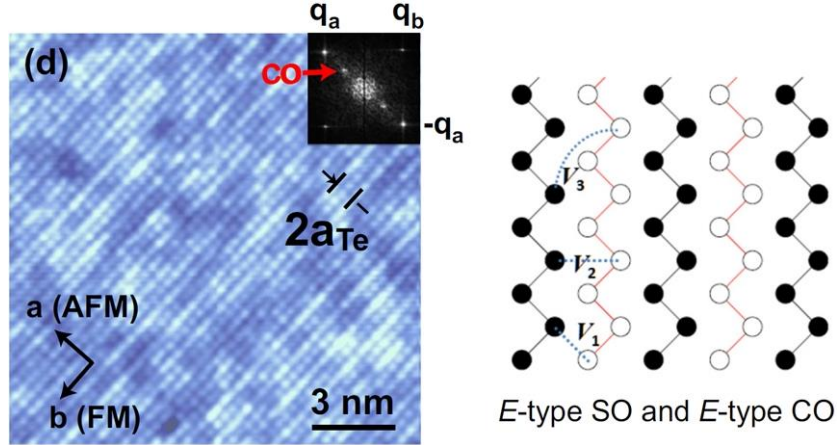


RHS: The geometry of the system that we consider: an (infinite) array of coupled chains of finite length. **LHS:** The log of the return probability of different quenches in an array of a 2D quantum Ising model. In quenches that pass through a phase boundary, we see the return probability has non-analyticities.

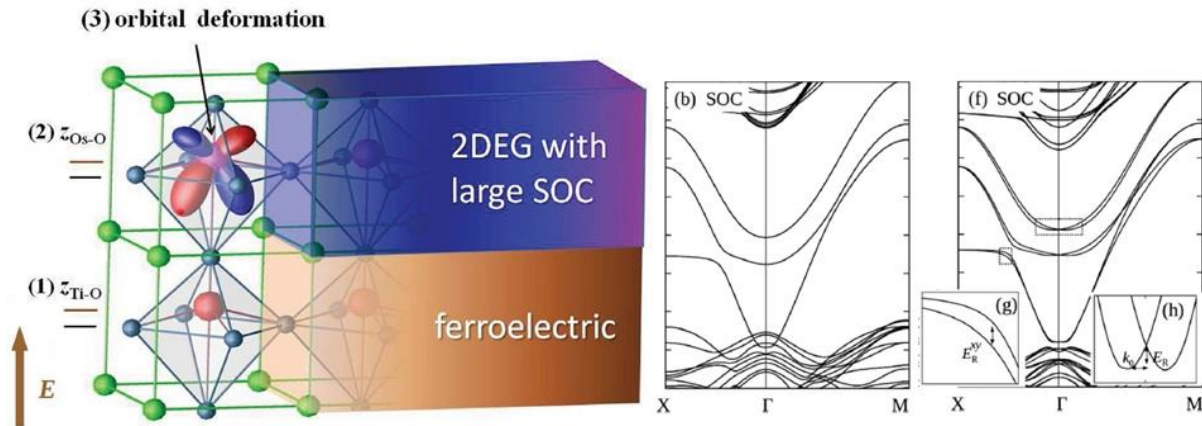
We have developed a method for simulating the real time evolution of extended quantum systems in two dimensions. The method combines the benefits of integrability and matrix product states in one dimension to avoid several issues that hinder other applications of tensor based methods in 2D. In particular it can be extended to infinitely long cylinders [19]. As an example application we have studied quantum quenches in the 2D quantum (2+1 dimensional) Ising model. In quenches that cross a phase boundary we find that the return probability shows non-analyticities in time.

Charge ordering in stoichiometric FeTe: Based on the unified picture proposed by us in PRL 105, 107004 (2010), we further predicted the existence of novel E -type charge ordering in FeTe. This was demonstrated with STM/STS measurements on FeTe films at Tsinghua

University as part of the DOE/BES-CAS (Chinese Academy of Sciences) collaborative research in quantum materials. These results imply that intersite interaction and charge fluctuations, so far much neglected, is essential to the understanding of iron-based superconductors [31].



Giant switchable Rashba effect in oxide heterostructures: By coupling ferroelectric BaTiO_3 and a 5d or 4d transition metal oxide with a large spin-orbit coupling, $\text{Ba}(\text{Os},\text{Ir},\text{Ru})\text{O}_3$, we show theoretically that giant Rashba spin splittings are possible and even controllable by an external electric field. Based on density functional theory and a microscopic tight binding understanding, it is concluded that the electric field is amplified and stored as a ferroelectric Ti-O distortion which, through the network of oxygen octahedra, induces a large (Os,Ir,Ru)-O distortion [14].



Interfacial coupling-induced ferromagnetic insulator phase in manganite film: We proposed a new route to interfacial coupling engineering via boosting quenched disorder by the surface phase transition of certain substrates. This was demonstrated with observation of a predicted disorder induced ferromagnetic-polaronic insulator in 12 nm $\text{Pr}_{2/3}\text{Sr}_{1/3}\text{MnO}_3$ film during the surface phase transition of SrTiO_3 substrate, by BNL electron microscopes group [30].

Probing single magnon excitations in Sr_2IrO_4 using oxygen K-edge resonant inelastic X-ray scattering (RIXS): For spin excitation in systems with heavy elements the energy resolution of commonly used L -edge RIXS in the hard x-ray region is usually poor. We proposed that single

magnon excitations can be measured with RIXS at the K -edge of the surrounding ligand atoms when the center heavy metal elements have strong spin-orbit coupling. This was demonstrated with oxygen K -edge RIXS experiments on Sr_2IrO_4 by BNL X-ray scattering group [15].

Future plans:

To develop a theory of composite order. The Kondo-Heisenberg model is known to possess an order parameter of a special type corresponding to the condensation of bound states of conduction electrons and local spins. The creation of such order goes hand in hand with gapped fractionalized excitations. We plan to extend this theory to other models.

To study the influence of nuclear spins on quantum critical systems. There are reasons to believe that the interaction between nuclear and electron spins in critical magnetic systems is strongly enhanced by the critical fluctuations. We are going to explore this.

To study the influence of retardation on the Spin-Fermion model. In collaboration with G. Kotliar we intend to construct an effective low energy theory which would allow to study corrections to the results obtained by single impurity DMFT. This model is likely to be a version of the famous Spin-Fermion model with frequency dependent spin-fermion coupling.

To study nonlinear optics and Raman scattering in 1D strongly correlated systems. We plan to use the nonperturbative techniques of theory of integrable systems to calculate multi-point correlation functions of various models describing nonlinear optics phenomena including resonance Raman scattering.

To study a possibility of realization of non-Abelian version of Kalmeyer-Laughlin state in microscopic models of chiral spin liquids. This state is an analogue of Fractional Quantum Hall effect for Mott insulators. We intend to find its non-Abelian generalizations such as a spin liquid analogue of Pfaffian state.

To continue the development of a two dimensional DMRG algorithms able to study the properties of two dimensional systems both in and out of equilibrium. We plan in particular to extend this work to two-dimensional lattice systems such as the two-dimensional Heisenberg model.

To explore novel physics in mixed 3d-4d-5d transition-metal compounds. The different strength of spin-orbit coupling on the 3d and 5d elements will dramatically change the pathway of superexchange, giving rise to novel mechanisms for spin anisotropy and spin frustration. We intend to establish theory-guided syntheses of new types of frustrated magnets.

To apply the aforementioned new route to interfacial coupling engineering to more heterostructure materials. We shall perform first-principles calculations and effective model analysis to guide experimental studies of cuprate/iridates superlattices.

To continue developing first-principles guided derivation of effective low-temperature Hamiltonians for material systems with multiple degrees of freedom. It will be applied to address the interplay of charge, orbital, spin, and anion polarization degrees of freedom in iron-based superconductors. An example problem is the orbital order without spin order in FeSe.

To study the ultrafast dynamics in strongly correlated materials in collaboration with the BNL X-ray scattering, photoemission, and UED groups. We shall first address the fundamental problem as to whether the electronic excitation pumped by the laser in recent pump-probe experiments on Sr₂IrO₄ is intra-site or inter-site transition. We will also consider modeling recent pump-probe ARPES experiments with a slave boson treatment of the two dimensional t-J model.

Publications

1. **Quantum Critical Fluctuations in Layered YFe₂Al₁₀,** L. S. Wu, M.-S. Kim, K. S. Park, A. M. Tsvelik, and M. C. Aronson, Proc. Nat. Academy of Sciences. pnas.1413112111.
2. **Multichannel Kondo impurity dynamics in a Majorana device,** A. Altland, B. Beri, R. Egger, A. M. Tsvelik, Phys. Rev. Lett. 113, 076401 Aug. 11 (2014) .
3. **Two-leg SU(2n) spin ladder: A low-energy effective field theory approach,** by P. Lecheminant and A. M. Tsvelik, Phys. Rev. B91, 174407 (2015).
4. **Spin liquid polymorphism in a correlated electron system on the threshold of superconductivity,** Igor A. Zaliznyak, A. T. Savici, M. Lumsden, A. M. Tsvelik, R. Hu, C. Petrovic, PNAS 1503559112, Aug. 3, 2015, doi 10.1073.
5. **Studying the Perturbed Wess-Zumino-Novikov-Witten SU(2)**k** Theory Using the Truncated Conformal Spectrum Approach,** R. M. Konik, T. Palmai, G. Takacs and A. M. Tsvelik, Nuclear Physics B 899, 547 (2015).
6. **Majorana boundary modes in Josephson junctions arrays with gapless bulk excitations,** M. Pino, A. M. Tsvelik, and L. B. Ioffe, Phys. Rev. Lett. 115, 197001 (2015).
7. **Quantum Phase Transition and Protected Ideal Transport in Kondo Chain,** A. M. Tsvelik and O. M. Yevtushenko, Phys. Rev. Lett. 115, 216402 (2015). *Editors Suggestion.*
8. **Low Energy Properties of the Kondo chain in the RKKY regime,** D. Schimmel, A. M. Tsvelik and O. M. Yevtushenko, New J. Phys. 18, 053004 (2016).

9. **Kondo physics from quasiparticle poisoning in Majorana devices**, S. Plugge, A. Zazunov, E. Eriksson, R. Egger, and A. M. Tsvelik, Phys. Rev. B 93, 104524 (2016).
10. **Orbital Exchange and Fractional Quantum Number Excitations in an f-electron Metal $\text{Yb}_2\text{Pt}_2\text{Pb}$** , L. S. Wu, W. J. Gannon, I. A. Zaliznyak, A. M. Tsvelik, M. Brockmann, J.-S. Caux, M.-S. Kim, Y. Qiu, J. R. D. Copley, G. Ehlers, A. Podlesnyak, M. C. Aronson, Science 352, 1206-1210 (2016).
11. **Particle Formation and Ordering in Strongly Correlated Fermionic Systems: Solving a Model of Quantum Chromodynamics**, P. Azaria, R. M. Konik, Ph. Lecheminant, T. Palmai, G. Takács, and A. M. Tsvelik, accepted to Phys. Rev. D, arXiv:1601.02979
12. **From Hund's insulator to Fermi liquid: Optical spectroscopy study of K doping in BaMn_2As_2** , McNally, D. E.; Zellman, S.; Yin, Z. P.; Post K.W., He H., Hao K., Kotliar G., Basov D., Homes C. C., Aronson M. C., Phys. Rev. B 92, 115142 (2015).
13. **$\text{CaMn}_2\text{Al}_{10}$: itinerant Mn magnetism on the verge of ferromagnetic order**, L. Steinke, J. W. Simonson, W.-G. Yin, G. J. Smith, J. J. Kistner-Morris, S. Zellman, A. Puri, M. C. Aronson, Phys. Rev. B 92, 020413 (2015).
14. **Giant switchable Rashba effect in oxide heterostructures**, Zhicheng Zhong, Liang Si, Qinfang Zhang, Wei-Guo Yin, Seiji Yunoki, Karsten Held, Adv. Mat. Interfaces, 2, issue 5 (2015).
15. **Probing single magnon excitations in Sr_2IrO_4 using OK-edge resonant inelastic X-ray scattering**, X. Liu, M. P. M. Dean, J. Liu, S. G. Chiubăian, N. Jaouen, A. Nicolaou, W. G. Yin, C. Rayan Serrao, R. Ramesh, H. Ding, J. P. Hill, J. Phys.: Condens. Matter 27, 202202 (2015).
16. **Separation of Timescales in a Quantum Newton's Cradle**, R. van den Berg, B. Wouters, S. Eliëns, J. De Nardis, R. M. Konik, J.-S. Caux, Phys. Rev. Lett. 116, 225302 (2016).
17. **Motion of a distinguishable impurity in the Bose gas: Arrested expansion without a lattice and impurity snaking**, N. J. Robinson, J.-S. Caux, R. M. Konik, Phys. Rev. Lett. 116, 145302 (2016).
18. **Giant Phonon Anomaly associated with Superconducting Fluctuations in the Pseudogap Phase of Cuprates**, Y. H. Liu, R. M. Konik, T. M. Rice, F. C. Zhang, Nat. Comm., 7, 10378 (2016).
19. **Quantum quenches in two spatial dimensions using chain array matrix product states**, A. J. A. James, R. M. Konik, Phys. Rev. B 92, 161111 (2015).

20. **Glimmers of a Quantum KAM Theorem: Insights from Quantum Quenches in One-Dimensional Bose Gases**, G. P. Brandino, J.-S. Caux, R. M. Konik, Phys. Rev. X, 5, 041043 (2015).
21. **Predicting excitonic gaps of semiconducting single-walled carbon nanotubes from a field theoretic analysis**, R. M. Konik, M. Y. Sfeir, J. Misewich, Phys. Rev. B 91, 075417 (2015).
22. **Itinerant effects and enhanced magnetic interactions in Bi-based multilayer cuprates**, M. P. M. Dean, A. J. A. James, A. C. Walters, V. Bisogni, I. Jarridge, M. Hucker, E. Giannini, M. Fujita, J. Pelliciari, Y. B. Huang, R. M. Konik, T. Schmitt, J. P. Hill, Phys. Rev. B 90, 220506, Dec 4 2014.
23. **Truncated conformal space approach for 2D Landau-Ginzburg theories**, A. Coser, M. Beria, G. P. Brandino, R. M. Konik, G. Mussardo. J. Stat. Mech – Theory and Experiment, P12010, Dec. 2014.
24. **Competing interactions in semiconductor quantum dots**, R. van den Berg, G. P. Brandino, O. El Araby, R. M. Konik, V. Gritsev, J.-S. Caux, Phys. Rev. B 90, 155117, Oct. 2014.
25. **What is the valence on Mn in Ga_{1-x}Mn_xN?** R. Nelson, T. Berlijn, J. Moreno, M. Jarrell, W. Ku, Phys. Rev. Lett. 115, 197203 (2015).
26. **Study of multiband disordered systems using the typical medium dynamical cluster approximation**, Yi Zhang, Hanna Terletska, C. Moore, Chinedu Ekuma, Ka-Ming Tam, Tom Berlijn, Wei Ku, Juana Moreno, Mark Jarrell, Phys. Rev. B 92, 205111 (2015).
27. **Weak phase stiffness and nature of the quantum critical point in the underdoped cuprates**, Yu. Yildirim, W. Ku, Phys. Rev. B 92, 180501 (2015).
28. **Itinerancy enhanced quantum fluctuation of magnetic moments in iron-based superconductors**, Yu-Ting Tam, Dao-Xin Yao, Wei Ku, Phys. Rev. Lett. 115, 117001 (2015).
29. **Surface-state-dominated transport in crystals of the topological crystalline insulator In-doped Pb_{1-x}Sn_xTe**, Ruidan Zhong, Xugang He, John A. Schneeloch, Cheng Zhang, Tiansheng Liu, Ivo Pletikosic, Qiang Li, Wei Ku, Tonica Valla, J. M. Tranquada, Genda Gu, Phys. Rev. B 91, 195321 (2015).
30. **Interfacial coupling-induced ferromagnetic insulator phase in manganite film**, B. Zhang, L. Wu, Wei-Guo Yin, C.-J. Sun, P. Yang, T. Venkatesan, J. Chen, Y. Zhu, and G. M. Chow, Nano Lett. (2016) DOI:10.1021/acs.nanolett.6b01056.

31. **Charge ordering in stoichiometric FeTe: Scanning tunneling microscopy and spectroscopy**, Wei Li, Wei-Guo Yin, Lili Wang, Ke He, Xucun Ma, Qi-Kun Xue, and Xi Chen, Phys. Rev. B 93, 041101(R) (2016).
32. **Bulk signatures of pressure-induced band inversion and topological phase transitions in Pb_{1-x}Sn_xSe**, X. Xi, X-G He, F. Guan, Z. Liu, R. D. Zhong, J. A. Schneeloch, T. S. Liu, G. D. Gu, D. Xu, Z. Chen, X. G. Hong, W. Ku, G. L. Carr, Phys. Rev. Lett. 113, 096401, 29 Aug. 2014.
33. **Electronic Structure Reconstruction across the Antiferromagnetic Transition in TaFe_{1.23}Te₃ Spin Ladder**, Xu, M; Wang, LM; Peng, R; Ge, QQ; Chen, F; Ye, ZR; Zhang, Y; Chen, SD; Xia, M; Liu, RH; Arita, M; Shimada, K; Namatame, H; Taniguchi, M; Matsunami, M; Kimura, S; Shi, M; Chen, XH; Yin, WG; Ku, W; Xie, BP; Feng, DL, Chinese Physics Letters 32, 027401, Feb. 2015.
34. **Intra-unit-cell nematic charge order in the titanium-oxypnictide family of superconductors**, Frandsen, BA; Bozin, ES; Hu, HF; Zhu, YM; Nozaki, Y; Kageyama, H; Uemura, YJ; Yin, WG; Billinge, SJL, Nature Comm. 5, 5761, Dec. 2014
35. **Interpretation of Scanning Tunneling Quasiparticle Interference and Impurity States in Cuprates**, Kreisel, A. and Choubey, Peayush and Berlijn, T. and Ku, W. and Andersen, B. M. and Hirschfeld, P. J., Phys. Rev. Lett. 114, 217002, 2015.

Collective charge and spin dynamics in low-dimensional itinerant electron systems with spin-orbit coupling

Carsten A. Ullrich

Department of Physics and Astronomy, University of Missouri, Columbia, MO 65211

Keywords: Two-dimensional electron gas, spin-orbit coupling, doped semiconductor quantum wells, exchange-correlation effects for noncollinear magnetism, spin waves in itinerant magnetic systems

Project Scope

This project aims to study the collective charge and spin excitations of itinerant quasi-2D electronic systems such as doped semiconductor nanostructures and carbon-based materials, in the presence of impurities and spin-orbit coupling (SOC). Earlier, we had discovered an interesting interplay between many-body effects and Rashba and Dresselhaus SOC: contrary to many situations in spintronics, collective spin modes are robust against SOC-induced (D'yakonov-Perel') decoherence. However, a full theoretical and practical exploration of the effect is still missing, and a wealth of new experimental data remains to be analyzed. The current project addresses three interrelated objectives: (1) We will develop a general theory of chiral spin waves in spin-polarized quasi-2D electron gases, in the presence of SOC. The goal will be to calculate spin-wave dispersions and linewidths that can be compared with experimental results from inelastic light scattering, and use this to understand how SOC and many-body effects influence each other. (2) Electronic many-body effects will be described using time-dependent density-functional theory. Doped quantum wells with SOC are noncollinear itinerant magnetic systems at the crossover between two and three dimensions, which poses novel challenges for standard exchange-correlation (xc) functionals such as the LDA. We will develop and test new orbital-dependent xc functionals for noncollinear magnetic systems using STLS and other approaches. (3) We will consider quantum well bilayer or multilayer systems with SOC, where the coupling between the quasi-2D electron systems leads to acoustic and optical modes. We will also study collective spin excitations in graphene and other carbon-based or topological materials in the presence of SOC and magnetic fields. Apart from the fundamental interest in the area of many-body physics, these projects may also uncover new practical ways of manipulating and controlling spin waves in low-dimensional itinerant electron systems, which could be used to encode, transport and process information.

Recent Progress

1. Spin-orbit twisted spin waves: group velocity control. This work was carried out in collaboration with Irene D'Amico (York, UK), Giovanni Vignale (Missouri), and the experimental group of Florent Perez (UPMC Paris). Following theoretical predictions [1], the fine structure of spin plasmons in quantum wells was first observed by inelastic light scattering in 2012 [2,3]. In the last couple of years, we have studied magnetized 2D electron gases in n-doped CdMnTe quantum wells. These systems have strong Rashba and Dresselhaus SOC, which affects the spin-wave dynamics in various interesting ways. Without SOC, the spin-wave dispersion has the form $\hbar\omega_s = Z + S_{sw}\hbar^2q^2/2m^*$, where Z is the bare Zeeman splitting, and S_{sw} is the spin-wave stiffness. Using an exact transformation of the many-body Hamiltonian, we have rigorously demonstrated that to lowest order in SOC the spin-wave stiffness is unchanged, but the dispersion in \mathbf{q} is shifted by a wave vector \mathbf{q}_s that depends on the strength of the SOC and on the propagation direction of the spin wave, thus lifting the chiral degeneracy. This effect can be understood as a spin wave propagating in a spin-orbit twisted reference frame. The spin-orbit twist can be controlled via the SOC or via changes in the carrier density. This offers practical ways of controlling the spin-wave group velocity, which may lead to novel applications in spin-wave routing devices or spin-wave lenses. These results could open up promising alternatives to magnonics in ferromagnetic thin films.

2. Spin waves in a chiral electron gas: Beyond Larmor's theorem. Very recently, we have carried out systematic theoretical studies of chiral 2D electron gases in the presence of SOC. This work was done by the PI and graduate student Shahrzad Karimi. Larmor's theorem states that in a system of interacting electrons in a

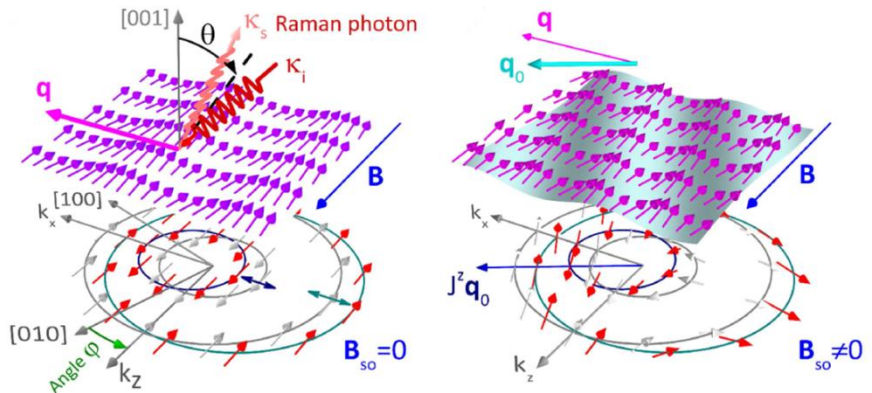


Fig.1. Left: Raman scattering geometry and spin wave in a magnetized 2DEG without SOC. Right: spin-orbit twisted spin wave.

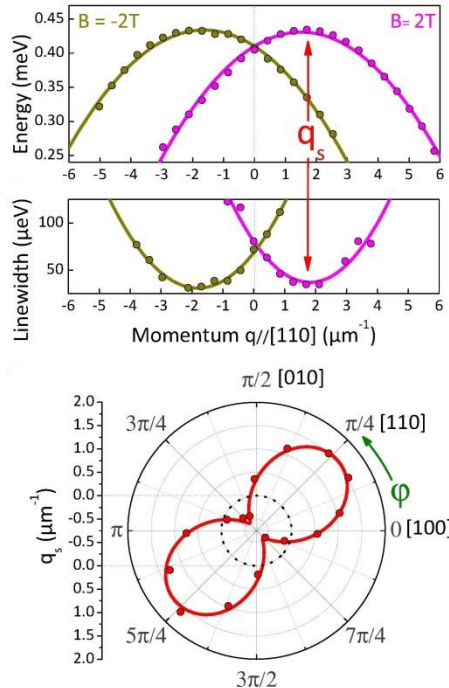


Fig.2. Momentum shift of the spin-wave dispersion and lifting of chiral degeneracy. The points are Raman scattering data, the lines are theory.

magnetic field \mathbf{B} , the electrons precess with frequency $\Omega_L = geB/2m^*$; therefore, the spin wave dispersion has the limit $\hbar\omega_s(q \rightarrow 0) = Z$. Based on Larmor's theorem, we have derived a novel constraint on the dynamical exchange-correlation potential in time-dependent density-functional theory which must be satisfied by approximate functionals, and we showed that it is indeed satisfied by local approximations. In the presence of SOC, Larmor's theorem is broken, and the spin-wave dispersion takes on the more general form $\hbar\omega_s = E_0 + E_1 q + E_2 q^2$ in the limit of small wave vectors. Figure 3 shows experimental results (obtained by F. Perez and F. Baboux in Paris) for the angular modulation of the coefficients E_0 , E_1 and E_2 , where the modulation amplitudes are determined by the SOC. We have carried out a systematic study of the spin waves in the presence of SOC, based on TDDFT linear response theory, and derived analytical expressions for E_0 and E_1 to lowest order in the Rashba and Dresselhaus coupling strengths. By comparing with experimental data, we are able to extract very accurately the strength of the dynamical exchange-correlation (xc) effects in the spin-polarized 2DEG. We discovered that there are significant deviations from the local-density approximation results, which shows that the development of more accurate (TD)DFT approaches for noncollinear spin systems remains an important and urgent task.

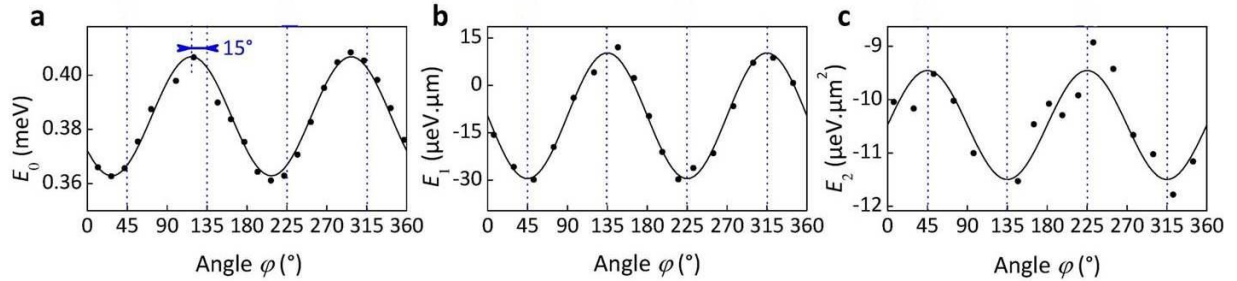


Fig.3. Experimental data for the angular modulation of the coefficients E_0 , E_1 and E_2 of the spin-wave dispersion of a 2DEG in the presence of SOC.

3. Three- to two-dimensional crossover in TDDFT.

The standard approximations in DFT are local and semilocal approximations (LDA, GGA). It has long been known for the ground state that LDA/GGA break down as a system transitions from 3D to 2D. We have performed the first systematic study in the dynamical case, where we investigated the xc kernel of TDDFT in various approximations. Specifically, we look at collective excitations of confined quasi-2D electron gases (inter- and intrasubband) as their width goes to zero. Semilocal xc kernels cause a breakdown at a critical width that is comparable to the 2D Wigner-Seitz radius of the electron gas. Fortunately, many practical applications for nanostructures are in a quasi-2D regime where local approximations are still valid. We also studied orbital functionals such as the Slater exchange functionals, and found them to be robust under 3D-2D crossover.

Future Plans

Spin waves in graphene. The PI and a graduate student, Matthew Anderson, are currently studying collective spin dynamics in doped graphene. The goal is to obtain spin-wave dispersions in the presence of SOC, and identify regimes and parameters where the expected modulation effects would be strong enough to facilitate experimental observation.

Linewidth of spin waves. The PI and a graduate student, Shahrzad Karimi, will develop a model to calculate the linewidth of spin waves in magnetized quasi-2DEGs in CdMnTe caused by spin-flip impurity scattering. For this purpose, we will generalize the memory-function formalism [4] for the spin-dependent case.

Spin-dependent STLS formalism. The PI will develop a generalization of the STLS formalism [5] to the case of noncollinear spins. This method will lead to a new and, hopefully, more accurate description of dynamical correlation effects in itinerant magnetic systems.

References

1. C. A. Ullrich and M. E. Flatté, *Anisotropic splitting of intersubband spin plasmons in quantum wells with bulk and structural inversion asymmetry*, Phys. Rev. B **68**, 235310 (2003)
2. F. Baboux, F. Perez, C. A. Ullrich, I. D'Amico, J. Gomez, and M. Bernard, *Giant collective spin-orbit field in a quantum well: fine structure of spin plasmons*, Phys. Rev. Lett. **109**, 166401 (2012)
3. F. Baboux, F. Perez, C. A. Ullrich, I. D'Amico, G. Karczewski, and T. Wojtowicz, *Coulomb-driven organization and enhancement of spin-orbit fields in collective spin excitations*, Phys. Rev. B **87**, 121303(R) (2013)
4. C. A. Ullrich and G. Vignale, *Time-dependent current density functional theory for the linear response of weakly disordered systems*, Phys. Rev. B **65**, 245102 (2002)
5. K. S. Singwi, M. P. Tosi, H. R. Land, and A. Sjölander, *Electron correlation at metallic densities*, Phys. Rev. **170**, 589 (1968)

Publications

1. Shahrzad Karimi and C. A. Ullrich, *Three- to two-dimensional crossover in time-dependent density-functional theory*, Phys. Rev. B **90**, 245304 (2014)
2. F. Baboux, F. Perez, C. A. Ullrich, G. Karczewski, and T. Wojtowicz, *Electron density magnification of the collective spin-orbit field in quantum wells*, Phys. Rev. B **92**, 125307 (2015)
3. F. Baboux, F. Perez, C. A. Ullrich, G. Karczewski, and T. Wojtowicz, *Spin-orbit stiffness of the spin-polarized electron gas*, Physica Status Solidi RLL **10**, 315-319 (2016)
4. F. Perez, F. Baboux, C. A. Ullrich, I. D'Amico, G. Vignale, G. Karczewski, and T. Wojtowicz, *Spin-orbit twisted spin waves: group velocity control*, submitted to Phys. Rev. Lett. (2016)
5. Shahrzad Karimi, F. Baboux, F. Perez, C. A. Ullrich, G. Karczewski, and T. Wojtowicz, *Spin precession and spin waves in a chiral electron gas: beyond Larmor's theorem*, in preparation for Phys. Rev. B (2016)

MATERIALS GENOME INNOVATION FOR COMPUTATIONAL SOFTWARE (**MAGICS**)

Priya Vashishta

Collaboratory for Advanced Computing and Simulations, Department of Chemical Engineering & Materials Science, Department of Physics & Astronomy, and Department of Computer Science, University of Southern California, Los Angeles, CA 90089-0242

Keywords: Computational synthesis; Reactive force fields; Non-adiabatic MD software; Thermal conductivity software; pump-probe ultra fast X-ray laser experiments for validation

MAGICS Center Team consists 11 investigators from 4 universities and 2 national laboratories. The Center supports 12 postdocs and software engineers, and 11 graduate students.

- **USC:** Priya Vashishta—PI, Malancha Gupta, Rajiv K. Kalia, Aiichiro Nakano, Oleg Prezhdo
- **Rice University:** Pulickel M. Ajayan
- **SLAC National Accelerator Laboratory:** Uwe Bergmann and David Fritz
- **California Institute of Technology:** William A. Goddard, III
- **Lawrence Berkeley National Laboratory:** Kristin A. Persson
- **University of Missouri:** David J. Singh

In addition, two unfunded senior investigators are also involved in the Center Jayakanth Ravichandran, **USC** and Aaron Lindenbergs, **Stanford**.

Project Scope

The **MAGICS** (*Materials Genome Innovation for Computational Software*) Center is about layered materials genome. Our goal is to develop and deliver validated first-principles based computational synthesis and characterization software, and carry out ultrafast pump-probe X-ray laser experiments at LCLS. The software will aid the synthesis of stacked LMs by chemical vapor deposition (CVD), exfoliation, and intercalation (Fig. 1). The software will provide function-property-structure relationships and will be sufficiently general to help synthesis and characterization of other functional nanomaterials. The **MAGICS** software stack will include plug-ins for a wide range of properties and processes including heat and mass transport, and various methods for free energy calculation.

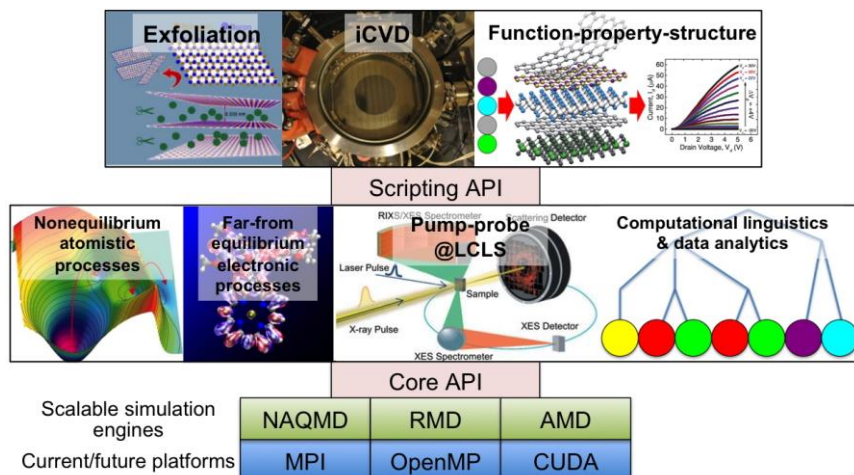
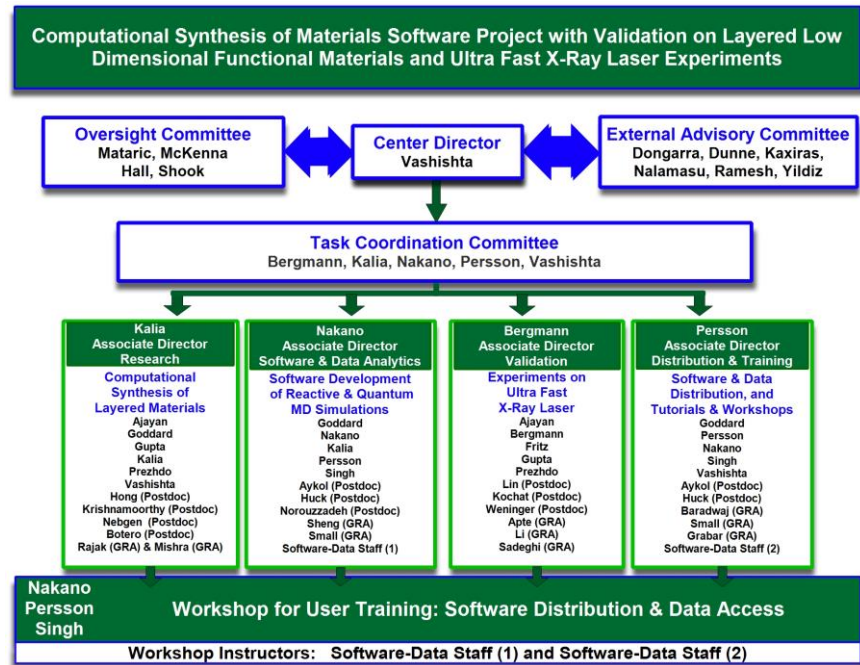


Fig. 1: Layered materials genome: Computational software for the synthesis and characterizations of stacked functional LMs. iCVD—initiated chemical vapor deposition; API—Application programming interface; LCLS—Linac Coherent Light Source; NAQMD—non-adiabatic quantum molecular dynamics; RMD—reactive molecular dynamics; AMD—accelerated molecular dynamics; MPI—Message passing interface; OpenMP—Open multi-processing; CUDA—Compute unified device architecture.



Recent Progress

Current status of research in computational synthesis, software development, experimental validation, and software & data distribution is described briefly in four parts.

1. NONADIABATIC MOLECULAR DYNAMICS SOFTWARE

Nonadiabatic molecular dynamics software: USC team (Kalia, Nakano & Prezhdo) is developing a method for efficiently simulating nonadiabatic molecular dynamics (NAMD) of condensed phase systems by combining the Fragment Molecular Orbital (FMO) approach with the NAMD techniques implemented with the PYXAID suite of programs. The method obtains electronic structure, including force and non-adiabatic coupling, with the FMO approach by splitting the system into fragments and computing properties of each fragment subject to the external field due to other all other fragments. The efficiency of the developed technique is being tested on transition metal complexes. The approach has been implemented within the Python extension for the *ab initio* dynamics (PYXAID) simulation package, which is an open source program designed to handle nanoscale materials.

2. DEVELOPMENT OF REACTIVE FORCE FIELD (REAXPQ)

Development of ReaxPQ: Goddard (Caltech), Kalia and Vashishta (USC) and their two postdocs and two grad students are continuing the development of the ReaxPQ method with the PQEq formalism that also includes polarization. In PQEq methodology each atom is represented by a variable charge plus two fixed charges (core and shell), modeled with a Gaussian charge distribution. Caltech-USC team is applying the QM and ReaxPQ methods to the synthesis of MoS₂ monolayers from the reaction of MoO₃ and Sulfur and related layered systems. We have started computational synthesis simulations to study the elementary processes during CVD growth of transition-metal dichalcogenide (TMDC) layers. Specifically, for the growth of MoS₂, we have simulated sulfidation of MoO₃. The simulation results revealed significant lowering of activation free energy due to sulfur vacancy, indicating an essential roles of vacancies for CVD growth. We have also started the training of force-field parameters for multimillion-atom

reactive molecular dynamics (RMD) using these QMD simulation results as a training set. A key component of this effort is validation by ultrafast experiments done at LCLS (Lindenberg, Bergmann and Fritz). We are collaborating with Adri van Duen (Penn State) in the ReaxFF force field development.

3. THERMAL CONDUCTIVITY SOFTWARE

Thermal conductivity software: Singh and his postdoc are developing a flexible thermal conductivity package to be used in conjunction with atomistic simulations. This will include a general thermal conductivity calculation based on Green-Kubo formalism. The software package – Thermal Analysis - ThermAl implements this along with a spectral analysis that will be of wide use in interpreting experimental data, especially with the ongoing development of experimental pump probe methods for energy and heat transport in materials. The code is being written in FORTRAN and incorporates a number of innovative features, especially as related to stochastic noise and sampling.

4. VALIDATION EXPERIMENTS

Ajayan (Rice) and Bergmann, Fritz (SLAC-LCLS-Stanford) and three postdocs and one grad student are leading the experimental research effort focused on layered materials and artificially stacked 2D layer structures, with specific focus on the growth and characterization of these materials. Integration of LM with polymeric materials will be carried out in Gupta's Lab at USC.

Time resolved X-ray studies at the Linac Coherent Light Source (LCLS): We used ultrafast x-ray diffraction to study how the electron-phonon interactions manipulate the atomic structure in TMDs. We used a 400 nm optical laser pulse to excite charge carriers above bandgap in the sample and detect the induced change in atomic structure by measuring position and intensity of x-ray Bragg reflections. The experiment makes use of the ultrafast time resolution that is available for pump-probe experiments at LCLS. We were able to observe centroid shifts of the (002) reflection in bulk WSe₂ after excitation with the pump laser. The data shows an initial compression of the layers followed by an expansion of the layers (see Fig. 2).

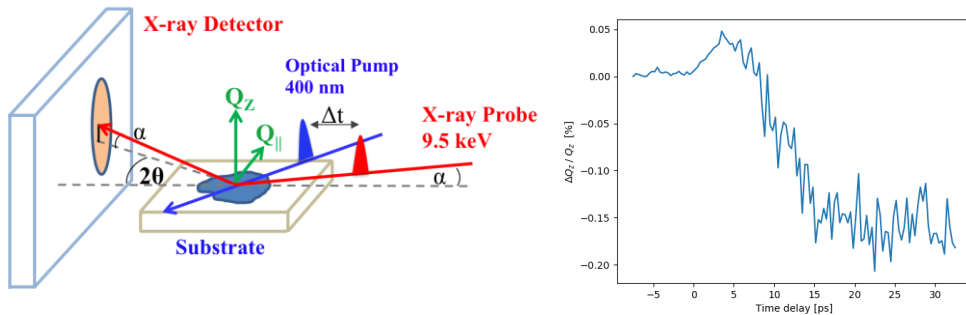


Fig. 2: (Left) Experimental setup. Incoming x-rays beam at 9.5 keV is focused on the sample in a grazing incident Bragg geometry. A 400 nm 50 fs laser pulse was used to excite carriers in the sample above the bandgap and the X-ray diffraction is detected with a CSPAD detector. (Right) Centroid position of the (002) peak as a function of pump-probe delay time.

Ultrafast electron diffraction (UED) at SLAC: We utilized the MeV ultrafast electron diffraction source at SLAC to explore the dynamics of charge carriers and lattice thermalization. The electron scattering cross section is 6 orders of magnitude larger than that of X-rays and subsequently yields a very good signal to noise ratio in the obtained diffraction patterns. This method allows us to measure incoherent lattice heat formation at different carrier density. Our initial results are shown in Fig. 3. We discover that this thermalization process of ~1 ps time

scale is independent of the carrier density and postulate that this is due to very efficient detect-assisted bimolecular recombination process.

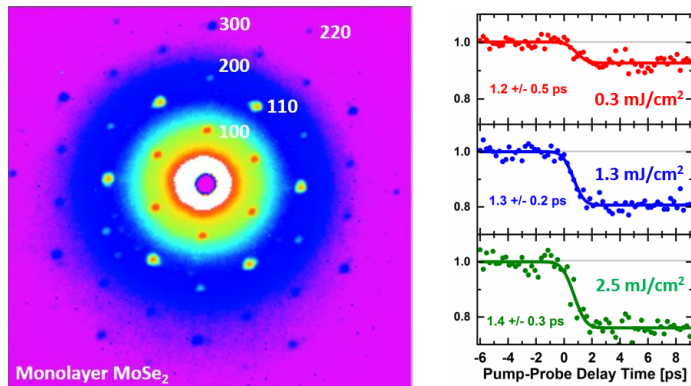


Fig. 3: Electron diffraction pattern from monolayer MoSe₂ (left) and Bragg peak time dependence (right).

5. SOFTWARE AND DATA DISTRIBUTION, AND TRAINING

Software management: We are developing an open source software toolkit for computational synthesis and characterization of materials and disseminate it to broad computational materials science community. MAGICS software will be based on a layered architecture that provides: (1) *simplicity and ease of use* through simple application programming interfaces (APIs) and powerful core library; (2) *extensibility*, where a community of users can add new features such as plugins without modifying the core library; and (3) *portable performance* across existing and future platforms. To allow seamless I/O integration and communication, a common interface and workflow environment will be developed by expanding the Pymatgen framework. The MAGICS software stack (Fig. 1) will consist of the following layers: (1) *scalable simulation engines on current and future computing platforms*: Our NAQMD, RMD, and AMD simulation engines combine global scalability and local computational efficiency; (2) *core library* is focused on the tasks that are common to many simulation scenarios: nonequilibrium atomistic processes, far-from equilibrium processes, and optical and X-ray pump-probe processes; and (3) *extensible plugins* will implement additional features beyond the core library. Community-developed plugins will be made available at software portal for general use. Key features of the software: (1) *exa-resilience* will be achieved by algorithmically restoring lost information without expensive checkpointing; (2) *high-throughput many-task computing (MTC)* to enable complex workflow of multiscale QMD/RMD/AMD simulations; (3) *in situ data-mining and statistical learning services* will be provided to examine NAQMD, RMD and AMD simulations, where queries will be performed on compressed data; *scalable visual analytics services* will be provided. For community code development and software distribution, bi-annual workshops have been budgeted, which train outside users and interfacing with the community of software developers. We will develop and maintain a scalable, open-source software package aimed for predictive computational synthesis. The software package will be available and distributed open-source to the community on Github.

Data Management: We will store and disseminate relevant data produced by the Center, such as computed and experimentally determined materials properties and synthesis parameters, reaction pathways, transition states, precursors and substrates, etc., through USC-HPC and **LBNL Materials Project (MP)**, adapting the flexibility of schemaless, or NoSQL, databases to support rapid evolution of requirements and scalability to large datasets.

Publications (2015-2016)

1. K. Nomura, R. K. Kalia, Y. Li, A. Nakano, P. Rajak, C. Sheng, K. Shimamura, F. Shimojo, and P. Vashishta, "Nanocarbon synthesis by high-temperature oxidation of nanoparticles," *Nature Scientific Reports* **6**, 24109 (2016).
2. T. Hakamata, K. Shimamura, F. Shimojo, R. K. Kalia, A. Nakano, and P. Vashishta, "The nature of free-carrier transport in organometal halide perovskites," *Nature Scientific Reports* **5**, 19599 (2016).
3. X. Fan, D. J. Singh, and W. T. Zheng, "Valence band splitting on multilayer MoS₂: mixing of spin-orbit coupling and interlayer coupling," *Journal of Physical Chemistry Letters* **7**, 2175 (2016).
4. X. Fan, D. J. Singh, Q. Jiang, and W.T. Zheng, "Pressure evolution of the potential barriers of phase transition of MoS₂, MoSe₂ and MoTe₂," *Physical Chemistry and Chemical Physics* **18**, 12080 (2016).
5. Y. Li, D. J. Singh, M.H. Du, Q. Xu, L. Zhang, W. Zheng, and Y. Ma, "Design of ternary alkaline earth Sn(II) oxides with potential good p-type conductivity," *Journal of Materials Chemistry C* **4**, 4592 (2016).
6. P. E. Small, R. K. Kalia, A. Nakano, and P. Vashishta, "Order-invariant real number summation: circumventing accuracy loss for multimillion summands on multiple parallel architectures," in *Proceedings of the International Parallel and Distributed Processing Symposium, IPDPS 2016* (IEEE, Chicago, IL, 2016) p. 152.
7. V. V. Chaban and O. V. Prezhdo "Energy storage in cubane derivatives and their real-time decomposition: computational molecular dynamics and thermodynamics," *ACS Energy Letters* **1**, 189 (2016).
8. V. V. Chaban and O. V. Prezhdo "Boron doping of graphene – pushing the limit," *Nanoscale*, in press, DOI: 10.1039/C6NR05309B.
9. N. A. Romero, A. Nakano, K. Riley, F. Shimojo, R. K. Kalia, P. Vashishta, and P. C. Messina, "Quantum molecular dynamics in the post-petaflop/s era," *IEEE Computer* **48**(11), 33-41 (2015).
10. K. Nomura, P. E. Small, R. K. Kalia, A. Nakano, and P. Vashishta, "An extended-Lagrangian scheme for charge equilibration in reactive molecular dynamics simulations," *Computer Physics Communications* **192**, 91 (2015).

Time-dependent density functional theories of charge, energy and spin transport and dynamics in nanoscale systems

GRANTS DE-FG02-05ER46203, DE-FG02-05ER46204

Principal Investigators:

Giovanni Vignale, Department of Physics, University of Missouri, Columbia
Massimiliano Di Ventra, Department of Physics, University of California, San Diego

Project scope

The focus of this research program is on developing density functional methods for the calculation of non-equilibrium phenomena of the transport type (finite wavelength, low frequency) and of the dynamical type (long wavelength, high frequency). One such method is the time-dependent current density functional theory, in which the evolution of the physical system is mimicked in a fictitious non-interacting system subjected to an effective one-particle potential, which we approximate as a function of the equilibrium density and non-equilibrium current density. A second approach is the quantum continuum mechanics □ an orbital-free method in which the quantum stress tensor is expressed as a functional of the non-equilibrium current density, leading to a closed equation of motion for the latter. Part of this work is done in collaboration with Max Di Ventra at UCSD. In the following we concentrate on the work we have recently done on extending the time-dependent density functional theory to thermoelectric transport phenomena, by introducing the (time-dependent) energy density as a new basic variable, and the Luttinger "gravitational" potential as its conjugate driving field. We have shown that this approach generalizes the standard Landauer-Büttiker formalism and offers a relatively simple way to include electron-electron interaction effects. Calculations on simple non-interacting models already reveal interesting effects arising from the inclusion of the Luttinger potential, such as the anomalous sign of the transient charge current driven by a thermal gradient and propagating quantum temperature oscillations. Including electron-electron interactions we have identified thermal corrections to the ordinary single-particle resistivity [5], and estimated their magnitude vis-a-vis the better known viscosity corrections, which we introduced a few years ago. We are presently working on the implementation of the adiabatic local density approximation for the effective exchange-correlation potentials. In a parallel effort, we have completed a many-body theoretical calculation of the thermal conductivity of the two-dimensional interacting electron liquid, showing the existence of a simple relation between the thermal transport time and the quasiparticle lifetime, and a strong violation of the conventional Wiedemann-Franz law [3].

Recent progress

1. Density Functional Theory of Thermoelectric Phenomena

The problem of calculating the thermal and electrical transport properties of nanoscale conductors is attracting great interest in the context of growing efforts to achieve efficient conversion of heat into electricity, and vice-versa. The recent development of scanning thermal microscopy, allowing for measurements of a local effective temperature on the atomic scale, provides strong motivation for extending the thermodynamic concept of temperature to non-equilibrium situation (standard hydrodynamics already does this, to a limited extent). Many years ago Luttinger took an important step in this direction by proposing that the thermoelectric transport properties of a macroscopic electron liquid could be calculated by subjecting the system

to a space- and time-varying potential field $\psi(\mathbf{r},t)$. The ψ potential was to be linearly coupled to the energy density, for which Luttinger chose one of several possible definitions — all equivalent in the long-wavelength limit. Luttinger's idea was that the dynamical response of the system to the varying ψ potential would be equivalent to the response to a temperature gradient in situations in which the latter is slowly varying, but would extend the concept of thermal response to situations in which the traditional notion of temperature is no longer meaningful. The gradient of this potential drives the thermal current, just as the gradient of the electric potential drives the electric current.

In a recent paper [1] we have developed Luttinger's idea into a full-fledged time-dependent density functional theory of local temperature and associated energy density variations, which should be useful for the ab-initio study of thermoelectric phenomena in electronic systems. We have identified the excess-energy density — i.e., the difference between the actual energy density and the energy that would be in equilibrium with the instantaneous particle density — as a second basic variable of the theory, in addition to the particle density. Both the particle density and the excess energy density are reproduced — exactly, in principle — in an effective non-interacting Kohn-Sham system. The time evolution of this effective system is driven by a new kind of Kohn-Sham equation, featuring a time-dependent and spatially varying mass, which represents local temperature variations. This is precisely how the Luttinger ψ -potential enters the Schrödinger equation of a noninteracting system. We have examined the two basic approximation strategies for the effective potentials that enter the Kohn-Sham equation. In the adiabatic approximation the interaction contribution to the Kohn-Sham effective potential is related to the entropy, the latter viewed as a functional of the particle and energy density of the homogeneous electron gas. In the first step beyond the adiabatic approximation the time derivatives of the density and energy density make their appearance as arguments of the potential functional. These quantities are related to the longitudinal parts of the particle and energy currents. In a homogeneous electron gas, the currents are related to their conjugate fields by a well-known matrix of thermoelectric transport coefficients. Based on this observation, we have been able to show that the leading dissipative contributions to the Kohn-Sham potential can be expressed in terms of the particle and thermal currents and of the thermoelectric linear transport coefficients of the homogeneous electron gas. The practical implementation of the adiabatic local density approximation (ALDA) is presently underway: the process is complicated by the existence of constraints on the admissible values of the energy density of a uniform electron gas, which can be locally violated in the inhomogeneous electron gas. In the meanwhile, making use of the leading dissipative corrections to the ALDA we have been able to estimate the magnitude of many-body thermal corrections to the resistivity. When an electric current passes through an inhomogeneous electronic system temperature gradients arise across inhomogeneities: these temperature gradients generate electric potential gradients (via the Peltier effect) and thus contribute to the total resistance of the structure. The magnitude of the effect is controlled by the thermal conductivity, which — in the absence of effective electron-impurity and electron-phonon collision — is defined by electron-electron interactions (this is why we characterize this as a many-body effect). Making use of our calculated values for the thermal conductivity of the interacting electron liquid [3], we have found the thermal correction to the resistivity to be comparable to, but generally smaller than the many-body viscous correction [6].

2. Model calculation for noninteracting systems

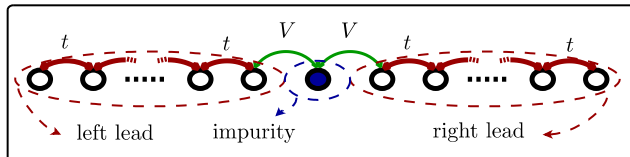


Fig. 1: Sketch of the model studied in Ref. [2]

In our recent papers we have worked out a few applications of Luttinger's ψ -potential idea to the calculation of thermal transport through a nanoscale junction. This means that we completely replace the different temperatures in the reservoirs by ψ potentials. The conventional statistical temperature remains constant throughout the system. To calculate the currents we closely follow the formulation of the non-equilibrium Green's function theory, in which the leads and the nanoscale system are initially in equilibrium with a unique reservoir at a single chemical potential and temperature. At the initial time different electric potentials and Luttinger fields are applied to the leads. The resulting electric and thermal currents are calculated in the long-time limit. Our main result is that, for a non-interacting system, in the linear response regime, the current calculated in this manner coincides with the current calculated in the Landauer-Büttiker (LB) approach. Furthermore we demonstrate that the LB result can be fully recovered in the non-linear regime, if the ψ potentials are applied during the initial preparation of the system, and turned off at the initial time. This is good news, which builds confidence in the general applicability of Luttinger's approach to nanoscale conductors. Many-body effects were not included in these calculations, but we expect to be able to handle them through the density-functional formalism of Ref. [1]. In practice, we have done our calculation for the simple model described in Fig. 1, describing a single impurity site coupled to semi-infinite leads, and we have carefully compared the results of the ψ -potential approach with those of the conventional LB approach, in both the linear and nonlinear regimes. Fig. 2 presents representative results for the thermal currents that flow in response to applied voltages and temperature gradients.

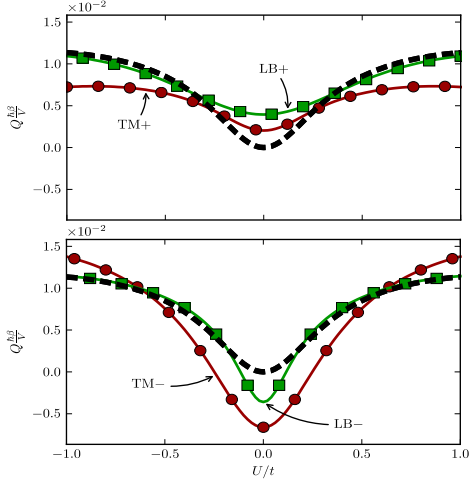


Fig. 2. Comparison of the steady-state heat current Q in the ψ -potential approach and in the LB approach. The currents are plotted against the potential bias U in units of the hopping t . The upper panel depicts the currents when the temperature in the left lead is raised to twice its initial value and the lower panel shows the heat current when the temperature in the left lead is reduced to half its initial value. The dashed, black curve is the heat current at zero relative temperature variation. The circles (red curve, labeled TM) correspond to the current in the ψ -potential approach and the squares (green curve, labeled LB) to the LB approach.

Fig. 3 presents additional results on the single impurity system, in which we now study the transient behavior of the current before a steady state is reached after a rapid increase of the temperature in one of the reservoirs [4].

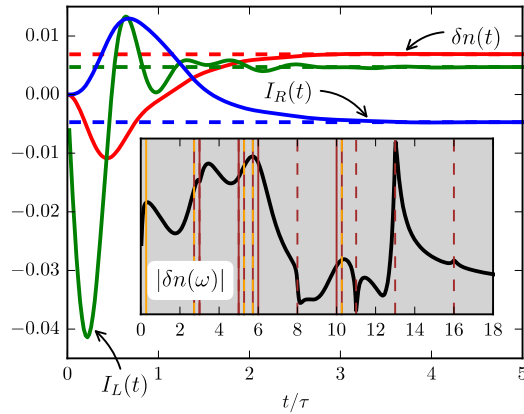


Fig. 3. Plot showing the transient density change, $\delta n(t)$, of the impurity site and the currents between left lead and impurity, $I_L(t)$, and right lead and impurity, $I_R(t)$, respectively. The corresponding steady-state values are indicated by the horizontal dashed lines. The inset shows the Fourier transform of the density change of the long-time tail. The structure of this power spectrum reflects the distribution of energy levels in the leads (from Ref. [4])

The most striking feature in this plot is the sign of the charge current I_L from the left reservoir, which is initially negative, indicating a counterintuitive transfer of charge from the impurity site to the left reservoir. What happens is that the sudden rise in temperature of the left reservoir requires a rapid redistribution of the electrons from below to above the chemical potential. The presence of the impurity assists—at short times—this redistribution by providing electrons above the chemical potential and the impurity density drops initially. At long times I_L and I_R settle to the intuitively expected values.

We have also calculated the energy propagation and the emergence of quantum temperature oscillations along a nanowire, modeled as a tight binding chain of 100 sites stretched between two reservoirs. Fig. 4a shows the propagation of the energy density following a temperature rise in the left reservoir, and Fig. 4b is the steady-state distribution of the temperature along the wire.

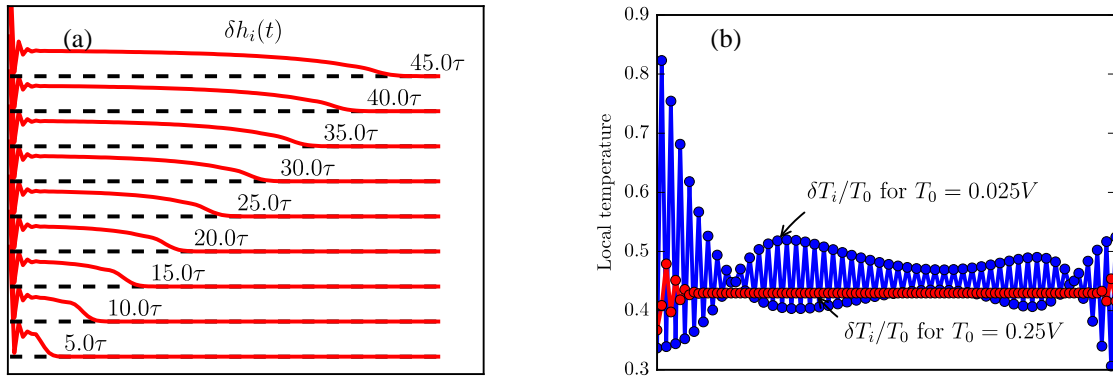


Fig. 4. (a) Plot of the transient energy wave propagating through the nanowire after a rise in the temperature of the left reservoir. t is the natural time scale for the hopping of an electron from the reservoir to the nanowire. (b) Steady-state local temperature distributions in the nanowire determined by a “probe” lead as in Fig. 2. The red lines correspond to an initial temperature of $k_B T_0 = 0.25V$ and the blue lines to $k_B T_0 = 0.025V$. The local temperature for the lower initial temperature exhibit typical $2k_F$ Friedel oscillations.

Planned activities

Our next step will be the implementation of the adiabatic local density approximation for the density functional method of Ref. [1]. This will be applied to the study of interaction effects in the propagation of heat pulses in quantum dots and nanowires.

Publications

1. *Density functional theory of thermoelectric phenomena*, F. G. Eich, M. Di Ventra, and G. Vignale, Phys. Rev. Lett. **112**, 196401 (2014).
2. *Luttinger field approach to thermoelectric transport in nanoscale conductors*, F. G. Eich, A. Principi, M. Di Ventra, and G. Vignale, Phys. Rev. B **90**, 115116 (2014).
3. *Violation of the Wiedemann-Franz law in clean graphene layers*, A. Principi and G. Vignale, Phys. Rev. Lett. **115**, 056603 (2015)
4. *Temperature-driven transient charge and heat currents in nanoscale conductors*, F.G. Eich, M. Di Ventra and G. Vignale, Phys. Rev. B **93**, 134309 (2016).
5. *Dynamical many-body corrections to the residual resistivity of metals*, V. U. Nazarov. G. Vignale, Y. -C. Chang, Phys. Rev. B **89**, 241108 (R) (2014).
6. *Functional theories of thermoelectric phenomena*, F. G. Eich, M. Di Ventra and G. Vignale, a review article submitted to Journal of Physics: Condensed Matter, July 2016.

Quantum Mesoscopic Materials

PI: Valerii Vinokur*; Co-PI: Andreas Glatz

Materials Science Division, Argonne National Laboratory, 9700 South Cass Avenue, Argonne, Illinois 60439

*vinokour@anl.gov

Project Scope

The synergistic research program “Quantum Mesoscopic Materials” conducts in-depth theoretical investigation into the physics of quantum mesoscopic materials. Our research is carried out in close collaboration with experimental groups around the globe. The *materials* of interest are systems, whose thermodynamics and statistics are controlled by quantum interference and quantum fluctuations and their interplay with quantum correlations, long-range interactions, and disorder. The main *objects* of our research are materials that exhibit effects of coherence on the meso- and macro-scales and mediate entanglement phenomena. Our immediate focus *objectives* are quantum coherent phase transitions and far from equilibrium phenomena. Exemplary recent accomplishments include the discovery and in-depth investigation of the novel low-temperature superinsulating state in strongly disordered superconducting films; the discovery of reentrant superconductivity in nano-patterned superconducting films and strips at high magnetic fields, a novel concept of critical superconductivity in nano-size systems and multiband superconductors, the discovery and in-depth investigation of the dynamic vortex Mott transition, and developing a systematic universal theory of nonequilibrium phase transitions based on non-Hermitian quantum mechanics. In what follows we highlight this new emergent direction, a theory of out-of-equilibrium phase transitions.

Recent Progress

Past years have seen marked progress along the program focus lines including the discovery of a novel critical superconductivity, breakthroughs in the description of the electric response of Cooper pair insulators, and entanglement and quantum interference effects in mesoscopic structures. Below we highlight one of the major achievements, the discovery of the dynamic vortex Mott transition and the related introduction of a universal approach to a predictive description of out-of-equilibrium instabilities and phase transitions.

Dynamic Mott transition – In collaboration with the experimental group at the University of Twente (Netherlands), we discovered a dynamic vortex Mott transition in proximity arrays of nano-scale superconducting islands [1] and revealed the related critical behavior.

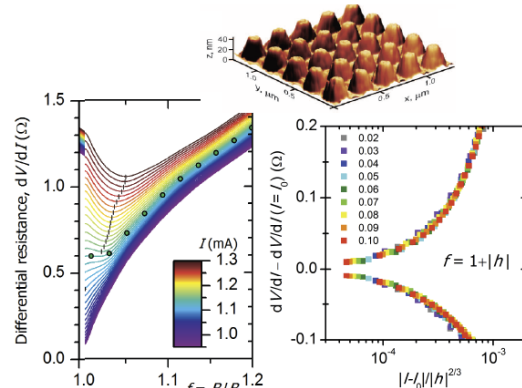


Fig. 1. Upper panel: Experimental system. Left: Differential vortex magnetoresistance near the matching magnetic field, where the numbers of vortices and traps match taken at different currents. Threshold current I_0 separating Mott insulator (dips) from Mott metal (peaks) is shown by dots. Right: same curves scaled as functions of $|I-I_0|/h^{2/3}$. Perfect scaling evidences the transition. Exponent 2/3 indicates that dynamic vortex Mott transition belongs to the universality class of the liquid-gas transition.

The non-equilibrium transition between vortex Mott insulating and metallic phases has been observed at commensurate fillings of the underlying square lattice of vortex traps upon increasing the applied electric current. The scaling exponents reveal different universality classes depending on the filling factor. In a subsequent work [2] we identified non-Hermitian quantum mechanics as a universal tool for the description of out-of-equilibrium phenomena in open dissipative systems. This allowed us to develop a theory for the dynamic Mott transition based on parity-time reversal (PT) symmetry breaking mechanism. Utilizing the Bethe ansatz treatment of the non-Hermitian extension of the Hubbard model, we derived the critical exponents of the Mott insulator-metal transition that are in an excellent agreement with experimental findings. Importantly, our findings open a route for the detailed investigation of strongly correlated quantum systems via experiments based on easily accessible tunable classic vortex arrays.

Spin-transfer torque-driven spin systems – Building on the success of the description of the dynamic Mott transition, we undertook the appealing task of constructing a similar non-Hermitian approach to out-of-equilibrium behavior to a completely different physical system demonstrating thus the universality of our technique. We succeeded in establishing a non-Hermitian generalization of the Hamiltonian description of the dissipative dynamics of non-equilibrium spin systems [3]. In our formulation the non-Hermiticity describes both, dissipation and action of non-conservative forces. In the classical limit, the novel approach revealed a driven spin-torque-transfer parity-time symmetry breaking phase transition between precessional and exponentially damped spin dynamics. The predicted effect has been verified by micromagnetic simulations and holds high promise as a platform for switching units in low-power spintronic devices.

Future Plans

We highlight the direction of research directly related to constructing a non-Hermitian theory of non-equilibrium phase transitions and instabilities. Our success in establishing non-Hermitian quantum mechanics as a universal tool for studying out-of-equilibrium physics allowed to tackle unresolved challenges that mark the emergence of new science that will push the frontiers of our knowledge well beyond the existing understanding of equilibrium physics and thermodynamics. The fundamental questions to resolve include:

- (i) What are similarities and differences between non-equilibrium phase transitions and their equilibrium counterparts in the same quantum system? If the transitions are continuous, what are their critical exponents? Which symmetries are broken, if any?
- (ii) What is the role of dissipative processes?
- (iii) Is it possible to develop a general non-Hermitian Hamiltonian formulation for the quantitative description of non-equilibrium steady states and phase transitions in open dissipative quantum systems?
- (iv) How does disorder affect dynamic phase transitions?

Importantly, in resolving these questions extensive large-scale computations are expected to play a prime role. Our discovery of the dynamic vortex Mott transition opened a route to investigate fundamental properties of strongly correlated quantum systems that are not

accessible by traditional means of exploring electronic systems suffering inevitable detrimental effects of disorder. We intend to investigate hybrid magnet/superconductor (M/SC) structures that will offer unprecedented opportunity for the cleanest tuning the properties of vortex arrays to realize Mott transitions. It will be possible to uncover mechanisms interconnecting localization, long-range interactions, and fluctuation effects. From the application point of view, the Mott metal-insulator transition (MIT) offers a new kind of transistor controlled by applied current or electric field. Our study of vortex systems controlled by tunable magnetization will reveal self-healing vortex patterns and their controlled manipulation. Their counterparts in the dual electronic system will enable MIT-based transistors. We intend to develop a theoretical/numerical technique for the quantitative description of hybrid SC/M structures employing a system of coupled time-dependent Ginzburg-Landau equations [6] for the dynamics of the superconducting order parameter and the Landau-Lifshitz-Gilbert equation describing the magnetization of the magnetic structure. Both sets are coupled through boundary conditions for the magnetic vector potential. Separate solutions for either superconductors or magnetic systems, are well known, but so far there are no solutions to the system of coupled dynamic equations applicable to realistic samples. We will study the dynamics in mesoscopic 3D hybrid SC/M structures involving a few billion degrees of freedom per system. We will implement the solver for the equation system targeting the upcoming next generation Intel Xeon Phi architecture (i.e., the new leadership class machines Theta & Aurora) to tackle this numerical challenge. Beside the fundamental insights, it will open pathways for energy-related applications and design of novel quantum electronics circuits.

Correspondingly, the main directions/goals of our future research integrating analytical and numerical methods are as follows:

- **Microscopic origin of imaginary vector potential (field):** We conjectured that the imaginary vector potential or field that measures the degree of non-Hermiticity is directly related to the applied driving field. We intend to reveal the microscopic origin of imaginary driving field. As a first step we will couple fermionic Hubbard models in the presence of an applied bias to a bosonic bath and integrate out the bath degrees of freedom and derive the emerging imaginary driving field.
- **Non-equilibrium Mott transition in the Ambegaokar-Eckern-Schön (AES) model of granular metals:** Transport in the insulating state of granular metals is governed by the competition of inter-grain tunneling with the Coulomb blockade effects which is also the key physical process governing Mott transitions in the Hubbard model. The standard approach is to eliminate the fermionic degrees of freedom in order to obtaining an effective action for the fluctuating electromagnetic phases on the individual grains, known as Ambegaokar-Eckern-Schön (AES) model. We will utilize this model to study the nonequilibrium Mott transition in the presence of a driving electric field and relate it to the PT-symmetry approach.
- **Non-linear dynamic Mott transition:** We will investigate underlying mechanisms of the dynamic Mott insulator-metal transitions in one- and two-dimensional quantum systems at fractional lattice fillings. We will study different universality classes of the phase transitions caused by spontaneous parity-time symmetry breaking and address the new effect of multiple dynamic Mott transitions in highly non-linear systems.

- **Coupled spin systems:** Based on the non-Hermitian Hamiltonian formalism developed for a single-spin system, we will investigate temporal dynamics and phase transitions in spin-chains and two-dimensional spin textures. We will utilize the result that action of spin-polarized current can be described as applied *imaginary* magnetic field to study Lee-Yang zeros in ferromagnetic Ising and Heisenberg models, and, more generally, dynamics and thermodynamics in the complex plane of physical parameters.
- **Instabilities in driven systems as parity-time symmetry-breaking phenomenon:** We will further apply non-Hermitian quantum mechanics to strongly correlated condensed matter systems out of equilibrium. We will investigate non-equilibrium phase transitions in parity-time-symmetric Bose-Fermi mixtures and unconventional superconductors, with the emphasis on current-driven dynamics of vortices.
- **Topological structures in ferroics:** We will closely collaborate with Axel Hoffmann's group at MSD that studies non-linear transitions in topologically non-trivial spin textures (e.g., skyrmions and domain walls). The developed non-Hermitian formalism offers a perfect tool for a non-perturbative description of topological spin excitations in magnetic systems. We will investigate skyrmions and toroidal dipoles, in ferroelectric materials as a platform for a new generation of ultra-low power information-storage and transmission elements in emergent oxide-based nanoelectronics. Protected by topological stability requirements, polarization skyrmions and toroidal dipoles, have long lifetimes that makes them most reliable information carriers. The polarization skyrmions are of about atomic size allowing to dramatically compactify information storage and increase the information processing speed.
- **Quantum tunneling of spins:** the non-Hermitian Hamiltonian formalism developed for single-spin systems will be generalized to a theory of quantum spin tunneling in open dissipative systems. The interest is motivated by the promise of using single-molecule nanomagnets as building blocks in spintronic devices. Geometric phase effects and topology play a crucial role in quantum spin dynamics, and the non-Hermitian formalism based on spin-coherent-state path integrals appears as the most adequate approach for this challenging problem.

Selected publications:

1. N. Poccia, V. Vinokur *et. al*, Science **349**, 1202 (2015).
2. A. Galda and V. Vinokur, PRB **94**, 020408(R) (2016).
3. V. Tripathi, A. Galda, H. Barman, and V. Vinokur, PRB **94**, 041104(R) (2016).
4. G.P. Papari, A.Glatz, F. Carillo, D. Stornaiuolo, D. Massarotti, V. Rouco, L. Longobardi, F. Beltram, V.M. Vinokur, and F. Tafuri, submitted to Nature Physics (2016).
5. M. Vasin, V. Ryzhov, and V. M. Vinokur, Scientific Reports **5**, 18600 (2015).
6. A. Sadovskyy, A. E. Koshelev, C. L. Phillips, D. A. Karpeev, and A. Glatz, J. of Comp. Phys. **294**, 639 (2015).
7. I. A. Sadovskyy, G. B. Lesovik, and V. M. Vinokur, New J. of Physics **17**, 103016 (2015).
8. M. Ortúñ, A. Somoza, V. M. Vinokur, and T. I. Baturina, Scientific Reports **5**, 9667 (2015).
9. I. L. Aleiner, A. V. Andreev, and V. M. Vinokur, PRL **114**, 076802 (2015).
10. I. Lukyanchuk, V. M. Vinokur, *et al*. Nature Physics **11**, 21 (2015).
11. A. Glatz, A. A. Varlamov, and V. M. Vinokur, EuroPhys Lett. **107**, 47004 (2014).
12. T. I. Baturina and V. M. Vinokur, Ann. Phys. **331**, 236 (2013).
13. R. Cordoba, T. I. Baturina, V. M. Vinokur, *et al*. Nature Comm. **4**, 1437 (2013).
14. O. G. Udalov, A. Glatz, I.S. Beloborodov, EuroPhys. Lett. **104**, 47004 (2013).

Accelerated molecular dynamics methods

Principal Investigator: Arthur F. Voter
Co-Principal Investigator: Danny Perez
Theoretical Division, Los Alamos National Laboratory
Los Alamos, NM 87545
afv@lanl.gov
danny_perez@lanl.gov

Project Scope

The primary goal of this project is to develop high-quality computational methods for reaching long time scales in the atomistic simulation of materials. While direct molecular dynamics (MD) is limited to roughly one microsecond, it is often crucial to understand the dynamics on longer time scales. We focus on infrequent-events, typically activated processes, as this characterizes the long-time dynamics of many materials of importance to LANL, BES and DOE missions. For this type of system, we can exploit the infrequent-event nature to shorten the time between successive events, and hence probe the behavior at much longer times. Largely under this BES program, we have developed the *accelerated molecular dynamics* (AMD) approach, in which we let the system trajectory itself find an appropriate way out of each state, eliminating the need to pre-specify, or to search for, all possible escape paths from a state. The key is to find the next escape path more quickly than MD would, while maintaining high accuracy in the resulting state-to-state dynamics. The methods in this AMD class are hyperdynamics, in which the potential surface is carefully modified to accelerate the escape dynamics, parallel-replica dynamics (ParRep), in which many replicas of the system are evolved simultaneously to effectively parallelize time, and temperature accelerated dynamics (TAD), in which a high-temperature trajectory is employed to quickly scan for the first escape that should occur at the lower temperature. With these core methods in place, our main focus now is on making them more powerful and efficient for a wide variety of systems, and on applying them to materials problems of relevance to DOE/BES as well as the DOE mission more broadly.

Recent Progress

Here are selected highlights from the past two years.

SpecTAD – We developed a new and powerful approach for parallelizing temperature accelerated dynamics: speculatively parallelized TAD (SpecTAD). The key concept is to use speculation on the outcome of a TAD simulation in order to expose additional parallelization opportunities. This is achieved by immediately spawning a child process in parallel each time an attempted escape event is observed, if it has a chance of later becoming the accepted event. This child process, a complete, independent TAD simulation in the state to which the system made its attempted escape, is continued as long as this event potentially may be accepted by the parent simulation. The result is a method that can move from one state to the next as quickly as the correct transition is seen at high temperature, giving significant speedup over conventional TAD (see Fig. 1). As an initial example, we simulated the deposition of one monolayer (ML) of Cu onto the Ag(100) surface, matching the experimental deposition rate of 0.04 ML/s and temperature of T=77K. Earlier TAD simulations on this same system required *months* of wall-

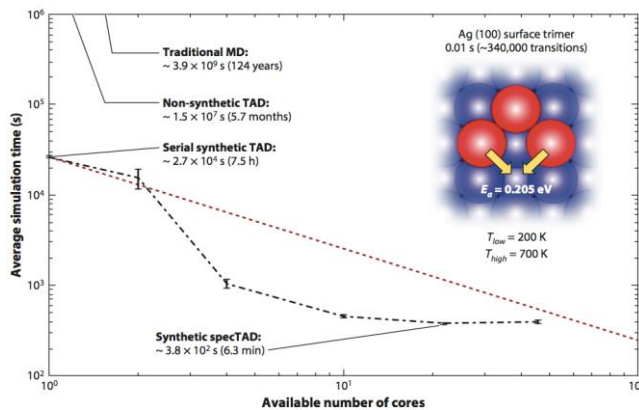


Figure 1: Simulation time versus number of cores showing the gains possible with SpecTAD compared to MD and standard TAD for a prototype low-barrier system.

interstitial formation on the mobility of the component defects in magnesium aluminate spinel (MgAl_2O_4), a ceramic with a range of technical applications including use as a radiation tolerant material in extreme environments. We found that the clustering of Al and O vacancies drastically reduces the mobility of both defects, while the clustering of Mg and O vacancies completely immobilizes them; this has consequences for stability under irradiation. The complex diffusion pathways (e.g., see Fig. 2) required extremely long simulations that would not have been feasible with pre-SpecTAD methods.

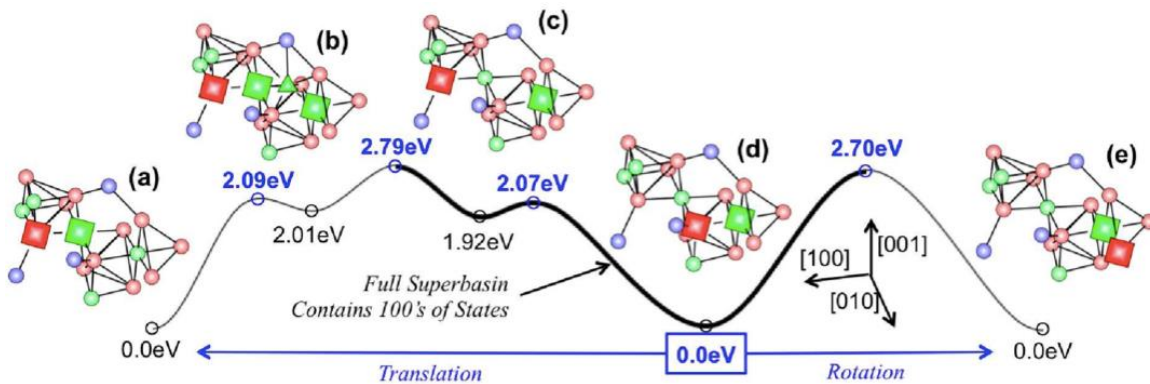


Figure 2: Dominant migration pathways for a dimer defect comprised of an oxygen vacancy and an aluminum vacancy in MgAl_2O_4 spinel. Elucidation of this process required evolving with SpecTAD for billions of transitions.

Accelerated quantum dynamics – Nuclear quantum effects – deviations from purely classical atomistic dynamics – are well known to be important in systems containing light elements at low temperature. While direct solution of the nuclear Schrodinger equation is prohibitive, semi-classical trajectory approaches, such as ring-polymer molecular dynamics (RPMD), are known to give a very good approximation to quantum zero-point and tunneling effects in activated escape processes. We have now shown that the ParRep method can be effectively combined with such approaches. The combined method is a powerful tool for reaching long time scales in complex infrequent-event systems where quantum dynamics are important. We demonstrated that it can be applied effectively to study interstitial helium diffusion in Fe and Fe-Cr alloy at low temperature (see Fig. 3).

clock time to reach one monolayer. By providing 128 cores for speculation, the same coverage was achieved by SpecTAD in ~10 hours for an overall boost factor of one billion.

Application of SpecTAD to Spinel – In collaboration with Blas P. Uberuaga’s BES program at LANL (*Phase Stability of Multi-Component Nanocomposites Under Irradiation*), we have applied SpecTAD to investigate the effects of di-vacancy and di-

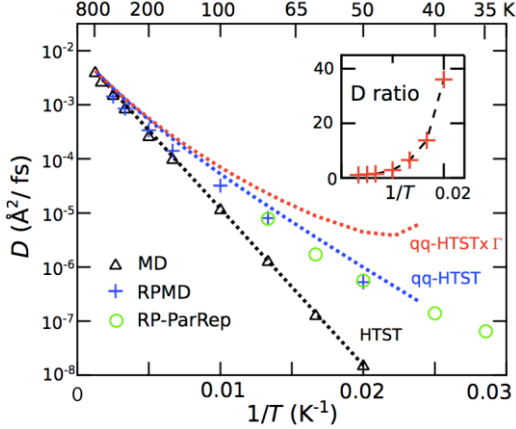


Figure 3: He diffusion in Fe, computed using ParRep combined with ring polymer MD (RPMD) showing the importance of quantum effects as well as the deficiency of standard quantum HTST approaches.

on a simple Ag surface system and demonstrated substantial increases in efficiency compared to ParRep (c.f. Fig. 4). This exceptional scalability was recently demonstrated on LANL’s Trinity supercomputer using up to 200,000 replicas. Note that the initial and key conceptual development of ParSplice was carried out under this BES program; current implementation efforts are supported by LANL/LDRD.

Future Plans

Our method development efforts will be focused on two main thrusts that we consider critical to the future development of AMD methods, namely, development of AMD methods for the exascale era, and further development of AMD methods for complex systems.

AMD at the exascale – The arrival of exascale computing, anticipated for just a few years from now, offers a great opportunity while also posing a daunting challenge. The raw computing power of such machines could enable MD simulation of materials on the timescale of seconds, but, in reality, the same microsecond timescale limit will persist when using traditional parallelization approaches. To meet this challenge, we plan to combine the ParSplice and SpecTAD methodologies into a unified, versatile framework for extreme scale simulations. We will also couple this new approach with spatial parallelization strategies in order to extend the range of size and time-scales that will be accessible at the exascale. We will also continue to advance our recently developed local hyperdynamics methodology, which allows hyperdynamics speedup on arbitrarily large systems (e.g., billions or trillions of atoms) with only a minor additional locality approximation.

ParSplice - We introduced a new AMD simulation technique, Parallel Trajectory Splicing (ParSplice), in which trajectory segments, generated in parallel, are spliced end-to-end to create a rigorously valid long-time trajectory. Segments are generated in proportion to the expected likelihood that they will be used to extend the state-to-state trajectory, which is estimated using a kinetic model that is built on the fly. This simultaneous generation of segments in multiple states leads to very good scalability. We validated the method

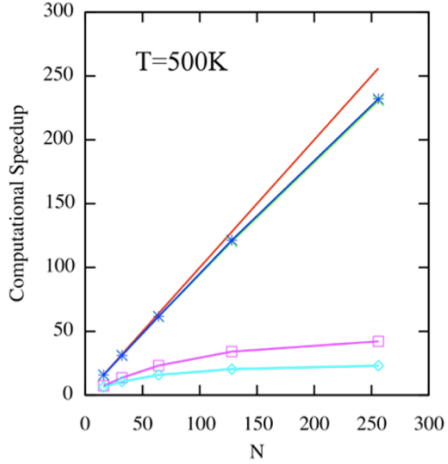


Figure 4: Computational speedup versus number of processors for simulating dynamics of an adatom trimer on the Ag(100) surface using ParRep (magenta and pale blue lines) or ParSplice (blue line). The red line denotes perfect parallel efficiency.

AMD for complex systems – An important and ongoing challenge facing AMD methods is to extend their applicability to encompass increasingly complex systems. We will focus on two approaches that should significantly extend the reach of AMD: the development of a generalized ParRep method based on the concept of quasi-stationary (QSD) distributions, and the further extension of AMD methods into the realm of quantum nuclear dynamics. The first of these builds on the recently developed understanding of the generality of ParRep and ParRep-based methods, allowing arbitrary definition of the states of the system. For the latter, we plan to adapt the TAD and hyperdynamics methods to RPMD.

Applications – Applications of AMD methods are essential to demonstrate the power of the methods but also to inform further development in a way that maximizes the impact on the problems of interest to DOE and on the field at large. We will continue our work with Blas Uberuaga’s BES program on simulating disordered oxides, and initiate a collaboration with Carlos Tomé’s BES on twin-twin interactions in HCP metals. We will also actively pursue our collaboration with an ongoing OFES/SciDAC program on plasma/surface interactions, and as well leverage the expertise of visitors in the group to investigate the long-time morphological stability of nanoparticles and dislocation/impurities interactions in metals.

Publications

- “The parallel replica dynamics method – Coming of age,” Danny Perez, Blas P. Uberuaga, and Arthur F. Voter, Computational Materials Science, **100**, 90 (2015).
- “Analysis of Transition State Theory Rates upon Spatial Coarse-Graining,” Andrew Binder, Mitchell Luskin, Danny Perez, and Arthur F. Voter, Multiscale Modeling and Simulation **13**, 890–915 (2015).
- “Hyperdynamics boost factor achievable with an ideal bias potential,” Chen Huang, Danny Perez, and Arthur F. Voter, J. Chem. Phys. **143**, 074113 (2015).
- “The Modern Temperature-Accelerated Dynamics Approach,” Richard J. Zamora, Blas P. Uberuaga, Danny Perez, and Arthur F. Voter, Annu. Rev. Chem. Biomol. Eng. **7**, 24 (2016).
- “Accelerating Ring-Polymer Molecular Dynamics with Parallel-Replica Dynamics,” Chun-Yaung Lu, Danny Perez, and Arthur F. Voter, J. Chem. Phys **144**, 244109 (2016)
- “The effects of cation-anion clustering on defect migration in MgAl₂O₄,” Richard Zamora, Arthur F. Voter, Danny Perez, Romain Periot, and Blas P. Uberuaga, Physical Chemistry Chemical Physics **18**, 19647 (2016).
- “Competing Kinetics and He Bubble Morphology in W,” Luis Sandoval, Danny Perez, Blas P. Uberuaga, and Arthur F. Voter, Physical Review Letters **114**, 105502 (2015).
- “Long-Time Dynamics through Parallel Trajectory Splicing,” Danny Perez, Ekin D. Cubuk, Amos Waterland, Efthimios Kaxiras, and Arthur F. Voter, Journal of Chemical Theory and Computation, **12**, 18 (2016)

Gutzwiller Density Functional Theory for First-Principles Calculation of Strongly Correlated Electron Systems

Principle Investigators: Cai-Zhuang Wang (FWP leader), Kai-Ming Ho, Yongxin Yao, Vladimir Antropov, Viatcheslav Dobrovitski
Ames Laboratory, Ames, Iowa, 50011
wangcz@ameslab.gov

Project Scope

“The *f*-electron challenge” in rare earth and actinide-bearing materials is one of the current scientific grand challenges in physics, chemistry, and materials science. While density functional theory (DFT) and computational codes based on the Kohn-Sham approach are highly effective and have been applied successfully to the prediction of the structures and properties of many materials, it fails for materials with strongly-correlated electrons. The scope of this project is to pursue the development of first-principles theory, algorithms and computational codes that are different from the approaches currently available for strongly correlated electron systems. We will develop a unified density functional theory and computational approach that can incorporate strong correlation effects in a truly first-principles, self-consistent manner without empirical Hubbard U and Hund’s J parameters. Computationally efficient and tractable algorithms and approaches for treating strong correlation, spin-orbit coupling, as well as crystal field effects under the new density functional formalism will also be developed and implemented to quantitatively describe the electronic properties and energetics of strongly correlated electron materials. Such a computational algorithm and code is highly desirable and would be widely applicable to many systems. This development is new and therefore should be considered as high risk, but it also has the potential for high payoff.

Recent Progress

Improved LDA+Gutzwiller approach and applications to Ce and Pu

Our development of first-principles theory and method for correlated electron systems is based on the Gutzwiller density functional theory (G-DFT) developed by Ho, Schmalian and Wang in 2008 (Phys. Rev. B, **77**, 073101). In contrast to the Kohn-Sham approach where the kinetic energy functional is introduced in reference to a non-interacting electron system, the G-DFT introduces a new kinetic energy functional in reference to an interacting electron system with exact treatment of the onsite kinetic energy and the Coulomb repulsion while using the Gutzwiller approximation for interactions between localized and delocalized electrons. This new energy functional yields a set of self-consistent one-particle Schrödinger equations analogous to LDA. At the same time, it also introduces additional variational degrees of freedom in the problem corresponding to the occupations of various local (many-body) electronic configurations in the system.

As an intermediate step towards the development of fully self-consistent G-DFT and computational code, we have developed a general efficient method to solve the equations associated with the local electronic configuration occupation probabilities $\{P_r\}$ under Gutzwiller approximation derived from the G-DFT. By combining this efficient Gutzwiller solver with DFT, we have developed an efficient LDA+Gutzwiller (LDA+G) method for calculating the electronic structure and total energy of strongly correlated electron systems [2,3,4,7]. Our improved LDA+G method goes beyond density-type Coulomb interactions and includes the full intra-atomic interactions. The method makes the on-site many electron interactions comply with Hund's rules and reproduces the essential features of low-lying multiplet excitations and incorporates the symmetry of the ligand field. Spin-orbit coupling and crystal field effects are also included. The LDA+G predict correctly the volume collapsed γ - α isostructural transition in Ce (PRL **111**, 196801 (2013)). We also applied the LDA+G method to the study of the energetics and electronic structure of plutonium, in collaboration with G. Kotliar's group at Rutgers [4]. Pu is the most exotic and mysterious element in the periodic table. It has six metallic allotropes and peculiar physical properties not yet understood. Using LDA+G, we have calculated the zero-temperature energies and equilibrium volumes of the six phases of Pu. The results of relative phase stability and equilibrium volumes of the phases compare well with experimental measurements [4] as one can see from Fig. 1. Our calculations also clarify how the electron correlations determine the unusual behavior of Pu solid.

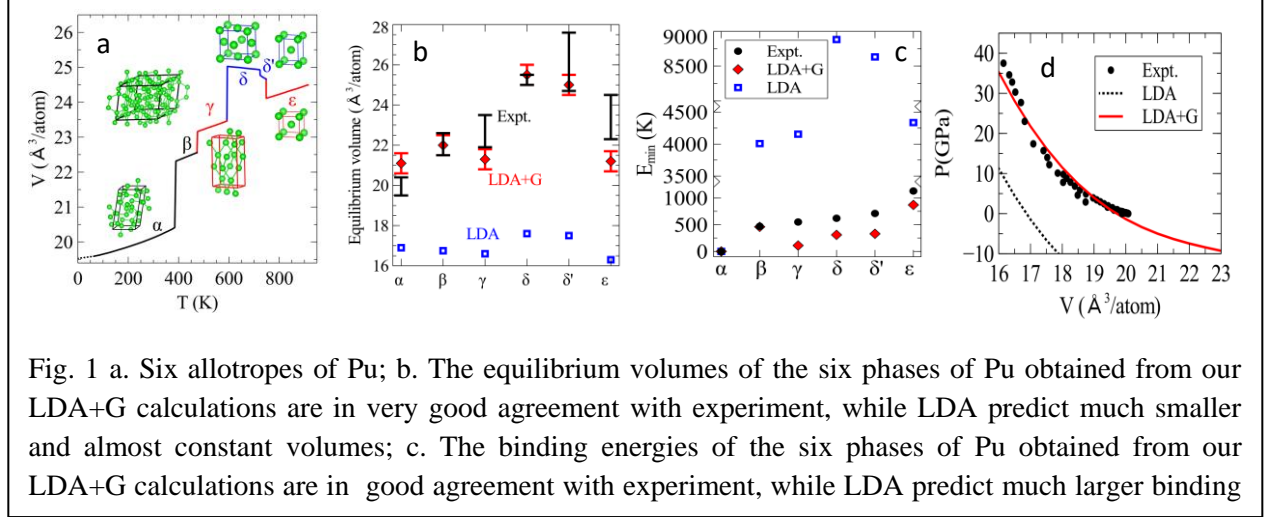


Fig. 1 a. Six allotropes of Pu; b. The equilibrium volumes of the six phases of Pu obtained from our LDA+G calculations are in very good agreement with experiment, while LDA predict much smaller and almost constant volumes; c. The binding energies of the six phases of Pu obtained from our LDA+G calculations are in good agreement with experiment, while LDA predict much larger binding

Correlation matrix renormalization (CMR) method for first-principles calculation of correlated electron systems without using empirical Hubbard U and Hund's J parameters

We also developed a correlation matrix renormalization (CMR) approximation [1, 6, 8, 9] to incorporate efficiently strong correlation effects into self-consistent first-principles calculations without using adjustable Hubbard U and Hund's J. In this approach, the commonly-adopted Gutzwiller approximation for evaluation of the one electron density matrix is extended to treat the evaluation of the two-electron correlation matrix of the system. Both one-electron density and two-electron correlation matrices evaluated from the Hartree-Fock (HF) calculations are renormalized according to the local electron correlation effects. The CMR method does not have the double counting problems commonly encountered in many previous many-body approaches.

The computational workload of our CMR method is similar to the Hartree-Fock approach while the results would be comparable to high-level quantum chemistry calculations. Moreover, the description of intersite electron interactions in CMR can be further improved by imposing the sum-rule between the one electron and two electron density matrices. The CMR method has been tested by studying the binding and dissociation behavior of various small molecules, where correlation changes from the weak to strong regime as the bond lengths between the atoms increase. We found the binding and dissociation behavior of the molecules calculated from the CMR method agrees well with the results from the high-level quantum chemistry CI calculations and available experimental data [8, 9] as one can also see from the examples shown in Fig. 2.

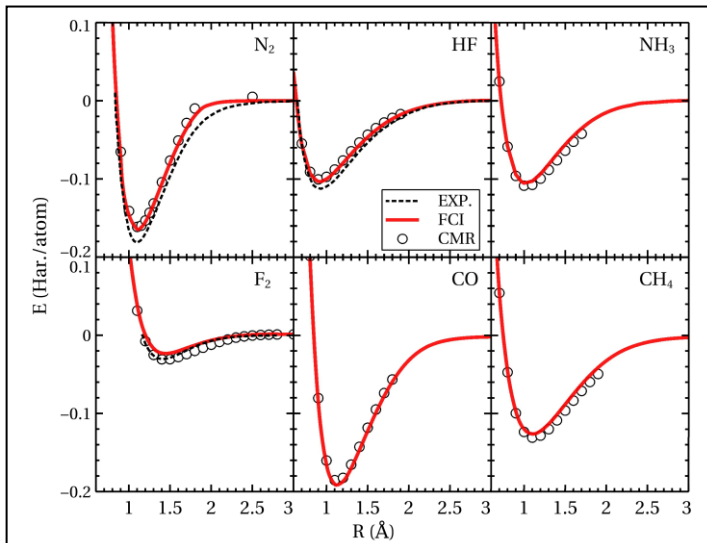


Fig. 2 Binding energy curves of N_2 , F_2 , HF , CO , NH_3 and CH_4 . The CMR and CI calculations are based on quasiamionic minimal basis orbitals (QUAMBOs). The results from CMR agree well with CI and experimental results.

Future Plans

In the future studies, we will focus on further development of the CMR method for accurate and efficient first-principles calculation of correlated electron systems without using empirical Hubbard U and Hund's J parameters.

- 1) We will continue to improve the CMR method for describing the binding and dissociation behavior of molecular systems. From the benchmark test results discussed in the recent progress section, we can see that the current CMR method describes well the binding and dissociation behavior of molecules with s and p electrons. While we will continue to test the scheme for more $s-p$ electron molecules, we will extend the method to treat molecules with d and f electrons. The prototype d and f electron molecules to be studied are Cr dimer and Ce dimer. It has been shown that accurate description of Cr is a very challenging and need careful treatments of electron correlations. Accurate bonding energy curve for Cr dimer from high-level quantum chemistry CI calculation is available. For Ce dimer, we will also compare the results from the CMR calculations with those from high-level quantum chemistry calculations. Through detail comparisons with the accurate quantum chemistry calculation results for these small molecules, we will learn how to accurately and efficiently treat the correlated d and f elections in our CMR approximations. The knowledge learned from such benchmark studies will help us to develop CMR method for bulk systems discussed below.

2) In parallel to the molecular calculations, we will develop the theory, computational algorithm, and code for CMR calculation of bulk systems. We will start the bulk CMR calculations for *s-p* electron systems where accurate results from the Kohn-Sham density functional theory are available for comparison. From such benchmark calculations and comparisons, we will learn how to accurately and efficiently incorporate the exchange-correlation functional from DFT with our CMR approach. The CMR bulk calculations will be extended to include *d* and *f* electrons once we learn more about how to treat *d* and *f* electron correlations from the molecular calculations discussed above.

Publications

- [1] “Correlation matrix renormalization approximation for total energy calculations of correlated electron systems”, Y. X. Yao, J. Liu, C. Z. Wang, and K. M. Ho, *Phys. Rev. B*, **89**, 045131 (2014).
- [2] “Principle of Maximum Entanglement Entropy and Local Physics of Strongly Correlate Materials”, Nicola Lanatà, Hugo U. R. Strand, Yongxin Yao, and Gabriel Kotliar. *Phys. Rev. Lett.* **113**, 036402 (2014).
- [3] “Interplay of spin-orbit and entropic effects in cerium”, Nicola Lanatà, Yong-Xin Yao, Cai-Zhuang Wang, Kai-Ming Ho, Gabriel Kotliar, *Phys. Rev. B* **90**, 161104 (R) (2014).
- [4] “Phase diagram and electronic structure of praseodymium plutonium”, Nicola Lanatà, Yong-Xin Yao, Cai-Zhuang Wang, Kai-Ming Ho, and Gabriel Kotliar, *Phys. Rev. X*, **5**, 011008 (2015).
- [5] “A coefficient average approximation towards Gutzwiller wavefunction formalism”, J. Liu, Y. X. Yao, C. Z. Wang, K. M. Ho, *J Phys- Condens. Matt.* **27**, 245604 (2015).
- [6] “Efficient and accurate treatment of electron correction with Correlation Matrix Renormalization theory”, Y. X. Yao, J. Liu, C. Liu, W. C. Lu, C. Z. Wang, and K. M. Ho, *Sci. Rep.* **5**, 13478 (2015).
- [7] “Gutzwiller renormalization group”, N. Lanata, Y.X. Yao, X. Y. Deng, C. Z. Wang, K. M. Ho, G. Kotliar, *Phys. Rev. B* **93**, 045103 (2016).
- [8] “Sum-rule corrections: A route to error cancellations in correlation matrix renormalization theory”, C. Liu, J. Liu, Y. X. Yao, C. Z. Wang, and K. M. Ho, *Mol. Phys.* under review.
- [9] “Correlation matrix renormalization theory: improved description of intersite electron interactions with sum-rule corrections”, C. Liu, J. Liu, Y. X. Yao, P. Wu, C. Z. Wang, and K. M. Ho, *J. Chem. Theory & Comp.* under review.

Disorder and Interaction in Correlated Electron Materials

Principal investigator: Ziqiang Wang
Department of Physics, Boston College, Chestnut Hill, MA 02467
wangzi@bc.edu

Project Scope

The program has two main themes. The first one investigates the correlated electronic structure, emergent quantum electronic states, low energy excitations, and unconventional superconductivity in transition metal oxides, pnictides, and chalcogenides. The focuses are on the high- T_c cuprates, the Fe-pnictides and Fe-chalcogenides superconductors, and the strongly spin-orbit coupled iridates. This part of the program is often motivated by and stays close to current experimental discoveries. The outcome will advance our theoretical understanding of the low-temperature collective quantum mechanical properties of the charge, spin, orbital, and lattice degrees of freedom in correlated electron materials. An important, integral part of the program has been the close and fruitful collaborations with experimental groups with expertise in, e.g., angle resolved photoemission (ARPES), scanning tunneling microscopy (STM); neutron scattering, and nuclear magnetic resonance (NMR). The second theme of the program investigates fundamental, yet unresolved problems of strong correlation by developing reliable, analytical methods and approaches. The primary focus has been on the "standard models" of correlated electrons in Mott-Hubbard systems; namely the Hubbard model and its necessary physical extensions. Examples include the Mott transition, the Mott insulator and the fractionalized spin liquids; the interplay between strong correlation and spin orbit coupling (SOC); the nature of the AF insulators; and the interplay between strong correlation, geometric frustration and topological order.

Issues that have been studied and addressed in the project recently includes: 1) combined experimental and theoretical study of the nature and the origin of the electron nematic order in FeSe superconductors, 2) electronic structure and hidden order in parent and electron doped perovskite iridates Sr_2IrO_4 with strong SOC, 3) the origin of the Mott transition and the fractionalized spin-liquid Mott insulator from an asymptotic solution of the Hubbard model; 4) correlation induced chiral spin density wave order and its topological properties in frustrated honeycomb and bilayer triangular lattices; (5) disorder and metal insulator transitions in Weyl semimetals.

Recent Progress

Below are some highlights of progress made in the past 2 years.

Nature of the electron nematicity in Fe-chalcogenide superconductor FeSe – The electron nematic order, a quantum state that breaks lattice rotational symmetry but not translation symmetry, is arguably the most unconventional and poorly understood phase in Fe-based superconductors (FeSC). In collaboration with Hong Ding's ARPES group, we

discovered some of the most novel properties of the nematic order in bulk FeSe. An important theoretical insight is that the rotational symmetry breaking associated with nematic order would remove the band degeneracies of the quantum electron states at certain high symmetry points in the Broullion zone. This offers a unique way to determine the nature of the nematicity by ARPES. We studied the temperature dependence, momentum space anisotropy, and the domain effects of the degeneracy splitting and concluded that the nematic order in FeSe is different from the commonly discussed local ferro-orbital order; it must involve spatially extended correlations and is consistent with a rotational symmetry breaking d-wave bond order termed as d-wave nematic bond order.

Interatomic Coulomb interaction as the origin for strong band renormalization and d-wave nematic bond order in FeSe – Motivated by our experimental findings, we investigated the microscopic origin of the nematic phase in FeSe. A complete symmetry analysis of the band degeneracy was carried out and all possible degeneracy lifting electronic orders are classified for FeSC. We found that there exists "hidden" antiunitary symmetries that protect the band degeneracies at Γ and M points. All possible degeneracy lifting electronic orders or interactions are then studied according to their symmetry and symmetry-breaking properties in connection to the experimental findings on the temperature dependence, momentum space anisotropy, and domain effects. We concluded that the observed nematic order in FeSe is associated with the degeneracy lifting at M point and corresponds ubiquitously to the d-wave nematic bond order involving the d_{xz}/d_{yz} and d_{xy} orbitals. The analysis also shows that the only interaction consistent with the observed degeneracy lifting at Γ point without breaking the four-fold rotation symmetry is the atomic spin-orbit coupling, which is indeed present even at high temperatures above the nematic transition as seen experimentally.

We then discovered that the Fe-Fe interatomic Coulomb repulsion V offers a natural explanation for the puzzling electron correlation effects in FeSe. It produces a strongly renormalized low-energy band structure where the van Hove singularity band touching degeneracy at M pint is driven to sit remarkably close (~ 25 meV) to the Fermi level in the high-temperature isotropic electron liquid phase as observed experimentally. Remarkably, this proximity enables the quantum fluctuations in V to induce a rotational symmetry breaking Pomeranchuk instability with electronic bond order in the d-wave channel. This emergent low-temperature d-wave nematic bond order, different from the commonly discussed ferro-orbital order and spin-nematicity, provides a microscopic explanation for the observed of nematicity in bulk and FeSe thin films, as well as its dependences on bulk and surface electron doping observed experimentally.

Chiral spin density wave order on frustrated honeycomb and bilayer triangle lattice – An important research direction for us has been to study electronic systems with both strong correlation and geometric frustration. These systems exhibit fascinating physics and hold great promise for finding (1) unconventional and topological magnetic states; (2) novel quantum spin-liquids; and (3) unconventional superconductivity. We have made considerable progress in developing the necessary theoretical framework and techniques for study these systems. An example is the textured quantum electronic phases with chiral

spin-density-wave (SDW) order in correlated systems with geometrical frustration. When the net spin chirality is nonzero, electrons accumulate Berry phase from the spontaneously generated internal magnetic field which gives rise to the anomalous Hall effect (AHE). A topological phase with quantum anomalous Hall effect (QAHE) can also arise in a chiral SDW insulator, where the gapped electron bands acquire nonzero Chern number. To this end, we studied the half-filled Hubbard model on the frustrated honeycomb lattice with nearest-neighbor hopping t_1 and second nearest-neighbor hopping t_2 , which is isomorphic to the bilayer triangle lattice. We showed that the Coulomb interaction U induces AF chiral spin density wave (χ -SDW) order in a wide range of $\kappa = t_2/t_1$ where both the two-sublattice AF order at small κ and the decoupled three-sublattice 120° order at large κ are strongly frustrated. The χ -SDW order leads to three distinct phases with different anomalous Hall responses. We find a continuous transition from a χ -SDW semimetal with the AHE to a topological chiral Chern insulator exhibiting the QAHE, followed by a discontinuous transition to a χ -SDW insulator with a zero total Chern number but an anomalous ac Hall effect. This is a concrete example where a topologically ordered insulating phase of correlated electrons arises in the absence of spin-orbit coupling. We conjectured that the χ -SDW is likely a generic phase of strongly correlated and highly frustrated hexagonal lattice electrons and discussed its connections and possible experimental realizations in hexagonal transition metal compounds. The method developed here to study noncollinear and ncoplanar magnetic order are very desirable for constructing strong coupling theories to study the interplay between electron correlation and the strong spin-orbit coupling in the transition metal iridates.

Doublon-holon binding as origin of Mott transition and fractionalized spin liquid: Asymptotic solution of the Hubbard model in the limit of large coordination – We have made significant progress in understanding and describing the Mott transition – the hallmark and the paradigm of the strong correlation problem. These include new ideas, reliable techniques, and the new physics beyond those obtainable in the dynamical mean field theory (DMFT). We showed that the excitonic binding between doubly occupied (doublon) and empty (holon) sites governs the incoherent Mott-Hubbard excitations. Using the slave-boson formulation, we constructed an asymptotically exact and analytical solution of the Mott transition and the emergent gapless spin liquid for the Hubbard model on the Bethe lattice in the large coordination number (z) limit. The Mott transition is shown to originate from doublon-holon binding as quantum corrections to the Brinkman-Rice transition. The doublon-holon binding theory allows a natural large- z limit where the intersite spin correlations survive the opening of the charge gap, giving rise to gapless spinons with a bandwidth of the order J . Quantitative comparisons are made to DMFT. We showed that the fermionic spinons are coupled to doublons and holons via a dissipative compact $U(1)$ gauge field that is in the deconfined phase, stabilizing the spin-charge separated gapless spin liquid Mott insulator. Thus, the doublon-holon binding unites the three important ideas of strong correlation: coherent quasiparticles, incoherent Hubbard bands, and deconfined Mott insulator.

Disorder and metal-insulator transitions in Weyl semimetals – The eigenstates of noninteracting lattice electrons in the presence of SOC can exhibit many interesting

topological properties, such as 2D and 3D topological insulators (TI), 2D quantum spin Hall insulator (QSHI), and 3D Weyl semimetals (WSM). We studied the effects of disorder and localization under such settings. Since many of these systems share close analogy to the 2D and multi-layer quantum Hall systems, our expertise in the quantum Hall transitions turns out to be very helpful. The WSM has Weyl nodes in bulk excitations and Fermi arc surface states. We found three exotic phase transitions. (I) Two Weyl nodes near the Brillouin zone boundary can be annihilated pairwise by disorder scattering, resulting in the opening of a topologically nontrivial gap and a transition from a WSM to 3D quantum anomalous Hall state. (II) When the two Weyl nodes are well separated in momentum space, the emergent bulk extended states can give rise to a direct transition from a WSM to a 3D diffusive anomalous Hall metal. (III) Two Weyl nodes can emerge near the zone center when the insulating gap closes with increasing disorder, enabling a direct transition from a normal band insulator to a WSM. We determined the phase diagram by computing the localization length and the Hall conductivity, and proposed that the phase transitions can be realized on a photonic lattice.

Future Plans

(1) We will study doping and hydrostatic pressure dependences of electronic nematic order in FeSe, as well as the interplay of magnetism, nematicity, and superconductivity in bulk FeSe crystals, multilayered FeSe films, and monolayer FeSe on STO substrates. Quantum nematic bond fluctuation induced superconductivity will be studied, as well as the T_c enhancement under electron doping and different layering conditions of FeSe. **(2)** The idea that the lifting of symmetry protected band degeneracies can be used to probe the novel quantum states and the underlying electronic order in correlated multiorbital electron materials will be further developed and employed to study the perovskite iridates Sr_2IrO_4 with large SOC. The highly spin-orbital entangled correlated electronic structure will be studied to describe a symmetry protected quadratic band-touching point observed just above the Fermi level, which may have remarkable consequences for recent experimental findings. We will study the effects of the lattice distortion, SOC, local and extended Coulomb and spin-exchange interactions, and provide a microscopic description of the canted AF insulating state with hidden coexisting electronic order, the collapse of the Mott gap due to electron doping and the emergence of the Fermi arc and antinodal pseudogap due to symmetry breaking electronic order, as well as the origin of an imminent SC state mediated by electronic fluctuations. **(3)** Our doublon-holon binding theory of the Mott transition and the asymptotic solution of the Hubbard model in the limit of large coordination number put us in a unique position to address several critical issues of strong correlation. We will investigate, using this reliable and systematic approach, the effects of spin-orbit coupling, multiorbitals and Hund's rule coupling, and carrier doping on the Mott transition and the Mott insulating states. The nature of the antiferromagnetic insulator and its interplay with the Mott gap will be thoroughly examined to provide the theoretical descriptions of the properties of Slater and Mott antiferromagnets relevant for current experimental efforts on the iridates and other strongly correlated materials. We will pursue a goal to develop a fully dynamical doublon-holon binding theory that can be promoted to a calculational tool for studying models and materials with strong correlation.

Publications Since 2014

1. Sen Zhou, Long Liang, and Ziqiang Wang, "Asymptotic solution of the Hubbard model in the limit of large coordination – Doublon-holon binding as origin of Mott transition and fractionalized spin liquid", arXiv:1605.03597 (2016).
2. Kun Jiang, Jiangping Hu, Hong Ding, and Ziqiang Wang, "Interatomic Coulomb interaction and electron nematic bond order in FeSe", Physical Review B**93**, 115138 (2016).
3. P. Zhang, T. Qian, P. Richard, X. P. Wang, H. Miao, B. Q. Lv, B. B. Fu, T. Wolf, C. Meingast, X. X. Wu, Z. Q. Wang, J. P. Hu, H. Ding, "Observation of two distinct d_{xz}/d_{yz} band splittings in FeSe", Physical Review B**91**, 214503 (2015).
4. Kun Jiang, Yi Zhang, Sen Zhou, and Ziqiang Wang, "Chiral spin density wave order on frustrated honeycomb and bilayer triangle lattice Hubbard model at half-filling", Physical Review Letters **114**, 216402 (2015).
5. Chui-Zhen Chen, Juntao Song, Hua Jiang, Qing-feng Sun, Ziqiang Wang, and X.C. Xie "Disorder and Metal-Insulator Transitions in Weyl Semimetals", Physical Review Letters **115**, 246603 (2015).
6. J.-X. Yin, Zheng Wu, J.-H. Wang, Z.-Y. Ye, Jing Gong, X. -Y. Hou, Lei Shan, Ang Li, X.-J. Liang, X.-X. Wu, Jian Li, C.-S. Ting, Z. Wang, J.-P. Hu, P.-H. Hor, H. Ding, S. H. Pan, "Observation of a Robust Zero-energy Bound State in Iron-based Superconductor Fe(Te,Se)", Nature Physics **11**, 543 (2015).
7. Y. M. Dai, H. Miao, L. Y. Xing, X. C. Wang, P. S. Wang, H. Xiao, T. Qian, P. Richard, X. G. Qiu, W. Yu, C. Q. Jin, Z. Wang, P. D. Johnson, C. C. Homes, H. Ding, "Spin-Fluctuation-Induced Non-Fermi-Liquid Behavior with suppressed superconductivity in $\text{LiFe}_{1-x}\text{Co}_x\text{As}$ ", Physical Review X **5**, 031035 (2015).
8. Ilija Zeljkovic, Kane L Scipioni, Daniel Walkup, Yoshinori Okada, Wenwen Zhou, Raman Sankar, Guoqing Chang, Yung Jui Wang, Hsin Lin, Arun Bansil, Fangcheng Chou, Ziqiang Wang, and Vidya Madhavan, "Nanoscale Determination of the Mass Enhancement Factor in the Lightly-Doped Bulk Insulator Lead Selenide", Nature Communications **6**, 6559 (2015).
9. Chui-Zhen Chen, Haiwen Liu, Hua Jiang, Qing-feng Sun, Ziqiang Wang, and X. C. Xie, "Tunable Anderson metal-insulator transition in quantum-spin Hall insulators", Physical Review B**91**, 214202 (2015).
10. Junfeng He, T. Hogan, Thomas R. Mion, H. Hafiz, Y. He, J. D. Denlinger, S.-K. Mo, C. Dhital, X. Chen, Qisen Lin, Y. Zhang, M. Hashimoto, H. Pan, D. H. Lu, M. Arita, K. Shimada, R.S. Markiewicz, Z. Wang, K. Kempa, M. J. Naughton, A. Bansil, S. D. Wilson, Rui-Hua He, "Spectroscopic evidence for negative electronic compressibility in a quasi-three dimensional spin-orbit correlated metal", Nature Materials **14**, 577 (2015).
11. Sen Zhou, Yupeng Wang, and Ziqiang Wang, "Doublon-holon binding, Mott transition, and fractionalized antiferromagnet in the Hubbard model". Physical Review B**89**, 195119 (2014).
12. Kun Jiang, Sen Zhou, and Ziqiang Wang, "Textured electronic states of the triangular-lattice Hubbard model and Na_xCoO_2 ". Physical Review B**90**, 165135 (2014).
13. Chetan Dhital, Tom Hogan, Wenwen Zhou, Xiang Chen, ZhenSong Ren, Mani Pokharel, Yoshinori Okada, M. Heine, Wei Tian, Z. Yamani, C. Opeil, J. S. Helton, J.W. Lynn, Ziqiang Wang, Vidya Madhavan, and Stephen D. Wilson, "Carrier localization and electronic phase separation in a doped spin-orbit-driven Mott phase in $\text{Sr}_3(\text{Ir}_{1-x}\text{Ru}_x)_2\text{O}_7$ ". Nature Communications **5**, 3377 (2014).
14. Long Liang, Ziqiang Wang, and Yue Yu, "Distinct-symmetry spin-liquid states and phase diagram of the Kitaev-Hubbard model". Physical Review B**90**, 075119 (2014).
15. H. Miao, L.-M. Wang, P. Richard, S.-F. Wu, J. Ma, T. Qian, L.-Y. Xing, X.-C. Wang, C.-Q. Jin, C.-P. Chou, Z. Wang, W. Ku, and H. Ding, "Coexistence of orbital degeneracy lifting and superconductivity in iron-based superconductors", Physical Review B**89**, 220503(R) (2014).
16. Yue Yu, Zhuxi Luo, and Ziqiang Wang, "Effects of dipole-dipole interaction between cigar-shaped BECs of cold alkali atoms: towards inverse-squared interactions". Journal of Physics: Condensed Matter **26**, 305402 (2014).
17. Chetan Dhital, Tom Hogan, Z. Yamani, Robert J. Birgeneau, W. Tian, M. Matsuda, A. S. Sefat, Ziqiang Wang, and Stephen D. Wilson, "Evolution of antiferromagnetic susceptibility under uniaxial pressure in $\text{Ba}(\text{Fe}_{1-x}\text{Co}_x)_2\text{As}_2$ ", Physical Review B**89**, 214404 (2014).
18. L. K. Zeng, X. B. Wang, J. Ma, P. Richard, S. M. Nie, H. M. Weng, N. L. Wang, Z. Wang, T. Qian, and H. Ding, "Observation of anomalous temperature dependence of spectrum on small Fermi surfaces in a BiS_2 -based superconductor", Physical Review B**90**, 054512 (2014).

Tensor networks and density functional theory for electronic structure

Principal Investigator: Professor Steven R. White

Department of Physics & Astronomy, University of California, Irvine, CA 92697

srwhite@uci.edu

Principal Investigator : Professor Kieron Burke

Department of Chemistry and of Physics, University of California, Irvine, CA 92697

kburke@uci.edu

Project Scope

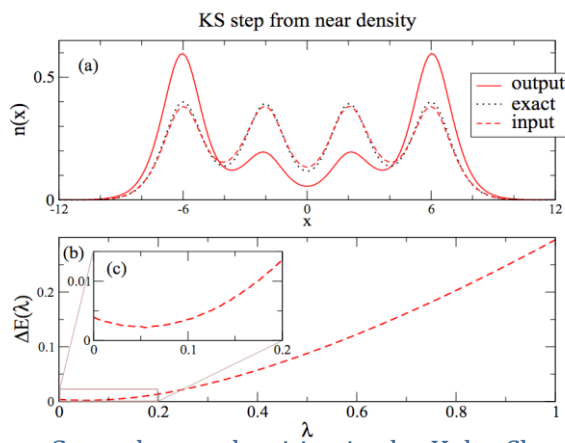
Density functional theory (DFT) and tensor networks (such as the density matrix renormalization group, DMRG) both exploit what Walter Kohn called the “nearsightedness” of many particle ground states—the idea that what happens physically at one point in space can’t depend in too much detail on what is happening at a point far away. DFT is a direct way to incorporate this idea in a formal theory, which also turns out to be extremely useful as a computational tool. Tensor networks are a much newer approach incorporating nearsightedness based on *entanglement* and recent developments in *quantum information*, which also leads directly to a set of powerful computational tools, the most famous being DMRG. The main idea of tensor networks is that instead of a wavefunction in $3N$ -dimensional space, where N is the number of particles, one describes quantum mechanics in the original space—1D, 2D, or 3D—but by putting a tensor—instead of complex number—at each point. Tensor networks are having a huge impact in studies of strongly correlated models, such as the Hubbard model. We are working to translate this success to practical electronic structure calculations, especially by combining methods and ideas from tensor networks, DFT, and also machine learning.

In the past few years we have developed tensor networks for electronic structure in *1D* very effectively. We are able to treat 1D “pseudosolids” with up to one hundred atoms, using a fine grid to represent the continuum instead of a basis, with chemical accuracy. In this case, the tensor network is DMRG, and on each grid point we have a tensor (in this case a matrix). Our algorithms and software have allowed us to test and develop DFT convergence and approximations in our 1D laboratory. Our current effort is directed towards extending this success to 3D. A 3D grid is too expensive for tensor networks, but to exploit nearsightedness using tensor networks it is essential to have a very localized orthogonal basis. As a first step we are developing new basis sets which start with wavelet bases, but adapt them, making them much more compact, using the occupied orbitals from a computationally cheap DFT calculation. Our approach is based on a close connection we have discovered between tensor networks and wavelets. This *wavelet coarse graining* (WCG) approach is being tested and developed in our 1D laboratory, and it is also being concurrently developed for linear chains of atoms in 3D. We are also developing algorithms to machine-learn the exact density functional and generate an optimized basis set on top of an approximate DFT result in the one dimensional test systems.

Recent Progress

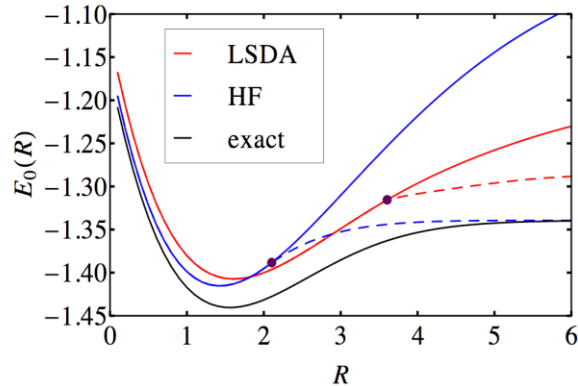
Software: The ITensor library for DMRG and tensor networks was developed by White and Miles Stoudenmire, who was a postdoc on this project. Miles has now become a researcher at UCI with about half of his time devoted to ITensor and software. ITensor just had a major new release and its use is growing rapidly. Graduate student Thomas E. Baker (supported by this project) has contributed substantially to ITensor documentation. ITensor is publicly available through its website (itensor.org) and on github.

One dimensional test laboratory - we have, with Lucas O. Wagner (former graduate student) and Stoudenmire, constructed a suitable system for comparing exact results from DMRG to approximate results from DFT. This involves suitably defined interaction potentials, software for DMRG and DFT, and correlation energy calculations performed by DMRG to parameterize the DFT approximations. With these tools we then benchmarked to properties of our 1D systems to show that the 1D systems approximate properties of real 3D systems.



Top: Ground state densities in the Kohn-Sham algorithm using the exact density functional, obtained with DMRG. Bottom: energy convergence versus convergence parameter (abscissa). The derivative about the input density is always negative, proving convergence.

functional derived from DMRG and were

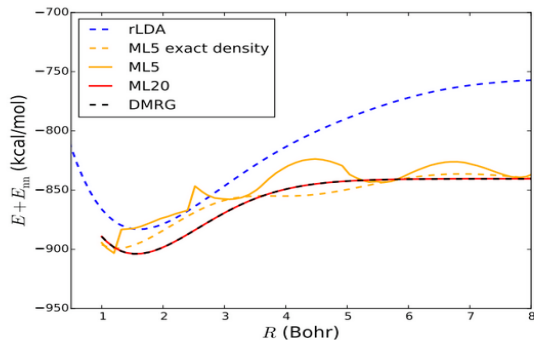


Dissociation curves for an H_2 pseudo-molecule for the local density approximation, Hartree-Fock, and DMRG. Dots denote the Coulson-Fischer points where restricted methods deviate from unrestricted (dashed) calculations. Qualitative features in this plot are very similar to real 3D calculations.

Errors in DFT approximations, such as the self-interaction error, misleading band gaps in the Kohn-Sham system, etc. are present in the approximate 1D functionals just as in real 3D calculations. In addition to the traditional soft-Coulomb interaction, we introduced a single exponential mimic the soft Coulomb potential (Baker, et. al.). The single exponential greatly reduces the computational cost of the DMRG calculations by reducing the size of the matrix product operator.

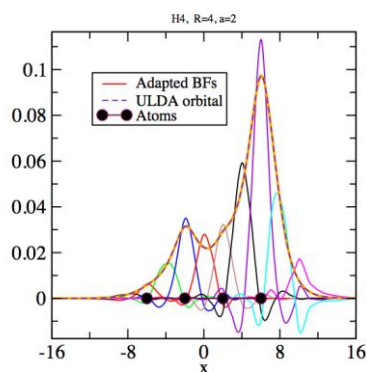
Convergence of the Kohn-Sham algorithm - the PIs, Wagner, and Stoudenmire analyzed convergence properties from the exact able to prove that the exact functional is

guaranteed to converge even in three dimensions as published in *Phys. Rev. Lett.* This answered an outstanding question for DFT for strongly correlated systems as well as showed the utility of the 1D comparison. This led to a comprehensive study of the convergence properties of DFT. An article was published in *Phys. Rev. B* showing very clear proofs of principle on the convergence of exact and approximate functionals that would be less clear for the community in real systems.



Dissociation plot of the machine learned functional for H_2 with LDA (blue) and DMRG (black) lines from previous figure. The dissociation curve is reproduced within chemical accuracy (red curve) while less training points give worse answered (orange lines).

Machine learning pure density functional theory - the PIs, Li Li (graduate student), and Baker undertook the task of using the recent exceedingly popular machine-learning techniques to learn the universal DFT functional, $F[n]$. While it was shown previously (*Phys. Rev. Lett.* **108**, 253002 (2012)) that the non-interacting Kohn-Sham system can be learned by machine learning methods, this is the first time the fully-interacting system has been learned. Useful proofs of principle, demonstrating that this can be done, and an entirely new atomic-centered basis set were developed to minimize the cost of using the exact functional in a self-consistent calculation. We are currently preparing to submit this to *Physical Review X* and expect this work to profoundly influence the direction of machine-learned calculations towards learning physics instead of merely data. Enough material has been derived to make this method immediately applicable to three dimensions.



Optimized basis set for an H_4 molecule.

Optimized basis sets: Wavelet Coarse Graining- White, along with Baker, Anna Kesselman, and Glen Evenly (post-doc, soon to be faculty at U. Sherbrooke), have developed an algorithm to adapt wavelet transformations to make optimized basis sets for a given quantum system. The goal is to use a low-level calculation such as DFT and then apply a series of wavelet transformations to reduce the effective number of basis functions and circumvent the need for, in some cases, thousands of basis set functions to obtain chemical accuracy. The software for this project is finished for the 1D case and tests are being performed and a manuscript is being written. We characterize the size of the basis by the number of functions per electron. Our goal is to have a basis with only 2-3 basis functions per electron, which is nevertheless able to produce chemically accurate results. In most cases in 1D this goal is being achieved, but

there are also cases where the DFT calculation used to adapt the basis is too inaccurate; these problem cases are being studied.

The adaptation of the basis to a set of occupied orbitals is based on a mapping between a special tensor network, the multi-scale entanglement renormalization ansatz (MERA), and wavelet transformations. This connection is being exploited in both directions. For use here, the algorithms for adapting a MERA can be applied to wavelets. In addition, we are using a novel set of wavelets developed with the MERA mapping, (Evenly and White [arXiv:1605.07312](https://arxiv.org/abs/1605.07312)) which are both compact and symmetric: something which is not possible with conventional wavelets. In work outside the scope of this project, the wavelet representation of MERA was used to produce the first analytic MERA, (White and Evenly, *Phys. Rev. Lett.* **116**, 140403 (2016)).

Future Plans

Wavelet Coarse Graining – The progression to 3D is the crucial part of this development, so we are now doing this concurrently with the 1D development. Our initial test case for a real 3D system is a linear chain of evenly spaced hydrogen atoms. For this system we are using the wavelet adaptation primarily only in the longitudinal direction; for the transverse directions ordinary Gaussians from a standard Gaussian basis set are used. The initial adaptation of the basis is performed on the standard Gaussian basis set itself; what that gives us is a basis which is orthogonal and local in one direction which spans the standard Gaussian basis set, but has a greater number of functions as required by the locality. The degree of locality obtained is much greater than one would obtain by simply orthogonalizing the Gaussians themselves. We are developing the algorithms and software to compute all the necessary integrals for this system. The most difficult are the two electron integrals. These are treated by writing the Coulomb interaction as a sum of about 100 specially fitted Gaussians; for each Gaussian term, the integrals separate into x, y, and z integrals which can then be evaluated numerically, utilizing FFT techniques. The final construction of any 3D two electron integral is then a sum of about 100 terms, each a product of tabulated 1D integrals. This computational approach appears fast enough so that integrals are not a bottleneck to our WCG calculations.

When DMRG is used in a quantum chemistry context, a key performance limitation comes from the N^4 two electron integrals that need to be put into the DMRG Hamiltonian. The high locality of the basis can be used to dramatically improve this: we find that integrals involving four different basis functions are small and can be treated at the mean-field level, leaving them out of the DMRG calculation. This small change improves the scaling by a factor of N. We plan to test and develop this idea over the next year.

Band gaps - One of the fundamental issues in DFT is the inability for common approximations to obtain reasonable band gaps. Using our low dimensional analogs, we are investigating this issue. It is hoped that a successful completion of the wavelet basis project will allow for faster computational time.

Publications

1. One-Dimensional Continuum Electronic Structure with the Density-Matrix Renormalization Group and Its Implications for Density-Functional Theory E.M. Stoudenmire, Lucas O. Wagner, Steven R. White, Kieron Burke, *Phys. Rev. Lett.* **109**, 056402 (2012).
2. Reference electronic structure calculations in one dimension Lucas O. Wagner, E.M. Stoudenmire, Kieron Burke, Steven R. White, *Phys. Chem. Chem. Phys.* **14**, 8581 - 8590 (2012)
3. Guaranteed Convergence of the Kohn-Sham Equations Lucas O. Wagner, E. M. Stoudenmire, Kieron Burke, Steven R. White, *Phys. Rev. Lett.* **111**, 093003 (2013)
4. Kohn-Sham calculations with the exact functional Lucas O. Wagner, Thomas E. Baker, E. M. Stoudenmire, Kieron Burke, Steven R. White, *Phys. Rev. B* **90**, 045109 (2014)
5. One-dimensional mimicking of electronic structure: The case for exponentials Thomas E. Baker, E. Miles Stoudenmire, Lucas O. Wagner, Kieron Burke, Steven R. White, *Phys. Rev. B* **91**, 235141 (2015)

Thermodynamic Stability and Elasticity of High Entropy Alloys

Principal investigator: Michael Widom
Department of Physics, Carnegie Mellon University
Pittsburgh, PA 15213
widom@cmu.edu

Project Scope

The goal of this program is to predict thermodynamic phase stability from first principles, with specific attention to high entropy alloys (HEA's) containing multiple elements that are chemically similar to each other so they can mix freely within a crystalline lattice. The resultant entropy of mixing might be able to stabilize simple crystal structures such as FCC and BCC relative to more complex intermetallic phases that occur frequently in binary or ternary alloys of less similar elements. Their simpler crystal structure lend advantageous mechanical properties such as high strength and hardness, which are moreover maintained at high temperatures. Owing to their complex stoichiometry, their design is highly flexible allowing specific properties to be tailored (e.g. for corrosion resistance) and opening opportunities for novel processing (e.g. through second phase precipitation).

This proposal addresses key questions in this developing field, specifically thermodynamic investigation of phase stability, and mechanical response of solid phases. The work utilizes first principles total energy calculations and molecular dynamics simulations, augmented with novel Monte Carlo techniques and data analysis methods. Emphasis is placed on developing computational methods and validating them with application to specific HEA-forming alloy systems.

Recent Progress

Novel first principles simulation techniques – In order to make first principles molecular dynamics a useful tool for study of substitutional solid solutions it is essential to circumvent the long time scale characteristic of atomic diffusion so as to efficiently sample configuration space. The defining character of a solid solution, namely random substitution of chemical species, suggests a hybrid approach supplementing conventional molecular dynamics (MD) with Monte Carlo swaps of chemical species (MC). In this MC/MD scheme the MD simulation is responsible for generating small atomic displacements associated with ordinary phonons, while the MC steps allow long-range diffusion of atomic species without the need to overcome diffusion barriers.

Computational efficiency dictates that first principles calculations will be performed on relatively small systems, leading to large fluctuations in quantities such as internal energy. These fluctuations can be exploited to further enhance sampling efficiency through the method of replica exchange, also known as parallel tempering. In this method runs ("replicas") proceed simultaneously at multiple temperatures. Periodically attempts are

made to swap temperatures among replicas with a Boltzmann-like probability. In this manner configurations trapped at low temperature can “diffuse” to a higher temperature where they escape the trap, then diffuse back to low temperature. Because replica exchange simulations produce equilibrium ensembles of structures at multiple temperatures, the resulting energy distributions can be analyzed using multiple histogram techniques to generate relative free energies as analytic functions over the entire simulated temperature range. These free energies include all contributions to the entropy (vibrational, discrete configurational, and electronic). Both MC/MD and the replica exchange variant are available for download at <http://alloy.phys.cmu.edu/mcmd.html>.

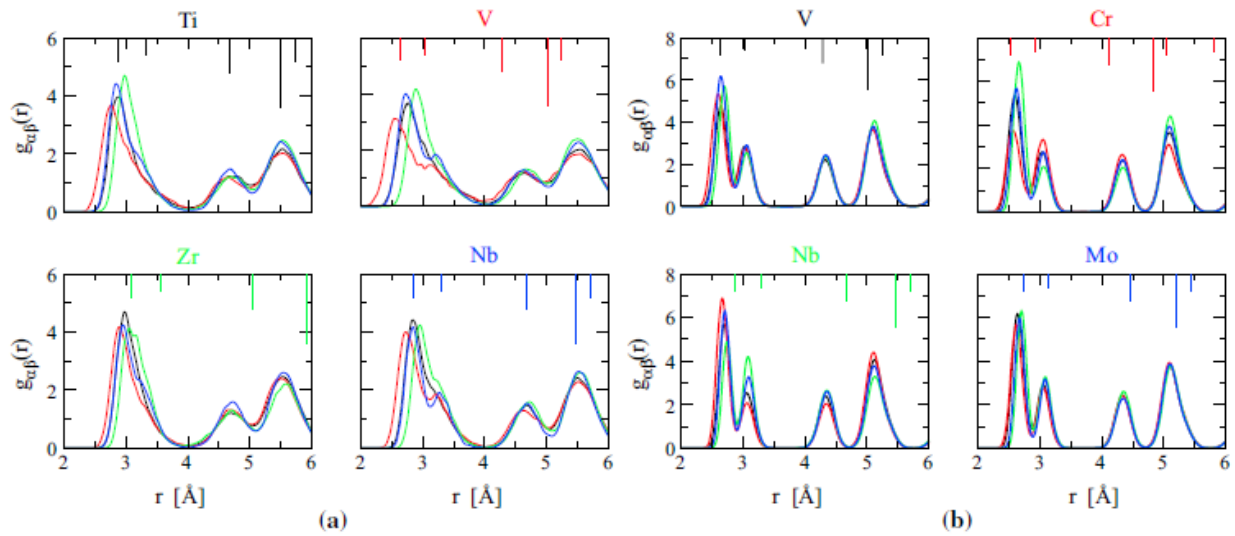


Figure 1 Pair correlation functions of high entropy alloys, (a) NbTiVZr and (b) CrMoNbV, equilibrated using MCMD at T=1200K then quenched to 300 K. The partials are color coded, e.g., in (a) for NbTiVZr, black indicates Ti, red indicates V, green indicates Zr, and blue indicates Nb. Thus, under Ti, the black curve is Ti-Ti and the red curve is Ti-V, etc.. Bars at top indicate the corresponding correlations in the pure BCC element. Note in (a) the loss of short-range BCC order for NbTiVZr while long-range order is preserved. Note in (b) the strong Cr-Nb pair correlations indicating short-range chemical order.

Configurational entropy estimates from first principles simulations – High entropy alloys contain multiple chemical species $\alpha = 1 \cdots N$ in nearly equal proportions. If there were N species, each with a fraction $x_\alpha = 1/N$, then the ideal entropy (or Bragg-Williams) of mixing $S_0 = -\sum x_\alpha \log x_\alpha$. However, differing preferences in chemical bonding among species create short-range chemical order that reduces the entropy by the amount of their “mutual information”, $I = \sum y_{\alpha\beta} \log y_{\alpha\beta} / x_\alpha x_\beta$, where $y_{\alpha\beta}$ are the bond frequencies between pairs of species α and β . The combination $S_0 - I$ is equivalent to Guggenheim’s quasichemical approximation and also to the Bethe cycle-free tree approximation. It represents the first step beyond Bragg-Williams in the cluster variation method (CVM) and can thus be extended systematically to include multi-site clusters. Even at the pair level, the mutual information provides a sizeable temperature-dependent correction to the entropy and has the advantage that it can be easily adapted to non-Bravais lattices such as the Laves phase that proves important for certain HEA’s. Further, pair correlation functions can be predicted with high accuracy (see Figure 1) using the simulation techniques described in the previous paragraph. Figure 2 illustrates the resulting configurational entropies.

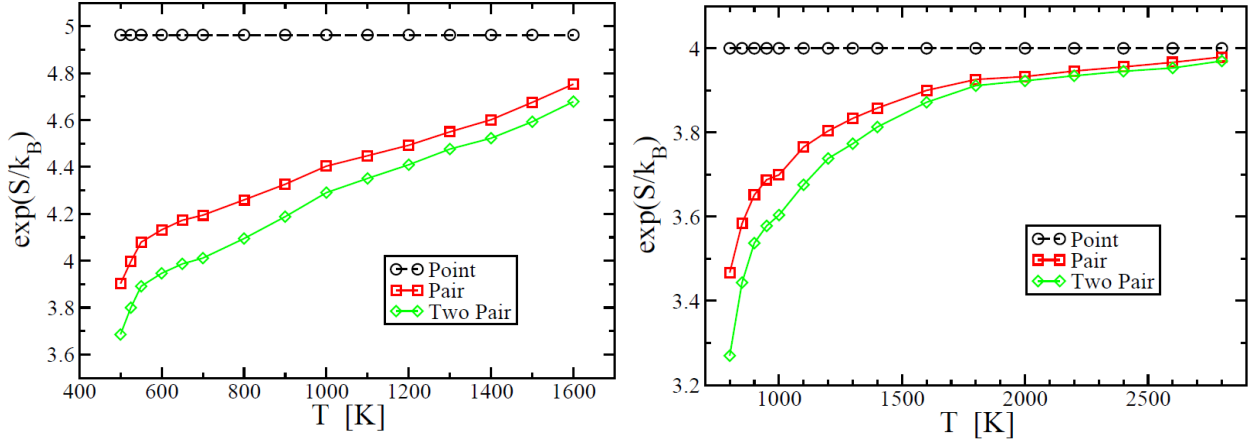


Figure 2 Temperature-dependent entropies in the point (Bragg Williams), pair (Bethe-Guggenheim) and two-pair (CVM) approximations. Left panel shows Al1.3CoCrFeNi, right panel shows MoNbTaW. High temperature slope and entropy deficit for Al1.3CoCrFeNi is due to preexisting B2 (CsCl) long-range order close to melting, while MoNbTaW entropy is nearly ideal at high T. Accelerating loss of entropy at low temperature for Al1.3CoCrFeNi may be due to segregation of CrFe, while in the case of MoNbTaW it reflects the onset of B2 short-range order.

Ground state identification in multicomponent refractory alloys – According to the Gibbs phase rule, at a fixed, generic temperature and pressure, the maximum number of phases coexisting equals the number of chemical species, N . We should thus expect up to N coexisting phases in the ground state of an N -component alloy. Cluster expansions of the first principles total energy enable an efficient search for ground states through a process automated in van de Walle’s ATAT toolkit. This method has been applied to two HEA-forming refractory compounds. We find that the alloy system MoNbTaW consists almost entirely of a single nearly equiatomic phase together with a slight excess of elemental Nb. This occurs because of the favorable (or at least neutral) interatomic interactions of all pairwise combinations. In contrast, CrMoNbV phase separates into a mixture of $N=4$ constituent phases. Three of these correspond to specific patterns of chemical ordering on the underlying body-centered cubic lattice, while the remaining case is a Laves phase formed from the equiatomic ternary CrNbV.

Predicted thermodynamic stability of a high entropy alloy – Most high entropy alloy-forming compounds are expected to phase separate at low temperatures, as noted above. A central theme of this project is to predict the phase behavior as a function of temperature. By combining multiple contributions to the free energy (electronic, vibrational and configurational, see Fig. 3) we show that the HEA is the equilibrium phase at high temperatures, while decomposition is expected below, notable precipitation of a Laves phase of approximate composition CrNbV. We predict a threshold of 1200K (900C) above which the HEA should be stable. Experiments by collaborator Peter Liaw (UTK) confirm formation of the HEA from the melt and verify its metastability at temperatures up to 1200C, but above 1200C the Laves phase precipitates out. This agrees moderately with our theory provided that the diffusional dynamics below 1200C are too slow to reach phase separated equilibrium. However, two problems remain – experiment observes continued existence of the Laves phase at temperatures above 1200C as well as multiple additional as-yet unidentified phases. Perhaps the additional phases are due to oxide

formation or some other form of decomposition not included in our model. Additional modeling efforts are underway to resolve the temperature for HEA stabilization.

Future Plans

Entropy contributions to HEA-forming families – The PI will continue his collaboration with Michael Gao of NETL to publish breakdowns of all entropy contributions to a large set of HEA-forming compounds. This work will include MCMD simulations with mutual information corrections, vibrational and electronic entropies. Separately he will investigate the formation of short-range chemical order in AlCoCrFeNi for comparison with experimental results of Peter Liaw.

Phase separation in CrMoNbV – The PI will continue thermodynamic modeling of the CrMoNbV compound to identify a possible third phase reported by collaborator Peter Liaw and his student Rui Zheng. This work will also involve collaboration with Michael Gao developing a CALPHAD model for the alloy system.

Lattice instability of HfNbTaZr – The PI and student Bojun Feng will simulate the formation of short-range chemical order, short-range mechanical instability of the BCC order, and phase separation in HfNbTaZr. This will be done in collaboration with Walter Steurer of ETH Zurich and his student Soumya Maiti.

High entropy non-Bravais lattice structures – The PI and collaborator Walter Steurer will extend the high entropy alloy concept to a new class of structures, in which high entropy exists within specific Wyckoff sites of non-Bravais lattice structures. Initial effort will be put towards the B2 (CsCl) structure type to identify aluminum-transition metal compounds in which the transition metals mix freely. Later we will apply this idea to Half-Heusler structures.

Publications

1. S. C. de la Barrera, Y.-C. Lin, S. Eichfeld, J. A. Robinson, Q. Gao, M. Widom, and R. M. Feenstra, "Thickness characterization of atomically-thin WSe₂ on epitaxial graphene by low-energy electron reflectivity oscillations", *J. Vac. Sci. Tech. B* **34** (2016) 04J106 (chosen as "Editors Pick")
2. H. Zhang, S. Yao and M. Widom, "Predicted phase diagram of B-C-N", *Phys. Rev. B* **93** (2015) 144107
3. M. Widom, "Entropy and diffuse scattering: comparison of NbTiVZr and CrMoNbV", *Met. Mat. Trans. A* **47** (2015) 3306-11
4. M. Widom, "Prediction of structure and phase transformations", chapter in *High Entropy Alloys: fundamentals and applications*, eds. M.C. Gao, J.-W. Yeh, P.K. Liaw and Y. Zhang (Springer, to be published 2015)

Thermodynamics and Kinetics of Phase Transformations in Energy Materials

Christopher Wolverton (PI)

Department of Materials Science and Engineering, Northwestern University

Email: c-wolverton@northwestern.edu

Vidvuds Ozolins (co-PI)

Department of Materials Science and Engineering, University of California, Los Angeles

Email: vidvuds@ucla.edu

Project Scope

The primary goal of this program is to develop computational tools and methodology for enabling a shift from empirical trial-and-error driven materials discovery towards data and information technology driven design of materials with targeted functional properties. Both thermodynamic and kinetic factors need to be taken into account when designing new materials. Thermodynamics sets the necessary-but-not-sufficient conditions for the suitability of a particular material in a given application, while the kinetics controls the rates of microscopic processes and hence the performance in energy applications (e.g., power in energy storage, conversion efficiencies in solar cells and thermoelectrics, chemical activity in catalysis). The complexity of these phenomena makes computational design difficult, not least due to the lack of suitable theoretical methods and computational tools. To address these needs, we develop systematic, quantitatively accurate first-principles methods to address two important problems: (i) predict and optimize the thermodynamics of materials over a large composition and structure space, and (ii) model kinetic processes such as mass and heat transport in crystalline solids under non-equilibrium conditions. These tasks are addressed by combining high-throughput computation with automatic construction of accurate lattice models using mathematically rigorous methods of information theory, such as compressive sensing and Bayesian inference.

Recent Progress (Highlights – Full Publication List Below)

Prediction of New Full Heusler Thermoelectrics

Computational discovery of new high-performance thermoelectrics is a challenging task since it requires a diverse set of theoretical tools that can assess the thermodynamic and structural stability, as well as electronic and thermal transport properties of complex multinary compounds. Our prior DOE-funded work has led to the development of such a set of computational tools, which we have now used to predict hitherto unknown stable materials that are promising new thermoelectrics. We performed a high-throughput *ab initio* search for thermodynamically stable full Heusler (FH) compounds with finite band gaps through elemental substitution within the Northwestern's qmpy (<https://pypi.python.org/pypi/qmpy>) framework in a chemical search space with 53 distinct elements. The Northwestern Open Quantum Materials Database (OQMD, <http://oqmd.org/>) was used to evaluate thermodynamic stability against all linear combination of (~400,000) compounds in the database, using the automated convex hull construction. Structural ground state searches for competing non-FH compounds were carried out using the minima hopping method (MHM) as implemented in the MINHOCAO package developed by the S.

Goedecker group in Basel. Lattice thermal conductivities were evaluated using the compressive sensing lattice dynamics (CSLD) package developed in UCLA.

FH compounds have received much less attention than the predominantly semiconducting half Heusler (HH) compounds XYZ because most of the known FH compounds are metals. Strikingly, we discovered a whole class of stable *semiconducting* FH compounds, which to our knowledge have not yet been reported in the literature. They contain ten valence electrons per formula unit with alkaline earth elements {Ba; Sr; Ca} in the X sublattice, whereas Y are noble metals {Au; Hg} and Z are main group elements {Sn; Pb; As; Sb; Bi}; we refer to these as “R compounds”. Unlike the known FH and HH compounds, our novel R compounds have one order of magnitude lower lattice thermal conductivities, approaching the theoretical lower limit that is achieved in glasses. The electronic transport properties of the new R compounds are comparable to the well-studied thermoelectric FH compound Fe₂VAl with high power factors due to flat and dispersive valence bands. This combination of thermal and electronic properties establishes the R compounds as a promising class of materials and calls for experimental verification of our predictions.

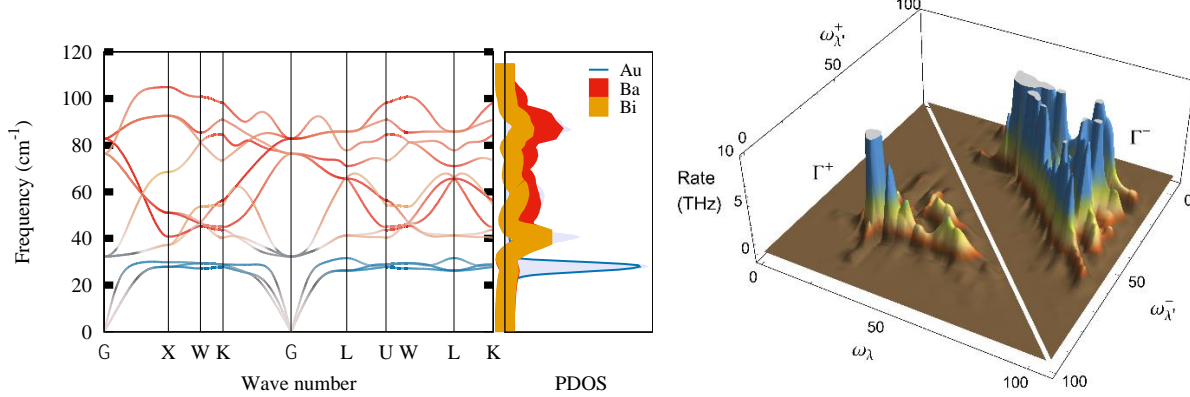


FIG. 1. Left panel: The phonon band structure of predicted full Heusler Ba₂AuBi compound. All bands are colored according to the amplitudes of the atomic displacements, where gray bands indicate an equal contribution of all atoms. The phonon density of states (PDOS) is shown on the right, with the shaded area indicating the total DOS. Right panel: Anharmonic scattering rates for three-phonon processes in Ba₂AuBi at 300 K. The lower left segment shows the absorption rates, whereas the upper right panel indicates the rates for emission processes. The corresponding phonon frequencies ω are given in units of cm^{-1} .

Phase Stability of PbTe-PbS alloys

The thermoelectric figure of merit (ZT) of semiconductors such as PbTe can be improved by forming nanostructures within the bulk of these materials. Alloying PbTe with PbS causes PbS-rich nanostructures to precipitate from the solid solution, scattering phonons and increasing ZT. Understanding the thermodynamics of this process is crucial to optimizing the efficiency gains of this technique. Previous calculations of the thermodynamics of PbS-PbTe alloys [(J. W. Doak and C. Wolverton, Phys. Rev. B 86, 144202 (2012)] found that mixing energetics alone were not sufficient to quantitatively explain the thermodynamic driving force for phase separation in these materials. In this work, we re-examine the thermodynamics of PbS-PbTe, including the effects of vibrational entropy in the free energy through frozen-phonon calculations of special quasirandom structures (SQS) to explain this discrepancy between first-principles and experimental phase stability. We find that vibrational entropy of mixing reduces the calculated maximum miscibility gap temperature TG of PbS-PbTe by 470 K, bringing the error between calculated and experimental TG down from 700 to 230 K. Our calculated vibrational spectra of PbS-PbTe SQS exhibit dynamic instabilities of S ions that corroborate reports of low-T ferroelectric-like phase transitions in solid solutions of PbS and PbTe, which are not present in either of the constituent compounds. We use our calculated vibrational spectra to obtain phase transition temperatures, which are in qualitative agreement with experimental results for PbTe-rich alloys, as well as to predict the existence of a low-T displacive phase transition in PbS-rich PbS-PbTe, which has not yet been experimentally investigated.

Future Plans

Clathrate Thermoelectrics – Type-I clathrate compounds are good thermoelectrics because they exhibit phonon-glass electron-crystal properties when their open cages are filled with guest atoms (“rattlers”). For validation, we have calculated lattice thermal conductivities for Si_{46} , $\text{Na}_8\text{Si}_{46}$ and $\text{Ba}_8\text{Si}_{46}$ and obtained good agreement with experimental measurements. We are now extending this work to novel clathrates with the aim of systematically searching for high thermoelectric performance.

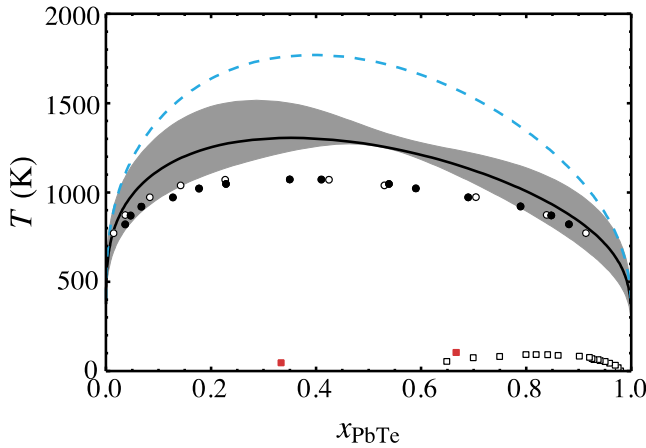


FIG. 2. Calculated high- and low-T solid-state phase diagrams of PbS–PbTe. The solid black line shows the miscibility gap calculated with vibrational entropy contributions the 90% confidence interval of the free energy fit shown as the gray shaded region. The dashed blue line shows a previously calculated miscibility gap for PbS–PbTe that neglects vibrational entropy. Red squares show calculated low-T phase transition temperatures, while circles show the experimentally measured miscibility gap of PbS–PbTe, and open squares show the experimentally measured low-T phase transitions.

Electronic Entropy in Thermochemical Water Splitting Materials – Large solid-state entropy of reduction is a requirement for realizing efficient thermochemical water splitting cycles (TWSC) with metal oxides, such as ceria (CeO_2). An overlooked source of entropy in TWSC materials arises from spin-orbit and crystal field induced splitting of *f* electron levels in lanthanide oxides. Preliminary calculations indicate that this neglected entropic contribution can even surpass the configurational entropy. This entropic analysis will allow us to design improved materials for thermochemical water splitting.

Publications

1. H. A. Hansen and C. Wolverton, "Kinetics and Thermodynamics of H_2O Dissociation on Reduced $CeO_2(111)$ ", J. Phys. Chem. C **118**, 27402 (2014).
2. Huang, Y.K.; Cain, J. D.; Peng, L.; Hao, S.; Chasapis, T.; Kanatzidis, M. G.; Wolverton, C.; Grayson, M.; and Dravid, V. P., "Evaporative Thinning: A Facile Synthesis Method for High Quality Ultrathin Layers of 2D Crystals", ACS Nano **8**, (2014) 10851.
3. M. Aykol and C. Wolverton, "Local environment dependent GGA+U method for accurate thermochemistry of transition metal compounds", Phys. Rev. B **90**, 115105 (2014).
4. J. W. Doak, C. Wolverton, and V. Ozolins, "Vibrational contributions to the phase stability of $PbS-PbTe$ alloys", Phys. Rev. B **92**, 174306 (2015).
5. L. Ward, K. Michel, and C. Wolverton, "Three new crystal structures in the Na-Pb system: solving structures without additional experimental input", Acta Cryst. A **71**, 542 (2015).
6. Y. Wang, K. Michel, Y. Zhang, and C. Wolverton, "Thermodynamic stability of transition metals on the Mg-terminated MgB_2 (0001) surface and their effects on hydrogen dissociation and diffusion" Phys. Rev. B **91**, 155431 (2015).
7. J. W. Doak, K. J. Michel, and C. Wolverton, "Determining dilute-limit solvus boundaries in multi-component systems using defect energetics: Na in $PbTe$ and PbS " J. Mater. Chem. C **3**, 10630 (2015).
8. S. Kirklin, J. Saal, B. Meredig, A. Thompson, J. Doak, M. Aykol, S. Ruhl, and C. Wolverton, "The Open Quantum Materials Database (OQMD): Assessing the Accuracy of DFT Formation Energies", npj Computational Materials **1**, 15010 (2015).
9. J. He, M. Amsler, Y. Xia, S. S. Naghavi, V. I. Hegde, S. Hao, S. Goedecker, V. Ozoliņš, and C. Wolverton, "Ultralow Thermal Conductivity in Full Heusler Semiconductors", Phys. Rev. Lett. **117**, 046602 (2016).
10. J. A. Flores-Livas, M. Amsler, C. Heil, A. Sanna, L. Boeri, G. Profeta, C. Wolverton, S. Goedecker, and E. K. U. Gross, "Superconductivity in metastable phases of phosphorus-hydride compounds under high pressure" Phys. Rev. B **93**, 020508(R) (2016).
11. M. Amsler, S. Goedecker, W. G. Zeier, G. J. Snyder C. Wolverton, and L. Chaput , "ZnSb polymorphs with improved thermoelectric properties", Chem. Mater. **28**, 2912 (2016).
12. L. Zhu, M. Amsler, T. Fuhrer, B. Schaefer, S. Faraji, S. Rostami, S. Alireza Ghasemi, A. Sadeghi, M. Grauzintyte, C. Wolverton, and S. Goedecker, "A fingerprint based metric for measuring similarities of crystalline structures" J. Chem. Phys. **144**, 034203 (2016).
13. S. Bajaj, H. Wang, J. W. Doak, C. Wolverton and G. J. Snyder, "Calculation of dopant solubilities and phase diagrams of X-Pb-Se (X = Br, Na) limited to defects with localized charge", J. Mater. Chem. C **4**, 1769 (2016).
14. Y. Wang, K. Michel, and C. Wolverton, "Hydrogen diffusion in bulk MgB_2 ", Scripta Mater. **117**, 86 (2016).
15. Z.-Q. Huang, W.-C. Chen, F.-C. Chuang, E. H. Majzoub, and V. Ozolins, "First-principles calculated decomposition pathways for $LiBH_4$ nanoclusters," Scientific Reports **6**, 26056 (2016).
16. A. A. Emery, J. E. Saal, S. Kirklin, V. I. Hegde, and C. Wolverton, "High-Throughput Computational Screening of Perovskites for Thermochemical Water Splitting Applications" Chem. Mater. (in press, 2016).
17. S. M. Clarke, J. P. S. Walsh, M. Amsler, C. D. Malliakas, T. Yu, S. Goedecker, Y. Wang, C. Wolverton, and D. E. Freedman, "Discovery of a Superconducting Cu-Bi Intermetallic Compound via High-pressure Synthesis" (submitted, 2016).
18. Z. Lin, A. Yin, Y. Xia, Q. He, V. Ozolins, Y. Huang, and X. Duan, "Symmetry-mismatched epitaxy in solution phase synthesized two-dimensional nanocrystals," submitted (2016).
19. H.-S. Kim, J. B. Cook, H. Lin, J. S. Ko, S. H. Tolbert, V. Ozolins, and B. Dunn, "The Use of Oxygen Vacancies to Enhance the Charge Storage Properties of MoO_{3-x} ," submitted (2016).

Probing fluctuation induced interactions in nanostructured materials

Principal investigator: Professor Lilia M. Woods

Department of Physics, University of South Florida, Tampa FL, 33620

lmwoods@usf.edu

Project Scope

The focus of this project is to bring forward the fundamental understanding of electromagnetic fluctuations interactions in novel materials at the nanoscale. Specifically, we pursue how van der Waals (vdW), Casimir, and related forces can be modified in terms of scaling, sign, and magnitude characteristics based on Dirac-like electronic and response properties in graphene systems. In addition, we also explore the role of such dispersive interactions on the structural, electronic and phonon properties of systems with chemically inert components, such as 2D layers and their quasi-1D derivatives. Although dispersive vdW/Casimir interactions are thought to be small, they can actually be dominant in many situations especially at the micro and nanoscale. Below we elaborate more on the common origin of such forces and their universality as highlighted in different materials. We also show that other fluctuation induced interactions, such as those originating from monopolar charges, can be present and even compete with the dipolar forces. The significant microscopic impact on the structural, electronic, optical, and phonon properties of vdW interactions in heterostructures is also discussed.

Recent Progress

Some highlights of our progress recently are provided below and an accompanying list of supporting publications is attached.

Common origin of van der Waals and Casimir interactions – In the past decade, many new materials have become available, which have stimulated the need of understanding their dispersive interactions. Perhaps the most popular examples are graphene and its related allotropes (carbon nanotubes and graphene nanoribbons), but other materials with Dirac-like spectra are also being investigated. For example, topological insulators, Chern insulators, and Weyl semimetals, are very interesting for the Casimir/vdW field as they have a range of electronic and optical response behaviors different than typical materials. The importance of the vdW interaction extends to organic and biological matter, where the organization of cellulose, lignin, and proteins relies on such a force. Many heterostructures, metamaterials, photonic crystals, and plasmonic nanostructures display unusual dispersive interaction effects [1-4]. The PI has played a leading role for the publication of an upcoming review article recognizing the common origin of Casimir and vdW interactions (Fig. 1) and summarizing related advances in the development and application of theoretical and computational techniques guided and motivated by progress in materials science [5]. A perspective for the future of this field as seen from condensed matter is especially useful especially for the broader fundamental applications of dispersive forces.

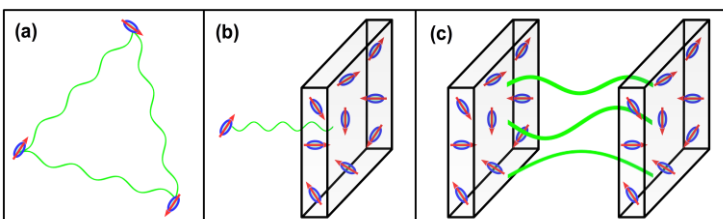


Fig. 1 Types of dispersive interactions: (a) dipolar vdW forces between atoms and molecules; (b) Casimir-Polder forces between atoms and substrates; (c) Casimir forces between large objects.

Fluctuation forces induced by real charges – In addition to dipolar fluctuation interactions, the fluctuations of other observables are also possible, which may give rise different interactions. We have realized that fluctuating charges transferred through wire connecting a graphene flake and a substrate can result in a new type of fluctuation force. The fundamental difference with the typical Casimir/vdW force lies in the origin. While the Casimir phenomenon is due to the electromagnetic excitations associated with the dielectric and magnetic response of each plate, the charge induced effect is due to *monopolar charge fluctuations* between the plates. We have developed a general theory to describe such novel interactions utilizing the capacitance concept and distinguishing between thermal and quantum mechanical effects through characteristic dependences on distance, temperature, and other factors [6]. Essentially we have a capacitor-like system, shown in Fig. 2a,b, which consists of a substrate and a graphene plate. The voltage fluctuations of the wire induce excess fluctuating charges on the capacitor plates. It is clear that this monopolar charge fluctuations force differs in origin from the dipolar fluctuation force giving rise to the well-established vdW/Casimir effect. The presented theory relies on the surface charge density response, fluctuation-dissipation theorem, and frequency-dependent capacitance of the system. Our detailed study shows that by changing the properties of the wire and graphene flake, there is a regime where the charge fluctuations force can be made dominant over the Casimir one. Fig. 2 (c,d) shows how the monopolar force can be controlled not only as a function of distance, but also the resistance and relaxation time of the wire. An experimental setting of how this force can be measured or tuned is also suggested in [6]. We further argue that charge fluctuation forces are always present in capacitor-like systems. They must be taken in conjunction with the standard Casimir interaction, which enables further probing of thermal and quantum mechanical effects of fluctuation induced phenomena in nanostructures.

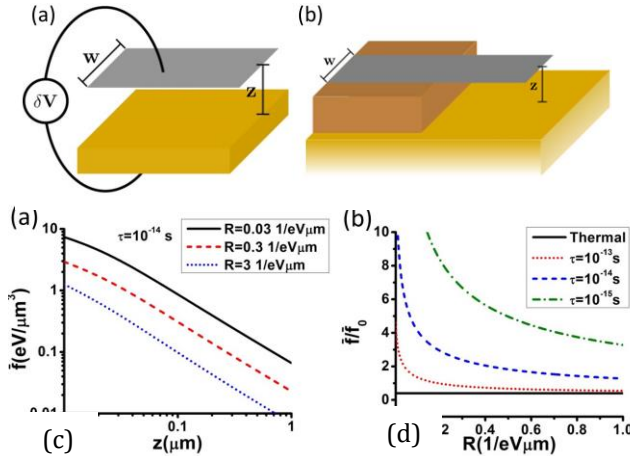


Fig. 2 (a) A parallel plate capacitor schematics where a connecting wire transfer voltage fluctuations δV to the plates. One of the plates can be a graphene flake with width w above a metallic thick substrate. (b) Experimentally realistic setting. The wire is represented by a metallic contact. Charge fluctuations force normalized by $\bar{f}_0 = -k_B T / (2Az)$ as a function of (c) distance z and (d) resistivity of the wire (A -capacitor area). Figure is taken from Ref. [6].

Van der Waals heterostructures and interlayer coupling – A new area of research directly related to vdW interactions has emerged, where 2D chemically inert layers are being stacked in a vertical manner. While strong chemical bonds are responsible for the in-plane stability of each layer, the relatively weak vdW interaction holds the heterostructure (HS) stack together. In this particular direction, we utilize first principles simulations within density functional theory implemented in the VASP code to study interface properties of graphene/silicene; graphene/MoS₂, and silicene/MoS₂ vdW heterostructures [7]. It turns out that the vdW interaction is of primary importance for the electronic and vibrational properties of such systems. On one hand, the vdW interaction together with the electronic orbital overlap leads to non-trivial changes in the deeper valence and higher conduction regions in terms of hybridization energy gaps. On the other hand, the vdW coupling is found to be necessary for the vibrational stability of the HS meaning that real phonon dispersion relations are achieved. Fig. 3 presents the unfolded band structure of the different systems. Fig. 3a shows distinct Dirac-like bands crossing the Fermi level, such that the linear

bands at the K-points belong to graphene, while the linear bands at the M-point belong to silicene. Another set of linear bands for silicene crossing at the Γ – point (barely visible in the graph) is also present. Similar additive features around the Fermi level are found for the other configurations. In addition to shifting of several characteristic bands, we find that the vdW interaction is responsible for opening of several band gaps in the conduction and valence regions of rather significant magnitude. Such gaps may have a common behavior as they occur for all studied systems but different energy locations. This suggests an approach for tuning optical transitions in a particular layer by simply choosing a suitable component for the HS. The vibrational properties are also studied showing a richness of the phonon dispersion as new breathing and shear modes are found, which can potentially be explored to control heat transfer in 2D systems.

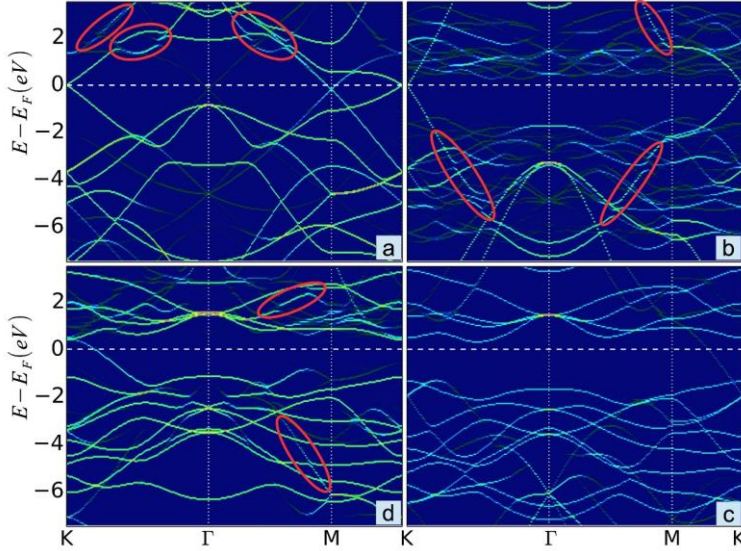


Fig. 3 Band structures for (a) GR/SIL projected on the SIL BZ; (b) GR/MoS₂ projected on the GR BZ; (c) GR/MoS₂ projected on the MoS₂ BZ; (d) SIL/MoS₂ projected on the MoS₂ BZ. The opening of some energy gaps due to interlayer hybridization are circled in red. (GR – graphene; SIL – silicene; BZ – Brillouin zone). Figure taken from Ref. [7].

Graphene Nanoribbons anchored to SiC substrates – Although considered to be weak, the vdW interaction is of decisive importance for other HS materials. One example are graphene nanoribbons (GNRs), a quasi-one dimensional planar graphene allotrope, chemically anchored to a SiC substrate [8]. We present electronic structure calculations using density functional theory with vdW-DF2 potential taken into account of zigzag graphene nanoribbons chemically attached via the edges to the Si or C terminated surfaces of the substrate. The edge characteristics are found to be rather robust in a sense that the spin polarization of the GNR zigzag edge is preserved such that the anchored ribbon is antiferromagnetic, similar to the case of free planar zigzag ribbons. What is interesting for the stability and electronic and structural properties, however, is the type of charge transfer, polarity of edge bonds, and vdW interaction. Specifically, our charge transfer calculations and density plots in Fig. 4 show that C-H and Si-H polarity introduce electrostatic interactions which can compete with the dispersive vdW coupling resulting in different bond lengths, signatures in the band structure, as well as stability of the ribbons anchored to the C or Si terminated sites.

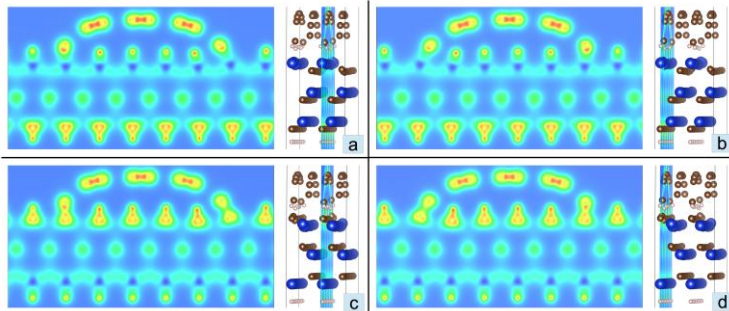


Fig. 4 (a) and (b) Charge density plots for GNRs anchored to Si terminated SiC substrate for two locations of the projected plane (right panels); (c) and (d) Charge density plots for GNRs anchored to C terminated SiC substrate for two locations of the projected plane (right panels). Figure taken from Ref. [8].

Future Plans

Casimir-Polder effects in multilayers – The PI plans on investigating the Casimir-Polder force in multilayered systems. This type of interaction characterizes how atoms couple to materials via electromagnetic fluctuations and it is of great relevance to novel phenomena such as trapping cold atoms, Bose-Einstein condensates, and quantum reflection [9]. We intend on giving a new perspective on this problem by exploring the role of multilayered graphene systems in order to provide insight in how number of layers, dielectric response, temperature, and other factors can be used to modulate this interaction.

Quantum Casimir interactions in silicene – It turns out that not only C, but other elements in the same group, such as Si, Ge, and Sn, also form stable 2D layered structures. Specifically, silicene (made of Si), germanene (made of Ge), and stanine (made of Sn) can be considered members of an expanded graphene family. Even though all of these are Dirac-like materials, the staggered lattice and strong spin orbit coupling make silicene distinct from graphene. The PI intends to pursue how different topological phases available in silicene (but not in graphene) via applied electric fields and/or circularly polarized light affect their long ranged dispersion interactions, a problem promising to give fundamental understanding in materials beyond graphene.

Thermal fluctuations in silicene – Another direction in the intermediate future of this project is how classical thermal fluctuations distinguish themselves from their quantum mechanical counterparts in Casimir related phenomena. It has been recognized recently that thermal fluctuation interaction are very sensitive to the specific model of the response properties of the materials as well as their dissipation [5]. In fact, for standard materials, it has been obtained that taking finite dissipation leads to significant quantitative differences in the interaction, an issue currently investigated by experimentalists. The PI intend to study this problem in the expanded graphene family in order to shed some light of how Dirac-like materials at the nanoscale and their dissipation affects thermal interactions.

Publications

1. L.M. Woods, A. Popescu, D. Drosdoff, and I.V. Bondarev, *Dispersion interactions in graphitic nanostructures*, Chem. Phys. **413**, 116 (2013);
2. A.D. Phan, T.X. Hoan, T.H. Nghiem, and L.M. Woods, *Surface plasmon resonances of protein-conjugated gold nanoparticles on graphitic substrates*, Appl. Phys. Lett. **103**, 163702 (2013);
3. D. Drosdoff and L.M. Woods, *Quantum and thermal dispersion forces: application to graphene nanoribbons*, Phys. Rev. Lett. **112**, 025501 (2014);
4. N. Khusnutdinov, R. Kashparov, and L.M. Woods, *Casimir effect for a stack of conductive planes*, Phys. Rev. D **92**, 045002 (2015);
5. L.M. Woods, D.A.R. Dalvit, A. Tkatchenko, P. Rodriguez-Lopez, A.W. Rodriguez, and R. Podgornik, *A materials perspective of Casimir and van der Waals interactions*, Rev. Mod. Phys., to be published (arXiv:1509:03338);
6. D. Drosdoff, I.V. Bondarev, A. Widom, R. Podgornik, and L.M. Woods, *Charge induced fluctuation forces in graphitic nanostructures*, Phys. Rev. X **6**, 011004 (2016);
7. N.B. Le, T.D. Huan, and L.M. Woods, *Interlayer interactions in van der Waals heterostructures: electron and phonon properties*, ACS Appl. Mater.&Interfaces **8**, 6286 (2016);
8. N.B. Le and L.M. Woods, *Graphene nanoribbons anchored to SiC substrates*, J. Phys.: Cond. Matt. **28**, 364001 (2016) (special issue, “Interfaces and heterostructures of van der Waals materials”);
9. N. Khusnutdinov, R. Kashparov, and L.M. Woods, *Casimir-Polder effect for a stack of conductive planes*, in progress.

First Principles Investigations for Magnetic Properties of Innovative Materials

Ruqian Wu, University of California, Irvine

1. Program scope

The main propose of this project is to address fundamental issues in molecular spintronics, spintronics and spin-topotronics. Explicitly, we study (1) topological band gaps of innovative two-dimensional materials for the realization of quantum spin Hall effect or quantum anomalous Hall effect; (2) magnetic anisotropy and spin dynamics in small structures including single molecular magnets; (3) origin of magnetic noise in “non-magnetic” qubits. The uniqueness of our density functional studies is the determination of magnetic anisotropy energies of large systems, which is essential for the understanding of spin dynamics and spintronics. It is our goal to conduct creative research on low-dimensional magnetic structures of fundamental importance, with an eye towards finding new materials and phenomena for technological breakthroughs.

2. Recent progress:

We have studied various systems/problems in the last year. Some important new results are summarized below.

2.1. Search for giant magnetic anisotropy in transition-metal dimers on defected hexagonal boron nitride sheet: Through systematic density functional calculations, the structural stability and magnetic properties of many transition-metal dimers embedded in a defected hexagonal boron nitride monolayer are investigated. We find twelve cases that may have magnetic anisotropy energies (MAEs) larger than 30meV. In particular, Ir-Ir@Dh-BN has both large MAE (~126 meV) and high structural stability, which makes it a promising candidate of magnetic unit in spintronics and quantum computing devices. We discuss the mechanism that leads to giant MAEs and elucidate the principles for the design of magnetic units at the atomic scale. This paper was published **J. Chem. Phys., 144, 204704 (2016)**, It acknowledged DOE support: “Work at UCI was supported by DOE-BES (Grant No. DE-FG02-05ER46237). Work at Fudan was supported by the Chinese National Science Foundation (Grant No. 11474056) and National Basic Research Program of China (Grant No. 2015CB921400). Computer simulations were partially performed on the U.S. Department of Energy Supercomputer Facility (NERSC). Several publications on the related topic are under preparation.

2.2. Spin wave diode and spin wave fiber. Spin waves are collective excitations propagating in the magnetic medium with ordered magnetizations. Magnonics, utilizing the spin wave (magnon) as information carrier, is a promising candidate for low-dissipation computation and communication technologies. We discover that, due to the Dzyaloshinskii-Moriya interaction, the scattering behavior of spin wave at a magnetic domain wall follows a generalized Snell’s law, where two magnetic domains work as two different mediums. Similar to optical total reflection that occurs at the water-air interfaces, spin waves may experience total reflection at magnetic domain walls when their incident angle larger than a critical value. We design a spin wave fiber using a magnetic domain structure with two domain walls, and demonstrate that such a spin wave fiber can transmit spin waves over long distance by total internal reflections, in analogy to an optical fiber. Our design of spin wave fiber opens up new possibilities in pure magnetic information processing. Figure 1 shows the schematic diagram (a) and

the magnetic simulations (b-f) for spin wave reflection and refraction at a magnetic domain wall. The black/white arrow denotes the magnetization direction in the left/right domain colored by yellow/orange (white/gray) in the schematic diagram (simulations). The work was submitted to **Physical Review B (Rapid communication)** with acknowledgment to DOE as "...R. W. was also supported by the Department of Energy (U. S.) under Grant No. DE-FG02-05ER46237."

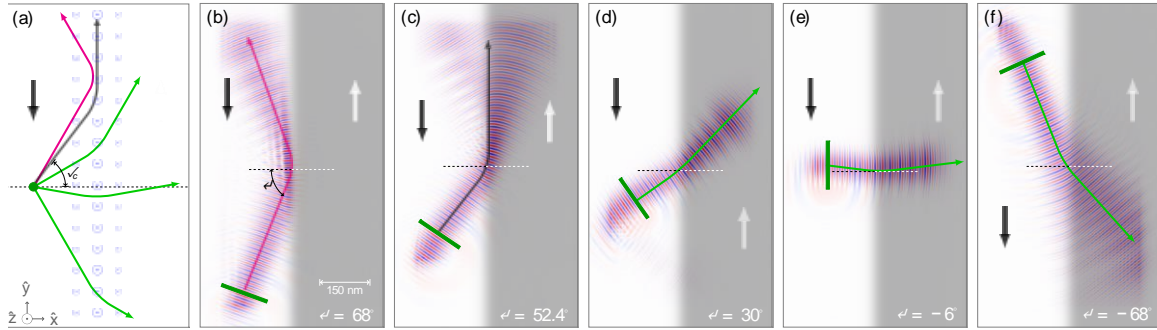


Fig. 1. (a) Schematic diagram of reflection/refraction behavior for spin wave incident from left domain with various incident angles. (b-f) Magnetic simulations with the incident angle $\alpha = 68^\circ$ (b), $\alpha = \theta_c$ (c), $\alpha = 30^\circ$ (d), $\alpha = -6^\circ$ (e), $\alpha = -68^\circ$ (f). In all panels: the domain wall width $w \sim 30\text{nm}$; the green bar denotes the exciting location of the spin wave; the exciting fields frequency is $f = 100\text{Ghz}$, and the critical angle is estimated to be $\theta_c = 52.4^\circ$.

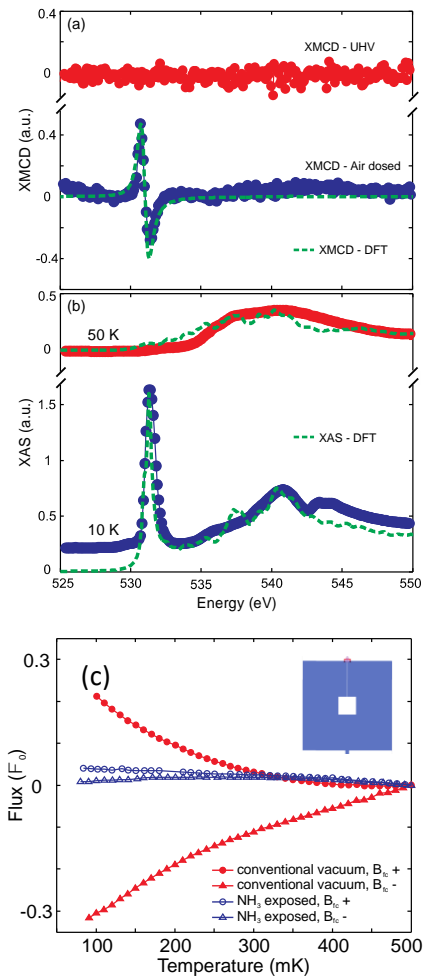
2.3. Two dimensional topological materials: Quantum spin Hall effect (QSHE) and quantum anomalous Hall effect (QAHE) in two-dimensional topological insulators are among the most interesting research topics of condensed matter physics and materials science. Through systematic density functional calculations and tight-binding simulations, we found that stanene on α -alumina surface may possess a sizeable topologically nontrivial band gap ($\sim 0.25\text{ eV}$) at the Γ point. Furthermore, stanene is atomically bonded to but electronically decoupled from the substrate, providing high structural stability and isolated QSH states to a large extent. The underlying physical mechanism is rather general, and this finding may lead to the opening of a new vista for the exploration of QSH insulators for room temperature device applications. This paper was published in **Physical Review B, 94, 035112 (2016)**, and acknowledged DOE as "Work at UCI was supported by DOE-BES (Grant No: DE-FG02-05ER46237 for HW and HF; SC0012670 for JK, SP, and HF)... Computer simulations were partially supported by NERSC."

We also demonstrated clear weak anti-localization (WAL) effect arising from induced Rashba spin-orbit coupling (SOC) in WS₂-covered single-layer and bilayer graphene devices, in close collaboration with experimental group of Prof. J. Shi (UCR) and theory group of J. Alicea (CalTech). At high carrier densities, we estimate the Rashba SOC relaxation rate to be $\sim 0.2\text{ps}^{-1}$ and show that it can be tuned by transverse electric fields. In addition to the Rashba SOC, we also predict the existence of a 'valley-Zeeman' SOC from first-principles calculations. The interplay between these two SOC's can open a non-topological but interesting gap in graphene; in particular, zigzag boundaries host four sub-gap edge states protected by time-reversal and crystalline symmetries. The graphene/WS₂ system provides a possible platform for these novel edge states. This

paper was submitted to **Two-dimensional Materials** and acknowledged DOE as “This work was supported by the DOE BES award No. DE-FG02-07ER46351 (BY and JS) and award No. DE-FG02-05ER46237 (JW and RW); ...”.

2.4. Origin and Reduction of 1/f Magnetic Flux Noise in Superconducting Device: A major obstacle to using superconducting quantum interference devices (SQUIDs) as qubits is flux noise. We propose that the heretofore mysterious spins producing flux noise could be O₂ molecules adsorbed on the surface. Using density functional theory calculations, we find that an O₂ molecule adsorbed on an α -alumina surface has a magnetic moment of $\square 1.8 \mu_B$. When the spin is oriented perpendicular to the axis of the O–O bond, the barrier to spin rotations is about 10 mK. Following the work we did in the last year [**PRL 115, 077002 (2015)**], we have a joint theoretical/experimental work with Prof. R. McDermott (UWM) and John Freeland (ANL), we demonstrate that adsorbed molecular O₂ is the dominant contributor to magnetism in superconducting thin films. We show that this magnetism can be suppressed by appropriate surface treatment or improvement in the sample vacuum environment. We observe a suppression of static spin susceptibility by more than an order of magnitude and a suppression of 1/f magnetic flux noise power spectral density of up to a factor of 5. These advances open the door to realization of superconducting qubits with improved quantum coherence. Figure 2 shows that agreement between theory and experiment for the x-ray absorption and x-ray magnetic circular dichroism spectra and the phenomenal reduction of magnetic susceptibility of the sample after the removal of surface oxygen molecules. This paper is under consideration for **Physical Review Letters** and it acknowledged DOE: “...DFT calculations at UCI (HW and RW) were supported by DOE-BES (Grant No. DE-FG02-05ER46237) and NERSC.”.

Fig. 2. (a) and (b) X-ray magnetic circular dichroism (XMCD) at the oxygen K-edge for a native Al film and an Al film exposed to air. Dashed lines are from DFT simulations. (c) Suppression of magnetic susceptibility. Temperature- dependent flux threading a square-washer Nb SQUID (350 pH; see inset) cooled in a conventional vacuum environment (closed red symbols) and cooled following vacuum bake and NH₃ passivation (blue open symbols).



3. Publications that acknowledged the DOE support (through 2015)

1. J. Hu, Z.Y. Zhu, and R.Q. Wu, “Chern Half Metal: The Case of Graphene With Co or Rh Adatom”, *Nano. Lett.* **15**, 2074 (2015).
2. J. Karel, J. Juraszek, J. Minar, C. Bordel, K.H. Stone, Y.N. Zhang, J. Hu, R.Q. Wu, H. Ebert, J.B. Kortright and F. Hellman, “The Effect of Chemical Order on

- the Magnetic and Electronic Properties of Epitaxial off-stoichiometry $\text{Fe}_x\text{Si}_{1-x}$ thin films”, Phys. Rev. B **91**, 144402 (2015).
3. J. Li, J. Hu, H. Wang and R.Q. Wu, “Rhenium-phthalocyanine molecular nanojunction with high magnetic anisotropy and high spin filtering efficiency”, Appl. Phys. Lett. **107**, 032404 (2015).
 4. H. Wang, C.T. Shi, J. Hu, C. Yu and R.Q. Wu, “Candidate source of flux noise in SQUIDs: adsorbed oxygen molecules”, Phys. Rev. Lett. **115**, 077002 (2015).
 5. A. Kabir, J. Hu, V. Turkowski, R.Q. Wu and T.S. Rahman, “Magnetic Anisotropy of FePt Nanoparticles”, Phys. Rev. B, **92**, 054424 (2015).
 6. J. Li, H. Wang, J. Hu and R.Q. Wu, “Search for giant magnetic anisotropy in transition-metal dimers on defected hexagonal boron nitride sheet”, J. Chem. Phys., **144**, 204704 (2016).
 7. B. Li, X. H. Luo, H. Wang, W. J. Ren, S. Yano, C.-W. Wang, J. S. Gardner, K.-D. Liss, P. Miao, S.-H. Lee, T. Kamiyama, R. Q. Wu, Y. Kawakita, and Z. D. Zhang, “Colossal negative thermal expansion induced by magnetic phase competition on frustrated lattices in Laves phase compound $(\text{Hf},\text{Ta})\text{Fe}_2$ ”, Phys. Rev. B 224405 (2016).
 8. H. Wang, S. T. Pi, J. Kim, Z. Wang, H. H. Fu and R. Q. Wu, “Possibility of Realizing Quantum Spin Hall Effect at Room Temperature in Stanene/ $\text{Al}_2\text{O}_3(0001)$ ”, Phys. Rev. B, 94, 035112 (2016).

4. Planned activities for next year

We have several research topics in the next phase.

1. Explore interactions between magnetic monolayers and dopants with 3D and 2D topological insulators, especially graphene with WS_2 and YIG.
2. Work on magnetic properties of oxide interfaces such as PZT/STO, LSMO/STO, and LCMO/LAO etc.
3. Develop new approaches to investigate the innovative phenomena such as valleytronics and Luttinger liquid behavior of electrons in 2D materials with defects and grain boundaries.
4. We will study the spin wave propagation in magnetic nanostructures.

Quantum Mechanical Simulations of Complex Nanostructures for Photovoltaic Applications

Principle investigator: Dr. Zhigang Wu
Department of Physics, Colorado School of Mines
1500 Illinois Street, Golden, CO 80401
zhiwu@mines.edu

I. Project Scope

In this proposal, the PI will first address the excited-state problem within the DFT framework to obtain quasiparticle energies from both Kohn-Sham (KS) eigenvalues and orbitals; and the electron-hole binding energy will be computed based on screened Coulomb interaction of corresponding DFT orbitals. The accuracy of these approaches will be examined against many-body methods of GW/BSE and quantum Monte Carlo (QMC). The PI will also work on improving the accuracy and efficiency of the GW/BSE and QMC methods in electronic excitation computations by using better KS orbitals obtained from orbital-dependent DFT as inputs. Then an extended QMC database of ground- and excited-state properties will be developed, and this will be spot checked and supplemented with data from GW/BSE calculations. The investigation will subsequently focus on the development of an improved exchange-correlation (XC) density functional beyond the current generalized gradient approximation (GGA) level of parameterization, with parameters fitted to the QMC database. This will allow the ground-state properties of focus systems to be more precisely predicted using DFT. These new developments will then be applied to investigate a chosen set of complex nanostructures that have great potential for opening new routes in designing materials with improved transport, electronic, and optical properties for PV and other optoelectronic usages: (1) Hybrid interfaces between materials with distinct electronic and optical properties, such as organic molecules (conjugated polymers, e.g. P3HT) and inorganic semiconducting materials (Si and ZnO). Complicated interface structures, including interface bonding configurations, compositional and geometrical blending patterns, interfacial defects, and various sizes and shapes of inorganic nanomaterials, will be considered for the purpose of understanding the working mechanisms of present organic/nano PV systems and designing optimum interface structures for fast charge separation and injection. (2) Complex-structured semiconducting nanomaterials that could induce charge separation without *pn*- or hetero-junctions. The new methodology will allow the PI to investigate the performance of realistic semiconducting nanomaterials of internal (impurities, defects, etc.) and external (uneven surface, mechanical twisting and bending, surface chemistry, etc.) complexities on optical absorption and charge transport against charge trapping and recombination. Of particular interest is whether such structural complexity in a single material could even be beneficial for PV usage, for example, charge separation through morphology control.

II. Recent Progress

1. Tunable Many-Body Interactions in Semiconducting Graphene: Giant Excitonic Effect and Strong Optical Absorption. How the long-range ordering and local defect configurations modify the electronic structure of graphene remains an outstanding problem in nanoscience, which precludes the practical method of patterning graphene from being widely adopted for making graphene-based electronic and optoelectronic devices, because a small variation in supercell geometry could change the patterned graphene from a semimetal to a semiconductor, or vice versa. We have solved this fundamental problem, using both an analytical tight-binding model and numerical DFT calculations, and we further investigated the many-body interactions in these semiconducting defected graphene structures, which affect their electronic and optical properties strongly. Employing the highly accurate many-body perturbation approach based on Green's functions, i.e., the GW approximation, we find a very large renormalization over independent particle methods of the fundamental band gaps of semiconducting graphene structures

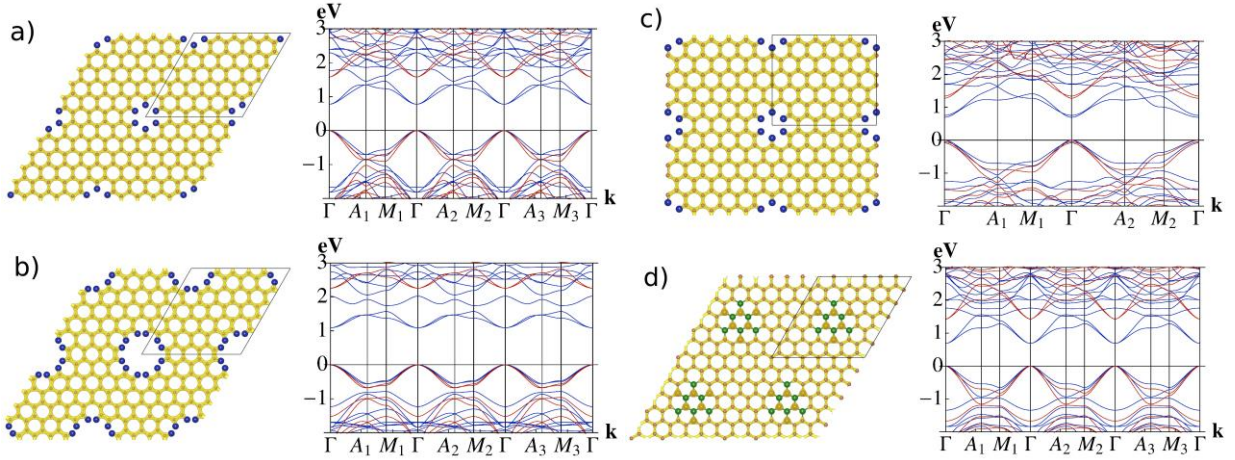


Figure 1. Crystal (left column) and electronic band (right column) structures of defected graphene structures. Yellow isosurfaces (left) indicate the total charge density. Blue and red lines (right) correspond to DFT and GW band structures, respectively. Hole edges are passivated by hydrogen (blue dots). Here (a), (b), (c) and (d) plot 4 semiconducting defected graphene structures for comparison.

with periodic defects, as illustrated in Figure 1, suggesting much enhanced many-body interactions in 2D materials.

In addition, their exciton binding energies are larger than 0.4 eV, showing significantly strengthened electron-electron and electron-hole interactions. Their absorption spectra (Figure 2) show two strong peaks whose positions are sensitive to the defect fraction and distribution. The strong near-edge optical absorption and excellent tunability make these two-dimensional materials promising for optoelectronic applications.

2. Giant band gap quantum spin Hall insulator with weak spin-orbit coupling. We also investigated the edge states of these semiconducting defected graphene. Previously, graphene was predicted as a quantum spin Hall (QSH) insulator due to the spin-orbit coupling (SOC). However, the weak SOC in graphene makes the bulk gap extremely small ($E_g \ll k_B T$ at room temperature), since a typical QSH insulator acquires its band gap through SOC. Thus it is useless for practical applications. Current investigations have mainly focused on adding heavy transition-metal atoms to graphene for dramatically increasing the spin-orbit coupling.

Here, we present a new method to open a giant band gap ($E_g > 1$ eV) in a QSH phase for arbitrarily weak SOC. We consider the tight-binding (TB) Kane-Mele model for the QSH insulator with the additional feature of periodic defects. By tuning the periodicity of structural defects, one can induce inter-valley scattering and open a large band gap. Surprisingly, the characteristic metallic edge modes of a QSH phase persist even with the inclusion of such periodic defects, as seen in Figures 3 and 4. We have performed TB calculations, showing the existence of a Z_2 odd QSH phase in a Kane-Mele model

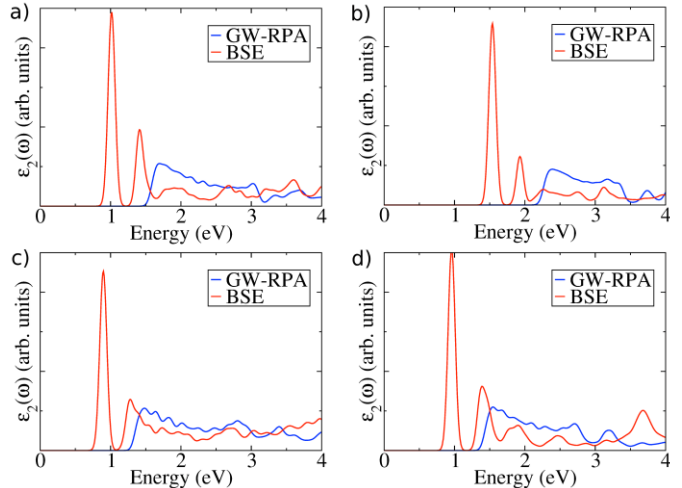


Figure 2. Imaginary part of the dielectric function for hexagonal systems with a (a) 6-C hole, (b) 12-C hole, (c) rectangular system with a 6-C hole, and (d) hexagonal system with 12 C atoms replaced by BN dopants.

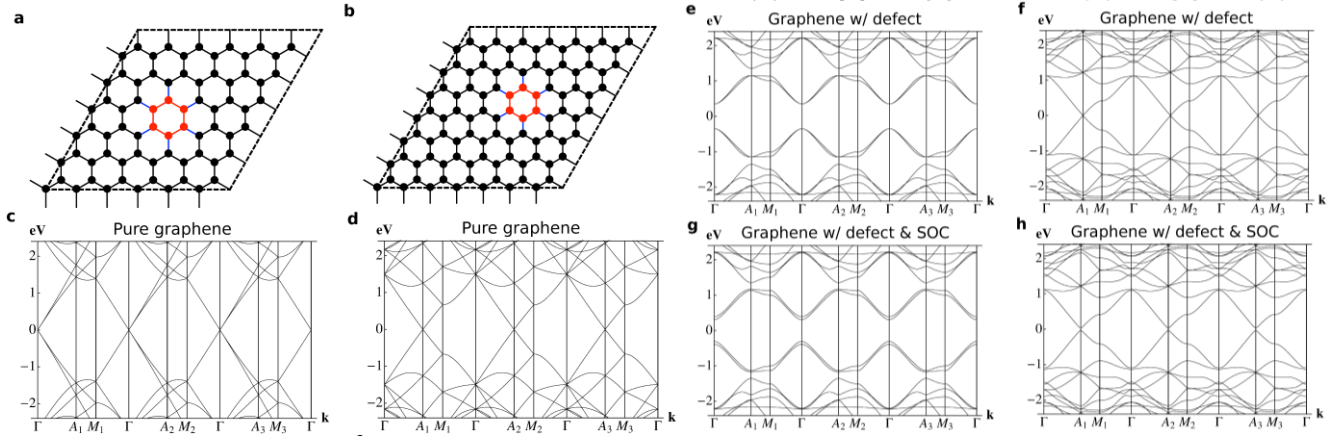


Figure 3: Bulk band structures with and without SOC. (a) and (b) Crystal structures of 6×6 and 7×7 graphene supercells subject to a single 6-C defect. In the (n_1, m_1, n_2, m_2) classification described in the manuscript, these are $(6, 0, 0, 6)$ and $(7, 0, 0, 7)$ supercells, respectively. Atom type 1 is represented by black dots while type 2 is red. In our model, hopping along red and blue bonds is turned off. (c) and (d) Band structures of 6×6 and 7×7 graphene supercells without any defect, i.e. pure graphene. (e) and (f) Band structures of 6×6 and 7×7 GNMs with a single 6-C defect. (g) and (h) Band structures of 6×6 and 7×7 GNMs with a single 6-C defect and SOC for C.

modified to include periodic defects, outlining the path to a giant band gap QSH insulator without enhancing intrinsic SOC.

3. Optical properties of Si allotropes with direct band gap and their nano-structures. Si is the most popular semiconductor for photovoltaics (PV) and integrated circuits industry. While it is abundant, inexpensive, and non-toxic, it has an indirect band gap, leading to poor absorption near band edge. In this project, we investigate Si allotropes with direct fundamental band gap and their nanostructures, whose E_g are close to the ideal value (1.1–1.8 eV) for PV, while the Si nanowires and QDs based on diamond Si have energy gaps too large for PV cells. Figure 5 summarizes two allotrope bulk structures and their optical absorption spectra, and they have direct band gaps.

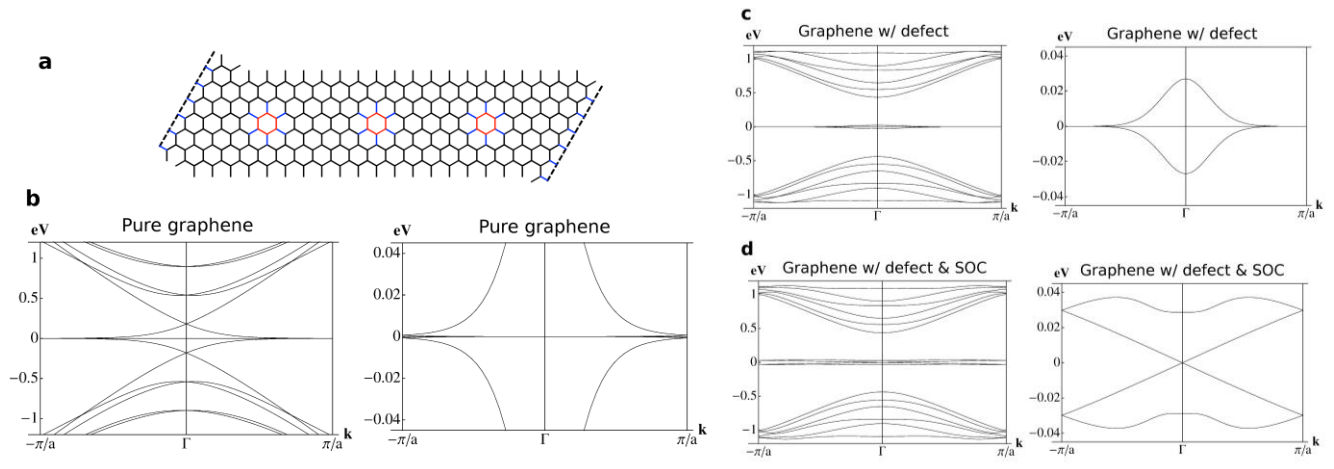


Figure 4: Ribbon band structures with and without spin-orbit coupling (SOC). (a) Crystal structure of a ribbon constructed from a 6×6 graphene nanomesh (GNM). Dashed lines indicate the periodic direction. Band structures for a ribbon of (b) pure graphene, (c) and GNM with SOC.

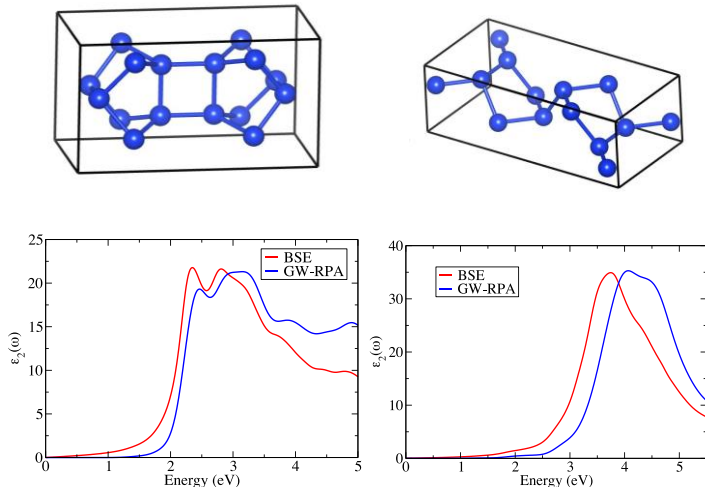


Figure 5. Crystal structure (top) and optical absorption spectra (bottom) of silicon allotropes with space groups of Fddd (left) and I4/mcm (right).

Material	ΔE_0 (ABINIT)	ΔE_0 (EPW)
C	-465	-615
Si	-61	-61
BN – Layered	-434	-560
BN – ZB	-362	-459
BN – WZ	-222	-305

Table I. Calculated band gap

renormalization (ΔE_0 in meV) for C, Si and BN of three different crystal structures, employing two different methods implemented in the ABINIT and the EPW packages. Here we studied the layered, zinc blende (ZB) and wurtzite (WZ) structures of BN.

4. Effects of electron-phonon interactions on electronic structures in nanostructures. Current electronic structure calculations mostly neglect the effects of electron-phonon interaction; however, it is substantial in certain bulk materials such as diamond and small nanoscale structures, in which quantum confinement might enhance it greatly. Table I summarizes the band gap normalization (ΔE_0) due to lattice vibrations in C, Si and boron nitride (BN). We find that the change in E_g can be as large as ~ 0.5 eV at room temperature, and it varies dramatically among different crystal structures.

We also found that two different methods currently implemented in the ABINIT and EPW packages predicted the same value of ΔE_0 (-61 meV) for Si, while for C and BN in which the electron-phonon coupling is much stronger, these two implementations generated significantly different values. We conclude that the EPW-implementation (using many unoccupied bands) predicts ΔE_0 comparable to experimental data, while the ABINIT-implementation (using only valence bands) underestimates ΔE_0 by about 20–30%. We are investigating the origin of this error.

IV. Selected Recent Publications Supported by This Fund

- [1] Marc Dvorak, Suhuai Wei, and Zhigang Wu, *Origin of the variation of exciton binding energy in semiconductors*, Phys. Rev. Lett. **110**, 016402 (2013).
- [2] Marc Dvorak, William Oswald, and Zhigang Wu, *Bandgap opening by patterning graphene*, (Nature) Scientific Reports **3**, 2289 (2013).
- [3] Paul Larson, Marc Dvorak, and Zhigang Wu, *Role of the plasmon-pole model in the GW approximation*, Phys. Rev. B **88**, 125205 (2013).
- [4] Huashan Li, Zhigang Wu, and Mark T. Lusk, *Dangling bond defects are the critical roadblock to efficient photoconversion in hybrid quantum dot solar cells*, J. Phys. Chem. C **118**, 46 (2014).
- [5] Huashan Li, Zhigang Wu, Tianlei Zhou, Alan Sellinger, and Mark T. Lusk, *Double superexchange in quantum dot mesomaterials*, Energy Environ. Sci. **7**, 1023 (2014).
- [6] Marc Dvorak, Xiao-Jia Chen and Zhigang Wu, *Quasiparticle energies and excitonic effects in dense solid hydrogen near metallization*, Phys. Rev. B **90**, 035103 (2014).
- [7] Marc Dvorak and Zhigang Wu, *Giant excitonic effect and tunable optical spectrum in graphene by defects patterning*, Phys. Rev. B **92**, 035422 (2015).
- [8] Marc Dvorak and Zhigang Wu, *Dirac point movement and topological phase transition in defected graphene*, Nanoscale **7**, 3645 (2015).
- [9] Xinquan Wang and Zhigang Wu, *Comment on "d+id' Chiral Superconductivity in Bilayer Silicene"*, Phys. Rev. Lett. **114**, 099701 (2015).

Interfacial Magnetic Skyrmions and Proximity Effects

Principal investigator: Jiadong Zang
Department of Physics, University of New Hampshire
Durham, NH 03824
Jiadong.Zang@unh.edu

Project Scope

Magnetic skyrmion is a nanostructured spin texture in which magnetic moments point in all directions wrapping a unit sphere. The aim of this project is to accurately manipulate skyrmions living on the interface of magnetic multilayers and control their dynamical behaviors. We are systematically exploring new approaches to create/annihilate skyrmions and studying their proximity effect once attached to other orders. Our theoretical efforts are supported by partnership with the experimental collaborator Dr. Axel Hoffmann from Argonne National Laborotory.

The skyrmion, being topologically nontrivial, not only attracts interests from fundamental physics, but also offers game-changing strategy in future low-dissipative information technology. However the major challenge is to realize precise control of skyrmions. To this end, the overarching investigations in this project highlight the creation of skyrmions in geometrical confinement, manipulations of skyrmions by phonons and magnons, and engineering of the semiconducting skyrmion properties.

As a zero-dimensional nano-sized object, the skyrmion provides a unique position to discuss the interplay between the dynamics of magnetic moments and quantum transport of electrons. Another goal of this project is to develop an algorithm coupling the Landau-Lifshitz-Gilbert dynamics of magnetization and the non-equilibrium Green's function of electrons. Dynamical properties of skyrmions can thus be tunable via band engineering.

Recent Progress

Direct imaging of magnetic field-driven transitions of skyrmions in nanodisks – the PI, in collaborations with the High Magnetic Field Laboratory in China, has extensively observed skyrmions in a few confined geometries, including nanoribbons, nanowires, and nanodisks. In this work, the skyrmion cluster in FeGe

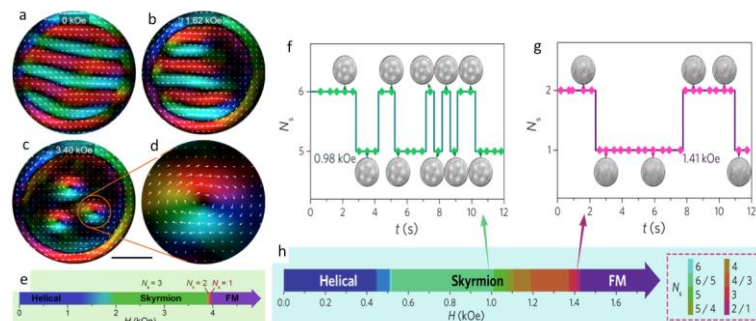


Fig. 1: (a-e) Imaging of skyrmions in FeGe nanodisks. (f-h) Telegraph noises in the transition of multi-skyrmion states at critical fields.

nanodisk and its transition to other orders are observed by high resolution Lorentz transmission electron microscopy, shown in Fig. 1. At elevated temperatures and certain

field, we also observed intermittent jumps between skyrmion cluster states, referred to as telegraph noise, which correspond to the coexisting states at the first order phase transition.

Field-driven oscillation of multi-skyrmion cluster in a nanodisk – Inspired by the observation of skyrmions in nanodisk reported in the work above, we used micromagnetic simulations to investigate the multi-skyrmion cluster in a small nanodisk. Under an in-plane static magnetic field, the multi-skyrmion cluster shows an oscillating behavior, as shown in Fig. 2, which resembles a torsional pendulum rotation about a perpendicular axis. In analogy to the rigid body theory, the skyrmion thus not only acquires particle properties like mass and velocity, as reported in numerous works, but also possesses the moment of inertia. Similar as the forced rotation of rigid bodies, the skyrmion cluster rotates under a rotation in-plane magnetic field. Interestingly, the frequency of the skyrmion rotation is a fraction of the field frequency, where the fractal coefficient is exactly the number of skyrmions in the nanodisk.

Quantum topological Hall effect in a Rashba spin-orbit electron gas coupled to the skyrmion crystal – The real space topology of the magnetic skyrmion gives rise to the Hall effect, dubbed as the topological Hall effect, of electrons traversing the texture. The PI, in collaboration with the University of California Riverside, predicted the quantized topological Hall effect (QTHE) in a Rashba spin-orbit coupled electron gas coupled to a skyrmion crystal. We showed that once its spin couples to the skyrmion texture via a weak Zeeman coupling, the electron will be driven into a quantum anomalous Hall insulating phase characterized by a nonzero integer Chern number and presence of chiral edge states shown in Fig. 3. Our calculations show that the nontrivial topological properties of the skyrmion spin texture can be imprinted on the two-dimensional electron gas system.

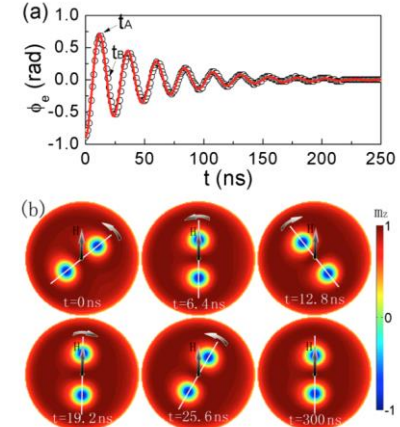


Fig. 2: (a) Damped oscillation of two-skyrmion-cluster driven by an in-plane magnetic field (b) Snapshots of m_z at different times after the field is turned on.

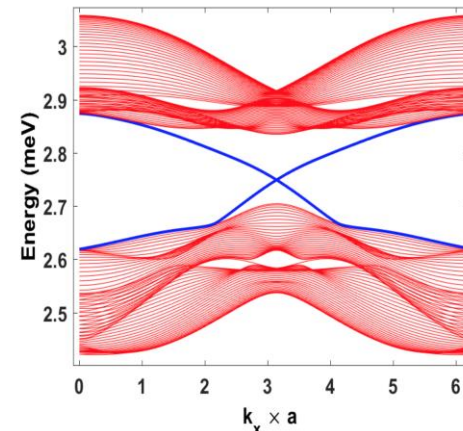


Fig. 3: Chiral edges states of Rashba electron gas subjected into a skyrmion crystal.

Future Plans

In the coming two years, we will mostly focus on the following problems in this new program.

Scattering of spin waves and skyrmions – the PI, in collaboration with the Argonne National Laboratory, will image the spin wave scattering of magnetic skyrmions. Due to the presence of the Dzyaloshinskii-Moriya interaction and inversion symmetry breaking, spin waves will be deflected transversely and result in a Hall effect. The trajectory of the spin wave can be imaged by the unique spatially resolved Brillouin light scattering (BLS) microscope in Argonne. Once scattered off an antiferromagnetic skyrmion, a spin wave version of the spin Hall effect, magnons of opposite chirality are deflected in opposite directions, will be observed, due to the presence of two sublattices and the non-Abelian emergent gauge field in antiferromagnets.

Phonon-driven skyrmion motion – The coupling between phonon and magnon has been preliminarily discussed in the context of ferromagnets. However, the non-collinear orders of helical and skyrmion phases introduce new physics. In these orders, the angle between neighboring spins depends on the ratio between the Heisenberg exchange J and the Dzyaloshinskii-Moriya interaction D . Once the lattice vibrates, the neighboring separation changes, the strength of J and D are affected, and the angle is consequently changed. This physical picture shows that a propagation of phonon will lead to the deviation of spin state away from its groundstate, as if the phonon excites magnons in the chiral magnets. We will perform a perturbation theory of the spin Hamiltonian in the presence of lattice vibration, and explore the phonon-driven spin wave transport and skyrmion motions.

Fine-tuning of skyrmion dynamics via band engineering – The interface of magnetic multilayer provides exciting tunability of the electron transport of the skyrmion materials. Alternatively, once the skyrmion material is attached to a semiconductor, band engineering of the latter can realize fine-tuning of the skyrmion's dynamical behavior. We will develop an advanced numerical approach by coupling the traditional micromagnetic simulation described by the Landau-Lifshitz-Gilbert (LLG) equation to the non-equilibrium Green's function (NEGF)- based quantum transport theory, in order to simulate the spin dynamics in nanomagnetism in general and semiconducting skyrmions in particular. Calculation of spin density from NEGF and micromagnetic evolution from LLG will be iterated. To further escalate the efficiency, perturbation approaches will be performed to avoid taking inverse of large matrices in the computation of NEGF.

Previous Publications

The list below contains selected previous publications by the PI that are relevant for the PI's new DOE-funded research program

1. X. Zhao, C. Jin, C. Wang, H. Du, J. Zang, Y. Zhang, M. Tian, R. Che, "Direct observation of cascading phase transitions in skyrmion cluster states within FeGe nanodisks", Proc. Natl. Acad. Sci, 201600197 (2016).
2. H. Du, R. Che, L. Kong, X. Zhao, C. Jin, C. Wang, J. Yang, W. Ning, R. Li, C. Jin, X. Chen, J. Zang, Y. Zhang, and M. Tian, 'Edge-mediated skyrmion chain and its collective dynamics in a confined geometry", *Nature Communications* **6**, 8504 (2015).
3. H. Du, D. Liang, C. Jin, L. Kong, M. J. Stolt, W. Ning, J. Yang, Y. Xing, J. Wang, R. Che, J. Zang, S. Jin, Y. Zhang, and M. Tian, 'Electrical probing of field-driven cascading

- quantized transitions of skyrmion cluster states in MnSi nanowires”, *Nature Communications*, **6**, 7637 (2015).
- 4. G. Yin, Y. Liu, Y. Barlas, J. Zang, and R. Lake, ‘Topological spin Hall effect from magnetic skyrmions”, *Phys. Rev. B* **92**, 024411 (2015).
 - 5. H. Hurst, D. Efimkin, J. Zang, and V. Galitski, ‘Charged skyrmions on the surface of a topological insulator”, *Phys. Rev. B* **91**, 060401(R) (2015)
 - 6. J. Kang and J. Zang, ‘Transport theory of metallic B20 helimagnets”, *Phys. Rev. B* **91**, 134401 (2015).
 - 7. J. S. White, et al., Electric field-induced skyrmion distortion and lattice rotation in the magnetoelectric insulator Cu₂OSeO₃”, *Phys. Rev. Lett.* **113**, 107203(2014), Editors' Suggestion.
 - 8. M. Mochizuki, et al., ‘Thermally driven ratchet motion of a skyrmion microcrystal and topological magnon Hall effect”, *Nature Materials*, **13**, 241 (2014).
 - 9. Lingyao Kong, and J. Zang, ‘Dynamics of insulating skyrmion under temperature gradient”, *Phys. Rev. Lett.* **111**, 067203 (2013).
 - 10. J. Zang, M. Mostovoy, J. H. Han, and N. Nagaosa, “Dynamics of skyrmion crystal in metallic thin films”, *Phys. Rev. Lett.* **107**, 136804 (2011).
 - 11. J. H. Han, J. Zang, Z. Yang, J. H. Park, and N. Nagaosa, “Skyrmion lattice in a two-dimensional chiral magnet”, *Phys. Rev. B* **82**, 094429 (2010).

Laser-induced ultrafast magnetization in ferromagnets

Principal investigator: Dr. Guoping Zhang
Department of Physics, Indiana State University
gpzhang@indstate.edu

Keywords: Ultrafast, laser, magnetization, reversal, magnetism

Project Scope

Our project focuses on a new frontier in magnetic storage. We explore the possibility to use a femtosecond (fs) laser pulse to manipulate the spin in magnetic media. This will have a direct impact on the future magnetic storage devices. The scope of this program is to investigate why an ultrafast laser pulse can induce so great demagnetization within so short time scales (a few hundred femtoseconds), by targeting the exchange interaction reduction. It has been known for a long time that the exchange interaction plays a significant role in magnetism, but its response on the fs time is very complex and largely unknown. Our objectives are (1) to reveal how the laser pulse can effectively reduce or even quench the exchange interaction, and (2) to establish the link between the exchange reduction and the spin moment change by solving time-dependent Liouville equation coupled with the exchange interaction change. This will enable us to reveal some of the intricate relations between the band excitation and correlation effects. One path that we take is to investigate how the band relaxation affects the exchange interaction. This band relaxation is due to the laser excitation. Another important path is that we explore the density functional itself for the excited states.

Recent Progress

Below are some highlights of progress made in the past 2 years (a more comprehensive publication list is appended below the highlights).

Ultrafast reduction in exchange interaction by a laser pulse: alternative path to femtomagnetism

Since the beginning of femtomagnetism [1,2], it has been hotly debated how an ultrafast laser pulse can demagnetize a sample and switch its spins within a few hundred femtoseconds, but no consensus has been reached. In this paper, we propose that an ultrafast reduction in the exchange interaction by a femtosecond laser pulse is mainly responsible for demagnetization and spin switching. The key physics is that the dipole selection rule demands two distinctive electron configurations for the ground and excited states and consequently changes the exchange interaction. Although the exchange interaction change is almost instantaneous, its effect on the spin is delayed by the finite spin wave propagation. Consistent with the experimental observation, the delay becomes longer with a stronger exchange interaction pulse. In spin-frustrated systems, the effect of the exchange interaction change is even more dramatic, where the spin can be directly switched from one direction to the other. Therefore, our theory has the potential to explain the essence of major observations in rare-earth transition metal

compounds for the last seven years. Our findings are likely to motivate further research in the quest of the origin of femtomagnetism.

Band-structure relaxation during photoexcitation diminishes magnetism

In contrast to previous theoretical studies, for the first time we go beyond the rigid band approximation and find that the band relaxation has a significant effect on the spin moment reduction and exchange splitting. Our study is performed in two steps. We first generate the initial excited state by promoting electrons from the valence band to the conduction band. Then we solve the Kohn-Sham equation self-consistently and, more importantly, allow the system to relax under this excited-state configuration. To our surprise, we find that in all the three 3d ferromagnetic metals, both the exchange splitting and the spin moment are sharply reduced. Then we compare our result with experiments, where good agreement is found.

Reducing electron exchange interaction on a femtosecond time

A decade ago Rhie et al [3] reported that when ferromagnetic nickel is subject to an intense ultrashort laser pulse, its exchange splitting is reduced quickly. But to simulate such reduction remains a big challenge. The popular rigid band approximation (RBA), where both the band structure and the exchange splitting are held fixed before and after laser excitation, is unsuitable for this purpose, while the time-dependent density functional theory could be time-consuming. To overcome these difficulties, we propose a time-dependent Liouville and density functional theory (TDLDF) that integrates the time-dependent Liouville equation into the density functional theory. As a result, the excited charge density is reiterated back into the Kohn-Sham equation, and the band structure is allowed to change dynamically. Even with the ground-state density functional, a larger demagnetization than RBA is found; after we expand Ortenzi's spin scaling method into an excited-state (laser) density functional, we find that the exchange splitting is indeed strongly reduced, as seen in the experiment. Both the majority and minority bands are shifted toward the Fermi level, but the majority shifts a lot more. The ultrafast reduction in exchange splitting occurs concomitantly with demagnetization. While our current theory is still unable to yield the same percentage loss in the spin moment as observed in the experiment, it predicts a correct trend that agrees with the experiments. With a better functional,

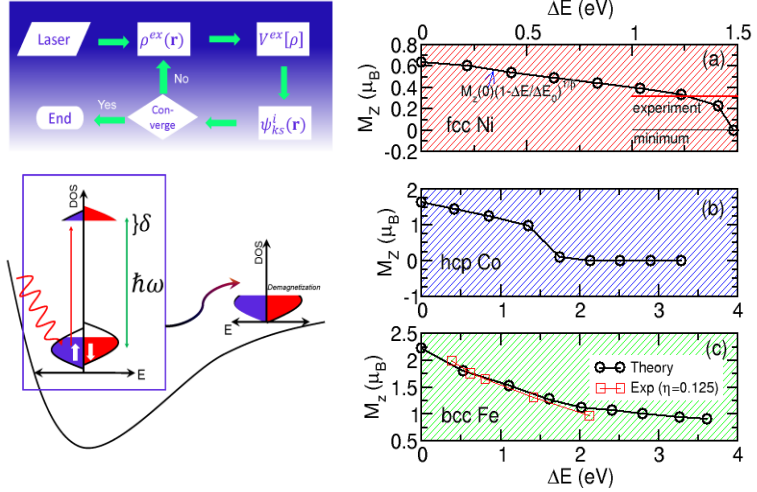


Figure 1. (Left) Theoretical scheme of our implementation. The laser creates an excited charge density and excited potential energy surface for the entire system. By solving the Kohn–Sham (KS) equation, we attain the KS wavefunction for the next iteration until convergence.

(Right) Spin moment decreases as the energy absorbed increases for (a) fcc Ni, (b) hcp Co and (c) bcc Fe.

we believe that our results can be further improved. Our work paves a novel way to address the exchange interaction reduction in other materials.

A new and simple model for magneto-optics uncovers an unexpected spin switching

In magneto-optics the spin angular momentum S_z of a sample is indirectly probed by the rotation angle and ellipticity [4], which are mainly determined by the off-diagonal susceptibility $\chi_{xy}^{(1)}$. Here we propose a new and simple model to establish such a much needed relation. Our model is based on the Hookean model, but includes spin-orbit coupling. Under continuous wave excitation, we show that $\chi_{xy}^{(1)}$ is indeed directly proportional to S_z for a fixed photon frequency ω . Such an elegant relation is encouraging, and we wonder whether our model can describe spin dynamics as well. By allowing the spin to change dynamically, to our surprise, our model predicts that an ultrafast laser pulse can induce a spin precession; with appropriate parameters, the laser can even reverse spin from one direction to another. We believe that our spin-orbit coupled model may find some important applications in spin switching processes [5], a hot topic in femtomagnetism [1,2].

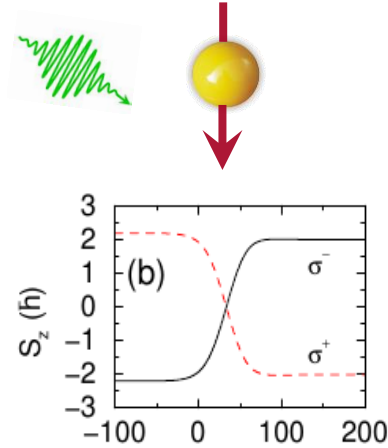


Figure 2. All-optical spin reversal. The σ^- pulse (solid line) only switches spin from down to up, while the σ^+ pulse (dashed line) only switches spin from up to down.

Future Plans

Band excitation – From the above study, we find that the band excitation is most likely to be the main course of the strong demagnetization. It is necessary to investigate how the transitions between these bands occur and how to implement them in the real materials. We expect the TDLDFT will have a broader impact not only in ferromagnets but also in high temperature superconductors, and more so than TDDFT.

Layered structures in Co system – Co layered structures have shown a strong magnetic moment. Since the structure can be tailored systematically, it also allows one to gradually change the spin moment. However, at this time, there are very few studies ever carried out. We plan to carry out additional calculations on this material. Our results can be compared with the experimental data directly.

Spin reversal – We will further investigate how the spin reversal occurs in regular magnetic systems. This requires a massively parallel investigation of a big and amorphous system, which has been a big challenge for the first-principles investigation. Our Hookean model will be employed to study the all-optical spin switching. This is one of the promising directions that may well lead to a direct application.

References

1. E. Beaurepaire, J.-C. Merle, A. Daunois, and J.-Y. Bigot, Ultrafast spin dynamics in ferromagnetic nickel, *Phys. Rev. Lett.* **76**, 4250–4253 (1996).
2. G. P. Zhang, W. Hübner, E. Beaurepaire and J.-Y. Bigot, Laser-Induced Ultrafast Demagnetization: Femtomagnetism, *Top. Appl. Phys.* **83** 245 (2002).
3. H.-S. Rhie, H. A. Dürr, and W. Eberhardt, Femtosecond Electron and Spin Dynamics in Ni/W(110) Films, *Phys. Rev. Lett.* **90**, 247201
4. G. P. Zhang, W. Hübner, G. Lefkidis, Y. Bai, and T. F. George, Paradigm of the time-resolved magneto-optical Kerr effect for femtosecond magnetism, *Nature Phys.* **5**, 499–502 (2009).
5. C. D. Stanciu, F. Hansteen, A. V. Kimel, A. Kirilyuk, A. Tsukamoto, A. Itoh, and Th. Rasing, All-Optical Magnetic Recording with Circularly Polarized Light, *Phys. Rev. Lett.* **99**, 047601 (2007).

Publications

1. Kai Lv, H. P. Zhu, J. Peng, G. P. Zhang and X. S. Wu, Electronic and magnetic properties of SrRuO₃ with Ru-vacancy: First-principle calculations, *EPL* **113**, 27001 (2016).
2. G. P. Zhang, Y. H. Bai, and Thomas F. George, Ultrafast reduction of exchange splitting in ferromagnetic nickel, *Journal of Physics: Condensed Matter* **27**, 236004 (2016).
3. M. S. Si, D. Z. Yang, D. S. Xue and G. P. Zhang, Femtosecond magnetism when the orbital angular momentum is quenched, *SPIN* **5**, 1540009 (2015).
4. G. P. Zhang, Y. H. Bai, and Thomas F. George, A new and simple model for magneto-optics uncovers an unexpected spin switching, *EPL* **112**, 27001 (2015).
5. G. P. Zhang, M. S. Si, Y. H. Bai, and Thomas F. George, Magnetic spin moment reduction in photoexcited ferromagnets through exchange interaction quenching: Beyond the rigid band approximation, *Journal of Physics: Condensed Matter* **27**, 206003 (2015).
6. G. P. Zhang, H. P. Zhu, Y. H. Bai, J. Bonacum, X. S. Wu, and Thomas F. George, Imaging superatomic molecular orbitals in a C₆₀ molecule through four 800-nm photons, *International Journal of Modern Physics B* **29**, 1550115 (2015).
7. G. P. Zhang, M. S. Si and T. F. George, Laser-induced ultrafast demagnetization time and spin moment in ferromagnets: First-principles calculation, *J. Appl. Phys.* **117**, 17D706 (2015).
8. M. S. Si, J. Y. Li, D. S. Xue, and G. P. Zhang, Probing ultrafast spin moment change of bcc iron in crystal-momentum space: A proposal, *Ultrafast Magnetism I*, edited by J.-Y. Bigot et al., Springer Proceedings in Physics Vol. **159**, 47 (2015).
9. Huiping Zhu, Guoping Zhang, and Xiaoshan Wu, Injection of spin polarization into Si from the heterostructure LaMnO₃/Si interface, *Applied Physics Express* **7**, 093003 (2014).
10. G. P. Zhang, Mingqiang Gu and X. S. Wu, Ultrafast reduction in exchange interaction by a laser pulse: Alternative path to femtomagnetism, *Journal of Physics: Condensed Matter* **26**, 376001 (2014).

Project Title: Theory of Defects in Electronic Materials

Principal Investigator: Shengbai Zhang

Department of Physics, Applied Physics & Astronomy, Rensselaer Polytechnic Institute, Troy, NY 12180

Email: zhangs9@rpi.edu

Project Scope:

The scope of this project includes theoretical development for accurate predictions of defects properties in electronic materials, and performing, in parallel, cutting-edge research in defect physics, such as non-equilibrium doping, deep-level engineering, excited-state properties, and defect-defect interaction and correlation, using first-principles theoretical tools with balanced accuracy and computation efficiency. We employ a comprehensive set of density functional theory (DFT) methods such as the local density approximation (LDA) and generalized gradient approximation (GGA)-based molecular dynamics (MD), time-dependent DFT (TDDFT), hybrid functional methods, and the many-body GW quasiparticle perturbation theory for accurate prediction of defect properties in electronic materials. We will examine, for charged defects, the response of the screening charge to the defect and the effects of the artificially introduced compensating jellium background, with the aim of eliminating unphysical interactions. Non-equilibrium doping is an active research topic of high current interest. We will study radiation damage, with a focus on the electronic excitation effect associated with ion implantation, and develop a theory for the recently-emerged and promising optical hyperdoping method. We will push the frontier of *ab initio* defect study from mainly isolated point defects to strongly interacting and correlated defects, e.g., clustering, and from mainly ground-state properties to excited-state properties. We will also explore possible paths to lower dopant ionization energy in ultrawide gap materials.

Recent Progress:

(1) *Multivalency-induced band gap opening at the edges of transition metal dichalcogenides* - Transition metal dichalcogenides (TMDs) such as MoS₂ have attracted considerable interest recently because of their unique properties and potential applications. Most of the proposed applications require the control of edge states. Metallic edges may allow leakage current, which is detrimental to device function. The armchair nanoribbons of MoS₂ have been theoretically shown to have a small gap (0.5-0.6 eV). However, armchair nanoribbons are usually not seen in experiment because zigzag ribbons have considerably lower energies. So far, theoretical calculations have shown that zigzag edges are metallic.

In Ref. [9], we solved the puzzle of whether the zigzag edge of monolayer MoS₂ is metallic or semiconducting. The answer in fact depends sensitively on S chemical potential and the polarization of the edges. We developed a generic electron counting model (ECM), which allows us to determine the 3x periodicity as the fundamental unit for semiconducting edges. We also demonstrated that the multivalency of Mo atoms is a critical factor for the reconstruction of

the edges to fulfill the ECM and to open the band gap (see Fig. 1). In addition, consistent with recent experiments, oxygen adsorption at edges results in even larger band gaps than the intrinsic edges. This concept of multivalency in TMD materials could also be generalized to understand point defects in TMDs or lateral junctions made of such materials.

(2) *Stacking fault defect in phosphorenes and black phosphorus* - Monolayer and few-layer phosphorenes (FLPs), which are fabricated from the layered material, black phosphorus (BP), have recently emerged as a candidate material for making field effect transistors, as well as other electronic devices such as photodetectors and even terahertz detectors. The electronic structures of FLPs have been the

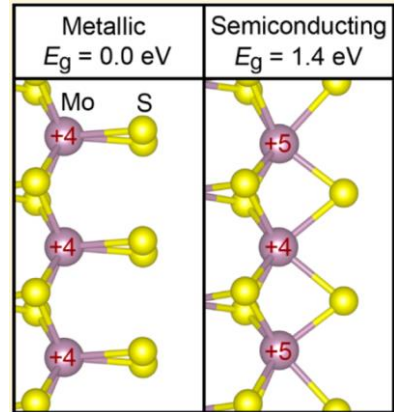


Fig. 1. Nominal charge states of Mo atoms at MoS₂ zigzag edges and the corresponding band

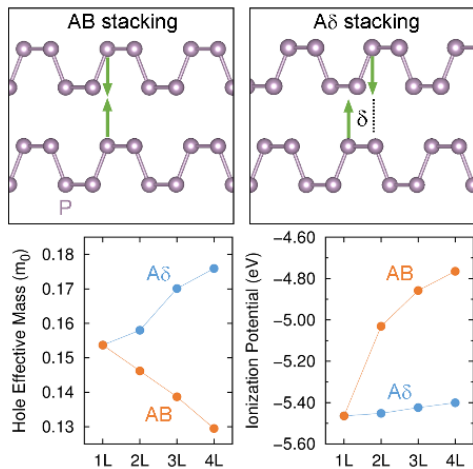


Fig. 2. Upper panels show the atomic structures of BP with the AB and A δ stacking. Lower panels show the hole effective mass and ionization potential of phosphorenes with the two stackings as a function of thickness (i.e., the number of monolayers nL).

manipulation of the stacking without any chemical modification.

subject of a number of theoretical studies. Most of the previous studies have focused on the stable stacking sequence as derived from the bulk BP, called AB stacking (see Fig. 2). In Ref. [6], we identify a new stacking (named A δ , see figure) between monolayer phosphorenes, which is found to be the only metastable stacking besides the stable AB stacking. Other stackings, such as AA and AC, which were proposed in two previous studies, are found to be unstable and will spontaneously transform into either AB or A δ stacking if symmetry constraint is lifted. The new A δ stacking is found to give rise to a whole zoo of enriched electronic and transport properties for FLPs and BP, including a direct-to-indirect transition in band gap, oppositely behaved effective masses as the layer thickness increases, and widely tunable band gap, electron affinity (EA), and ionization potential (IP). Important applications in nanoelectronics are expected by employing such enhanced properties. In particular, lateral junctions with type-I, II, and III alignments could all be realized by a single material simply by

(3) *Charge transfer at the MoS₂/WS₂ interface* - The success of van der Waals heterostructures made of layered materials hinges on the understanding of charge transfer across the interface as the foundation for new device concepts. In contrast to conventional heterostructures, where a strong interfacial coupling is essential to charge transfer, recent experimental findings indicate that van der Waals heterostructures can exhibit ultrafast charge transfer despite the weak binding of these heterostructures. In Ref. [2], we find, using TDDFT-molecular dynamics (MD), the timescale of the charge transfer across the MoS₂/WS₂ heterostructure depends

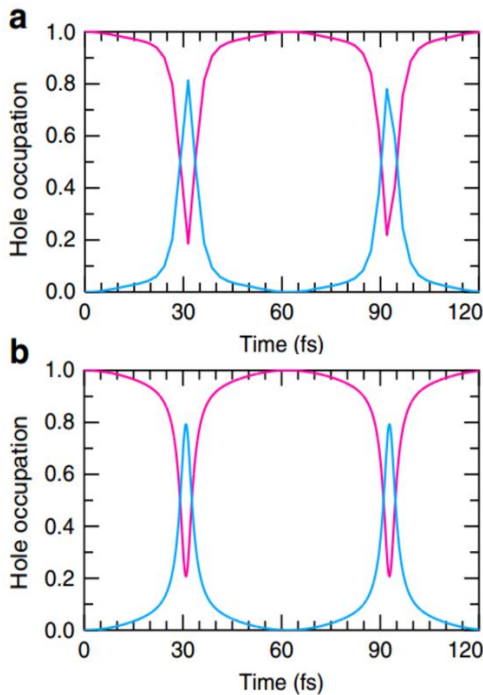


Fig. 3. Projection of hole wavefunction onto MoS_2 (red) and WS_2 (blue) layers based on TDDFT-MD (a) and model calculation (b).

dynamic coupling, leading to the much longer charge transfer times associated with the alternate stacking (3R and AB') patterns found in the TDDFT-MD calculations.

Future Plans (2016-2017):

(1) *Carrier transport through bounded defect states* - Our recent work [Phys. Rev. Lett. 114, 196801 (2015)] suggests that defects in two-dimensional (2D) semiconductors such as MoS_2 are unlikely to be shallow due to reduced screening in the third dimension. This finding raises the fundamental question how charge carrier transport takes place in 2D systems. While the presence of a substrate is widely believed to affect the position of the defect levels inside the band gap and hence the ability to transport charged carriers, here we will explore the effect due to interactions between bounded defect states.

(2) *Molecular intercalation in layered materials* - Small molecules inside solids have attracted considerable attention recently. It ranges from organic-inorganic hybrid photovoltaic semiconductors, to molecular doping of semiconductors [14], to molecular ion intercalation in graphite [M.-C. Lin, et al., Nature 520, 324 (16 April 2015)]. Here we will explore this scenario further by examining the mystery behind AlCl_4 intercalation into graphite. Not only will the study offer physical insights into the experimental observations but also point to possible new directions in manipulating the materials properties through defect / impurity engineering.

greatly on the nature of the stacking. 2H stacking was found to exhibit ultrafast (within 100 fs) charge transfer, while little to no charge was transferred in this timescale for either the 3R or AB' stacking configurations.

To understand the nature of the charge transfer, we constructed a simple analytic model of the van der Waals heterostructure, and we find that the oscillating dipole associated with the coherent motion of holes plays an essential role in the charge transfer. The rapid charge oscillations found through TDDFT-MD calculations are well represented in the model calculation, as shown in Fig. 3 (a) and (b). Further, by analyzing the model, we find that there is unexpected critical behavior in the system. When the dipole matrix coupling associated with the hole transfer, $M_z = \langle \text{MoS}_2 | z | \text{WS}_2 \rangle$, is above a critical value, rapid charge oscillations take place. However, when M_z drops below the critical value, the magnitude of the oscillations drop discontinuously from approximately 75% to 5% of the hole population. This reduction of the dipole oscillation significantly weakens the

(3) *Topological carbon for future electronics* - In the past year, through first-principles calculations and tight-binding modeling [5, 11, 12, Phys. Rev. Lett. 113, 085501 (2014)], we have established the generic topological nature of three-dimensional (3D) carbon networks with mixed sp^2 and sp^3 characteristics. The key difference between the carbon-based topological physics is different from that of standard topological insulators in the sense that it does not rely on the spin-orbit coupling, which is intrinsically small for carbon, but on the orbital physics of the π electrons. Recently, such 3D carbon networks, known as carbon honeycombs, have been experimentally synthesized. We will build on our past successes and proceed to explore the exotic topological properties in such carbon structures and related materials for potential applications never envisioned before.

List of key publications (2015-2016):

- (1) L. Seixas, D. West, A. Fazzio & S. B. Zhang, "Vertical twinning of the Dirac cone at the interface between topological insulators and semiconductors", *Nature Comm.* **6**, 7630 (2015).
- (2) H. Wang, J. Bang, Y. Y. Sun, L. Liang, D. West, V. Meunier, and S. B. Zhang, "The role of collective motion in the ultrafast charge transfer in van der Waals heterostructures", *Nature Comm.* **7**, 11504 (2016).
- (3) Y. Y. Sun, M. L. Agiorgousis, P. Zhang, and S. B. Zhang, "Chalcogenide perovskites for photovoltaics", *Nano Lett.* **15**, 581 (2015).
- (4) Y. Jiang, X. Zhang, Y. Wang, N. Wang, D. West, S. Zhang, and Z. Zhang, "Vertical/Planar Growth and Surface Orientation of Bi_2Te_3 and Bi_2Se_3 Topological Insulator Nanoplates", *Nano Lett.* **15**, 3147 (2015).
- (5) Y.-P. Chen, Y. Xie, S. A. Yang, H. Pan, F. Zhang, M. L. Cohen, and S. Zhang, "Nanostructured carbon allotropes with Weyl-like loops and points", *Nano Lett.* **15**, 6974 (2015).
- (6) S. Lei, H. Wang, L. Huang, Y. Y. Sun, and S. B. Zhang, "Stacking fault enriching the electronic and transport properties of few-layer phosphorenes and black phosphorus", *Nano Lett.* **16**, 1317 (2016).
- (7) W. Liu, D. West, L. He, Y. Xu, J. Liu, K. Wang, Y. Wang, G. van der Laan, R. Zhang, S. Zhang, and K. L. Wang, "Atomic-Scale Magnetism of Cr-Doped Bi_2Se_3 Thin Film Topological Insulators", *ACS Nano* **9**, 10237 (2015).
- (8) D. Wang, D. Han, X.-B. Li, S.-Y. Xie, N.-K. Chen, W. Q. Tian, D. West, H.-B. Sun, and S. B. Zhang, "Determination of Formation and Ionization Energies of Charged Defects in Two-Dimensional Materials", *Phys. Rev. Lett.* **114**, 196801 (2015).
- (9) M. C. Lucking, J. Bang, H. Terrones, Y. Y. Sun, and S. B. Zhang, "Multivalency-induced band gap opening at MoS_2 edges", *Chem. Mater.* **27**, 3326 (2015).
- (10) Y. Y. Sun, J. Shi, J. Lian, W. Gao, M. L. Agiorgousis, P. Zhang, and S. B. Zhang, "Discovering lead-free perovskite solar materials with a split-anion approach", *Nanoscale* **8**, 6284 (2016).
- (11) C. Zhong, Y. Chen, Y. Xie, S. A. Yang, M. L. Cohen and S. B. Zhang, "Towards three-dimensional Weyl-surface semimetals in graphene networks", *Nanoscale* **8**, 7232 (2016).
- (12) Y. Gao, Y. Chen, C. Zhong, Z. Zhang, Y. Xie, S. Zhang, "Electron and phonon properties and gas storage in carbon honeycombs", *Nanoscale* **8**, 12863 (2016).
- (13) J. Bang, Y. Y. Sun, J.-H. Song, and S. B. Zhang, "Carrier-induced transient defect mechanism for non-radiative recombination in InGaN light-emitting devices", *Sci. Rep.* **6**, 24404 (2016).

- (14) J. Bang, Y. Y. Sun, D. West, B. K. Meyer and S. B. Zhang, "Molecular doping of ZnO by ammonia: a possible shallow acceptor", *J. Mater. Chem. C* **3**, 339 (2015).

Electronic Structure and Fundamental Physics of Semiconductor Nanostructures (8/2014-8/2016)

PI: Alex Zunger; University of Colorado, Boulder, Colorado 80309
Alex.Zunger@Colorado.edu

Key Words: Quantum dots, Wires, Quantum Materials, Topological Insulators, Inverse Design.

Project scope:

Testing our fundamental understanding of the basic many body interactions that govern the electronic properties of semiconductor nanostructures requires access to spectroscopically rich and highly resolved data. Alas, such high quality spectroscopy tends to exist mostly in rather *large* nanostructures (that have good structural perfection, nearly perfect passivation and isolation from the environment). Such are the self-assembled epitaxial systems containing typically 100,000 or 1,000,000 atoms per computational unit cell, or colloidal QD containing ~ 10,000 per cell. This size regime is well outside the range of DFT methodologies. At the same time, continuum-like effective-mass methods (based on envelope functions) that can handle large nanostructures lack the atomistic resolution needed to describe the underlying electronic structure phenomenology. Our method is tailored at such structures. Using our previously developed screened- pseudopotential plus configuration interaction approach we can directly address million-atom nanostructures of the sort described above. Our scope is to use this methodology for understanding fundamental electronic processes in nano- and eventually *mesoscopic systems*.

The project is now transitioning to study ‘Quantum Materials’ including defects, doping and design DDD). A new renewal proposal has been submitted and approved for funding starting 8/2016. The transition to this focus is already apparent in late 2015 and early 2016 (subject C below) .

Recent Progress (2014-2016):

- A. *2D Quantum wells and super lattice nanostructures [1]-[2]:*
- B. *Silicon Nano crystals [3]-[4]:*
- C. *‘Quantum materials’ and Design of structures with target properties [5]-[10]*

Subject A. 2D Quantum wells and super lattice nanostructures [1]-[2]:

Split Dirac cones in HgTe/CdTe quantum wells due to symmetry-enforced level anticrossing at interfaces [1]

HgTe is a band-inverted compound, which forms a two-dimensional topological insulator if sandwiched between CdTe barriers for a HgTe layer thickness above the critical value. We describe the fine structure of Dirac states in the HgTe/CdTe quantum wells of critical and close-to-critical thicknesses and show that the necessary creation of interfaces brings in another important physical effect: the opening of a significant anticrossing gap between the tips of the Dirac cones. The level repulsion driven by the natural interface inversion asymmetry of zinc-blende heterostructures considerably modifies the electron states and dispersion but preserves the topological transition at the critical thickness. By combining symmetry analysis, atomistic

calculations, and extended $\mathbf{k} \cdot \mathbf{p}$ theory with interface terms, we obtain a quantitative description of the energy spectrum and extract the interface-mixing coefficient. We discuss how the fingerprints of the predicted zero-magnetic-field splitting of the Dirac cones could be detected experimentally by studying magnetotransport phenomena, cyclotron resonance, Raman scattering, and THz radiation absorption.

2D Superlattices for $\text{PbTiO}_3\text{-SrTiO}_3$ ferroelectric-dielectric cation ordering induced polarization enhancement [2]

An efficient computational material design approach (cluster expansion) is employed for the ferroelectric $\text{PbTiO}_3/\text{SrTiO}_3$ system. Via exploring a configuration space including over 3×10^6 candidates, two special cation ordered configurations—either perfect or mixed 1/1 (011) superlattice—are identified with the mostly enhanced ferroelectric polarization by up to about 95% in comparison with the (001) superlattice. We find that the exotic couplings between the antiferrodistortive (AFD) and ferroelectric (FE) modes which is absent from the PTO and STO, as the origin for the best polarization property of the two superlattices. This understanding should provide fresh ideas to design multifunctional perovskite heterostructures

Subject B. Silicon Nano crystals [3]-[4]:

Single-Dot Absorption Spectroscopy and Theory of Silicon Nanocrystals [3]

A major question in field of nanostructures has been whether an indirect bulk compound such as Si can become direct, or strongly absorbing, at reduced dimensionality. The modern theory of nanostructures treats nanostructures atomistically as a giant molecule rather than via continuum-based effective mass methods. However, such high-resolution theoretical calculations cannot be compared with experimental data from *ensemble* measurements, where size (and shape) dispersion even at a very small scale smears out discrete features both in emission and absorption. So far only PLE of individual quantum dots was demonstrated only for direct band gap materials, but it is much more difficult to perform on single Si nanocrystals due to their low emission rate, stemming from $\sim \mu\text{s}$ exciton lifetime. Here we report the first successful single dot spectra for Si in parallel with single dot excitonic calculations. We provide a detailed and full interpretation of the various excitonic transitions in Si nanocrystals showing the system can not be described as direct.

Quasi-Direct Optical Transitions in Silicon Nano crystals exceeding the intensity of bulk transitions [4]

Comparison of the measured absolute absorption cross section on a per Si atom basis of plasma-synthesized Si nanocrystals (NCs) with the absorption of bulk crystalline Si shows that while near the band edge the NC absorption is weaker than the bulk, yet above ~ 2 eV the NC absorbs up to 5 times more than the bulk. Using atomistic screened pseudopotential calculations we show that this enhancement arises from interface-induced scattering that enhances the quasi-direct, zero-phonon transitions by mixing direct Γ -like wavefunction character into the indirect X-like conduction band states. The absorption enhancement factor increases exponentially with decreasing NC size and is correlated with the exponentially increasing direct Γ -like wavefunction character mixed into the NC conduction states. This observation and its theoretical understanding could lead to engineering of Si and other indirect band gap NC materials for optical and optoelectronic applications.

Subject C: ‘Quantum materials’ and Design of structures with target properties [5]-[10]

Our work here centered on using first-principles calculations to study special intriguing effects in so called ‘Quantum Materials’. Recent results include:

- (a) Discovering that the interfacial charge and magnetism at the junction between two insulators LaAlO₃ and SrTiO₃ originates from polarity-induced spontaneous defect formation, not from ‘polarization catastrophe’ [5]. This realization creates a different design principle for achieving conductivity between insulators.
- (b) Design of a never before made compound that is a transparent, 3 eV band gap conductor (made from heavy elements Ta,Ir,Ge normally not associated with large band gaps) ,and experimental verification (measured mobility of 2700 at room temperature) [6].This suggests a different way of thinking about what creates wide gaps in heavy element compounds (a different kind of band anti crossing), and what can lead to conductivity in the presence of a wide gap (easily formed Ge-on-Ta anti site defect that releases plenty of mobile holes).
- (c) Sorting of numerous never before made (‘missing compounds’) of the 1:1:1 family into ‘missing predicted stable’ and ‘missing predicted unstable’ and successful synthesis of 18 members of the former class with structures agreeing in all cases with the predicted ones [7]. This collaboration created some confidence in our method of predicting lowest energy structures (e.g via our Global Space Group Optimization (GSGO) DFT method as well as high throughput tests),and created a list of never before made interesting compounds including TI and transparent conductors.
- (d) Design of a new prototype compound Rb(CuTe) made from 2D like Cu-Te nanoribbons embedded in a 3D ordinary lattice (of Rb atoms), such that external strain is ‘absorbed’ via rotation of the nanoribbons rather than by a large increase in stress [8]. This opens an interesting avenue for strain tolerant compounds containing a ‘molecular like’ component that has internal (e,g rotational) degrees of freedom.
- (e) Design of a topological superlattice InSb/CdTe from component materials that are not topological [9]. Here the idea is to utilize the internal electric field set up by these *non- isovalent* components (a III-V such as InSb and a II-VI such as CdTe) to create a Stark effect that leads to band inversion.This permits making TI from non band inverted components.

Future Directions:

- (a) Investigating whether a metal (with Fermi level intersecting a band) can nevertheless be transparent (ie designing forbidden transitions at photon energies below 2-3 eV.
- (b) Study the bulk properties and defects Hybrid Organic-inorganic Perovskites with Target Intrinsic Photovoltaic Functionalities
- (c) Investigating whether oxides can be simultaneously topological insulators and thermodynamically stable: Co-evaluation of topological insulation and structural stability of ABO₃ oxide perovskites

(d) Using defect DFT theory to study the origin of spontaneous off stoichiometry in quantum materials including transition metals, such as half-Heusler compounds

Ten Publications (August 2014 – July 2016) supported by BES (additional publications and developments can be found in our web page <http://www.colorado.edu/zunger-materials-by-design/>)

A. 2D Quantum wells and super lattice nanostructures:

- [1] S.A. Tarasenko, M.V. Durnev, M.O. Nestoklon, E.L. Ivchenko, J.-W. Luo, **A. Zunger**, "Split Dirac cones in HgTe/CdTe quantum wells due to symmetry-enforced level anticrossing at interfaces", Phys. Rev. B. **Rapid Communication** **91** (2015) 081302
- [2] J. Deng, A. Zunger, J.Z. Liu, "Cation ordering induced polarization enhancement for PbTiO₃-SrTiO₃ ferroelectric- dielectric superlattices", Phys. Rev. **Rapid Communication** B. **91** (2015) 081301.

B. Silicon Nano crystals:

- [3] I. Sychugov, F. Pevere, Jun-Wei Luo, Alex Zunger , Jan Linnros "Single-dot Absorption Spectroscopy and Theory of Silicon Nanocrystal", Phy. Rev.B. **Rapid Communication** **93**, 161413 (2016).
- [4] Benjamin G. Lee, Jun Wei Luo, Nathan R. Neale, Matthew C. Beard, Daniel Hiller Margit Zacharias, Alex Zunger, Pauls Stradins "Quasi-Direct Optical Transitions in Silicon Nano crystals exceeding the intensity of bulk transitions" **Nano Letters** **16**, 1583-1589 (2016)

C. ‘Quantum Materials’ and Design of structures with target properties

- [5] L. Yu, A. Zunger,"A polarity-induced defect mechanism for conductivity and magnetism at polar-nonpolar oxide interfaces," **Nature Communications** **5**, 5118 (2014).
- [6] F. Yan, X. Zhang, Yonggang Yu, L.Yu, A. Nagaraja, T.O. Mason, and Alex Zunger" Design and discovery of a novel Half- Heusler transparent hole conductor made of all metallic heavy elements" **Nature Communication** **6**, 7308 (2015).
- [7] R. Gautier, X. Zhang, L. Hu, L. Yu, Y. Lin, T. O. L. Sunde, D. Chon, K. R. Poeppelmeier, A. Zunger,"Prediction and accelerated laboratory discovery of previously unknown 18-electron ABX compounds", **Nature Chemistry** **7**, 308-316 (2015)
- [8] Michael J. Vermeer, Xiuwen Zhang, Giancarlo Trimarchi, Peter J. Chupas, Kenneth R. Poeppelmeier and Alex Zunger "Prediction and Synthesis of Strain Tolerant RbCuTe Crystals Based on Rotation of One-Dimensional Nano Ribbons within a Three-Dimensional Inorganic Network" **J. Am. Chem. Soc.** **137**, 11383 (2015).
- [9] Q. Liu, X. Zhang, L. B. Abdalla and A. Zunger, "Transforming common III-V and II-VI semiconductor compounds into two-dimensional topological heterostructures: The case of CdTe/InSb superlattices" **Advaced Functiona Materials** **26**, 3259-3267 (2015)
- [10] Jino Im, Giancarlo Trimarchi, Kenneth Poeppelmeier, and Alex Zunger "Incomplete Peierls-like chain dimerization as a mechanism for intrinsic conductivity and optical transparency: A La-Cu-O-S phase with mixed-anion layers as a case study" **Phys. Rev B** **92**, 235139 (2015)

Unconventional Spin and Orbital Ordering in Semiconductor Nanostructures

Principal investigator: Professor Igor Zutic

Department of Physics, University at Buffalo, State University of New York

Buffalo, NY 14260 zigor@buffalo.edu

Project Scope

Semiconductor nanostructures, such as quantum dots (QDs), provide an interesting interplay of interaction effects in confined geometries and novel opportunities to control the spin and orbital ordering at the nanoscale. However, owing to the computational complexity of including even a small number of magnetic impurities (~ 10), there is a need to apply various approximation schemes to accurately describe magnetic QDs. Unfortunately, a widely used mean-field theory leads to spurious phase transitions and an incorrect description of the carrier density in small magnetic systems. These difficulties impede the progress in understanding the fundamental properties and potential applications of semiconductor nanostructures. To systematically address this situation, our main objectives are: (i) developing a comprehensive framework suitable to study the interplay of many-body effects and quantum confinement in small magnetic systems, focusing on the inclusion of spin fluctuations and developing computational methods beyond the mean-field approximation. (ii) exploring novel possibilities for the control of spin and orbital ordering in semiconductor nanostructures, as well as to providing proposals for their experimental implementation.

Recent Progress

Below are some highlights of progress made in the past 2 years (our publication list and used references are given below the highlights).

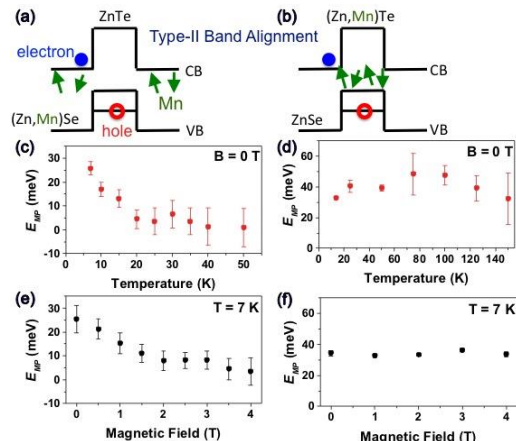


Fig. 1 Type-II band alignment in (a) $(\text{Zn},\text{Mn})\text{Se}/\text{ZnTe}$ and (b) $\text{ZnSe}/(\text{Zn},\text{Mn})\text{Te}$ QDs. (c), (d) Temperature dependence of the MP energy. (e), (f) B-field dependence of the MP energy [1].

Unconventional Magnetic Polaron Formation in (II,Mn)VI Quantum Dots

The formation of a magnetic polaron (MP) can be viewed as a cloud of localized impurity spins, aligned through exchange interaction with a confined carrier spin. It leads to an energy gain by MP formation, E_{MP} , and a red shift in the photoluminescence. Almost all previous MP studies in QDs used a spatially direct Type-I band alignment. Electrons and holes are confined in the same region, since the position of a conduction band (CB) minimum and valence band (VB) maximum coincide. Such QDs promote fast electron-hole recombination and thus suppress the carrier-mediated magnetic ordering. With experimentalists at U. Buffalo [1], we explored paths

to overcome those limitations by focusing on spatially indirect Type-II QDs (Fig. 1). A strong electron-hole spatial separation leads to much longer radiative lifetimes, i.e., the carriers have more time to align nearby Mn-spins. Surprisingly, in two closely related MBE grown Type-II QD systems [Figs. 1(a) and (b)], the MP formation displays a strikingly different behavior based on the location of Mn ions. A conventional MP behavior, i.e., a strong E_{MP} suppression with temperature (T) and magnetic field (B) is observed for Mn-doping outside of the QD [Figs. 1(c)

and (e)]. Both thermal disorder and B-field [partially pre-aligns Mn spins and thus the energy gain through the subsequent exchange-driven alignment is suppressed], give the expected behavior. In contrast, a qualitatively different behavior of robust MPs is seen for Mn-doping in the QDs with a strong hole-Mn overlap [Figs. 1(d) and (f)]. We have qualitatively explained such a peculiar $E_{MP}(T,B)$ behavior, attributed to a large difference in the magnitude of the exchange field.

Magnetic Ordering in Quantum Dots: Open vs. Closed Shells

Changing the carrier occupancy, from open to closed shells, leads to qualitatively different forms of carrier-mediated magnetic ordering in QDs. While it is common to study such nanomagnets within a mean field approximation (MFA), excluding the spin fluctuations can mask important phenomena and lead to spurious thermodynamic phase transitions in small magnetic systems [2].

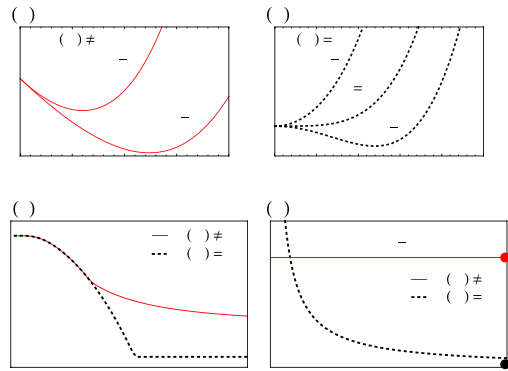


Fig. 2 Magnetic ordering in nanomagnets. A system that (a) does not and (b) does display a phase transition. The free energy, Eq. (1), is shown as a function of the order parameter at various T applicable to both (a) and (b). (c) The T -evolution of the order parameter for the free energy described in (a) and (b). (d) For high T , there are two qualitatively different finite-size scalings for the normalized order parameter which also extrapolate to distinct thermodynamic limits (circles) [2].

By employing coarse-grained, variational, and Monte Carlo methods on singly and doubly occupied QDs to include spin fluctuations, we have studied the relevance of the MFA and identified different finite-size scaling. To qualitatively distinguish magnetic ordering in different systems, we use a simple description in which the relevant free energy functional is reduced to a MFA free energy, F , given as a function of the order parameter X , and T ,

$$F(X,T) = g_0 + g_1 X + \alpha X^2/2 + g_4 X^4/4, \quad (1)$$

where the coefficients, g_0 , g_1 , α , and g_4 are functions of T , see Fig. 2. The quadratic and quartic terms in X describe the entropy of the magnetic ions. In contrast to the conventional Ginzburg-Landau form, Eq. (1) contains the linear term in X in the absence of an applied B-field. We explain the origin of this term by

a careful choice of the order parameter, which should be an observable quantity, such as the exchange energy [2] and not the widely used magnetization which leads to spurious phase transitions in nanomagnets.

Magnetoanisotropic Andreev Reflection in Ferromagnet/Superconductor Junctions

We reveal [3] how the spin-orbit coupling (SOC) and crystalline anisotropy influence the process of Andreev reflection (AR), in which the reflected particle carries the information about the phase of the incident particle and the macroscopic phase of the superconductor to which a Cooper pair is being transferred, see Fig. 3. AR spectroscopy is known as a sensitive probe of signatures of a superconducting pairing and carrier spin polarization in F/S junctions. While the anisotropy of the AR was previously attributed to the anisotropy of the superconducting pair potential, we show [3] that it can also arise due to interfacial SOC, even with an isotropic s-wave pairing. We ascribe behavior to the change in direction

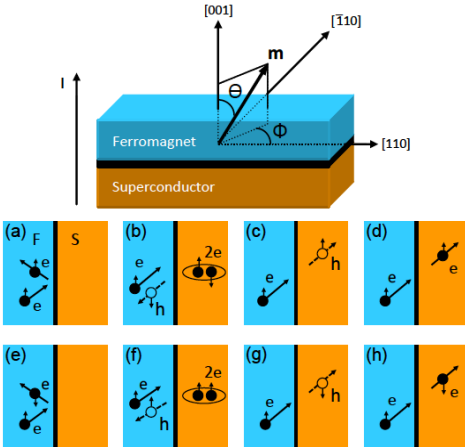


Fig. 3 Top: F/S junction. Magnetization vector \mathbf{m} is given by the spherical angles Θ , Φ . Current, I , flows normal to the interface. Bottom: Scattering processes at the F/S interface with SOC. Electrons (holes): full (empty) circles. Vertical arrows denote the spin. The processes for a spin up incoming electron: (a) Specular reflection, AR, (c) hole-like AR [3].

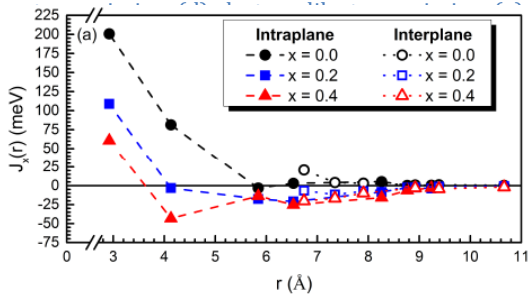


Fig. 4 The magnetic interaction's doping dependence as a function of distance between Mn pairs for different hole doping, x in $(\text{Ba},\text{K})(\text{Zn},\text{Mn})_2\text{As}_2$. A corresponding sign change, as a function distance, reveals the competition of the antiferromagnetic short-range superexchange and ferromagnetic carrier-mediated indirect changes, leading to frustrated magnetism [4].

coupling, J_{eff} . The key difference between the classical double exchange and the actual interaction in DMS is that an effective J_{eff} , as opposed to the standard Hund's coupling J , depends on the Mn d-band position with respect to the Fermi level, and thus allows tuning of the magnetic interactions. We predict a path to enhance T_c in novel DMS with an already record-high T_c .

Future Plans

Experimental Realization of Magnetoanisotropic Andreev Reflection Results in high-quality Fe/MgO/S junctions by Farkhad Aliev (UNAM) show MAAR/TAMR>600, consistent with our predictions initially focused on S/semiconductor junctions [3]. We will modify our approach for F/MgO/S junctions and generalize our MAAR model [3] neglecting the orbital effect, induced by the B-field needed to rotate the magnetization. The inclusion of the B-field will be also important to explain a peculiar long-range proximity effect.

Transport and Magnetic Patterns in Quantum Dots While spin-dependent transport in has been studied in various QDs, it assumed the absence of magnetism in closed-shell systems. This

of magnetization in the F region. Remarkably, the resulting magneto-anisotropic AR (MAAR), leads to anisotropic out-of-plane resistance [3],

$$\text{MAAR}=[R(90^\circ)-R(0^\circ)]/R(90^\circ), \quad (2)$$

orders of magnitude larger than its normal-state counterpart, tunneling anisotropic magnetoresistance (TAMR) in highly spin-polarized F. This is because AR (with no analog in the normal-state TAMR) is very sensitive to interfacial SOC fields. Our findings, recently experimentally confirmed, establish AR spectroscopy as a probe of interfacial SOC in F/S junctions.

Theory of Novel Mn-doped II-II-V Semiconductors

A novel II-II-V magnetic semiconductor $(\text{Ba},\text{K})(\text{Zn},\text{Mn})_2\text{As}_2$, isostructural to 122 Fe-based superconductors, with its decoupled spin and charge doping, provides a unique opportunity to elucidate the microscopic origin of the magnetic interaction and ordering in dilute magnetic semiconductors (DMS). We show that (i) the conventional density functional theory accurately describes this material, and (ii) the magnetic interaction emerges from the competition of the short-range superexchange and the longer-range spin-spin interaction mediated by the itinerant As holes, depicted in Fig. 4 [4]. The carrier-mediated interaction can be viewed as a high-doping extrapolation of double exchange with the Schrieffer-Wolff p-d interaction representing an effective Hund's rule

assumption contradicts our findings of two-carrier generalization of the MPs. We will study magnetic QDs with a tunable carrier occupancy that we expect would lead to nontrivial changes in magnetic ordering and the appearance of magnetic patterns.

Tunneling Planar Hall Effect in Topological Insulators In 3D topological insulators that have helical surface states with spin-momentum locking, we have predicted a novel tunneling planar Hall effect [9] arising from an electrostatic control of a magnetic barrier. Using first-principles calculations, we will examine suitable materials systems to verify our predictions and explore the coexistence of trivial and topological surface states.

Publications

1. B. Barman, R. Oszwa Idowski, L. Schweidenback, A. H. Russ, W.-C. Chou, W.-C. Fan, J. R. Murphy, A. N. Cartwright, I. R. Sellers, A. G. Petukhov, I. Zutic and B. D. McCombe, and A. Petrou, Time Resolved Magneto-Photoluminescence Studies of Magnetic Polaron Dynamics in Type-II Quantum Dots, PRB **92**, 035430 (2015).
2. J. M. Pientka, R. Oszwaldowski, A. G. Petukhov, J. E. Han, and I. Zutic, Magnetic Ordering in Quantum Dots: Open vs. Closed Shells, PRB **92**, 155402 (2015).
3. P. Hogl, A. Matos-Abiague, I. Zutic, and J. Fabian, Magnetoanisotropic Andreev Reflection in Ferromagnet/Superconductor Junctions, PRL **115**, 116601 (2015).
4. J. K. Glasbrenner, I. Zutic, and I. I. Mazin, Theory of Mn-doped II-II-V Semiconductors, PRB **90**, 140403(R) (2014).
5. J. Lee, K. Vyborny, J. Han, and I. Zutic, Nodal 'Ground State' and Orbital Textures in Quantum Dots, PRB **89**, 045315 (2014).
6. A. Khaetskii, V. N. Golovach, X. Hu, and I. Zutic, A Phonon Laser Using Quantum Dot Spin States, PRL **111**, 186601 (2013).
7. B. Scharf and I. Zutic, Probing Majorana-Like States in Quantum Dots and Quantum Rings, PRB **91**, 144505 (2015).
8. G. L. Fatin, A. Matos-Abiague, B. Scharf, and I. Zutic, Wireless Majorana Bound States: From Magnetic Tunability to Braiding, arXiv:1510.08182, PRL (in press).
9. B. Scharf, A. Matos-Abiague, J. E. Han, E. M. Hankiewicz, and I. Zutic, Tunneling Planar Hall Effect in Topological Insulators: Spin-Valves and Amplifiers, arXiv:1601.01009 (PRL under review).
10. A. Matos-Abiague and J. Fabian, Tunneling Anomalous Hall and Spin Hall Effects, PRL **115**, 056602 (2015).
11. B. Scharf, A. Matos-Abiague, I. Zutic, and J. Fabian, Probing Topological Transitions in HgTe/ CdTe Quantum Wells by Magneto-Optical Measurements, PRB **91**, 235433 (2015).
12. B. Scharf, T. Frank, M. Gmitra, J. Fabian, I. Zutic, and V. Perebeinos, Excitonic Stark Effect in MoS₂ Monolayers, arXiv:1606.03902 (PRB under review).
13. B. Scharf, Z. Wang, D. V. Tuan, J. Shan, K. F. Mak, I. Zutic, and H. Dery, Probing Many-Body Inter-actions in Monolayer Transition-Metal Dichalcogenides, arXiv:1606.0710 (PRL under review).
14. P. Lazic, K. D. Belashchenko, and I. Zutic, Effective Gating and Tunable Magnetic Proximity Effects in Two-Dimensional Heterostructures, PRB **93**, 241401(R) (2016).
15. I. Zutic and P. E. F. Junior, Semiconductor Lasers Taken for a Spin, Nat. Nanotech. **9**, 750 (2014).
16. N. Tesarova, T. Ostatnický, V. Novak, K. Olejník, J. Subrt, H. Reichlova, A. M. C. T. Ellis, J. Lee, G. M. Sipahi, J. Sinova, J. Hamrle, T. Jungwirth, P. Nemec, J. Černé, and K. Vyborny, Systematic Study of Magnetic Linear Dichroism and Birefringence in (Ga,Mn)As, PRB **89**, 085203 (2014).
17. I. Zutic and A. Matos-Abiague, Fluid Spintronics: Cause a Stir, Nat. Phys. **12**, 24 (2016).

Author Index

Allen, Philip B.....	1
Antropov, Vladimir	338
Balents, Leon.....	5
Bansil, Arun	9
Baranger, Harold U.	13
Barraza-Lopez, Salvador.....	17
Bellaiche, Laurent	23
Benali, Anouar	150
Bernholc, J.	27
Bhatt, Ravindra N.....	32
Bondarev, Igor.....	38
Burke, Kieron.....	347
Ceperley, David M.....	150
Chamon, Claudio	42
Chan, Garnet Kin-Lic.....	46
Chelikowsky, James R.	50
Cheng, Hai-Ping.....	54
Chernyshev, Alexander	59
Chudnovsky, Eugene M.	63
Cohen, Marvin L.	184
Coleman, Piers	68
Cooper, Valentino R.....	72, 220
Dagotto, Elbio	77
Daw, Murray S.	81
Di Ventra, Massimiliano	325
Dobrovitski, Viatcheslav.....	338
Du, M. H.	220
Dufty, J. W.	295
Eisenbach, Markus	251
Feiguin, Adrian	86
Fernandes, Rafael M.	90
Finkel'stein, Alexander.....	95
Fishman, Randy	77
Freericks, J. K.	99
Fry, James N.	54
Fu, Liang	103
Galitski, Victor M.	106
Galli, Giulia.....	110, 113, 125
Glatz, Andreas.....	330
Glazman, Leonid.....	117
Gull, Emanuel	121
Gygi, Francois	125
Haas, Stephan.....	129
Haldane, F. Duncan M.	32
Harris, F. E.	295
Heinonen, Olle	230
Hermele, Michael.....	133
Ho, Kai-Ming	338
Jain, Anubhav.....	141
Jain, Jainendra K.	137
Johnson, Duane D.	145
Kamenev, Alex.....	117
Kent, Paul R. C.	150
Kettemann, Stefan	129
Kim, Eun-Ah	154
Konik, R. M.	307
Koshelev, Alex	230
Kotliar, Gabriel	158
Kovalev, Alexey.....	162
Krogl, Jaron T.....	251
Ku, Wei	307
Lambrecht, Walter R. L.	166
Landman, Uzi.....	171
Lee, Dung-Hai.....	184
Lee, Patrick A.	175
Lindsay, L. R.	220
Littlewood, Peter	230
Liu, Andrea J.	180
Louie, Steven G.....	184
Lyanda-Geller, Yuli	188
MacDonald, Allan H.	192
Markiewicz, Robert S.....	9
Martin, Ivar	230
Matveev, Kostya	230
Mele, Eugene.....	196
Millis, A. J.	200
Mishchenko, Eugene	204
Mitas, Lubos.....	208
Mitra, Aditi.....	212
Morales, Miguel A.	150
Moreo, Adriana	77
Morr, Dirk K.	216
Morris, J. R.	220
Nagel, Sidney	226
Neaton, Jeffrey B.	184
Niu, Qian	192
Norman, Mike	230
Okamoto, Satoshi	77
Ozolins, Vidvuds.....	356
Parker, D. S.	220
Perez, Danny	334
Pickett, Warren E.	234

Pleimling, Michel.....	287
Raghu, Srinivas	238
Rahman, Talat S.....	243
Rappe, Andrew M.....	247
Reboreda, Fernando A.....	251
Rehr, John J.....	257
Rezayi, Edward H.....	32
Runge, K.....	295
Saleur, Hubert	129
Satpathy, Sashi	261
Scalettar, Richard	265
Schlottmann, Pedro	268
Schwegler, Eric	125
Shastry, Sriram.....	272
Sheng, Donna N.....	276
Shulenburger, Luke	150
Stafford, Charles A.....	282
Stocks, G. Malcolm.....	251
Täuber, Uwe C.....	287
Todadri, Senthil.....	291
Trickey, Samuel B.....	295
Trivedi, Nandini	299
Tserkovnyak, Yaroslav	303
Tsvelik, Alexei M.....	307
Ullrich, Carsten A.....	316
Vashishta, Priya	320
Vignale, Giovanni	325
Vinokur, Valerii	330
Voter, Arthur F.....	334
Wang, Cai-Zhuang	338
Wang, Lin-Wang.....	184
Wang, Ziqiang.....	342
White, Steven R.....	347
Widom, Michael.....	352
Wolverton, Christopher.....	356
Woods, Lilia M.....	361
Wu, Ruqian	365
Wu, Zhigang.....	369
Yang, Kun	32
Yao, Yongxin	338
Yin, Weiguo	307
Zang, Jiadong	373
Zhang, Guoping	377
Zhang, Shengbai.....	381
Zunger, Alex	386
Zutic, Igor.....	390

Participant List

<u>Name</u>	<u>Organization</u>	<u>Email</u>
Allen, Philip	Stony Brook University	philip.allen@stonybrook.edu
Balents, Leon	University of California, Santa Barbara	balents@kitp.ucsb.edu
Bansil, Arun	Northeastern University	ar.bansil@neu.edu
Baranger, Harold	Duke University	baranger@phy.duke.edu
Barraza-Lopez, Salvador	University of Arkansas	sbarraza@uark.edu
Bellaiche, Laurent	University of Arkansas	laurent@uark.edu
Benali, Anouar	Argonne National Laboratory	benali@anl.gov
Bernholc, Jerzy	North Carolina State University	bernholc@ncsu.edu
Bondarev, Igor	North Carolina Central University	ibondarev@nccu.edu
Chamon, Claudio	Boston University	chamon@bu.edu
Chan, Garnet	California Institute of Technology	gkc1000@gmail.com
Chelikowsky, James	University of Texas, Austin	jrc@utexas.edu
Chubukov, Andrey	University of Texas, Austin	huachen@physics.utexas.edu
Chudnovsky, Eugene	University of Minnesota	achubuko@umn.edu
Coleman, Piers	City University of New York	Eugene.Chudnovsky@Lehman.CUNY.edu
Cooper, Valentino	Rutgers University	coleman@physics.rutgers.edu
Dagotto, Elbio	Oak Ridge National Laboratory	coopervr@ornl.gov
Daw, Murray	ORNL / University of Tennessee	edagotto@utk.edu
Devereaux, Tom	Clemson University	daw@clemson.edu
Eisenbach, Markus	Stanford University	tpd@stanford.edu
Feiguin, Adrian	Oak Ridge National Laboratory	eisenbachm@ornl.gov
Fernandes, Rafael	Northeastern University	a.feiguin@northeastern.edu
Finkel'stein, Alexander	University of Minnesota	rfernand@umn.edu
Fu, Liang	Texas A&M University	finkelstein@physics.tamu.edu
Galli, Giulia	Massachusetts Institute for Technology	liangfu@mit.edu
Glatz, Andreas	University of Chicago	gagalli@uchicago.edu
Glazman, Leonid	Argonne National Laboratory	glatz@anl.gov
Gull, Emanuel	Yale University	leonid.glazman@yale.edu
Gygi, Francois	University of Michigan	egull@umich.edu
Haas, Stephan	University of California, Davis	fgygi@ucdavis.edu
Heinonen, Olle	University of Southern California	shaas@usc.edu
Hermele, Michael	Argonne National Laboratory	heinonen@anl.gov
Hirschfeld, Peter	University of Colorado, Boulder	michael.hermele@colorado.edu
Ho, K M	University of Florida	pjh@phys.ufl.edu
Jain, Anubhav	Ames Laboratory	kmh@iastate.edu
Jain, Jainendra	Lawrence Berkeley National Laboratory	ajain@lbl.gov
Johnson, Duane	Pennsylvania State University	jkj2@psu.edu
Kargarian, Mehdi	Ames Laboratory/Iowa State University	DDJ@AmesLab.gov
Kent, Paul	University of Maryland, College Park	mehdi.kargarian@gmail.com
Klironomos, Alexios	Oak Ridge National Laboratory	kentpr@ornl.gov
Kotliar, Gabriel	National Science Foundation	aklirono@nsf.gov
Kovalev, Alexey	BNL /Rutgers University	kotliar@physics.rutgers.edu
Lambrecht, Walter	University of Nebraska, Lincoln	alexey.kovalev@unl.edu
Landman, Uzi	Case Western Reserve University	walter.lambrecht@case.edu
Lee, Patric	Georgia Institute of Technology	uzi@gatech.edu
Liu, Andrea	Massachusetts Institute for Technology	palee@mit.edu
Louie, Steven	University of Pennsylvania	ajliu@physics.upenn.edu
Lyanda-Geller, Yuli	LBNL / University of California, Berkeley	sglouie@berkeley.edu
Markiewicz, Robert	Purdue University	yuli@purdue.edu
	Northeastern University	markiewic@neu.edu

Martin, Ivar	Argonne National Laboratory	ivar@anl.gov
Mele, Eugene	University of Pennsylvania	mele@physics.upenn.edu
Millis, Andrew	Columbia University	millis@phys.columbia.edu
Mitas, Lubos	North Carolina State University	lmitas@ncsu.edu
Mitra, Aditi	New York University	aditi.mitra@nyu.edu
Morr, Dirk	University of Illinois, Chicago	dkmorr@uic.edu
Morris, James	Oak Ridge National Laboratory	morrisj@ornl.gov
Nagel, Sidney	University of Chicago	srnagel@uchicago.edu
Neaton, Jeffrey	LBLN / University of California, Berkeley	jbneaton@lbl.gov
Niu, Qian	University of Texas, Austin	niu@physics.utexas.edu
Norman, Michael	Argonne National Laboratory	norman@anl.gov
Ochoa de Eguileor, Hector	University of California, Los Angeles	hector.ochoa@physics.ucla.edu
Ozolins, Vidvuds	University of California, Los Angeles	vidvuds@ucla.edu
Perez, Danny	Los Alamos National Laboratory	danny_perez@lanl.gov
Perry, Kelly	Oak Ridge National Laboratory	perryka@ornl.gov
Pickett, Warren	University of California, Davis	wepickett@ucdavis.edu
Raghу, Srinivas	Stanford University	sraghu@stanford.edu
Rahman, Talat	University of Central Florida	talat.rahman@ucf.edu
Rappe, Andrew	University of Pennsylvania	rappe@sas.upenn.edu
Reboredо, Fernando	Oak Ridge National Laboratory	reboredofa@ornl.gov
Rehr, John	University of Washington	jjr@uw.edu
Satpathy, Sashi	University of Missouri	satpathys@missouri.edu
Scalettаr, Richard	University of California, Davis	scalettar@physics.ucdavis.edu
Schlottmann, Pedro	Florida State University	schlottmann@physics.fsu.edu
Shastry, Sriram	University of California, Santa Cruz	sriram@physics.ucsc.edu
Stafford, Charles	University of Arizona	staffordphysics92@gmail.com
Sumpter, Bobby	Oak Ridge National Laboratory	sumpterbg@ornl.gov
Täuber, Uwe	Virginia Technology	tauber@vt.edu
Todadri, Senthil	Massachusetts Institute for Technology	senthil@mit.edu
Trickey, Samuel	University of Florida	trickey@qtp.ufl.edu
Trivedi, Nandini	The Ohio State University	trivedi.15@osu.edu
Tsvelik, Alexei	Brookhaven National Laboratory	tsvelik@gmail.com
Ullrich, Carsten	University of Missouri	ullrichc@missouri.edu
Vashishta, Priya	University of Southern California	priyav@usc.edu
Vignale, Giovanni	University of Missouri	vignaleg@missouri.edu
Vinokour, Valerii	Argonne National Laboratory	vinokour@anl.gov
Voter, Arthur	Los Alamos National Laboratory	afv@lanl.gov
Wang, Ziqiang	Boston College	wangzi@bc.edu
Wang, Cai-Zhuang	Ames Laboratory	wangcz@ameslab.gov
White, Steven	University of California, Irvine	srwhite@uci.edu
Widom, Michael	Carnegie Mellon University	widom@cmu.edu
Woods, Lilia	University of South Florida	lmwoods@usf.edu
Wu, Ruqian	University of California, Irvine	wur@uci.edu
Wu, Zhigang	Colorado School of Mines	zhiwu@mines.edu
Yang, Kun	Florida State University	kunyang@magnet.fsu.edu
Zang, Jiadong	University of New Hampshire	jiadong.zang@unh.edu
Zhang, Shengbai	Rensselaer Polytechnic Institute	zhangs9@rpi.edu
Zhang, Guoping	Indiana State University	gpzhang@magneto.indstate.edu